Diversity, disparity and the temporal dynamics of eco-morphological adaptation in the cichlid radiation of Lake Tanganyika

Inauguraldissertation

zur

Erlangung der Würde eines Doktors der Philosophie

vorgelegt der

Philosophisch-Naturwissenschaftlichen Fakultät

der Universität Basel

von

Fabrizia Nina Ronco

aus Basel, Schweiz

2021

Genehmigt von der Philosophisch-Naturwissenschaftlichen Fakultät auf Antrag von

Prof. Dr. Walter Salzburger, Prof. Dr. George Turner

(Mitglieder des Dissertationskomitees: Fakultätsverantwortliche/r, Dissleiter/in, Korreferent/in)

Basel, den 25. Juni 2019

(Datum der Genehmigung durch die Fakultät)

Prof. Dr. Martin Spiess

Dekanin/Dekan

Diversity, disparity and the temporal dynamics of eco-morphological adaptation in the cichlid radiation of Lake Tanganyika

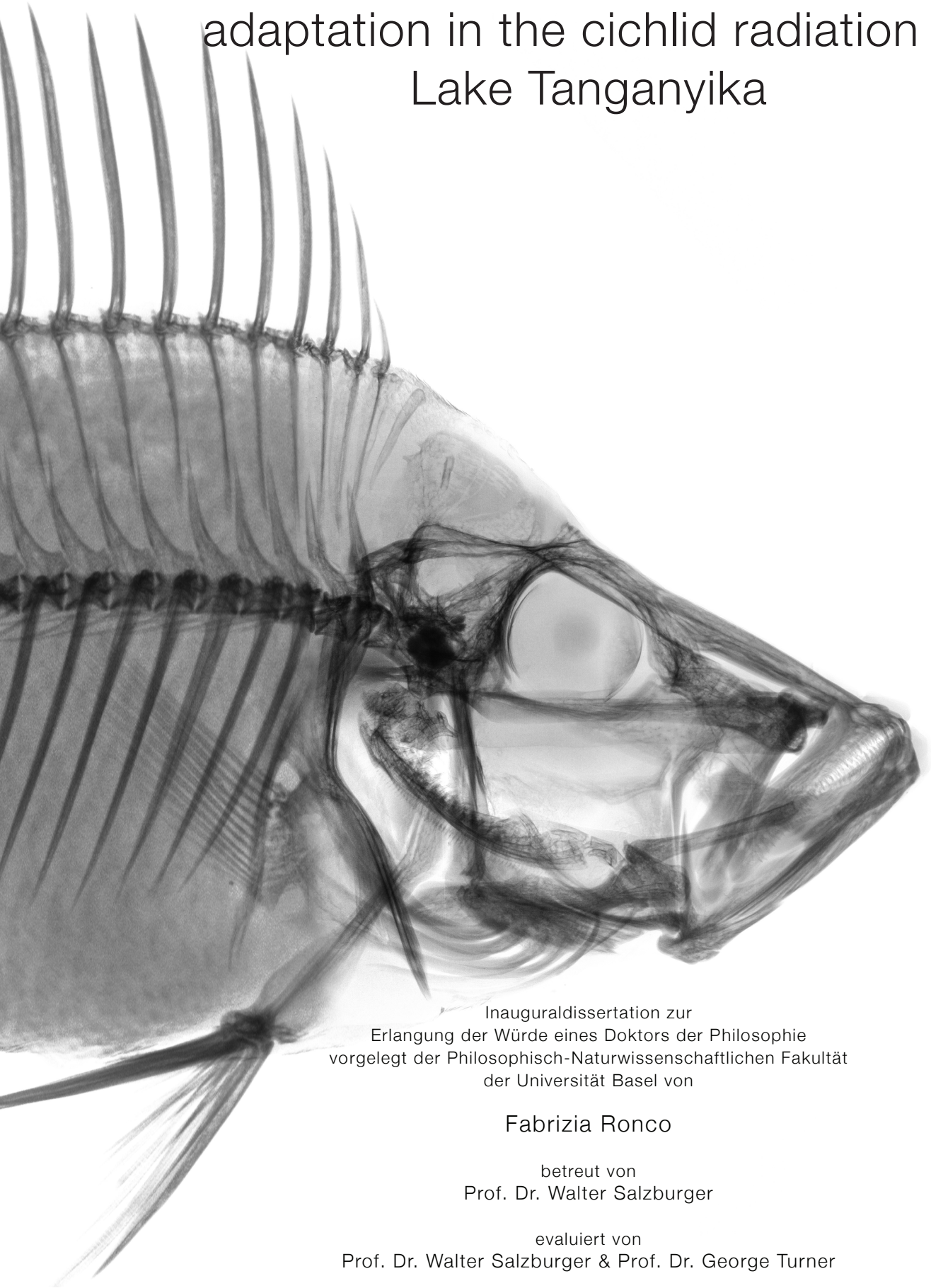

Inauguraldissertation zur
Erlangung der Würde eines Doktors der Philosophie
vorgelegt der Philosophisch-Naturwissenschaftlichen Fakultät
der Universität Basel von

Fabrizia Ronco

betreut von
Prof. Dr. Walter Salzburger

evaluiert von
Prof. Dr. Walter Salzburger & Prof. Dr. George Turner

Preface

"(...) how the innumerable species inhabiting this world have been modified, so as to acquire that perfection of structure and coadaptation which justly excites our admiration." — Charles Darwin, *The Origin of Species*

Charles Darwin's words from the introduction of *The Origin of Species* – the genesis of evolutionary biology – get right to the heart of what inevitably crosses one's mind when dipping your head into the warm waters of one of the East African Great Lakes: The incredible diversity, the abundance, the degree of specialization. Cichlid fishes as far as the eye can see – the entire ecosystem seems to be governed by cichlids. All forms and shapes one can think of how to modify a fishes' body plan. Each member of the species flock appears to be specialized in order to maximize the number of species fitting in the lake.

To me, the Lake Tanganyika radiation has become more than only an ideal model system to approach different questions of evolutionary biology, it exemplifies what inspires me to be a biologist: The fascination for nature's diversity and the curiosity in trying to comprehend it – understand how the elusive biodiversity we find on this planet arose, how it adapts and how it persists. Why do some lineages in the tree of life, show more diversity and specializations than others? I hope that my scientific contribution provides an additional step towards a better understanding of the processes and mechanisms of evolution by combining technologies of modern research with the mind of a naturalist.

Fabrizia Ronco, June 2019

Contents

Introduction

Even one hundred sixty years after the initial release of Charles Darwin's '*The Origin of Species*' (Darwin, 1859), evolutionary biologists are still seeking to understand the origin of the incredible diversity of live on Earth. Without doubts, there have been great advances in the field, but some fundamental questions on how species arise, adapt and persist, and what contributes to the dynamics and patterns of diversity, are still a main focus of modern evolutionary research. One particular pattern stands out regarding the distribution of diversity in the tree of life: some lineages diversified (or are still diversifying) more than others. Many of these extremely species-rich groups are the product of one of the most remarkable features of evolution – *adaptive radiations*. Adaptive radiation describes the process that a single lineage rapidly diversifies into a variety of phenotypically diverse species, well adapted to their ecological niches (Schluter, 2000). This typically results in a vast number of species in a relatively short period of time and is likely the source of a great portion of the biodiversity we find today (Gavrilets and Losos, 2009; Schluter, 2000). Among the most famous and best studied examples of adaptive radiations are the species assemblages of the Galapagos finches (Grant and Grant, 2007), the Caribbean anole lizards (Losos, 2009), the Hawaiian silverswords (Baldwin and Sanderson, 1998), and the impressive species flocks of the East African cichlid fishes (Fryer and Iles, 1972; Salzburger, 2018), which are the focus of this PhD thesis. In the East African Great Lakes Tanganyika, Malawi, and Victoria over a thousand cichlid species evolved through independent adaptive radiations in the last few millions to several thousands of years (Kocher, 2004; Salzburger, 2018). This unique setting of parallel radiations makes the East African cichlids one of the prime model systems of evolutionary biology – or in the words of Gorge Barlow: *'nature's grand experiment in evolution'* (Barlow, 2000). The Lake Tanganyika adaptive radiation, however, stands out from these: It is the oldest of the radiations and – although not the most species-rich – exhibits the highest degree of morphological, ecological as well as behavioural diversity (Fryer and Iles, 1972; Salzburger et al., 2014).

In the classical view, adaptive radiations are considered the consequence of 'ecological opportunity' that opens when a new environment with abundant and underutilized resources is colonized. This can happen when a new environment emerges (typically the formation of a new lake or island), when a variety of niche space is freed (i.e. after a mass-extinction event), or with the emergence of a so called 'key-innovation' – a novel trait which enables a lineage to colonize new niche space (Schluter, 2000; Simpson, 1953).

Besides the production of taxonomic diversity, the second important component of an adaptive radiation is *adaptation* to a variety of niches (Gavrilets and Losos, 2009; Schluter, 2000). Hence a crucial feature of an adaptive radiation is a close link between phenotype and environment. This relationship has been established for several adaptive radiations, for example, the shape and size of the beak in the different Galapagos finches reflects specialization in their diet (Grant and Grant, 2007), and the various anole eco-morphs on the Caribbean islands differ in their habitat use (Losos, 2009). Also within the East African cichlid radiations several adaptive traits have been identified, reflecting different trajectories of niche exploitation (reviewed for Tanganyika cichlids in (Takahashi and Koblmüller, 2011)). For instance, overall body shape plays an important role in swimming performance and thus mainly reflects divergence along the benthic-limnetic axis (Barluenga et al., 2006; Muschick et al., 2014). Further, head morphology, including gill raker morphology are associated with trophic adaptation (Clabaut et al., 2007; Muschick et al., 2014, 2012). Gill rakers are spine-like, bony protrusions of the branchial gill arches in fishes and are important for uptake and handling of food particles in the buccal cavity (Sanderson et al., 2001). The cichlids' jaws, however, have received particular attention: Besides the oral jaw apparatus, cichlids possess a second set of jaws situated in the pharynx. This pharyngeal jaw apparatus is used to masticate and process food items and is functionally decoupled from the oral jaw apparatus (Hulsey, 2006; Liem, 1973; see Figure 1). The highly specialized pharyngeal jaw apparatus of cichlids is often referred to as a key-innovation (Hulsey, 2006; Liem, 1973), and modifications in its morphology have been associated with a shift in resource use (Hulsey, 2006; Muschick et al., 2012; Salzburger, 2009). Importantly, the combination of several such adaptive traits may have contributed to the build-up of reproductive isolation between species (see Nosil, 2012) and allow for the co-occurrence of closely related taxa (Takahashi and Koblmüller, 2011).

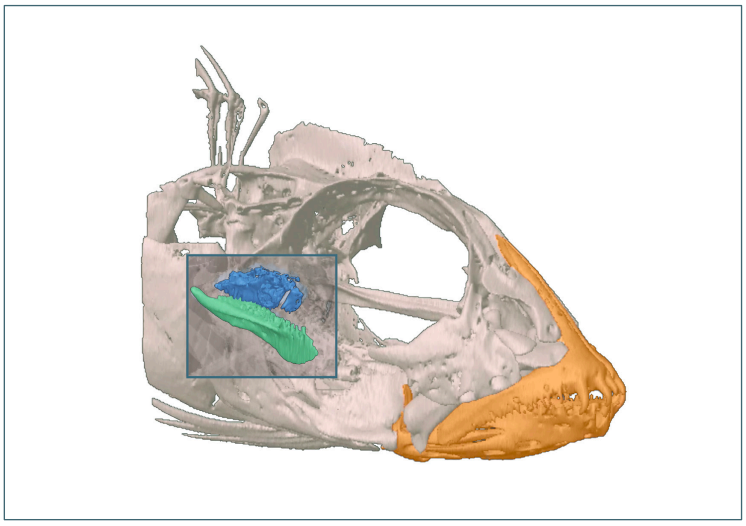

Figure 1: Three-dimensional reconstruction (based on X-ray computed tomography) of the head of the cichlid species *Neolamprologus furcifer*. The oral jaw apparatus is highlighted in orange. A section of the skull was virtually removed (blue box) to uncover the pharyngeal jaw apparatus (the upper pharyngeal jaw bones are highlighted in blue and the lower pharyngeal jaw in green).

The major goal of this thesis is to provide a better understanding of the importance and the dynamics of eco-morphological adaptations in the Lake Tanganyika cichlid adaptive radiation and to identify drivers of diversity and morphological disparity. The first part of my thesis (Part I: Main Body of Work) covers three chapters representing the main focus of my PhD work on taxonomic, eco-morphological and genetic diversity of the Lake Tanganyika cichlid adaptive radiation.

One of the approaches of this thesis towards a better understanding of the contribution of eco-morphological adaptation to a radiation was to conduct an integrative analysis of the *entire* Lake Tanganyika cichlid radiation (see Chapter 2 & 8). Thus, as a first step we compiled an up-to-date inventory of the taxonomic diversity of Lake Tanganyika's cichlid fishes (Chapter 1: The taxonomic diversity of the cichlid fish fauna of ancient Lake Tanganyika, East Africa). This compilation not only provides a complete list of all currently valid described cichlid species of Tanganyika, but also lists putative species (undescribed) as well as local varieties on the basis of the available literature as well as extensive observations and collections around the lake. I further review the taxonomic history of the Tanganyika cichlids assemblage and discuss some of the major taxonomic challenges regarding this species flock.

Based on theoretical work and empirical studies a variety of predictions on the outcome and the dynamics of adaptive radiations have been postulated (Gavrilets and Losos, 2009; Schluter, 2000). One of the ensuing main features of adaptive radiations is a phenotype-environment correlation reflecting phenotypic specialisation to the exploited ecological niches (Schluter, 2000). Mathematical models predict that eco-morphological diversification and speciation arise early in the radiation, declining over time as the available niche space is filled (Gavrilets and Losos, 2009). Further adaptation is expected to proceed in stages – a characteristic ordering of divergence along different selective trajectories (Danley and Kocher, 2001; Gavrilets and Losos, 2009; Streelman and Danley, 2003). Both the 'early burst' model and the 'stages' model have received little empirical support so far (Gavrilets and Losos, 2009). However, they had never been tested on a large radiation with a complete taxon sampling. Therefore, Chapter 2 (Drivers, dynamics and progression of a massive adaptive radiation in African cichlid fish) focuses on the in-depth investigation of nearly the entire taxonomic diversity of the Tanganyika cichlid adaptive radiation (see Chapter 1): We combined whole genome sequencing, multivariate morphological measurements (based on three-dimensional and two-dimensional X-ray imaging) of several morphological traits, and stable isotope analysis as a proxy for niche use in virtually all species of the Lake Tanganyika cichlid radiation. Based on this extensive dataset we present the most comprehensive phylogenetic hypothesis of Lake Tanganyika cichlids to date and investigate the association of niche use and body shape as well as oral jaw morphology and lower pharyngeal jaw shape. Combining the phylogenetic framework with the eco-morphological data we trace back patterns of eco-morphological evolution through the phylogenetic history of the radiation and test predictions of the adaptive radiation theory.

The third chapter (A functional trade-off between trophic adaptation and parental care predicts sexual dimorphism in cichlid fish) focuses on another important trophic trait in fish – the gill raker apparatus. In this study, we first investigate how differences in gill raker length relate to trophic ecology across 65 Tanganyika cichlid species. Further, we provide an alternative perspective on the diversity of trophic morphology in Lake Tanganyika cichlids – the too often neglected contribution of sexual dimorphism. We hypothesize that gill rakers are not only involved in food uptake and handling, but also in mouthbrooding. By contrasting the different breeding modes of Lake Tanganyika cichlids (uni-parental mouthbrooders, bi-parental mouthbrooders, and nest guarding species) we investigate how the interplay of mouthbrooding and trophic ecology might have led to sexual dimorphism in gill raker length.

The second part of the thesis (Part II: Side Projects) comprises five chapters, to which I contributed on different aspects of speciation research using Tanganyika cichlids as a model system. In Chapter 4 and 5 (Adaptive divergence between lake and stream populations of

an East African cichlid fish and Variation of anal fin egg-spots along an environmental gradient in a haplochromine cichlid fish) we zoom into the speciation continuum of different populations of the haplochromine species *Astatotilapia burtoni* by investigating population divergence along an environmental gradient in a replicated lake and stream system.

Chapter 6 introduces Point-Combination Transect (PCT): Incorporation of small underwater cameras to study fish communities, a newly developed method for community assessment. We later applied this method to a large-scale survey in Lake Tanganyika to investigate habitat differentiation and co-occurrence patters of Lake Tanganyika cichlids (Chapter 7: Community assembly patterns and niche evolution in the species-flock of cichlid fishes from the East African Lake Tanganyika).

Chapter 8 focuses on yet another component of speciation – the evolution of sex chromosomes: Tempo and mode of sex chromosome turnovers in an adaptive radiation.

The last part of my thesis (Part III: Outreach) is a perspective (dispatch) on a paper investigating speciation in an African crater lake (Malinsky et al., 2015).

The three parts of the thesis are followed by an overall discussion of the results obtained from the three main chapters (part I). I would like to emphasize that all the work I present here is the product of various collaborations, my personal contribution to each chapter can be taken from the respective authors contribution section.

References

Baldwin, B.G., Sanderson, M.J., 1998. Age and rate of diversification of the Hawaiian silversword alliance (Compositae). Proc. Natl. Acad. Sci. U. S. A. 95, 9402–9406.

Barlow, G., 2000. The Cichlid fishes: Nature's Grand Experiment in Evolution. Perseus Publishing, Cambridge, Massachusetts.

Barluenga, M., Stölting, K.N., Salzburger, W., Muschick, M., Meyer, A., 2006. Sympatric speciation in Nicaraguan crater lake cichlid fish. Nature 439, 719–723. https://doi.org/10.1038/nature04325

Clabaut, C., Bunje, P.M.E., Salzburger, W., Meyer, A., 2007. Geometric morphometric analyses provide evidence for the adaptive character of the Tanganyikan cichlid fish radiations. Evolution 61, 560–578. https://doi.org/10.1111/j.1558-5646.2007.00045.x

Danley, P.D., Kocher, T.D., 2001. Speciation in rapidly diverging systems: lessons from Lake Malawi. Mol. Ecol. 10, 1075–1086.

Darwin, C., 1859. On the Origin of Species by Means of Natural Selection. London.

Fryer, G., Iles, T.D., 1972. The Cichlid Fishes of the Great Lakes of Africa. T.F.H. Publications, Neptune City, NJ.

Gavrilets, S., Losos, J.B., 2009. Adaptive Radiation: Contrasting Theory with Data. Science (80-.). 323, 732–737.

Grant, P.R., Grant, B.R., 2007. How and Why Species Multiply: The Radiation of Darwin's Finches. Princeton University Press, Princeton.

Hulsey, C.D., 2006. Function of a key morphological innovation: fusion of the cichlid pharyngeal jaw. Proc. Biol. Sci. 273, 669–675. https://doi.org/10.1098/rspb.2005.3375

Kocher, T.D., 2004. Adaptive evolution and explosive speciation: the cichlid fish model. Nat. Rev. Genet. 5, 288–298. https://doi.org/10.1038/nrg1316

Liem, K.F., 1973. Evolutionary Strategies and Morphological Innovations: Cichlid Pharyngeal Jaws. Syst. Zool. 22, 425–441.

Losos, J., 2009. Lizards in an Evolutionary Tree: Ecology and Adaptive Radiation of Anoles. University of California Press, Berkeley.

Malinsky, M., Challis, R.J., Tyers, A.M., Schiffels, S., Terai, Y., Ngatunga, B.P., Miska, E.A., Durbin, R., Genner, M.J., Turner, G.F., 2015. Genomic islands of speciation separate cichlid ecomorphs in an East African crater lake. Science (80-.). 350, 1493–1498. https://doi.org/10.1126/science.aac9927

Muschick, M., Indermaur, A., Salzburger, W., 2012. Convergent evolution within an adaptive radiation of cichlid fishes. Curr. Biol. 22, 2362–8. https://doi.org/10.1016/j.cub.2012.10.048

Muschick, M., Nosil, P., Roesti, M., Dittmann, M.T., Harmon, L., Salzburger, W., 2014. Testing the stages model in the adaptive radiation of cichlid fishes in East African Lake Tanganyika. Proc. R. Soc. B Biol. Sci. 281, 20140605–20140605. https://doi.org/10.1098/rspb.2014.0605

Nosil, P., 2012. Ecological Speciation. Oxforn Series in Ecology and Evolution.

Salzburger, W., 2018. Understanding explosive diversification through cichlid fish genomics. Nat. Rev. Genet. 19, 705–717. https://doi.org/10.1038/s41576-018-0043-9

Salzburger, W., 2009. The interaction of sexually and naturally selected traits in the adaptive radiations of cichlid fishes. Mol. Ecol. 18, 169–85. https://doi.org/10.1111/j.1365-294X.2008.03981.x

Salzburger, W., Van Bocxlaer, B., Cohen, A.S., 2014. Ecology and Evolution of the African Great Lakes and Their Faunas. Annu. Rev. Ecol. Evol. Syst. 45, 519–545. https://doi.org/10.1146/annurev-ecolsys-120213-091804

Sanderson, S.L., Cheer, A.Y., Goodrich, J.S., Graziano, J.D., Callan, W.T., 2001. Crossflow filtration in suspension-feeding fishes. Nature 412, 439–441. https://doi.org/10.1038/35086574

Schluter, D., 2000. The ecology of adaptive radiation. Oxford University Press, New York.

Simpson, G.G., 1953. The Major Features of Evolution. Columbia University Press, New York.

Streelman, J.T., Danley, P.D., 2003. The stages of vertebrate evolutionary radiation. Trends Ecol. Evol. 18, 126–131. https://doi.org/10.1016/S0169-5347(02)00036-8

Takahashi, T., Koblmüller, S., 2011. The Adaptive Radiation of Cichlid Fish in Lake Tanganyika: A Morphological Perspective. Int. J. Evol. Biol. 1–14. https://doi.org/10.4061/2011/620754

Part I | Main Body of Work

Chapter 1

The taxonomic diversity of the cichlid fish fauna of ancient Lake Tanganyika, East Africa

Fabrizia Ronco, Heinz H. Büscher, Adrian Indermaur & Walter Salzburger

Journal of Great Lakes Research | Special Issue:
Speciation in Ancient Lakes (2020)

Journal of Great Lakes Research 46 (2020) 1067–1078

Contents lists available at ScienceDirect

Journal of Great Lakes Research

journal homepage: www.elsevier.com/locate/ijglr

Review

The taxonomic diversity of the cichlid fish fauna of ancient Lake Tanganyika, East Africa

Fabrizia Ronco *, Heinz H. Büscher, Adrian Indermaur, Walter Salzburger

Zoological Institute, University of Basel, Vesalgasse 1, 4051 Basel, Switzerland

ARTICLE INFO

Article history:
Received 29 January 2019
Received in revised form 10 April 2019
Accepted 29 April 2019
Available online 30 June 2019

Communicated by Björn Stelbrink

Keywords:
Biodiversity
Ichthyodiversity
Great Lakes
Undescribed species

ABSTRACT

Ancient Lake Tanganyika in East Africa houses the world's ecologically and morphologically most diverse assemblage of cichlid fishes, and the third most species-rich after lakes Malawi and Victoria. Despite long-lasting scientific interest in the cichlid species flocks of the East African Great Lakes, for example in the context of adaptive radiation and explosive diversification, their taxonomy and systematics are only partially explored; and many cichlid species still await their formal description. Here, we provide a current inventory of the cichlid fish fauna of Lake Tanganyika, providing a complete list of all valid 208 Tanganyikan cichlid species, and discuss the taxonomic status of more than 50 undescribed taxa on the basis of the available literature as well as our own observations and collections around the lake. This leads us to conclude that there are at least 241 cichlid species present in Lake Tanganyika, all but two are endemic to the basin. We finally summarize some of the major taxonomic challenges regarding Lake Tanganyika's cichlid fauna. The taxonomic inventory of the cichlid fauna of Lake Tanganyika presented here will facilitate future research on the taxonomy and systematics and the ecology and evolution of the species flock, as well as its conservation.

Contents

Introduction

Ancient lakes, defined here as lakes that have continuously existed for much of the Quaternary period or longer, are well known as biodiversity hot-spots. These long persisting freshwater bodies are typically very deep and rather isolated and usually house extremely species-rich biological communities featuring exceptional levels of endemism (Brooks, 1950; Martens, 1997). The extraordinary species richness of these lakes is often the product of intralacustrine adaptive radiations, in the course of which a common ancestor diversifies rapidly into new, phenotypically distinct, species that occupy the available ecological niche space (Schluter, 2000; Salzburger et al., 2014). As a matter of fact, some of the most impressive cases of adaptive radiations are known from ancient lakes, as exemplified by the species flocks of cichlid

* Corresponding author.
E-mail address: fabrizia.ronco@unibas.ch (F. Ronco).

https://doi.org/10.1016/j.jglr.2019.05.009
0380-1330/

fishes in the East African Great Lakes (Fryer and Iles, 1972; Seehausen, 2015; Salzburger, 2018) or the amphipods in Lake Baikal (Macdonald et al., 2005). Besides being hot-spots of organismal diversity, ancient lakes may also serve as species reservoirs over time (Salzburger et al., 2002; Schelly and Stiassny, 2004; Wilson et al., 2004).

Scientific interest in ancient lakes and their faunas is manifold (e.g. Albrecht and Wilke, 2008; Larson and Schaetzl, 2001; Salzburger et al., 2014; Timoshkin et al., 2016; von Rintelen et al., 2014); yet, the different ancient lakes have received different levels of scientific attention. While Lake Baikal and the Laurentian Great Lakes are considered the best studied lakes in the world, the East African Great Lakes are under-studied in various aspects, for example with respect to their faunas and especially when it comes to taxa other than the cichlids (Salzburger et al., 2014). But even for the cichlid species flocks of the East African Great Lakes, which have been in the focus of taxonomic and speciation research for more than a century, the basic taxonomic structure is often poorly investigated. In Lake Malawi, for example, less than half of the estimated number of 800–1000 species are nominally described (Snoeks, 2000, 2004). Likewise, in Lake Victoria, only about 25% of the estimated amount of endemic species are described (Snoeks, 2000).

The situation is somewhat different for Lake Tanganyika, for which a much more comprehensive taxonomic record for cichlids is available (Snoeks et al., 1994). This is – at least to some extent – because the Tanganyikan cichlid species show greater differences to each other facilitating their classification (Snoeks, 2000), which can in turn be attributed to the relatively greater age of the lake's species flock compared to those of lakes Victoria (ca. 100–150 ka; Verheyen et al., 2003) and Malawi (ca. 700–800 ka; Malinsky et al., 2018; Meyer et al., 2017) and because of the polyphyletic nature of the Tanganyikan cichlid assemblage (Salzburger et al., 2002, 2005). Besides, there have been distinct periods of increased collection and classification activities with respect to the Tanganyikan cichlid fauna (see below).

Lake Tanganyika is the oldest (~9–12 Ma) of the East African Great Lakes and represents – by means of water volume – the largest body of freshwater in Africa (32,600 km^2 with a maximum depth of 1470 m) (Cohen et al., 1993; Salzburger et al., 2014). Lake Tanganyika's markedly diverse ichthyofauna is composed of 22 different fish families (Koblmüller et al., 2006; Fermon et al., 2017), including what is arguably the phenotypically most diverse cichlid assemblage in the world (Fryer and Iles, 1972; Salzburger et al., 2014). Apart from the cichlids, Lake Tanganyika is unique among the East African Great Lakes in having the by far highest proportion of endemic and morphologically diverse genera in groups of organisms other than cichlids (Salzburger et al., 2014). It is the Tanganyikan cichlids, however, that rank among the most noted model systems in evolutionary and speciation research (e.g. Irisarri et al., 2018; Muschick et al., 2012; Salzburger, 2018; Theis et al., 2017; Winkelmann et al., 2014), behavioural biology (e.g. Jungwirth et al., 2015; Theis et al., 2012; Young et al., 2019), and the study of the molecular mechanisms of trait evolution (e.g. Böhne et al., 2016; Santos et al., 2014). Despite the general interest in Tanganyikan cichlids, most previous studies have either focused on one particular species, on a sub-group of species (e.g. a genus or a tribe), or on a subset of taxa occurring in a particular area of the lake as a representative for the Tanganyikan cichlid radiation. As a consequence, some species and/or geographic regions are thoroughly investigated, whereas others remain understudied. Overall, the scientific literature is vague when it comes to the actual number of cichlid species found in Lake Tanganyika, and even more so for other African Great Lakes. Well established online databases – such as FishBase (Froese and Pauly, 2019) or the Catalog of Fishes (Fricke et al., 2019) – are of moderate help in this context as these are restricted to contain information about described species and their level of completeness depends on their curation, whereas undescribed species and varieties of existing species have mainly been discussed in extensive monographs (Konings, 2015) and/or hobbyists' journals.

Here we provide a concise overview of the currently described, valid cichlid species of Lake Tanganyika and list so far undescribed species as well as local varieties, taking into consideration the available literature including all first descriptions of cichlid species from the lake, as well as personal observations during many years of field collections (1980–2018) covering the majority of the shoreline of Lake Tanganyika (see Fig. 1). Note that we only considered species which we observed, and/or which have been reported to occur in the lake itself (i.e. lacustrine species), whereas purely riverine species are not discussed.

We do not aim to challenge or revise the taxonomic status of any of the described cichlid species from Lake Tanganyika. Instead, we (*i*) provide an up-to-date inventory of all Lake Tanganyika cichlid species considered valid in the light of the International Code of Zoological Nomenclature; (*ii*) report candidate taxa for future descriptions as new species based on personal observations and opinions; and (*iii*) identify the major areas of taxonomic uncertainty with regard to the cichlid species flock of Lake Tanganyika. The species inventory of Lake Tanganyika cichlids, compiled to

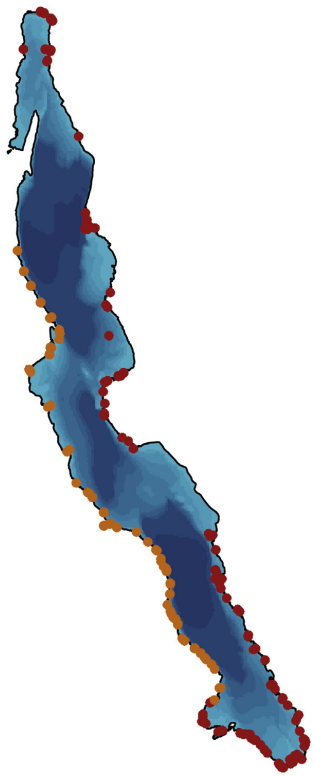

Fig. 1. Map of Lake Tanganyika with indicated localities visited for collection and diving activities. Orange circles represent sites visited before 1998 by only one author (HHB), red circles indicate locations sampled between 2007 and 2018 by all authors. Darker areas in the lake illustrate the three sub-basins of Lake Tanganyika. (For interpretation of the references to colour in this figure legend, the reader is referred to the web version of this article.)

the best of our knowledge, will serve as valuable resource for the scientific community interested in the Tanganyikan cichlid fish fauna.

Cichlid taxonomy

Before reviewing the current taxonomy of the cichlid fauna of Lake Tanganyika, we briefly discuss some of the general problems associated with the delineation of species in cichlids, in which, for various reasons, the classic species concepts are often not effective (reviewed in Salzburger, 2018). A first challenge emerges from the species-richness of the cichlid species flocks themselves, as it is often difficult for taxonomists to keep track of this diversity and to identify unambiguous characters on the basis of which species can be distinguished (Kornfield and Smith, 2000; Snoeks, 2000). The various cichlid species in the East African Great Lakes are very closely related, as a consequence of their origin via rapid adaptive radiation, which adds another level of complexity to taxonomic work (see e.g. Shaffer and Thomson, 2007; Van Steenberge et al., 2018). Furthermore, since the cichlid adaptive radiations are still ongoing, the boundaries between populations of the same species and two distinct species are often transitional (see e.g. Theis et al., 2014; Pauquet et al., 2018), making it difficult to draw a line between the alternatives that two sister-taxa are two species, rather than just one. Species delineation is further complicated by past introgressive hybridization events and ongoing gene flow between species, which appear to be rather common in cichlids (Anseeuw et al., 2012; Gante et al., 2016; Meier et al., 2017; Meyer et al., 2017; Irisarri et al., 2018). Finally, different approaches towards cichlid classification have been adopted over time, among taxonomists, and also among the radiations. What is considered a species thus differs among the cichlid species flocks of lakes Victoria, Malawi and Tanganyika. For example, whereas in lakes Victoria and Malawi, a difference in male nuptial colouration can be the sole diagnostic character distinguishing two species, different 'colour-morphs' are typically combined into the same species in Lake Tanganyika. This situation might partially reflect differences in the contribution of underlying evolutionary processes among the cichlid adaptive radiations in the East African Great Lakes (Van Steenberge et al., 2018). However, also within Lake Tanganyika, different criteria have been used in the delineation of cichlid species, and some valid species are separated by minor differences only. For example, *Neolamprologus longior* (Staeck, 1980) differs from its congener *N. leleupi* (Poll, 1956) by slight differences in body proportions and colouration only. Note that *N. longior,* among many other species, has initially been described as a sub-species. However, Poll (1986) refuted this concept for Lake Tanganyika cichlids and elevated all previously existing sub-species to the species level.

Species delineation in general, and in cichlids in particular is not an easy task and should incorporate the available suite of methods in an integrative framework (see Van Steenberge et al., 2015, 2018). Clearly, a uniform treatment in species delineation would be desirable; even if, at the end, each case has to be studied thoroughly and assessed individually. A re-evaluation of the Tanganyikan cichlid species and/or the revision of the taxonomic status of certain species is beyond the scope of this work. Instead, we aim to provide an overview of the current taxonomic status of the cichlid fish fauna of Lake Tanganyika. In the following, we subdivide the taxonomic diversity of Tanganyikan cichlids into the two categories 'described' and 'undescribed' species, whereby the former category includes what we classify as 'questionable species' and 'museum species'. This subdivision is to account for the situation that some Tanganyikan cichlids have been studied in much more detail than others, with many of them still awaiting formal description, while again others have not been observed since their first description.

Described Tanganyikan cichlid species

It took a bit more than 30 years after Richard F. Burton (1821–1890) and John H. Speke (1827–1864) – in search of the source of the Nile – discovered Lake Tanganyika in 1858 (Burton, 1860) until the first lacustrine cichlids of Lake Tanganyika were described (Günther, 1894). Among them was *Astatotilapia burtoni* (Günther, 1894), a haplochromine species inhabiting the vegetated littoral zone of the lake as well as adjacent rivers and swamps. This widespread species has become one of the best studied cichlids and a common model species for behavioural, developmental and molecular studies (e.g. Böhne et al., 2016; Santos et al., 2014; Theis et al., 2012; Weitekamp and Hofmann, 2017).

After the first species descriptions by Albert K. L. G. Günther (1830–1914) in 1894, the number of formally described species increased rapidly around 1900 due to the comprehensive taxonomic work by George A. Boulenger (1858–1937) based on collections from expeditions to Lake Tanganyika conducted between 1894 and 1905 (see Fig. 2 and Table 1). A second major increase in species descriptions occurred between the 1940s and the 1980s through the extensive work of Max Poll (1908–1991) on the collections of the Belgian expedition to the lake between 1946 and 1947 (see Fig. 2 and Table 1). It was also Poll (Poll, 1986) who grouped the – at the time – 173 described Tanganyikan cichlid species into 12 tribes based on meristic and anatomical characters (note that in taxonomy a tribe is the rank between the genus and the family level). Subsequent taxonomic and molecular phylogenetic work erected additional tribes for some genera, while merging other tribes (Takahashi, 2003; Takahashi and Koblmüller, 2011; Dunz and Schliewen, 2013). According to our accounts, 208 cichlid species belonging to 57 genera and 16 tribes are described from Lake Tanganyika to date (including valid, lacustrine species only), while new taxa are added nearly every year (see Fig. 2 and Table 1). Our assignment of species into tribes largely follows the

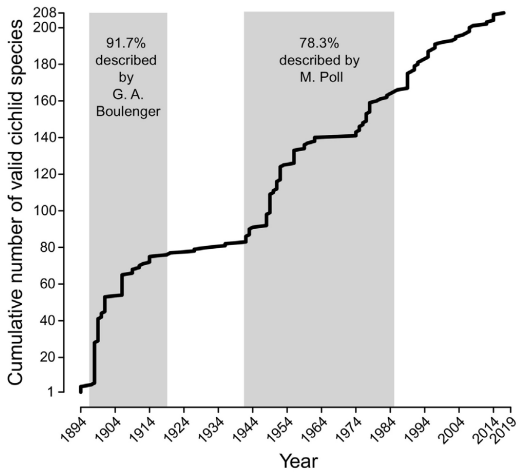

Fig. 2. Cumulative number of described cichlid species over time. The number of described species increased over the years steadily with a major increment around 1900, by the extensive work by George Boulenger, followed by a second steep ascent between the 1940's and the 1980's due to Max Poll's contributions. Note that only currently valid species are included, all later synonymized species are not considered in this study (see Table 1 for references).

Table 1
List of described, valid, lacustrine cichlid species of Lake Tanganyika. For each of the 208 species the tribe assignment, the initial name upon description, and the reported type locality are provided. If no holotype has been assigned, the sampling localities of the syntypes are listed. Note that for the two species *L. kungweensis* and *N. brichardi* the species name has changed and therefore both names and references are listed. Only native and still valid species have been considered. Superscript notation: [1] Species we consider as 'museum species'; [2] Species we consider as 'questionable species'; [3] Species with affinity to rivers, occurring in the lake and in the Lake Tanganyika basin; [4] Species not endemic to the Lake Tanganyika basin. LT = Lake Tanganyika; BUR = Burundi; DRC = Democratic Republic of Congo; TAN = Tanzania; ZAM = Zambia.

tribe	valid name	description	initial name upon description	type locality
Bathybatini	*Bathybates fasciatus*	Boulenger, 1901	*Bathybates fasciatus*	West Coast
	Bathybates ferox	Boulenger, 1898	*Bathybates ferox*	Kinyamkolo (= Mpulungu, ZAM)
	Bathybates graueri	Steindachner, 1911	*Bathybates graueri*	LT
	Bathybates hornii	Steindachner, 1911	*Bathybates horni*	LT
	Bathybates leo	Poll, 1956	*Bathybates leo*	Nyanza Lac (BUR)
	Bathybates minor	Boulenger, 1906	*Bathybates minor*	Kituta (= Chituta Bay, ZAM), Lofu (= Lufubu, ZAM)
	Bathybates vittatus	Boulenger, 1914	*Bathybates vittatus*	Kilewa Bay (DRC)
	Hemibates koningsi	Schedel and Schliewen, 2017	*Hemibates koningsi*	Mpulungu (ZAM)
	Hemibates stenosoma	(Boulenger, 1901)	*Paratilapia stenosoma*	south end of LT (ZAM) and Maswa, south of Ujiji (TAN)
Benthochromini	*Benthochromis horii*	Takahashi, 2008	*Benthochromis horii*	Mtondwe Island (= Mutondwe Island, ZAM)
	Benthochromis melanoides	(Poll, 1984)	*Haplotaxodon melanoides*	Albertville (= Kalemie, DRC)
	Benthochromis tricoti	(Poll, 1948)	*Haplotaxodon tricoti*	Karema (TAN), Moba Bay (DRC)
Boulengerochromini	*Boulengerochromis microlepis*	(Boulenger, 1899b)	*Tilapia microlepis*	Moliro (DRC)
Coptodini	*Coptodon rendalli* [3,4]	(Boulenger, 1897)	*Chromis rendalli*	Upper Shire River (Malawi)
Cyphotilapiini	*Ctenochromis benthicola*	(Matthes, 1962)	*Haplochromis benthicola*	Kalundu (DRC)
	Cyphotilapia frontosa	(Boulenger, 1906)	*Paratilapia frontosa*	Kigoma (TAN)
	Cyphotilapia gibberosa	Takahashi and Nakaya, 2003	*Cyphotilapia gibberosa*	Kasenga (ZAM)
Cyprichromini	*Cyprichromis coloratus*	Takahashi and Hori, 2006	*Cyprichromis coloratus*	Wonzye Point (ZAM)
	Cyprichromis leptosoma	(Boulenger, 1898)	*Paratilapia leptosoma*	Mbity Rocks (= Mbita Rocks, ZAM), Kinyamkolo (= Mpulungu, ZAM)
	Cyprichromis microlepidotus	(Poll, 1956)	*Limnochromis microlepidotus*	Ubwari (DRC)
	Cyprichromis pavo	Büscher, 1994	*Cyprichromis pavo*	Tembwe (DRC)
	Cyprichromis zonatus	Takahashi et al., 2002	*Cyprichromis zonatus*	Kasenga (ZAM)
	Paracyprichromis brieni	(Poll, 1981)	*Cyprichromis brieni*	Ubwari (DRC)
	Paracyprichromis nigripinnis	(Boulenger, 1901)	*Paratilapia nigripinnis*	Msambu (= Msamba, TAN)
Ectodini	*Asprotilapia leptura*	Boulenger, 1901	*Asprotilapia leptura*	Msambu (= Msamba, TAN)
	Aulonocranus dewindti	(Boulenger, 1899b)	*Paratilapia dewindti*	Moliro (DRC)
	Callochromis macrops	(Boulenger, 1898)	*Paratilapia macrops*	Mbity Rocks (= Mbita Rocks, ZAM), Kinyamkolo (= Mpulungu, ZAM)
	Callochromis melanostigma	(Boulenger, 1906)	*Pelmatochromis melanostigma*	Uvira (DRC), Kaboge (DRC), Niamkolo (= Mpulungu, ZAM), Lofu (= Lufubu, ZAM), Kituta (= Chituta Bay, ZAM)
	Callochromis pleurospilus	(Boulenger, 1906)	*Pelmatochromis pleurospilus*	Mpala (DRC), Tembwi (= Cap Tembwe, DRC)
	Cardiopharynx schoutedeni	Poll, 1942	*Cardiopharynx schoutedeni*	Usumbura (= Bujumbura, BUR)
	Cunningtonia longiventralis	Boulenger, 1906	*Cunningtonia longiventralis*	Niamkolo (= Mpulungu, ZAM)
	Cyathopharynx foae	(Vaillant, 1899)	*Ectodus foae*	LT, south
	Cyathopharynx furcifer	(Boulenger, 1898)	*Paratilapia furcifer*	Kinyamkolo (= Mpulungu, ZAM)
	Ectodus descampsii	Boulenger, 1898	*Ectodus descampsii*	LT
	Enantiopus melanogenys	(Boulenger, 1898)	*Ectodus melanogenys*	LT
	Grammatotria lemairii	Boulenger, 1899b	*Grammatotria lemairii*	Moliro (DRC)
	Lestradea perspicax	Poll, 1943	*Lestradea perspicax*	Rumonge (BUR)
	Lestradea stappersii	(Poll, 1943)	*Ophthalmotilapia stappersii*	Kilewa Bay (DRC)
	Microdontochromis rotundiventralis	Takahashi et al., 1997	*Microdontochromis rotundiventralis*	Nkumbula Island (ZAM)
	Microdontochromis tenuidentata	(Poll, 1951b)	*Xenotilapia tenuidentata*	Baie de Vua (= Livua, DRC)
	Ophthalmotilapia boops	(Boulenger, 1901)	*Tilapia boops*	Msambu (= Msamba, TAN)
	Ophthalmotilapia heterodonta	(Poll and Matthes, 1962)	*Oph. ventralis heterodontus*	Mboko Island (DRC)
	Ophthalmotilapia nasuta	(Poll and Matthes, 1962)	*Ophthalmochromis nasutus*	Kalungwe (DRC)
	Ophthalmotilapia ventralis	(Boulenger, 1898)	*Paratilapia ventralis*	Mbity Rocks (= Mbita Rocks, ZAM), Kinyamkolo (= Mpulungu, ZAM)
	Xenotilapia bathyphilus	(Poll, 1956)	*Xenotilapia ochrogenys bathyphilus*	Sumbu (ZAM)
	Xenotilapia boulengeri	(Poll, 1942)	*Enantiopus boulengeri*	Rumonge (BUR)
	Xenotilapia burtoni	(Poll, 1951a)	*Xenotilapia longispinis burtoni*	Burton Bay (DRC)
	Xenotilapia caudafasciata	Poll, 1951b	*Xenotilapia caudafasciata*	Moba Bay (DRC)
	Xenotilapia flavipinnis	Poll, 1985	*Xenotilapia flavipinnis*	Bujumbura (BUR)
	Xenotilapia longispinis	Poll, 1951a	*Xenotilapia longispinis*	Ruzizi (BUR)
	Xenotilapia nasus	De Vos et al., 1995	*Xenotilapia nasus*	Gitaza, 29km south of Bujumbura (BUR)
	Xenotilapia nigrolabiata	Poll, 1951b	*Xenotilapia nigrolabiata*	M'Samba (= Msamba, TAN)
	Xenotilapia ochrogenys	(Boulenger, 1914)	*Enantiopus ochrogenys*	Kilewa Bay (DRC)
	Xenotilapia ornatipinnis	Boulenger, 1901	*Xenotilapia ornatipinnis*	Kibwesi (= Kibwesa/ Sibwesa, TAN)
	Xenotilapia papilio	Büscher, 1990	*Xenotilapia papilio*	Tembwe, (DRC)
	Xenotilapia sima	Boulenger, 1899b	*Xenotilapia sima*	Moliro (DRC)
	Xenotilapia singularis	(Boulenger, 1914)	*Stappersia singularis*	Kilewa Bay (DRC), Tulo (DRC)
	Xenotilapia spilopterus	Poll and Stewart, 1975	*Xenotilapia spilopterus*	Nkumbula Island (ZAM)
Eretmodi	*Eretmodus cyanostictus*	Boulenger, 1898	*Eretmodus cyanostictus*	Mbity Rocks (= Mbita Rocks, ZAM), Kinyamkolo (= Mpulungu, ZAM)
	Eretmodus marksmithi	Burgess, 2012	*Eretmodus marksmithi*	Makombe (BUR)
	Spathodus erythrodon	Boulenger, 1900	*Spathodus erythrodon*	Albertville (= Mtoa, DRC)
	Spathodus marlieri	Poll, 1950	*Spathodus marlieri*	Uvira (DRC)
	Tanganicodus irsacae	Poll, 1950	*Tanganicodus irsacae*	Uvira (DRC)
Haplochromini	*Astatotilapia burtoni* [3]	(Günther, 1894)	*Chromis burtoni*	LT
	Astatoreochromis straeleni [3]	(Poll, 1944)	*Haplochromis straeleni*	Lukuga river
	Haplochromis stappersii [3]	Poll, 1943	*Haplochromis stappersii*	Lufuku river (= Mpala, DRC)
Tropheini	*Ctenochromis horei*	Günther, 1894	*Chromis horei*	LT
	Gnathochromis pfefferi	(Boulenger, 1898)	*Paratilapia pfefferi*	Kinyamkolo (= Mpulungu, ZAM)
	Interochromis loocki	(Poll, 1949)	*Limnotilapia loocki*	Kigoma (TAN)
	Limnotilapia dardennii	(Boulenger, 1899b)	*Tilapia dardennii*	Moliro (DRC)
	Lobochilotes labiatus	(Boulenger, 1898)	*Tilapia labiata*	Kinyamkolo (= Mpulungu, ZAM)
	Petrochromis ephippium	(Brichard, 1989)	*Petrochromis trewavasae ephippium*	LT
	Petrochromis famula	Matthes and Trewavas, 1960	*Petrochromis famula*	LT
	Petrochromis fasciolatus	Boulenger, 1914	*Petrochromis fasciolatus*	Kapampa (DRC), Kilewa Bay (DRC)
	Petrochromis horii	Takahashi and Koblmüller, 2014	*Petrochromis horii*	Kasenga (ZAM)
	Petrochromis macrognathus	Yamaoka, 1983	*Petrochromis macrognathus*	Luhanga (DRC)
	Petrochromis orthognathus	Matthes, 1959a	*Petrochromis orthognathus*	Bemba (DRC)
	Petrochromis polyodon	Boulenger, 1898	*Petrochromis polyodon*	Mbity Rocks (= Mbita Rocks, ZAM), Kinyamkolo (= Mpulungu, ZAM)
	Petrochromis trewavasae	Poll, 1948	*Petrochromis trewavasae*	Moliro (DRC)
	Pseudosimochromis babaulti	(Pellegrin, 1927b)	*Simochromis babaulti*	Ouvira (= Uvira (DRC)
	Pseudosimochromis curvifrons	(Poll, 1942)	*Simochromis curvifrons*	Nyanza Lac (BUR)
	Pseudosimochromis margaretae [1]	(Axelrod and Harrison, 1978)	*Simochromis margaretae*	Kigoma (TAN)
	Pseudosimochromis marginatus	(Poll, 1956)	*Simochromis marginatus*	Manga (= Cape Banza area, DRC)
	Simochromis diagramma	(Günther, 1894)	*Chromis diagramma*	LT
	Tropheus annectens	Boulenger, 1900	*Tropheus annectens*	Albertville (= Mtoa, DRC)
	Tropheus brichardi	Nelissen and Thys van den Audenaerde, 1975	*Tropheus brichardi*	Nyanza Lac (BUR)
	Tropheus duboisi	Marlier, 1959	*Tropheus duboisi*	Bemba (DRC)
	Tropheus kasabae [2]	(Nelissen, 1977)	*Tropheus moorii kasabae*	Kasaba Bay (= Kala Bay, ZAM)
	Tropheus moorii	Boulenger, 1898	*Tropheus moorii*	Kinyamkolo (= Mpulungu, ZAM)
	Tropheus polli [2]	Axelrod, 1977	*Tropheus polli*	Bulu Island (= Karilani Island, TAN)

tribe	valid name	description	initial name upon description	type locality
Lamprologini	*Altolamprologus calvus*	(Poll, 1978)	*Lamprologus calvus*	Chipimbi (ZAM)
	Altolamprologus compressiceps	(Boulenger, 1898)	*Lamprologus compressiceps*	Kinyamkolo (= Mpulungu, ZAM)
	Chalinochromis brichardi	Poll, 1974	*Chalinochromis brichardi*	south of Bujumbura (BUR)
	Chalinochromis cyanophleps	Kullander et al., 2014a	*Chalinochromis cyanophleps*	Namansi (TAN)
	Chalinochromis popelini	Brichard, 1989	*Chalinochromis popelini*	Moba (DRC)
	Julidochromis dickfeldi	Staeck, 1975	*Julidochromis dickfeldi*	between Cape Kachese and Cape Kamwankoko (ZAM)
	Julidochromis marksmithi	Burgess, 2014	*Julidochromis marksmithi*	Kerenge Island (TAN)
	Julidochromis marlieri	Poll, 1956	*Julidochromis marlieri*	Makobola (DRC)
	Julidochromis ornatus	Boulenger, 1898	*Julidochromis ornatus*	Mbity Rocks (= Mbita Rocks, ZAM)
	Julidochromis regani	Poll, 1942	*Julidochromis regani*	Nyanza Lac (BUR)
	Julidochromis transcriptus	Matthes, 1959b	*Julidochromis transcriptus*	Makobola (DRC)
	Lamprologus callipterus	Boulenger, 1906	*Lamprologus callipterus*	Mpala (DRC), Niamkolo (= Mpulungu, ZAM)
	Lamprologus finalimus [1]	Nichols and LaMonte, 1931	*Lamprologus finalimus*	Uvira (DRC)
	Lamprologus kungweensis	Poll, 1956	*Lam. ocellatus* (Poll, 1952) > *Lam. kungweensis* (Poll, 1956)	Kungwe Bay (TAN)
	Lamprologus laparogramma	Bills and Ribbink, 1997	*Lamprologus laparogramma*	Mpulungu (ZAM)
	Lamprologus lemairii	Boulenger, 1899b	*Lamprologus lemairii*	Moliro (DRC)
	Lamprologus meleagris	Büscher, 1991b	*Lamprologus meleagris*	Bwassa (DRC)
	Lamprologus ocellatus	(Steindachner, 1909b)	*Julidochromis ocellatus*	LT
	Lamprologus ornatipinnis	Poll, 1949	*Lamprologus ornatipinnis*	south of Mtoto, before Moba (DRC)
	Lamprologus signatus	Poll, 1952	*Lamprologus signatus*	Moba (DRC)
	Lamprologus speciosus	Büscher, 1991b	*Lamprologus speciosus*	Bwassa (DRC)
	Lamprologus stappersi [1]	Pellegrin, 1927a	*Lamprologus stappersi*	Sambala River (DRC)
	Lepidiolamprologus attenuatus	(Steindachner, 1909b)	*Lamprologus attenuatus*	LT
	Lepidiolamprologus cunningtoni	(Boulenger, 1906)	*Lamprologus cunningtoni*	Moliro (DRC)
	Lepidiolamprologus elongatus	(Boulenger, 1898)	*Lamprologus elongatus*	Mbity Rocks (= Mbita Rocks, ZAM), Kinyamkolo (= Mpulungu, ZAM)
	Lepidiolamprologus kamambae	Kullander et al., 2012	*Lepidiolamprologus kamambae*	Kamamba Island (TAN)
	Lepidiolamprologus kendalli	(Poll and Stewart, 1977)	*Lamprologus kendalli*	Mutondwe Island (ZAM)
	Lepidiolamprologus mimicus	Schelly et al., 2007	*Lepidiolamprologus mimicus*	Chituta Bay (ZAM)
	Lepidiolamprologus nkambae [2]	(Staeck, 1978)	*Lamprologus nkambae*	Nkamba Bay (ZAM)
	Lepidiolamprologus profundicola	(Poll, 1949)	*Lamprologus profundicola*	Cap Tembwe (DRC)
	Neolamprologus bifasciatus	Büscher, 1993	*Neolamprologus bifasciatus*	Lunangwa (DRC)
	Neolamprologus boulengeri	(Steindachner, 1909b)	*Julidochromis boulengeri*	LT
	Neolamprologus brevis	(Boulenger, 1899a)	*Lamprologus brevis*	Albertville (= Mtoa, DRC), in the mouth of a Catfish
	Neolamprologus brichardi	Poll, 1974	*Lam. savoryi elongatus* (Trewavas and Poll, 1952) > *N. brichardi* (Poll, 1974)	Kisoje (= Cape Kungwe area, TAN)
	Neolamprologus buescheri	(Staeck, 1983)	*Lamprologus buescheri*	Cape Kachese (ZAM)
	Neolamprologus calliurus	(Boulenger, 1906)	*Lamprologus calliurus*	Tembwi (= Cap Tembwe, DRC)
	Neolamprologus cancellatus [2]	Aibara et al., 2005	*Neolamprologus cancellatus*	Wonzye Point (ZAM)
	Neolamprologus caudopunctatus	(Poll, 1978)	*Lamprologus caudopunctatus*	Cape Kabeyeye (ZAM)
	Neolamprologus chitamwebwai	Verburg and Bills, 2007	*Neolamprologus chitamwebwai*	Cape Bangwe (TAN)
	Neolamprologus christyi	(Trewavas and Poll, 1952)	*Lamprologus christyi*	Mtosi (TAN)
	Neolamprologus crassus	(Brichard, 1989)	*Lamprologus crassus*	Luhanga Bay (DRC)
	Neolamprologus cylindricus	Staeck and Seegers, 1986	*Neolamprologus cylindricus*	Chipwa (ZAM)
	Neolamprologus falcicula	Brichard, 1989	*Lamprologus falcicula*	Magara (BUR)
	Neolamprologus fasciatus	(Boulenger, 1898)	*Lamprologus fasciatus*	Kinyamkolo (= Mpulungu, ZAM)
	Neolamprologus furcifer	(Boulenger, 1898)	*Lamprologus furcifer*	Mbity Rocks (= Mbita Rocks, ZAM), Kinyamkolo (= Mpulungu, ZAM)
	Neolamprologus gracilis	(Brichard, 1989)	*Lamprologus gracilis*	Masanza (DRC)
	Neolamprologus hecqui [1]	(Boulenger, 1899a)	*Lamprologus hecqui*	Albertville (= Mtoa, DRC), in the mouth of a Catfish
	Neolamprologus helianthus	Büscher, 1997	*Neolamprologus helianthus*	Kamakonde (DRC)
	Neolamprologus leleupi	(Poll, 1956)	*Lamprologus leleupi*	Luhanga (DRC)
	Neolamprologus leloupi	(Poll, 1948)	*Lamprologus leloupi*	Mtoto (DRC)
	Neolamprologus longicaudatus	Nakaya and Gashagaza, 1995	*Neolamprologus longicaudatus*	Cape Banza, Ubwari Peninsula (DRC)
	Neolamprologus longior	(Staeck, 1980)	*Neolamprologus leleupi longior*	between Kabogo point and Kibwe Bay (TAN)
	Neolamprologus marunguensis	Büscher, 1989	*Neolamprologus marunguensis*	Kapampa (DRC)
	Neolamprologus meeli	(Poll, 1948)	*Lamprologus meeli*	Katibili (DRC)
	Neolamprologus modestus	(Boulenger, 1898)	*Lamprologus modestus*	Mbity Rocks (= Mbita Rocks, ZAM), Kinyamkolo (= Mpulungu, ZAM)
	Neolamprologus mondabu	(Boulenger, 1906)	*Lamprologus mondabu*	Kaboge (= Kabogo, TAN)
	Neolamprologus multifasciatus	(Boulenger, 1906)	*Lamprologus multifasciatus*	Niamkolo Bay (= Mpulungu, ZAM)
	Neolamprologus mustax	(Poll, 1978)	*Lamprologus mustax*	Cape Nundo (ZAM)
	Neolamprologus niger	(Poll, 1956)	*Lamprologus niger*	Luhanga (DRC)
	Neolamprologus nigriventris	(Büscher, 1992b)	*Lamprologus nigriventris*	Lunangwa (DRC)
	Neolamprologus obscurus	(Poll, 1978)	*Lamprologus obscurus*	Cape Chipimbi (ZAM)
	Neolamprologus olivaceous	(Brichard, 1989)	*Lamprologus olivaceous*	Luhanga Bay (= Lunangwa Bay, DRC)
	Neolamprologus pectoralis	Büscher, 1991a	*Neolamprologus pectoralis*	Tembwe (DRC)
	Neolamprologus petricola	Poll, 1949	*Lamprologus petricola*	Mtoto Bay (DRC)
	Neolamprologus pleuromaculatus	(Trewavas and Poll, 1952)	*Lamprologus pleuromaculatus*	Usumbura (= Bujumbura, BUR)
	Neolamprologus prochilus	(Bailey and Stewart, 1977)	*Lamprologus prochilus*	Nyika Bay, Nkumbula Island, 2km north of Mpulungu (ZAM)
	Neolamprologus pulcher	(Trewavas and Poll, 1952)	*Lamprologus savoryi pulcher*	Kasanga (TAN)
	Neolamprologus savoryi	(Poll, 1949)	*Lamprologus savoryi*	Kigoma (TAN)
	Neolamprologus schreyeni	(Poll, 1974)	*Lamprologus schreyeni*	La chute (= 35 km south of Bujumbura, BUR)
	Neolamprologus sexfasciatus	(Trewavas and Poll, 1952)	*Lamprologus sexfasciatus*	Mtoto (DRC)
	Neolamprologus similis	Büscher, 1992a	*Neolamprologus similis*	Zongwe (DRC)
	Neolamprologus splendens	(Brichard, 1989)	*Lamprologus splendens*	Cape Zongwe (DRC)
	Neolamprologus tetracanthus	(Boulenger, 1899a)	*Lamprologus tetracanthus*	Albertville (= Mtoa, DRC)
	Neolamprologus timidus	Kullander et al., 2014b	*Neolamprologus timidus*	Ulwile Island (TAN)
	Neolamprologus toae	(Poll, 1949)	*Lamprologus toae*	Kavala Island, Braconé Bay (= Bilila Island, DRC)
	Neolamprologus tretocephalus	(Boulenger, 1899a)	*Lamprologus tretocephalus*	Albertville (= Mtoa, DRC)
	Neolamprologus variostigma	Büscher, 1995b	*Neolamprologus variostigma*	Tembwe (DRC)
	Neolamprologus ventralis	Büscher, 1995a	*Neolamprologus ventralis*	Tembwe (DRC)
	Neolamprologus walteri	Verburg and Bills, 2007	*Neolamprologus walteri*	Tembo Rock (TAN)
	Neolamprologus wauthioni [1]	(Poll, 1949)	*Lamprologus wauthioni*	between Camp Jaques (Albertville = Kalemie, DRC) & Katibili (DRC)
	Telmatochromis bifrenatus	Myers, 1936	*Telmatochromis bifrenatus*	Kigoma (TAN)
	Telmatochromis brachygnathus	Hanssens and Snoeks, 2003	*Telmatochromis brachygnathus*	Cape Chaitika (ZAM)
	Telmatochromis brichardi	Louisy, 1989	*Telmatochromis brichardi*	Usumbura (= Bujumbura, BUR)
	Telmatochromis dhonti	(Boulenger, 1919)	*Lamprologus dhonti*	Albertville (= Kalemie, DRC)
	Telmatochromis temporalis	Boulenger, 1898	*Telmatochromis temporalis*	Mbity Rocks (= Mbita Rocks, ZAM), Kinyamkolo (= Mpulungu, ZAM)
	Telmatochromis vittatus	Boulenger, 1898	*Telmatochromis vittatus*	Mbity Rocks (= Mbita Rocks, ZAM)
	Variabilichromis moorii	(Boulenger, 1898)	*Lamprologus moorii*	Mbity Rocks (= Mbita Rocks, ZAM), Kinyamkolo (= Mpulungu, ZAM)

tribe	valid name	description	initial name upon description	type locality
Limnochromini	*Baileychromis centropomoides*	(Bailey and Stewart, 1977)	*Leptochromis centropomoides*	3-4km west of Mpulungu (ZAM)
	Gnathochromis permaxillaris	(David, 1936)	*Limnochromis permaxillaris*	Rumonge (BUR)
	Greenwoodochromis bellcrossi	(Poll, 1976)	*Hemibates bellcrossi*	Mutondwe Island (ZAM)
	Greenwoodochromis christyi	(Trewavas, 1953)	*Limnochromis christyi*	LT
	Limnochromis abeelei	Poll, 1949	*Limnochromis abeelei*	between Cap Bwana Denge and Moni (DRC)
	Limnochromis auritus	(Boulenger, 1901)	*Paratilapia aurita*	Msambu (= Msamba, TAN)
	Limnochromis staneri	Poll, 1949	*Limnochromis staneri*	between Cap Bwana Denge and Moni (DRC)
	Reganochromis calliurus	(Boulenger, 1901)	*Paratilapia calliura*	Kalambo (TAN/ZAM)
	Tangachromis dhanisi	(Poll, 1949)	*Limnochromis dhanisi*	south of Mtoto, before Moba (DRC)
	Triglachromis otostigma	(Regan, 1920)	*Limnochromis otostigma*	Msambu (= Msamba, TAN), Mshale
Oreochromini	*Oreochromis niloticus eduardianus*[3,4]	(Boulenger, 1912)	*Tilapia eduardiana*	South-eastern slope of Mount Ruwenzoni (Uganda)
	Oreochromis tanganicae	(Günther, 1894)	*Chromis tanganicae*	LT
Perissodini	*Haplotaxodon microlepis*	Boulenger, 1906	*Haplotaxodon microlepis*	Niamkolo (= Mpulungu, ZAM), Kasawa (= Kasama, ZAM), Kasanga (TAN)
	Haplotaxodon trifasciatus	Takahashi and Nakaya, 1999	*Haplotaxodon trifasciatus*	Nkumbula Island (ZAM)
	Perissodus eccentricus	Liem and Stewart, 1976	*Perissodus eccentricus*	Chituta Bay (ZAM)
	Perissodus microlepis	Boulenger, 1898	*Perissodus microlepis*	Mbity Rocks (= Mbita Rocks, ZAM)
	Plecodus elaviae	Poll, 1949	*Plecodus elaviae*	Usumbura (= Bujumbura, BUR)
	Plecodus multidentatus	Poll, 1952	*Plecodus multidentatus*	Moba (DRC)
	Plecodus paradoxus	Boulenger, 1898	*Plecodus paradoxus*	LT
	Plecodus straeleni	Poll, 1948	*Plecodus straeleni*	Cap Tembwe (DRC)
	Xenochromis hecqui	Boulenger, 1899a	*Xenochromis hecqui*	Albertville (= Mtoa, DRC)
Trematocarini	*Trematocara caparti*	Poll, 1948	*Trematocara caparti*	Karema (TAN)
	Trematocara kufferathi	Poll, 1948	*Trematocara kufferathi*	Karema (TAN)
	Trematocara macrostoma	Poll, 1952	*Trematocara macrostoma*	Moba (DRC)
	Trematocara marginatum	Boulenger, 1899b	*Trematocara marginatum*	Moliro (DRC)
	Trematocara nigrifrons	Boulenger, 1906	*Trematocara nigrifrons*	Sumbu (ZAM)
	Trematocara stigmaticum	Poll, 1943	*Trematocara stigmaticum*	LT
	Trematocara unimaculatum	Boulenger, 1901	*Trematocara unimaculatum*	Usambura (= Bujumbura, BUR)
	Trematocara variabile	Poll, 1952	*Trematocara variabile*	Moba (DRC)
	Trematocara zebra	De Vos et al., 1996	*Trematocara zebra*	between Luhanga and Pemba (DRC)
Tylochromini	*Tylochromis polylepis*	(Boulenger, 1900)	*Pelmatochromis polylepis*	Albertville (= Mtoa, DRC), Kinyamkolo (= Mpulungu, ZAM)

molecular phylogenetics-based studies by Muschick et al. (2012) and Dunz and Schliewen (2013).

We would like to note that this compilation only contains those species, which are still valid; whereas, species that were synonymized subsequent to their description are not considered. Furthermore, we only report native species. Therefore, we did not include the Nile Tilapia, *Oreochromis niloticus* (Linnaeus, 1758). This species was introduced on several occasions in and around Lake Tanganyika but failed to successfully colonize the lacustrine zone of the lake and is mainly found in adjacent rivers. On the other hand, the subspecies *O. niloticus eduardianus* (Boulenger, 1912) was included in our list (see Table 1), as this taxon is considered native in the northern part of Lake Tanganyika.

'Museum species'

Most of the 208 described cichlid species of Lake Tanganyika can more or less readily be encountered while SCUBA diving or snorkelling, or bought on local fish markets. For example, in the last five years alone, we were able to collect specimens of 182 out of the 208 described Tanganyikan cichlid species during fieldwork campaigns in Burundi, the Democratic Republic of Congo (DRC), Tanzania and Zambia, and a similar number of species was photographically documented by a single biologist during ca. 750 h of underwater observations (Konings, 2015). On the other hand, there are five cichlid species that, following their initial description, have never been reported again from the wild (to the best of our knowledge). Here, we refer to these species as 'museum species', since they are only known from the type material in museum collections (see Table 1).

Three of these species, *L. stappersi* Pellegrin, 1927(a), *Neolamprologus hecqui* (Boulenger, 1899a), and *N. wauthioni* (Poll, 1949) have been collected from the western shoreline of Lake Tanganyika and only very little is known about the species' ecology, behaviour or distribution. The assessment of *L. stappersi and N. hecqui* is further complicated by the fact that for these species only the holotypes exist in museum collections. This makes it difficult to compare them to other taxa, as no within-species variance can be determined. On top of this, the only available specimen of *N. hecqui* was collected from the mouth of a catfish (Poll, 1956) and is, hence, not in particularly good shape. Subsequent specimens collected as *N. hecqui* were all re-assigned as *L. meeli* and *L. boulengeri*, respectively (Van Wijngaarden, 1995; Konings, 2015). For *N. wauthioni*, a paratype series comprising 13 specimens collected between 1946 and 1947 has been deposited. Still, this species has never been collected again (except for some incorrectly identified specimens later assigned to *L. ocellatus* (Steindachner, 1909b) by Büscher (2007)). At this time and without new collections, it is difficult to judge whether these three species have unusually small distribution ranges restricted to under-explored sections of the shoreline or may, given their similarity to species described later, be senior synonyms of other taxa.

In contrast, there are two species supposedly occurring in well accessible areas of Lake Tanganyika, which have not been reported again after their descriptions and which we consequently list as additional 'museum species'. *Pseudosimochromis margaretae* (Axelrod and Harrison, 1978) was described on the basis of four specimens collected at a depth of three to six meters in the bay off Kigoma, Tanzania. While members of this genus are generally fairly easy to observe while snorkelling, we failed to collect or observe this species, despite intensive sampling, diving, and snorkelling activities at the reported type locality or elsewhere. The other species is *Lamprologus finalimus* Nichols and LaMonte, 1931 for which only the holotype exists. Intensive collection and research activities at and around the type locality in more recent years (see e.g. Van Steenberge et al., 2011; Mushagalusa et al., 2014; Fermon et al., 2017) did not reveal any further specimen of this species. In both cases the type material indicates a clear distinction from their congeners. This suggests that *P. margaretae* and *N. finalimus* are either extremely rare, have a very cryptic life style, or might have become extinct.

Additionally, we would like to mention here *Xenotilapia burtoni* (Poll, 1951a), although, according to our definition, this species does not entirely qualify as 'museum species'. A substantial type

series for this species was collected between 1946 and 1947 in the Burton Bay, DRC. However, to our knowledge this species was only reported again once after its initial description (Fermon, 2007).

'Questionable species'

Three out of the 208 formally described cichlid species of Lake Tanganyika are categorized as 'questionable species' here: *Tropheus kasabae* (Nelissen, 1977), *T. polli* Axelrod, 1977, and *N. cancellatus* Aibara et al., 2005. The former two species were previously suggested, based on literature but not on morphological measurements, to be junior synonyms of *T. moori* Boulenger, 1898 and *T. annectens* Boulenger, 1900, respectively (Konings and Dieckhoff, 1992; Konings, 2013). We here agree that their species status is questionable, as in both cases the newly described species was never directly compared to the type material of *T. moori* and *T.*

Table 2
List of undescribed species and local varieties. The categorization is based on our personal opinions and observations from fieldwork and collection activities. The notation of the cheironyms follows the conventions explained in Snoeks (2000). LT = Lake Tanganyika; aff. = species affinis, suggesting that the taxon is similar, but distinct from the mentioned nominal species; cf. = conferre, suggesting the taxon to be comparable with the mentioned nominal species (Table 2).

tribe	cheironym	category	comment	distribution	references
Benthochromini	*Benthochromis* sp. "horii mahale"	variety	*cf. Benthochromis horii*	Mahale area	Konings, 2015
Cyphotilapiini	*Cyphotilapia* sp. "5-bar frontosa"	variety	*cf. Cyphotilapia frontosa*	northern LT	Genevelle, 2004; Konings, 2015; Takahashi et al., 2007 (referred to as: *Cyphotilapia* sp. "6-bar frontosa")
Cyprichromini	*Cyprichromis* sp. "dwarf jumbo"	potential species	*aff. Cyprichromis coloratus*: much smaller in body size and differs in colouration	northern LT	Konings, 2015; Tawil, 2008
	Cyprichromis sp. "jumbo"	potential species	*aff. Cyprichromis coloratus*: differs in colouration	southern LT	Konings, 2015
	Cyprichromis sp. "kibishi"	potential species	*aff. Cyprichromis zonatus*: differs in colouration and disconjunct distribution	Kibishi area	Konings, 2015
	Paracyprichromis sp. "tembwe"	potential species	aff. *Paracyprichromis nigripinnis*: differs in caudal fin shape	Tembwe area (~40km south of Moba)	first report
	Paracyprichromis sp. "brieni south"	variety	*cf. Paracyprichromis brieni*	southern LT	Konings, 2015
Ectodini	*Ophthalmotilapia* sp. "paranasuta"	potential species	*aff. Ophthalmotilapia nasuta*: differs in head and fin shape, differs in behaviour	northern LT	Konings, 2015
	Ophthalmotilapia sp. "white cap"	potential species	*aff. O. ventralis* and *aff. O. heterodonta*	Tanzanian coast	Staeck, 2014
	Xenotilapia sp. "kilesa"	potential species	aff. *Enantiopus melanogenys*: differs in melanin patterns	Kilesa area	Konings, 2015 (referred to as *Enantiopus* sp. "kilesa")
	Xenotilapia sp. "papilio sunflower"	potential species	*aff. Xenotilapia papilio:* differs in shape and colouration of the dorsal fin	southern LT	Koblmüller et al., 2004; Konings, 2015
	Ectodus sp. "north"	variety	*cf. Ectodus descampsi*	northern LT	Koblmüller et al., 2004; Konings, 2015
	Xenotilapia sp. "spilopterus north"	variety	*cf. Xenotilapia spilopterus*	northern LT	Konings, 2015
Haplochromini	*Haplochromis* sp. "chipwa"	potential species	*aff. Haplochromis stappersii*: genetic data shows strong divergence	southern tributaries and estuaries	Meyer and Indermaur et al., 2015
Tropheini	*Petrochromis* sp. "giant"	in preparation	description in preparation	Mahale to Kipili area	Mattsson, 2018, bioRxiv preprint
	Petrochromis sp. "kazumbae"	in preparation	description in preparation	Kigoma area	Mattsson, 2018, bioRxiv preprint
	Petrochromis sp. "macrognathus rainbow"	in preparation	description in preparation	Kipili area	Mattsson, 2018, bioRxiv preprint
	Petrochromis sp. "polyodon texas"	in preparation	description in preparation	Mahale to Kipili area	Mattsson, 2018, bioRxiv preprint
	Petrochromis sp. "red"	in preparation	description in preparation	Mahale area	Mattsson, 2018, bioRxiv preprint
	Tropheus sp. "black", *Tropheus* sp. "kirschfleck"	in preparation	description in preparation	northern LT	Van Steenberge, 2014
	Tropheus sp. "lunatus"	in preparation	description in preparation	Cape Kabogo, Maswa area	Van Steenberge, 2014
	Tropheus sp. "mpimbwe"	in preparation	description in preparation	Cape Mpimbwe	Van Steenberge, 2014; Van Steenberge et al., 2018
	Tropheus sp. "murago"	in preparation	description in preparation	Wapembwe area	Konings, 2015; Van Steenberge, 2014
	Tropheus sp. "red"	in preparation	description in preparation	south-western LT	Konings, 2015; Van Steenberge, 2014; Van Steenberge et al., 2011, 2018;
	Petrochromis sp. "kipili brown"	potential species	*aff. Petrochromis horii*: similar ecology, but has only 7 vertical bars in dorsal fin (versus 8 in *P. horii*)	Kipili area	Konings, 2015
	Petrochromis sp. "moshi yellow"	variety	*cf. Petrochromis ephippium*	Mahale to Kipili area	Konings, 2015
	Petrochromis sp. "orthognathus ikola"	variety	*cf. Petrochromis orthognathus*	Ikola area	Koblmüller et al., 2010; Konings, 2015
	Tropheus sp. "brichardi kipili"	variety	*cf. Tropheus brichardi*	Kipili area	Karlsson and Karlsson, 2015; Van Steenberge et al., 2018
	Tropheus sp. "lukuga"	variety	*cf. Tropheus brichardi*	Lukuga area and central Tanzanian coast	Karlsson and Karlsson, 2015
Lamprologini	*Altolamprologus* sp. "compressiceps shell"	potential species	*aff. Altolamprologus compressiceps*: distinct in body size and colouration	Lake wide on shell beds	Koblmüller et al., 2007, 2017; Konings, 2015; Konings and Dieckhoff 1992;
	Chalinochromis sp. "bifrenatus"	potential species	*aff. Chalinochromis brichardi*: distinct differences in colouration and caudal fin shape	southern Tanzanian coast	Konings, 2015; Van Steenberge et al., 2011
	Julidochromis sp. "kombe"	potential species	*aff. Julidochromis transcriptus:* differs in colouration and body shape and discontinuous distribution	Kombe area	Brichard, 1989; Konings, 2015
	Julidochromis sp. "unterfels"	potential species	*aff. Julidochromis spp.*: differs in behaviour from all known *Julidchromis* spp., mouth distinctly terminal, high body		first report
	Lamprologus sp. "ornatipinnis congo"	potential species	aff. *Lamprologus ornatipinnis:* more pronounced sexual size dimorphism, distinct dorsal fin shape	southern DRC coast	first report
	Neolamprologus sp. "caudopunctatus kipili"	potential species	*aff. Neolamprologus leloupi*: missing black margin on the caudal fin, larger body size; differs in body shape	Kipili area	Konings, 2015; Snoeks et al., 1994
	Neolamprologus sp. "cygnus"	potential species	*aff. Neolamprologus falcicula*: found in deeper waters, differs in behaviour and juvenile colouration	southern Tanzanian coast	Konings, 2015
	Neolamprologus sp. "eseki"	potential species	*aff. Neolamprologus mondabu:* differs in shape and colour of the caudal fin	Kipili area	Konings, 2015, 2005
	Neolamprologus sp. "falcicula mahale"	potential species	*aff. Neolamprologus falcicula:* differs in fin colouration and juvenile colouration, syntopic with *N.* sp. "gracilis tanzania"	Mahale area	first report
	Neolamprologus sp. "gracilis tanzania"	potential species	aff. *Neolamprologus gracilis*: differs in shape of the caudal fin, disconjunct distribution, syntopic with *N.* sp. "falcicula mahale"	Mahale area	first report, see Konings, 2015 for distribution of *N. gracilis*
	Neolamprologus sp. "kombe"	potential species	*aff. N. savoryi and aff. N. brichardi:* shares traits of both species, potentially of hybrid origin	Kombe area	Büscher, 2018
	Neolamprologus sp. "ventralis stripe"	potential species	*aff. Neolamprologus ventralis*: differs in body colouration	western Zambia	first report
	Telmatochromis sp. "longola"	potential species	*aff. Telmatochromis spp.*	Longola area	first report
	Chalinochromis sp. "ndobhoi"	variety	*cf. Chalinochromis brichardi*	Maswa and Kungwe Bay	Brichard, 1989; Konings, 2015
	Julidochromis sp. "marlieri south"	variety	*cf. Julidochromis marlieri*	southern LT	see Konings, 2015 for distribution of *J. marlieri*
	Julidochromis sp. "regani south"	variety	*cf. Julidochromis regain*	southern LT	see Konings, 2015 for distribution of *J. regani*
	Lamprologus sp. "ornatipinnis zambia"	variety	*cf. Lamprologus ornatipinnis*	southern LT	Gordon and Bills, 1999; Konings, 2015
	Lepidiolamprologus sp. "meeli kipili"	variety	*cf. Lepidiolamprologus attenuatus*	Kipili area	Konings, 2015
	Neolamprologus sp. "brevis magara"	variety	*cf. Neolamprologus brevis*	Magara area	Herrmann, 1987
	Neolamprologus sp. "daffodil"	variety	*cf. Neolamprologus pulcher*	Samazi / Kantalamba area	Konings, 2015
	Neolamprologus sp. "furcifer ulwile"	variety	*cf. Neolamprologus furcifer*	Ulwile area	Kullander et al., 2014
	Neolamprologus sp. "modabu mahale"	variety	*cf. Neolamprologus mondabu*	Mahale area	first report
	Telmatochromis sp. "dhonti north"	variety	*cf. Telmatochromis dhonti*	northern LT	Konings, 2015, *cf. T. caninus* (Poll, 1942), junior. syn. of *T. dhonti*, (Poll, 1986)
	Telmatochromis sp. "dhonti twiyu"	variety	*cf. Telmatochromis dhonti*	southern Tanzanian coast	*cf. T. macrolepis* (Borodin,1931), junior syn. of *T. dhonti* (Hanssens & Snoeks, 2001)
	Telmatochromis sp. "shell"	variety	*cf. Telmatochromis temporalis*	Lake wide on shell beds	Konings, 2015; Takahashi et al., 2012; Winkelmann et al., 2014
Trematocarini	*Trematocara* sp. "north"	potential species	*aff. T. unimaculatum,* differs in fin colouration, head morphology and various meristic counts	Unknown, one specimen purchased on a fish market in Bujumbura.	first report

annectens, respectively, for which additionally the certainty of their type localities is under debate (see Konings, 2013; Konings and Dieckhoff, 1992 for details). At this stage, these two species should be considered valid until a solid revision of the genus *Tropheus* is available, which is currently in preparation (Van Steenberge, personal communication). The third species we consider a 'questionable species', *N. cancellatus,* is reported from a single location in Zambia only. It has previously been suggested based on morphological grounds that this species might represent a hybrid between members of the genus *Telmatochromis* and *Lamprologus* (sensu lato) (Konings, 2015). Recent genetic data (Ronco et al., unpublished) lend support to this hypothesis, so that we consider *N. cancellatus* an occasional, natural hybrid and thus list it as 'questionable species', needing further investigation.

Undescribed Tanganyikan cichlid species

In addition to the 208 formally described cichlid species (including 'museum species' and 'questionable species'), a substantial number of so far undescribed species have been identified, partly in the scientific literature, yet to a much larger extent in hobbyists' journals and in the ornamental fish trade (note that cichlids are very popular among aquarists). Lacking any proper scientific description, these putative species (or local varieties) are usually referred to under cheironyms, such as trade names or the names of their location of origin. Quite a number of these undescribed species have been incorporated in scientific studies so that data on their morphology, ecology and/or behaviour as well as on their phylogenetic position and/or population structure exist (see e.g. Koblmüller et al., 2004, 2007; Egger et al., 2007; Meyer et al., 2015). However, their taxonomic status remains undefined. In Table 2, we list 55 undescribed cichlid species or local varieties reported from Lake Tanganyika in the scientific and/or popular literature, all of which we were able to observe and collect in the field and were subject to subsequent examinations. We have classified these taxa into the two categories 'local variety' or 'potential new species', based on personal observations and opinion (see Table 2). We do not claim here that this has any nomenclatural implications. Instead, our main intention is to emphasize the urgency of taxonomic revisions of many genera of Lake Tanganyika cichlids to clarify the status of the taxa mentioned in Table 2.

Taxonomic challenges in Lake Tanganyika cichlids

The taxonomy of cichlid fishes in general, and that of the cichlid species flocks in the East Africa Great Lakes in particular, is highly

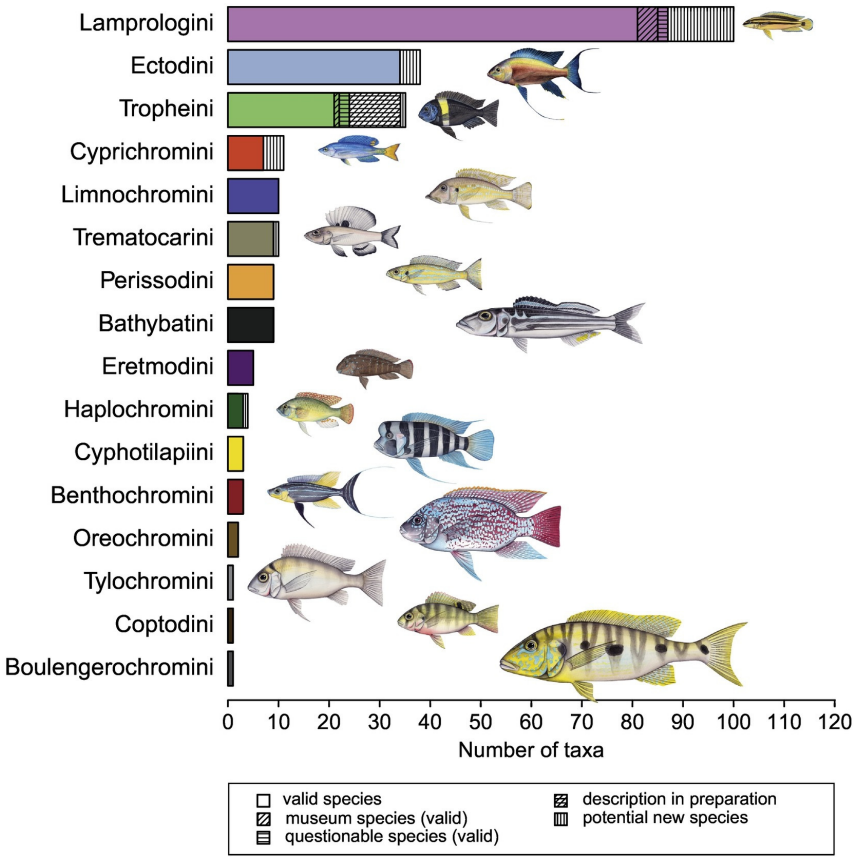

Fig. 3. Taxonomic diversity of Lake Tanganyika cichlids per tribe. Coloured partitions in the bar plot indicate the number of described species, different hatchings are used to highlight 'questionable species' and 'museum species'. White partitions refer to so far undescribed species of the two categories 'description in preparation' and what we classify as 'potential species'.

challenging (Snoeks et al., 1994; Snoeks, 2000), which is partly due to the sheer number of species present and their close relatedness. In Lake Tanganyika this is further complicated by cases of convergent evolution within the radiation (Muschick et al., 2012), which might have contributed to several generic misplacements. Additionally, many Tanganyikan cichlid species show complex distribution patterns, presumably shaped by the patchy distribution of habitats along the lake's shoreline in combination with major lake level fluctuations (among other reasons) (see e.g. Sturmbauer et al., 2001). During periods of the most extreme low water stands, the lake was subdivided into three sub-basins (Salzburger et al., 2014). This previous separation of the lake in sub-basins is reflected today by many sister-species pairs showing a north versus south distribution (probably reflecting allopatric diversification in the sub-basins) or an east versus west distribution (probably reflecting dispersal along the paleo shore lines). However, the current taxonomy of Lake Tanganyika cichlids does not treat such cases consistently. In some cases, vicariant species-pairs were nominally described as two species (e.g. *N. leleupi* (Poll, 1956) from the West and *N. longior* (Staeck, 1980) from the East); in other cases, these were initially described as two species (e.g. *Telmatochromis dhonti* (Boulenger, 1919) from the South and *T. caninus* Poll, 1942 from the North) but later synonymized (Poll, 1986); while again in other cases only one species had been described (e.g. *N. gracilis* (Brichard, 1989) from the West with reports from a local variant at the eastern shore, *N.* sp. "gracilis tanzania", see Table 2). Especially the East-West species pairs need revision, aiming at a more uniform taxonomic treatment of such sister-species pairs. Lake-wide sampling and phylogeographic studies (Rüber et al., 1999; Pauquet et al., 2018; Koblmüller et al., 2019) could serve as useful tool for future taxonomic revisions dealing with such difficult cases. Further, such studies can also contribute to the detection of yet unknown species. For example, a lake-wide genetic study of the tribe Eretmodini uncovered a distinct lineage within the genus *Eretmodus* (Rüber et al., 1999) which was later described as *Eretmodus marksmithi* Burgess, 2012.

Cases calling for revisions

Among Lake Tanganyika cichlids, several species are known to have been misplaced at the genus level. For example, Poll (1981) grouped two species, *Gnathochromis permaxillaris* (David, 1936) (type species of the genus *Gnathochromis*) and *G. pfefferi* (Boulenger, 1898) into the new genus *Gnathochromis*, based on morphological characteristics. Molecular work, however, placed *G. pfefferi* robustly within the Tropheini and *G. permaxillaris* within the Limnochromini (Salzburger et al., 2002; Takahashi, 2003). Yet, their generic name remains so far unchanged. The same applies to the genus *Ctenochromis* Pfeffer, 1893: Molecular data showed that *C. horei* (Günther, 1894) belongs to the Tropheini, while *C. benthicola* (Matthes, 1962) groups within the Cyphotilapiini (Muschick et al., 2012). In this case, none of the Tanganyikan species is the type species of the genus *Ctenochromis*. In both cases the generic misplacement affects only one or two species, respectively. However, within the Lamprologini the current genus assignment seems to disagree with the phylogenetic knowledge of the tribe for numerous taxa (see e.g. Colombo et al., 2016; Schelly et al., 2006). Those cases exemplify the need for a large-scale taxonomic revision of Lake Tanganyika cichlids.

Conclusions

We present a systematic overview of the taxonomic diversity of the lacustrine cichlid species flock from ancient Lake Tanganyika, East Africa. In particular, we provide an inventory of the valid cichlid fish species from Lake Tanganyika and list putatively undescribed species as well as local varieties. Based on this compilation, we estimate that Lake Tanganyika's cichlid species flock comprises at least 241 species, of which 208 (~86%) are nominally described and all but two (99.2%) are endemic to the basin (see Tables 1 and 2). To emphasize the demand for taxonomic revision, we highlighted some taxa at the species, genus and tribe level, needing further investigation.

Although Lake Tanganyika seems to be one of the most thoroughly examined aquatic ecosystems in tropical Africa, basic systematic work is pressing. Solid taxonomic knowledge is not only the basis for scientific study but also for nature conservation. As many other biodiversity hotspots, the unique ecosystem of Lake Tanganyika faces numerous anthropogenic threats. For example, the lake has become the focus of attention for future oil drilling projects (see Verheyen, 2016). A comprehensive understanding of the biological diversity of Lake Tanganyika is the basic prerequisite for any conservation measure, for example the delineation of small-scale protected areas (Sturmbauer, 2008). Although the IUCN Red List (International Union for Conservation of Nature's Red List of Threatened Species) accepts varieties and sub-population with reservations, valid species or subspecies are easier to assess in the system (IUCN Standards and Petitions Subcommittee, 2006).

Acknowledgements

We would like to thank Adolfe Irakoze, Gerald Katai, George Kazumbe, Dinny Mwanakulya, Jimmy Sichilima, and Humphry D. Sichilima Jr., for their help and support during field work; Victoria Huwiler, Mireille Schreyen-Brichard, Humphry D. Sichilima, and Craig Zytkow for providing infrastructure on site; Julie Himes for fish illustrations in Fig. 3; Gaspard Banyankimbona (University of Burundi), Nshombo Muderhwa and Pascal Masilya (Centre de Recherche en Hydrobiologie, Uvira, DR Congo), Ishmael Kimirei (TAFIRI, Kigoma, Tanzania), and Taylor Banda and Lawrence Makasa (Department of Fisheries, Mpulungu, Zambia) for assistance with research permits; Yves Fermon for his help in the field and valuable discussions on cichlid taxonomy; and Lukas Rüber and an anonymous reviewer for valuable comments to improve this manuscript. The authors would further like to acknowledge funding through the University of Basel, the Swiss National Science Foundation and the European Research Council (ERC).

References

Aibara, M., Takahashi, T., Nakaya, K., 2005. Neolamprologus cancellatus, a new cichlid fish from Lake Tanganyika, Africa. Ichthyol. Res. 52, 354–359. https://doi.org/10.1007/s10228-005-0296-0.

Albrecht, C., Wilke, T., 2008. Ancient Lake Ohrid: biodiversity and evolution. Hydrobiologia 615, 103–140. https://doi.org/10.1007/s10750-008-9558-y.

Anseeuw, D., Nevado, B., Busselen, P., Snoeks, J., Verheyen, E., 2012. Extensive introgression among ancestral mtDNA lineages: phylogenetic relationships of the Utaka within the Lake Malawi cichlid flock. Int. J. Evol. Biol. 2012, 1–9. https://doi.org/10.1155/2012/865603.

Axelrod, G.S., 1977. A new species of Tropheus (Pisces: Cichlidae) from Lake Tanganyika. The J.L.B. Smith Institute of Ichthyology 17, 1–12.

Axelrod, G.S., Harrison, J.A., 1978. Simochromis margaretae, a new species of cichlid fish from Lake Tanganyika. The J.L.B. Smith Institute of Ichthyology 19, 1–16.

Bailey, R.M., Stewart, D.J., 1977. Cichlid fishes from Lake Tanganyika: additions to the Zambian fauna including two new species. Occasional Papers of the Museum of Zoology University of Michigan 679, 1–30.

Bills, R.I., Ribbink, A.J., 1997. Description of Lamprologus laparogramma sp. nov., and rediagnosis of Lamprologus signatus Poll 1956 and Lamprologus kungweensis Poll 1952, with notes on their ecology and behaviour (Teleostei: Cichlidae). S. Afr. J. Sci. 93, 555–564.

Böhne, A., Wilson, C.A., Postlethwait, J.H., Salzburger, W., 2016. Variations on a theme: genomics of sex determination in the cichlid fish Astatotilapia burtoni. BMC Genomics 17, 1–12. https://doi.org/10.1186/s12864-016-3178-0.

Borodin, N.A., 1931. Some new cichlid fishes from lakes Nyasa, Tanganyika and Viktoria in Central Africa. Proceedings of the New England Zoological Clob 12, 49–54.

Boulenger, G.A., 1897. Descriptions of new fishes from the Upper Shiré River, British Central Africa, collected by Dr. Percy Rendall, and presented to the British Museum by Sir Harry H. Johnston, K.C.B. Proceedings of the Zoological Society of London, 915–920.

Boulenger, G.A., 1898. Report on the collection of fishes made by Mr. J. E. S. Moore in Lake Tanganyika during his expedition, 1895–96. Transactions of the Zoological Society of London 15, 1–30.

Boulenger, G.A., 1899a. Poissons nouveaux du Congo. Cinquième Partie. Cyprins, Silures, Cyprinodontes, Acanthoptérygiens. Annales du Musée du Congo Belge 1, 15–127.

Boulenger, G.A., 1899b. Second contribution to the ichthyology of Lake Tanganyika. On the fishes obtained by the Congo Free State Expedition under Lieut. Lemaire in 1898. Transactions of the Zoological Society of London 15, 87–96.

Boulenger, G.A., 1900. Matériaux pour la faune du Congo. Poissons nouveaux du Congo. Sixième Partie. Mormyres, Characins, Cyprins, Silures, Acanthoptérygiens, Dipneustes. Annales du Musée du Congo Belge, Zoologie, Série 1, 129–164.

Boulenger, G.A., 1901. Diagnoses of new fishes discovered by Mr. J. E. S. Moore in lakes Tanganyika and Kivu. Ann. Mag. Nat. Hist. 7, 1–6.

Boulenger, G.A., 1906. Fourth contribution to the ichthyology of Lake Tanganyika. Report on the collection of fishes made by Dr. W. A. Cunnington during the Third Tanganyika Expedition, 1904–1905. Transactions of the Zoological Society of London 17, 537–601.

Boulenger, G.A., 1912. Descriptions of three new African cichlid fishes of the genus Tilapia, preserved in the British Museum. Ann. Mag. Nat. Hist. 10, 138–140.

Boulenger, G.A., 1914. Mission Stappers au Tanganyika-Moero. Diagnoses de poissons nouveaux. I. Acanthoptérygiens, Opisthomes, Cyprinodontes, Revue de Zoologie Africaine 3, 442–447.

Boulenger, G.A., 1919. On a collection of fishes from Lake Tanganyika, with descriptions of three new species. Proceedings of the Zoological Society of London, 17–20.

Brichard, P., 1989. Cichlids and all the other fishes of Lake Tanganyika. T.F.H. Publications, Neptune City, NJ.

Brooks, J.L., 1950. Speciation in ancient lakes. Q. Rev. Biol. 25, 131–176.

Burgess, W.E., 2012. A new species of goby cichlid of the genus Eretmodus, E. marksmithi, (Pisces: Cichlidae) from the Northern part of Lake Tanganyika, *Tanganika Magazyn* 12, 23–31.

Burgess, W.E., 2014. Juidochromis marksmithi, A New Species of Julidochromis from the Tanzanian Coast of Lake Tanganyika. Tanganika Magazyn 15, 40–49.

Burton, R.F., 1860. The lake Regions of Central Africa. Longman, Green, Longman, and Roberts, London 2, 1–468.

Büscher, H.H., 1989. Ein neuer Tanganjika-Cichlide aus Zaire: Neolamprologus marunguensis n. sp. (Cichlidae, Lamprologini). Die Aquarien- und Terrarienzeitschrift (DATZ) 42, 739–743.

Büscher, H.H., 1990. Xenotilapia papilio n. sp., ein neuer Cichlide aus dem Tanganjikasee (Cichlidae, Ectodini). Die Aquarien- und Terrarienzeitschrift (DATZ) 43, 289–293.

Büscher, H.H., 1991a. Ein neuer Tanganjikasee-Cichlide aus Zaire: Neolamprologus pectoralis n. sp. (Cichidae, Lamprologini). Die Aquarien- und Terrarienzeitschrift (DATZ) 44, 784–789.

Büscher, H.H., 1991b. Neue Schneckencichliden aus dem Tanganjikasee: Lamprologus meleagris n. sp. und L. speciosus n. sp. (Cichidae, Lamprologini). Die Aquarien- und Terrarienzeitschrift (DATZ) 44, 374–382.

Büscher, H.H., 1992a. Ein neuer Cichlide aus dem Tanganjikasee: Neolamprologus similis n. sp. Die Aquarien- und Terrarienzeitschrift (DATZ) 45, 520–525.

Büscher, H.H., 1992b. Neolamprologus nigriventris n. sp.: Ein neuer Tanganjikasee-Cichlide (Cichidae, Lamprologini). Die Aquarien- und Terrarienzeitschrift (DATZ) 45, 778–783.

Büscher, H.H., 1993. Neolamprologus bifasciatus n. sp.: Ein neuer Tanganjikasee-Cichlide (Cichidae, Lamprologini). Die Aquarien- und Terrarienzeitschrift (DATZ) 46, 385–389.

Büscher, H.H., 1994. Cyprichromis pavo n. sp.: Ein neuer Cichlide aus dem Tanganjikasee. Die Aquarien- und Terrarienzeitschrift (DATZ) 46, 257–264.

Büscher, H.H., 1995a. Ein neuer Cichlide aus dem Tanganjikasee: Neolamprologus ventralis n. sp. (Cichlidae, Lamprologini). Die Aquarien- und Terrarienzeitschrift (DATZ) 48, 379–382.

Büscher, H.H., 1995b. Ein neuer Cichlide von der zairischen Küste des Tanganjikasees: Neolamprologus variostigma n.sp. (Cichlidae, Lamprologini). Die Aquarien- und Terrarienzeitschrift (DATZ) 48, 794–797.

Büscher, H.H., 1997. Ein neuer Cichlide aus dem Tanganjikasee: Neolamprologus helianthus (Cichlidae, Lamprologini). Die Aquarien- und Terrarienzeitschrift (DATZ) 50, 701–706.

Büscher, H.H., 2007. Ein verschollener Buntbarsch, Die Aquarien- und Terrarienzeitschrift (DATZ) 6, 58–61.

Büscher, H.H., 2018. Eine mysteriöse Neolamprologus-Art aus Sambia. DCG-Informationen 49, 254–259.

Cohen, A.S., Soreghan, M.J., Scholz, C.A., 1993. Estimating the age of formation of lakes: an example from Lake Tanganyika, East African Rift system. Geology 21, 511–514.

Colombo, M., Indermaur, A., Meyer, B.S., Salzburger, W., 2016. Habitat use and its implications to functional morphology: niche partitioning and the evolution of locomotory morphology in Lake Tanganyikan cichlids (Perciformes: Cichlidae). Biol. J. Linn. Soc. 118, 536–550. https://doi.org/10.1111/bij.12754.

David, L., 1936. Contribution à l'étude de la faune ichthyologique du lac Tanganyka. Revue de Zoologie et de Botanique Africaines 28, 149–160.

De Vos, L., Risch, L., Thys van den Audenaerde, D., 1995. Xenotilapia nasus, nouvelle espèce de poisson des zones sous-littorale et benthique du Nord du lac Tanganyika (Perciformes: Cichlidae). Ichthyological Exploration of Freshwaters 6, 377–384.

De Vos, L., Nshombo, M., Thys van den Audenaerde, D., 1996. Trematocara zebra (Perciformes; Cichlidae), nouvelle espèce du nord-ouest du Lac Tanganyika (Zaïre). Belgian Journal Of Zoology 126, 3–20.

Dunz, A.R., Schliewen, U.K., 2013. Molecular phylogeny and revised classification of the haplotilapiine cichlid fishes formerly referred to as "Tilapia". Mol. Phylogenet. Evol. 68, 64–80. https://doi.org/10.1016/j.ympev.2013.03.015.

Egger, B., Koblmüller, S., Sturmbauer, C., Sefc, K.M., 2007. Nuclear and mitochondrial data reveal different evolutionary processes in the Lake Tanganyika cichlid genus Tropheus. BMC Evol. Biol. 7, 1–14. https://doi.org/10.1186/1471-2148-7-137.

Fermon, Y., 2007. Étude de l'État des lieux de la partie nord du lac Tanganyika dans le cadre du Programme Pêche d'Action Contre la Faim en République Démocratique du Congo. Action Against Hunger, USA.

Fermon, Y., Nshombo, M., Muzumani, R., Benoît, J., 2017. Guide de la faune des poissons de la côte congolaise d'Ubwari à la Ruzizi, Lac Tanganyika. Editions de l'Association France Cichlid, F-31540 Fontourbière Saint Julia.

Fricke, R., Eschmeyer, W.N., van der Laan, R., 2019. Eschmeyer's Catalog of Fishes: Genera, Species, References http://researcharchive.calacademy.org/research/ichthyology/catalog/fishcatmain.asp, .

Froese, R., Pauly, D., 2019. FishBase: www.fishbase.org.

Fryer, G., Iles, T.D., 1972. The cichlid fishes of the Great Lakes of Africa. T.F.H. Publications, Neptune City, NJ.

Gante, H.F., Matschiner, M., Malmstrøm, M., Jakobsen, K.S., Jentoft, S., Salzburger, W., 2016. Genomics of speciation and introgression in Princess cichlid fishes from Lake Tanganyika. Mol. Ecol. 25, 6143–6161. https://doi.org/10.1111/mec.13767.

Genevelle, E., 2004. Distribution écologie et collecte du genre Cyphotilapia Regan, 1920. L'an Cichlidé 4, 53–66.

Gordon, A.K., Bills, I.R., 1999. Aspects of the feeding and reproductive biology of the Lake Tanganyikan cichlid, Lamprologus ornatipinnis (Pisces, Cichlidae). Environ. Biol. Fish 55, 431–441. https://doi.org/10.1023/A:1007540121262.

Günther, A.C.L.G., 1894. Descriptions of reptiles and fishes collected by Mr. E. Coode-Hore on Lake Tanganyika, Proceedings of the Zoological Society of London 1893, 628–632.

Hanssens, M., Snoeks, J., 2001. A revised synonymy of Telmatochromis temporalis (Teleostei, Cichlidae) from Lake Tanganyika (East Africa). J. Fish Biol. 58, 639–655. https://doi.org/10.1006/jfbi.2000.1475.

Hanssens, M., Snoeks, J., 2003. A new species and geographical variation in the Telmatochromis temporalis complex (Teleostei, Cichlidae) from Lake Tanganyika. J. Fish Biol. 63, 593–616. https://doi.org/10.1046/j.1095-8649.2003.00173.x.

Herrmann, H.J., 1987. Die Buntbarsche der Alten Welt -Tanganjikasee. Kernen, Germany.

Irisarri, I., Singh, P., Koblmüller, S., Torres-Dowdall, J., Henning, F., Franchini, P., Fischer, C., Lemmon, A.R., Lemmon, E.M., Thallinger, G.G., Sturmbauer, C., Meyer, A., 2018. Phylogenomics uncovers early hybridization and adaptive loci shaping the radiation of Lake Tanganyika cichlid fishes. Nat. Commun. 9, 1–12. https://doi.org/10.1038/s41467-018-05479-9.

IUCN Standards and Petitions Subcommittee, 2006. Guidelines for Using the IUCN Red List - Categories and Criteria.

Jungwirth, A., Brena, P.F., Keller, I., Taborsky, M., 2015. Polygyny affects paternal care, but not survival, pair stability, and group tenure in a cooperative cichlid. Behav. Ecol. 0, 1–9. https://doi.org/10.1093/beheco/arv194.

Karlsson, M., Karlsson, M., 2015. Anmerkungen zu Brichards Tropheus: Tropheus brichardi, Tropheus sp. "Crescentic", Tropheus sp. "Lukuga" und "Kushangaza". DCG-Informationen 46, 146–161.

Koblmüller, S., Salzburger, W., Sturmbauer, C., 2004. Evolutionary relationships in the sand-dwelling cichlid lineage of Lake Tanganyika suggest multiple colonization of rocky habitats and convergent origin of biparental mouthbrooding. J. Mol. Evol. 58, 79–96. https://doi.org/10.1007/s00239-003-2527-1.

Koblmüller, S., Sturmbauer, C., Verheyen, E., Meyer, A., Salzburger, W., 2006. Mitochondrial phylogeny and phylogeography of East African squeaker catfishes (Siluriformes: Synodontis). BMC Evol. Biol. 6, 1–16. https://doi.org/10.1186/1471-2148-6-49.

Koblmüller, S., Duftner, N., Sefc, K.M., Aibara, M., Stipacek, M., Blanc, M., Egger, B., Sturmbauer, C., 2007. Reticulate phylogeny of gastropod-shell-breeding cichlids from Lake Tanganyika - the result of repeated introgressive hybridization. BMC Evol. Biol. 7, 1–13. https://doi.org/10.1186/1471-2148-7-7.

Koblmüller, S., Egger, B., Sturmbauer, C., Sefc, K.M., 2010. Rapid radiation, ancient incomplete lineage sorting and ancient hybridization in the endemic Lake Tanganyika cichlid tribe Tropheini. Mol. Phylogenet. Evol. 55, 318–334. https://doi.org/10.1016/j.ympev.2009.09.032.

Koblmüller, S., Nevado, B., Makasa, L., Van Steenberge, M., Vanhove, M.P.M., Verheyen, E., Sturmbauer, C., Sefc, K.M., 2017. Phylogeny and phylogeography of Altolamprologus: ancient introgression and recent divergence in a rock-dwelling Lake Tanganyika cichlid genus. Hydrobiologia 791, 35–50. https://doi.org/10.1007/s10750-016-2896-2.

Koblmüller, S., Zangl, L., Börger, C., Daill, D., Vanhove, M.P.M., Sturmbauer, C., Sefc, K.M., 2019. Only true pelagics mix: comparative phylogeography of deepwater bathybatine cichlids from Lake Tanganyika. Hydrobiologia 832, 93–103. https://doi.org/10.1007/s10750-018-3752-3.

Konings, A., 2005. Back to Nature Guide to Tanganyika cichlids (2nd Editio. ed. Fohrmann Aquaristik).
Konings, A., 2013. Tropheus in their natural habitat. Cichlid press, El Paso.
Konings, A., 2015. Tanganyika Cichlids in their natural habitat, 3th Editio. ed. Cichlid Press, El Paso.
Konings, A., Dieckhoff, H.W., 1992. Tanganyika Secrets. Cichlid press, El Paso.
Kornfield, I., Smith, P.F., 2000. African cichlid fishes: model systems for evolutionary biology. Annu. Rev. Ecol. Evol. Syst. 31, 163–196.
Kullander, S.O., Karlsson, M., Karlsson, M., 2012. Lepidiolamprologus kamambae, a new species of cichlid fish (Teleostei: Cichlidae) from Lake Tanganyika. Zootaxa 3492, 30–48.
Kullander, S.O., Karlsson, M., Karlsson, M., Norén, M., 2014a. Chalinochromis cyanophleps, a new species of cichlid fish (Teleostei: Cichlidae) from Lake Tanganyika. Zootaxa 3790, 425–438. https://doi.org/10.11646/zootaxa.3790.3.2.
Kullander, S.O., Norén, M., Karlsson, M., Karlsson, M., 2014b. Description of Neolamprologus timidus, new species, and review of N. Furcifer from Lake Tanganyika (Teleostei: Cichlidae). Ichthyological Exploration of Freshwaters 24, 301–328.
Larson, G., Schaetzl, R., 2001. Origin and evolution of the Great Lakes. J. Great Lakes Res. 27, 518–546. https://doi.org/10.1016/S0380-1330(01)70665-X.
Liem, K.F., Stewart, D.J., 1976. Evolution of the scale-eating cichlid fishes of Lake Tanganyika: a generic revision with a description of a new species. Bulletin of the Museum of Comparative Zoology 147, 319–350.
Louisy, P., 1989. Description de Telmatochromis brichardi (Pisces, Cichlidae, Lamprologini), espèce nouvelle du lac Tanganyika. Revue française d'aquariologie 15, 79–85.
Macdonald, K.S., Yampolsky, L., Duffy, J.E., 2005. Molecular and morphological evolution of the amphipod radiation of Lake Baikal. Mol. Phylogenet. Evol. 35, 323–343. https://doi.org/10.1016/j.ympev.2005.01.013.
Malinsky, M., Svardal, H., Tyers, A.M., Miska, E.A., Genner, M.J., Turner, G.F., Durbin, R., 2018. Whole-genome sequences of Malawi cichlids reveal multiple radiations interconnected by gene flow. Nature Ecology & Evolution 2, 1940–1955. https://doi.org/10.1038/s41559-018-0717-x.
Marlier, G., 1959. Observations sur la biologie littorale du Lac Tanganika. Revue de Zoologie et de Botanique Africaines 59, 164–183.
Martens, K., 1997. Speciation in ancient lakes. Trends Ecol. Evol. 12, 177–182.
Matthes, H., 1959a. Un cichlide nouveau du Lac Tanganyika: Petrochromis orthognathus n. sp. Revue de Zoologie et de Botanique Africaines 60, 335–341.
Matthes, H., 1959b. Un cichlide nouveaux du lac Tanganika Julidochromis transcriptus n. sp. Revue de Zoologie et de Botanique Africaines 60, 126–130.
Matthes, H., 1962. Poissons nouveaux ou intéressants du lac Tanganika et du Ruanda. Annales, Musée Royal de l'Afrique Centrale, Tevuren, Belgique. Série in 80. Sciences Zoologique 111, 27–88.
Matthes, H., Trewavas, E., 1960. Petrochromis famula n. sp., a cichlid fish of Lake Tanganyika. Revue de Zoologie et de Botanique Africaines 61, 349–357.
Mattsson, C., 2018. A Morphological and Molecular Analysis of the Species Diversity of the Cichlid Genus Petrochromis from Lake Tanganyika (Teleostei: Cichlidae). bioRxiv Preprint. https://doi.org/10.1101/280263.
Meier, J.I., Marques, D.A., Mwaiko, S., Wagner, C.E., Excoffier, L., Seehausen, O., 2017. Ancient hybridization fuels rapid cichlid fish adaptive radiations. Nat. Commun. 8, 1–11. https://doi.org/10.1038/ncomms14363.
Meyer, B.S., Indermaur, A., Ehrensperger, X., Egger, B., Banyankimbona, G., Snoeks, J., Salzburger, W., 2015. Back to Tanganyika: a case of recent trans-species-flock dispersal in East African haplochromine cichlid fishes. R. Soc. Open Sci. 2, 1–5. https://doi.org/10.1098/rsos.140498.
Meyer, B.S., Matschiner, M., Salzburger, W., 2017. Disentangling incomplete lineage sorting and introgression to refine species-tree estimates for Lake Tanganyika cichlid fishes. Syst. Biol. 66, 531–550. https://doi.org/10.1093/sysbio/syw069.
Muschick, M., Indermaur, A., Salzburger, W., 2012. Convergent evolution within an adaptive radiation of cichlid fishes. Curr. Biol. 22, 2362–2368. https://doi.org/10.1016/j.cub.2012.10.048.
Mushagalusa, C.D., Nshombo, M., Lushombo, M., 2014. Littoral fisheries on Cichlidae (Pisces) from the northwestern part of Lake Tanganyika, East Africa. Aquat. Ecosyst. Health Manag. 17, 41–51.
Myers, G.S., 1936. Report on the fishes collected by H. C. Raven in Lake Tanganyika in 1920. Proceedings of the United States National Museum 84, 1–15.
Nakaya, K., Gashagaza, M.M., 1995. Neolamprologus longicaudatus, a New Cichlid Fish from the Zairean Coast of Lake Tanganyika. Japanese Journal of Ichthyology 42, 39–43.
Nelissen, M.H.J., 1977. Description of Tropheus moorii kasabae n. sspec. (Pisces, Cichlidae) from the south of Lake Tanganyika. Revue de Zoologie Africaine 91, 237–242.
Nelissen, M.H.J., Thys van den Audenaerde, D., 1975. Description of Tropheus brichardi sp. nov. from Lake Tanganyika (Pisces, Cichlidae). Revue de Zoologie Africaine 89, 974–980.
Nichols, J.T., LaMonte, F.R., 1931. A new Lamprologus from Lake Tanganyika. Am. Mus. Novit. 478, 1–2.
Pauquet, G., Salzburger, W., Egger, B., 2018. The puzzling phylogeography of the haplochromine cichlid fish Astatotilapia burtoni. Ecology and Evolution 8, 5637–5648. https://doi.org/10.1002/ece3.4092.
Pellegrin, J., 1927a. Description de Cichlidés et d'un Mugilidé nouveaux du Congo belge. Revue de Zoologie Africaine 15, 52–57.
Pellegrin, J., 1927b. Mission Guy Babault, poissons du lac Tanganyika. Bulletin du Muséum National d'Histoire Naturelle 33, 499–501.
Pfeffer, G., 1893. Ostafrikanische Fische gesammelt von Herrn Dr. F. Stuhlmann im Jahre 1888 and 1889. In: Jahrbuch Der Hamburgischen Wissenschaftlichen Anstalten, pp. 127–177.
Poll, M., 1942. Cichlidae nouveaux du lac Tanganika appartenant aux collections du Musée du Congo. Revue de Zoologie et de. Botanique Africaines 36, 343–360.
Poll, M., 1943. Descriptions de poissons nouveaux du Lac Tanganika, appartenant aux familles des Clariidae et Cichlidae. Revue de Zoologie et de Botanique Africaines 37, 305–318.
Poll, M., 1944. Descriptions de poissons nouveaux recueillis dans la région d'Albertville (Congo belge) par le Dr. G. Pojer, Bulletin du Musée Royal d'Histoire Naturelle de Belgique 20, 1–12.
Poll, M., 1948. Descriptions de Cichlidae nouveaux recueillis par la mission hydrobiologique belge au Lac Tanganika (1946-1947). Bulletin du Musée Royal d'Histoire Naturelle de Belgique 24, 1–31.
Poll, M., 1949. Deuxième série de Cichlidae nouveaux recueillis par la mission hydrobiologique belge en Lac Tanganika (1946-1947). Bulletin de l'Institut Royal des Sciences Naturelles de Belgique 25, 1–55.
Poll, M., 1950. Description de deux Cichlidae pétricoles du lac Tanganika. Revue de Zoologie et de Botanique Africaines 43, 292–302.
Poll, M., 1951a. Troisième série de Cichlidae nouveaux recueillis par la mission hydrobiologique belge au lac Tanganika (1946-1947). Bulletin de l'Institut Royal des Sciences Naturelles de Belgique 27, 1–11.
Poll, M., 1951b. Troisième série de Cichlidae nouveaux recueillis par la mission hydrobiologique belge au lac Tanganika (1946-1947) (suite 1+2). Bulletin de l'Institut Royal des Sciences Naturelles de Belgique 27, 1–12; 1–7.
Poll, M., 1952. Quatrième série de Cichlidae nouveaux recueillis par la mission hydrobiologique belge au lac Tanganika (1946-1947). Bulletin de l'Institut Royal des Sciences Naturelles de Belgique 28, 1–20.
Poll, M., 1956. Poissons Cichlidae. In: Exploration Hydrobiologique Du Lac Tanganika, pp. 1946–1947 (Résultats Scientifiques).
Poll, M., 1974. Contribution à la faune ichthyologique du lac Tanganika, d'après les récoltes de P. Brichard. Revue de Zoologie Africaine 88, 99–110.
Poll, M., 1976. Hemibates bellcrossi sp. n. du lac Tanganika. Revue de Zoologie Africaine 90, 1017–1020.
Poll, M., 1978. Contribution à la connaissance du genre Lamprologus Schth. Description de quatre espèces nouvelles, réhabilitation de Lamprologus mondabu et synopsis remanié des espèces du lac Tanganika. Bulletin de al classe des sciences Académie Royale de Belgique (série 5) (64), 725–758.
Poll, M., 1981. Contribution à la faune ichthyologique du lac Tanganika. Révision du genre Limnochromis Regan, 1920. Description de trois genres nouveaux et d'une espèce nouvelle: Cyprichromis brieni. Annales de la Société royale zoologique de Belgique 111, 163–179.
Poll, M., 1984. Haplotaxodon melanoides sp. n. du lac Tanganika (Pisces, Cichlidae). Revue de Zoologie Africaine 98, 677–681.
Poll, M., 1985. Description de Xenotilapia flavipinnis sp.n. du lac Tanganika (Pisces, Cichlidae) *Revue de Zoologie Africaine* 99, pp. 105–109.
Poll, M., 1986. Classification des Cichlidae du lac Tanganika, Tribus, genres et espéces (Brussels).
Poll, M., Matthes, H., 1962. Trois poissons remarquables du Lac Tanganika. Annales, Musée Royal de l'Afrique Centrale, Tevuren, Belgique. Série in 80, Sciences Zoologique 111.
Poll, M., Stewart, D.J., 1975. A new cichlid fish of the genus Xenotilapia from Lake Tanganyika, Zambia (Pisces, Chichlidae). RevZoolAfr 89, 919–924.
Poll, M., Stewart, D., 1977. Un nouveau Lamprologus du sud du Lac Tanganika (Zambia) (Pisces, Cichlidae). Revue de Zoologie Africaine 91, 1047–1056.
Regan, C.T., 1920. On a new cichlid fish from Lake Tanganyika. Ann. Mag. Nat. Hist. 9, 152.
Renn, S.C.P., Machado, H.E., Duftner, N., Sessa, A.K., Harris, R.M., Hofmann, H.A., 2018. Gene expression signatures of mating system evolution. Genome 61, 287–297. https://doi.org/10.1139/gen-2017-0075.
Rüber, L., Verheyen, E., Meyer, A., 1999. Replicated evolution of trophic specializations in an endemic cichlid fish lineage from Lake Tanganyika. Proc. Natl. Acad. Sci. 96, 10230–10235. https://doi.org/10.1073/pnas.96.18.10230.
Salzburger, W., 2018. Understanding explosive diversification through cichlid fish genomics. Nat. Rev. Genet. 19, 705–717. https://doi.org/10.1038/s41576-018-0043-9.
Salzburger, W., Meyer, A., Baric, S., Verheyen, E., Sturmbauer, C., 2002. Phylogeny of the Lake Tanganyika cichlid species flock and its relationship to the Central and East African haplochromine cichlid fish faunas. Syst. Biol. 51, 113–135. https://doi.org/10.1080/106351502753475907.
Salzburger, W., Mack, T., Verheyen, E., Meyer, A., 2005. Out of Tanganyika: genesis, explosive speciation, key-innovations and phylogeography of the haplochromine cichlid fishes. BMC Evol. Biol. 5, 1–15. https://doi.org/10.1186/1471-2148-5-17.
Salzburger, W., Van Bocxlaer, B., Cohen, A.S., 2014. Ecology and evolution of the African Great Lakes and their faunas. Annu. Rev. Ecol. Evol. Syst. 45, 519–545. https://doi.org/10.1146/annurev-ecolsys-120213-091804.
Santos, M.E., Braasch, I., Boileau, N., Meyer, B.S., Sauteur, L., Böhne, A., Belting, H.G., Affolter, M., Salzburger, W., 2014. The evolution of cichlid fish egg-spots is linked with a cis-regulatory change. Nat. Commun. 5. https://doi.org/10.1038/ncomms6149.
Schedel, F.D.B., Schliewen, U.K., 2017. Hemibates koningsi spec. nov: a new deep-water cichlid (Teleostei: Cichlidae) from Lake Tanganyika. Zootaxa 4312, 92–112. https://doi.org/10.11646/zootaxa.4312.1.4.

Schelly, R.C., Stiassny, M.L.J., 2004. Revision of the Congo river Lamprologus Schilthuis, 1891 (Teleostei: Cichlidae), with descriptions of two new species. *Am. Mus. Novit.* 3451, 1–40. doi:https://doi.org/10.1206/0003-0082(2004)451.

Schelly, R., Salzburger, W., Koblmüller, S., Duftner, N., Sturmbauer, C., 2006. Phylogenetic relationships of the lamprologine cichlid genus Lepidiolamprologus (Teleostei: Perciformes) based on mitochondrial and nuclear sequences, suggesting introgressive hybridization. Mol. Phylogenet. Evol. 38, 426–438. https://doi.org/10.1016/j.ympev.2005.04.023.

Schelly, R., Takahashi, T., Bills, R., Hori, M., 2007. The first case of aggressive mimicry among lamprologines in a new species of Lepidiolamprologus (Perciformes: Cichlidae) from Lake Tanganyika. Zootaxa 1638, 39–49.

Schluter, D., 2000. The Ecology of Adaptive Radiation. Oxford University Press, New York.

Seehausen, O., 2015. Process and pattern in cichlid radiations - inferences for understanding unusually high rates of evolutionary diversification. New Phytol. 207, 304–312. https://doi.org/10.1111/nph.13450.

Shaffer, H.B., Thomson, R.C., 2007. Delimiting species in recent radiations. Syst. Biol. 56, 896–906.

Snoeks, J., 2000. How well known is the Ichthyodiversity of the Large East African Lakes? Adv. Ecol. Res. 31, 17–38.

Snoeks, J., 2004. The cichlid diversity of Lake Malawi/Nyasa/Niassa: identification, distribution and taxonomy. Cichlid Press, El Paso, TX, U.S.A.

Snoeks, J., Rüber, L., Verheyen, E., 1994. The Tanganyika problem: comments on the taxonomy and distribution patterns of its cichlid fauna. Archiv für Hydrobiologie–Beiheft Ergebnisse der Limnologie 44, 355–372.

Staeck, W., 1975. A New Cichlid Fish From Lake Tanganyika: Julidochromis Dickfeldi sp. n. (Pisces, Cichlidae) *Revue de Zoologie Africaine*, 89, pp. 981–986.

Staeck, W., 1978. Ein neuer Cichlide aus dem südlichen Tanganjikasee: Lamprologus nkambae n. sp. Revue de Zoologie Africaine 92, 436–441.

Staeck, W., 1980. Ein neuer Cichlide vom Ostufer des Tanganjikasees: Lamprologus leleupi longior n. ssp. (Pisces, Cichlidae). Revue de Zoologie Africaine 94, 11–14.

Staeck, W., 1983. Lamprologus buescheri n. sp. from the Zambian part of Lake Tanganyika (Pisces: Cichlidae). Senckenberg. Biol. 63, 325–328.

Staeck, W., 2014. Eine neue geografische Farbvariante von Ophthalmotilapia sp. "Whitecap", 46. *DCG-Informationen*, pp. 136–138.

Staeck, W., Seegers, L., 1986. Neolamprologus cylindricus spec. nov. Beschreibung eines neuen Tanganjikacichliden aus dem südlichen Tansania und dem östlichen Sambia. Die Aquarien- und Terrarienzeitschrift (DATZ) 39, 448–451.

Steindachner, F., 1909a. Über eine neue Tilapia- und Lamprologus-Art aus dem Tanganyikasee und über Brachyplatystoma (Taenionema) platynema Blgr. aus der Umgebung von Pará, *Anzeiger der Akademie für Wissenschaftlichen, Wien*. Mathematisch-Naturwissenschaftlichen Klasse 46, 443–447.

Steindachner, F., 1909b. Über einige neue Fischarten aus dem Tanganyikasee. Anzeiger der Kaiserlichen Akademie der Wissenschaften in Wien, Mathematisch-Naturwissenschaftlichen Klasse 46, 399–404.

Steindachner, F., 1911. Beiträge zur Kenntnis der Fischfauna des Tanganyikasees und des Kongogebietes. Sitzungsberichte der Kaiserlichen Akademie der Wissenschaften, Mathematisch-Naturwissenschaftlichen Klasse 120, 1171–1186.

Sturmbauer, C., 2008. The Great Lakes in East Africa: biological conservation considerations for species flocks. Hydrobiologia 615, 95–101. https://doi.org/10.1007/s10750-008-9554-2.

Sturmbauer, C., Baric, S., Salzburger, W., Rüber, L., Verheyen, E., 2001. Lake level fluctuations synchronize genetic divergences of cichlid fishes in African Lakes. Mol. Biol. Evol. 18, 144–154. https://doi.org/10.1093/oxfordjournals.molbev.a003788.

Takahashi, T., 2003. Systematics of Tanganyikan cichlid fishes (Teleostei: Perciformes). Ichthyol. Res. 50, 367–382. https://doi.org/10.1007/s10228-003-0181-7.

Takahashi, T., 2008. Description of a new cichlid fish species of the genus Benthochromis (Perciformes: Cichlidae) from Lake Tanganyika. J. Fish Biol. 72, 603–613. https://doi.org/10.1111/j.1095-8649.2007.01727.x.

Takahashi, T., Hori, M., 2006. Description of a new Lake Tanganyikan cichlid fish of the genus Cyprichromis (Perciformes: Cichlidae) with a note on sexual dimorphism. J. Fish Biol. 68, 174–192. https://doi.org/10.1111/j.0022-1112.2006.001055.x.

Takahashi, T., Koblmüller, S., 2011. The adaptive radiation of cichlid fish in Lake Tanganyika: a morphological perspective. Int. J. Evol. Biol., 1–14 https://doi.org/10.4061/2011/620754.

Takahashi, T., Koblmüller, S., 2014. A new species of Petrochromis (Perciformes: Cichlidae) from Lake Tanganyika. Ichthyol. Res. 61, 252–264. https://doi.org/10.1007/s10228-014-0396-9.

Takahashi, T., Nakaya, K., 1999. New species of Haplotaxodon (Perciformes : Cichlidae) from Lake Tanganyika, Africa. Copeia, 101–106.

Takahashi, T., Nakaya, K., 2003. New species of Cyphotilapia (Perciformes: Cichlidae) from Lake Tanganyika, Africa. American Society of Ichthyologists and Herpetologists 2003, 824–832.

Takahashi, T., Yanagisawa, Y., Nakaya, K., 1997. Microdontochromis rotundiventralis, a new cichlid fish (Perciformes: Cichlidae) from Lake Tanganyika. Ichthyol. Res. 44, 109–117. https://doi.org/10.1007/BF02678689.

Takahashi, T., Hori, M., Nakaya, K., 2002. New species of Cyprichromis (Perciformes: Cichlidae) from Lake Tanganyika, Africa. Copeia, 1029–1036.

Takahashi, T., Ngatunga, B., Snoeks, J., 2007. Taxonomic status of the six-band morph of Cyphotilapia frontosa (Perciformes: Cichlidae) from Lake Tanganyika, Africa. Ichthyol. Res. 54, 55–60. https://doi.org/10.1007/s10228-006-0374-y.

Takahashi, T., Ota, K., Kohda, M., Hori, M., 2012. Some evidence for different ecological pressures that constrain male and female body size. Hydrobiologia 684, 35–44.

Tawil, P., 2008. The Exquisite Cyprichromis from Kigoma, a "dwarf jumbo". Cichlid News Magazine 17, 6–16.

Theis, A., Salzburger, W., Egger, B., 2012. The function of anal fin egg-spots in the cichlid fish Astatotilapia burtoni. PLoS One 7,. https://doi.org/10.1371/journal.pone.0029878 e29878.

Theis, A., Ronco, F., Indermaur, A., Salzburger, W., Egger, B., 2014. Adaptive divergence between lake and stream populations of an East African cichlid fish. Mol. Ecol. 23, 5304–5322. https://doi.org/10.1111/mec.12939.

Theis, A., Roth, O., Cortesi, F., Ronco, F., Salzburger, W., Egger, B., 2017. Variation of anal fin egg-spots along an environmental gradient in a haplochromine cichlid fish. Evolution 71, 766–777. https://doi.org/10.1111/evo.13166.

Timoshkin, O.A., Samsonov, D.P., Yamamuro, M., Moore, M.V., Belykh, O.I., Malnik, V. V., Sakirko, M.V., Shirokaya, A.A., Bondarenko, N.A., Domysheva, V.M., Fedorova, G.A., Kochetkov, A.I., Kuzmin, A.V., Lukhnev, A.G., Medvezhonkova, O.V., Nepokrytykh, A.V., Pasynkova, E.M., Poberezhnaya, A.E., Potapskaya, N.V., Rozhkova, N.A., Sheveleva, N.G., Tikhonova, I.V., Timoshkina, E.M., Tomberg, I. V., Volkova, E.A., Zaitseva, E.P., Zvereva, Y.M., Kupchinsky, A.B., Bukshuk, N.A., 2016. Rapid ecological change in the coastal zone of Lake Baikal (East Siberia): is the site of the world's greatest freshwater biodiversity in danger? J. Great Lakes Res. 42, 487–497. https://doi.org/10.1016/j.jglr.2016.02.011.

Trewavas, E., 1953. A new species of the cichlid genus Limnochromis of Lake Tanganyika. Bulletin du Musée Royal d'Histoire Naturelle de Belgique 29, 1–3.

Trewavas, E., Poll, M., 1952. Three new species and two new subspecies of the genus Lamprologus, Cichlid fishes of Lake Tanganyika. Bulletin de l'Institut Royal des Sciences Naturelles de Belgique 28, 1–16.

Vaillant, L.L., 1899. Protopterus retropinnis et Ectodus foae. Bulletin du Muséum National d'Histoire Naturelle 5, 219–222.

Van Steenberge, M., Vanhove, M.P.M., Muzumani Risasi, D., Mulimbwa N'Sibula, T., Muterezi Bukinga, F., Pariselle, A., Gillardin, C., Vreven, E., Raeymaekers, J.A.M., Huyse, T., Volckaert, F.A.M., Nshombo Muderhwa, V., Snoeks, J., 2011. A recent inventory of the fishes of the north-western and central western coast of Lake Tanganyika (Democratic Republic Congo). Acta Ichthyol. Piscat. 41, 201–214.

Van Steenberge, M., Pariselle, A., Huyse, T., Volckaert, F.A.M., Snoeks, J., Vanhove, M. P.M., 2015. Morphology, molecules, and monogenean parasites: an example of an integrative approach to cichlid biodiversity. PLoS One 10, 1–42. https://doi.org/10.1371/journal.pone.0124474.

Van Steenberge, M., Raeymaekers, J.A.M., Hablützel, P.I., Vanhove, M.P.M., Koblmüller, S., Snoeks, J., 2018. Delineating species along shifting shorelines: Tropheus (Teleostei, Cichlidae) from the southern subbasin of Lake Tanganyika. Front. Zool. 15, 1–18. https://doi.org/10.1186/s12983-018-0287-4.

Van Steenberger, M., 2014. Species and Speciation in Tropheus, Simochromis and Pseudosimochromis: A Multidisciplinary Approach to a Cichlid Radiation from Lake Tanganyika. KU Leuven.

Van Wijngaarden, C., 1995. Distributiepatronen van de Lamprologinen. KU Leuven, Belgium.

Verburg, P., Bills, R., 2007. Two new sympatric species of Neolamprologus (Teleostei: Cichlidae) from Lake Tanganyika, East Africa. Zootaxa 1612, 25–44.

Verheyen, E., 2016. Oil extraction imperils Africa's Great Lakes. Science 354, 561–562. https://doi.org/10.1126/science.aal1722.

Verheyen, E., Salzburger, W., Snoeks, J., Meyer, A., 2003. Origin of the superflock of cichlid fishes from Lake Victoria, East Africa. Science 300, 325–329. https://doi.org/10.1126/science.1080699.

von Rintelen, T., Marwoto, R.M., Haffner, G.D., Herder, F., 2014. Preface: speciation research in ancient lakes – classic concepts and new approaches. Hydrobiologia 739, 1–6. https://doi.org/10.1007/s10750-014-2028-9.

Weitekamp, C.A., Hofmann, H.A., 2017. Neuromolecular correlates of cooperation and conflict during territory defense in a cichlid fish. Horm. Behav. 89, 145–156. https://doi.org/10.1016/j.yhbeh.2017.01.001.

Wilson, A.B., Glaubrecht, M., Meyer, A., 2004. Ancient lakes as evolutionary reservoirs: evidence from the thalassoid gastropods of Lake Tanganyika. Proc. R. Soc. B 271, 529–536. https://doi.org/10.1098/rspb.2003.2624.

Winkelmann, K., Genner, M.J., Takahashi, T., Rüber, L., 2014. Competition-driven speciation in cichlid fish. Nat. Commun. 5. https://doi.org/10.1038/ncomms4412.

Yamaoka, K., 1983. A revision of the cichlid fish genus petrochrommis from Lake Tanganyika, with description of a new species. Japanese Journal of Ichthyology 30, 129–141.

Young, R.L., Ferkin, M.H., Ockendon-Powell, N.F., Orr, V.N., Phelps, S.M., Pogány, Á., Richards-Zawacki, C.L., Summers, K., Székely, T., Trainor, B.C., Urrutia, A.O., Zachar, G., O'Connell, L.A., Hofmann, H.A., 2019. Conserved transcriptomic profiles underpin monogamy across vertebrates. PNAS 116, 1331–1336. https://doi.org/10.1073/PNAS.1813775116.

Chapter 2

Drivers and dynamics of a massive adaptive radiation in African cichlid fishes

Fabrizia Ronco, Michael Matschiner, Astrid Böhne, Anna Boila, Heinz H. Büscher, Athimed El Taher, Adrian Indermaur, Milan Malinsky, Virginie Ricci, Ansgar Kahmen, Sissel Jentoft & Walter Salzburger

Nature (2021)

Article

Drivers and dynamics of a massive adaptive radiation in cichlid fishes

https://doi.org/10.1038/s41586-020-2930-4

Received: 4 February 2020

Accepted: 20 August 2020

Published online: 18 November 2020

Check for updates

Fabrizia Ronco[1]✉, Michael Matschiner[1,2,3], Astrid Böhne[1,4], Anna Boila[1], Heinz H. Büscher[1], Athimed El Taher[1], Adrian Indermaur[1], Milan Malinsky[1], Virginie Ricci[1], Ansgar Kahmen[5], Sissel Jentoft[3] & Walter Salzburger[1,3]✉

Adaptive radiation is the likely source of much of the ecological and morphological diversity of life[1–4]. How adaptive radiations proceed and what determines their extent remains unclear in most cases[1,4]. Here we report the in-depth examination of the spectacular adaptive radiation of cichlid fishes in Lake Tanganyika. On the basis of whole-genome phylogenetic analyses, multivariate morphological measurements of three ecologically relevant trait complexes (body shape, upper oral jaw morphology and lower pharyngeal jaw shape), scoring of pigmentation patterns and approximations of the ecology of nearly all of the approximately 240 cichlid species endemic to Lake Tanganyika, we show that the radiation occurred within the confines of the lake and that morphological diversification proceeded in consecutive trait-specific pulses of rapid morphospace expansion. We provide empirical support for two theoretical predictions of how adaptive radiations proceed, the 'early-burst' scenario[1,5] (for body shape) and the stages model[1,6,7] (for all traits investigated). Through the analysis of two genomes per species and by taking advantage of the uneven distribution of species in subclades of the radiation, we further show that species richness scales positively with per-individual heterozygosity, but is not correlated with transposable element content, number of gene duplications or genome-wide levels of selection in coding sequences.

At the macroevolutionary level, the diversity of life has been shaped mainly by two antagonistic processes: evolutionary radiations increase, and extinction events decrease, organismal diversity over time[5,8,9]. Evolutionary radiations are referred to as adaptive radiations if new lifeforms evolve rapidly through adaptive diversification into a variety of ecological niches, which typically presupposes ecological opportunity[1–3,10]. Whether or not an adaptive radiation occurs depends on a variety of extrinsic and intrinsic factors as well as on contingency, whereas the magnitude of an adaptive radiation is determined by the interplay between its main components, speciation (minus extinction) and adaptation to distinct ecological niches[1,2,4,11]. Despite considerable scientific interest in the phenomenon of adaptive radiation as the cradle of organismal diversity[1,2,10,12,13], many predictions regarding its drivers and dynamics remain untested, particularly in exceptionally species-rich instances. Here, we examine what some consider as the "most outstanding example of adaptive radiation"[14], the species flock of cichlid fishes in Lake Tanganyika. This cichlid assemblage comprises about 240 species[15], which together feature an extraordinary degree of morphological, ecological and behavioural diversity[14–17]. We construct a species tree of Lake Tanganyika's cichlid fauna on the basis of genome-wide data, demonstrate the adaptive nature of the radiation, reconstruct eco-morphological diversification along the species tree, and test general and cichlid-specific predictions related to adaptive radiation.

In situ radiation in Lake Tanganyika

To establish the phylogenetic context of cichlid evolution in Lake Tanganyika, we estimated the age of the radiation through divergence time analyses based on cichlid and other teleost fossils[18], and constructed time-calibrated species trees using 547 newly sequenced cichlid genomes (Supplementary Table 1). Our new phylogenetic hypotheses (Fig. 1, Extended Data Figs. 1–4, Supplementary Figs. 1, 2) support the assignment of the Tanganyikan cichlid fauna into 16 subclades—corresponding to the taxonomic grouping of species into tribes[15]—and confirm that the Tanganyikan representatives of the tribes Coptodonini, Oreochromini and Tylochromini belong to more ancestral and widespread lineages that have colonized the lake secondarily[12,15,19] (Supplementary Discussion). It has been under debate whether all endemic Tanganyikan cichlid tribes evolved within the confines of Lake Tanganyika or whether some of them evolved elsewhere before the formation of the lake[20–22]. Our time calibrations establish that the most recent common ancestor of the cichlid radiation in Lake Tanganyika lived around 9.7 million years ago (Ma) (95% highest-posterior-density

[1]Zoological Institute, Department of Environmental Sciences, University of Basel, Basel, Switzerland. [2]Palaeontological Institute and Museum, University of Zurich, Zurich, Switzerland. [3]Centre for Ecological and Evolutionary Synthesis (CEES), Department of Biosciences, University of Oslo, Oslo, Norway. [4]Centre for Molecular Biodiversity Research (ZMB), Zoological Research Museum Alexander Koenig, Bonn, Germany. [5]Botany, Department of Environmental Sciences, University of Basel, Basel, Switzerland. ✉e-mail: fabrizia.ronco@unibas.ch; walter.salzburger@unibas.ch

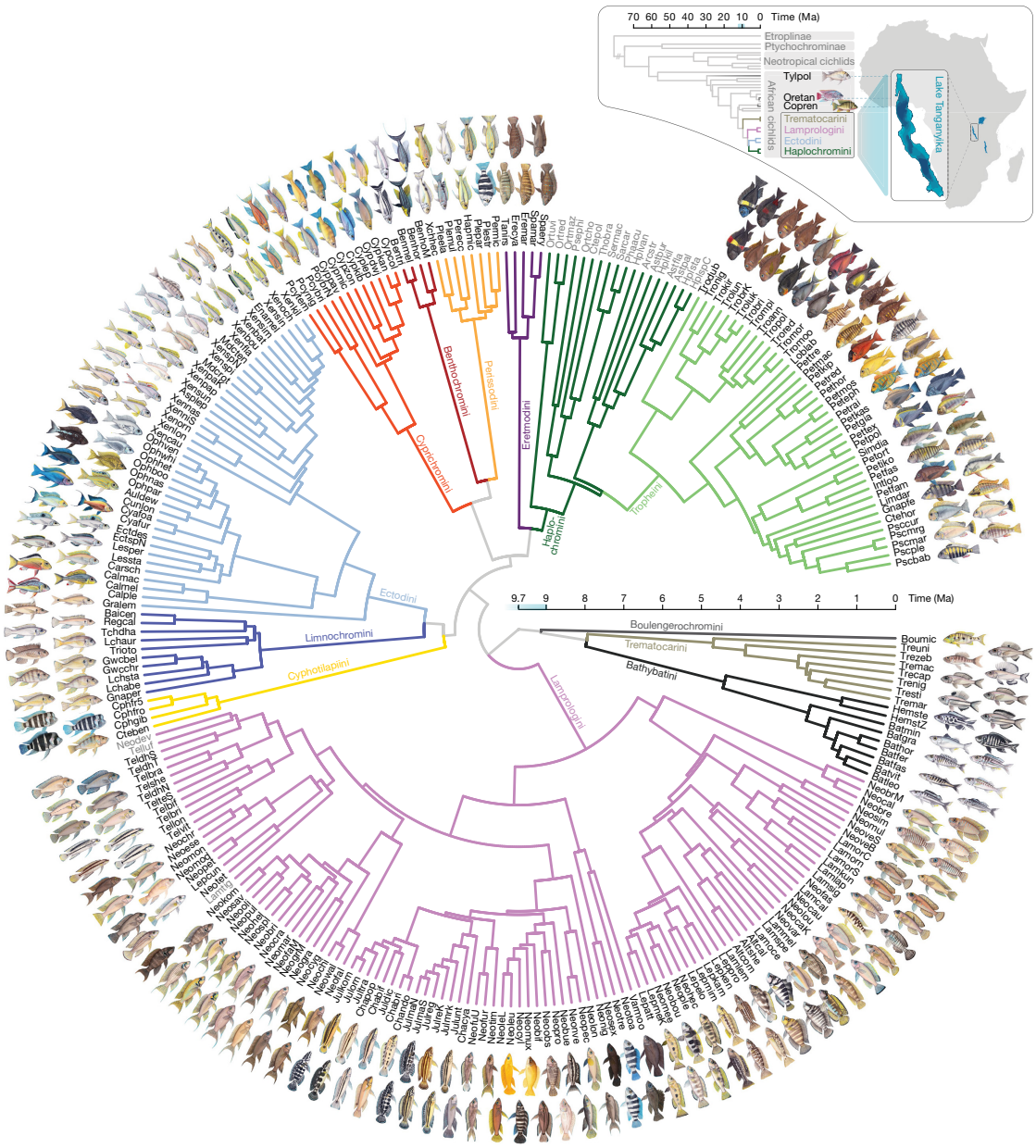

Fig. 1 | Time-calibrated species tree of the cichlid fishes of African Lake Tanganyika. The species tree was time calibrated with a relaxed-clock model and is based on a maximum-likelihood topology inferred from genome-wide SNPs. Species names are abbreviated using a six-letter code, whereby the first three letters represent the genus and the last three letters the species name (Supplementary Table 1; see Extended Data Fig. 2 for the phylogeny with full species names). Branches are coloured according to tribes, and for all lake species an illustration is shown. Representatives of riverine cichlids (grey font) are nested within the radiation. The inset shows the time-calibrated phylogeny of more ancestral cichlid lineages (estimated under the multi-species coalescent model, Extended Data Fig. 1), highlighting the phylogenetic positions of the Tanganyikan representatives of the tribes Coptodonini (*Coptodon rendalli* (Copren)), Oreochromini (*Oreochromis tanganicae* (Oretan)) and Tylochromini (*Tylochromis polylepis* (Tylpol)), which colonized the lake secondarily. The schematic map of the African continent shows the position of the three Great Lakes Victoria, Malawi and Tanganyika, with a magnified section of Lake Tanganyika. The presumed age of Lake Tanganyika[23] (9–12 Myr) is indicated in blue along the time axes. Species trees based on alternative topologies are presented in Extended Data Figs. 2–4, and uncalibrated nuclear and mitochondrial phylogenies on the specimen level are shown in Supplementary Figs. 1, 2.

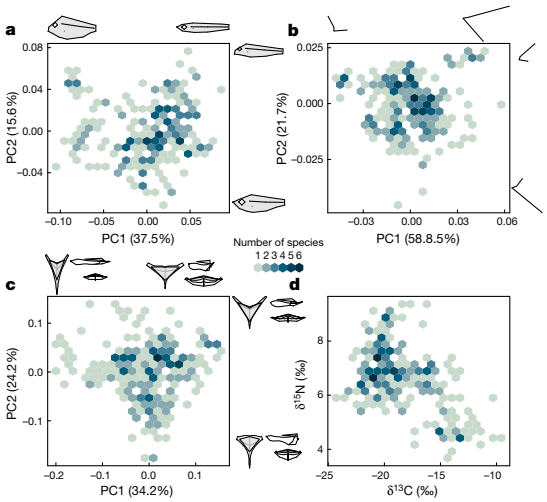

Fig. 2 | Morphospace and ecospace occupation of the cichlid fishes of Lake Tanganyika. a–c, PCA of body shape (**a**, $n = 242$ taxa; 2,197 specimens), upper oral jaw morphology (**b**, $n = 242$ taxa; 2,197 specimens) and lower pharyngeal jaw shape (**c**, $n = 239$ taxa, 1,168 specimens) along with the associated shape changes. **d**, Ecospace spanned by the stable C and N isotope composition (δ^{13}C and δ^{15}N values; $n = 236$ taxa; 2,259 specimens). The colour scale indicates the number of species in 20 by 20 bins across the trait space (see Extended Data Figs. 6, 7 for PCA and stable-isotope biplots with a focus on morpho- and ecospace occupation per tribe).

age interval: 10.1–9.1 Ma) (Fig. 1), which coincides with the appearance of lacustrine conditions in the Tanganyikan Rift[23]. This suggests that the radiation commenced shortly after the lake had formed and that all endemic cichlid tribes have evolved and diversified in situ, that is, within the temporal and geographical context of Lake Tanganyika.

Phenotypes correlate with environments

Because—in the case of adaptive radiation—diversification occurs via niche specialization, a strong association is expected in the extant fauna between the environment occupied by a species and the specific morphological features used to exploit it[2,3]. To quantify eco-morphological diversification across the radiation, we investigated three trait complexes through landmark-based morphometric analyses. Specifically, we quantified body shape and upper oral jaw morphology using 2D landmarks acquired from X-ray images and the shape of the lower pharyngeal jaw bone based on 3D landmarks derived from micro-computed tomography (μCT) scans (Extended Data Fig. 5). To approximate the ecological niche of each species, we used the carbon and nitrogen stable-isotope composition of muscle tissue, which provides information about the relative position along the benthic–pelagic axis (δ^{13}C value) and the relative trophic level (δ^{15}N value), respectively[16,24]—a pattern that we corroborate here for Lake Tanganyika (Extended Data Fig. 6a, Supplementary Discussion). The major axes of shape variation for each trait complex were identified through a principal component analysis (PCA). To test for phenotype–environment correlations and to identify the ecologically most relevant components of each of these trait complexes, we performed a two-block partial least-square analysis (PLS) with the stable-isotope measurements, and applied a phylogenetic generalized least-square analysis (pGLS) to account for phylogenetic dependence.

The quantification of variation in body shape revealed that principal component 1 (PC1) represented mainly differences in aspect ratio, whereas PC2 was loaded with changes in head morphology (Fig. 2a). The changes in aspect ratio (comparable to PC1) were correlated with the δ^{13}C and δ^{15}N values (PLS: Pearson's $r = 0.69$, $R^2 = 0.48$, $P = 0.001$; pGLS: $R^2 = 0.12$, $P < 0.001$, $\lambda_{pGLS} = 1.007$). PC1 of upper oral jaw morphology mainly represented changes in the orientation and relative size of the premaxilla, which was also the main correlate to the stable C and N isotope composition (PLS: Pearson's $r = 0.62$, $R^2 = 0.38$, $P = 0.001$; pGLS: $R^2 = 0.09$, $P < 0.001$, $\lambda_{pGLS} = 1.023$), whereas PC2 was defined by changes in the ratio of the rostral versus the lateral part of the bone (Fig. 2b). For lower pharyngeal jaw shape, we found that PC1 reflected mainly changes in the aspect ratio of the jaw bone in combination with an increased posterior thickness, whereas PC2 involved similar shifts in thickness, yet in this case in combination with changes in the lengths of the postero-lateral horns that act as muscle-attachment structures[25] (Fig. 2c). The PLS revealed that shape changes similar to PC2 are best associated with stable-isotope values (PLS: Pearson's $r = 0.67$, $R^2 = 0.45$, $P = 0.001$; pGLS: $R^2 = 0.16$, $P < 0.001$, $\lambda_{pGLS} = 1.018$). The PCAs further revealed that the occupied area of the morphospace and ecospace scales with the number of species in the tribes (Extended Data Figs. 6, 7; ecospace: Pearson's $r = 0.88$, d.f. = 9, $P < 0.001$; body shape: Pearson's $r = 0.91$, d.f. = 9, $P < 0.001$; upper oral jaw morphology: Pearson's $r = 0.88$, d.f. = 9, $P < 0.001$; lower pharyngeal jaw shape: Pearson's $r = 0.83$, d.f. = 9, $P = 0.002$), a pattern that is not driven by sample size only (Supplementary Discussion).

Overall, the significant association between each of the three traits and the stable C and N isotope composition underpins their adaptive value (Extended Data Fig. 8a–c). A joint consideration points out that deep-bodied cichlids with inferior mouths and thick lower pharyngeal jaws with short horns are associated with higher stable-isotope projections (high δ^{13}C and low δ^{15}N values), indicating that such fishes occur predominantly in the benthic/littoral zone of the lake and feed on plants and algae, whereas more elongated species with more superior mouths and longer and thinner lower pharyngeal jaws are generally associated with lower stable-isotope projections (low δ^{13}C and high δ^{15}N values), suggesting a more pelagic lifestyle and a higher position in the food chain.

Pulses of morphological diversification

Next, we investigated the temporal dynamics of how the observed eco-morphological disparity emerged over the course of the radiation. In addition to the three eco-morphological traits, we also scored male pigmentation patterns to approximate disparity along the signalling axis—another potentially important component of diversification in adaptive radiations[1,6,7,26]. For all four traits, we estimated morphospace expansion through time using ancestral-state reconstructions along the time-calibrated species tree and applying a variable-rates model of trait evolution[27,28] (Extended Data Fig. 8d, e). We calculated morphological disparity as the extent of occupied morphospace in time intervals of 0.15 million years (Myr) in comparison to a null model that assumes Brownian motion. Likewise, evolutionary rates through time were calculated as mean evolutionary rates derived from the variable-rates model, sampled at the same time points along the phylogeny.

Our analyses uncovered a pattern of discrete pulses in morphospace expansion, which were followed, in most cases, by morphospace packing (Fig. 3). The timing of these pulses differed among the traits. For body shape, we found a pulse of rapid morphospace expansion early in the radiation, alongside the first pulse of lower pharyngeal jaw shape diversification (Fig. 3b, c); this early phase of the radiation also features the highest evolutionary rates for body shape (Fig. 3d). The pulse in upper oral jaw diversification occurred in the middle phase of the radiation. Evolutionary rates were increased during this period, and were even higher at a later phase that was dominated by packing of the upper oral jaw morphospace rather than its expansion (Fig. 3b–d). This

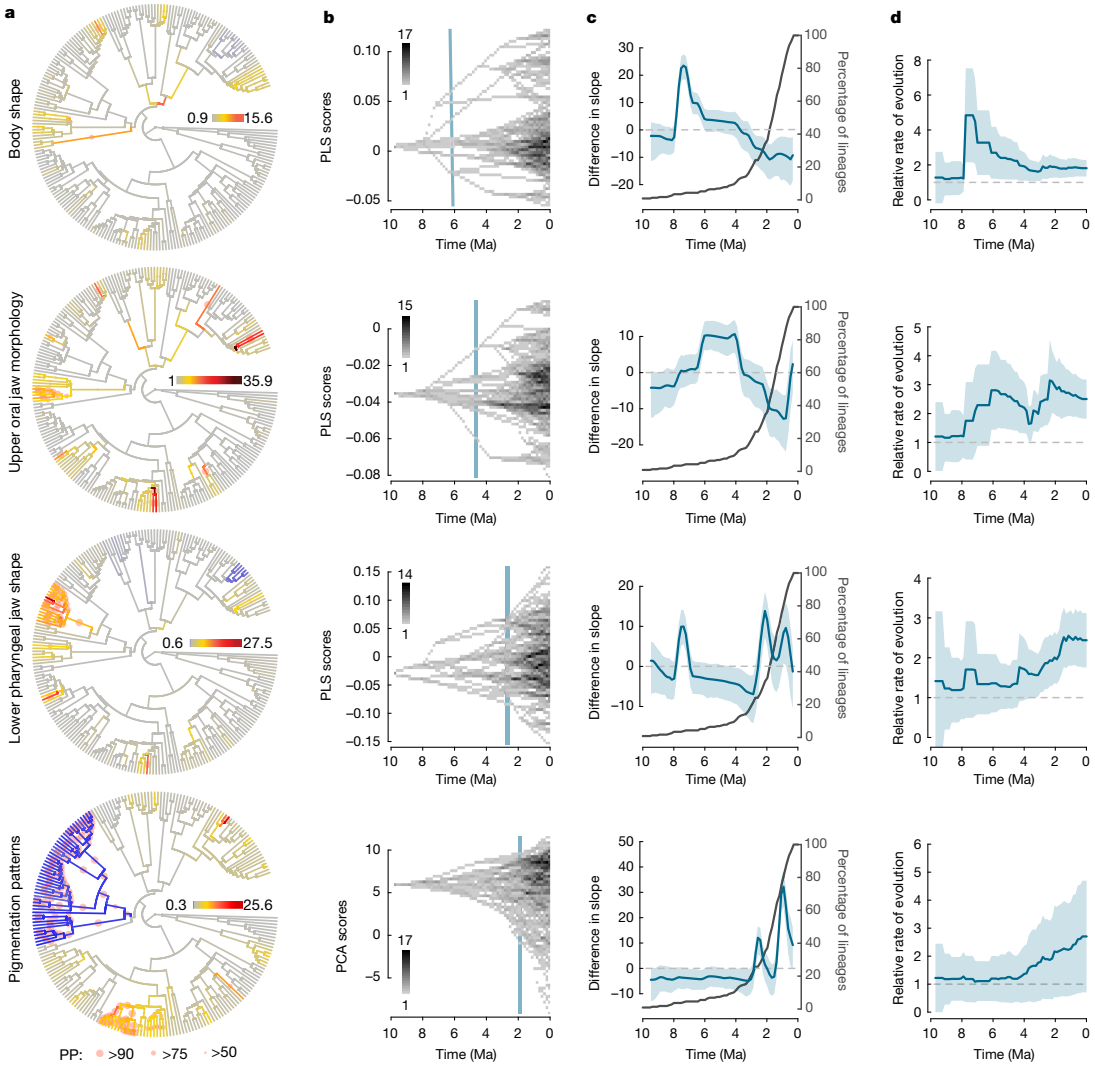

Fig. 3 | Temporal dynamics of morphological diversification in the adaptive radiation of cichlid fishes in Lake Tanganyika. a–d, First row: body shape, $n = 232$ taxa, 2,164 specimens; second row: upper oral jaw morphology, $n = 232$ taxa, 2,164 specimens; third row: lower pharyngeal jaw shape, $n = 232$ taxa, 1,148 specimens; fourth row: pigmentation patterns, $n = 218$ taxa, 1,016 specimens. **a**, Species tree (Fig. 1) with branches coloured according to the mean relative rates of trait evolution for each trait. PP, posterior probability for rate shift. **b**, Morphospace densities (number of lineages) through time for each trait. Blue lines indicate the point in time when 50% of the extant morphospace had become occupied. **c**, Comparison of slopes (blue) of morphospace expansion over time between the observed data and the Brownian motion null model of trait evolution (mean across 500 Brownian motion simulations with 95% quantiles). A difference in slopes above zero represents morphospace expansion and values below zero indicate morphospace packing relative to the null model. Lineage accumulation through time derived from the species tree is shown in dark grey. **d**, Mean relative rates of trait evolution over time with standard deviation (blue).

suggests that, in that later phase, rapidly evolving lineages diverged into pre-occupied regions of the morphospace, ultimately resulting in convergent forms[16]. The second pulse in lower pharyngeal jaw morphospace expansion happened late in the radiation when evolutionary rates were also highest for this trait (Fig. 3b–d). Thus, the theoretical prediction that eco-morphological diversification is rapid early in an adaptive radiation and slows down through time as the available niche space becomes filled[1,5] applies only to body shape. Yet, this early burst in body shape diversification was not connected to a substantial increase in lineage accumulation (Fig. 3c).

Pigmentation patterns showed a single pulse of diversification and increased evolutionary rates late in the radiation—a signature unlikely to be caused by a high turnover rate in this trait (Supplementary Discussion). This late pulse of diversification in pigmentation patterns, together with the consecutive pulses of morphospace expansion in the eco-morphological traits, is in agreement with the prediction that

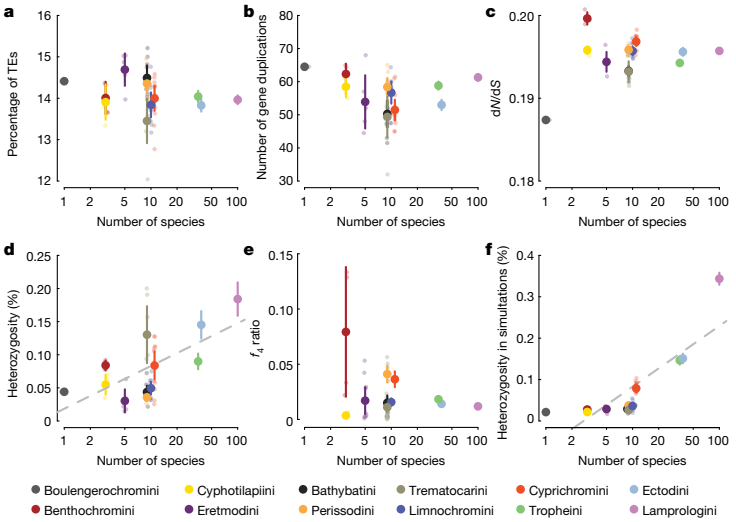

Fig. 4 | Association between genomic features and species richness across the cichlid tribes in Lake Tanganyika. Each genomic summary statistic was tested for a correlation with species richness per tribe (log transformed). To account for phylogenetic structure in the data, we calculated phylogenetic independent contrasts for each variable. Data points are coloured according to tribes; large points are tribe means shown with 95% confidence intervals, small points represent species means and are only shown for group sizes <40. **a**, Percentage of the genome identified as transposable elements (TEs) (Pearson's $r = -0.31$, d.f. = 10, $P = 0.33$; tribe means are based on one genome per species; Extended Data Fig. 9a). **b**, Number of duplicated genes (Pearson's $r = -0.27$, d.f. = 10, $P = 0.40$; tribe means are based on species means). **c**, Genome-wide d*N*/d*S* ratios as a measure of selection on coding sequences (Pearson's $r = 0.26$, d.f. = 10, $P = 0.42$; tribe means are based on species means across a set of 15,294 genes per genome; Extended Data Fig. 9b). **d**, Percentage of heterozygous sites per genome (Pearson's $r = 0.70$, d.f. = 10, $P = 0.012$; tribe means are based on species means). **e**, f_4-ratio statistics as a measure of gene flow among species within each tribe (Pearson's $r = -0.35$, d.f. = 9, $P = 0.29$; tribe means are based on all species triplets within each tribe; see Extended Data Fig. 10 for a summary of the f_4-ratio statistics for all species comparisons). **f**, Mean percentage of heterozygous sites in simulations with within-tribe migration rates sampled from the observed f_4-ratio statistics (Pearson's $r = 0.84$, d.f. = 10, $P = 0.00067$; tribe means are based on species means across 20 simulations; Extended Data Fig. 9c).

diversification in an adaptive radiation proceeds in discrete temporal stages—first in macrohabitat use, then by trophic specialization, followed by a final stage of divergence along the signalling axes[1,6,7]. However, in contrast to the conventional stages model, the most recent stage of the cichlid adaptive radiation in Lake Tanganyika, which coincides with a large number of speciation events (Fig. 3c), is characterized by temporally overlapping pulses of diversification in both a putative signalling trait and in an ecologically relevant trait. The lower pharyngeal jaw shape is the only trait complex showing two discrete pulses of morphospace expansion—one early in the radiation and one late when niche space already became limited. This later pulse suggests that diversification in the pharyngeal jaw apparatus facilitated fine-scaled resource partitioning after body shape and upper oral jaw morphospaces had been explored, resulting in the densely packed niche space observed today (Figs. 2, 3b).

Genomic features and species richness

Finally, we examined whether the diversity patterns arising over the course of the radiation are linked with particular genomic features. It has previously been suggested—on the basis of five reference cichlid genomes—that the radiating African cichlid lineages are characterized by increased transposable element counts, increased levels of gene duplications, and genome-wide accelerated coding-sequence evolution[13]. Because of the phylogenetic substructure of Lake Tanganyika's cichlid fauna and the widely differing species numbers among tribes, our data offered the opportunity to examine genomic features for an association with per-tribe species richness within a large-scale radiation. We did not find evidence that members of species-rich tribes exhibit greater numbers of transposable elements (Fig. 4a) or more duplicated genes in their genomes (Fig. 4b), nor do they feature elevated genome-wide signatures of selection in coding sequences (Fig. 4c) (see also Extended Data Fig. 9). However, we found that a tribe's species richness scales positively with a common measure of genetic diversity: genome-wide heterozygosity (Fig. 4d). That genetic diversity is linked to species richness has been previously suggested, although the nature of this relationship and the determinants of genetic diversity are under debate[29,30].

Elevated levels of heterozygosity could potentially result from hybridization[31], which has itself been suggested as a trigger of cichlid radiations[22,32,33]. In Tanganyikan cichlids, the level of gene flow within tribes (estimated using f_4-ratio values[34]) does not correlate with a tribe's species richness (Fig. 4e, Extended Data Fig. 10). Nevertheless, much of the variation in heterozygosity as well as its correlation with species richness can be explained by the observed levels of gene flow within tribes in combination with the reduced gene flow among them: through coalescent simulations of genome evolution along the species tree we show that variation in migration rates, sampled from the empirical f_4-ratio estimates, can produce levels of heterozygosity that are similar to the ones observed in nature (Fig. 4f). Hence, the correlation between species richness and heterozygosity can be explained by gene flow and phylogenetic structure, which is consistent with the expectation that the effect of gene flow scales positively with the number of hybridizing species and the divergence among these. In the cichlid radiation in Lake Malawi, which is an order of magnitude younger than the one in Lake Tanganyika, heterozygosity levels vary much less among lineages and

do not scale with species richness, which—according to our findings—can be explained by the much lower levels of genetic differentiation between the hybridizing species[33].

Conclusion

On the basis of a comprehensive dataset on cichlid fishes from African Lake Tanganyika, we tested predictions related to the phenomenon of adaptive radiation. We establish that the Tanganyikan cichlid radiation unfolded within the temporal and spatial confines of the lake, giving rise to an endemic fauna consisting of about 240 species in 52 genera and 13 tribes in less than 10 Myr. Although the ancestors of these tribes initially found comparable ecological opportunity, present-day species numbers differ by two orders of magnitude among these phylogenetic sublineages. Our analyses of morphological, ecological and genomic information revealed that, taken as a whole, species-rich tribes occupy larger fractions of the morphospace and ecospace and contain species that are, at the per-genome level, genetically more diverse, which appears to be linked to gene flow. We demonstrate a phenotype–environment association in three trait complexes (body shape, upper oral jaw morphology and lower pharyngeal jaw shape) and pinpoint their most relevant adaptive components. We show that eco-morphological diversification was not gradual over the course of the radiation. Instead, we identified trait-specific pulses of accelerated phenotypic evolution, whereby only diversification in body shape shows an early burst[1,5]. The sequence of the trait-specific pulses essentially follows the pattern postulated in the stages model of adaptive radiation[1,6,7], with the extension that the most recent stage of the cichlid adaptive radiation in Lake Tanganyika, which is characterized by a large number of speciation events, is defined by increased diversification in both an ecological (lower pharyngeal jaw) and a signalling (pigmentation) trait. To what extent the observed diversity and disparity patterns were shaped by past environmental fluctuations and extinction dynamics cannot be answered conclusively through the investigation of the extant fauna alone.

Online content

Any methods, additional references, Nature Research reporting summaries, source data, extended data, supplementary information, acknowledgements, peer review information; details of author contributions and competing interests; and statements of data and code availability are available at https://doi.org/10.1038/s41586-020-2930-4.

1. Gavrilets, S. & Losos, J. B. Adaptive radiation: contrasting theory with data. *Science* **323**, 732–737 (2009).
2. Schluter, D. *The Ecology of Adaptive Radiation* (Oxford Univ. Press, 2000).
3. Simpson, G. G. *The Major Features of Evolution* (Columbia Univ. Press, 1953).
4. Glor, R. E. Phylogenetic insights on adaptive radiation. *Annu. Rev. Ecol. Evol. Syst.* **41**, 251–270 (2010).
5. Foote, M. The evolution of morphological diversity. *Annu. Rev. Ecol. Syst.* **28**, 129–152 (1997).
6. Danley, P. D. & Kocher, T. D. Speciation in rapidly diverging systems: lessons from Lake Malawi. *Mol. Ecol.* **10**, 1075–1086 (2001).
7. Streelman, J. T. & Danley, P. D. The stages of vertebrate evolutionary radiation. *Trends Ecol. Evol.* **18**, 126–131 (2003).
8. Benton, M. J. Diversification and extinction in the history of life. *Science* **268**, 52–58 (1995).
9. Sepkoski, J. J., Jr. Rates of speciation in the fossil record. *Phil. Trans. R. Soc. Lond. B* **353**, 315–326 (1998).
10. Berner, D. & Salzburger, W. The genomics of organismal diversification illuminated by adaptive radiations. *Trends Genet.* **31**, 491–499 (2015).
11. Wagner, C. E., Harmon, L. J. & Seehausen, O. Ecological opportunity and sexual selection together predict adaptive radiation. *Nature* **487**, 366–369 (2012).
12. Salzburger, W. Understanding explosive diversification through cichlid fish genomics. *Nat. Rev. Genet.* **19**, 705–717 (2018).
13. Brawand, D. et al. The genomic substrate for adaptive radiation in African cichlid fish. *Nature* **513**, 375–381 (2014).
14. Fryer, G. & Iles, T. D. *The Cichlid Fishes of the Great Lakes of Africa* (T.F.H. Publications, 1972).
15. Ronco, F., Büscher, H. H., Indermaur, A. & Salzburger, W. The taxonomic diversity of the cichlid fish fauna of ancient Lake Tanganyika, East Africa. *J. Gt. Lakes Res.* **46**, 1067–1078 (2020).
16. Muschick, M., Indermaur, A. & Salzburger, W. Convergent evolution within an adaptive radiation of cichlid fishes. *Curr. Biol.* **22**, 2362–2368 (2012).
17. Salzburger, W., Van Bocxlaer, B. & Cohen, A. S. Ecology and evolution of the African Great Lakes and their faunas. *Annu. Rev. Ecol. Evol. Syst.* **45**, 519–545 (2014).
18. Matschiner, M., Böhne, A., Ronco, F. & Salzburger, W. The genomic timeline of cichlid diversification across continents. *Nat. Commun.* https://doi.org/10.1038/s41467-020-17827-9 (2020).
19. Koch, M. et al. Evolutionary history of the endemic Lake Tanganyika cichlid fish *Tylochromis polylepis*: A recent intruder to a mature adaptive radiation. *J. Zool. Syst. Evol. Res.* **45**, 64–71 (2007).
20. Salzburger, W., Meyer, A., Baric, S., Verheyen, E. & Sturmbauer, C. Phylogeny of the Lake Tanganyika cichlid species flock and its relationship to the Central and East African haplochromine cichlid fish faunas. *Syst. Biol.* **51**, 113–135 (2002).
21. Schedel, F. D. B., Musilova, Z. & Schliewen, U. K. East African cichlid lineages (Teleostei: Cichlidae) might be older than their ancient host lakes: new divergence estimates for the east African cichlid radiation. *BMC Evol. Biol.* **19**, 94 (2019).
22. Irisarri, I. et al. Phylogenomics uncovers early hybridization and adaptive loci shaping the radiation of Lake Tanganyika cichlid fishes. *Nat. Commun.* **9**, 3159 (2018).
23. Cohen, A. S., Soreghan, M. J. & Scholz, C. A. Estimating the age of formation of lakes: an example from Lake Tanganyika, East African Rift system. *Geology* **21**, 511–514 (1993).
24. Post, D. M. Using stable isotopes to estimate trophic position: models, methods, and assumptions. *Ecology* **83**, 703–718 (2002).
25. Liem, K. F. Evolutionary strategies and morphological innovations: cichlid pharyngeal jaws. *Syst. Zool.* **22**, 425–441 (1973).
26. Salzburger, W. The interaction of sexually and naturally selected traits in the adaptive radiations of cichlid fishes. *Mol. Ecol.* **18**, 169–185 (2009).
27. Venditti, C., Meade, A. & Pagel, M. Multiple routes to mammalian diversity. *Nature* **479**, 393–396 (2011).
28. Cooney, C. R. et al. Mega-evolutionary dynamics of the adaptive radiation of birds. *Nature* **542**, 344–347 (2017).
29. Ellegren, H. & Galtier, N. Determinants of genetic diversity. *Nat. Rev. Genet.* **17**, 422–433 (2016).
30. Schluter, D. & Pennell, M. W. Speciation gradients and the distribution of biodiversity. *Nature* **546**, 48–55 (2017).
31. Grant, P. R. & Grant, B. R. *40 Years of Evolution: Darwin's Finches on Daphne Major Island* (Princeton Univ. Press, 2014).
32. Meier, J. I. et al. Ancient hybridization fuels rapid cichlid fish adaptive radiations. *Nat. Commun.* **8**, 14363 (2017).
33. Malinsky, M. et al. Whole-genome sequences of Malawi cichlids reveal multiple radiations interconnected by gene flow. *Nat. Ecol. Evol.* **2**, 1940–1955 (2018).
34. Patterson, N. et al. Ancient admixture in human history. *Genetics* **192**, 1065–1093 (2012).

Article

Methods

No statistical methods were used to predetermine sample size. The experiments were not randomized. The investigators were not blinded to allocation during experiments and outcome assessment.

Sampling

Sampling was conducted between 2014 and 2017 at 130 locations at Lake Tanganyika. To maximise taxon coverage, we included additional specimens from previous expeditions (4.9% of the samples) as well as from other collections (0.8%). The final dataset (301 taxa; $n = 2{,}723$ specimens) contained an almost complete taxon sampling of the cichlid fauna of Lake Tanganyika, as well as 18 representative cichlid species from nearby waterbodies, and 32 outgroup species. All analyses described below are based on the same set of typically 10 specimens per species, or subsets thereof (Supplementary Tables 1, 2, Supplementary Methods).

Whole-genome sequencing

Genomic DNA of typically one male and one female specimen per species ($n = 547$) was extracted from fin clips preserved in ethanol using the E.Z.N.A. Tissue DNA Kit (Omega Bio-Tek) and sheared on a Covaris E220 (60 µl with 10% duty factor, 175 W, 200 cycles for 65 s). Individual libraries were prepared using TruSeq DNA PCR-Free Sample Preparation kit (Illumina; low sample protocol) for 350-bp insert size, pooled (six per lane), and sequenced at 126-bp paired-end on an Illumina HiSeq 2500 (Supplementary Table 1 contains information on read depths).

Assessing genomic variation

After adaptor removal with Trimmomatic[35] (v.0.36), reads of 528 genomes (all species belonging to the cichlid radiation in Lake Tanganyika plus additional species nested within this radiation and some selected outgroup species; Supplementary Table 1) were mapped to the Nile tilapia reference genome (RefSeq accession GCF_001858045.1[36]) using BWA-MEM[37] (v.0.7.12). Variant calling was performed with HaplotypeCaller and GenotypeGVCF tools[38] (v.3.7) (GATK), applying a minimum base quality score of 30. Variant calls were filtered with BCFtools[39] (v.1.6; FS < 20, QD > 2, MQ > 20, DP > 4,000, DP < 8,000, ReadPosRankSum > −0.5, MQRankSum > −0.5). We applied a filter to sites in proximity to indels with a minor allele count greater than 2, depending on the size of the indel. With SNPable (http://lh3lh3.users.sourceforge.net/snpable.shtml), we determined all sites within regions of the Nile tilapia reference genome in which read mapping could be ambiguous and masked these sites. Using VCFtools[40] (v.0.1.14) we further masked, per individual, genotypes with a read depth below 4 or a genotype quality below 20. Sites that were no longer polymorphic after the filtering steps were excluded, resulting in a dataset of 57,751,375 SNPs. Called variants were phased with the software beagle[41] (v.4.1). The phasing of *Neolamprologus cancellatus*, which appeared to be F_1 hybrids, was further improved with a custom script. Further details are provided in the Supplementary Methods.

De novo genome assemblies

De novo genome assemblies were generated from the raw-read data for each individual following an approach described previously[42,43], using CeleraAssembler[44] (v.8.3) and FLASH[45] (v.1.2.11). Eight genomes repeatedly failed to assemble and were therefore excluded from further analyses (specimen vouchers: A188, IRF6, IZC5, JWE7, JWG1, JWG2, LJD3 and LJE8). Assembly quality was assessed with QUAST[46] (v.4.5) and completeness was determined with BUSCO[47] (v.3). Assembly statistics summarized with MultiQC[48] (v.1.7) are available on Dryad.

Determining the age of the radiation

To determine the age of the cichlid radiation in Lake Tanganyika, we applied phylogenomic molecular-clock analyses for representatives of all cichlid subfamilies and the most divergent tribes, together with non-cichlid outgroups (44 species; Extended Data Fig. 1). Following Matschiner et al.[18] we identified and filtered orthologue sequences from genome assemblies and compiled 'strict' and 'permissive' datasets that contained alignments for 510 and 1,161 genes and had total alignment lengths of 542,922 and 1,353,747 bp, respectively. We first analysed the topology of the species with the multi-species coalescent model implemented in ASTRAL[49] (v.5.6.3), based on gene trees that we estimated for both datasets with BEAST2[50] (v.2.5.0). As undetected past introgression can influence divergence-time estimates in molecular clock analyses, we further tested for signals of introgression in the form of asymmetric species relationship in gene trees and excluded five species (*Fundulus heteroclitus*, *Tilapia brevimanus*, *Pelmatolapia mariae*, *Tilapia sparrmanii*, and *Steatocranus* sp. 'ultraslender') potentially affected by introgression from all subsequent molecular-clock analyses. We then estimated divergence times among the most divergent cichlid tribes and the age of the cichlid radiation in Lake Tanganyika with the multi-species coalescent model in StarBEAST2[51] (v.0.15.5), using the 'strict' set of gene alignments (Extended Data Fig. 1). Further details are provided in the Supplementary Methods.

Phylogenetic inference

To infer a complete phylogeny of the cichlid radiation in Lake Tanganyika (the Tanganyikan representatives of the more ancestral tribes Coptodonini, Oreochromini and Tylochromini were excluded) from genome-wide SNPs we applied additional filters, retaining only SNPs with <40% missing data and between-SNP distances of at least 100 bp. The remaining 3,630,997 SNPs were used to infer a maximum-likelihood phylogeny with RAxML[52] (v.8.2.4; Fig. 1, Extended Data Fig. 2, Supplementary Fig. 1). The species-tree topology was further estimated under the multi-species coalescent model from a set of local phylogenies with ASTRAL (Extended Data Fig. 3); these local phylogenies were inferred with IQ-TREE[53] (v.1.7-beta7) from alignments for 1,272 genomic regions determined to be particularly suitable for phylogenetic analysis (see Supplementary Methods). We also applied the multi-species coalescent model implemented in SNAPP[54] (v.1.4.2) to the dataset of genome-wide SNPs (Extended Data Fig. 4). Species-level phylogenies resulting from these different approaches were used as topological constraints in subsequent relaxed-clock analyses of divergence times (see below). In addition, we estimated the mitochondrial phylogeny based on maximum-likelihood with RAxML (Supplementary Fig. 2). Further details are provided in the Supplementary Methods.

Divergence time estimates within the radiation

For relaxed-clock analyses, the 1,272 alignments were further filtered by applying stricter thresholds on the proportion of missing data and the strength of recombination signals. Ten remaining alignments with a length greater than 2,500 bp and less than 130 hemiplasies (total length: 30,738 bp; completeness: 95.8%), were then used jointly to estimate divergence times with the uncorrelated-lognormal relaxed-clock model implemented in BEAST2. To account for phylogenetic uncertainty in downstream phylogenetic comparative analyses, we performed three separate sets of relaxed clock analyses, in which the topology was either fixed to the species-level phylogeny inferred with RAxML (Fig. 1, Extended Data Fig. 2), the species tree inferred with ASTRAL (Extended Data Fig. 3) or the Bayesian species tree inferred with SNAPP (Extended Data Fig. 4). Further details are provided in the Supplementary Methods.

Morphometrics

To quantify body shape and upper oral jaw morphology, we applied a landmark-based geometric morphometric approach to digital X-ray images (for the full set of 10 specimens per species whenever possible; $n = 2{,}197$). We selected 21 landmarks, of which 17 were distributed across the skeleton and four defined the premaxilla (Extended Data Fig. 5a).

Landmark coordinates were digitized using FIJI[55] (v2.0.0-rc-68/1.521i). To extract overall body shape information, we excluded landmark 16, which marks the lateral end of the premaxilla, hence minimizing the impact of the orientation of the upper oral jaw. We then applied a Procrustes superimposition to remove the effect of size, orientation, and translational position of the coordinates.

For upper oral jaw morphology, we used a subset of four landmarks. A crucial feature of the oral jaw morphology is the orientation of the mouth relative to the body axes. However, this component of the upper oral jaw morphology would be lost in a classical geometric morphometric analysis, in which only pure shape information is retained. To overcome this, we extracted the premaxilla-specific landmarks (1, 2, 16 and 21) after Procrustes superimposition of the entire set of landmarks and subsequently recentred the landmarks to align the specimens without rotation. Thus, the resulting landmark coordinates do not represent the pure shape of the premaxilla but additionally contain information on its orientation and size in relation to body axes and body size, respectively.

To quantify lower pharyngeal jaw bone shape in 3D, a landmark-based geometric morphometric approach was applied on μCT scans of the head region of five specimens per species (n = 1,168). To capture all potential functionally important structures of the lower pharyngeal jaw bone, we selected a set of 27 landmarks (10 true landmarks and 17 sliding semi-landmarks) well distributed across the left side of the bone (Extended Data Fig. 5b). Landmark coordinates were acquired using TINA[56] (v.6.0). To retain the lateral symmetric properties of the shape data during superimposition, we reconstructed the right side of the lower pharyngeal jaw bone by mirroring the landmark coordinates across the plane of bilateral symmetry fitted through all landmarks theoretically lying on this plane. We then superimposed the resulting 42 landmarks while sliding the semi-landmarks along the curves by minimizing Procrustes distances and retained the symmetric component only.

To identify the major axes of shape variation across the multivariate datasets we performed a PCA for each trait. We also calculated morphospace size per tribe as the square root of the convex hull area spanned by species means of the PC1 and PC2 scores. We then tested for a correlation between morphospace size and estimated species richness of a tribe[15] (log-transformed to obtain normal distribution). To account for phylogenetic non-independence, we calculated phylogenetic independent contrasts with the R package ape[57] (v.5.2) using the species tree (Fig. 1) pruned to the tribe level. We then calculated Pearson's correlation coefficients for independent contrasts using the function cor.table of the R package picante[58] (v.1.8).

All landmark coordinates for geometric morphometric analyses were processed and analysed in R[59] (v.3.5.2) using the packages geomorph[60] (v.3.0.7) and Morpho[61] (v.2.6). Further details are provided in the Supplementary Methods.

Stable-isotope analysis

To approximate ecology for each species, we measured the stable carbon (C) and nitrogen (N) isotope composition of all available specimens from Lake Tanganyika (n = 2,259). We analysed a small (0.5–1 mg) dried muscle sample of each specimen with a Flash 2000 elemental analyser coupled to a Delta Plus XP continuous-flow isotope ratio mass spectrometer (IRMS) via a Conflo IV interface (Thermo Fisher Scientific). Carbon and nitrogen isotope data were normalized to the VPDB (Vienna Pee Dee Belemnite) and Air-N_2 scales, respectively, using laboratory standards which were calibrated against international standards. Values are reported in standard per-mil notation (‰), and long-term analytical precision was 0.2‰ for $\delta^{13}C$ values and 0.1‰ for $\delta^{15}N$ values. Note that we have used some of these stable-isotope values in a previous study[62].

To confirm interpretability of the $\delta^{13}C$ and $\delta^{15}N$ values, we additionally collected and analysed baseline samples covering several trophic levels from the northern and the southern basin of Lake Tanganyika (Supplementary Methods, Supplementary Discussion).

To test for a correlation of ecospace size with species richness of the tribes, we applied the same approach as described above to the $\delta^{13}C$ and $\delta^{15}N$ values.

Phenotype–environment association

For each trait (body shape, upper oral jaw, lower pharyngeal jaw) we performed a two-block PLS analysis based on species means of the Procrustes aligned landmark coordinates and the stable C and N isotope compositions using the function two.b.pls in geomorph. To account for phylogenetic dependence of the data we applied a pGLS as implemented in the R package caper[63] (v.1.0.1) across the two sets of PLS scores (each morphological axis and the stable-isotope projection) using the time-calibrated species tree based on the maximum-likelihood topology. The strength of phylogenetic signal in the data was accounted for by optimising the branch length transformation parameter lambda using a maximum-likelihood approach.

Scoring pigmentation patterns

To quantify a putative signalling trait in cichlids, we scored the pigmentation patterns in typically five male specimens per species (n = 1,016), on the basis of standardized images taken in the field after capture of the specimens (see Supplementary Methods). Following the strategy described in Seehausen et al.[64], the presence or absence of 20 pigmentation features was recorded, whereby we extended number of scored features to include additional body and fin pigmentation patterns (Extended Data Fig. 5c). We then applied a logistic PCA implemented in the R package logisticPCA[65] (v.0.2) and used the PC1 scores as univariate proxy for differentiation along the signalling axes for further analyses.

Trait evolution modelling and disparity estimates

To investigate the temporal dynamics of morphological diversification over the course of the radiation we essentially followed the strategy of Cooney et al.[28] (which is based on measurements on extant taxa and assumes constant niche space and no or constant extinction over the course of the radiation), using the PLS scores of body shape, upper oral jaw morphology, and lower pharyngeal jaw shape and the PC1 scores of pigmentation patterns as well as the time-calibrated maximum-likelihood species tree topology. For each trait we assessed the phylogenetic signal in the data by calculating Pagel's lambda and Blomberg's K with the R package phytools[66] (v.0.6-60). We then tested the fit of four models of trait evolution for each of the four traits. We applied a white noise model, a Brownian motion model, a single-optimum Ornstein–Uhlenbeck model and an early burst model of trait evolution using the function fitContinuous of the R package geiger[67] (v.2.0.6.1). Additionally, we fitted a variable-rates model (a Brownian motion model which allows for rate shift on branches and nodes) using the software BayesTrait (http://www.evolution.rdg.ac.uk/; v.3) with uniform prior distributions adjusted to our dataset (alpha: −1–1, sigma: 0–0.001 for morphometric traits; alpha: 0–10, sigma: 0–10 for pigmentation pattern) and applying single-chain Markov-chain Monte Carlo runs with one billion iterations. We sampled parameters every 100,000th iteration, after a pre-set burnin of 10,000,000 iterations. We then tested for each trait for convergence of the chain using a Cramer–von Mises statistic implemented in the R package coda[68] (v.0.19-3). The models were compared by calculating their log-likelihood and Akaike information criterion (AIC) difference (Extended Data Fig. 8d). Based on differences in AIC, the variable-rates model was best supported for all traits but body shape, which showed a strong signal of an early burst of trait evolution (Extended Data Fig. 8d, note that the variable-rates model has the highest log-likelihood for body shape as well). We nevertheless focused on the variable-rates model for further analyses of all traits to be able to compare temporal patterns of trait evolution among the traits.

Article

To estimate morphospace expansion through time we used a maximum-likelihood ancestral-state reconstruction implemented in phytools. To account for differences in the rate of trait evolution along the phylogeny, we reconstructed ancestral states using the mean rate-transformed tree derived from the variable-rates model. We then projected the ancestral states onto the original species tree and calculated the morphospace extent (that is, the range of trait values) in time intervals of 0.15 million years (note that this is an arbitrary value; however, differently sized time intervals had no effect on the interpretation of the results). For each time point we extracted the branches existing at that time and predicted the trait value linearly between nodes. We then compared the resulting morphospace expansion over time relative to a null model of trait evolution. We therefore simulated 500 datasets (PLS and PC1 scores) under Brownian motion given the original species tree with parameters derived from the Brownian motion model fit to the original data. For each simulated dataset we produced morphospace-expansion curves using the same approach as described above. We then compared the slopes of our observed data with each of the null models by calculating the difference of slopes through time (Fig. 3) using linear models fitted for each time interval with the two subsequent time intervals. Note that for body shape we also estimated morphospace expansion through time using the early burst model for ancestral-state reconstruction, which resulted in a very similar pattern of trait diversification.

Unlike other metrics of disparity (for example, variance or mean pairwise distances) morphospace extent is not sensitive to the density distribution of measurements within the morphospace and captures its full range[69]. Hence, comparing the extent of morphospace between observed data and the null model directly unveils the contribution of morphospace expansion relative to the null model; and because the increase in lineages over time is identical in the observed and the simulated data, this comparison also provides an estimate for morphospace packing.

To summarize evolutionary rates we calculated the mean rate of trait evolution inferred by the variable-rates model in the same 0.15 million years intervals along the phylogeny.

To account for phylogenetic uncertainty in the tree topology we repeated the analyses of trait evolution using the time-calibrated trees based on tree topologies estimated with ASTRAL and SNAPP (Extended Data Figs. 3, 4; Supplementary Methods; Supplementary Discussion). Furthermore, to also account for uncertainty in branch lengths, we repeated the analysis on 100 trees from the Bayesian posterior distribution for each of the three trees (Extended Data Fig. 8d, e, results are provided on Dryad).

Further details can be found in the Supplementary Methods.

Characterization of repeat content

For the repeat content analysis, we randomly selected one de novo genome assembly per species of the radiation ($n = 245$). We performed a de novo identification of repeat families using RepeatModeler (v.1.0.11; http://www.repeatmasker.org). We then combined the RepeatModeler output library with the available cichlid-specific libraries (Dfam and RepBase; v.27.01.2017; http://www.repeatmasker.org; 258 ancestral and ubiquitous sequences, 161 cichlid-specific repeats, and 6 lineage-specific sequences; 65,118, 273,530 and 6,667 bp in total, respectively) and used the software RepeatMasker (v.4.0.7; http://www.repeatmasker.org) (-xsmall -s -e ncbi -lib combined_libraries.fa) to identify and soft-mask interspersed repeats and low complexity DNA sequences in each assembly. The reported summary statistics were obtained using RepeatMasker's buildSummary.pl script (Fig. 4a, Extended Data Fig. 9a, results per genome are provided on Dryad).

Gene duplication estimates

Per genome, gene duplication events were identified with the structural variant identification pipeline smoove (population calling method; https://github.com/brentp/smoove, docker image cloned 20/12/2018), which builds upon lumpy[70], svtyper[71] and svtools (https://github.com/hall-lab/svtools). Variants were called per sample ($n = 488$ genomes, 246 taxa of the Tanganyika radiation) from the initial mapping files against the Nile tilapia reference genome with the function 'call'. The union of sites across all samples was obtained with the function 'merge', then all samples were genotyped at those sites with the function 'genotype', and depth information was added with --duphold. Genotypes were combined with the function 'paste' and annotated with 'annotate' and the reference genome annotation file. The obtained VCF file was filtered with BCFtools to keep only duplications longer than 1 kb and of high quality (MSHQ >3 or MSHQ = −1, FMT/DHFFC[0] > 1.3, QUAL >100). The resulting file was loaded into R (v.3.6.0) with vcfR[72] (v.1.8.0) and filtered to keep only duplications with less than 20% missing genotypes. Next, we removed duplication events with a length outside 1.5 times the interquartile range above the upper quartile of all duplication length, resulting in a final dataset of 476 duplications (Fig. 4b).

Analyses of selection on coding sequence

To predict genes within the de novo genome assemblies, we used AUGUSTUS[73] (v.3.2.3) with default parameters and 'zebrafish' as species parameter ($n = 485$ genomes, 245 taxa). For each prediction we inferred orthology to Nile tilapia genes (GCF_001858045.1_ASM185804v2) with GMAP (GMAP-GSNAP[74]; v.2017-08-15) applying a minimum trimmed coverage of 0.5 and a minimum identity of 0.8. We excluded specimens with less than 18,000 tilapia orthologous genes detected (resulting in $n = 471$ genomes, 243 taxa). Next, we kept only those tilapia protein coding sequences that had at least one of their exons present in at least 80% of the assemblies (260,335 exons were retained, representing 34,793 protein coding sequences). Based on the Nile tilapia reference genome annotation file, we reconstructed for each assembly the orthologous coding sequences. Missing exon sequences were set to Ns. We then kept a single protein coding sequence per gene (the one being present in the maximum number of species with the highest percentage of sequence length), resulting in 15,294 protein coding sequences. Per gene, a multiple sequence alignment was then produced using MACSE[75] (v.2.01). We calculated for each specimen and each gene the number of synonymous (S) and non-synonymous (N) substitutions by pairwise comparison to the orthologue tilapia sequence using codeml with runmode −2 within PAML[76] (v.4.9e). To obtain an estimate of the genome-wide sequence evolution rate that is independent of filtering thresholds, we calculated the genome-wide dN/dS ratio for each specimen based on the sum of dS and dN across all genes (Fig. 4c, Extended Data Fig. 9b).

Signals of past introgression

We used the f_4-ratio statistic[34] to assess genomic evidence for interspecific gene exchange. We calculated the f_4-ratio for all combinations of trios of species on the filtered VCF files using the software Dsuite[77] (v.0.2 r20), with *T. sparrmanii* as outgroup species (we excluded *N. cancellatus* as all specimens of this species appeared to be F_1 hybrids; Supplementary Methods). The f_4-ratio statistic estimates the admixture proportion, that is, the proportion of the genome affected by gene flow. The results presented in this study (Fig. 4e, Extended Data Fig. 10) are based on the 'tree' output of the Dsuite function Dtrios, with each trio arranged according to the species tree on the basis of the maximum-likelihood topology. The per-tribe analyses (Fig. 4e) were based only on comparisons where all species within a trio belong to the same tribe ($n = 243$ taxa).

In addition to the f_4-ratio we also identified signals of past introgression among species using a phylogenetic approach by testing for asymmetry in the relationships of species trios in 1,272 local maximum-likelihood trees generated using IQ-TREE (Supplementary Methods; Extended Data Fig. 10).

Heterozygosity

We calculated the number of heterozygous sites per genome ($n = 488$ genomes, 246 taxa from the Tanganyika radiation) from the VCF files using the BCFtools function stats and then quantified the percentage of heterozygous sites among the number of callable sites per genome (see above) (Fig. 4d).

To explore if the observed levels of heterozygosity per tribe can be explained by the levels of gene flow within tribes we performed coalescent simulations with msprime[78] (v.0.7.4). We simulated genome evolution of all species of the radiation following the time-calibrated species tree (Fig. 1), assuming a generation time of 3 years[79] and a constant effective population size of 20,000 individuals. Species divergences were implemented as mass migration events and introgression within tribes as migration between species pairs with rates set according to their introgression (f_4-ratio) signals inferred with Dsuite. To convert the f_4-ratio values into migration rates, we applied a scaling factor of 5×10^{-6}, which results in a close correspondence in magnitude of the simulated introgression signals to those observed empirically (Fig. 4, Extended Data Fig. 9c). In each of 20 separate simulations, we randomly sampled one pairwise f_4-ratio value for each pair of species (there are many f_4 ratios per species pair—one for each possible third species added to the test trio; the maximum values per pair are shown in Extended Data Fig. 10). The simulated data consisted of one chromosome of 100 kb (mutation rate: 3.5×10^{-9} per bp per generation[33], recombination rate: 2.2×10^{-8} per bp per generation; see Supplementary Methods). Levels of heterozygosity were calculated for all simulated datasets as described for the empirical data.

To account for between-tribe gene flow we further performed simulations in which migration between tribes was also sampled from the empirical f_4-ratio distribution. For simplicity in setting up the simulation model, we assume that gene flow between tribes is ongoing until present day, which is clearly an overestimate (see Supplementary Discussion). Nevertheless, the results of these simulations support our hypothesized scenario, confirming that much of the variation in heterozygosity as well as its correlation with species richness can be explained by the observed levels of gene flow.

Correlation of genome-wide statistics with species richness

We tested for a correlation between tribe means (based on species means) of each genomic summary statistics (transposable element counts, number of gene duplications, genome-wide dN/dS ratio, per-genome heterozygosity, and f_4-ratio, as well as the heterozygosity and f_4-ratio statistics derived from simulated genome evolution) and species richness of the tribes, applying the same approach as described above for tests of correlation between morpho- and ecospace size and species richness.

Reporting summary

Further information on research design is available in the Nature Research Reporting Summary linked to this paper.

Data availability

All newly sequenced genomes for this study and their raw reads are available from NCBI under the BioProject accession number PRJNA550295 (https://www.ncbi.nlm.nih.gov/bioproject/). The VCF file, tree files, summary statistics of the assembled genomes and phenotypic datasets generated and analysed during this study are available as downloadable files on Dryad (https://doi.org/10.5061/dryad.9w0vt4bbf). The Nile tilapia reference genome used is available under RefSeq accession GCF_001858045.1. All X-ray data are available on MorphoSource under the project number P1093. Source data are provided with this paper.

Code availability

Code used to analyse the data is available on GitHub (https://github.com/cichlidx/ronco_et_al), except for analyses where single commands from publicly available software were used and where all settings are fully reported in the Methods and/or Supplementary Methods.

35. Bolger, A. M., Lohse, M. & Usadel, B. Trimmomatic: a flexible trimmer for Illumina sequence data. *Bioinformatics* **30**, 2114–2120 (2014).
36. Conte, M. A., Gammerdinger, W. J., Bartie, K. L., Penman, D. J. & Kocher, T. D. A high quality assembly of the Nile Tilapia (*Oreochromis niloticus*) genome reveals the structure of two sex determination regions. *BMC Genomics* **18**, 341 (2017).
37. Li, H. & Durbin, R. Fast and accurate short read alignment with Burrows–Wheeler transform. *Bioinformatics* **25**, 1754–1760 (2009).
38. McKenna, A. et al. The Genome Analysis Toolkit: a MapReduce framework for analyzing next-generation DNA sequencing data. *Genome Res*. **20**, 1297–1303 (2010).
39. Li, H. A statistical framework for SNP calling, mutation discovery, association mapping and population genetical parameter estimation from sequencing data. *Bioinformatics* **27**, 2987–2993 (2011).
40. Danecek, P. et al. The variant call format and VCFtools. *Bioinformatics* **27**, 2156–2158 (2011).
41. Browning, S. R. & Browning, B. L. Rapid and accurate haplotype phasing and missing-data inference for whole-genome association studies by use of localized haplotype clustering. *Am. J. Hum. Genet*. **81**, 1084–1097 (2007).
42. Böhne, A. et al. Repeated evolution versus common ancestry: Sex chromosome evolution in the haplochromine *Pseudocrenilabrus philander*. *Genome Biol. Evol*. **11**, 439–458 (2019).
43. Malmstrøm, M., Matschiner, M., Tørresen, O. K., Jakobsen, K. S. & Jentoft, S. Data descriptor: Whole genome sequencing data and de novo draft assemblies for 66 teleost species. *Sci. Data* **4**, 1–13 (2017).
44. Myers, E. W. et al. A whole-genome assembly of *Drosophila*. *Science* **287**, 2196–2204 (2000).
45. Magoč, T. & Salzberg, S. L. FLASH: fast length adjustment of short reads to improve genome assemblies. *Bioinformatics* **27**, 2957–2963 (2011).
46. Gurevich, A., Saveliev, V., Vyahhi, N. & Tesler, G. QUAST: quality assessment tool for genome assemblies. *Bioinformatics* **29**, 1072–1075 (2013).
47. Simão, F. A., Waterhouse, R. M., Ioannidis, P., Kriventseva, E. V. & Zdobnov, E. M. BUSCO: assessing genome assembly and annotation completeness with single-copy orthologs. *Bioinformatics* **31**, 3210–3212 (2015).
48. Ewels, P., Magnusson, M., Lundin, S., Käller, M. & Multi, Q. C. MultiQC: summarize analysis results for multiple tools and samples in a single report. *Bioinformatics* **32**, 3047–3048 (2016).
49. Zhang, C., Rabiee, M., Sayyari, E. & Mirarab, S. ASTRAL-III: polynomial time species tree reconstruction from partially resolved gene trees. *BMC Bioinformatics* **19** (Suppl 6), 153 (2018).
50. Bouckaert, R. et al. BEAST 2.5: An advanced software platform for Bayesian evolutionary analysis. *PLOS Comput. Biol*. **15**, e1006650 (2019).
51. Ogilvie, H. A., Bouckaert, R. R. & Drummond, A. J. StarBEAST2 brings faster species tree inference and accurate estimates of substitution rates. *Mol. Biol. Evol*. **34**, 2101–2114 (2017).
52. Stamatakis, A. RAxML version 8: a tool for phylogenetic analysis and post-analysis of large phylogenies. *Bioinformatics* **30**, 1312–1313 (2014).
53. Nguyen, L.-T., Schmidt, H. A., von Haeseler, A. & Minh, B. Q. IQ-TREE: a fast and effective stochastic algorithm for estimating maximum-likelihood phylogenies. *Mol. Biol. Evol*. **32**, 268–274 (2015).
54. Bryant, D., Bouckaert, R., Felsenstein, J., Rosenberg, N. A. & RoyChoudhury, A. Inferring species trees directly from biallelic genetic markers: bypassing gene trees in a full coalescent analysis. *Mol. Biol. Evol*. **29**, 1917–1932 (2012).
55. Schindelin, J. et al. Fiji: an open-source platform for biological-image analysis. *Nat. Methods* **9**, 676–682 (2012).
56. Schunke, A. C., Bromiley, P. A., Tautz, D. & Thacker, N. A. TINA manual landmarking tool: software for the precise digitization of 3D landmarks. *Front. Zool*. **9**, 6 (2012).
57. Paradis, E., Claude, J. & Strimmer, K. APE: Analyses of phylogenetics and evolution in R language. *Bioinformatics* **20**, 289–290 (2004).
58. Kembel, S. W. et al. Picante: R tools for integrating phylogenies and ecology. *Bioinformatics* **26**, 1463–1464 (2010).
59. R Development Core Team. R: A language and environment for statistical computing. *R Foundation for Statistical Computing* (2018).
60. Adams, D. C. & Otárola-Castillo, E. Geomorph: An R package for the collection and analysis of geometric morphometric shape data. *Methods Ecol. Evol*. **4**, 393–399 (2013).
61. Schlager, S. in *Statistical Shape and Deformation Analysis* (eds Zheng, G., Li, S. & Szekely, G.) 217–256 (Academic Press, 2017).
62. Ronco, F., Roesti, M. & Salzburger, W. A functional trade-off between trophic adaptation and parental care predicts sexual dimorphism in cichlid fish. *Proc. R. Soc. Lond. B* **286**, 20191050 (2019).
63. Orme, D. *The Caper Package: Comparative Analysis of Phylogenetics and Evolution in R* https://cran.r-project.org/web/packages/caper/vignettes/caper.pdf (2018).
64. Seehausen, O., Mayhew, P. J. & Van Alphen, J. J. M. Evolution of colour patterns in East African cichlid fish. *J. Evol. Biol*. **12**, 514–534 (1999).
65. Landgraf, A. J. & Lee, Y. Dimensionality reduction for binary data through the projection of natural parameters. *J. Multivar. Anal*. 104668 (2020).
66. Revell, L. J. phytools: An R package for phylogenetic comparative biology (and other things). *Methods Ecol. Evol*. **3**, 217–223 (2012).

Article

67. Harmon, L. J., Weir, J. T., Brock, C. D., Glor, R. E. & Challenger, W. GEIGER: investigating evolutionary radiations. *Bioinformatics* **24**, 129–131 (2008).
68. Plummer, M., Best, N., Cowles, K. & Vines, K. CODA: convergence diagnosis and output analysis for MCMC. *R News* **6**, 7–11 (2005).
69. Ciampaglio, C. N., Kemp, M. & McShea, D. W. Detecting changes in morphospace occupation patterns in the fossil record: characterization and analysis of measures of disparity. *Paleobiology* **27**, 695–715 (2001).
70. Layer, R. M., Chiang, C., Quinlan, A. R. & Hall, I. M. LUMPY: a probabilistic framework for structural variant discovery. *Genome Biol.* **15**, R84 (2014).
71. Chiang, C. et al. SpeedSeq: ultra-fast personal genome analysis and interpretation. *Nat. Methods* **12**, 966–968 (2015).
72. Knaus, B. J. & Grünwald, N. J. vcfr: a package to manipulate and visualize variant call format data in R. *Mol. Ecol. Resour.* **17**, 44–53 (2017).
73. Stanke, M., Schöffmann, O., Morgenstern, B. & Waack, S. Gene prediction in eukaryotes with a generalized hidden Markov model that uses hints from external sources. *BMC Bioinformatics* **7**, 62 (2006).
74. Wu, T. D. & Watanabe, C. K. GMAP: a genomic mapping and alignment program for mRNA and EST sequences. *Bioinformatics* **21**, 1859–1875 (2005).
75. Ranwez, V., Douzery, E. J. P., Cambon, C., Chantret, N. & Delsuc, F. MACSE v2: Toolkit for the alignment of coding sequences accounting for frameshifts and stop codons. *Mol. Biol. Evol.* **35**, 2582–2584 (2018).
76. Yang, Z. PAML 4: phylogenetic analysis by maximum likelihood. *Mol. Biol. Evol.* **24**, 1586–1591 (2007).
77. Malinsky, M., Matschiner, M. & Svardal, H. Dsuite–fast *D*-statistics and related admixture evidence from VCF files. *Methods Ecol. Evol.* https://doi.org/10.1111/1755-0998.13265 (2020).
78. Kelleher, J., Etheridge, A. M. & McVean, G. Efficient coalescent simulation and genealogical analysis for large sample sizes. *PLOS Comput. Biol.* **12**, e1004842 (2016).
79. Malinsky, M. et al. Genomic islands of speciation separate cichlid ecomorphs in an East African crater lake. *Science* **350**, 1493–1498 (2015).

Acknowledgements We thank the University of Burundi, the Ministère de l'Eau, de l'Environnement, de l'Amenagement du Territoire et de l'Urbanisme, Republic of Burundi, the Centre de Recherche en Hydrobiologie (CRH), Uvira, DR Congo, the Tanzania Commission for Science and Technology (COSTECH), the Tanzania Fisheries Research Institute (TAFIRI), the Tanzania National Parks Authority (TANAPA), the Tanzania Wildlife Research Institute (TAWIRI), the Lake Tanganyika Research Unit, Department of Fisheries, Republic of Zambia, and the Zambian Department for Immigration for research permits; G. Banyankimbona, H. Mwima, G. Hakizimana, N. Muderhwa, P. Masilya, I. Kimirei, M. Mukuli Wa-Teba, G. Moshi, A. Mwakatobe, C. Katongo, T. Banda and L. Makasa for assistance with obtaining research permits; the boat crews of the *Chomba* (D. Mwanakulya, J. Sichilima, H. D. Sichilima Jr and G. Katai) and the *Maji Makubwa II* (G. Kazumbe and family) for navigation, guidance and company; the boat drivers M. Katumba and T. Musisha; the car drivers A. Irakoze and J. Leonard; M. Schreyen-Brichard, M. Mukuli Wa-Teba, G. Kazumbe, I. Kimirei, D. Schlatter, R. Schlatter, M. K. Dominico, H. Sichilima Sr, C. Zytkow, P. Lassen and V. Huwiler for logistic support; G. Banyankimbona, N. Boileau, B. Egger, Y. Fermon, G. Kazumbe, G. Katai, R. Lusoma, K. Smailus, L. Widmer and numerous fishermen at Lake Tanganyika for help during sampling; V. Huwiler, Charity, O. Mangwangwa and the Zytkow family for lodging; people of innumerable villages on the shores of Lake Tanganyika for providing workspace, shelter for night-camps and access to village infrastructure; M. Barluenga, H. Gante, Z. Musilová, F. Schedel, J. Snoeks, M. Stiassny, H. Tanaka, G. Turner and M. Van Steenberge for providing additional samples and/or specimens; M. Sánchez, A. Schweizer and A. Wegmann for assistance with the μCT scanning of large specimens; C. Moes for help with radiographs; V. Evrard for help with stable isotopes; I. Nissen and E. Burcklen for assistance with DNA shearing; M. Conte and T. D. Kocher for sharing the RepeatMasker annotations for Nile tilapia; C. Klingenberg and M. Sánchez for discussions on the morphometric approach; A. Tooming-Klunderud and team at the Norwegian Sequencing Centre and C. Beisel and team at the Genomics Facility Basel at the ETH Zurich Department of Biosystems Science and Engineering (D-BSSE), Basel, for assistance with next-generation sequencing; M. Jacquot, E. Pujades and T. Sengstag for the setup and assistance with the collection database system (LabKey); and J. Johnson and A. Viertler for fish illustrations in Fig. 1 and Extended Data Fig. 5, respectively. Calculations were performed at sciCORE (http://scicore.unibas.ch/) scientific computing centre at University of Basel (with support by the SIB/Swiss Institute of Bioinformatics) and the Abel computer cluster, University of Oslo. This work was funded by the European Research Council (ERC, Consolidator Grant Nr. 617585 'CICHLID-X' jointly hosted by the University of Basel and the University of Oslo) and the Swiss National Science Foundation (SNSF, grants 156405 and 176039) to W.S. A. Böhne was supported by the SNSF (Ambizione grant 161462).

Author contributions F.R., A.I. and W.S. designed this study (with input from H.H.B., A.K. and S.J.). F.R., A.I., H.H.B. and W.S. collected the specimens in the field. F.R. and A. Böhne extracted DNA and prepared the libraries for sequencing. S.J. coordinated sequencing. M. Matschiner performed the mapping, variant calling, phylogenetic analyses and coalescent simulations. M. Malinsky contributed to the variant calling pipelines and performed the f_4-ratio statistics. A. Böhne assembled the genomes and quantified gene duplications, A.E.T. conducted the dN/dS analyses and V.R. analysed transposable elements. A. Boila assessed stable-isotope compositions, H.H.B. radiographed the specimens and W.S. scored pigmentation patterns. F.R. curated the samples and performed μCT scanning, geometric morphometric analyses, and all analyses incorporating morphological and ecological data as well as correlations with species richness. F.R. and W.S. wrote the manuscript with contributions and/or feedback from all authors. All authors read and approved the final version of the manuscript.

Competing interests The authors declare no competing interests.

Additional information

Supplementary information is available for this paper at https://doi.org/10.1038/s41586-020-2930-4.

Correspondence and requests for materials should be addressed to F.R. or W.S.

Peer review information *Nature* thanks the anonymous reviewer(s) for their contribution to the peer review of this work.

Chapter 2 | Extended Data

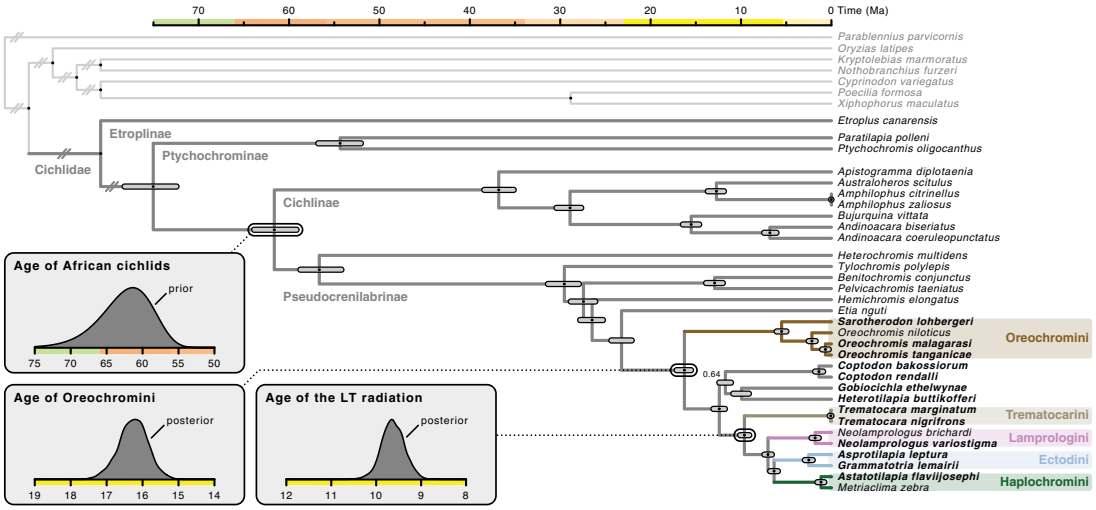

Extended Data Fig. 1 | Age of the adaptive radiation of cichlid fishes in African Lake Tanganyika. Time-calibrated species tree of species representing divergent tribes and subfamilies within cichlids as well as closely-related non-cichlid outgroups, generated with the multi-species coalescent model in StarBEAST2. Nodes marked with a black dot were constrained according to species-tree analyses with ASTRAL. Node bars indicate 95% highest-posterior density age intervals. Outgroup divergence times are not drawn to scale. Insets visualize the prior distribution applied for the age of African cichlids according to Matschiner et al.[18], as well as posterior age estimates for Oreochromini and the cichlid adaptive radiation in Lake Tanganyika (LT).

Article

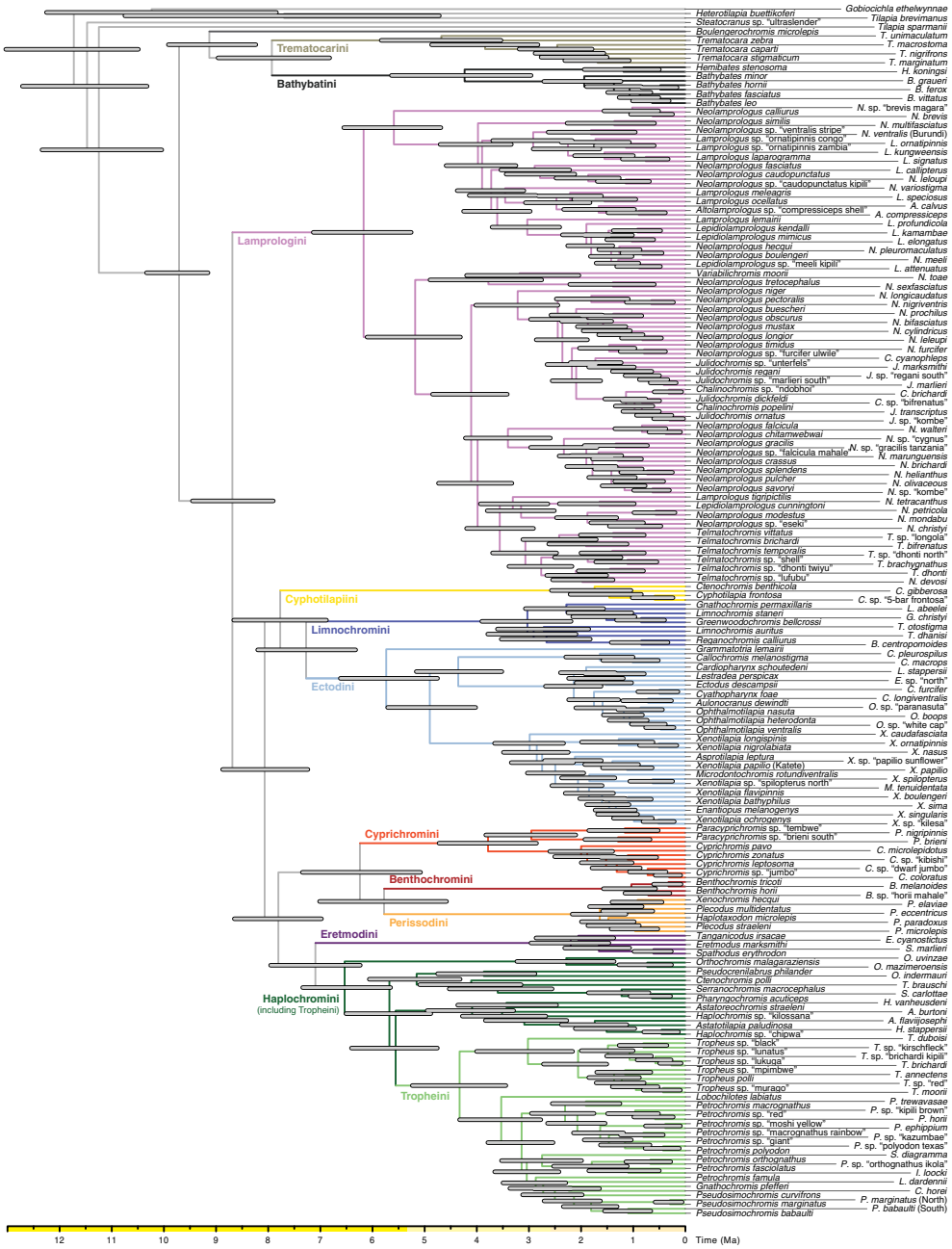

Extended Data Fig. 2 | Time-calibrated species tree of the cichlid adaptive radiation in Lake Tanganyika. The species tree is based on the maximum-likelihood topology estimated with RAxML (Fig. 1) and was time-calibrated using a relaxed-clock model in BEAST2, applied to a selected set of alignments.

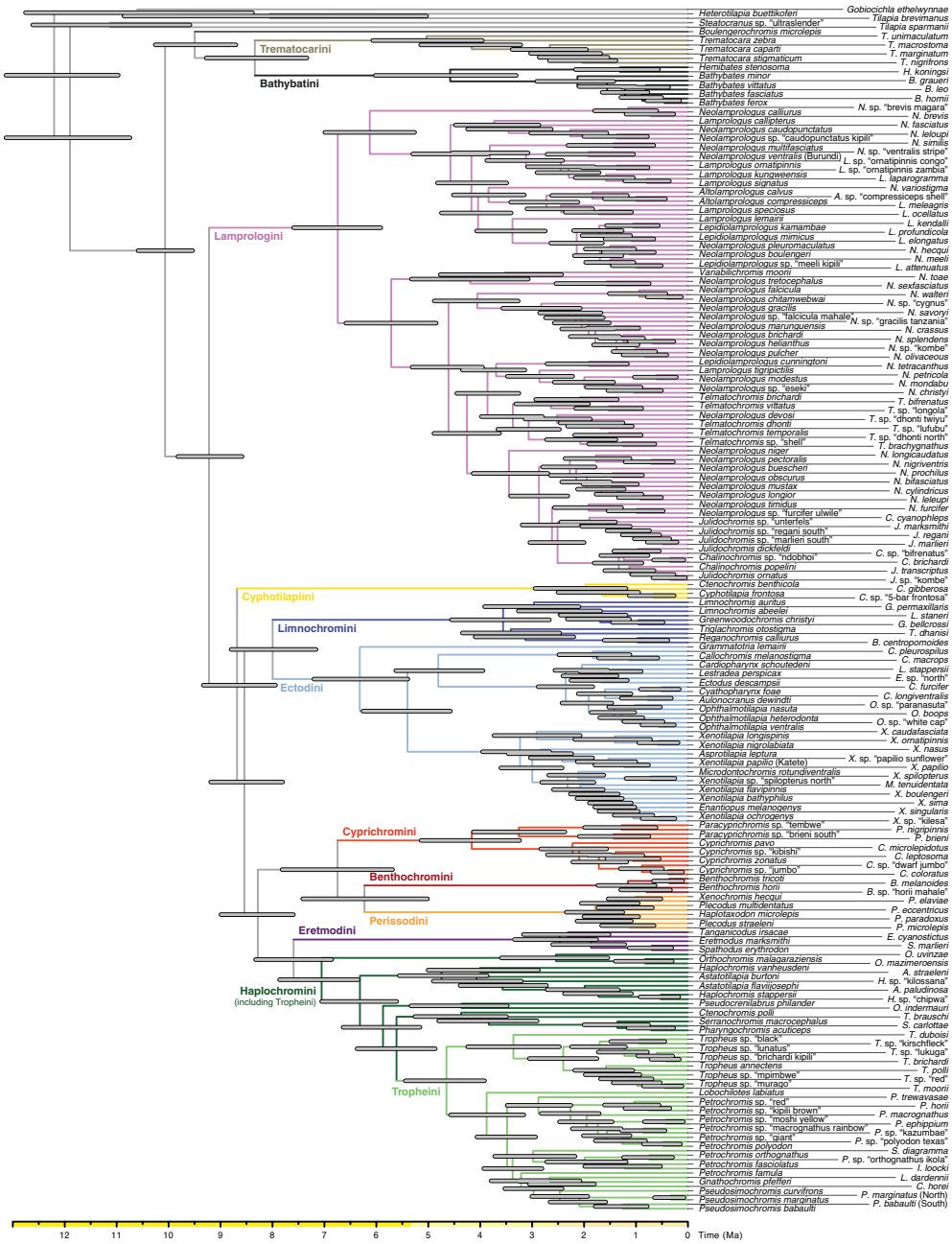

Extended Data Fig. 3 | Alternative time-calibrated species tree of the cichlid adaptive radiation in Lake Tanganyika. The species tree is based on the topology estimated with ASTRAL and was time-calibrated using a relaxed-clock model in BEAST2, applied to a selected set of alignments.

Article

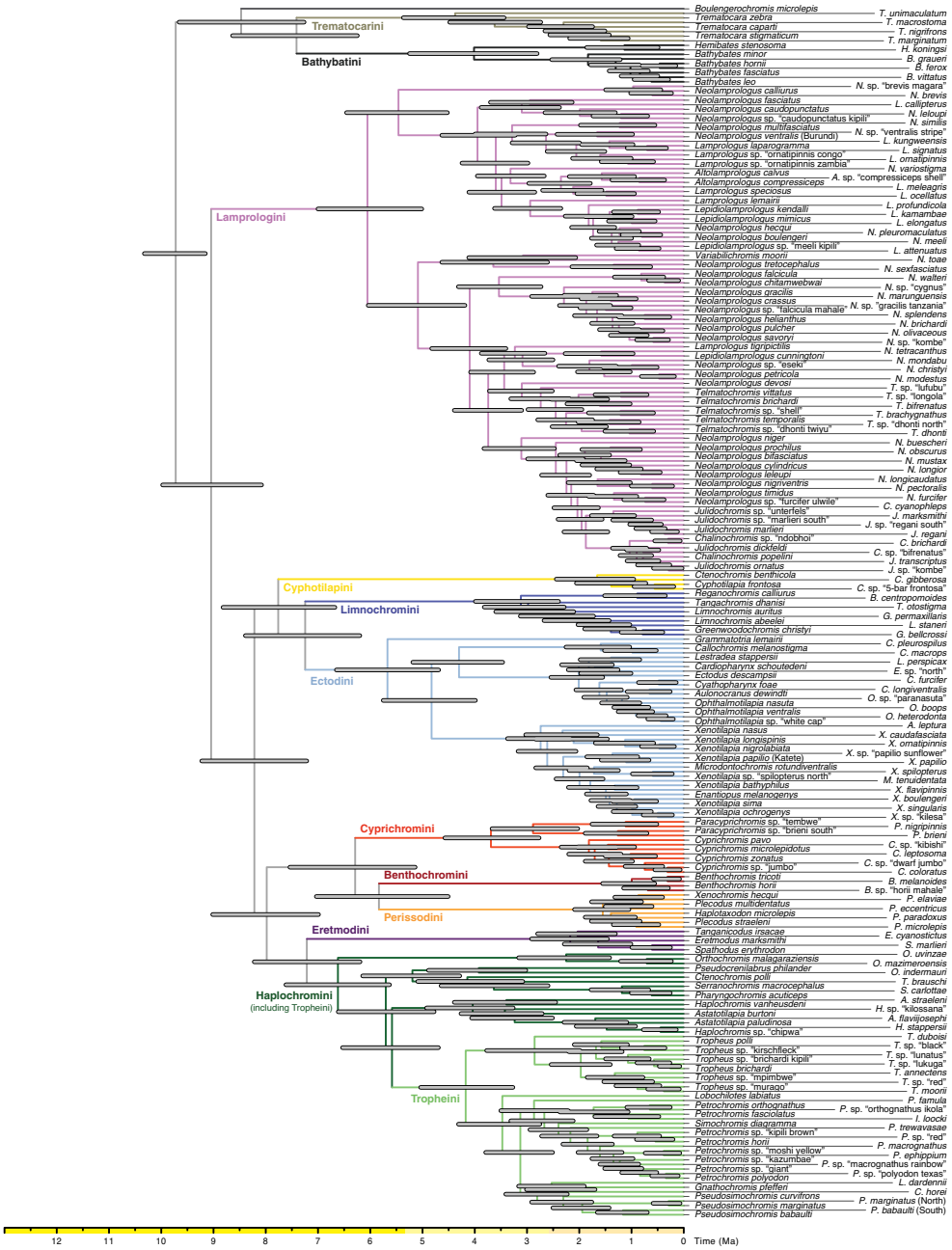

Extended Data Fig. 4 | Alternative time-calibrated species tree of the cichlid adaptive radiation in Lake Tanganyika. The species tree is based on the topology estimated with SNAPP and was time-calibrated using a relaxed-clock model in BEAST2, applied to a selected set of alignments.

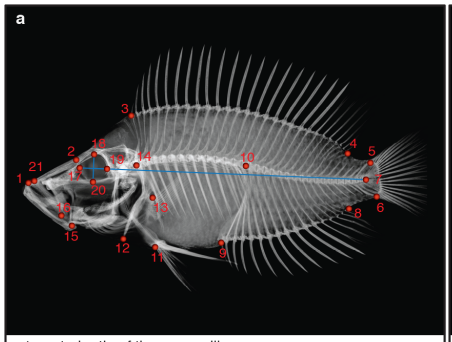

1 anterior tip of the premaxilla
2 dorsal tip of the premaxilla
3 basis of the first dorsal fin spine
4 basis of the last dorsal fin ray
5 tip of the last neural spine (branching off the pre-ural centre 3; marking the dorsal basis of the caudal fin)
6 tip of the last haemal spine (branching off the pre-ural centre 3; marking the ventral basis of the caudal fin)
7 centre of the last caudal vertebra (urostyle)
8 basis of the last anal fin ray
9 basis of the first anal fin spine
10 centre of the first caudal vertebra
11 basis of the pelvic fin spine
12 ventral tip of the cleithrum
13 basis of the first (dorsal) pectoral fin ray
14 centre of the first abdominal vertebra
15 joint of the articular and the quadrate
16 lateral end of the premaxilla
17 anterior margin of the eye
18 dorsal margin of the eye
19 posterior margin of the eye
20 ventral margin of the eye
21 angular point on the anterior ridge of the premaxilla

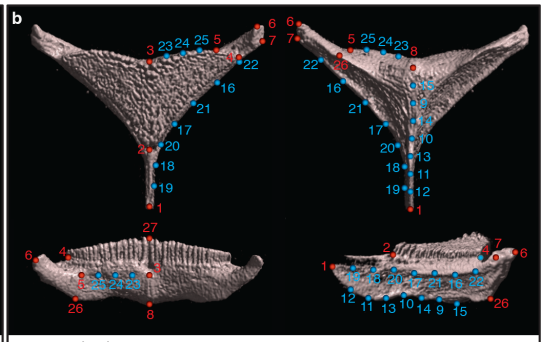

1 anterior tip
2 end of dentition anterior
3 dorsal-posterior centre (~base of first tooth)
4 end of dentition left posterior towards horn
5 angular point centre-to-horn
6 left horn tip sagittal
7 left horn tip lateral
8 ventral-posterior centre
9 ventral sagittal line posterior
10 ventral sagittal line centre
11 ventral sagittal line anterior
12 ventral sagittal line centre in most anterior segment
13 ventral sagittal line centre in centre-anterior segment
14 ventral sagittal line centre in centre-posterior segment
15 ventral sagittal line centre in most posterior segment
16 lateral left line posterior
17 lateral left line centre
18 lateral left line anterior
19 lateral left line centre in most anterior segment
20 lateral left line centre in centre-anterior segment
21 lateral left line centre in centre-posterior segment
22 lateral left line centre in most posterior segment
23 posterior line sagittal
24 posterior line center
25 posterior line lateral
26 angular point ventral-horn-ridge
27 tooth height posterior sagittal

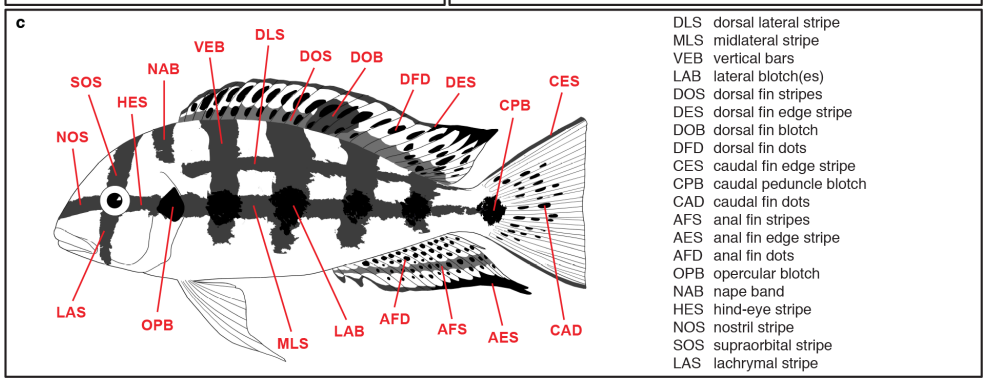

DLS dorsal lateral stripe
MLS midlateral stripe
VEB vertical bars
LAB lateral blotch(es)
DOS dorsal fin stripes
DES dorsal fin edge stripe
DOB dorsal fin blotch
DFD dorsal fin dots
CES caudal fin edge stripe
CPB caudal peduncle blotch
CAD caudal fin dots
AFS anal fin stripes
AES anal fin edge stripe
AFD anal fin dots
OPB opercular blotch
NAB nape band
HES hind-eye stripe
NOS nostril stripe
SOS supraorbital stripe
LAS lachrymal stripe

Extended Data Fig. 5 | Phenotyping of the specimens. a, Two-dimensional landmarks placed on X-ray images of the specimens. To quantify overall body shape we excluded landmark 16 (to minimise the effect of the orientation of the oral jaw). To analyse upper oral jaw morphology we used landmarks 1, 2, 16 and 21. **b**, Three-dimensional landmarks used to analyse lower pharyngeal jaw shape on µCT scans of the heads. True landmarks are indicated in red, sliding semi-landmarks are indicated in blue. **c**, Body regions scored for presence/absence of pigmentation patterns.

Article

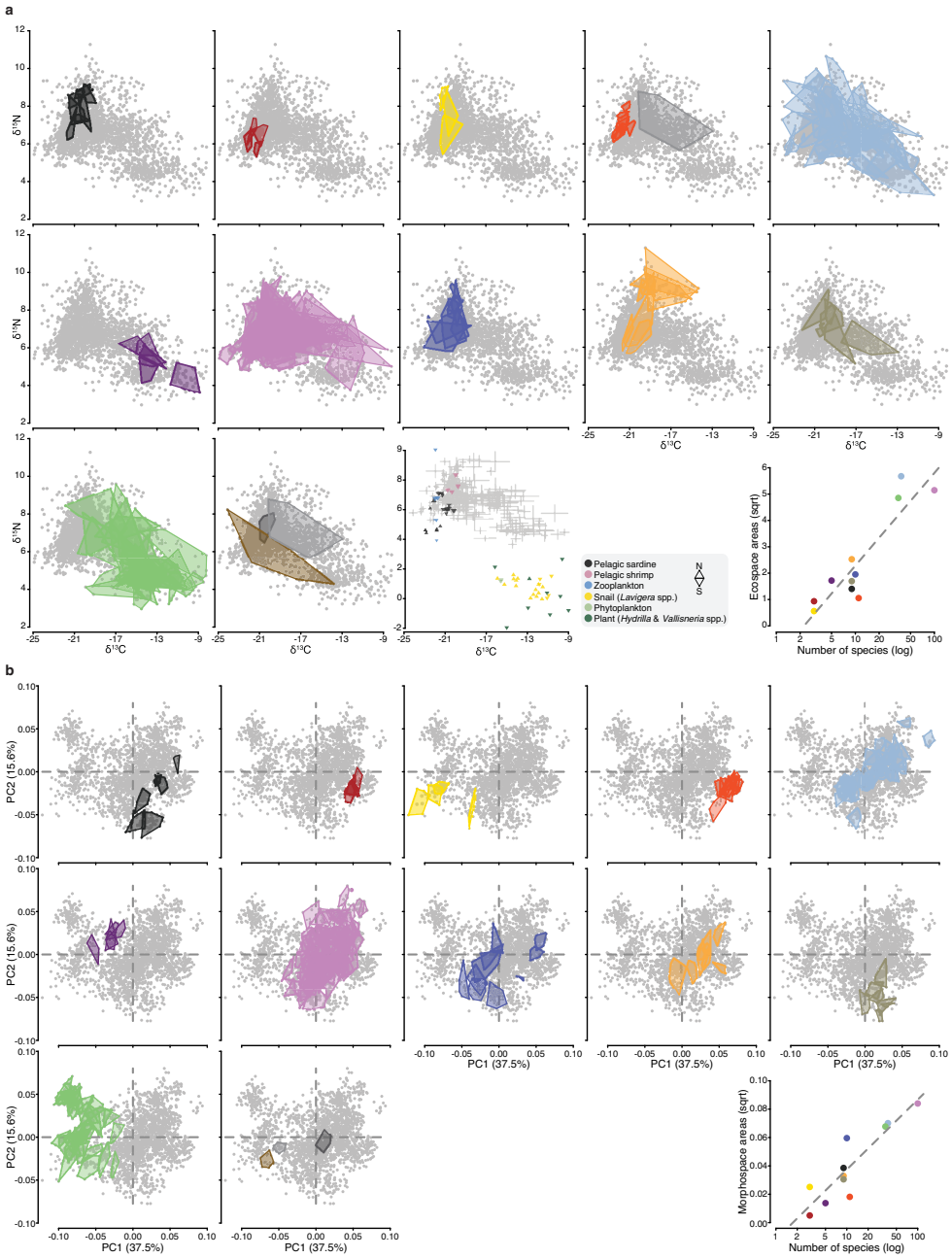

Extended Data Fig. 6 | Ecospace and morphospace occupation of the cichlid adaptive radiation in Lake Tanganyika. Scatter plots for each focal tribe (indicated with colours, see Fig. 1 for colour key) against the total eco-and morphospace (grey). Species ranges are indicated with convex hulls. **a**, Stable N and C isotope compositions ($\delta^{15}N$ and $\delta^{13}C$ values). The additional plot shows $\delta^{15}N$ and $\delta^{13}C$ values of a baseline dataset which confirms the interpretability of the stable N and C isotope composition in Lake Tanganyika (see Supplementary Methods and Discussion). **b**, PC1 and PC2 of body shape (for shape changes associated with the PC axes see Fig. 2). The last plot for each trait shows the size of the traitspace per tribe in relation to species numbers (stable isotopes: Pearson's $r = 0.88$, d.f. = 9, $P = 0.0004$; body shape: Pearson's $r = 0.91$, d.f. = 9, $P = 0.0001$). Traitspace size was calculated as the square root of the convex hull area spanned by species means.

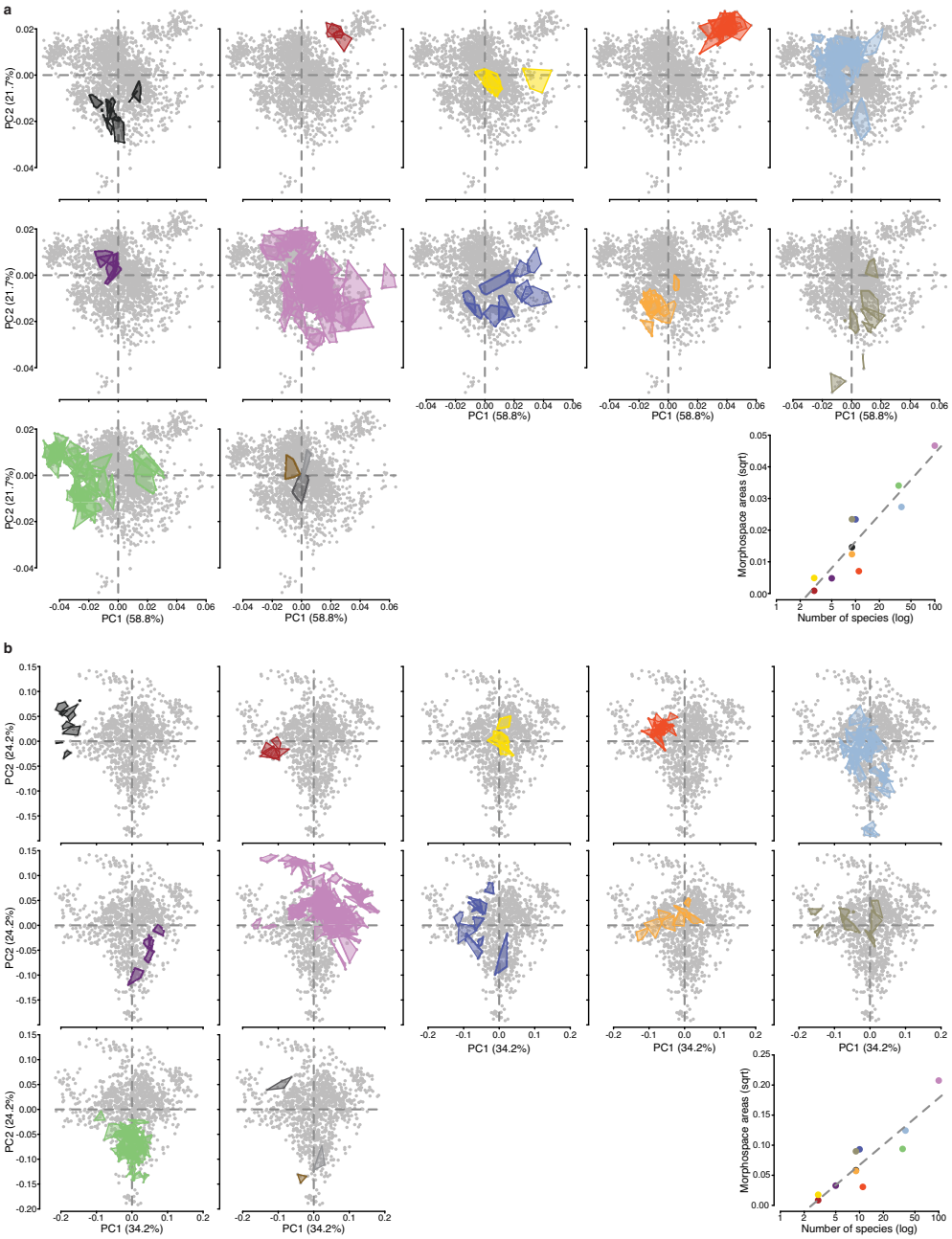

Extended Data Fig. 7 | Morphospace occupation of the cichlid adaptive radiation in Lake Tanganyika. a, **b**, Scatter plots of PC1 and PC2 for upper oral jaw morphology (**a**) and lower pharyngeal jaw shape per tribe (**b**) (indicated with colours, see Fig. 1 for colour key) against the total morphospace (grey). Species ranges are indicated with convex hulls. For shape changes associated with the respective PC-axis see Fig. 2. The last plot for each trait shows the size of the morphospace per tribe in relation to species numbers (upper oral jaw morphology: Pearson's $r = 0.88$, d.f. = 9, $P = 0.0003$; lower pharyngeal jaw shape: Pearson's $r = 0.83$, d.f. = 9, $P = 0.0017$). Morphospace size was calculated as the square root of the convex hull area spanned by species means.

Article

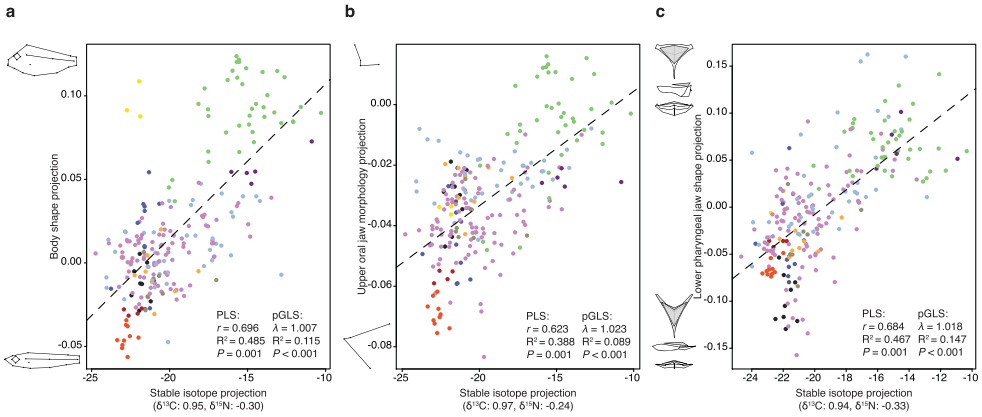

d

Tree topology	Trait	Model comparison log-likelihood difference (AIC difference)					Phylogenetic signal	
		White noise	Brownian motion	Ornstein-Uhlenbeck	Early burst	Variable rates	λ	K
Maximum-likelihood (RAxML)	Body shape	256 (477)	21 (8)	21 (10)	16 (**0**)	**0** (22)	*1.01*	*2.14*
	Upper oral jaw morphology	228 (390)	53 (40)	53 (42)	49 (35)	**0** (**0**)	*1.02*	*1.34*
	Lower pharyngeal jaw shape	193 (330)	44 (32)	44 (34)	44 (34)	**0** (**0**)	*1.02*	*1.13*
	Pigmentation pattern	101 (146)	53 (49)	45 (36)	53 (51)	**0** (**0**)	*0.94*	*0.44*
Multi-species coalescent (ASTRAL)	Body shape	258 (483)	23 (11)	23 (13)	16 (**0**)	**0** (21)	*1.02*	*2.28*
	Upper oral jaw morphology	228 (390)	54 (41)	54 (43)	50 (36)	**0** (**0**)	*1.03*	*1.42*
	Lower pharyngeal jaw shape	191 (325)	46 (35)	46 (37)	46 (37)	**0** (**0**)	*1.03*	*1.14*
	Pigmentation pattern	99 (143)	49 (43)	42 (32)	49 (45)	**0** (**0**)	*0.94*	*0.47*
Multi-species coalescent (SNAPP)	Body shape	259 (487)	19 (9)	19 (11)	14 (**0**)	**0** (25)	*1.01*	*2.12*
	Upper oral jaw morphology	225 (386)	48 (31)	48 (33)	44 (26)	**0** (**0**)	*1.02*	*1.32*
	Lower pharyngeal jaw shape	190 (324)	42 (28)	42 (30)	42 (30)	**0** (**0**)	*1.02*	*1.04*
	Pigmentation pattern	101 (147)	50 (44)	43 (32)	50 (46)	**0** (**0**)	*0.94*	*0.43*

e

Tree topology	Trait	Model comparison (AIC difference)					Phylogenetic signal		
		White noise	Brownian motion	Ornstein-Uhlenbeck	Early burst	Variable rates	λ	K	Root age
Maximum-likelihood (RAxML)	Body shape	453-486	2-11	4-13	**0**	5-30	*1-1*	*1.8-2.3*	8.8 - 10.4
	Upper oral jaw morphology	373-398	23-54	25-56	20-55	**0**	*1-1*	*1.1-1.5*	
	Lower pharyngeal jaw shape	319-337	14-65	16-63	16-67	**0**	*0.9-1*	*0.9-1.2*	
	Pigmentation pattern	133-158	37-85	27-59	39-87	**0**	*0.9-1*	*0.3-0.5*	
Multi-species coalescent (ASTRAL)	Body shape	461-494	4-13	6-15	**0**	10-28	*1-1*	*2-2.4*	9.4 - 10.9
	Upper oral jaw morphology	377-397	24-53	26-55	19-52	**0**	*1-1*	*1.2-1.5*	
	Lower pharyngeal jaw shape	316-330	13-60	15-60	15-62	**0**	*1-1*	*0.9-1.3*	
	Pigmentation pattern	130-149	30-83	24-54	32-85	**0**	*0.9-1*	*0.3-0.5*	
Multi-species coalescent (SNAPP)	Body shape	467-498	3-10	5-12	**0**	13-35	*1-1*	*1.9-2.2*	9.0 - 10.5
	Upper oral jaw morphology	371-392	14-43	16-45	10-43	**0**	*1-1*	*1.1-1.4*	
	Lower pharyngeal jaw shape	316-330	10-64	12-61	12-66	**0**	*1-1*	*0.8-1.1*	
	Pigmentation pattern	136-154	35-119	24-71	37-121	**0**	*0.9-1*	*0.3-0.5*	

Extended Data Fig. 8 | PLS fit for each multivariate trait against the stable N and C isotope compositions ($\delta^{15}N$ and $\delta^{13}C$ values) and models of trait evolution. a–**c**, PLS fits for body shape (**a**), upper oral jaw morphology (**b**) and lower pharyngeal jaw shape (**c**). Associated shape changes and loadings of the respective stable isotope projection are indicated next to the axes. Data points represent species means and are coloured according to tribe. **d**, Comparison of model fits for different models of trait evolution and phylogenetic signal for each trait complex using three time-calibrated species trees with alternative topologies. **e**, Overview of the model fits and phylogenetic signal inferred using 100 trees sampled from the posterior distributions of the time calibrations for each of the three alternative tree topologies.

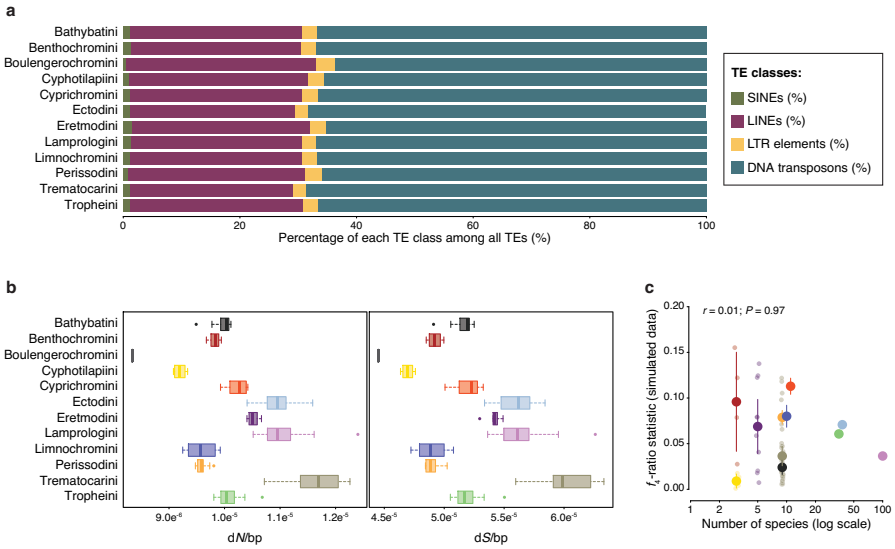

Extended Data Fig. 9 | Genome-wide statistical analyses. a, Proportion of the different classes of transposable elements (TE) among all TE for each tribe (one genome per species, $n = 245$). **b**, Species means of d*N* (left) and d*S* (right) values over alignment length for each tribe ($n = 243$ taxa, 471 genomes). The boxes' centre lines show median, box limits show first and third quartiles, and whiskers show the 1.5 × interquartile ranges. **c**, f_4-ratio statistics among species within each tribe in simulated data (tribe means are based on the mean across 20 simulations of each species triplet). Data points are coloured according to tribes; large points are tribe means shown with 95% confidence intervals, small points represent species means and are only shown for group sizes <40 species. To test for a correlation with species richness per tribe (log-transformed), we calculated phylogenetic independent contrasts for each variable and inferred Pearson's *r* through the origin.

Article

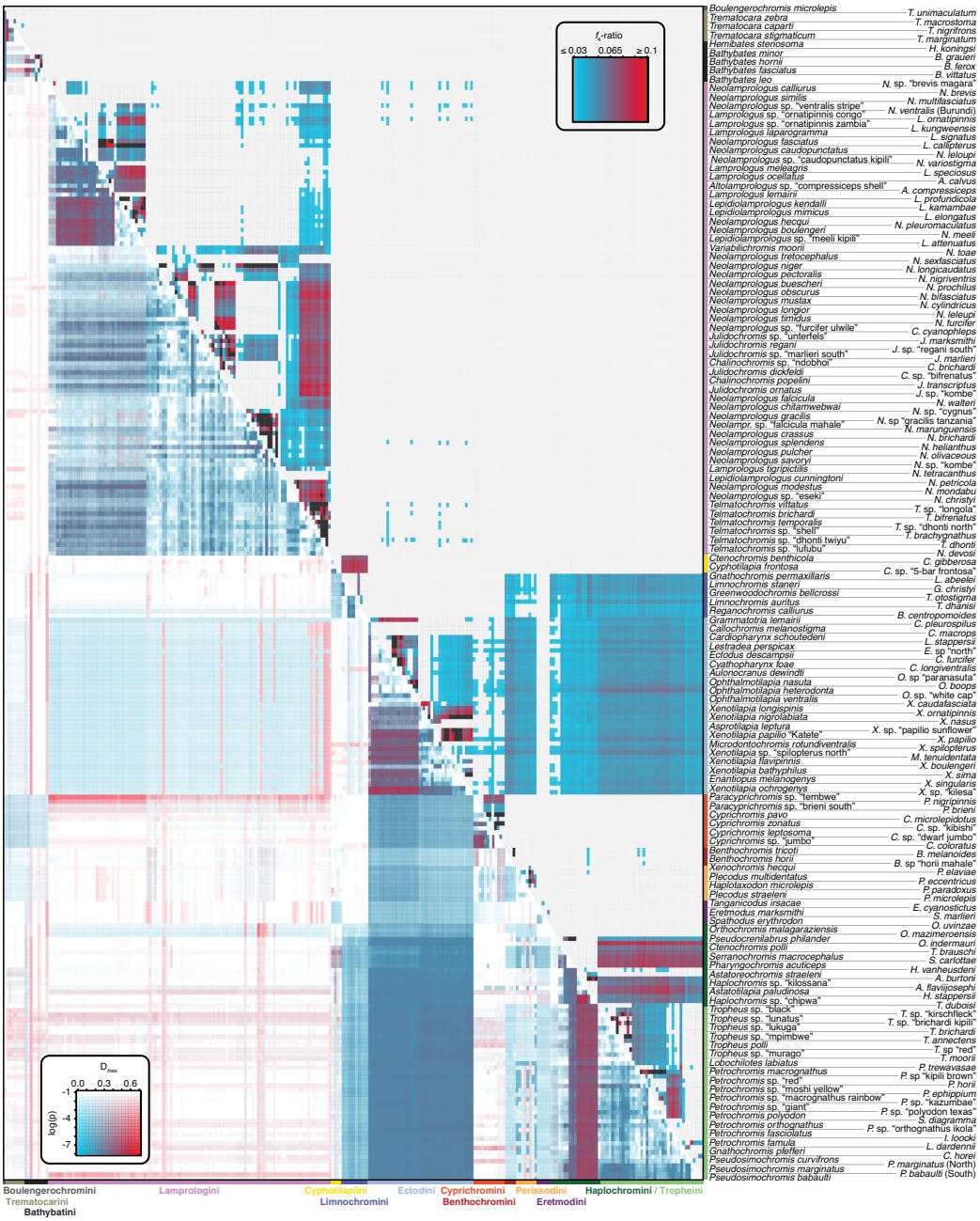

Extended Data Fig. 10 | Signals of introgression among Lake Tanganyika cichlid species. Upper matrix: maximum values of the f_4-ratio statistics between all pairs of species, derived from calculations across all combinations of species trios with *T. sparrmanii* fixed as the outgroup. The f_4-ratio estimates the proportion of the genome affected by gene flow, all presented values are statistically significant (one-sided block-jackknife tests: $P < 5 \times 10^{-5}$ after Benjamini–Hochberg correction for multiple testing). Lower matrix: D_{tree}-statistics (hue) with corresponding *P*-value (two-tailed binomial test, not adjusted for multiple testing; log-transformed; saturation) based on a phylogenetic approach testing for asymmetry in the relationships of species trios in 1,272 local maximum-likelihood trees (see Supplementary Methods). The two different approaches uncovered little gene flow among the tribes (see Supplementary Discussion).

Chapter 2 | Supplementary information

nature research

https://doi.org/10.1038/s41586-020-2930-4

Supplementary information

Drivers and dynamics of a massive adaptive radiation in cichlid fishes

1. Supplementary Methods

Sampling

Sampling at Lake Tanganyika was conducted during a total of ca. nine months of fieldwork between 2014 and 2017 at 130 locations in the Republic of Burundi, the Republic of Zambia, and the United Republic of Tanzania. Fishes were either caught with barrier nets while snorkelling or Scuba diving, or purchased from local fishermen. After euthanasia with clove oil, each specimen was photographed using Nikon D5000 digital cameras (Nikon Corporation, Tokyo, Japan) and a fin clip was taken and preserved in 100% ethanol for later DNA extraction. For initial fixation of the specimens, we used 10-20% formalin (depending on the size of the fish). To fix the specimens in a standardized way, we placed the fish with their right body side facing down in a plane plastic container. The body was straightened and fins were erected while covering the specimen with formalin-soaked paper towels. To ensure adequate fixation, we additionally injected formalin into the body cavity. Once specimens were fully fixed (usually after 4 days) they were rinsed and placed in water (overnight), and transferred for long-term storage into 70% ethanol. All specimens were integrated into the *Ichthyological collection on Tanganyikan cichlids of the University of Basel* (https://www.unibas.ch/de/Universitaet/Administration-Services/Generalsekretariat/Archive-Sammlungen/Wissenschaftliche-Sammlungen/Alphabetisch-sortiert/Buntbarsch-Sammlung.html).

To maximize taxon sampling, we included additional specimens from previous expeditions (4.9% of the samples) as well as from other collections (0.8%). The final dataset (301 taxa; n = 2,723 specimens) contained an almost complete taxon sampling of the cichlid fauna of Lake Tanganyika including 201 of the 208 formally described species (96.6%; note that five of the missing species have never been found since description or their species status is under discussion[15]) and all undescribed species which have been reported in a recent species inventory for Lake Tanganyika cichlids[15]. Further, we included 18 representative cichlid species from nearby waterbodies and 32 outgroup species. These additional taxa were used for phylogenetic analysis only except for *Oreochromis tanganicae* and *Tylochromis polylepis*, which occur in Lake Tanganyika and were thus included in the overall characterisation of morphospace and ecospace (PCA, Fig. 2). All analyses described below are based on the same set of typically 10 preserved specimens per species, or subsets thereof (see Supplementary Table 1; a full list of individual specimen vouchers including details on sampling location is provided as Supplementary Table 2).

Whole genome sequencing

Genomic DNA of typically one male and one female specimen per species (n = 547) was extracted from fin-clips preserved in ethanol using the E.Z.N.A. Tissue DNA Kit (Omega Bio-Tek) and sheared on a Covaris E220 (60 µl with 10% duty factor, 175 W, 200 cycles for 65 sec). Individual libraries were prepared using Illumina's TruSeq DNA PCR-Free Sample Preparation kit (Low Sample Protocol) for 350 bp insert size, pooled (six libraries per lane), and sequenced at 126 bp paired-end on an Illumina HiSeq 2500 (see Supplementary Table 1 for information on read depths).

Assessing genomic variation

To obtain a dataset of genome-wide SNPs for all species of the cichlid radiation of Lake Tanganyika, species nested within the radiation, as well as selected closely-related outgroup species (*n* = 528; see Supplementary Table 1 for a species list and read depth), we trimmed adapters with Trimmomatic[35] (v.0.36), mapped the reads against the Nile tilapia reference genome (*Oreochromis niloticus;* RefSeq accession GCF_001858045.1[36]), and performed variant calling.

Details on mapping, variant calling, and filtering. We customised the Nile tilapia reference genome by concatenating lexicographically all unplaced scaffolds into an 'UNPLACED' super chromosome. After mapping with BWA-MEM[37] (v.0.7.12), duplicate reads were marked with Picard-tools (http://broadinstitute.github.io/picard/; v.2.7.1), indels were realigned with GATK[38] (v.3.6), and the final alignment files in BAM format were indexed with SAMtools[82] (v.1.3.1). The per-individual read coverage distribution was determined with BEDtools[83] (v.2.21.0), and variant calling was performed with GATK's HaplotypeCaller and GenotypeGVCF tools[38] (v.3.7), applying a minimum base quality score of 30.

Variant calls were filtered according to a strict pipeline to ensure high call reliability. Sites were excluded with BCFtools[39] (v.1.6) if the Phred-scaled *P*-value of Fisher's exact test for strand bias was greater than 20, if the quality score normalised by read depth was below 2, if the root mean square mapping quality was below 20, or if the overall read depth across all 528 samples was either below 4,000 or above 8,000. Sites were further excluded if the Mann-Whitney-Wilcoxon rank sum test produced a test statistic below -0.5 for either site position bias within reads or mapping quality bias between reference and alternative alleles. Indels were normalised with BCFtools. As the dataset contained a large number of indels, we did not remove all SNPs within a fixed distance to indels. Instead, we applied a filter to sites in proximity to indels with a minor allele count greater than 2, depending on the size of the indel: For indels with a size of 5 bp or larger, we excluded sites within 10 bp of the indel, but sites were only excluded within 5, 3, or 2 bp if the indel size was 3-4, 2, or 1 bp, respectively. To reduce the number of indels in the dataset we also excluded nine of the outgroup species (specimen vouchers: Z03, Z07, Z09, Z17, JAB6, JAC7, KYH4, JWE6, and JWF2).

We further masked sites within regions of the Nile tilapia reference genome in which read mapping was likely to be ambiguous. To determine these regions, we used the SNPable pipeline (http://lh3lh3.users.sourceforge.net/snpable.shtml). The approach implemented in this tool divides the reference genome into overlapping fragments (in our case 100 bp fragments that overlapped by 99 bp) that are then mapped back to the reference, allowing a count of how many fragments map correctly at each site. Based on the results of this approach, we excluded all sites from regions in which less than 90 out of 100 fragments mapped back correctly. For each individual independently, we masked genotypes with a read depth below 4 or a genotype quality below 20 using VCFtools[40] (v.0.1.14). Finally, sites that were no longer polymorphic after the previous filtering steps were excluded, resulting in a dataset of 57,751,375 SNPs (VCF file available on Dryad; https://doi.org/10.5061/dryad.9w0vt4bbf). We additionally generated a more strictly filtered SNP dataset with all filtering steps as described above, but applying a minimum genotype quality of 30

instead of 20 and masking all sites of the Nile tilapia genome in which less than 95 of 100 fragments mapped back correctly. This more strictly filtered dataset included 54,048,145 SNPs.

Phasing. Called variants were phased with the software beagle[41] (v.4.1). Genotypes that had been missing or masked before the imputation step of phasing with beagle were masked again after the imputation. At this step we excluded one sample from a museum collection (specimen voucher: Bel33; *Trematocara variabile*) from further analysis, due to signs of contamination and/or DNA degradation.

Identification of first-generation hybrids

On the basis of the results of an initial application of *D* statistics[84] to the SNP dataset (see below) and the previous suggestion that *Neolamprologus cancellatus* is a hybrid species involving *Telmatochromis vittatus* as one parent[85], we analysed the genotypes of the two *N. cancellatus* specimens (specimen vouchers: LJC9 and LJD1) included in our dataset at sites that are fixed for alternative alleles in pairs of candidate parental species. We found that the two *N. cancellatus* specimens were heterozygous at 5,792 out of 5,912 sites (98%) that are fixed for alternative alleles in *T. vittatus* and *Neolamprologus fasciatus*, indicating that these two species – or lineages very closely related to them – are the parents of the two *N. cancellatus* specimens and that these two specimens represent first-generation (F1) inter-specific hybrids. As the mitochondrial genomes of the two *N. cancellatus* specimens cluster with those of the two *N. fasciatus* specimens (Supplementary Fig. 2), we further conclude that the mother of both was a *Neolamprologus* (most likely *N. fasciatus*) and the father a *Telmatochromis* (most likely *T. vittatus*), which is in agreement with field observations of male *T. vittatus* spawning at the opening of shells or cavities occupied by female *N. fasciatus*[86].

We then used this information to improve the genotype phasing for the *N. cancellatus* specimens, separating all heterozygous genotypes so that one of the two resulting haplotypes approximated the nucleotide sequence of *T. vittatus* and the other one that of *N. fasciatus*.

As the inclusion of F1 hybrids between two rather distantly related species can strongly influence phylogenetic inference, we consequently excluded *N. cancellatus* from all phylogenetic analyses at the species levels (species-tree inference and all subsequent phylogenetic comparative analyses). For individual-based phylogenetic inference we used separately the phased haplotypes of *N. cancellatus* that were obtained as described above.

De novo genome assemblies

De novo genome assemblies were generated from the Illumina raw read data for each individual following an approach described previously[42,43] using CeleraAssembler[44] (v.8.3) and FLASH[45] (v.1.2.11). Eight genomes repeatedly failed to assemble and were therefore excluded from further assembly-based analyses (specimen vouchers: A188, IRF6, IZC5, JWE7, JWG1, JWG2, LJD3, and LJE8). Assembly quality was assessed with QUAST[46] (v.4.5) and completeness was determined with BUSCO[47] (v.3; -l actinopterygii_odb9, -sp zebrafish). Assembly statistics were summarised with MultiQC[48] (v.1.7). Summary statistics are available on Dryad; https://doi.org/10.5061/dryad.9w0vt4bbf: 04_genomeAssemblies_multiQC_busco.csv, 04_genomeAssemblies_multiQC_quast.csv.

Determining the age of the radiation

To determine the age of the radiation of cichlid fishes in Lake Tanganyika, we applied phylogenomic molecular-clock analyses for representatives of all cichlid subfamilies together with non-cichlid outgroups (in total 44 species, Extended Data Fig. 1).

Selection of nuclear markers for phylogenetic analyses. The selection of nuclear markers suitable for molecular-clock analyses followed the strategy described in Matschiner *et al.*[18] and was initially based on the annotated genomes of medaka (*Oryzias latipes*), midas cichlid (*Amphilophus citrinellus*), Nile tilapia (*O. niloticus*), lyretail cichlid (*Neolamprologus brichardi*), Burton's mouthbrooder (*Astatotilapia burtoni*), and zebra mbuna (*Metriaclima zebra*) in release 94 of the ENSEMBL database[87]. We identified 3,781 genes that each had no deletions or duplications among cichlids according to ENSEMBL's gene tree information and that were composed of at least three exons longer than 150 bp. In total, the 3,781 genes contained 22,251 exons with this minimum length. For each of these exons, we quantified the sequence similarity between medaka, which we used as an outgroup, and the six cichlid species by their pairwise TBLASTN[88] bitscores. Based on this quantification, we excluded all exons for which one or more of the pairwise bitscores between orthologs were below 50 or less than 20 units greater than the largest bitscores with other genomic regions (that is, potential paralogs). This ensured that true orthologs of the exons in the dataset are recognizable by their TBLASTN bitscores, a property that we exploited in the subsequent identification of orthologs from the newly assembled cichlid genome sequences. Finally, we excluded all exons if no more than one further exon of the same gene remained in the dataset, to allow tests of within-gene exon tree concordance in the subsequent ortholog identification. The resulting dataset contained 10,590 exons of 2,081 genes. For each of these exons, we retrieved the medaka amino-acid sequence together with the exon-specific TBLASTN bitscore value that we had determined as a threshold for recognition of potential orthologs from cichlid assemblies.

Selection of species for phylogenomic analyses. To enable reliable phylogenetic time calibrations based on multiple constraints on outgroup divergences, we included not just the most divergent cichlid lineages but also representatives of closely-related outgroups within Ovalentaria[89]. As in Matschiner *et al.*[18], we included the rock-pool blenny (*Parablennius parvicornis*) to represent the order Blenniiformes, medaka (*O. latipes*) to represent the order Beloniformes, and six representatives of the order Cypriniformes: mangrove rivulus (*Kryptolebias marmoratus*), sheepshead minnow (*Cyprinodon variegatus*), mummichog (*Fundulus heteroclitus*), turquoise killifish (*Nothobranchius furzeri*), Amazon molly (*Poecilia formosa*), and platyfish (*Xiphophorus maculatus*). The genome assemblies of the rock-pool blenny and turquoise killifish were taken from Malmstrøm *et al.*[90] and Reichwald *et al.*[91], respectively, all other genome assemblies were taken from ENSEMBL release 94. We further included 36 cichlid species representing all subfamilies, the most divergent lineages of African cichlids (subfamily Pseudocrenilabrinae), and four tribes of cichlids deriving from the earliest splits of the Tanganyikan cichlid radiation. The subfamilies Etroplinae, Ptychochrominae, and Cichlinae were represented by the same species as in Matschiner *et al.*[18]: *Etroplus canarensis*, *Ptychochromis oligocanthus*, *Paratilapia polleni* "Andapa", *Apistogramma diplotaenia*, *Andinoacara biseriatus*, *Bujurquina vittata*, *Andinoacara coeruleopunctatus*, *Amphilophus citrinellus*, *Amphilophus zaliosus*,

and *Australoheros scitulus*. As in Matschiner *et al.*[18], genome assemblies of *A. citrinellus* and *A. coeruleopunctatus* were taken from ENSEMBL release 94 and from the Cambridge Cichlid Browser (http://cichlid.gurdon.cam.ac.uk/Andinoacara_coeruleopunctatus_final_min1000bp_scaffolds.fa.gz), respectively; genome assemblies of the other eight species were generated by Matschiner *et al.*[18]. Within the subfamily Pseudocrenilabrinae, we included six members of the divergent West African cichlid tribes Heterochromini, Tylochromini, Chromidotilapiini, Hemichromini, and Etiini: *Heterochromis multidens*, *Tylochromis polylepis*, *Benitochromis conjunctus*, *Pelvicachromis taeniatus*, *Hemichromis elongatus*, and *Etia nguti*. The genome assemblies of these six species were taken from Matschiner *et al.*[18]. We further included *O. niloticus* as well as three additional representatives of the tribe Oreochromini: *O. tanganicae*, *O. malagarasi*, and *Sarotherodon lohbergeri*. Of these, the genome assembly of *O. niloticus* was taken from Conte *et al.*[92], while genome assemblies for the other three species were newly generated (specimen vouchers: JAB6, KYH4, and Z05, respectively). Eight more cichlid species from outside Lake Tanganyika were included, representing the tribes Tilapiini, Steatocranini, Gobiocichlini, Pelmatolapiini, Heterotilapiini, and Coptodonini: *Tilapia sparrmanii*, *Steatocranus* sp. "ultraslender", *Gobiocichla ethelwynae*, '*Tilapia' brevimanus*, *Pelmatolapia mariae*, *Heterotilapia buttikoferi*, *Coptodon bakossiorum*, and *Coptodon rendalli*. Genome assemblies of all these species were newly generated (specimen vouchers: JWF7, JWE8, JWE7, JWF9, JWF2, JWE3, JWE5, and JWE6, respectively). Finally, four tribes nested within the Tanganyikan cichlid radiation – Trematocarini, Ectodini, Lamprologini, and Haplochromini – were represented by *Trematocara marginatum*, *Trematocara nigrifrons*, *Asprotilapia leptura*, *Grammatotria lemairii*, *Neolamprologus variostigma*, *N. brichardi*, *Astatotilapia flaviijosephi*, and *Metriaclima zebra*. With the exception of *N. brichardi* and *M. zebra*, for which genome assemblies were taken from ENSEMBL release 94 and Conte *et al.*[92], respectively, the assemblies of these species were newly generated (specimen vouchers: ISA3, IUE5, INF2, JDD7, JWA5, and LJD2). The four tribes from Lake Tanganyika were selected so that their splits included the earliest divergence within the radiation (the separation of Trematocarini from the other three tribes) while avoiding tribes for which earlier studies had inferred signals of introgression (e.g. Boulengerochromini, Bathybatini, Perissodini, and Cyprichromini)[93]. The particular samples per tribe were selected based on their comparatively high read depth (see Supplementary Table 1) or isolated geographic distribution reducing the probability of hybridisation (specimen voucher: LJD2; *A. flaviijosephi* occurring in Jordan and Israel). In total, we used genome assemblies of 44 species to determine the age of the adaptive radiation of cichlid fishes in Lake Tanganyika.

Targeted assembly of potential orthologs. To improve the contiguity of potential ortholog sequences, we complemented the 17 newly generated genome assemblies used for divergence-time estimations with targeted assemblies using both Kollector[94] (v.1.0.1) and aTRAM[95] (v.2.0.alpha.5) as described in Matschiner *et al.*[18]. As targets, we used a set of 10,373 sequences from the Nile tilapia (*O. niloticus*) genome assembly[92], each of which was the most similar homolog to one of the 10,590 selected medaka exons (no sufficiently similar homologs could be identified for 217 exons). Details on these analyses are provided in Matschiner *et al.*[18]. Targeted assemblies were merged with the whole-genome assemblies of the same species prior to further analysis.

Compilation of ortholog sequences. The identification and filtering of ortholog sequences followed the workflow first established in Malmstrøm *et al.*[90] and further developed by Musilova *et al.*[96] and Matschiner *et al.*[18]. In brief, this workflow uses exon sequences of an outgroup query together with exon-specific bitscore thresholds to identify potential orthologs, which are further filtered by dN/dS ratios, proportion of missing data, alignment reliability, GC-content variation, genomic position, within-gene exon-tree discordance, and substitution-rate variation to select the most suitable orthologs for phylogenetic divergence-time estimation. Accordingly, we used the 10,590 selected medaka exon sequences as queries in TBLASTN searches to identify potential orthologs from the 44 genome assemblies listed above. Subject sequences were accepted as candidate orthologs if their bitscore was above the exon-specific threshold determined during marker selection; this was the case for a total of 448,364 sequences. Per exon, we generated alignments of nucleotide exon sequences with MAFFT[97] (v.7.300), guided by their amino-acid translation to ensure the integrity of codon triplets.

The 10,590 exon-sequence alignments were then subjected to the following filters to select the most suitable paralog-free alignments for the subsequent phylogenomic analyses:

1) Per exon, TBLASTN bitscores of all sequences were compared and those sequences with bitscores lower than 0.9 times the highest bitscore observed for any ingroup species were discarded. For exon sequences that evolve clock-like, true orthologs should all be similarly distant to outgroup sequences; thus, this filter is expected to remove sequences that are either paralogous or do not evolve in a clock-like fashion – two properties that both render the sequences unsuitable for divergence-time estimation.
2) In pairwise comparisons with the medaka exon sequences, dN/dS ratios were calculated for all ingroup sequences using *codeml* of the PAML package[78] (v.4.6) with runmode –2, and sequences with dN/dS ratios greater than 0.25 were excluded, as this could indicate positive selection on certain branches or sites, which would imply departures from clock-like evolution.
3) We excluded all exon-sequence alignments in which sequences were missing for more than 10 of the 44 species. This filter removed 2,504 alignments.
4) We used the software BMGE[98] (v.1.1) to assess local alignment reliability and removed codons if one or more sites of the codon had a proportion of missing data greater than 20% or a smoothed entropy-like score above 0.5.
5) We excluded exon alignments that had become shorter than 150 bp after the above filtering steps; this filter removed 206 of the remaining 8,086 alignments.
6) We quantified GC content per exon sequence and removed alignments with an among-sequence standard deviation in GC content greater than 0.04, as high GC-content variation has been shown to affect phylogenetic inference[99]. This filter removed 34 of the remaining 7,880 exon alignments.
7) To allow subsequent analyses of within-gene exon-tree discordance, we retained only those exons for which at least two more exons assigned to the same gene and located within 100,000 bp of each other on the same medaka chromosome remained in the dataset. This requirement removed 1,332 of the remaining 7,846 exon alignments.
8) We tested for within-gene exon-tree discordance with the software Concaterpillar[100] (v.1.7.2). Although our phylogenetic analyses of cichlid divergence times did allow for among-gene tree

discordance, we conservatively assumed that within-gene exon-tree discordance was more likely the result of paralogy than of within-gene recombination (due to incomplete lineage sorting, see below). If at least three exons of a gene had trees that were concordant with each other, these were concatenated into gene alignments; all other exon alignments were discarded. After applying this filter, 1,293 genes with a total of 6,076 exons remained in the dataset.

9) To characterize how fast and clock-like genes evolve, we estimated the mean and the standard deviation of the substitution rate across species for each gene, using the Bayesian software BEAST 2[50] (v.2.5.0) with an uncorrelated lognormal (UCLN) relaxed molecular clock model[101] and the bModelTest add-on package[102] (v.1.1.2) to average over substitution models. Each analysis was set to run for 10 million Markov chain Monte Carlo (MCMC) iterations. This produced effective sample sizes (ESS) for all parameters of at least 200 for 1,121 of the 1,293 genes and ESS values of at least 100 for all parameters for all but 80 genes.
10) Gene alignments were inspected visually for potential homology errors[103] and five alignments were excluded due to possible misalignment.
11) Finally, the remaining 1,288 gene alignments were filtered in a 'strict' and 'permissive' way to select genes with low substitution rates (reducing the probability of homoplasies), comparatively clock-like evolution, and a strong and consistent phylogenetic signal. This selection was thus based on threshold values for the estimated substitution rate, the estimated coefficient of rate variation, and the minimum ESS value resulting from the analysis (as inconsistent phylogenetic signal within a gene, potentially resulting from misalignment or paralogy, can lead to low ESS values). In the 'strict' selection of genes, we required a substitution-rate estimate below 0.0015 per site and million year, a coefficient of rate variation below 0.4, and a minimum ESS value of at least 200. In contrast, our 'permissive' selection of genes allowed substitution-rate estimates up to 0.002 per site and million year, coefficients of rate variation up to 0.6, and minimum ESS values of at least 100.

The resulting 'strict' and 'permissive' datasets contained 510 and 1,161 genes and had total alignment lengths of 542,922 and 1,353,747 bp, respectively. For subsequent analyses, we generated maximum-clade-credibility consensus trees with node heights set to mean age estimates for each gene from the posterior tree distributions estimated with BEAST 2, using the program TreeAnnotator (v.2.5.0), which is part of the BEAST 2 package[50].

Species-tree inference. As a first test of the among-species relationships supported by our datasets, we performed species-tree analyses with the multi-species coalescent model implemented in the program ASTRAL[49] (v.5.6.3), separately for the 'strict' and 'permissive' sets of maximum-clade-credibility consensus gene trees. Both sets of gene trees supported exactly the same species-tree topology that fully agreed with the monophyly of all ingroup and outgroup genera, tribes, subfamilies, families, suborders, and orders, as well as the previously established sequence of tribal divergence events within Neotropical and African cichlids[22,104]. Moreover, the species trees received very high support, with posterior probabilities of 100% for all but one node. The exception was the monophyly of the outgroup species *C. variegatus* and *F. heteroclitus*, which received 56% posterior probability with the 'strict' set of gene trees and 76% with the 'permissive' set of trees.

To verify that homoplasies did not affect the reliability of our inferred species trees, we also reconstructed species relationships based on indels as markers with low frequency of homoplasies[99]. We identified indels from exon alignments of all genes in the 'strict' and 'permissive' datasets, using the versions of the exon alignments generated by step 1) of the above-described filtering sequence as some of the filtering steps would have removed indels. We only recorded non-overlapping indels that did not change the exon's reading frame and excluded those indels for which the presence or absence could not be determined in more than five species due to missing sequences. The matrices resulting from the 'strict' and 'permissive' datasets included presence or absence for 654 and 2,253 indels, respectively, of which 191 and 707 indels were parsimony-informative. We used PAUP*[105] (v.4.0a164) to reconstruct maximum-parsimony trees for the 'strict' and 'permissive' indel matrices, which had parsimony scores of 715 and 2,467, respectively. The consensus trees for the 'strict' and 'permissive' indel matrices contained 24 and 35 bifurcating nodes that were all fully concordant with the species trees inferred with the multi-species coalescent model, except for the position of *C. variegatus*, which appeared more closely related to *P. formosa* and *X. maculatus* than to *F. heteroclitus* in the maximum-parsimony trees.

Identification of species with signals of past introgression. As undetected past introgression can influence divergence-time estimates in molecular clock analyses, we tested for signals of introgression among the species in our dataset in the form of asymmetric species relationship in exon or gene trees. For each trio of species A, B, and C, one of the three possible pairs A,B, A,C, or B,C forms a sister group in the true species tree. In the absence of introgression, the multi-species coalescent model predicts this pair to have the highest frequency in a set of local phylogenies and the other two pairs to have frequencies that are similar and reflect the amount of incomplete lineage sorting (ILS). Thus, significant differences in the frequencies of the two alternative pairs can be taken as indication that introgression may have occurred; however, those differences can also arise from other model violations[106]. We tested exhaustively for significant differences between the second-highest and third-highest pair frequencies in all possible trios among the 44 species in our dataset, and then investigated specific signals of introgression further, based on genealogy interrogation[107,108]. We performed these analyses separately for four sets of trees generated with the program IQ-TREE[53] (v.1.6.8) for all gene alignments from both the 'strict' and 'permissive' sets of markers, and for sets of the exon alignments that had been concatenated for the 'strict' and 'permissive' gene alignments. Maximum-likelihood tree inference with IQ-TREE employed the program's standard model selection and two search repetitions per analysis. In agreement with recent phylogenomic studies of teleosts[18,90,96,109], we specified the blenniiform *P. parvicornis* as the outgroup to all other species, except for markers where the *P. parvicornis* sequence was missing; in those cases, all members of Cyprinodontiformes and Beloniformes were used as the outgroup. For each generated tree, we converted nodes separated by branches shorter than 0.001 substitutions per site into polytomies with the function *di2multi* of the R package ape[57] (v.5.2). The resulting tree sets were then queried for the relationships of each possible species trio, and we quantified support for introgression in the tree by applying a statistic that we call D_{tree} to highlight that the statistic is in principle related to Patterson's D statistic[84,110], only that pairs of tips are counted in sets of trees instead of shared alleles along the genome: $D_{tree} = (f_{2nd} - f_{3rd}) / (f_{2nd} +$

f_{3rd}), where f_{2nd} is the frequency of the second-most frequent pairing of two of the three species in the tree set, and f_{3rd} is the frequency of the third-most frequent (i.e. the least frequent) pairing of two species. High values of D_{tree} support introgression between the two species involved in the pair with the second-highest frequency. For example, if species A and B are found as a pair in 900 trees, species A and C form a pair in 80 trees and B and C form a pair in 20 trees, then $f_{2nd} = 80$, $f_{3rd} = 20$, and $D_{tree} = (80 - 20) / (80 + 20) = 0.6$, supporting introgression between species A and C. The significance of the difference between f_{2nd} and f_{3rd} is calculated using a one-sided binomial test. Trees in which the three species form a polytomy are ignored.

The analyses based on the 'strict' and 'permissive' tree sets generally produced the same patterns of D_{tree} variation among trios, but as expected, those based on the larger 'permissive' tree sets were statistically more significant. From the combination of our D_{tree} analyses, we formed nine hypotheses of introgression that we then investigated further with genealogy interrogation[107,108]:

1) Introgression between *H. multidens* and members of the Neotropical cichlid subfamily Cichlinae; supported e.g. by $D_{tree} = 0.19$ ($P < 10^{-6}$) for the species trio *G. ethelwynae*, *H. multidens*, and *A. zaliosus* in the 'strict' set of exon trees.
2) Introgression between *F. heteroclitus* and Poecilidae, supported e.g. by $D_{tree} = 0.25$ ($P < 10^{-4}$) for the species trio *C. variegatus*, *F. heteroclitus*, and *X. maculatus* in the 'strict' set of gene trees or $D_{tree} = 0.10$ ($P < 10^{-8}$) for the same trio in the 'permissive' set of exon trees.
3) Introgression between the Malagasy cichlid subfamily Ptychochrominae and the African subfamily Pseudocrenilabrinae, supported e.g. by $D_{tree} = 0.42$ ($P < 10^{-8}$) for the species trio *G. ethelwynae*, *H. multidens*, and *P. oligocanthus* in the 'strict' set of exon trees.
4) Introgression between the Neotropical cichlid subfamily Cichlinae and the Indian subfamily Etroplinae or the Malagasy subfamily Ptychochrominae, supported e.g. by $D_{tree} = 0.18$ ($P < 10^{-4}$) for the species trio *G. ethelwynae*, *A. coeruleopunctatus*, and *E. canarensis* in the 'strict' set of exons.
5) Introgression between '*T.*' *brevimanus* and *P. mariae*, supported e.g. by $D_{tree} = 0.33$ ($P < 10^{-8}$) for the species trio *H. buttikoferi*, '*T.*' *brevimanus*, and *P. mariae* in the 'permissive' set of gene trees.
6) Introgression between *G. ethelwynae* and *P. mariae*, supported e.g. by $D_{tree} = 0.25$ ($P < 10^{-5}$) for the species trio *H. buttikoferi*, *P. mariae*, and *G. ethelwynae* in the 'permissive' set of gene trees.
7) Introgression between the cichlid tribe Coptodonini and a clade formed by *T. sparrmanii*, *Steatocranus* sp. "ultraslender", and all members of the Lake Tanganyika radiation, supported e.g. by $D_{tree} = 0.45$ ($P < 10^{-8}$) for the species trio *G. ethelwynae*, *M. zebra*, and *C. rendalli* in the 'permissive' set of gene trees.
8) Introgression between the Indian cichlid subfamily Etroplinae and the Malagasy subfamily Ptychochrominae, supported e.g. by $D_{tree} = 0.23$ ($P < 10^{-8}$) for the species trio *G. ethelwynae*, *P. polleni* "Andapa", and *E. canarensis* in both the 'strict' and 'permissive' sets of exon trees.
9) Introgression between a clade formed by *T. sparrmanii* and *Steatocranus* sp. "ultraslender" and a clade formed by *G. ethelwynae*, '*T.*' *brevimanus*, *P. mariae*, and *H. buttikoferi*, supported by e.g. $D_{tree} = 0.34$ ($P < 10^{-8}$) for the species trio *A. leptura*, *Steatocranus* sp. "ultraslender", and *G. ethelwynae* in the 'permissive' set of exon trees.

We tested each of the nine hypotheses of introgression with genealogy interrogation as described in Barth *et al.*[108]. In brief, we specified for each hypothesis three alternative topology constraints and reran IQ-TREE for each marker of each set with each of the three constraints to compare the relative likelihoods of the constrained trees. For example, to test hypothesis 1), we prepared three constraints where the first enforced monophyly of the African cichlid subfamily Pseudocrenilabrinae, the second enforced monophyly of the Neotropical subfamily Cichlinae and *H. multidens*, and the third enforced monophyly of Pseudocrenilabrinae and Cichlinae without *H. multidens*. While no or only weak and inconsistent support was found for the hypotheses 1), 3), 4), 7), and 8), the results consistently supported hypotheses 2), 5), 6), and 9):

2) With all sets of trees, a majority of markers has a higher likelihood when *F. heteroclitus* is constrained to form a monophyletic group with Poecilidae, compared to when *C. variegatus* (the sister to *F. heteroclitus* in the species trees inferred with ASTRAL) is forced into the same position.
5) With all sets of trees, a majority of markers has a higher likelihood when *'T.' brevimanus* is constrained to form a monophyletic group with *P. mariae*, compared to when *H. buttikoferi* (the sister to *'T.' brevimanus* in the species trees) is forced into the same position.
6) With all sets of trees, a majority of markers has a higher likelihood when *P. mariae* is constrained to form a monophyletic group with *G. ethelwynae*, compared to when *'T.' brevimanus* and *H. buttikoferi* (which together form the sister group to *P. mariae* in the species trees) are forced into the same position.
9) In all sets of trees, a majority of markers have a higher likelihood when *T. sparrmanii* and *Steatocranus* sp. "ultraslender" are jointly constrained to form a monophyletic group with *G. ethelwynae*, *'T.' brevimanus*, *P. mariae*, and *H. buttikoferi*, compared to when all members of the Lake Tanganyika radiation (which together form the sister group to *T. sparrmanii* and *S.* sp. "ultraslender" in the species trees) are forced into the same position.

Based on the corroborated evidence for four cases of past introgression, we excluded the species *F. heteroclitus*, *'T.' brevimanus*, *P. mariae*, *T. sparrmanii,* and *Steatocranus* sp. "ultraslender" from all subsequent molecular-clock analyses.

We repeated the introgression tests described above with further tree sets based on ortholog exons and genes identified in an entirely independent round of the orthology identification workflow that relied on Nile tilapia exon sequences as queries instead of medaka sequences. In this separate application of the ortholog identification workflow, we thus used Nile tilapia as outgroup and excluded all other members of Oreochromini as well as all species more distant to the radiation in Lake Tanganyika than the Oreochromini. Instead, we included newly generated genome assemblies for three additional representatives of the radiation: *Boulengerochromis microlepis* (voucher JCF2), *Bathybates fasciatus* (ITH3), and *Hemibates koningsi* (IZA5) to allow a better focus on possible introgression events connected to the early lineages of Lake Tanganyika. In this round of ortholog identification, the application of 'strict' filters resulted in sets of 2,381 exons and 536 genes with a total alignment length of 591,993 bp, whereas 'permissive' filters produced sets that comprised 3,466 exons and 762 genes with a total of 956,463 bp. The introgression tests confirmed the above-listed hypotheses 5), 6), and 9)

and did not produce consistent signals for further introgression events involving the three additional Lake Tanganyika species.

Phylogenetic divergence-time estimation. As we expected that ILS could have occurred among the species included in our molecular-clock analyses, we estimated divergence times among cichlid fishes and the age of the cichlid adaptive radiation in Lake Tanganyika under the multi-species coalescent model, using the StarBEAST2[51] (v.0.15.5) add-on package for BEAST 2. However, despite recent speed improvements, StarBEAST2 remains computationally demanding as it estimates all marker trees jointly with the species tree. To achieve feasible run times, we therefore had to streamline the analysis in the following ways:

- We only used the 'strict' set of genes.
- We constrained the monophyly in the species tree of 34 groups that are unambiguously supported by recent phylogenomic studies[18,22,96].
- We performed parallel analyses with different fixed population sizes (see below) instead of estimating the population size from the data.
- We applied the strict molecular clock model instead of a relaxed-clock model, assuming that substitution rates are comparable at least among the Neotropical and African cichlid subfamilies Cichlinae and Pseudocrenilabrinae and that errors that could potentially result from rate variation between cichlids and outgroups do not propagate to age estimates within the subfamilies as long as the ages of subfamilies themselves are correctly constrained.
- We used the Generalised time-reversible (GTR) substitution model with gamma-distributed among-site rate variation instead of performing Bayesian model averaging.
- Instead of estimating all parameters independently for each gene, we linked the absolute substitution rates, the GTR model's relative substitution rates and base frequencies, and the alpha parameter of the gamma-distributed among-site rate variation according to partitioning schemes estimated with the program PartitionFinder[111] (v.2.1.1). Prior to these analyses with PartitionFinder, we split all gene alignments by codon position and excluded third codon positions to avoid possible effects of alignment saturation. Data blocks of first codon positions per gene and blocks of second codon positions per gene were used in separate PartitionFinder analyses (but per gene, the block composed of first codon positions and the block composed of second codon positions were forced to share the same gene tree in the subsequent StarBEAST2 analysis). The PartitionFinder analyses were repeated twice so that data blocks were first clustered by their absolute substitution rates and then by the fitted parameters of the GTR model with gamma-distributed among-site rate variation. In all PartitionFinder analyses, we employed the 'rcluster' algorithm with clustering based on the Akaike information criterion (AIC), we assumed linked branch lengths, and we required a minimum of 10,000 sites in each partition. These settings grouped the first codon position blocks into 13 partitions when clustering was based on absolute substitution rates and into six partitions when clustering was based on the GTR model parameters. The second codon position blocks were also grouped into 13 partitions when clustering was based on absolute substitution rates and into nine partitions when GTR model parameters were considered; when generating the settings file for the

StarBEAST2 analyses, the model parameters of different data blocks were linked exactly according to these partitions.

The settings for the StarBEAST2 analysis further included the birth-death model of diversification with extinction[112] and five different age constraints to calibrate divergence times, each of which was in accordance with the timeline estimated by Matschiner *et al.*[18] and implemented through a lognormal prior distribution: The age of the root was set to 92.0 Ma (with a standard deviation in log space of 0.05), the divergence of cichlids was set to 87.5 Ma (with a standard deviation of 0.06), the divergence between Beloniformes and Cyprinodontiformes was set to 74.9 Ma (with a standard deviation of 0.09), the divergence of Etroplinae was set to 76.8 (with a standard deviation of 0.07), and the divergence of Pseudocrenilabrinae and Cichlinae was set to 62.1 Ma (with a standard deviation of 0.21). We performed 19 replicate analyses for each of four assumed effective population sizes: 83,333, 166,667, 333,333, and 666,667 (in each case also assuming a generation time of 3 years[33]). Despite our model simplifications, the analyses of our dataset, which was unusually large for StarBEAST2 analyses with 510 genes and a total alignment length of 542,922 bp, required up to 10 billion MCMC iterations and a run time (wall time) of around 50 days for each of the 76 replicates to reach convergence (ESS values above 200 for all model parameters). We removed the first 55% of each completed MCMC chain as burn-in, merged the posterior distributions of the 19 replicate analyses per assumed effective population size, and thinned each merged posterior distribution to 1,000 MCMC states. From these, we generated maximum-clade-credibility consensus trees with the program TreeAnnotator. With an assumed effective population size of 666,667, the divergence of the Neotropical cichlid subfamily Cichlinae and the African subfamily Pseudocrenilabrinae was estimated at 61.6 Ma with a 95% highest-posterior-density (HPD) interval from 63.9-56.2 Ma, in agreement with the constraint centred on 62.1 Ma that we had placed on this node according to the timeline estimated by Matschiner *et al.*[18]. The age of the adaptive radiation of cichlid fishes in Lake Tanganyika, marked by the divergence between Trematocarini and the combined Lamprologini, Ectodini, and Haplochromini, was estimated in these analyses at 9.6 Ma with a 95% HPD interval from 10.1-9.1 Ma (Extended Data Fig. 1). Thus, even though the age of Lake Tanganyika, which has long been assumed to lie between 12-9 Ma[17,23], was not used as an age constraint in our analyses, our results are fully consistent with an endemic adaptive radiation of cichlid fishes soon after the early colonization of the lake by a single lineage.

In the analyses based on smaller assumed effective population sizes, the estimated age for the divergence of Cichlinae and Pseudocrenilabrinae was younger than the constraint that we had placed on this node, namely between 49.5 and 47.5 Ma instead of around 61.6 Ma[18]. We attribute this discrepancy to a conflict with the older age constraints caused by substitution-rate variation in the outgroups that was not accounted for in our analysis. After scaling the age estimates of these alternative analyses so that the divergence between Cichlinae and Pseudocrenilabrinae matches the previously determined age of around 62.1 Ma[18], the age estimates for the Lake Tanganyika radiation were 9.6 Ma, 9.4 Ma, and 9.5 Ma with assumed effective population sizes of 83,333, 166,667, and 333,333, respectively, thus corroborating our conclusion of a radiation onset around 9.6 Ma.

Phylogenetic inference

To investigate the phylogenetic structure of the cichlid radiation of Lake Tanganyika, we performed phylogenetic analyses based on genome-wide nuclear SNPs as well as assembled mitochondrial genome sequences.

Maximum-likelihood inference of among-sample relationships from genome-wide nuclear SNPs. Nuclear SNPs were used to infer a phylogeny of 518 individuals (including both phased haplotypes for each of the two *N. cancellatus* specimens) with the software RAxML[52] (v.8.2.4), using the GTRCAT substitution model. For this phylogenetic analysis, the dataset of 57,751,375 SNPs was further filtered with BCFtools to exclude sites with more than 40% missing data, followed by thinning of the dataset with VCFtools so that no two SNPs were closer than 100 bp to each other, and by discarding the second of the phased alleles of each genotype. This resulted in a dataset of 3,630,997 SNPs. The analysis accounted for the absence of invariable sites with the ascertainment bias correction developed by Felsenstein[113] and implemented in RAxML. To apply this correction, we determined the number of omitted invariant sites as the difference between the number of all callable sites (sites that were neither masked due to potentially ambiguous read mapping nor due to proximity to indels; see above) and the number of variable sites, considering the additional filtering and thinning of the dataset. To assess reliability of the results, we performed five replicates of this analysis. The phylogeny was rooted using the outgroup taxa *S.* sp. "ultraslender", *G. ethelwynae*, '*T.' brevimanus*, *P. mariae*, and *H. buttikoferi*.

Instead of applying bootstrapping, which can lead to inflated support values when concatenated alignments are used[114], we estimated node support by dividing the dataset of sites with less than 40% missing data into 100 non-overlapping subsets that each contained 471,991 SNPs, and inferring a phylogeny separately from each of these subsets. We then quantified node support for every node in the phylogeny inferred with the dataset of 3,630,997 SNPs, as the number of subset phylogenies that supported this node (Extended Data Fig. 2; tree file available on Dryad; https://doi.org/10.5061/dryad.9w0vt4bbf: 05_RAxML.tre)

A species-level tree was generated from this sample-level phylogeny by excluding for each species all tips except the one for the sample with the lowest proportion of missing data. This species-level maximum-likelihood tree inferred with RAxML was subsequently used as the first out of three topological constraints in relaxed-clock analyses of divergence times within the radiation (see below in section "Divergence time estimates within the radiation").

Species-tree inference from selected genomic regions. From the full dataset containing 57,751,375 SNPs, we generated sequence alignments for each non-overlapping window of a length of 5,000 bp (excluding the sequences of the two *N. cancellatus* specimens). For sites that were not included in the SNP dataset, it was assumed that these were invariable and identical to the corresponding site in the Nile tilapia reference genome. However, to account for potential unidentified variation, parts of all sequences were masked according to whether variation could have been detected if it existed. Thus, all regions excluded from the SNP dataset due to potentially ambiguous mapping or proximity to indels were again masked, but in addition, we also masked regions in which the overall read depth across all samples was either below 4,000 or above 8,000, and we masked, per individual, those regions where

less than 4 reads had sufficient quality for variant calling with GATK. Window alignments were further filtered according to multiple criteria to identify the most suitable alignments for phylogenetic inference: First, alignments were discarded if the overall proportion of missing data was above 70% or if the standard deviation of the proportion of missing data across tribes was above 0.02; the latter filter was applied to exclude windows with tribe-specific deletions. Second, the local phylogeny was inferred for each alignment with RAxML based on the GTRCAT substitution model, after excluding alignment regions that had a gap rate above 0.2 or an entropy score above 0.5; these values were determined with BMGE. For each local phylogeny, the Robinson-Foulds distance[115] to the phylogeny inferred from genome-wide SNPs with RAxML was calculated with the Python (v.2.7.10) package ete3[116] (v.3.1.1), and the alignment was excluded from further analysis if the calculated distance was above 700. Third, after reducing all alignments to sequences of the one individual per species that had the lowest proportion of missing data, we calculated the number of hemiplasies per alignment, assuming that this number can serve as an indicator of within-alignment recombination[117]. The number of hemiplasies was calculated as the difference between the number of variable sites and the parsimony score, which was determined with PAUP* (v.4.0a163). Subsequently, the most suitable alignments for phylogenetic inference were selected from the ones remaining in the dataset as those characterized by an alignment length greater than 2,000 bp after filtering, a number of variable sites greater than 400, and a number of hemiplasies below 200. These criteria were met by 1,272 alignments, which had a total length of 3,219,018 bp and an overall completeness of 95.1%. For each of these 1,272 alignments, maximum-likelihood trees were generated with IQ-TREE (v.1.7-beta7), assuming the GTR substitution model with gamma-distributed among-site rate variation. The maximum-likelihood trees generated by IQ-TREE were then used as input for species-tree inference under the multi-species coalescent model with ASTRAL. This species tree inferred with ASTRAL was subsequently used as the second out of three topological constraints in relaxed-clock analyses of divergence times within the radiation (see below in section "Divergence time estimates within the radiation").

Bayesian inference of the species tree from genome-wide nuclear SNPs. We performed Bayesian species tree inference with the SNP-based molecular-clock approach of Stange *et al.*[118], using the SNAPP[54] (v.1.4.2) add-on package for BEAST 2. However, due to the high computational demand of SNAPP analyses caused by the mathematical integration over all possible trees at each SNP, we could not analyse all species of the cichlid adaptive radiation of Lake Tanganyika in a single analysis. Instead, we performed one backbone analysis with representatives of the two most divergent lineages per tribe and then used the resulting age estimates for the first within-tribe divergences as secondary age constraints for per-tribe analyses.

We selected 27 samples for the backbone analysis, so that all tribes of the radiation, except for the monotypic Boulengerochromini, were represented by at least two species descending from opposite sides of the first within-tribe divergence according to the species-level trees inferred with RAxML and ASTRAL (see above in section "Maximum-likelihood inference of among-sample relationships from genome-wide nuclear SNPs" and "Species-tree inference from selected genomic regions", respectively). Wherever we could opt between multiple samples, we selected the one with the highest read depth after mapping. For Boulengerochromini, we included sample JCF2. In both the RAxML and

ASTRAL trees, the first divergence within Trematocarini separated *Trematocara unimaculatum* from the remaining Trematocarini; thus, we selected the *T. unimaculatum* sample with the highest read depth (IXA6) together with the sample with the highest read depth among the remaining Trematocarini, which was a *T. marginatum* (ISA3). For Bathybatini, the RAxML and ASTRAL trees agreed that the first within-tribe divergence occurred between the genera *Hemibates* and *Bathybates*; thus, we selected the samples with the highest read depth of each of the two genera, a *Hemibates koningsi* (IZA5) and a *Bathybates fasciatus* (ITH3). For Lamprologini, both trees strongly supported the same two monophyletic subgroups that included 37 and 70 species, respectively; we selected one *N. variostigma* (JWA6) and one *Julidochromis* sp. "unterfels" (JWA2) as the samples with the highest read depths in each of the two subgroups. For Cyphotilapiini, the two trees both supported *Ctenochromis benthicola* as the sister group to three species of the genus *Cyphotilapia*; thus, we selected a *Ctenochromis benthicola* (DMD1) and a *Cyphotilapia* sp. "5-bar frontosa" (KDG2). For Limnochromini, the two trees disagreed in the composition of the two clades descending from the first within-tribe divergence; however, both trees placed *Triglachromis otostigma*, *Tangachromis dhanisi*, *Reganochromis calliurus*, and *Baileychromis centropomoides* on one side of the first within-tribe divergence and *Gnathochromis permaxillaris*, *Limnochromis abeelei*, *L. staneri*, and two species of *Greenwoodochromis* on the other side; thus, we selected a *T. dhanisi* (LJA8) and a *L. staneri* (ITA6). For Ectodini, both trees placed *G. lemairii* as the sister species to a clade formed by all other members of the tribe; thus, we selected a *G. lemairii* (JDD7) and a *Xenotilapia flavipinnis* (JAF7). For Cyprichromini, both trees agreed that the first divergence occurred between the genera *Cyprichromis* and *Paracyprichromis*; thus, we selected a *Cyprichromis coloratus* (JEC7) and a *Paracyprichromis* sp. "tembwe" (JWD1). For Benthochromini, both trees placed *Benthochromis tricoti* and *B. melanoides* on one side of the first within-tribe divergence and *B. horii* and *B*. sp. "horii mahale" on the other side; thus, we selected a *B. melanoides* (ILG3) and a *B*. sp. "horii mahale" (LEF2). For Perissodini, both trees placed the first divergence between *Xenochromis hecqui*, *Plecodus elaviae*, *Plecodus multidentatus*, and *Perissodus eccentricus* on one side and *Haplotaxodon microlepis*, *H. trifasciatus*, *Plecodus paradoxus*, *P. straeleni*, and *Perissodus microlepis* on the other side; thus, we selected a *P. multidentatus* (IZA8) and a *P. straeleni* (INE8). For Eretmodini, both trees agreed that the first divergence occurred between *Tanganicodus irsacae* and *Eretmodus cyanostictus* on the one side and *Eretmodus marksmithi*, *Spathodus marlieri*, and *S. erythrodon* on the other side; thus, we selected an *E. cyanostictus* (IZH7) and an *E. marksmithi* (JXE9). For Tropheini, both trees supported the same two subgroups composed of 13 and 27 species, respectively; we selected a *Tropheus annectens* (JWG4) and a *Petrochromis trewavasae* (IWC9) as representatives of these two subgroups. Finally, the remaining lineages traditionally assigned to Haplochromini formed four strongly supported subgroups in both trees: The first included all *Orthochromis* species except *O. indermauri*, the second included *O. indermauri* together with *Pseudocrenilabrus philander*, the third included *Ctenochromis polli*, *Thoracochromis brauschi*, *Serranochromis macrocephalus*, *Sargochromis carlottae*, and *Pharyngochromis acuticeps*, and the fourth was composed of eight species of the genera *Haplochromis*, *Astatotilapia*, and *Astatoreochromis*. We included one representative of each of these four subgroups in our backbone analyses. These were an *Orthochromis uvinzae* (KYE7), an *O. indermauri* (HXC6), a *S. macrocephalus* (JWF5), and an *A. burtoni* (IZC5).

We generated all input files for SNAPP analyses with the script 'snapp_prep.rb'[118] and constrained the divergence between the three tribes Boulengerochromini, Trematocarini, and Bathybatini and all other tribes with a normally distributed prior that was centred at 9.7 Ma and had a standard deviation of 0.3, according to our estimates of the age of the cichlid adaptive radiation in Lake Tanganyika. To achieve feasible run times with SNAPP, we limited the analysis to a maximum of 10,000 variable sites, which were randomly sampled from all sites that were variable among the 27 species included in the backbone analysis. Unlike in the other phylogenetic analyses based on SNP data described above, we used the more strictly filtered SNP dataset with a minimum genotype quality of 30 for our analyses with SNAPP. As the starting tree topology, we selected the one resulting from the RAxML analysis, pruned to include the 27 species only. We performed 10 replicate SNAPP analyses, each with a run length of 1 million MCMC iterations. Convergence of MCMC chains was assessed visually with the program Tracer[119] (v.1.7.1) by comparing parameter traces across replicate analyses, and confirmed by ESS values greater than 200. After discarding the first 10% of each MCMC chain as burn-in, we merged the posterior distributions of all replicates and used these to generate maximum-clade-credibility trees with TreeAnnotator.

The ages of the first within-tribe divergences were estimated at 3.09 Ma (95% HPD: 3.42-2.77 Ma) for Trematocarini, 4.94 Ma (95% HPD: 5.40-4.53 Ma) for Bathybatini, 4.55 Ma (95% HPD: 4.93-4.13 Ma) for Lamprologini, 2.26 Ma (95% HPD: 2.60-1.93 Ma) for Cyphotilapiini, 3.73 Ma (95% HPD: 4.14-3.34 Ma) for Limnochromini, 4.35 Ma (95% HPD: 4.76-4.01 Ma) for Ectodini, 2.79 Ma (95% HPD: 3.11-2.48 Ma) for Cyprichromini, 0.21 Ma (95% HPD: 0.29-0.13 Ma) for Benthochromini, 1.31 Ma (95% HPD: 1.52-1.11 Ma) for Perissodini, 1.20 Ma (95% HPD: 1.37-1.03 Ma) for Eretmodini, and 3.02 (95% HPD: 3.34-2.68 Ma) for Tropheini. Of the four representatives of subgroups traditionally assigned to Haplochromini, *O. uvinzae* was estimated to have diverged from all other haplochromine lineages at 5.84 Ma (95% HPD: 6.29-5.44 Ma), *O. indermauri* and *S. macrocephalus* were estimated to have diverged at 4.65 Ma (95% HPD: 5.03-4.31 Ma), and *A. burtoni* was estimated to have diverged from Tropheini at 4.39 Ma (95% HPD: 4.75-4.03 Ma).

These age estimates were subsequently used to define normally-distributed priors as age constraints on the first within-tribe divergence in tribe-specific SNAPP analyses that used the same settings as the backbone analysis. For all tribes for which the RAxML and ASTRAL trees agreed on the exact composition of the two subgroups descending from the first within-tribe divergence (thus, all tribes except Limnochromini; see above), we constrained the monophyly of each of these two subgroups. In the case of Trematocarini, where the RAxML analyses suggested the possible presence of substitution-rate variation between the lineages descending from the first within-tribe divergence, we added two species of Bathybatini, *H. koningsi* (IZA5) and *B. fasciatus* (ITH3), as outgroups, and added monophyly constraints for both the ingroup and the outgroup to ensure the correct placement of the within-tribe root position. As a consequence of the outgroup addition, the age constraint was in this case not placed on the very first divergence of the tree, but only on the first divergence within the tribe Trematocarini. We also added outgroup species in the analyses of each of the four subgroups of lineages traditionally assigned to Haplochromini, as this allowed us to constrain their divergence times based on the backbone

analysis even though the backbone analysis had only included a single representative of each of the four subgroups.

As each of the three tribes Lamprologini, Ectodini, and Tropheini were too large to allow the joint analysis of all their members with SNAPP, we divided these tribes into sets of unambiguously supported subgroups and performed another layer of backbone analyses within these tribes as well as separate analyses of each subgroup. For Lamprologini, we identified five subgroups that were strongly supported by both the RAxML and ASTRAL trees: The first of these included 8 species, of which 6 were of the genus *Lamprologus* (e.g. *L. kungweensis*) and 2 were of the genus *Neolamprologus* (e.g. *N. ventralis*). The second subgroup counted 19 species, including 3 species of the genus *Altolamprologus* (e.g. *A. compressiceps*), 4 species of the genus *Lamprologus* (e.g. *L. ocellatus*), 7 species of the genus *Lepidiolamprologus* (e.g. *L. elongatus*), and 5 species of the genus *Neolamprologus* (e.g. *N. meeli*). The third subgroup counted 16 species, all of which were of the genus *Neolamprologus* (e.g. *N. brichardi*). The fourth subgroup counted 20 species, including *Lamprologus tigripictilis*, *Lepidiolamprologus cunningtoni*, 7 species of the genus *Neolamprologus* (e.g. *N. modestus*), and all 11 species of the genus *Telmatochromis*. The fifth subgroup counted 29 species, including 14 species of the genus *Neolamprologus* (e.g. *N. buescheri*), all 5 species of the genus *Chalinochromis*, and all 10 species of the genus *Julidochromis*. In total, the five subgroups included all but 15 species of Lamprologini. For our within-tribe backbone analysis, we thus selected the 15 species that were not included in any subgroup as well as two representatives of each subgroup. Like for our overall backbone analysis, these two representatives were selected so that their divergence was the first within-subgroup divergence and their read depths were maximized. Thus, we selected one *Neolamprologus ventralis* (Burundi) (KAG8) and one *Lamprologus ornatipinnis* (JZF3) as representatives of the first subgroup, a *N. variostigma* (JWA6) and a *Neolamprologus pleuromaculatus* (JZF2) as representatives of the second subgroup, a *Neolamprologus falcicula* (JXD7) and a *Neolamprologus gracilis* (JWH2) as representatives of the third subgroup, a *Lepidiolamprologus cunningtoni* (IOH5) and a *Telmatochromis* sp. “dhonti twiyu” (LHC1) as representatives of the fourth subgroup, and a *Neolamprologus pectoralis* (JWA7) and a *Julidochromis* sp. "unterfels" (JWA2) as representatives of the fifth subgroup.

For Ectodini, we used two subgroups that were unambiguously supported by both the RAxML and ASTRAL trees. The first of these contained 15 species and included all species of the genera *Ophthalmotilapia* (6 spp.), *Ectodus* (2 spp.), *Cyathopharynx* (2 spp.), *Lestradea* (2 spp.), as well as *Cardiopharynx schoutedeni*, *Aulonocranus dewindti*, and *Cunningtonia longiventralis.* The second subset counted 21 species and included all species of the genera *Xenotilapia* (17 spp.), *Microdontochromis* (2 spp.), as well as *A. leptura* and *Enantiopus melanogenys*. *G. lemairii* and three species of the genus *Callochromis* were not included in these subsets. Thus, we used these latter four species as well as two representatives of each of the two subgroups in our within-tribe backbone analysis. As representatives, we selected *C. schoutedeni* (KAF2), *O.* sp. “paranasuta” (JYF7), *X. caudafasciata* (IXB9), and *X. flavipinnis* (JAF7), again based on the same criteria as for the other backbone analyses. To ensure correct placement of the within-tribe root position, we further added two outgroups from the tribe Limnochromini, namely a *L. staneri* (ITA6) and a *T. dhanisi* (LJA8).

We also used two unambiguously supported subgroups for Tropheini. The first of these included all 13 species of the genus *Tropheus*, while the second counted 27 species including all species of the genera *Petrochromis* (16 spp.) and *Pseudosimochromis* (5 spp.) as well as *Lobochilotes labiatus*, *Interochromis loocki*, *Limnotilapia dardennii*, *Gnathochromis pfefferi*, *Ctenochromis horei*, and *Simochromis diagramma*. As representatives of these subgroups in the within-tribe backbone analysis, we used a *Tropheus duboisi* (KHA5), a *T. annectens* (JWG4), a *L. labiatus* (ISD8), and a *Petrochromis trewavasae* (IWC9). We further added an *Astatoreochromis straeleni* (KAE8) and an *A. burtoni* (IZC5) as outgroups.

For the fifth subgroup of Lamprologini and the second subgroup of Tropheini, fewer than 1,000 sites were variable and sufficiently complete within the group, due to the requirement for SNAPP analyses that all sites must have data for at least one sample of each species. For the SNAPP analyses of these two groups, we therefore used the SNP dataset with a minimum genotype quality of 20, instead of the more strictly filtered one with a quality threshold of 30 that was used for all other SNAPP analyses. This change allowed us to use the maximum amount of 10,000 variable sites for the SNAPP analyses of the two subgroups.

We again performed ten replicate analyses per group, each of which included 1 million MCMC iterations, and we resumed these for another 1 million iterations in a few cases in which the MCMC chains had not sufficiently converged after the first million iterations. The proportion of each MCMC chain that was discarded as burn-in was again set to a minimum of 10% and increased if the visual inspection of traces indicated a longer burn-in phase. For each set of analyses, we generated a combined posterior distribution by sampling 1,000 states from the post-burn-in MCMC chains of the ten analysis replicates.

Finally, the backbone and tribe-specific trees resulting from the SNAPP analyses were combined to produce complete species trees of the Lake Tanganyika cichlid radiation. Instead of combining only summary trees from all SNAPP analyses, we combined all 1,000 trees of the posterior tree distributions of each analysis to form a distribution of 1,000 trees including all species. The tree combination was done iteratively – integrating the tribe-specific trees into the backbone trees one by one – by replacing the placeholder tips in the backbone trees with the trees (after pruning the outgroups if any were used) from tribe-specific analyses. Instead of simply integrating the nth tree from the tribe-specific posterior distribution into the nth tree from the backbone posterior distribution, we made the replacement under consideration of the age of the connection node in the two trees. Thus, prior to each integration of a tribe-specific tree distribution into the backbone tree distribution, we ranked both the 1,000 trees from the tribe-specific distribution and the 1,000 trees from the backbone distribution by the age of the connection node, and then integrated tribe-specific trees into the backbone trees according to this rank. For example, prior to integrating the tribe-specific trees for Bathybatini into the backbone trees, the 1,000 backbone trees were ranked by the age of the two placeholder species *Hemibates koningsi* and *Bathybates fasciatus*. Similarly, the 1,000 tribe-specific trees were ranked by the age of their root node, at which *Hemibates* and *Bathybates* diverge. The two placeholder species in the first-ranked backbone tree were then replaced with the first-ranked of the tribe-specific trees and so forth. At the end of this process, all placeholder species in the backbone trees were replaced with (pruned) tribe-specific trees,

forming 1,000 species-complete trees of Lake Tanganyika cichlid fishes. From this tree distribution, we generated a maximum-clade-credibility tree with the program TreeAnnotator.

Even though the SNAPP analysis produced age estimates for every divergence event, these were based on the strict molecular clock model (the only clock model available in SNAPP) and may therefore be misleading in the presence of substitution-rate variation. For this reason, we estimated divergence times within the radiation separately with a relaxed-clock model; however, as relaxed-clock models can so far not be applied to genome-wide SNPs, these analyses were based on selected genomic regions (see below in section "Divergence time estimates within the radiation"). Nevertheless, we used the results of the SNAPP analysis to inform the relaxed-clock analyses by providing the maximum-clade-credibility tree as the third out of three topological constraints in the divergence time analyses.

Quartet inference of the species tree from genome-wide nuclear SNPs. The thinned dataset generated for phylogenetic inference from nuclear SNPs was also used to infer the species tree of 270 species included in the SNP dataset (and with both phased haplotypes for each of the two *N. cancellatus* specimens), using the quartet approach of SVDQuartets[120] implemented in the program PAUP* (v.4.0a161). A maximum of 300 million randomly selected quartets (about a third of all possible quartets) were analysed in the inference. The support for nodes in the resulting species tree was again quantified based on the 100 subsets of the SNP data generated for phylogenetic inference from nuclear SNPs (data not shown; tree files available on Dryad; https://doi.org/10.5061/dryad.9w0vt4bbf: 05_SVDquartets.tre, 05_SVDquartets_sub1.tre, 05_SVDquartets_strictlyfiltered.tre, 05_SVDquartets_strictlyfiltered_sub1.tre).

Inference of the mitochondrial phylogeny. For each individual, reads mapping to the mitochondrial genome of Nile tilapia (NCBI accession NC_013663.1) were extracted from BAM files, converted into FASTQ format with Picard-tools, and assembled with the iterative MITObim[121] (v.1.8) approach based on the MIRA[122] (v.4.0.2) assembler. The assembled mitochondrial genome sequences of all 528 individuals (including the two *N. cancellatus* samples) were then used to generate a multiple sequence alignment with MAFFT[97] (v.7.300). The mitochondrial genome-wide alignment was divided into separate alignments for each of the 12 mitochondrial protein-coding genes except *ND6*. These alignments were further split according to codon position, and the 36 resulting alignments were used to define partitions for maximum-likelihood phylogenetic inference, performed with RAxML on the basis of the GTRCAT substitution model (Supplementary Fig. 2; tree file and mitochondrial genomes are available on Dryad; https://doi.org/10.5061/dryad.9w0vt4bbf: 03_mitochondrial_assemblies.tgz, 05_mitogenome.tre).

Divergence time estimates within the radiation

We used a selected set of the phylogenetically most suitable alignments for divergence time estimation under the relaxed-molecular-clock model. The alignments were selected from the genome-wide set of alignments described above, using the same settings as for the selection of alignments for species-tree inference with ASTRAL (see above), except that the minimum alignment length was set to 2,500 bp after filtering with BMGE, and the maximum number of hemiplasies was set to 130. These criteria were met by ten alignments, which had a total length of 30,738 bp and a completeness of 95.8%.

Divergence times were inferred with BEAST 2, and the bModelTest package was used to average over substitution models for each alignment separately. We assumed a birth-death process of diversification[112] and applied the uncorrelated lognormal relaxed-clock model[101] to account for branch-rate variation. To achieve feasible run times with the computationally demanding relaxed-clock analyses, we were forced to constrain the tree topology; however, we accounted for phylogenetic uncertainty by performing three separate sets of analyses in which the topology was either fixed to the species-level phylogeny inferred with RAxML from the dataset of genome-wide SNPs (see above in section "Maximum-likelihood inference of among-sample relationships from genome-wide nuclear SNPs", Extended Data Fig. 2), the species tree inferred with ASTRAL from selected genomic regions (see above in section "Species-tree inference from selected genomic regions"; Extended Data Fig. 3), or the Bayesian species tree inferred with SNAPP from genome-wide SNPs (see above in section "Bayesian inference of the species tree from genome-wide nuclear SNPs"; Extended Data Fig. 4). In each case, the age of the root was calibrated with a normal prior distribution centred at 9.7 Ma[18]. Ten replicate BEAST 2 analyses were performed with each tree topology, with chain lengths of 20 million MCMC iterations per replicate. Convergence of MCMC chains was supported by ESS values greater than 200 for all model parameters. The posterior distributions of all replicate analyses were merged and maximum-clade-credibility trees were produced with TreeAnnotator (Fig. 1, Extended Data Figs. 2-4, tree files available on Dryad; https://doi.org/10.5061/dryad.9w0vt4bbf: 05_BEAST_RAxML.tre, 05_BEAST_ASTRAL.tre, 05_BEAST_SNAPP.tre).

2D-Morphometrics

To quantify body shape and upper oral jaw morphology, we applied a landmark-based geometric morphometric approach to digital X-ray images (for the full set of 10 specimens per species whenever possible; n = 2,197).

X-ray imaging. We acquired X-ray images of the full body of the specimens using a Faxitron Digital Specimen Radiography System LX-60, with 35 kV tube voltage and 0.3 mA tube current. Exposure times varied between 10-20 sec depending on the size of the specimen.

Landmark placing. We selected 21 landmarks, of which 17 were distributed across the skeleton and four defined the premaxilla (see Extended Data Fig. 5a). Landmark coordinates were digitized by a single person (to avoid investigator bias) using the software FIJI[55] (v2.0.0-rc-68/1.521i).

Body shape. To extract overall body shape information, we excluded landmark 16, which marks the lateral end of the premaxilla, hence minimizing the impact of the orientation of the upper oral jaw. We then applied a Procrustes superimposition to remove the effect of size, orientation, and translational position of the coordinates, followed by a PCA. Landmark coordinates were processed and analysed in R[59] (v.3.5.2) using the package geomorph[60] (v.3.0.7).

Upper oral jaw morphology. For upper oral jaw morphology, we used a subset of four landmarks. A crucial feature of the oral jaw morphology is the orientation of the mouth relative to the body axes. However, this component of the upper oral jaw morphology would be lost in a classical geometric morphometric analysis, in which only pure shape information is retained. To overcome this, we

extracted the premaxilla-specific landmarks (1, 2, 16, and 21) *after* Procrustes superimposition of the entire set of landmarks and subsequently re-centred the landmarks to align the specimens without rotation. Thus, the resulting landmark coordinates do not represent the pure shape of the premaxilla but additionally contain information on its orientation and size in relation to body axes and body size, respectively. We then performed a PCA to identify the major axes of shape variation across the multivariate dataset. Landmark coordinates were processed and analysed in R using the package geomorph.

3D-Morphometrics

To quantify lower pharyngeal jaw bone shape in 3D, a landmark-based geometric morphometric approach was applied on µCT-scans of the head region of five specimens per species (n = 1,168).

CT-scanning. We acquired CT-scans of typically five specimens per species (n = 1,168) on a Bruker Skyscan 1174v2, at 50 kV and 800 µA. Depending on the size of the specimens, we used different filtering options ranging from no filter up to 1 mm aluminium filter; exposure time was adjusted accordingly. Voxel size ranged between 6.6 µm and 29.9 µm with typically 400 projections. Reconstruction was performed using NRecon (v.1.6.10.2), while parameter settings were adjusted to optimize each scan individually. For very large specimens (> 25 cm SL) we used a Nikon XT H 225 ST with a rotating target for scanning and CT Pro 3D (V5.1.6054.18526) for reconstruction.

Landmark placing. To capture all potential functionally important structures of the lower pharyngeal jaw bone, we selected a set of 27 landmarks (10 true landmarks and 17 sliding semi-landmarks) well distributed across the left side of the bone (see Extended Data Fig. 5b). Landmark coordinates were acquired by a single person using the TINA manual landmarking tool[56], which allows digitization of 3D landmarks directly in the volume (image stack). To place semi-landmarks equally distant along ridges (ventral sagittal ridge, lateral ridge, and posterior ridge), we used three plane points to span a grid intersecting the respective ridge.

Landmark superimposition. To retain the lateral symmetric properties of the shape data during superimposition, we reconstructed the right side of the lower pharyngeal jaw bone by mirroring the landmark coordinates across the plane of bilateral symmetry fitted through all landmarks theoretically lying on this plane. The resulting set of 42 landmarks was then superimposed while sliding the semi-landmarks along the curves by minimizing Procrustes distances. To remove the remaining asymmetric component of shape variation (produced by the deviation of the non-paired landmarks from the fitted plane of bilateral symmetry), we extracted the symmetric component using the function *bilat.symmetry*, followed by a PCA. Landmark coordinates were processed and analysed in R using the package geomorph.

Stable isotope analysis

To approximate ecology for each species, we measured the stable carbon (C) and nitrogen (N) isotope composition of all available individuals per species (n = 2,259). We analysed a small (0.5 – 1 mg) dried muscle sample of each specimen with a Flash 2000 elemental analyser coupled to a Delta Plus XP continuous-flow isotope ratio mass spectrometer (IRMS) via a Conflo IV interface (Thermo Fisher

Scientific, Bremen, Germany). Carbon and nitrogen isotope data were normalised to the VPDB (Vienna Pee Dee Belemnite) and Air-N_2 scales, respectively, using laboratory standards that were calibrated against international standards. Values are reported in standard per-mil notation (‰), and long-term analytical precision was 0.2‰ for $\delta^{13}C$ values and 0.1‰ for $\delta^{15}N$ values. Note that we have used some of these stable isotope values in a previous study[62].

Baseline data. As the carbon and nitrogen stable isotope composition can be influenced by the varying biochemistry of the local environment, we additionally collected and analysed a baseline dataset covering several trophic levels form the northern and the southern basin of the lake to assure interpretability of the measured stable isotope values in cichlids. This baseline dataset included benthic samples (plants (*Hydrilla* and *Vallisneria* spp.), snails (*Lavigeria* spp.), and phytoplankton; collected near-shore in water depths of less than 5 m) as well as pelagic samples (pelagic shrimps, lake sardines (*Stolothrissa tanganicae*), and zooplankton; collected offshore).

Further, we used the stable isotope dataset of the cichlids (n = 2,259) to test whether there is a general trend in the stable isotope data that can be explained by the latitudinal and longitudinal gradient of the sampling localities. To do so, we fitted multiple regression models with stable isotope values as response variable ($\delta^{15}N$ and $\delta^{13}C$, respectively) and longitude, latitude, and species as covariates – allowing interaction (isotope ~ latitudinal * longitudinal * species). We then applied an ANOVA on each of the fitted models to calculate for each covariate and their interactions the percentage of variance explained. Additionally, we grouped the different cichlid species into ecological categories (based on the available literature[85] as well as our own observations during specimen collection) according to their trophic level (i.e. scale eaters, piscivores, fish and invertebrate feeder, fry and plankton feeder, plankton feeder, plankton feeder and invertebrate feeder, invertebrate feeder, omnivore, aufwuchs and invertebrate feeder, aufwuchs and algae feeder, and algae scraper) and their habitat (i.e. pelagic, deep-benthic, intermediate-benthic, shallow-benthic, and littoral). We applied the same linear regression models but using trophic categories instead of the species covariate for $\delta^{15}N$ ($\delta^{15}N$ ~ latitudinal * longitudinal * trophic) and using habitat categories instead of the species covariate for $\delta^{13}C$ ($\delta^{13}C$ ~ latitudinal * longitudinal * habitat).

As an alternative test of whether N and C stable isotope data show a shift depending on the sampling location, we filtered our dataset for species with a lake-wide distribution of which we had collected specimens at different geographic locations (in the northern and southern part of the lake). This subset included species (n = 19) across all trophic levels and ecologies along the benthic-pelagic trajectory (*Plecodus multidentatus, Perissodus microlepis, Bathybates fasciatus, Bathybates minor, Bathybates leo, Lepidiolamprologus profundicola, Lepidiolamprologus elongatus, Lepidiolamprologus attenuatus, Benthochromis horii, Neolamprologus savoryi, Altolamprologus compressiceps, Limnochromis auritus, Triglachromis otostigma, Neolamprologus furcifer, Ophthalmotilapia nasuta, Xenotilapia boulengeri, Ctenochromis horei, Petrochromis famula*, and *Petrochromis polyodon*). We then tested if – across this set of species – the northern and southern samples differ in their $\delta^{15}N$ and $\delta^{13}C$ stable isotope composition using a two-sided t-test across all the per-basin species means.

All statistical analyses of the stable isotope data were conducted in R. The results of all the above tests are detailed in the Supplementary Discussion section below.

Trait space occupation per tribe

We calculated, per tribe, morpho- and ecospace size as the square root of the convex hull area spanned by species means of the PC1 and PC2-scores and $\delta^{13}C$ and $\delta^{15}N$ values, respectively. We then tested for a correlation of trait space size and estimated species richness of a tribe[15] (log-transformed to obtain normal distribution). To account for phylogenetic non-independence among the data points we calculated phylogenetic independent contrasts with the R package ape[57] (v.5.2) using the species tree presented in Fig. 1 pruned to the tribe level. We then calculated Pearson's correlation coefficients for independent contrasts using the function *cor.table* of the R package picante[58] (v.1.8).

Phenotype-environment association

For each trait complex (body shape, upper oral jaw morphology, and lower pharyngeal jaw shape) we performed a two-block PLS analysis based on species means of the Procrustes aligned landmark coordinates and the stable C and N isotope compositions using the function *two.b.pls* of the R package geomorph. Similar to a PCA, in a PLS the multivariate shape data are rotated, but in this case to identify the major axes of covariation between two blocks of multivariate data. To account for phylogenetic dependence of the data we applied a phylogenetic generalized least square analysis (pGLS) as implemented in the R package caper[63] (v.1.0.1) across the two sets of PLS scores (each morphological axis with the stable isotope projection) using the time-calibrated species tree based on the maximum-likelihood topology (Fig. 1). The strength of phylogenetic signal in the data was accounted for by optimising the branch length transformation parameter lambda using a maximum-likelihood approach.

Scoring pigmentation patterns

To quantify a putative signalling trait in cichlids, we scored the pigmentation patterns typically in five male specimens per species (n = 1,016), on the basis of standardized images taken in the field after capture of the specimens (see above). Following the strategy described in Seehausen *et al.*[64], the presence/absence of 20 pigmentation features was recorded by a single person, whereby we extended the scoring method to also include additional body and fin pigmentation patterns present in Tanganyikan cichlids (Extended Data Fig. 5c). We then applied a logistic PCA implemented in the R package logisticPCA[65] (v.0.2) and used the PC1 scores as univariate proxy for differentiation along the signalling axes for further analyses.

Trait evolution modelling and disparity estimates

To investigate the temporal dynamics of diversification over the course of the cichlid adaptive radiation in Lake Tanganyika, we analysed the four trait complexes (body shape, upper oral jaw morphology, lower pharyngeal jaw shape, and pigmentation pattern) by applying a phylogenetic comparative approach to the PLS- and the PCA-scores, respectively, using the time-calibrated species tree based on the maximum-likelihood topology (Fig. 1). We therefore compared the fit of several models of trait evolution to the four traits investigated and reconstructed morphospace dynamics and evolutionary rate patterns through time essentially following the strategy described in Cooney *et al.*[28], which is based on

measurements on extant taxa and assumes constant niche-space and no (or constant) extinction over the course of the radiation. All analyses were conducted in R, unless stated otherwise. We used PLS-scores as univariate measure for the eco-morphological traits because the PLS-fit (see above) allows to identify the shape changes associated with the ecological trajectories and thus most likely represent the adaptive components of each trait complex. However, we additionally applied the same approach using PC1-scores for all traits, yielding very similar results and biological interpretations as the PLS-based analyses (results are provided on Dryad; https://doi.org/10.5061/dryad.9w0vt4bbf: 07_Temporal_patterns_complementary_results.pdf).

Phylogenetic signal. For each trait we calculated the phylogenetic signal in the data by calculating Pagel's Lambda and Blomberg's K using the function *phylosig* of the R package phytools[66] (v.0.6-60).

Fitting models of trait evolution. We tested the fit of four models of trait evolution along the time-calibrated species tree to the PLS- and the PCA-scores, respectively, for each of the four phenotypic trait complexes. We applied a white noise model, a Brownian motion (BM) model, a single-optimum Ornstein-Uhlenbeck model, and an 'early burst' model of trait evolution using the function *fitContinuous* of the R package geiger[67] (v.2.0.6.1). Additionally, we fitted a variable rates model (a BM model of trait evolution that allows for rate shifts on branches and nodes) using the software BayesTrait (http://www.evolution.rdg.ac.uk/, v.3) with uniform prior distributions adjusted to our dataset (alpha: -1 – 1, sigma: 0 – 0.001 for morphometric traits; alpha: 0 – 10, sigma: 0 – 10 for pigmentation pattern) and applying single-chain Markov chain Monte Carlo runs with one billion iterations. We sampled parameters every 100,000th iteration, after a pre-set burnin of 10,000,000 iterations. We then tested, in each separate analysis, for convergence of the chain using a Cramer-von-Mises statistic as implemented in the R package coda[68] (v.0.19-3). As all chains passed the test, we further thinned the converged chain to 5,900 post-burnin samples and summarised the results by calculating the mean rate shift and the posterior probabilities for a shift per branch. The different models were compared by calculating their log-likelihood and Akaike Information Criterion (AIC) difference (see Extended Data Fig. 8d, e). Based on difference in AIC, the variable rates model was best supported for all traits but body shape, which showed a strong signal of an early burst of trait evolution (see Extended Data Fig. 8d, e, note that the variable rates model has the highest log-likelihood for body shape as well). We nevertheless focused on the variable rates model for further analyses of all traits to be able to compare temporal patterns of trait evolution among the traits.

Morphospace expansion through time. To estimate morphospace expansion through time we used the maximum-likelihood ancestral state reconstruction implemented in the R package phytools. To account for differences in the rate of trait evolution along the phylogeny, we reconstructed ancestral states using the mean rate-transformed tree derived from the variable rates model (see above). We then projected the ancestral states onto the original species tree and calculated the morphospace extent (i.e. the range of trait values [$value_{maximum}$ - $value_{minimum}$]) in time intervals of 0.15 million years (note that this is an arbitrary value; however, differently sized time intervals had no effect on the interpretation of the results). For each time point, we extracted the branches existing at that time and predicted the trait value linearly between nodes. We then compared the resulting morphospace expansion over time relative to a null model of trait evolution. For this, we simulated 500 datasets (PLS and PC1 scores)

under BM given the original species tree with parameters derived from the BM model fit to the original data. For each simulated dataset we produced disparity-through-time curves using the same approach as described above. We then compared the slopes of our observed data with each of the null models by calculating the difference of slopes through time (Fig. 3) using linear models fitted for each time interval with the two subsequent time intervals. Note that for body shape we also estimate morphospace expansion through time using the early burst model for ancestral state reconstruction, which resulted in a very similar pattern for trait diversification and led to the same conclusion.

Unlike other metrics of disparity (e.g. variance or mean pairwise distances) morphospace extent is not sensitive to the density distribution of measurements within the morphospace and captures its full range[69]. Hence, comparing the extent of morphospace between observed data and the null model directly unveils the contribution of morphospace expansion relative to the null model; and because the increase in lineages over time is identical in the observed and the simulated data, this comparison also provides an estimate for morphospace packing.

Evolutionary rates through time. To summarise, for each trait, how the evolutionary rates changed over the course of the radiation, we calculated the mean rate of trait evolution inferred with the variable rates model in the same 0.15 million years intervals along the phylogeny. A graphical representation of evolutionary rates per tribe are available on Dryad; https://doi.org/10.5061/dryad.9w0vt4bbf: 07_Temporal_patterns_complementary_results.pdf.

Accounting for phylogenetic uncertainty. To account for phylogenetic uncertainty in the tree topology we repeated the analyses of trait evolution using the time-calibrated species trees based on tree topologies estimated with ASTRAL and SNAPP (see above and Supplementary Discussion for a comparison of the three topologies). To also account for uncertainty in branch lengths, we repeated the analysis on 100 trees from the Bayesian posterior distributions for each of the three trees. The results based on these alternative trees are provided on Dryad; https://doi.org/10.5061/dryad.9w0vt4bbf: 07_Temporal_patterns_complementary_results.pdf).

Characterisation of repeat content

For the repeat content analysis, we randomly selected one *de novo* genome assembly per species of the radiation (n = 245). We performed a *de novo* identification of repeat families using RepeatModeler[70] (v.1.0.11). We then combined the RepeatModeler output library with the available cichlid-specific libraries[71] (Dfam and RepBase; v.27.01.2017; 258 ancestral and ubiquitous sequences, 161 cichlid-specific repeats, and 6 lineage-specific sequences; 65,118, 273,530, and 6,667 bp in total, respectively) and used the software RepeatMasker[71] (v.4.0.7) (-xsmall -s -e ncbi -lib combined_libraries.fa) to identify and soft-mask interspersed repeats and low complexity DNA sequences in each assembly. The reported summary statistics were obtained using RepeatMasker's 'buildSummary.pl' script (Fig. 4a, Extended Data Fig. 9a, results per genome are provided on Dryad; https://doi.org/10.5061/dryad.9w0vt4bbf: 08_Transposable_elements.pdf).

Gene duplication estimates

Per genome, gene duplication events were identified with the structural variant identification pipeline smoove following the population calling method (https://github.com/brentp/smoove, docker image cloned 20/12/2018), which builds upon lumpy[72], svtyper[73], and svtools (https://github.com/hall-lab/svtools). Variants were called per sample (n = 488 genomes, 246 taxa of the Tanganyika radiation) from the initial mapping files against the Nile tilapia reference genome with the function *call*. The union of sites across all samples was obtained with the function *merge,* then all samples were genotyped at those sites with the function *genotype*, and depth information was added with --duphold. Genotypes were combined with the function *paste* and annotated with *annotate* and the reference genome annotation file. The obtained VCF file was filtered with BCFtools to keep only duplications longer than 1 kb and of high quality (MSHQ > 3 or MSHQ == -1, FMT/DHFFC[0] > 1.3, QUAL > 100). The resulting file was loaded into R (v.3.6.0) with vcfR[74] (v.1.8.0) and filtered to keep only duplications with less than 20% missing genotypes. Next, we removed duplication events with a length outside 1.5 times the interquartile range above the upper quartile of all duplication length, resulting in a final dataset of 476 duplications (Fig. 4b).

Analyses of selection on coding sequence

To predict genes within the *de novo* genome assemblies, we used AUGUSTUS[75] (v.3.2.3) with default parameters and 'zebrafish' as --species parameter (n = 485 genomes, 245 taxa). For each prediction we inferred orthology to Nile tilapia genes (GCF_001858045.1_ASM185804v2) with GMAP (GMAP-GSNAP[76]; v.2017-08-15) applying a minimum trimmed coverage of 0.5 and a minimum identity of 0.8. We excluded specimens with less than 18,000 Nile tilapia orthologous genes detected (resulting in 471 genomes, 243 taxa). Next, we kept only those tilapia protein coding sequences that had at least one of their exons present in at least 80% of the assemblies (260,335 exons were retained, representing 34,793 protein coding sequences). Based on the tilapia reference genome annotation file, we reconstructed for each assembly the orthologous coding sequences. Missing exon sequences were set to 'N's. We then kept a single protein coding sequence per gene (the one being present in the maximum number of species with the highest percentage of sequence length), resulting in 15,294 protein coding sequences. Per gene, a multiple sequence alignment was then produced using MACSE[77] (v.2.01). We calculated for each specimen and each gene the number of synonymous (S) and non-synonymous (N) substitutions by pairwise comparison to the ortholog Nile tilapia sequence using *codeml* with runmode -2 within PAML[78] (v.4.9e). To obtain an estimate of the genome-wide sequence evolution rate that is independent of filtering thresholds, we calculated the genome-wide dN/dS ratio for each specimen based on the sum of dS and dN across all genes (Fig. 4c, Extended Data Fig. 9b).

Signals of past introgression

We used the f_4-ratio statistic[34] to assess genomic evidence for interspecific gene exchange. We calculated the f_4-ratio for all combinations of trios of species on the filtered VCF file using the software Dsuite[79] (v.0.2 r20), with *T. sparrmanii* as outgroup species (note that we excluded *N. cancellatus* as all specimens of this species appeared to be F1 hybrids; see above). The f_4-ratio statistic (in combination with its associated P-value) estimates the 'admixture proportion', i.e. the proportion of the genome

affected by gene flow. The results presented in this manuscript (Fig. 4e, Extended Data Fig. 10) are based on the 'tree' output of the Dsuite function *Dtrios*, with each trio arranged according to the species tree based on the maximum-likelihood topology (Fig. 1). For the per tribe analyses shown in Fig. 4e we only used comparisons where all species within the trio come from the same tribe and belong to the cichlid adaptive radiation in Lake Tanganyika (n = 243 taxa).

In addition to the f_4-ratio we also identified signals of past introgression among species using a phylogenetic approach by testing for asymmetry in the relationships of species trios in 1,272 local maximum-likelihood trees generated using IQ-TREE (see above; Extended Data Fig. 10).

Heterozygosity

Empirical data. We calculated the number of heterozygous sites per genome (n = 488 genomes, 246 taxa from the Tanganyika radiation) from the VCF files using the BCFtools function *stats*. We then calculated the percentage of heterozygous sites among the number of callable sites per genome (considering mappability, proximity to indels, overall read depth, and read depth per individual; see the description of masking in the section "Details on mapping, variant calling, and filtering") (Fig. 4d).

Simulations. To explore if the observed levels of heterozygosity per tribe can be explained by the levels of gene flow within tribes, we performed coalescent simulations with the software msprime[80] (v.0.7.4) to assess the expected levels of heterozygosity in species of the Lake Tanganyika cichlid radiation given the inferred introgression signals. We simulated the evolution of all species of the radiation following the time-calibrated species tree (based on the maximum-likelihood tree topology; Fig 1), assuming a generation time of 3 years, as in Malinsky *et al.*[81], and a constant effective population size of 20,000 individuals. Each species divergence event was implemented as a mass migration between the two descendent species where all individuals of one species migrate to the other one (when viewed backwards in time). The time points of these mass migration events were set according to the corresponding divergence times in the species tree. Migration rates between pairs of species within tribes were set according to their introgression (f_4-ratio) signals inferred with Dsuite. To convert the f_4-ratio values inferred by Dsuite into migration rates, we applied a scaling factor of 5×10^{-6}, which results in a close correspondence in magnitude of the simulated introgression signals to those observed empirically (Fig. 4f, Extended Data Fig. 9c). In each of twenty separate simulations, we randomly sampled one pairwise f_4-ratio value for each pair of species for conversion to migration rates (there are many f_4-ratios per a pair of species – one for each possible third species added to the test trio; the maximum values per pair are shown in Extended Data Fig. 10). The simulated data consisted of a single chromosome of 100 kb in length with a mutation rate of 3.5×10^{-9} per bp and generation[33]. The recombination rate was set to 2.2×10^{-8} per bp per generation, based on the genome of approximately 1 Gb consisting of 22 chromosomes. As the number of chromosome arms is an excellent predictor of the total amount of recombination events[123], assuming one recombination event per chromosome is a reasonable first order approximation. Levels of heterozygosity were calculated for all simulated datasets as described for the empirical data. To confirm appropriate scaling between the empirically observed f_4-ratios and the migration rates applied in simulations, we recalculated f_4-ratios from the simulated datasets, again using Dsuite with the same settings as for the empirical dataset.

To account for between-tribe gene flow we further performed simulations in which migration between tribes was also sampled from the empirical f_4-ratio distribution. For simplicity in setting up the simulation model, we assume that gene flow between tribes is ongoing until the present day, which is clearly an overestimate (see Supplementary Discussion). Nevertheless, the results of these simulations support our hypothesized scenario, confirming that much of the variation in heterozygosity as well as its correlation with species richness can be explained by the observed levels of gene flow.

Correlation of genome-wide statistics with species richness

We tested for a correlation between tribe means of each genomic summary statistics (TE counts, number of gene duplications, genome-wide dN/dS ratio, per-genome heterozygosity, and f_4-ratio, as well as the heterozygosity and f_4-ratio statistics derived from simulated genome evolution) and species richness of the tribes. Estimated species richness for each tribe[15] was log-transformed to obtain normal distribution. To account for phylogenetic non-independence among the data points we calculated phylogenetic independent contrasts as implemented in the R package ape[57] (v.5.2) using the species tree presented in Fig. 1 (the time-calibrated species tree based on the maximum-likelihood tree topology) pruned to the tribe level. We then calculated Pearson's correlation coefficients for independent contrasts (through the origin) using the function *cor.table* of the R package picante[58] (v.1.8). Note that accounting for clade age of the tribes did not change the conclusions on the observed associations (results not shown).

2. Supplementary Discussion

The age of the cichlid radiation in Lake Tanganyika

Our phylogenomic divergence time estimates based on cichlid and other teleost fossils and without taking into consideration biogeographic assumptions such as the presumed ages of lakes[18] revealed an age of the cichlid radiation in Lake Tanganyika of 9.7 (± 0.5) Ma (Fig. 1), which is in line with the estimated age of Lake Tanganyika itself[23]. This suggests that the tribes Bathybatini, Benthochromini, Boulengerochromini, Cyphotilapiini, Cyprichromini, Ectodini, Eretmodini, Lamprologini, Limnochromini, Perissodini, Trematocarini, and the Tropheini evolved and diversified within Lake Tanganyika. Together, these tribes make up the adaptive radiation of cichlid fishes in Lake Tanganyika.

Three cichlid species endemic to Lake Tanganyika from three different tribes (*Coptodon rendalli*, *Oreochromis tanganicae*, and *Tylochromis polylepis*) are not part of the evolutionary radiation of cichlid fishes in this lake (Fig. 1). Earlier studies[19,22,124] as well as our own time-calibrated phylogenomic analyses support the interpretation that these species are secondary colonisers to Lake Tanganyika: First, the three tribes to which these species belong (Coptodonini, Oreochromini, and Tylochromini) are not the most closely-related lineages to the cichlid radiation in Lake Tanganyika. Second, our estimations of the divergence times of these tribes are older than the age of Lake Tanganyika, ranging from 12.4 Ma (Coptodonini) to 29.5 Ma (Tylochromini) (Extended Data Fig. 1). Finally, these tribes contain 18-37 species each, of which all but one species each occur only outside of Lake Tanganyika, and the single Tanganyikan representatives are phylogenetically deeply nested within their respective tribe.

Phylogenetic inference

We applied three complementary strategies to reconstruct the phylogenetic relationships among all species belonging to the adaptive radiation of cichlid fishes in Lake Tanganyika (that is, all cichlid species occurring in the lake, except *C. rendalli*, *O. tanganicae*, and *T. polylepis*; see above) from the genome-wide data and time-calibrated the resulting phylogenetic hypotheses using a relaxed-clock model. More specifically, we (*i*) inferred a maximum-likelihood (ML) phylogeny with RAxML using 3,630,997 SNPs; (*ii*) constructed a species tree based on 1,272 genomic regions with ASTRAL; and (*iii*) applied the multi-species coalescent model implemented in SNAPP using genome-wide biallelic SNPs. In addition, we applied a quartet inference approach to the SNP data and calculated a maximum-likelihood phylogeny on the basis of the mitochondrial genomes.

The phylogenetic hypotheses based on genome-wide data (ML, Fig. 1, Extended Data Fig. 2; ASTRAL, Extended Data Fig. 3; SNAPP, Extended Data Fig. 4) were largely congruent with each other and shared a majority of the internal nodes: 217 nodes (out of 264) were shared between ML and SNAPP (>82%, Robinson-Foulds distance: 94), 222 between ML and ASTRAL (>84%, Robinson-Foulds distance: 84), and 207 between SNAPP and ASTRAL (>78%, Robinson-Foulds distance: 114). Also, the quartet inference topology was rather similar to the ML, ASTRAL, and SNAPP trees (200 shared nodes with ML, Robinson-Foulds distance: 126). The topology based on the mitochondrial genomes (Supplementary Fig. 2) was more distinct, sharing 101 nodes with ML (>38%, Robinson-Foulds distance: 324), 97 with ASTRAL (>36%, Robinson-Foulds distance: 332), and 98 with SNAPP (>36%, Robinson-Foulds distance: 330). In only six cases, the representatives of a species were not resolved as monophyletic clade in the individual-level maximum-likelihood tree inferred from nuclear SNPs (Supplementary Fig. 1).

In all phylogenetic hypotheses – be it on the basis of genome-wide or mitochondrial sequence data – the respective members of a tribe formed a monophyletic group, supporting the taxonomic assignment of the Tanganyikan cichlid fauna into tribes[15]. The hypothesised evolutionary relationships among the tribes belonging to the radiation were identical between the ML and the SNAPP topology: A clade formed by the monotypic tribe Boulengerochromini plus the Trematocarini and Bathybatini was placed as sister group to the Lamprologini and the remaining tribes, in which the Cyphotilapiini plus the Limnochromini and Ectodini were resolved as sister group to the Cyprichromini, Benthochromini, and Perissodini and the Eretmodini plus the Haplochromini/Tropheini (Extended Data Figs. 2, 4). The only difference – at the level of phylogenetic relationships among tribes – between the ML and SNAPP topologies on the one hand and the ASTRAL tree on the other hand was that, in the ASTRAL tree (Extended Data Fig. 3), the Cyphotilapiini were placed as sister group to the derived clade of mouthbrooders containing the Limnochromini+Ectodini, the Cyprichromini, Benthochromini+Perissodini, and the Eretmodini+Haplochromini/Tropheini, whereas the Cyphotilapiini were part of a clade with the Limnochromini+Ectodini in the ML and SNAPP trees.

The hypothesised evolutionary relationships within the tribes of the adaptive radiation of cichlid fishes in Lake Tanganyika were also largely congruent between the topologies obtained with ML, ASTRAL, and SNAPP (see Extended Data Figs. 2-4). Qualitative differences between the phylogenetic hypotheses typically involved the placement of individual species relative to their congeners (for

example, *Lepidiolamprologus profundicola* in the ASTRAL topology) or particular subclades in a tribe (for example, *Reganochromis calliurus* and *Baileychromis centropomoides* were resolved as sister group to the remaining Limnochromini species in the SNAPP topology; the "*Neolamprologus brichardi/pulcher* clade" was placed as sister to the clade containing *Telmatochromis* in the ML topology). The relative placement to one another of some *Xenotilapia* and *Petrochromis* species differed among the three topologies as well.

In the maximum-likelihood phylogeny on the basis of the mitochondrial genomes (Supplementary Fig. 2), the monotypic Boulengerochromini were placed as sister lineages to all remaining tribes of the radiation (albeit bootstrap node support for these remaining tribes was only 79), in which the Trematocarini+Bathybatini were resolved as sister group to all other tribes. Among these, the Eretmodini formed the sister group to the Limnochromini and a clade in which the Cyphotilapiini were placed as sister clade to the Ectodini plus a clade formed by the Cyprichromini, Perissodini, and Benthochromini, and the Haplochromini/Tropheini. Thus, the general structure of the tribal relationships was comparable between the mitochondrial phylogeny and the trees inferred from genome-wide markers, with the exception of the placement of the Eretmodini. In previous studies using smaller sets of mitochondrial markers, the Eretmodini were placed as sister lineage to the Lamprologini or as sister group to the Lamprologini and a clade of mouthbrooders (see e.g.[20,125–127]).

Taken together, the different phylogenetic hypotheses reconstructed from genome-wide data of virtually all species of the adaptive radiation of cichlid fishes in Lake Tanganyika are highly congruent, and support a common scenario of the course of the radiation as well as its timeline. All our analyses (including those involving distant outgroup species to determine the age of the radiation) support monophyly of the tribes belonging to the radiation. There is also agreement between the topologies based on genome-wide markers that 14 (out of the 57) genera of cichlid fishes in Lake Tanganyika are not monophyletic, partly reflecting convergent morphological evolution within this species flock[16], once more illustrating that taxonomic revisions are needed[15].

Stable isotopes analysis

As carbon (C) and nitrogen (N) stable isotope composition can be influenced by the varying biochemistry of the local environment, we additionally collected and analysed baseline datasets covering several trophic levels from the northern and the southern basin of the lake (see Extended Data Fig. 6a). Comparing the baseline data with the stable isotope composition of the cichlids revealed a clear trophic signal in $\delta^{15}N$ with the typical ~3‰ increase from one trophic level to the next, supporting the interpretation that $\delta^{15}N$ stable isotopes values can be used as a proxy for the trophic level in Lake Tanganyika. Likewise, the $\delta^{13}C$ stable isotope values clearly discriminate between pelagic and littoral baseline samples as well as between pelagic and littoral cichlids (see Extended Data Fig. 6a).

When testing for a general trend in stable isotope composition along the latitudinal and longitudinal gradient of the sampling locations with species as additional covariate we found a significant effect for of the sampling locality ($\delta^{15}N$: $F_{latitude} = 12.92$, $P_{latitude} < 0.001$, $F_{longitude} = 749.7$, $P_{longitude} < 0.001$; $\delta^{13}C$: $F_{latitude} = 0.087$, $P_{latitude} = 0.77$, $F_{longitude} = 328.3$, $P_{longitude} < 0.001$). Likewise, when we used the ecological categories as covariate the sampling locality showed, in most cases, a significant effect in the multiple

regression model ($\delta^{15}N$: $F_{latitude} = 4.46$, $P_{latitude} = 0.035$, $F_{longitude} = 258.86$, $P_{longitude} < 0.001$; $\delta^{13}C$: $F_{latitude} = 0.016$, $P_{latitude} = 0.9$, $F_{longitude} = 59.2$, $P_{longitude} < 0.001$). However, only very little variance was explained by the sampling locations in the models ($\delta^{15}N$: latitude = 0.07%, longitude = 4.27%; $\delta^{13}C$: latitude = 0.0003%, longitude = 1.26%). Importantly, the latitude and longitude of the sampling locality showed a significant interaction with species ($\delta^{15}N$: $F_{latitude:species} = 3.3$, $P_{latitude:species} < 0.001$, $F_{longitude:species} = 5.04$, $P_{longitude:species} < 0.001$; $\delta^{13}C$: $F_{latitude:species} = 2.67$, $P_{latitude:species} < 0.001$, $F_{longitude:species} = 3.70$, $P_{longitude:species} < 0.001$) and ecological category ($\delta^{15}N$: $F_{latitude:trophic} = 7.32$, $P_{latitude: trophic} < 0.001$, $F_{longitude:trophic} = 7.71$, $P_{longitude:trophic} < 0.001$; $\delta^{13}C$: $F_{latitude:habitat} = 4.97$, $P_{latitude:habitat} < 0.001$, $F_{longitude:habitat} = 12.92$, $P_{longitude:habitat} < 0.001$). Hence, no general correction for sampling locality over the dataset is applicable to the stable isotope compositions.

Testing for a difference in stable isotope compositions between northern and southern samples across a set of species representing all trophic levels and occurring along the entire spectrum of the benthic-pelagic axis revealed no difference ($\delta^{15}N$: t = -1.56, DF = 35.1, $P = 0.13$; $\delta^{13}C$: t = 1.61, DF = 33.5, $P = 0.12$), suggesting that across contrasting ecologies the biogeochemistry is sufficiently similar among sampling locations in Lake Tanganyika to interpret the $\delta^{15}N$ and $\delta^{13}C$ stable isotope values with respect to the trophic axis and the benthic-pelagic axis.

Taken together, we conclude that, while the biogeochemical variance across sampling locations might add some additional variance to the data, the ecological signal clearly dominates in the stable isotope data. Importantly, we confirm that, across our cichlid dataset, the $\delta^{15}N$ value informs about the relative trophic level of the species and the $\delta^{13}C$ value can be interpreted as the relative position along the benthic-pelagic axis.

Trait space occupation per tribe

When comparing the size of morpho- and ecospace per tribe, we found a strong correlation between occupied trait space and species richness of a tribe (Extended Data Figs. 6, 7). To test if this pattern is mainly driven by sample size, we repeated the per-tribe morpho- and ecospace occupation analyses using a resampling strategy. We sampled 1,000 times four species per tribe and re-calculated the trait space occupation. This confirmed the positive association of morphospace occupation and tribe size for upper oral jaw morphology (Pearson's $r = 0.64$, df = 9, $P = 0.04$) and lower pharyngeal jaw shape (Pearson's $r = 0.69$, df = 9, $P = 0.02$). For body shape, the pattern was only confirmed when excluding the Limnochromini (Pearson's $r = 0.69$, df = 9, $P = 0.03$), which occupy a very large fraction of the morphospace relative to their number of species (Extended Data Figs. 6, 7). For the ecospace occupation, the resampling procedure using four species was only possible for 10 tribes (due to missing data for one of the Cyphotilapiini), which confirms the general pattern (Pearson's $r = 0.60$, df = 8, $P = 0.06$). Overall, this supports that larger tribes occupy larger areas of the morphospace – irrespective of sample size.

Late burst in diversification of pigmentation pattern

For pigmentation pattern we detected a pulse of diversification along with increasing evolutionary rates late in the radiation. This signal could potentially also occur under a scenario of a rapid turnover in this

trait, characterised by high evolutionary rates and convergent evolution. Colour patterns are known to evolve rapidly in cichlids[26,64]. However, the Ornstein-Uhlenbeck model of trait evolution which models this scenario has very low support given the data (Extended Data Fig. 8d, e). Moreover, our analysis showed that two tribes (Ectodini and Limnochromini) stand out with constantly low rates of trait evolution in pigmentation pattern throughout – suggesting that high turnover rate in this trait is not a general feature of the cichlid radiation in Lake Tanganyika. In spite of this, a late burst emerged as the general trend of trait evolution for pigmentation pattern for the remaining tribes (Fig. 3).

Signals of past introgression

To assess the extent of genetic introgression among cichlids of the radiation in Lake Tanganyika, we calculated the f_4-ratio values as well as Patterson's D statistic and its associated P-values (based on block jack-knifing) across all combinations of trios of species within the radiation (n = 265 species), resulting in 3,066,580 values for each statistic. The outgroup was in all cases fixed (*T. sparrmanii*).

We focus on the f_4-ratios because this statistic is designed to estimate the 'admixture fraction' and therefore is a suitable measure of the level of gene flow, especially when applied within the cichlid tribes of Lake Tanganyika, where the effect of any variation in overall substitution rates is unlikely to be pronounced. The distributions of all the f_4-ratio values within tribes were therefore chosen for correlation with species richness of tribes (Fig. 4e), and also served as a basis for the simulations that show how the observed levels of gene flow might have led to elevated heterozygosity in the more species-rich tribes (Fig. 4f).

There are a number of challenges associated with an interpretation of a system of over 3 million f_4-ratio estimates and in pinpointing specific introgression events from these results[79]. First, the f_4-ratio estimates the admixture fraction between a pair of species. However, it is based on trios of species (and an outgroup), and the value of the estimate depends on which other species is included in the trio and on the assumed relationship among the species in each trio. We constrained the relationships using the maximum-likelihood tree topology (Fig. 1). Therefore, the estimates rely on this phylogeny being correct. Second, a single ancestral introgression event can be responsible for many elevated f_4-ratios between multiple taxa which share drift (i.e. branches on the true phylogeny).

In Extended Data Fig. 10 we show, for each pair of species, the maximum value of the statistic across all trios in which an estimate for the pair was obtained. Therefore, in this sense we present the upper bound of the admixture fraction estimate for each pair. We show f_4-ratio values greater than 3%; the associated P-values show that the imbalance in allele sharing that is the basis of these f_4-ratio values is statistically significant ($P < 5\times10^{-5}$ after Benjamini-Hochberg correction for multiple testing). The vast majority of introgression signals are within tribes, with two exceptions: 1) between Cyphotilapiini and Limnochromini (where f_4-ratio values are around 8%) and 2) between the group comprising Limnochromini+Ectodini and the tribes Haplochromini/Tropheini, Benthochromini, and Perissodini (f_4-ratios around 4 to 5%). The uniformity of these signals across all pairs of species from these groups suggests that the gene flow is likely to have happened between the common ancestors of these tribes/groups. Interestingly, the f_4-ratios do not exceed 3% between Cyphotilapiini and Tropheini, where gene flow evidence was reported previously by Irisarri *et al.*[22] on the basis of Patterson's D statistic. In

this context we note that at the between-tribe level, the *D* statistic is more likely to be influenced by variation in overall substitution rates[128], which we also observed in our dataset.

We also see signals of introgression between Tropheini and many of the haplochromine species sampled from rivers outside of Lake Tanganyika, with admixture fractions estimated by f_4-ratios ranging between 3 and 8%. These signals come mainly in two blocks, suggesting introgression between the common ancestor of all Tropheini and the common ancestors of two riverine haplochromine lineages.

The signatures of introgression within tribes are numerous. There are 229 pairs of species with admixture proportion estimates of more than 10% (144 in Lamprologini, 43 in Ectodini, 19 in Tropheini, 11 in Cyprichromini, two in Perissodini, two in Benthochromini, two in Bathybatini, and six among the riverine haplochromines). Some of these signals confirm previous reports (e.g. strong introgression among the 'Princess cichlid' species[129]), but many of the putative hybridisation events are new findings, which we envisage as a starting point for future, more detailed, investigations.

3. References

82. Li, H. *et al.* The Sequence Alignment/Map format and SAMtools. *Bioinformatics* **25**, 2078–2079 (2009).
83. Quinlan, A. R. & Hall, I. M. BEDTools: a flexible suite of utilities for comparing genomic features. *Bioinformatics* **26**, 841–842 (2010).
84. Durand, E. Y., Patterson, N., Reich, D. & Slatkin, M. Testing for ancient admixture between closely related populations. *Mol. Biol. Evol.* **28**, 2239–2252 (2011).
85. Konings, A. *Tanganyika Cichlids in their natural habitat*. (Cichlid Press, 2015).
86. Büscher, H. H. *Neolamprologus cancellatus*, eine Chimäre aus dem Tanganjikasee. *DCG-Informationen* **50**, 282–288 (2019).
87. Zerbino, D. R. *et al.* Ensembl 2018. *Nucleic Acids Res.* **46**, D754–D761 (2017).
88. Altschul, S. F., Gish, W., Miller, W., Myers, E. W. & Lipman, D. J. Basic local alignment search tool. *J. Mol. Biol.* **215**, 403–410 (1990).
89. Wainwright, P. C. *et al.* Evolution of pharyngognathy: a phylogenetic and functional appraisal of the pharyngeal jaw key innovation in labroid fishes and beyond. *Syst. Biol.* **61**, 1001–1027 (2012).
90. Malmstrøm, M. *et al.* Evolution of the immune system influences speciation rates in teleost fishes. *Nat. Genet.* **48**, 1204–1210 (2016).
91. Reichwald, K. *et al.* Insights into sex chromosome evolution and aging from the genome of a short-lived fish. *Cell* **163**, 1527–1538 (2015).
92. Conte, M. A. *et al.* Chromosome-scale assemblies reveal the structural evolution of African cichlid genomes. *Gigascience* **8**, 288 (2019).
93. Meyer, B. S., Matschiner, M. & Salzburger, W. Disentangling incomplete lineage sorting and introgression to refine species-tree estimates for Lake Tanganyika cichlid fishes. *Syst. Biol.* **66**, 531–550 (2017).
94. Kucuk, E. *et al.* Kollector: transcript-informed, targeted de novo assembly of gene loci. *Bioinformatics* **33**, 1782–1788 (2017).
95. Allen, J. M., LaFrance, R., Folk, R. A., Johnson, K. P. & Guralnick, R. P. aTRAM 2.0: An improved, flexible locus assembler for NGS data. *Evol. Bioinforma.* **14**, 1176934318774546 (2018).
96. Musilova, Z. *et al.* Vision using multiple distinct rod opsins in deep-sea fishes. *Science* **364**, 588–592 (2019).
97. Katoh, K. & Standley, D. M. MAFFT multiple sequence alignment software version 7: improvements in performance and usability. *Mol. Biol. Evol.* **30**, 772–780 (2013).
98. Criscuolo, A. & Gribaldo, S. BMGE (Block Mapping and Gathering with Entropy): a new software for selection of phylogenetic informative regions from multiple sequence alignments. *BMC Evol. Biol.* **10**, 210 (2010).
99. Jarvis, E. D. *et al.* Whole-genome analyses resolve early branches in the tree of life of modern birds. *Science* **346**, 1320–1331 (2014).
100. Leigh, J. W., Susko, E., Baumgartner, M. & Roger, A. J. Testing congruence in phylogenomic analysis. *Syst. Biol.* **57**, 104–115 (2008).

101. Drummond, A. J., Ho, S. Y. W., Philips, M. J. & Rambaut, A. Relaxed phylogenetics and dating with confidence. *PLOS Biol.* **4**, e88 (2006).

102. Bouckaert, R. R. & Drummond, A. J. bModelTest: Bayesian phylogenetic site model averaging and model comparison. *BMC Evol. Biol.* **17**, 42 (2017).

103. Springer, M. S. & Gatesy, J. On the importance of homology in the age of phylogenomics. *Syst. Biodivers.* **16**, 210–228 (2018).

104. López-Fernández, H., Winemiller, K. O. & Honeycutt, R. L. Multilocus phylogeny and rapid radiations in Neotropical cichlid fishes (Perciformes: Cichlidae: Cichlinae). *Mol. Phylogenet. Evol.* **55**, 1070–1086 (2010).

105. Swofford, D. L. PAUP*. Phylogenetic analysis using parsimony (*and other methods). Version 4. (2003).

106. Mailund, T., Munch, K. & Schierup, M. H. Lineage sorting in apes. *Annu. Rev. Genet.* **48**, 519–535 (2014).

107. Arcila, D. *et al.* Genome-wide interrogation advances resolution of recalcitrant groups in the tree of life. *Nat. Ecol. Evol.* **1**, 1–10 (2017).

108. Barth, J. *et al.* Stable species boundaries despite ten million years of hybridization in tropical eels. *Nat. Commun.* **11,** 1433 (2020).

109. Betancur-R, R. *et al.* Phylogenetic classification of bony fishes. *BMC Evol. Biol.* **17**, 162 (2017).

110. Green, R. E. *et al.* A draft sequence of the Neandertal genome. *Science* **328**, 710–722 (2010).

111. Lanfear, R., Frandsen, P. B., Wright, A. M., Senfeld, T. & Calcott, B. PartitionFinder 2: New methods for selecting partitioned models of evolution for molecular and morphological phylogenetic analyses. *Mol. Biol. Evol.* **34**, 772–773 (2017).

112. Gernhard, T. The conditioned reconstructed process. *J. Theor. Biol.* **253**, 769–778 (2008).

113. Felsenstein, J. Phylogenies from restriction sites: A maximum-likelihood approach. *Evolution (N. Y).* **46**, 159–173 (1992).

114. Liu, L., Xi, Z., Wu, S., Davis, C. C. & Edwards, S. V. Estimating phylogenetic trees from genome-scale data. *Ann. N. Y. Acad. Sci.* **1360**, 36–53 (2015).

115. Robinson, D. F. & Foulds, L. R. Comparison of Phylogenetic Trees. *Math. Biosci.* **51**, 131–147 (1981).

116. Huerta-Cepas, J., Serra, F. & Bork, P. ETE 3: Reconstruction, analysis, and visualization of phylogenomic data. *Mol. Biol. Evol.* **33**, 1635–1638 (2016).

117. Maynard Smith, J. & Smith, N. H. Detecting recombination from gene trees. *Mol. Biol. Evol.* **15**, 590–599 (1998).

118. Stange, M., Sánchez-Villagra, M. R., Salzburger, W. & Matschiner, M. Bayesian divergence-time estimation with genome-wide SNP data of sea catfishes (Ariidae) supports Miocene closure of the Panamanian Isthmus. *Syst. Biol.* **67**, 681–699 (2018).

119. Rambaut, A., Drummond, A. J., Xie, D., Baele, G. & Suchard, M. A. Posterior summarization in Bayesian phylogenetics using Tracer 1.7. *Syst. Biol.* **67**, 901–904 (2018).

120. Chifman, J. & Kubatko, L. S. Quartet inference from SNP data under the coalescent model. *Bioinformatics* **30**, 3317–3324 (2014).

121. Hahn, C., Bachmann, L. & Chevreux, B. Reconstructing mitochondrial genomes directly from genomic next-generation sequencing reads--a baiting and iterative mapping approach. *Nucleic Acids Res.* **41**, e129--e129 (2013).

122. Chevreux, B., Wetter, T. & Suhai, S. Genome sequence assembly using trace signals and additional sequence information. *Comput. Sci. Biol. Proc. Ger. Conf. Bioinforma.* 1–12 (1999).

123. Coop, G. & Przeworski, M. An evolutionary view of human recombination. *Nat. Rev. Genet.* **8**, 23–34 (2007).

124. Dunz, A. R. & Schliewen, U. K. Molecular phylogeny and revised classification of the haplotilapiine cichlid fishes formerly referred to as 'Tilapia'. *Mol. Phylogenet. Evol.* **68**, 64–80 (2013).

125. Kocher, T. D., Conroy, J. A., McKaye, K. R., Stauffer, J. R. & Lockwood, S. F. Evolution of NADH dehydrogenase subunit 2 in east african cichlid fish. *Molecular Phylogenetics and Evolution* vol. 4 420–432 (1995).

126. Day, J. J., Cotton, J. A. & Barraclough, T. G. Tempo and mode of diversification of Lake Tanganyika cichlid fishes. *PLoS One* **3**, e1730 (2008).

127. Meyer, B. S. *et al.* Back to Tanganyika: A case of recent trans-species-flock dispersal in East African haplochromine cichlid fishes. *R. Soc. Open Sci.* **2**, 1–5 (2015).

128. Pease, J. B. & Hahn, M. W. Detection and Polarization of Introgression in a Five-Taxon Phylogeny. *Syst. Biol.* **64**, 651–662 (2015).

129. Gante, H. F. *et al.* Genomics of speciation and introgression in Princess cichlid fishes from Lake Tanganyika. *Mol. Ecol.* **25**, 6143–6161 (2016).

4. Supplementary Figures and Tables

Supplementary Fig. 1 continues on the next page

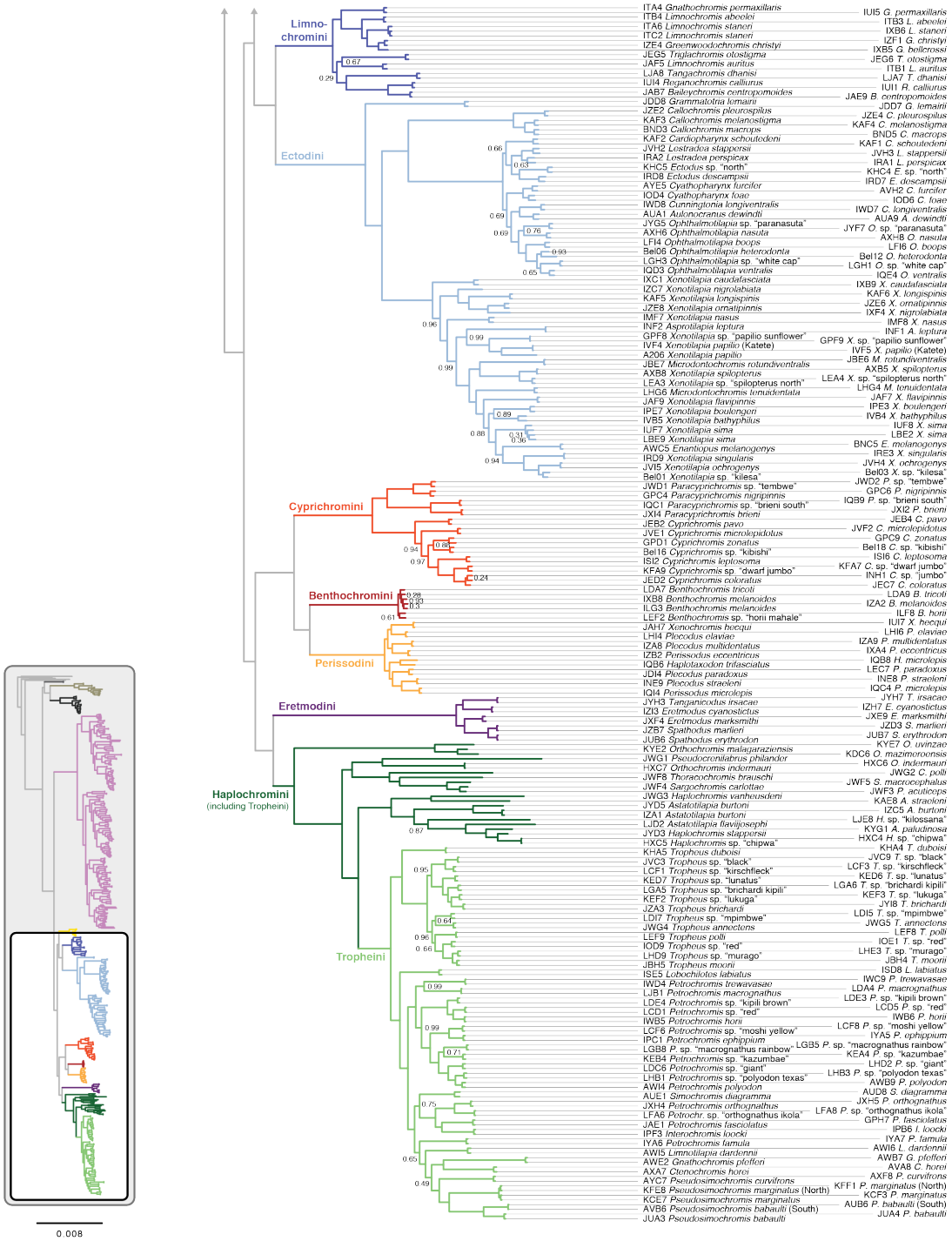

Supplementary Fig. 1 | Individual-level phylogeny for the cichlid adaptive radiation in Lake Tanganyika. Maximum-likelihood tree inferred from nuclear SNPs. Node labels indicate the proportion of data subsets supporting a clade (equal to 1 for all nodes without labels).

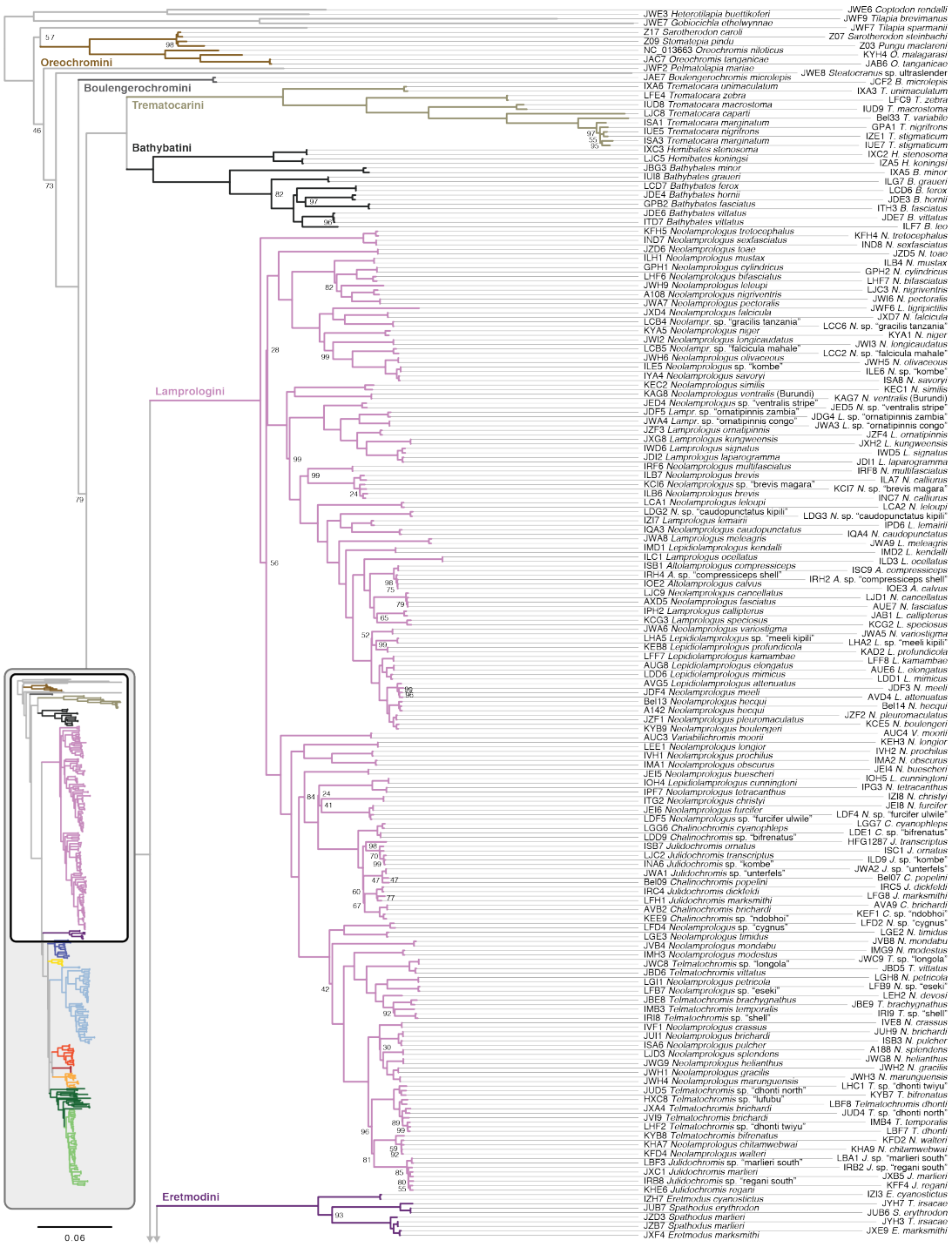

Supplementary Fig. 2 continues on the next page

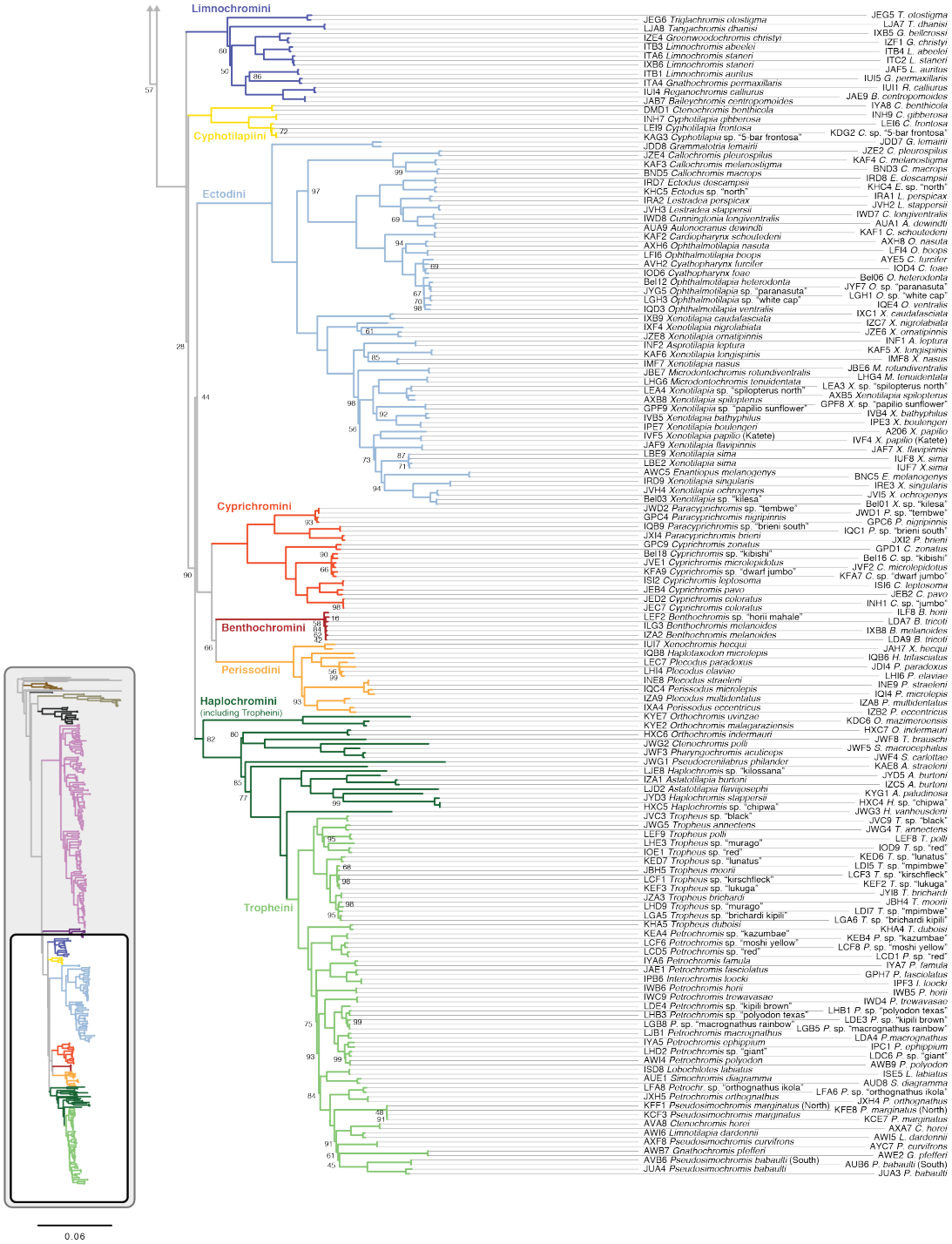

Supplementary Fig. 2 | Individual-level mitochondrial phylogeny for the cichlid adaptive radiation in Lake Tanganyika. Maximum-likelihood tree inferred from mitochondrial genomes. Node labels represent bootstrap values (100 for all nodes without labels).

Supplementary Table 1 | Sample size information per species. For each analysis the total sample size is given whereas the number in brackets indicates the number of specimens used uniquely for the respective analysis. All genomes and raw sequences are available at NCBI under the BioProject accession number PRJNA550295. A full list of individual specimen vouchers including details on sampling location is provided as Supplementary Table 2. AMNH = American Museum of Natural History (New York, USA); MRAC = Royal Museum for Central Africa (Tervuren, Belgium); HHB = Private collection of one of the authors, H.H.B.

Species abbr.	Full name	Tribe	Origin	Sample source	Stable isotope	Body & OJ morphology	LPJ shape	Pigmentation pattern	Genomes	Total specimens	Comment	Read depth after mapping to the Nile Tilapia reference genome (mean|median)
Batfas	*Bathybates fasciatus*	Bathybatini	LT	own collection	10	8	5	5	2 (1)	11	LT radiation	GPB2: 7.17\7; ITH3: 10.79\12
Batfer	*Bathybates ferox*	Bathybatini	LT	own collection	10	10	5	5	2	10	LT radiation	LCD6: 6.42\6; LCD7: 6.07\6
Batgra	*Bathybates graueri*	Bathybatini	LT	own collection	10	10	5	5	2 (2)	12	LT radiation	ILG7: 9.42\10; IUI8: 7.23\7
Bathor	*Bathybates hornii*	Bathybatini	LT	own collection	1	1	1	1	2 (2)	3	LT radiation	JDE3: 8.09\8; JDE4: 10.61\11
Batleo	*Bathybates leo*	Bathybatini	LT	own collection	10 (3)	7	5	5	1 (1)	11	LT radiation	ILF7: 6.73\7
Batmin	*Bathybates minor*	Bathybatini	LT	own collection	10	10	5	5	2 (1)	11	LT radiation	IXA5: 7.45\7; IBG3: 6.96\7
Batvit	*Bathybates vittatus*	Bathybatini	LT	own collection	10 (3)	5	5	5	3 (3)	13	LT radiation	ITD7: 7.43\7; JDE6: 9.41\10; JDE7: 9.36\9
HemstZ	*Hemibates koningsi*	Bathybatini	LT	own collection & F. Schedel	2	2	2	2	2 (1)	3	LT radiation	IZA5: 12.52\14; LJC5: 8.82\7
Hemste	*Hemibates stenosoma*	Bathybatini	LT	own collection	9	9	5	5	2 (2)	11	LT radiation	IXC2: 6.85\7; IXC3: 7.11\7
Benhor	*Benthochromis horii*	Benthochromini	LT	own collection	10	10	5	5	1 (1)	11	LT radiation	ILF8: 9.0\9
Benmel	*Benthochromis melanoides*	Benthochromini	LT	own collection	10	10	5	5	3 (3)	13	LT radiation	ILG3: 9.14\9; IXB8: 7.35\7; IZA2: 7.37\7
BenhoM	*Benthochromis* sp. "horii mahale"	Benthochromini	LT	own collection	10	10	5	5	1	10	LT radiation	LEF2: 11.86\13
Bentri	*Benthochromis tricoti*	Benthochromini	LT	own collection	10	10	5	5	2	10	LT radiation	LDA7: 7.43\7; LDA9: 7.83\8
Boumic	*Boulengerochromis microlepis*	Boulengerochromini	LT	own collection	10	10	5	5	2 (2)	12	LT radiation	IAE7: 14.67\16; JCF2: 15.43\17
Ctenben	*Ctenochromis benthicola*	Cyphotilapiini	LT	own collection	0	6 (1)	5	0	2 (2)	8	LT radiation	DMD1: 8.43\8; IYA8: 7.35\7
Cphfro	*Cyphotilapia frontosa*	Cyphotilapiini	LT	own collection	10	10	5	4	2	10	LT radiation	LEI6: 7.05\7; LEI9: 6.98\7
Cphgib	*Cyphotilapia gibberosa*	Cyphotilapiini	LT	own collection	10	10	5	5	2 (2)	12	LT radiation	INH7: 10.12\10; INH9: 9.6\10
Cphfr5	*Cyphotilapia* sp. "5-bar frontosa"	Cyphotilapiini	LT	own collection	10	10	5	3	2 (2)	12	LT radiation	KAG3: 10.33\11; KDG2: 13.12\14
Cypcol	*Cyprichromis coloratus*	Cyprichromini	LT	own collection	10	10	5	5	2 (1)	11	LT radiation	JEC7: 15.66\18; JED2: 14.4\16
Cyplep	*Cyprichromis leptosoma*	Cyprichromini	LT	own collection	10	10	5	5	2 (2)	12	LT radiation	ISI2: 8.9\9; ISI6: 8.08\8
Cypmic	*Cyprichromis microlepidotus*	Cyprichromini	LT	own collection	10	10	5	5	2 (2)	12	LT radiation	JVE1: 6.1\6; JVF2: 6.7\7
Cyppav	*Cyprichromis pavo*	Cyprichromini	LT	own collection	10	10	5	5	2 (2)	12	LT radiation	JEB2: 9.01\9; JEB4: 7.66\7
Cypdwj	*Cyprichromis* sp. "dwarf jumbo"	Cyprichromini	LT	own collection	10	10	5	5	2 (2)	12	LT radiation	KFA7: 12.84\14; KFA9: 10.64\11
Cypkan	*Cyprichromis* sp. "jumbo"	Cyprichromini	LT	own collection	10	10	5	5	1	10	LT radiation	INH1: 9.78\10
Cypkib	*Cyprichromis* sp. "kibishi"	Cyprichromini	LT	MRAC	0	0	0	0	2 (2)	2	LT radiation	Bel16: 6.63\6; Bel18: 7.33\7
Cypzon	*Cyprichromis zonatus*	Cyprichromini	LT	own collection	10	10	5	5	2	10	LT radiation	GPC9: 9.73\10; GPD1: 6.35\6
PcytbrN	*Paracyprichromis brieni*	Cyprichromini	LT	own collection	10	10	5	5	2 (2)	12	LT radiation	JXI2: 7.1\7; JXI4: 6.03\6
Pcynig	*Paracyprichromis nigripinnis*	Cyprichromini	LT	own collection	10	10	5	5	2 (2)	12	LT radiation	GPC4: 12.88\14; GPC6: 6.45\6
Pcybri	*Paracyprichromis* sp. "brieni south"	Cyprichromini	LT	own collection	10	10	5	5	2 (2)	12	LT radiation	IQB9: 8.27\8; IQC1: 5.99\6
Pcytem	*Paracyprichromis* sp. "tembwe"	Cyprichromini	LT	HHB	0	0	0	0	2 (2)	2	LT radiation	JWD1: 16.84\19; JWD2: 16.05\18
Asplep	*Asprotilapia leptura*	Ectodini	LT	own collection	10	10	5	5	2 (2)	12	LT radiation	INF1: 9.8\10; INF2: 14.13\16
Auldew	*Aulonocranus dewindti*	Ectodini	LT	own collection	10	10	5	5	2 (2)	12	LT radiation	AUA1: 7.93\8; AUA9: 7.81\8
Calmac	*Callochromis macrops*	Ectodini	LT	own collection	10	10	5	5	2 (2)	12	LT radiation	BND3: 7.9\8; BND5: 8.5\9
Calmel	*Callochromis melanostigma*	Ectodini	LT	own collection	10	10	5	5	2 (2)	12	LT radiation	KAF3: 7.6\8; KAF4: 7.64\8
Calple	*Callochromis pleurospilus*	Ectodini	LT	own collection	10	10	5	5	2 (2)	12	LT radiation	JZE2: 8.02\8; JZE4: 14.8\17
Carsch	*Cardiopharynx schoutedeni*	Ectodini	LT	own collection	10	10	5	2	2 (2)	12	LT radiation	KAF1: 7.3\7; KAF2: 12.46\14
Cunlon	*Cunningtonia longiventralis*	Ectodini	LT	own collection	10	10	5	5	2 (2)	12	LT radiation	IWD7: 6.48\6; IWD8: 7.71\8
Cyafoa	*Cyathopharynx foae*	Ectodini	LT	own collection	10	10	5	5	2 (2)	12	LT radiation	IOD4: 6.88\7; IOD6: 5.79\5
Cyafur	*Cyathopharynx furcifer*	Ectodini	LT	own collection	10	10	5	5	2 (2)	12	LT radiation	AVH2: 8.11\8; AYE5: 8.2\8
Ectdes	*Ectodus descampsii*	Ectodini	LT	own collection	10	10	5	3	2 (2)	12	LT radiation	IRD7: 9.87\10; IRD8: 6.84\7
EctspN	*Ectodus* sp. "north"	Ectodini	LT	own collection	10	10	5	3	2 (2)	12	LT radiation	KHC4: 6.7\7; KHC5: 6.55\6
Enamel	*Enantiopus melanogenys*	Ectodini	LT	own collection	10	10	5	5	2 (2)	12	LT radiation	AWC5: 8.35\8; BNC5: 9.07\9
Gralem	*Grammatotria lemairii*	Ectodini	LT	own collection	10 (1)	9	5	5	2 (2)	12	LT radiation	JDD7: 12.78\14; JDD8: 7.04\7
Lesper	*Lestradea perspicax*	Ectodini	LT	own collection	10	10	5	5	2 (2)	12	LT radiation	IRA1: 6.01\6; IRA2: 8.29\8
Lessta	*Lestradea stappersii*	Ectodini	LT	own collection	10	10	5	5	2 (2)	12	LT radiation	JVH2: 6.8\7; JVH3: 5.54\5
Mdcrot	*Microdontochromis rotundiventralis*	Ectodini	LT	own collection	10	10	5	5	2 (2)	12	LT radiation	JBE6: 7.47;.JBE7: 12.3\14
Mdcten	*Microdontochromis tenuidentata*	Ectodini	LT	own collection	10	10	5	5	2 (2)	12	LT radiation	LHG4: 9.78\10; LHG6: 11.17\12
Ophboo	*Ophthalmotilapia boops*	Ectodini	LT	own collection	10	10	5	5	2	10	LT radiation	LFI4: 7.64\8; LFI6: 7.41\7
Ophhet	*Ophthalmotilapia heterodonta*	Ectodini	LT	own collection & MRAC	0	1	0	1	2 (2)	3	LT radiation	Bel06: 6.54\6; Bel12: 7.2\7
Ophnas	*Ophthalmotilapia nasuta*	Ectodini	LT	own collection	10	10	5	5	2 (2)	12	LT radiation	AXH6: 8.05\8; AXH8: 8.39\8
Ophpar	*Ophthalmotilapia* sp. "paranasuta"	Ectodini	LT	own collection	10	10	5	5	2 (2)	12	LT radiation	JYF7: 9.87\10; JYG5: 7.98\8
Ophwhi	*Ophthalmotilapia* sp. "white cap"	Ectodini	LT	own collection	10	9	5	5	2	10	LT radiation	LGH1: 8.25\8; LGH3: 7.51\7
Ophven	*Ophthalmotilapia ventralis*	Ectodini	LT	own collection	10	10	5	5	2 (2)	12	LT radiation	IQD3: 7.78\8; IQE4: 7.13\7
Xenbat	*Xenotilapia bathyphilus*	Ectodini	LT	own collection	10	10	5	5	2 (2)	12	LT radiation	IVB4: 8.98\9; IVB5: 7.15\7
Xenbou	*Xenotilapia boulengeri*	Ectodini	LT	own collection	10	10	5	5	2 (2)	12	LT radiation	IPE3: 7.56\7; IPE7: 7.34\7
Xencau	*Xenotilapia caudafasciata*	Ectodini	LT	own collection	10	9	5	5	2 (2)	12	LT radiation	IXB9: 7.85\8; IXC1: 7.27\7
Xenfla	*Xenotilapia flavipinnis*	Ectodini	LT	own collection	10	10	5	5	2 (2)	12	LT radiation	JAF7: 14.97\17; JAF9: 13.26\15
Xenlon	*Xenotilapia longispinis*	Ectodini	LT	own collection	10	10	5	5	2 (2)	12	LT radiation	KAF5: 8.69\9; KAF6: 9.6\10
Xennas	*Xenotilapia nasus*	Ectodini	LT	own collection	10	10	5	5	2 (2)	12	LT radiation	IMF7: 6.93\7; IMF8: 11.1\12
XenniS	*Xenotilapia nigrolabiata*	Ectodini	LT	own collection	10	10	5	5	2 (1)	11	LT radiation	IXF4: 14.05\16; IZC7: 7.51\7
Xenoch	*Xenotilapia ochrogenys*	Ectodini	LT	own collection	10	10	5	5	2 (2)	12	LT radiation	JVH4: 9.13\9; JVI5: 10.73\12
Xenorn	*Xenotilapia ornatipinnis*	Ectodini	LT	own collection	10	10	5	3	2 (2)	12	LT radiation	JZE6: 8.5\9; JZE8: 7.9\18
XenorS	*Xenotilapia ornatipinnis* (South)	Ectodini	LT	own collection	1	1	1	0	0	1	LT radiation	
XenpaK	*Xenotilapia papilio*	Ectodini	LT	HHB	10 (4)	4	5	0	1 (1)	11	LT radiation	A206: 9.77\9
Xenpap	*Xenotilapia papilio* (Katete)	Ectodini	LT	own collection	10	10	5	5	2 (2)	12	LT radiation	IVF4: 11\12; IVF5: 6.57\6
Xensim	*Xenotilapia sima*	Ectodini	LT	own collection	10	10	5	5	4 (2)	12	LT radiation	IUF7: 8.56\9; IUF8: 8.66\9; LBE2: 8.69\9; LBE9: 6.79\7
Xensin	*Xenotilapia singularis*	Ectodini	LT	own collection	10	10	5	5	2	10	LT radiation	IRD9: 7.34\7; IRE3: 6.79\6
Xenkil	*Xenotilapia* sp. "kilesa"	Ectodini	LT	MRAC	0	0	0	0	2 (2)	2	LT radiation	Bel01: 10.43\11; Bel03: 5.99\6
Xensun	*Xenotilapia* sp. "papilio sunflower"	Ectodini	LT	own collection	10	10	5	5	2 (2)	12	LT radiation	GPF8: 7.28\7; GPF9: 8.1\8
XenspN	*Xenotilapia* sp. "spilopterus north"	Ectodini	LT	own collection	10	10	5	0	2 (2)	12	LT radiation	LEA3: 6.78\7; LEA4: 6.59\6
Xenspi	*Xenotilapia spilopterus*	Ectodini	LT	own collection	10	10	5	5	2 (2)	12	LT radiation	AXB5: 7.69\8; AXB8: 7.6\8
Ereoya	*Eretmodus cyanostictus*	Eretmodini	LT	own collection	10	10	5	4	2 (2)	12	LT radiation	IZH7: 18.76\22; IZI3: 12.02\13
Eremar	*Eretmodus marksmithi*	Eretmodini	LT	own collection	10	10	5	3	2 (2)	12	LT radiation	JXE9: 10.01\11; JXF4: 6.34\6
Spaery	*Spathodus erythrodon*	Eretmodini	LT	own collection	10	10	5	5	2 (2)	12	LT radiation	JUB6: 7.13\7; JUB7: 8.44\9
Spamar	*Spathodus marlieri*	Eretmodini	LT	own collection	10	10	5	5	2 (2)	12	LT radiation	JZE7: 6.16\6; JZD3: 10.18\11
Tanirs	*Tanganicodus irsacae*	Eretmodini	LT	own collection	10	10	5	5	2 (2)	12	LT radiation	JYH3: 9.71\10; JYH7: 7.17\7
Altcal	*Altolamprologus calvus*	Lamprologini	LT	own collection	10	10	5	5	2 (2)	12	LT radiation	IOE2: 7.92\8; IOE3: 9.38\10
Altcom	*Altolamprologus compressiceps*	Lamprologini	LT	own collection	10	10	5	5	2 (2)	12	LT radiation	ISB1: 8.29\8; ISC9: 9.3\10
Altshe	*Altolamprologus* sp. "compressiceps shell"	Lamprologini	LT	own collection	10	10	5	5	2 (2)	12	LT radiation	IRH2: 5.78\5; IRH4: 6.04\6
Chabri	*Chalinochromis brichardi*	Lamprologini	LT	own collection	10	10	5	5	2 (2)	12	LT radiation	AVA9: 7.76\8; AVB2: 7.5\8
Chacya	*Chalinochromis cyanophleps*	Lamprologini	LT	own collection	10	10	5	5	2	10	LT radiation	LGG6: 8.11\8; LGG7: 7.72\8
Chapop	*Chalinochromis popelini*	Lamprologini	LT	MRAC	0	0	0	0	2 (2)	2	LT radiation	Bel07: 7.68\7; Bel09: 6.9\7
Chabif	*Chalinochromis* sp. "bifrenatus"	Lamprologini	LT	own collection	10	10	5	5	2	10	LT radiation	LDD9: 7.53\8; LDE1: 7.59\8
Chando	*Chalinochromis* sp. "ndobhor"	Lamprologini	LT	own collection	10	10	5	3	2 (2)	12	LT radiation	KEE9: 7.16\7; KEF1: 7.39\7
Julcic	*Julidochromis dickfeldi*	Lamprologini	LT	own collection	10	10	5	5	2 (2)	12	LT radiation	IRC4: 10\11; IRC5: 7.3\7
Julmrk	*Julidochromis marksmithi*	Lamprologini	LT	own collection	10	9	5	5	2	10	LT radiation	LFG8: 6.77\7; LFH1: 8.69\9
JulmaN	*Julidochromis marlieri*	Lamprologini	LT	own collection	10	10	5	5	2 (2)	12	LT radiation	JXB5: 9.12\10; JXC1: 8.81\9
Julorn	*Julidochromis ornatus*	Lamprologini	LT	own collection	10	10	5	5	2 (2)	12	LT radiation	ISB7: 6.61\6; ISC1: 8.5\10
JulreK	*Julidochromis regani*	Lamprologini	LT	own collection	10	10	5	1	2 (2)	12	LT radiation	KFF4: 7.47\8; KHE6: 7.01\7
Julkom	*Julidochromis* sp. "kombe"	Lamprologini	LT	own collection	10	10	5	5	2 (2)	12	LT radiation	ILD9: 7.18\7; INA6: 6.64\6
JulmaS	*Julidochromis* sp. "marlieri south"	Lamprologini	LT	own collection	10	10	5	4	2	10	LT radiation	LBA1: 8.22\8; LBF3: 8.72\9
Julreq	*Julidochromis* sp. "regani south"	Lamprologini	LT	own collection	10	10	5	5	2 (2)	12	LT radiation	IRB2: 6.63\6; IRB8: 7.63\8
Julunt	*Julidochromis* sp. "unterfels"	Lamprologini	LT	HHB	9 (3)	5	5	0	2 (2)	11	LT radiation	JWA1: 14.33\16; JWA2: 16.05\18
Jultra	*Julidochromis transcriptus*	Lamprologini	LT	H. Gante	0	0	0	0	2 (2)	2	LT radiation	HFG1287: 11\12; LJC2: 9.91\10
Lamcal	*Lamprologus callipterus*	Lamprologini	LT	own collection	10	10	5	4	2 (2)	12	LT radiation	IPH2: 10.05\11; JAB1: 7.77\8
Lamfin	*Lamprologus finalimus*	Lamprologini	LT	AMNH	0	1 (1)	0	0	0	1	LT radiation	
Lamkun	*Lamprologus kungweensis*	Lamprologini	LT	own collection	9	10 (1)	5	5	2 (2)	12	LT radiation	JXG8: 12.91\14; JXH2: 12.97\14
Lamlap	*Lamprologus laparogramma*	Lamprologini	LT	own collection	10 (1)	9	5	5	2 (2)	12	LT radiation	JDI1: 7.72\8; JDI2: 9.52\10
Lamlem	*Lamprologus lemairii*	Lamprologini	LT	own collection	10	10	5	5	2 (2)	12	LT radiation	IPD6: 6.46\6; IZI7: 7.93\8
Lammel	*Lamprologus melasgris*	Lamprologini	LT	HHB	10 (3)	8 (1)	5	0	2 (2)	13	LT radiation	JWA8: 5.66\5; JWA9: 10.88\11
Lamoce	*Lamprologus ocellatus*	Lamprologini	LT	own collection	10 (1)	9	5	5	2 (2)	12	LT radiation	ILC1: 6.88\7; ILD3: 8.02\8
Lamorn	*Lamprologus ornatipinnis*	Lamprologini	LT	own collection	10	9	5	5	2 (2)	12	LT radiation	JZF3: 14.59\16; JZF4: 12.01\13
Lamsig	*Lamprologus signatus*	Lamprologini	LT	own collection	10	10	5	5	2 (2)	12	LT radiation	IWD5: 8.1\8; IWD6: 9.37\10
LamorC	*Lamprologus* sp. "ornatipinnis congo"	Lamprologini	LT	HHB	1	5	5	0	2 (2)	7	LT radiation	JWA3: 6.8\7; JWA4: 6.58\6
LamorS	*Lamprologus* sp. "ornatipinnis zambia"	Lamprologini	LT	own collection	9	9	5	5	2 (2)	11	LT radiation	JDF5: 8.1\8; JDG4: 6.46\6
Lamspe	*Lamprologus speciosus*	Lamprologini	LT	own collection	10	10	5	5	2 (2)	12	LT radiation	KCG2: 9.72\10; KCG3: 13.48\15
Lepatt	*Lepidiolamprologus attenuatus*	Lamprologini	LT	own collection	10	10	5	5	2 (2)	12	LT radiation	AVD4: 7.38\7; AVG5: 8.1\8
Lepcun	*Lepidiolamprologus cunningtoni*	Lamprologini	LT	own collection	10	10	5	5	2	10	LT radiation	IOH4: 8.18\8; IOH5: 13.28\15
Lepelo	*Lepidiolamprologus elongatus*	Lamprologini	LT	own collection	10	10	5	5	2 (2)	12	LT radiation	AUE6: 7.25\7; AUG8: 7.6\8
Lepkam	*Lepidiolamprologus kamambae*	Lamprologini	LT	own collection	10	10	5	5	2	10	LT radiation	LFF7: 5.92\6; LFF8: 8.2\8
Lepken	*Lepidiolamprologus kendalli*	Lamprologini	LT	own collection	10	10	5	5	2 (2)	12	LT radiation	IMD1: 13.55\15; IMD2: 7.72\8
Lepmim	*Lepidiolamprologus mimicus*	Lamprologini	LT	own collection	10	10	5	5	2	10	LT radiation	LDD1: 7.63\8; LDD6: 7.6\8
Lepnka	*Lepidiolamprologus nkambae*	Lamprologini	LT	own collection	0	1 (1)	0	0	0	1	LT radiation	
Leppro	*Lepidiolamprologus profundicola*	Lamprologini	LT	own collection	10 (1)	8	5	4	2	10	LT radiation	KAD2: 8.55\9; KEB8: 8.61\9
LepmeK	*Lepidiolamprologus* sp. "meeli kipili"	Lamprologini	LT	own collection	10 (2)	7	5	5	2	10	LT radiation	LHA2: 7.43\7; LHA5: 7.9\8
Neobif	*Neolamprologus bifasciatus*	Lamprologini	LT	own collection	10	10	5	5	2	10	LT radiation	LHF6: 7.29\7; LHF7: 7.25\7
Neobou	*Neolamprologus boulengeri*	Lamprologini	LT	own collection	10	10	5	5	2 (2)	12	LT radiation	KCE5: 6.92\7; KYB9: 7.69\8
Neobre	*Neolamprologus brevis*	Lamprologini	LT	own collection	10 (1)	9	5	5	2 (2)	12	LT radiation	ILB6: 6.49\6; ILB7: 6.76\7
Neobri	*Neolamprologus brichardi*	Lamprologini	LT	own collection	10	10	5	5	2 (2)	12	LT radiation	JUH9: 8.39\9; JUI1: 6.18\6
Neobue	*Neolamprologus buescheri*	Lamprologini	LT	own collection	10	10	5	4	2 (2)	12	LT radiation	JEI4: 7.87; JEI5: 7.36\7
Neocal	*Neolamprologus callilurus*	Lamprologini	LT	own collection	10	10	5	5	2 (2)	12	LT radiation	ILA7: 9.77\10; INC7: 8.19\8
Neocan	*Neolamprologus cancellatus*	Lamprologini	LT	H. Tanaka & HHB	1	2	2	0	2	2	LT radiation	LJC9: 6.8\6; LJD1: 6.28\5
Neocau	*Neolamprologus caudopunctatus*	Lamprologini	LT	own collection	10	10	5	5	2 (2)	12	LT radiation	IQA3: 14.65\16; IQA4: 7.62\8
Neochi	*Neolamprologus chitamwebwai*	Lamprologini	LT	own collection	10	10	5	4	2 (2)	12	LT radiation	KHA7: 7.04\7; KHA9: 5.95\6
Neochr	*Neolamprologus christyi*	Lamprologini	LT	own collection	10	10	5	5	2 (2)	12	LT radiation	ITG2: 8.33\9; IZ8: 6.6\6
Neocra	*Neolamprologus crassus*	Lamprologini	LT	own collection	10	10	5	5	2 (2)	12	LT radiation	IVE8: 8.83\9; IVF1: 8.7\8\9
Neocyl	*Neolamprologus cylindricus*	Lamprologini	LT	own collection	10	10	5	5	2	10	LT radiation	GPH1: 13.67\15; GPH2: 9.64\10
Neofal	*Neolamprologus falcicula*	Lamprologini	LT	own collection	10	10	5	5	2 (2)	12	LT radiation	JXD4: 9.12\9; JXD7: 11.1\12
Neofas	*Neolamprologus fasciatus*	Lamprologini	LT	own collection	10	10	5	5	2 (2)	12	LT radiation	AUE7: 10.06\11; AXD5: 8.03\8
Neofur	*Neolamprologus furcifer*	Lamprologini	LT	own collection	10	10	5	5	2 (2)	12	LT radiation	JEI6: 10.2\11; JEI8: 12.9\14
Neogra	*Neolamprologus gracilis*	Lamprologini	LT	HHB	10 (5)	5	5	0	2 (2)	12	LT radiation	JWH1: 11.41\12; JWH2: 13\14
Neohec	*Neolamprologus hecqui*	Lamprologini	LT	HHB & MRAC	0	0	0	0	3 (3)	3	LT radiation	A142: 11.49\12; Bel13: 6.44\6; Bel14: 6.86\7
Neohel	*Neolamprologus helianthus*	Lamprologini	LT	HHB	10 (5)	5	5	0	2 (2)	12	LT radiation	JWG8: 5.51\5; JWG9: 10.62\11
NeoleL	*Neolamprologus leleupi*	Lamprologini	LT	HHB	5	3	5	0	1 (1)	6	LT radiation	JWH9: 10.69\11
Neolou	*Neolamprologus leloupi*	Lamprologini	LT	own collection	10	10	5	5	2 (2)	12	LT radiation	LCA1: 7.31\7; LCA2: 8.16\8
Neolon	*Neolamprologus longicaudatus*	Lamprologini	LT	own collection	0	0	0	0	2 (2)	2	LT radiation	JWI2: 8.17\8; JWI3: 10.7\11
Neolou	*Neolamprologus longior*	Lamprologini	LT	own collection	10	10	5	5	2 (2)	12	LT radiation	KEH3: 12.67\14; LEE1: 7\7
Neomar	*Neolamprologus marunguensis*	Lamprologini	LT	HHB	10 (5)	5	5	0	2 (2)	12	LT radiation	JWH3: 10.92\12; JWH4: 11.28\12
Neomee	*Neolamprologus meeli*	Lamprologini	LT	own collection	10	10	5	4	2 (2)	12	LT radiation	JDF3: 6.75\6; JDF4: 13.81\15
Neomod	*Neolamprologus modestus*	Lamprologini	LT	own collection	10	10	5	5	2 (1)	11	LT radiation	IMG9: 8.35\8; IMH3: 9.78\10
Neomon	*Neolamprologus mondabu*	Lamprologini	LT	own collection	10	10	5	5	2 (2)	12	LT radiation	JVB4: 10.78\11; JVB8: 9.08\9
Neomul	*Neolamprologus multifasciatus*	Lamprologini	LT	own collection	10	10	5	5	2 (2)	12	LT radiation	IRF6: 6.96\7; IRF8: 6.26\6
Neomux	*Neolamprologus mustax*	Lamprologini	LT	own collection	10	10	5	5	2 (2)	12	LT radiation	ILB4: 8.5\9; ILH1: 6.41\6
Neonig	*Neolamprologus niger*	Lamprologini	LT	own collection	10	10	5	5	2	10	LT radiation	KYA1: 6.37\6; KYA5: 6.78\7
Neonve	*Neolamprologus nigriventris*	Lamprologini	LT	HHB	4	5	5	0	2 (2)	7	LT radiation	A108: 9.75\10; LJC3: 10.85\11
Neoobs	*Neolamprologus obscurus*	Lamprologini	LT	own collection	10	10	5	5	2 (2)	12	LT radiation	IMA1: 7.43\7; IMA2: 6.5\6
Neooli	*Neolamprologus olivaceus*	Lamprologini	LT	HHB	10 (4)	6	5	0	2 (2)	12	LT radiation	JWH5: 10.81\11; JWH6: 11.65\12
Neopec	*Neolamprologus pectoralis*	Lamprologini	LT	HHB	5	6 (1)	5	0	2 (2)	8	LT radiation	JWA7: 11.23\12; JWI6: 11.19\12
Neopet	*Neolamprologus petricola*	Lamprologini	LT	own collection	10	10	5	5	2	10	LT radiation	LGH8: 7.71\8; LGI1: 8\8

Species abbr.	Full name	Tribe	Origin	Sample source	Stable isotope	Body & OJ morphology	LPJ shape	Pigmentation pattern	Genomes	Total specimens	Comment	Read depth after mapping to the Nile Tilapia reference genome (mean|median)
Neople	*Neolamprologus pleuromaculatus*	Lamprologini	LT	own collection	4	4	4	3	2 (2)	6	LT radiation	JZF1: 8.12|8; JZF2: 14.36|16
Neopro	*Neolamprologus prochilus*	Lamprologini	LT	own collection	10	10	5	5	2 (2)	12	LT radiation	IVH1: 7.93|8; IVH2: 7.43|7
Neopul	*Neolamprologus pulcher*	Lamprologini	LT	own collection	10	10	5	5	2 (2)	12	LT radiation	ISA8: 6.8|7; ISB3: 7.7|8
Neosav	*Neolamprologus savoryi*	Lamprologini	LT	own collection	10	10	5	5	2 (2)	12	LT radiation	ISA8: 8.7|8; IYA4: 6.6|6
Neosex	*Neolamprologus sexfasciatus*	Lamprologini	LT	own collection	10	10	5	5	2 (2)	12	LT radiation	IND7: 8.09|8; IND8: 7.6|8
Neosim	*Neolamprologus similis*	Lamprologini	LT	own collection	10	10	5	5	2 (2)	12	LT radiation	KEC1: 8.62|9; KEC2: 7.62|8
NeobrM	*Neolamprologus* sp. "brevis magara"	Lamprologini	LT	own collection	10	10	5	5	2 (2)	12	LT radiation	KCI6: 13.74|15; KCI7: 7.38|7
NeocaK	*Neolamprologus* sp. "caudopunctatus kipili"	Lamprologini	LT	own collection	10	10	5	4	2	10	LT radiation	LDG2: 7.11|7; LDG3: 8.03|8
Neocyq	*Neolamprologus* sp. "cygnus"	Lamprologini	LT	own collection	10	10	5	5	2	10	LT radiation	LFD2: 8.28|8; LFD4: 8.07|8
Neoese	*Neolamprologus* sp. "eseki"	Lamprologini	LT	own collection	10	10	5	5	2	10	LT radiation	LFB7: 6.1|6; LFB9: 8.1|8
NeofaM	*Neolamprologus* sp. "falicicula mahale"	Lamprologini	LT	own collection	11	11	5	5	2 (1)	12	LT radiation	LCB5: 6.24|6; LCC2: 6.11|6
NeofuU	*Neolamprologus* sp. "furcifer uwile"	Lamprologini	LT	own collection	10	10	5	4	2	10	LT radiation	LDF4: 7.62|6; LDF5: 7.7|8
NeogrM	*Neolamprologus* sp. "gracilis tanzania"	Lamprologini	LT	own collection	10	10	5	5	2 (1)	11	LT radiation	LCB4: 6.67|7; LCC6: 6.8|7
Neokom	*Neolamprologus* sp. "kombe"	Lamprologini	LT	own collection	10	10	5	5	2 (2)	12	LT radiation	ILE5: 5.79|5; ILE6: 8.1|8
NeoveS	*Neolamprologus* sp. "ventralis stripe"	Lamprologini	LT	own collection	7	7	5	5	2	7	LT radiation	JED4: 8.09|8; JED5: 14.11|16
Neospl	*Neolamprologus splendens*	Lamprologini	LT	HHB	10 (5)	5	5	0	2 (2)	12	LT radiation	A188: 7.1|24; LJD3: 8.6|36
Neotet	*Neolamprologus tetracanthus*	Lamprologini	LT	own collection	10	10	5	5	2 (2)	12	LT radiation	IPF7: 6.91|7; IPG3: 10.43|11
Neotim	*Neolamprologus timidus*	Lamprologini	LT	own collection	10	10	5	2	2	10	LT radiation	LGE2: 7.67|8; LGE3: 6.29|6
Neotoa	*Neolamprologus toae*	Lamprologini	LT	own collection	10	10	5	5	2 (2)	12	LT radiation	JZD5: 8.46|9; JZD6: 9.24|10
Neotre	*Neolamprologus tretocephalus*	Lamprologini	LT	own collection	10	10	5	4	2 (2)	12	LT radiation	KFH4: 7.73|8; KFH5: 7.72|8
Neovar	*Neolamprologus variostigma*	Lamprologini	LT	HHB	0	0	0	0	2 (2)	2	LT radiation	JWA5: 14.61|16; JWA6: 16.21|19
NeoveB	*Neolamprologus ventralis* (Burundi)	Lamprologini	LT	own collection	6	6	5	0	2 (2)	8	LT radiation	KAG7: 14.64|16; KAG8: 15.74|18
Neowal	*Neolamprologus walteri*	Lamprologini	LT	own collection	10 (1)	9	5	4	2 (2)	12	LT radiation	KFD2: 7.45|7; KFD4: 7.3|7
Telbif	*Telmatochromis bifrenatus*	Lamprologini	LT	own collection	10	10	5	5	2 (2)	12	LT radiation	KYB7: 7.15|7; KYB8: 7.3|7
Telbra	*Telmatochromis brachygnathus*	Lamprologini	LT	own collection	9	9	5	5	2 (2)	11	LT radiation	JBE8: 6.74|6; JBE9: 7.03|7
Telbri	*Telmatochromis brichardi*	Lamprologini	LT	own collection	10	10	5	5	2 (2)	12	LT radiation	JVI9: 8.27|8; JXA4: 8.1|8
TeldhS	*Telmatochromis dhonti*	Lamprologini	LT	own collection	10	10	5	5	2 (2)	12	LT radiation	LBF7: 6.9|7; LBF8: 6.5|6
TeldhN	*Telmatochromis* sp. "dhonti north"	Lamprologini	LT	own collection	9	9	5	5	2 (2)	11	LT radiation	JUD4: 6.13|6; JUD5: 12.21|13
TeldhT	*Telmatochromis* sp. "dhonti tiwiyu"	Lamprologini	LT	own collection	10	10	5	5	2 (1)	11	LT radiation	LHC1: 13.1|14; LHF2: 11.7|12
Tellon	*Telmatochromis* sp. "longola"	Lamprologini	LT	HHB	0	1	1	0	2 (2)	3	LT radiation	JWC8: 7|7; JWC9: 12.5|14
Telshe	*Telmatochromis* sp. "shell"	Lamprologini	LT	own collection	10	10	5	5	2 (2)	12	LT radiation	IRI8: 8.46|9; IRI9: 6.8|7
TelteS	*Telmatochromis temporalis*	Lamprologini	LT	own collection	10	10	5	5	2 (2)	12	LT radiation	IMB3: 5.86|6; IMB4: 8.4|9
Telvit	*Telmatochromis vittatus*	Lamprologini	LT	own collection	10	10	5	5	2 (2)	12	LT radiation	JBD5: 7.11|7; JBD6: 7.5|8
Varmoo	*Variabilichromis moorii*	Lamprologini	LT	own collection	10	10	5	5	2 (2)	12	LT radiation	AUC3: 9.38|10; AUC4: 7.5|8
Baicen	*Baileychromis centropomoides*	Limnochromini	LT	own collection	10	9	5	5	2 (1)	11	LT radiation	JAB7: 7.04|7; JAE9: 10.1|10
Gnaper	*Gnathochromis permaxillaris*	Limnochromini	LT	own collection	10	10	5	5	2 (2)	12	LT radiation	ITA4: 9.04|9; IUI5: 8.5|9
Gwcbel	*Greenwoodochromis bellcrossi*	Limnochromini	LT	own collection	10	10	5	5	1 (1)	11	LT radiation	IXB5: 10.09|10
Gwcchr	*Greenwoodochromis christyi*	Limnochromini	LT	own collection	10	10	5	5	2 (2)	12	LT radiation	IZE4: 9.92|10; IZF1: 7.3|7
Lchabe	*Limnochromis abeelei*	Limnochromini	LT	own collection	10	10	5	5	2 (2)	12	LT radiation	ITB3: 8.47|9; ITB4: 7.35|7
Lchaur	*Limnochromis auritus*	Limnochromini	LT	own collection	10	10	5	5	2 (2)	12	LT radiation	ITB1: 7.96|8; JAF5: 8.2|8
Lchsta	*Limnochromis staneri*	Limnochromini	LT	own collection	10	10	5	5	3 (3)	13	LT radiation	ITA6: 14.89|17; ITC2: 7.08|7; IXB6: 7.61|7
Regcal	*Reganochromis calliurus*	Limnochromini	LT	own collection	10	10	5	5	2 (2)	12	LT radiation	IUI1: 6.7|16; IUI4: 7.6|8
Tchdha	*Tangachromis dhanisi*	Limnochromini	LT	own collection	3	3	3	1	2	3	LT radiation	LJA7: 6.2|26; LJA8: 12.4|13
Tricto	*Triglachromis otostigma*	Limnochromini	LT	own collection	10	10	5	5	2	10	LT radiation	JEG5: 9.14|9; JEG6: 6.8|7
Haprnic	*Haplotaxodon microlepis*	Perissodini	LT	own collection	10 (2)	7	5	4	1 (1)	11	LT radiation	IQB8: 13.04|14
Haptri	*Haplotaxodon trifasciatus*	Perissodini	LT	own collection	0	0	0	0	1 (1)	1	LT radiation	IQB6: 8.1|8
Perecc	*Perissodus eccentricus*	Perissodini	LT	own collection	10 (1)	9	5	5	2 (2)	12	LT radiation	IXA4: 8.38|9; IZB2: 12.39|13
Permic	*Perissodus microlepis*	Perissodini	LT	own collection	8	10 (1)	5	5	2 (2)	12	LT radiation	IQC4: 9.19|10; IQ4: 6.9|7
Pleela	*Plecodus elavier*	Perissodini	LT	own collection	10 (1)	9	5	5	2	10	LT radiation	LHI4: 7.8|8; LHI6: 8.0|8
Plemul	*Plecodus multidentatus*	Perissodini	LT	own collection	8	8	5	5	2 (2)	10	LT radiation	IZA8: 13.81|15; IZA9: 9.8|10
Plepar	*Plecodus paradoxus*	Perissodini	LT	own collection	10	10	5	5	2 (1)	11	LT radiation	JDI4: 8.65|9; LEC7: 6.8|7
Plestr	*Plecodus straeleni*	Perissodini	LT	own collection	10	10	5	5	2 (2)	12	LT radiation	INE8: 14.44|16; INE9: 9.22|10
Xchhec	*Xenochromis hecqui*	Perissodini	LT	own collection	10 (1)	9	5	5	2 (2)	12	LT radiation	IUI7: 6.75|7; JAH7: 9.58|10
Trecap	*Trematocara caparti*	Trematocarini	LT	H. Tanaka	3	3	3	0	1	3	LT radiation	LJC8: 6.9|15
Tremac	*Trematocara macrostoma*	Trematocarini	LT	own collection	10	10	5	5	2 (2)	12	LT radiation	IUD8: 10.72|11; IUD9: 9.7|10
Tremar	*Trematocara marginatum*	Trematocarini	LT	own collection	12 (2)	10	5	4	2 (2)	14	LT radiation	ISA1: 6.2|8; ISA3: 11.6|13
Treniq	*Trematocara niquifrons*	Trematocarini	LT	own collection	10	10	5	2	2 (2)	12	LT radiation	GPA1: 6.3|16; IUE5: 11.7|11
Trespn	*Trematocara* sp. "north"	Trematocarini	LT	own collection	0	1	1	0	0	1	LT radiation	
Tresti	*Trematocara stigmaticum*	Trematocarini	LT	own collection	6	6	5	5	2 (2)	8	LT radiation	IUE7: 8.8|28; IZE1: 8.8|39
Treuni	*Trematocara unimaculatum*	Trematocarini	LT	own collection	9	9	5	5	2 (2)	11	LT radiation	IXA3: 9.5|10; IXA6: 9.3|9
Trevar	*Trematocara variabile*	Trematocarini	LT	MRAC	0	0	0	0	1 (1)	1	LT radiation	Bel33: 6.4|86
Trezeb	*Trematocara zebra*	Trematocarini	LT	own collection	10	10	5	2	2	10	LT radiation	LFC9: 5.9|65; LFE4: 6.2|36
Ctehor	*Ctenochromis horei*	Tropheini	LT	own collection	10	10	5	5	2 (2)	12	LT radiation	AVA8: 7.9|18; AXA7: 8.2|68
Gnapfe	*Gnathochromis pfefferi*	Tropheini	LT	own collection	10	10	5	5	2 (2)	12	LT radiation	AWB7: 7.49|8; AWE2: 7.2|47
Intioo	*Interochromis loocki*	Tropheini	LT	own collection	10	10	5	5	2 (2)	12	LT radiation	IPB6: 9.08|9; IPF3: 7.2|27
Limdar	*Limnotilapia dardennii*	Tropheini	LT	own collection	10	9	5	9	2 (2)	12	LT radiation	AWI5: 7.84|8; AWI6: 7.99|8
Loblab	*Lobochilotes labiatus*	Tropheini	LT	own collection	10	9	5	5	2 (2)	12	LT radiation	ISD8: 7.5|7; ISE5: 6.5|66
Peteph	*Petrochromis ephippium*	Tropheini	LT	own collection	10 (1)	9	5	5	2 (2)	12	LT radiation	IPC1: 7.44|7; IYA5: 5.9|66
Petfam	*Petrochromis famula*	Tropheini	LT	own collection	10	10	5	5	2 (2)	12	LT radiation	IYA6: 5.92|6; IYA7: 8.2|18
Petfas	*Petrochromis fasciolatus*	Tropheini	LT	own collection	10	10	5	5	2 (2)	12	LT radiation	GPH7: 8|8; JAE1: 7.9|38
Pethor	*Petrochromis horii*	Tropheini	LT	own collection	10	10	5	2	2 (1)	11	LT radiation	IWB5: 7.38|7; IWB6: 9.7|110
Petmac	*Petrochromis macrognathus*	Tropheini	LT	own collection	10	10	5	5	2	10	LT radiation	LDA4: 7.1|17; LJB1: 6.3|36
Petort	*Petrochromis orthognathus*	Tropheini	LT	own collection	10	10	5	3	2	10	LT radiation	JXH4: 4.17|4; JXH5: 12.62|14
Petpol	*Petrochromis polyodon*	Tropheini	LT	own collection	10	9	5	5	2 (2)	12	LT radiation	AWB9: 7.76|8; AWI4: 7.8|38
Petgia	*Petrochromis* sp. "giant"	Tropheini	LT	own collection	10 (1)	3	5	5	2	10	LT radiation	LDC6: 8.22|8; LHD2: 7.6|8
Petkas	*Petrochromis* sp. "kazumbae"	Tropheini	LT	own collection	10	10	5	5	2 (2)	12	LT radiation	KEA4: 8.39|8; KEB4: 8.6|39
Petkip	*Petrochromis* sp. "kipili brown"	Tropheini	LT	own collection	10	10	5	4	2	10	LT radiation	LDC3: 6.5|6; LDE4: 7.4|97
Petrai	*Petrochromis* sp. "macrognathus rainbow"	Tropheini	LT	own collection	10	10	5	5	2	10	LT radiation	LGB5: 7.5|7; LGB8: 7.5|8
Petmos	*Petrochromis* sp. "moshi yellow"	Tropheini	LT	own collection	10	10	5	3	2	10	LT radiation	LCF6: 7.8|18; LCF8: 7.2|77
Petiko	*Petrochromis* sp. "orthognathus ikola"	Tropheini	LT	own collection	10	10	5	5	2	10	LT radiation	LFA6: 7.4|7; LFA8: 7.6|98
Pettex	*Petrochromis* sp. "polyodon texas"	Tropheini	LT	own collection	10	10	5	5	2	10	LT radiation	LHB11: 8.1|28; LHB3: 9.99|10
Petred	*Petrochromis* sp. "red"	Tropheini	LT	own collection	10	10	5	5	2	10	LT radiation	LCD1: 6.5|6; LCD5: 6.5|36
Pettre	*Petrochromis trewavasae*	Tropheini	LT	own collection	10	10	5	5	2	10	LT radiation	IWC9: 14.43|16; IWD4: 8.3|48
Pscbab	*Pseudosimochromis babaulti*	Tropheini	LT	own collection	10	10	5	5	2 (2)	12	LT radiation	JUA3: 8.2|88; JUA4: 12.6|114
Pscple	*Pseudosimochromis babaulti* (South)	Tropheini	LT	own collection	10 (1)	9	5	5	2 (2)	12	LT radiation	AUB6: 9.64|10; AVB6: 9.6|210
Psccur	*Pseudosimochromis curvifrons*	Tropheini	LT	own collection	10	10	5	5	2 (2)	12	LT radiation	AXF8: 9.07|9; AYC7: 9.9|10
Pscmar	*Pseudosimochromis marginatus*	Tropheini	LT	own collection	10	10	5	5	2 (1)	11	LT radiation	KCE7: 9.9|11; KCF3: 15.2|17
Pscmrg	*Pseudosimochromis marginatus* (North)	Tropheini	LT	own collection	8 (1)	9 (1)	5	5	2 (2)	12	LT radiation	KFE8: 7.2|97; KFF1: 7.6|68
Simdia	*Simochromis diagramma*	Tropheini	LT	own collection	10	10	5	5	2 (2)	12	LT radiation	AUD8: 10.21|11; AUE1: 9.5|110
Troann	*Tropheus annectens*	Tropheini	LT	MRAC	0	0	0	0	2 (2)	2	LT radiation	JWG4: 14.12|16; JWG5: 7.9|48
Trobri	*Tropheus brichardi*	Tropheini	LT	own collection	10	10	5	5	2 (2)	12	LT radiation	JYI8: 8.73|9; JZA3: 8.6|9
Trodub	*Tropheus duboisi*	Tropheini	LT	own collection	10	10	5	3	2 (2)	12	LT radiation	KHA4: 7.66|8; KHA5: 8.1|8
Tromoo	*Tropheus moorii*	Tropheini	LT	own collection	10	10	5	5	2 (2)	12	LT radiation	JBH4: 6.83|7; JBH5: 7.8|68
Tropol	*Tropheus polli*	Tropheini	LT	own collection	10	9	5	2	2 (2)	12	LT radiation	LEF8: 11.96|13; LEF9: 11.86|13
Tronig	*Tropheus* sp. "black"	Tropheini	LT	own collection	10	10	5	5	2 (2)	12	LT radiation	JVC3: 10.56|11; JVC9: 8.5|29
TrobrK	*Tropheus* sp. "brichardi kipili"	Tropheini	LT	own collection	10	10	5	1	2	10	LT radiation	LGA5: 7.4|17; LGA6: 7.9|78
Trokir	*Tropheus* sp. "kirschfleck"	Tropheini	LT	own collection	10	10	5	5	2	10	LT radiation	LCF1: 7.38|7; LCF3: 6.7|37
Troluk	*Tropheus* sp. "lukuga"	Tropheini	LT	own collection	10	10	5	3	2 (2)	12	LT radiation	KEF2: 11.91|13; KEF3: 7.4|7
Trolun	*Tropheus* sp. "lunatus"	Tropheini	LT	own collection	10	10	5	5	2 (2)	12	LT radiation	KED6: 7.5|17; KED7: 7.9|98
Trompi	*Tropheus* sp. "mpimbwe"	Tropheini	LT	own collection	10	10	5	5	2	10	LT radiation	LDI5: 7.1|7; LDI7: 6.4|36
Tromor	*Tropheus* sp. "murago"	Tropheini	LT	own collection	10	10	5	5	2	10	LT radiation	LHD9: 7.74|8; LHE9: 7.4|57
Trored	*Tropheus* sp. "red"	Tropheini	LT	own collection	10	10	5	5	2 (2)	12	LT radiation	IOD9: 9.13|9; IOE1: 7.6|98
Arcstr	*Astatoreochromis straeleni*	Haplochromini	LT & affluent	own collection	0	0	0	0	1 (1)	1	nested within the LT radiation	KAE8: 7.2|97
Astbur	*Astatotilapia burtoni*	Haplochromini	LT & affluent	own collection	0	0	0	0	3 (3)	3	nested within the LT radiation	IZA1: 7.97|8; IZC5: 15.42|17; JYD5: 5.11|5
Astfla	*Astatotilapia flavijosephi*	Haplochromini	Jordan	Aquaria Trade	0	0	0	0	1 (1)	1	nested within the LT radiation	LJD2: 5.4|85
Astpal	*Astatotilapia paludinosus*	Haplochromini	LT affluent	own collection	0	0	0	0	1 (1)	1	nested within the LT radiation	KVG1: 6.1|26
Ctepol	*Ctenochromis polli*	Haplochromini	Congo River	Aquaria Trade	0	0	0	0	1 (1)	1	nested within the LT radiation	JWG2: 14.02|15
HplspC	*Haplochromis* sp. "chipwa"	Haplochromini	LT & affluent	own collection	0	0	0	0	2 (2)	2	nested within the LT radiation	HXC4: 6.32|6; HXC5: 9.04|9
Hplkil	*Haplochromis* sp. "kilossana"	Haplochromini	Warni River	G. Turner	0	0	0	0	1 (1)	1	nested within the LT radiation	LJE8: 18.52|22
Hplsta	*Haplochromis stappersii*	Haplochromini	LT & affluent	own collection	0	0	0	0	1 (1)	1	nested within the LT radiation	JYD3: 11.77|13
Hplvan	*Haplochromis vanheusdeni*	Haplochromini	Ruaha River	F. Schedel	0	0	0	0	1 (1)	1	nested within the LT radiation	JWG3: 6.9|17
Ortcho	*Orthochromis indermauri*	Haplochromini	LT affluent	own collection	0	0	0	0	2 (2)	2	nested within the LT radiation	HXC6: 15.22|17; HXC7: 6.2|6
Ortred	*Orthochromis malagarazienses*	Haplochromini	LT affluent	own collection	0	0	0	0	1 (1)	1	nested within the LT radiation	KYE2: 6.7|47
Ortmaz	*Orthochromis mazimeroensis*	Haplochromini	LT affluent	own collection	0	0	0	0	1 (1)	1	nested within the LT radiation	KDC6: 6.6|36
Ortuvi	*Orthochromis uvinzae*	Haplochromini	LT affluent	own collection	0	0	0	0	1 (1)	1	nested within the LT radiation	KYE7: 6.6|17
Psephi	*Pseudocrenilabrus philander*	Haplochromini	LT affluent	own collection	0	0	0	0	1 (1)	1	nested within the LT radiation	JWG1: 15.96|18
Thobra	*Thoracochromis brauschi*	Haplochromini	Lake Fwa	Aquaria Trade	0	0	0	0	1 (1)	1	nested within the LT radiation	JWF8: 14.7|16
Lamtig	*Lamprologus tigripictilis*	Lamprologini	Congo River	Aquaria Trade	0	0	0	0	1 (1)	1	nested within the LT radiation	JWF6: 14.1|16
Neodev	*Neolamprologus devosi*	Lamprologini	LT affluent	own collection	0	0	0	0	1 (1)	1	nested within the LT radiation	LEH2: 9.8|10
Telluf	*Telmatochromis* sp. "lufubu"	Lamprologini	LT affluent	own collection	0	0	0	0	1 (1)	1	nested within the LT radiation	HXC8: 8.1|18
Ampzal	*Amphilophus zaliosus*	Amphilophini	Lake Apoyo	M. Barluenga	0	0	0	0	1 (1)	1	outgroup	not mapped
Bencon	*Benitochromis conjunctus*	Chromidotilapini	Cameroon	own collection	0	0	0	0	1 (1)	1	outgroup	not mapped
Peltae	*Pelvicachromis taeniatus*	Chromidotilapini	Cameroon	own collection	0	0	0	0	2 (2)	2	outgroup	not mapped
Andbis	*Andinoacara biseriatus*	Cichlasomini	Ecuador	Z. Musilová	0	0	0	0	1 (1)	1	outgroup	not mapped
Bujvit	*Bujurquina vittata*	Cichlasomini	Paraguay	Z. Musilová	0	0	0	0	1 (1)	1	outgroup	not mapped
Copbak	*Coptodon bakossiorum*	Coptodonini	Cameroon	own collection	0	0	0	0	1 (1)	1	outgroup	not mapped
Copren	*Coptodon rendalli*	Coptodonini	LT	own collection	0	0	0	0	1 (1)	1	outgroup	JWE6: 16.0|17
Etingu	*Etia nguti*	Etini	Cameroon	own collection	0	0	0	0	1 (1)	1	outgroup	not mapped
Etrcan	*Etroplus canarensis*	Etroplini	India	Aquaria Trade	0	0	0	0	1 (1)	1	outgroup	not mapped
Apidip	*Apistogramma diplotaenia*	Geophagini	Brazil	Z. Musilová	0	0	0	0	1 (1)	1	outgroup	not mapped
Gobeth	*Gobiocichla ethelwynae*	Gobiocichlini	Cameroon	own collection	0	0	0	0	1 (1)	1	outgroup	JWE7: 13.5|15
Tilbre	*Tilapia brevimanus*	Gobiocichlini	Western Africa	Aquaria Trade	0	0	0	0	1 (1)	1	outgroup	JWF9: 15.58|16
Hchelo	*Hemichromis elongatus*	Hemichromini	Cameroon	own collection	0	0	0	0	1 (1)	1	outgroup	not mapped
Aussci	*Australoheros scitutus*	Heroini	Uruguay	Aquaria Trade	0	0	0	0	1 (1)	1	outgroup	not mapped
Htcmul	*Heterochromis multidens*	Heterochromini	Cameroon	own collection	0	0	0	0	1 (1)	1	outgroup	not mapped
Hetbut	*Heterotilapia buttikofferi*	Heterotilapini	Western Africa	Aquaria Trade	0	0	0	0	1 (1)	1	outgroup	JWE3: 7.9|18
Oremal	*Oreochromis malagarazi*	Oreochromini	LT affluent	own collection	0	0	0	0	1 (1)	1	outgroup	KYH4: 8.0|68
Oretan	*Oreochromis tanganicae*	Oreochromini	LT	own collection	10	10 (1)	5	0	2 (2)	13	outgroup	JAB6: 18.1|18; JAC7: 17.23|17
Sthcar	*Sarotherodon caroli*	Oreochromini	Lake Barombi Mbo	own collection	0	0	0	0	1 (1)	1	outgroup	Z17: 10.30|10
Sthloh	*Sarotherodon lohbergeri*	Oreochromini	Lake Barombi Mbo	own collection	0	0	0	0	2 (2)	2	outgroup	not mapped
Sthste	*Sarotherodon steinbachi*	Oreochromini	Lake Barombi Mbo	own collection	0	0	0	0	1 (1)	1	outgroup	Z07: 10.7|11
Stopin	*Stomatepia pindu*	Oreochromini	Lake Barombi Mbo	own collection	0	0	0	0	1 (1)	1	outgroup	Z09: 11.02|11
Pummac	*Pungu maclareni*	Oreochromini	Lake Barombi Mbo	own collection	0	0	0	0	1 (1)	1	outgroup	Z03: 10.8|11
Parpol	*Paratilapia polleni*	Paratilapini	Madagascar	Zoo Zurich	0	0	0	0	1 (1)	1	outgroup	not mapped
Pelmar	*Pelmatolapia mariae*	Pelmatolapini	Cameroon	own collection	0	0	0	0	1 (1)	1	outgroup	JWF2: 15.8|17
Pyoli	*Pychochromis oligocanthus*	Pychochromini	Madagascar	Zoo Zurich	0	0	0	0	1 (1)	1	outgroup	not mapped
Phsacu	*Pharyngochromis aculeops*	Serranochromini	Zambezi River	own collection	0	0	0	0	1 (1)	1	outgroup	JWF3: 14.5|16
Sarcar	*Sargochromis carlottae*	Serranochromini	Zambezi River	own collection	0	0	0	0	1 (1)	1	outgroup	JWF4: 13.8|15
Sermac	*Serranochromis macrocephalus*	Serranochromini	Kafue River	own collection	0	0	0	0	1 (1)	1	outgroup	JWF5: 17.3|20
Steult	*Steatocranus* sp. "ultraslender"	Steatocranini	Congo River	Aquaria Trade	0	0	0	0	1 (1)	1	outgroup	JWE8: 12.0|13
Tilspa	*Tilapia sparmanii*	Tilapiini	Lake Chila	own collection	0	0	0	0	1 (1)	1	outgroup	JWF7: 16.5|18
Tylpol	*Tylochromis polylepis*	Tylochromini	LT	own collection	10 (1)	9	5	0	2 (2)	12	outgroup	not mapped
Total	**301 taxa**	**33 tribes**			**2259 (60)**	**2197 (9)**	**1168 (0)**	**1016**	**547 (439)**	**2723**		

Supplementary Table 2 | Specimen list. Overview over all cichlid specimens used in this study with taxonomic information and sampling locations.

ID	Sex	SpeciesID	CollectionDate	CollectionLocation	latitude	longitude
9689	NA	Lamfin	NA	Uvira	NA	NA
20A1	NA	Cteben	09.08.10	Mpulungu Fishmarket	-8.76047	31.11219
88-05-a	NA	Neospl	03.10.88	Kafitilila DRC	-7.71522	30.23414
88-05-b	NA	Neospl	03.10.88	Kafitilila DRC	-7.71522	30.23414
88-06	NA	Neonve	03.10.88	Kafitilila DRC	-7.71522	30.23414
88-09	NA	Tellon	05.10.88	Longola	-7.48194	30.21778
88-10	NA	Lammel	06.10.88	Kalubamba DRC	-7.37944	30.18972
88-11-a	NA	Lammel	06.10.88	Kalubamba DRC	-7.37944	30.18972
88-11-b	NA	Lammel	06.10.88	Kalubamba DRC	-7.37944	30.18972
88-19	NA	Neogra	06.10.88	Kibushi	-7.66667	30.21667
89-02	NA	Neomar	26.09.89	Kafitilila DRC	-7.71522	30.23414
89-05-a	NA	Neomar	27.09.89	Kafitilila DRC	-7.71522	30.23414
89-05-b	NA	Neomar	27.09.89	Kafitilila DRC	-7.71522	30.23414
89-05-c	NA	Neomar	27.09.89	Kafitilila DRC	-7.71522	30.23414
89-07-a	NA	Neogra	27.09.89	Kafitilila DRC	-7.71522	30.23414
89-07-b	NA	Neogra	27.09.89	Kafitilila DRC	-7.71522	30.23414
89-07-c	NA	Neogra	27.09.89	Kafitilila DRC	-7.71522	30.23414
89-07-d	NA	Neogra	27.09.89	Kafitilila DRC	-7.71522	30.23414
89-15-b	NA	Neohel	30.09.89	Kalo DRC	-7.79528	30.26639
89-15-c	NA	Neohel	30.09.89	Kalo DRC	-7.79528	30.26639
89-15-d	NA	Neohel	30.09.89	Kalo DRC	-7.79528	30.26639
89-16-a	NA	Neomar	03.10.89	Kalo DRC	-7.79528	30.26639
89-16-b	NA	Neomar	03.10.89	Kalo DRC	-7.79528	30.26639
89-17	NA	Neogra	03.10.89	Kalo DRC	-7.79528	30.26639
89-28-a	NA	Lammel	07.10.89	Kalubamba DRC	-7.37944	30.18972
89-28-b	NA	Lammel	07.10.89	Kalubamba DRC	-7.37944	30.18972
89-28-c	NA	Lammel	07.10.89	Kalubamba DRC	-7.37944	30.18972
89-30-a	NA	Neospl	07.10.89	Kasu	-7.31667	30.15000
89-30-b	NA	Neospl	07.10.89	Kasu	-7.31667	30.15000
89-30-c	NA	Neospl	07.10.89	Kasu	-7.31667	30.15000
89-30-d	NA	Neospl	07.10.89	Kasu	-7.31667	30.15000
89-30-e	NA	Neospl	07.10.89	Kasu	-7.31667	30.15000
89-31-a	NA	Neonve	01.10.89	Kalo DRC	-7.79528	30.26639
89-31-b	NA	Neonve	01.10.89	Kalo DRC	-7.79528	30.26639
89-31-c	NA	Neonve	01.10.89	Kalo DRC	-7.79528	30.26639
90-01-a	NA	XenpaK	02.08.90	Tembwe DRC	-7.23972	30.11944
90-01-b	NA	XenpaK	02.08.90	Tembwe DRC	-7.23972	30.11944
90-02-a	NA	XenpaK	02.08.90	Tembwe DRC	-7.23972	30.11944
90-02-b	NA	XenpaK	02.08.90	Tembwe DRC	-7.23972	30.11944
90-07	NA	Neospl	22.08.90	Tembwe DRC	-7.23972	30.11944
90-08-a	NA	Neospl	22.08.90	Tembwe DRC	-7.23972	30.11944
90-08-b	NA	Neospl	22.08.90	Tembwe DRC	-7.23972	30.11944
90-10	NA	Neopec	23.08.90	Tembwe DRC	-7.23972	30.11944
90-84	NA	Neomar	07.09.90	Myunga	-7.94611	30.39444
90-92-b	NA	Neonve	09.09.90	Kamakonde DRC	-7.87361	30.30389
91-06-a	NA	Neopec	20.04.91	Tembwe DRC	-7.23972	30.11944
91-06-b	NA	Neopec	20.04.91	Tembwe DRC	-7.23972	30.11944
91-15	NA	Neohel	25.04.91	Kalo DRC	-7.79528	30.26639
91-21	NA	Neomar	26.04.91	Kamakonde DRC	-7.87361	30.30389
91-23-a	NA	Neohel	26.04.91	Kamakonde DRC	-7.87361	30.30389
91-23-b	NA	Neohel	26.04.91	Kamakonde DRC	-7.87361	30.30389
91-44-a	NA	XenpaK	09.05.91	Tembwe DRC	-7.23972	30.11944
91-44-b	NA	XenpaK	09.05.91	Tembwe DRC	-7.23972	30.11944
91-52-a	NA	Neogra	11.05.91	Tembwe DRC	-7.23972	30.11944
91-52-b	NA	Neogra	11.05.91	Tembwe DRC	-7.23972	30.11944
93-03-a	NA	Neogra	25.04.93	Tembwe DRC	-7.23972	30.11944
93-03-b	NA	Neogra	25.04.93	Tembwe DRC	-7.23972	30.11944
93-14	NA	LamorC	29.04.93	Kisongwa DRC	-7.23361	30.11250
93-18-a	NA	LamorC	02.05.93	Kisongwa DRC	-7.23361	30.11250
93-18-b	NA	LamorC	02.05.93	Kisongwa DRC	-7.23361	30.11250
93-38-a	NA	Neohel	12.05.93	Kamakonde DRC	-7.87361	30.30389
93-38-b	NA	Neohel	12.05.93	Kamakonde DRC	-7.87361	30.30389
93-38-c	NA	Neohel	12.05.93	Kamakonde DRC	-7.87361	30.30389
93-43-b	NA	Neohel	13.05.93	Kamakonde DRC	-7.87361	30.30389
93-47-a	NA	Lammel	15.05.93	Kalubamba DRC	-7.37944	30.18972
93-47-b	NA	Lammel	15.05.93	Kalubamba DRC	-7.37944	30.18972
93-47-c	NA	Lammel	15.05.93	Kalubamba DRC	-7.37944	30.18972
93-53	NA	Neopec	17.05.93	Kisongwa DRC	-7.23361	30.11250
93-54-a	NA	Neooli	19.05.93	Kyeso DRC	-6.81667	29.61472
93-54-b	NA	Neooli	19.05.93	Kyeso DRC	-6.81667	29.61472
93-55-a	NA	Neooli	19.05.93	Kyeso DRC	-6.81667	29.61472
93-55-b	NA	Neooli	19.05.93	Kyeso DRC	-6.81667	29.61472
93-55-c	NA	Neooli	19.05.93	Kyeso DRC	-6.81667	29.61472
93-60-8	NA	Neopec	26.04.93	Tembwe DRC	-7.23972	30.11944
94-18-a	NA	NeoleL	24.05.94	Litimba DRC	-8.02583	30.47889
94-18-b	NA	NeoleL	24.05.94	Litimba DRC	-8.02583	30.47889
94-25-a	NA	Neomar	26.05.94	Mulinde	-7.76833	30.27167
94-25-b	NA	Neomar	26.05.94	Mulinde	-7.76833	30.27167
94-51	NA	LamorC	02.06.94	Kisongwa DRC	-7.23361	30.11250
94-60	NA	LamorC	02.06.94	Kisongwa DRC	-7.23361	30.11250
94-77-a	NA	NeoleL	09.06.94	Kitumba DRC	-6.82361	29.62694
94-77-b	NA	NeoleL	09.06.94	Kitumba DRC	-6.82361	29.62694
94-78	NA	NeoleL	09.06.94	Kitumba DRC	-6.82361	29.62694
94-85-a	NA	Neooli	11.06.94	Kyeso DRC	-6.81667	29.61472
94-85-b	NA	Neooli	11.06.94	Kyeso DRC	-6.81667	29.61472
94-86-a	NA	Neooli	11.06.94	Kyeso DRC	-6.81667	29.61472
94-86-b	NA	Neooli	11.06.94	Kyeso DRC	-6.81667	29.61472
95-04-a	NA	Neooli	29.04.95	Kyeso DRC	-6.81667	29.61472
95-07-a	NA	Julunt	29.04.95	Kyeso DRC	-6.81667	29.61472
95-07-b	NA	Julunt	29.04.95	Kyeso DRC	-6.81667	29.61472
95-07-c	NA	Julunt	29.04.95	Kyeso DRC	-6.81667	29.61472
95-15	NA	Neopec	04.05.95	Tembwe DRC	-7.23972	30.11944
95-22-a	NA	Lammel	06.05.95	Kalubamba DRC	-7.37944	30.18972
95-22-b	NA	Lammel	06.05.95	Kalubamba DRC	-7.37944	30.18972
95-27-a	NA	XenpaK	08.05.95	Kasenga	-8.71525	31.14186
95-27-b	NA	XenpaK	08.05.95	Kasenga	-8.71525	31.14186
95-27-c	NA	XenpaK	08.05.95	Kasenga	-8.71525	31.14186
95-27-d	NA	XenpaK	08.05.95	Kasenga	-8.71525	31.14186
96-36	NA	Julunt	08.10.96	Kyeso DRC	-6.81667	29.61472
96-37-a	NA	Julunt	09.10.96	Kyeso DRC	-6.81667	29.61472
96-37-b	NA	Julunt	09.10.96	Kyeso DRC	-6.81667	29.61472
96-37-c	NA	Julunt	09.10.96	Kyeso DRC	-6.81667	29.61472
98-31-a	NA	Julunt	04.05.98	Kyeso DRC	-6.81667	29.61472
98-31-b	NA	Julunt	04.05.98	Kyeso DRC	-6.81667	29.61472
A108	F	Neonve	NA	NA	NA	NA
A142	M	Neohec	NA	NA	NA	NA
A188	M	Neospl	NA	Kasu	-7.31667	30.15000
A206	F	XenpaK	NA	Tembwe DRC	-7.23972	30.11944
AUA1	F	Auldew	19.07.11	Toby's Place	-8.62322	31.20044
AUA9	F	Auldew	19.07.11	Toby's Place	-8.62322	31.20044
AUB6	M	Pscple	19.07.11	Toby's Place	-8.62322	31.20044
AUC3	F	Varmoo	19.07.11	Toby's Place	-8.62322	31.20044
AUC4	M	Varmoo	19.07.11	Toby's Place	-8.62322	31.20044
AUD8	F	Simdia	19.07.11	Toby's Place	-8.62322	31.20044
AUE1	M	Simdia	19.07.11	Toby's Place	-8.62322	31.20044
AUE6	M	Lepelo	20.07.11	Toby's Place	-8.62322	31.20044
AUE7	M	Neofas	20.07.11	Toby's Place	-8.62322	31.20044
AUG8	F	Lepelo	20.07.11	Toby's Place	-8.62322	31.20044
AVA8	M	Ctehor	21.07.11	Toby's Place	-8.62322	31.20044
AVA9	F	Chabri	21.07.11	Toby's Place	-8.62322	31.20044
AVB2	M	Chabri	21.07.11	Toby's Place	-8.62322	31.20044
AVB6	F	Pscple	21.07.11	Toby's Place	-8.62322	31.20044
AVD4	M	Lepatt	23.07.11	Toby's Place	-8.62322	31.20044
AVG5	F	Lepatt	24.07.11	Toby's Place	-8.62322	31.20044
AVH2	M	Cyafur	24.07.11	Toby's Place	-8.62322	31.20044
AWB7	M	Gnapfe	25.07.11	Toby's Place	-8.62322	31.20044
AWB9	M	Petpol	25.07.11	Toby's Place	-8.62322	31.20044
AWC5	M	Enamel	25.07.11	Toby's Place	-8.62322	31.20044
AWE2	F	Gnapfe	26.07.11	Toby's Place	-8.62322	31.20044
AWI4	F	Petpol	26.07.11	Toby's Place	-8.62322	31.20044
AWI5	F	Limdar	26.07.11	Toby's Place	-8.62322	31.20044
AWI6	M	Limdar	26.07.11	Toby's Place	-8.62322	31.20044
AXA7	F	Ctehor	27.07.11	Toby's Place	-8.62322	31.20044
AXB5	M	Xenspi	27.07.11	Toby's Place	-8.62322	31.20044
AXB8	F	Xenspi	27.07.11	Toby's Place	-8.62322	31.20044
AXD5	F	Neofas	28.07.11	Toby's Place	-8.62322	31.20044
AXF8	F	Psccur	28.07.11	Toby's Place	-8.62322	31.20044
AXH6	M	Ophnas	29.07.11	Toby's Place	-8.62322	31.20044
AXH8	F	Ophnas	29.07.11	Toby's Place	-8.62322	31.20044
AYC7	M	Psccur	30.07.11	Toby's Place	-8.62322	31.20044
AYE5	F	Cyafur	01.08.11	Toby's Place	-8.62322	31.20044
Bel01	M	Xenkil	NA	Kilesa near Kasenga	-5.73333	29.36667
Bel03	M	Xenkil	NA	Kilesa near Kasenga	-5.73333	29.36667
Bel06	M	Ophhet	NA	Kyanza	-7.11139	29.97583
Bel07	M	Chapop	NA	Mugayo	-6.77833	29.55833
Bel09	F	Chapop	NA	Mtoto	-6.96278	29.73333
Bel12	M	Ophhet	NA	Kitoka	-5.45000	29.28333
Bel13	NA	Neohec	NA	Kalemie	-5.93240	29.20032
Bel14	NA	Neohec	NA	Kalemie	-5.93240	29.20032
Bel16	M	Cypkib	NA	Milila	-5.68333	29.38333
Bel18	F	Cypkib	NA	Milila	-5.68333	29.38333
Bel33	F	Trevar	NA	Kalemie	-5.93240	29.20032
BNC5	F	Enamel	05.08.11	Toby's Place	-8.62322	31.20044
BND3	M	Calmac	05.08.11	Toby's Place	-8.62322	31.20044
BND5	F	Calmac	05.08.11	Toby's Place	-8.62322	31.20044
DMC6	NA	Cteben	16.09.11	Mpulungu Fishmarket	-8.76047	31.11219
DMC7	NA	Cteben	16.09.11	Mpulungu Fishmarket	-8.76047	31.11219
DMC8	NA	Cteben	11.09.11	Mpulungu Fishmarket	-8.76047	31.11219
DMC9	NA	Cteben	16.09.11	Mpulungu Fishmarket	-8.76047	31.11219
DMD1	M	Cteben	16.09.11	Mpulungu Fishmarket	-8.76047	31.11219
DMD2	NA	Cteben	16.09.11	Mpulungu Fishmarket	-8.76047	31.11219
FPO1	M	Ptyoli	NA	NA	NA	NA
GPA1	F	Trenig	02.09.14	Mpulungu Fishmarket	-8.76047	31.11219
GPA5	F	Tremar	02.09.14	Mpulungu Fishmarket	-8.76047	31.11219
GPA7	M	Tremar	02.09.14	Mpulungu Fishmarket	-8.76047	31.11219
GPA8	M	Tremar	02.09.14	Mpulungu Fishmarket	-8.76047	31.11219
GPA9	F	Tremar	02.09.14	Mpulungu Fishmarket	-8.76047	31.11219
GPB1	M	Tremar	02.09.14	Mpulungu Fishmarket	-8.76047	31.11219
GPB2	F	Batfas	02.09.14	Mbita Island W	-8.75333	31.08631
GPB3	NA	Batfas	02.09.14	Mbita Island W	-8.75333	31.08631
GPB4	M	Tylpol	02.09.14	Mpulungu Fishmarket	-8.76047	31.11219
GPB5	F	Tylpol	02.09.14	Mpulungu Fishmarket	-8.76047	31.11219
GPB6	F	Limdar	02.09.14	Mpulungu Fishmarket	-8.76047	31.11219
GPB7	F	Limdar	02.09.14	Mpulungu Fishmarket	-8.76047	31.11219
GPB8	F	Limdar	02.09.14	Mpulungu Fishmarket	-8.76047	31.11219
GPB9	F	Limdar	02.09.14	Mpulungu Fishmarket	-8.76047	31.11219
GPC1	M	Limdar	02.09.14	Mpulungu Fishmarket	-8.76047	31.11219
GPC2	M	Limdar	02.09.14	Mpulungu Fishmarket	-8.76047	31.11219
GPC3	M	Limdar	02.09.14	Mpulungu Fishmarket	-8.76047	31.11219
GPC4	M	Pcynig	03.09.14	Chituta	-8.72361	31.15000
GPC6	F	Pcynig	03.09.14	Chituta	-8.72361	31.15000
GPC8	NA	Neopro	03.09.14	Kasenga Fishermen	-8.71389	31.14028
GPC9	M	Cypzon	03.09.14	Chituta	-8.72361	31.15000
GPD1	F	Cypzon	03.09.14	Chituta	-8.72361	31.15000
GPD5	NA	Xensun	03.09.14	Chituta	-8.72361	31.15000
GPD6	NA	Xensun	03.09.14	Chituta	-8.72361	31.15000
GPD7	NA	Xensun	03.09.14	Chituta	-8.72361	31.15000
GPD8	M	Pcynig	03.09.14	Chituta	-8.72361	31.15000
GPD9	M	Pcynig	03.09.14	Chituta	-8.72361	31.15000
GPE1	M	Pcynig	03.09.14	Chituta	-8.72361	31.15000
GPE2	NA	Pcynig	03.09.14	Chituta	-8.72361	31.15000
GPE3	NA	Pcynig	03.09.14	Chituta	-8.72361	31.15000
GPE4	NA	Pcynig	03.09.14	Chituta	-8.72361	31.15000
GPE5	NA	Pcynig	03.09.14	Chituta	-8.72361	31.15000
GPE6	F	Pcynig	03.09.14	Chituta	-8.72361	31.15000
GPE7	F	Pcynig	03.09.14	Chituta	-8.72361	31.15000
GPE8	F	Pcynig	03.09.14	Chituta	-8.72361	31.15000
GPF2	NA	Gwcchr	03.09.14	Chituta	-8.72361	31.15000
GPF3	NA	Tromoo	03.09.14	Chituta	-8.72361	31.15000
GPF4	NA	Tromoo	03.09.14	Chituta	-8.72361	31.15000
GPF5	NA	Limdar	03.09.14	Chituta	-8.72361	31.15000
GPF6	NA	Petfas	03.09.14	Chituta	-8.72361	31.15000
GPF8	M	Xensun	04.09.14	Isanga	-8.65456	31.19183
GPF9	F	Xensun	04.09.14	Isanga	-8.65456	31.19183
GPG2	NA	Xensun	04.09.14	Isanga	-8.65456	31.19183
GPG3	NA	Xensun	04.09.14	Isanga	-8.65456	31.19183
GPG4	NA	Xensun	04.09.14	Isanga	-8.65456	31.19183
GPG5	NA	Xensun	04.09.14	Isanga	-8.65456	31.19183
GPG6	NA	Xensun	04.09.14	Isanga	-8.65456	31.19183
GPG7	NA	Xensun	04.09.14	Isanga	-8.65456	31.19183
GPG8	NA	Xensun	04.09.14	Isanga	-8.65456	31.19183
GPG9	M	Neochr	04.09.14	Isanga	-8.65456	31.19183

ID	Sex	SpeciesID	CollectionDate	CollectionLocation	latitude	longitude
GPH1	M	Neocyl	04.09.14	Isanga	-8.65456	31.19183
GPH2	F	Neocyl	04.09.14	Isanga	-8.65456	31.19183
GPH3	F	Neocyl	04.09.14	Isanga	-8.65456	31.19183
GPH4	NA	Petfas	04.09.14	Isanga	-8.65456	31.19183
GPH6	M	JulmaS	05.09.14	Toby's Place	-8.62322	31.20044
GPH7	M	Petfas	05.09.14	Toby's Place	-8.62322	31.20044
GPH8	M	Petfas	05.09.14	Toby's Place	-8.62322	31.20044
GPH9	F	Petfas	05.09.14	Toby's Place	-8.62322	31.20044
GPI1	NA	Petfas	05.09.14	Toby's Place	-8.62322	31.20044
GPI2	F	Petfas	05.09.14	Toby's Place	-8.62322	31.20044
GPI3	M	Petfas	05.09.14	Toby's Place	-8.62322	31.20044
GPI4	NA	Pethor	05.09.14	Toby's Place	-8.62322	31.20044
GPI5	NA	Pethor	05.09.14	Toby's Place	-8.62322	31.20044
GPI6	NA	Petmac	05.09.14	Toby's Place	-8.62322	31.20044
HFG1287	M	Jultra	NA	NA	NA	NA
HXC4	M	HplspC	NA	Kalambo Lake / Chipwa	-8.60174	31.18701
HXC5	F	HplspC	NA	Kalambo Lake / Chipwa	-8.60174	31.18701
HXC6	F	Ortcho	NA	Lufubu River 2 (Chomba)	-8.68594	30.56442
HXC7	M	Ortcho	NA	Lufubu River 2 (Chomba)	-8.68594	30.56442
HXC8	M	Telluf	NA	Lufubu River 2 (Chomba)	-8.68594	30.56442
ILA1	NA	Lamlem	15.08.14	Katoto	-8.80611	31.02667
ILA2	M	Neocal	15.08.14	Katoto	-8.80611	31.02667
ILA3	M	Neocal	15.08.14	Katoto	-8.80611	31.02667
ILA4	M	Neocal	15.08.14	Katoto	-8.80611	31.02667
ILA5	M	Neocal	15.08.14	Katoto	-8.80611	31.02667
ILA6	M	Neocal	15.08.14	Katoto	-8.80611	31.02667
ILA7	M	Neocal	15.08.14	Katoto	-8.80611	31.02667
ILA9	M	Neocal	15.08.14	Katoto	-8.80611	31.02667
ILB1	M	Neocal	15.08.14	Katoto	-8.80611	31.02667
ILB2	M	Lamlap	15.08.14	Katoto	-8.80611	31.02667
ILB3	F	Lamlap	15.08.14	Katoto	-8.80611	31.02667
ILB4	F	Neomux	15.08.14	Kombe	-8.79389	31.01583
ILB6	M	Neobre	15.08.14	Kombe	-8.79389	31.01583
ILB7	F	Neobre	15.08.14	Kombe	-8.79389	31.01583
ILC1	M	Lamoce	15.08.14	Kombe	-8.79389	31.01583
ILC2	M	Neobre	15.08.14	Kombe	-8.79389	31.01583
ILC3	M	Neobre	15.08.14	Kombe	-8.79389	31.01583
ILC4	M	Neobre	15.08.14	Kombe	-8.79389	31.01583
ILC5	M	Neobre	15.08.14	Kombe	-8.79389	31.01583
ILC6	M	Neobre	15.08.14	Kombe	-8.79389	31.01583
ILC7	M	Neobre	15.08.14	Kombe	-8.79389	31.01583
ILC8	F	Neobre	15.08.14	Kombe	-8.79389	31.01583
ILC9	F	Neobre	15.08.14	Kombe	-8.79389	31.01583
ILD1	F	Neobre	15.08.14	Kombe	-8.79389	31.01583
ILD2	F	Neobre	15.08.14	Kombe	-8.79389	31.01583
ILD3	F	Lamoce	15.08.14	Kombe	-8.79389	31.01583
ILD4	M	Lamoce	15.08.14	Kombe	-8.79389	31.01583
ILD5	M	Lamoce	15.08.14	Kombe	-8.79389	31.01583
ILD6	M	Lamoce	15.08.14	Kombe	-8.79389	31.01583
ILD7	M	LamorS	15.08.14	Kombe	-8.79389	31.01583
ILD9	M	Julkom	15.08.14	Kombe	-8.79389	31.01583
ILE4	M	Neomod	15.08.14	Kombe	-8.79389	31.01583
ILE5	M	Neokom	15.08.14	Kombe	-8.79389	31.01583
ILE6	F	Neokom	15.08.14	Kombe	-8.79389	31.01583
ILE7	M?	Neokom	15.08.14	Kombe	-8.79389	31.01583
ILE8	M?	Neokom	15.08.14	Kombe	-8.79389	31.01583
ILE9	NA	Neokom	15.08.14	Kombe	-8.79389	31.01583
ILF1	NA	Neokom	15.08.14	Kombe	-8.79389	31.01583
ILF2	NA	Neokom	15.08.14	Kombe	-8.79389	31.01583
ILF3	NA	Neokom	15.08.14	Kombe	-8.79389	31.01583
ILF4	NA	Neokom	15.08.14	Kombe	-8.79389	31.01583
ILF5	NA	Neokom	15.08.14	Kombe	-8.79389	31.01583
ILF6	NA	Neokom	15.08.14	Kombe	-8.79389	31.01583
ILF7	F	Batleo	16.08.14	Kombe Fishermen	-8.79333	31.01833
ILF8	M	Benhor	16.08.14	Kombe Fishermen	-8.79333	31.01833
ILG3	F	Benmel	16.08.14	Kombe Fishermen	-8.79333	31.01833
ILG7	M	Batgra	16.08.14	Kombe Fishermen	-8.79333	31.01833
ILH1	M	Neomux	16.08.14	Kombe	-8.79389	31.01583
ILH2	NA	Lchabe	16.08.14	Kombe Fishermen	-8.79333	31.01833
ILH3	M	Gralem	16.08.14	Kombe Fishermen	-8.79333	31.01833
ILH4	M	Benhor	16.08.14	Kombe Fishermen	-8.79333	31.01833
ILH5	M	Benhor	16.08.14	Kombe Fishermen	-8.79333	31.01833
ILH6	M	Benhor	16.08.14	Kombe Fishermen	-8.79333	31.01833
ILH7	M	Benhor	16.08.14	Kombe Fishermen	-8.79333	31.01833
ILH8	M	Benhor	16.08.14	Kombe Fishermen	-8.79333	31.01833
ILH9	M	Benhor	16.08.14	Kombe Fishermen	-8.79333	31.01833
ILI1	F	Benhor	16.08.14	Kombe Fishermen	-8.79333	31.01833
ILI2	F	Benhor	16.08.14	Kombe Fishermen	-8.79333	31.01833
ILI3	F	Benhor	16.08.14	Kombe Fishermen	-8.79333	31.01833
ILI4	F	Benhor	16.08.14	Kombe Fishermen	-8.79333	31.01833
ILI5	NA	Boumic	16.08.14	Kombe Fishermen	-8.79333	31.01833
ILI6	NA	Boumic	16.08.14	Kombe Fishermen	-8.79333	31.01833
ILI7	NA	Neomux	16.08.14	Kombe	-8.79389	31.01583
ILI8	NA	Neosex	16.08.14	Kombe	-8.79389	31.01583
IMA1	F	Neoobs	18.08.14	Kabwensolo	-8.60972	30.82917
IMA2	M	Neoobs	18.08.14	Kabwensolo	-8.60972	30.82917
IMA3	NA	Neoobs	18.08.14	Kabwensolo	-8.60972	30.82917
IMA4	F	Neocal	18.08.14	Kabwensolo	-8.60972	30.82917
IMA5	M	Plestr	18.08.14	Kabwensolo	-8.60972	30.82917
IMA6	M	Plestr	18.08.14	Kabwensolo	-8.60972	30.82917
IMA7	M	Plestr	18.08.14	Kabwensolo	-8.60972	30.82917
IMA9	NA	Tromoo	18.08.14	Kabwensolo	-8.60972	30.82917
IMB1	NA	Pscple	18.08.14	Kabwensolo	-8.60972	30.82917
IMB2	NA	TelteS	18.08.14	Kabwensolo	-8.60972	30.82917
IMB3	M	TelteS	18.08.14	Kabwensolo	-8.60972	30.82917
IMB4	F	TelteS	18.08.14	Kabwensolo	-8.60972	30.82917
IMB6	F	Neomux	18.08.14	Kabwensolo	-8.60972	30.82917
IMB7	M	Neomux	18.08.14	Kabwensolo	-8.60972	30.82917
IMB8	M	Neomux	18.08.14	Kabwensolo	-8.60972	30.82917
IMB9	F	Neomux	18.08.14	Kabwensolo	-8.60972	30.82917
IMC1	F	Plestr	18.08.14	Kabwensolo	-8.60972	30.82917
IMC2	M	Plestr	18.08.14	Kabwensolo	-8.60972	30.82917
IMC6	NA	Neomod	18.08.14	Kabwensolo	-8.60972	30.82917
IMD1	M	Lepken	19.08.14	Kabwensolo	-8.60972	30.82917
IMD2	F	Lepken	19.08.14	Kabwensolo	-8.60972	30.82917
IMD3	M	Lepken	19.08.14	Kabwensolo	-8.60972	30.82917

ID	Sex	SpeciesID	CollectionDate	CollectionLocation	latitude	longitude
IMD4	F	Lepken	19.08.14	Kabwensolo	-8.60972	30.82917
IMD5	M	Lepken	19.08.14	Kabwensolo	-8.60972	30.82917
IMD6	F	Limdar	19.08.14	Kabwensolo	-8.60972	30.82917
IMD7	M	Neomod	19.08.14	Kabwensolo	-8.60972	30.82917
IMD8	M	Neomod	19.08.14	Kabwensolo	-8.60972	30.82917
IMD9	M	Neomod	19.08.14	Kabwensolo	-8.60972	30.82917
IME3	M	Altcal	19.08.14	Kabwensolo	-8.60972	30.82917
IME4	M	Altcal	19.08.14	Kabwensolo	-8.60972	30.82917
IME6	F	Plestr	19.08.14	Kabwensolo	-8.60972	30.82917
IME7	NA	Boumic	19.08.14	Kabwensolo Fishermen	-8.60697	30.82981
IME8	NA	Boumic	19.08.14	Kabwensolo Fishermen	-8.60697	30.82981
IME9	NA	Neomux	19.08.14	Kabwensolo	-8.60972	30.82917
IMF1	M	Cyafoa	19.08.14	Kabwensolo Fishermen	-8.60697	30.82981
IMF2	NA	Chabri	19.08.14	Kabwensolo	-8.60972	30.82917
IMF3	NA	Altcom	19.08.14	Kabwensolo	-8.60972	30.82917
IMF4	NA	Lamcal	19.08.14	Kabwensolo	-8.60972	30.82917
IMF5	NA	Tromoo	19.08.14	Kabwensolo	-8.60972	30.82917
IMF6	NA	Neoobs	19.08.14	Kabwensolo	-8.60972	30.82917
IMF7	M	Xennas	19.08.14	Chitweshiba	-8.59583	30.80750
IMF8	F	Xennas	19.08.14	Chitweshiba	-8.59583	30.80750
IMF9	M	Xenbat	19.08.14	Chitweshiba	-8.59583	30.80750
IMG1	F	Xennas	19.08.14	Chitweshiba	-8.59583	30.80750
IMG2	F	Xennas	19.08.14	Chitweshiba	-8.59583	30.80750
IMG3	M	Xennas	19.08.14	Chitweshiba	-8.59583	30.80750
IMG4	M	Xennas	19.08.14	Chitweshiba	-8.59583	30.80750
IMG5	NA	Xennas	19.08.14	Chitweshiba	-8.59583	30.80750
IMG6	NA	Tromoo	19.08.14	Chitweshiba	-8.59583	30.80750
IMG7	F	Chabri	19.08.14	Chitweshiba	-8.59583	30.80750
IMG8	M	Chabri	19.08.14	Chitweshiba	-8.59583	30.80750
IMG9	M	Neomod	19.08.14	Chitweshiba	-8.59583	30.80750
IMH1	M	Neomod	19.08.14	Chitweshiba	-8.59583	30.80750
IMH2	F	Neomod	19.08.14	Chitweshiba	-8.59583	30.80750
IMH3	F	Neomod	19.08.14	Chitweshiba	-8.59583	30.80750
IMH6	F	Xenbat	20.08.14	Chitweshiba	-8.59583	30.80750
IMH7	F	Xennas	20.08.14	Chitweshiba	-8.59583	30.80750
IMH8	M	Xennas	20.08.14	Chitweshiba	-8.59583	30.80750
IMH9	M	Xennas	20.08.14	Chitweshiba	-8.59583	30.80750
IMI1	NA	Xennas	20.08.14	Chitweshiba	-8.59583	30.80750
IMI2	F	Lepmim	20.08.14	Chitweshiba	-8.59583	30.80750
IMI3	NA	Batfas	20.08.14	Chitweshiba	-8.59583	30.80750
IMI4	NA	Plestr	20.08.14	Chitweshiba	-8.59583	30.80750
IMI5	NA	Altcal	20.08.14	Chitweshiba	-8.59583	30.80750
IMI6	NA	Lepken	20.08.14	Chitweshiba	-8.59583	30.80750
IMI7	NA	Lepken	20.08.14	Chitweshiba	-8.59583	30.80750
IMI9	NA	Gralem	20.08.14	Chitweshiba	-8.59583	30.80750
INA1	NA	Plemul	16.08.14	Kombe	-8.79389	31.01583
INA2	NA	Neokom	16.08.14	Kombe	-8.79389	31.01583
INA4	M	Julkom	16.08.14	Kombe	-8.79389	31.01583
INA5	NA	Julkom	16.08.14	Kombe	-8.79389	31.01583
INA6	F	Julkom	16.08.14	Kombe	-8.79389	31.01583
INA7	M	Lamoce	16.08.14	Chezi	-8.77944	31.00556
INA8	M	Lamoce	16.08.14	Chezi	-8.77944	31.00556
INA9	M	Lamoce	16.08.14	Chezi	-8.77944	31.00556
INB1	M	Lamoce	16.08.14	Chezi	-8.77944	31.00556
INB2	F	Lamoce	16.08.14	Chezi	-8.77944	31.00556
INB3	M	Neomux	16.08.14	Chezi	-8.77944	31.00556
INB4	F	Neomux	16.08.14	Chezi	-8.77944	31.00556
INB5	NA	Neosex	16.08.14	Chezi	-8.77944	31.00556
INB6	NA	Neosex	16.08.14	Chezi	-8.77944	31.00556
INB8	NA	Julkom	16.08.14	Chezi	-8.77944	31.00556
INB9	NA	Julkom	16.08.14	Chezi	-8.77944	31.00556
INC1	NA	Julkom	16.08.14	Chezi	-8.77944	31.00556
INC2	NA	Julkom	16.08.14	Chezi	-8.77944	31.00556
INC3	NA	Julkom	16.08.14	Chezi	-8.77944	31.00556
INC4	NA	Julkom	16.08.14	Chezi	-8.77944	31.00556
INC5	NA	Julkom	16.08.14	Chezi	-8.77944	31.00556
INC6	NA	Julkom	16.08.14	Chezi	-8.77944	31.00556
INC7	F	Neocal	16.08.14	Chezi	-8.77944	31.00556
INC8	M	Neocal	16.08.14	Chezi	-8.77944	31.00556
INC9	F	Neocal	16.08.14	Chezi	-8.77944	31.00556
IND2	M	TelteS	16.08.14	Chezi	-8.77944	31.00556
IND3	M	TelteS	16.08.14	Chezi	-8.77944	31.00556
IND4	M	TelteS	16.08.14	Chezi	-8.77944	31.00556
IND5	M	TelteS	16.08.14	Chezi	-8.77944	31.00556
IND6	M	TelteS	16.08.14	Chezi	-8.77944	31.00556
IND7	M	Neosex	17.08.14	Kanfonki	-8.70278	30.92250
IND8	F	Neosex	17.08.14	Kanfonki	-8.70278	30.92250
INE1	M	Neosex	17.08.14	Kanfonki	-8.70278	30.92250
INE2	M	Neosex	17.08.14	Kanfonki	-8.70278	30.92250
INE3	M	Neomux	17.08.14	Kanfonki	-8.70278	30.92250
INE4	NA	Neomux	17.08.14	Kanfonki	-8.70278	30.92250
INE5	M	Cphgib	17.08.14	Kanfonki	-8.70278	30.92250
INE6	F	Lamlem	17.08.14	Kanfonki	-8.70278	30.92250
INE7	M	Lamlem	17.08.14	Kanfonki	-8.70278	30.92250
INE8	F	Plestr	17.08.14	Kanfonki	-8.70278	30.92250
INE9	M	Plestr	17.08.14	Kanfonki	-8.70278	30.92250
INF1	F	Asplep	17.08.14	Kanfonki	-8.70278	30.92250
INF2	M	Asplep	17.08.14	Kanfonki	-8.70278	30.92250
INF4	M	Asplep	17.08.14	Kanfonki	-8.70278	30.92250
INF5	M	Asplep	17.08.14	Kanfonki	-8.70278	30.92250
INF6	F	Asplep	17.08.14	Kanfonki	-8.70278	30.92250
INF7	M	Asplep	17.08.14	Kanfonki	-8.70278	30.92250
INF8	F	Asplep	17.08.14	Kanfonki	-8.70278	30.92250
INF9	F	Asplep	17.08.14	Kanfonki	-8.70278	30.92250
ING1	M	Asplep	17.08.14	Kanfonki	-8.70278	30.92250
ING2	F	Asplep	17.08.14	Kanfonki	-8.70278	30.92250
ING3	F	Asplep	17.08.14	Kanfonki	-8.70278	30.92250
ING4	NA	Permic	17.08.14	Kanfonki	-8.70278	30.92250
ING5	NA	Permic	17.08.14	Kanfonki	-8.70278	30.92250
ING6	M	Chabri	17.08.14	Kanfonki	-8.70278	30.92250
ING7	NA	Neomod	17.08.14	Kanfonki	-8.70278	30.92250
ING8	M	Telbra	17.08.14	Kanfonki	-8.70278	30.92250
ING9	M	Telbra	17.08.14	Kanfonki	-8.70278	30.92250
INH1	M	Cypkan	17.08.14	Kanfonki	-8.70278	30.92250
INH2	M	Cypkan	17.08.14	Kanfonki	-8.70278	30.92250
INH3	M	Cypkan	17.08.14	Kanfonki	-8.70278	30.92250

ID	Sex	SpeciesID	CollectionDate	CollectionLocation	latitude	longitude
INH4	NA	Cypkan	17.08.14	Kanfonki	-8.70278	30.92250
INH5	NA	Cypkan	17.08.14	Kanfonki	-8.70278	30.92250
INH6	NA	Cypkan	17.08.14	Kanfonki	-8.70278	30.92250
INH7	M	Cphgib	17.08.14	Kanfonki	-8.70278	30.92250
INH9	F	Cphgib	17.08.14	Kanfonki	-8.70278	30.92250
INI2	M	Neosex	17.08.14	Kanfonki	-8.70278	30.92250
INI3	M	Neosex	17.08.14	Kanfonki	-8.70278	30.92250
INI4	F	Neosex	17.08.14	Kanfonki	-8.70278	30.92250
INI5	F	Neosex	17.08.14	Kanfonki	-8.70278	30.92250
INI6	M	Neosex	17.08.14	Kanfonki	-8.70278	30.92250
INI8	M	Plestr	17.08.14	Kanfonki	-8.70278	30.92250
IOA1	M	Neobue	23.08.14	Kachese	-8.49053	30.47750
IOA2	M	Neobue	23.08.14	Kachese	-8.49053	30.47750
IOA3	F	Neobue	23.08.14	Kachese	-8.49053	30.47750
IOA4	F	Neobue	23.08.14	Kachese	-8.49053	30.47750
IOA5	M	Neobue	23.08.14	Kachese	-8.49053	30.47750
IOA6	F	Neobue	23.08.14	Kachese	-8.49053	30.47750
IOA7	NA	Neobue	23.08.14	Kachese	-8.49053	30.47750
IOA8	NA	Neobue	23.08.14	Kachese	-8.49053	30.47750
IOA9	NA	Neobue	23.08.14	Kachese	-8.49053	30.47750
IOB1	F	Julreg	23.08.14	Kachese	-8.49053	30.47750
IOB2	F	Julreg	23.08.14	Kachese	-8.49053	30.47750
IOB3	F	Julreg	23.08.14	Kachese	-8.49053	30.47750
IOB4	M	Lamoce	23.08.14	Ntingila	-8.48139	30.46139
IOB5	NA	Altcal	23.08.14	NA	NA	NA
IOB6	NA	Altcal	23.08.14	NA	NA	NA
IOB7	NA	Loblab	23.08.14	Kachese	-8.49053	30.47750
IOB8	NA	Loblab	23.08.14	Kachese	-8.49053	30.47750
IOB9	M	Neofas	23.08.14	Kachese	-8.49053	30.47750
IOC1	M	Lepken	23.08.14	Kachese	-8.49053	30.47750
IOC2	NA	Tromoo	23.08.14	Kachese	-8.49053	30.47750
IOC3	NA	Altcal	23.08.14	Kachese	-8.49053	30.47750
IOC4	NA	Altcal	23.08.14	Kachese	-8.49053	30.47750
IOC5	NA	Altcal	23.08.14	Kachese	-8.49053	30.47750
IOC6	NA	Neoobs	23.08.14	Kachese	-8.49053	30.47750
IOC7	NA	Neoobs	23.08.14	Kachese	-8.49053	30.47750
IOC8	NA	Neoobs	23.08.14	Kachese	-8.49053	30.47750
IOC9	NA	Neoobs	23.08.14	Kachese	-8.49053	30.47750
IOD2	NA	Gralem	23.08.14	Kachese	-8.49053	30.47750
IOD3	NA	Gralem	23.08.14	Kachese	-8.49053	30.47750
IOD4	F	Cyafoa	24.08.14	Chimba	-8.42611	30.45667
IOD6	M	Cyafoa	24.08.14	Chimba	-8.42611	30.45667
IOD9	M	Trored	24.08.14	Chimba	-8.42611	30.45667
IOE1	F	Trored	24.08.14	Chimba	-8.42611	30.45667
IOE2	M	Altcal	24.08.14	Chimba	-8.42611	30.45667
IOE3	F	Altcal	24.08.14	Chimba	-8.42611	30.45667
IOE4	M	Altcal	24.08.14	Chimba	-8.42611	30.45667
IOE5	NA	Altcal	24.08.14	Chimba	-8.42611	30.45667
IOE6	M	Plepar	24.08.14	Chimba	-8.42611	30.45667
IOE7	M	Plepar	24.08.14	Chimba	-8.42611	30.45667
IOE8	NA	Trored	24.08.14	Chimba	-8.42611	30.45667
IOE9	F	Trored	24.08.14	Chimba	-8.42611	30.45667
IOF1	NA	Trored	24.08.14	Chimba	-8.42611	30.45667
IOF2	NA	Trored	24.08.14	Chimba	-8.42611	30.45667
IOF3	M	Trored	24.08.14	Chimba	-8.42611	30.45667
IOF4	M	Trored	24.08.14	Chimba	-8.42611	30.45667
IOF5	M	Trored	24.08.14	Chimba	-8.42611	30.45667
IOF6	M	Trored	24.08.14	Chimba	-8.42611	30.45667
IOF7	F	Trored	24.08.14	Chimba	-8.42611	30.45667
IOF8	M	Ophnas	24.08.14	Chimba	-8.42611	30.45667
IOF9	M	Ophnas	24.08.14	Chimba	-8.42611	30.45667
IOG3	M	Cyafoa	24.08.14	Chimba	-8.42611	30.45667
IOG4	M	Cyafoa	24.08.14	Chimba	-8.42611	30.45667
IOG5	M	Cyafoa	24.08.14	Chimba	-8.42611	30.45667
IOG6	M	Cyafoa	24.08.14	Chimba	-8.42611	30.45667
IOG7	M	Cyafoa	24.08.14	Chimba	-8.42611	30.45667
IOG8	F	Cyafoa	24.08.14	Chimba	-8.42611	30.45667
IOG9	F	Cyafoa	24.08.14	Chimba	-8.42611	30.45667
IOH1	F	Cyafoa	24.08.14	Chimba	-8.42611	30.45667
IOH2	F	Cyafoa	24.08.14	Chimba	-8.42611	30.45667
IOH4	F	Lepcun	24.08.14	Chimba	-8.42611	30.45667
IOH5	M	Lepcun	24.08.14	Chimba	-8.42611	30.45667
IOH6	M	Regcal	24.08.14	Chimba	-8.42611	30.45667
IOH7	M	Regcal	24.08.14	Chimba	-8.42611	30.45667
IOH8	M	Lesper	24.08.14	Chimba	-8.42611	30.45667
IOH9	F	Lesper	24.08.14	Chimba	-8.42611	30.45667
IOI1	M	Lesper	24.08.14	Chimba	-8.42611	30.45667
IOI2	F	Lesper	24.08.14	Chimba	-8.42611	30.45667
IOI3	M	Lesper	24.08.14	Chimba	-8.42611	30.45667
IOI4	F	Lesper	24.08.14	Chimba	-8.42611	30.45667
IOI5	NA	Lesper	24.08.14	Chimba	-8.42611	30.45667
IOI6	M	Lesper	24.08.14	Chimba	-8.42611	30.45667
IOI7	F	Lesper	24.08.14	Chimba	-8.42611	30.45667
IOI8	F	Lesper	24.08.14	Chimba	-8.42611	30.45667
IOI9	M	Psccur	24.08.14	Chimba	-8.42611	30.45667
IPA1	M	Cyafur	20.07.14	Toby's Place	-8.62322	31.20044
IPA3	M	Chabri	20.07.14	Toby's Place	-8.62322	31.20044
IPA4	F	Cyafur	20.07.14	Toby's Place	-8.62322	31.20044
IPA6	F	Cyafur	20.07.14	Toby's Place	-8.62322	31.20044
IPA8	NA	Permic	20.07.14	Toby's Place	-8.62322	31.20044
IPA9	NA	Xenspi	20.07.14	Toby's Place	-8.62322	31.20044
IPB1	NA	Auldew	20.07.14	Toby's Place	-8.62322	31.20044
IPB3	M	Neosav	20.07.14	Toby's Place	-8.62322	31.20044
IPB4	M	Lepelo	20.07.14	Toby's Place	-8.62322	31.20044
IPB5	F	Intloo	20.07.14	Toby's Place	-8.62322	31.20044
IPB6	F	Intloo	20.07.14	Toby's Place	-8.62322	31.20044
IPB7	M	Intloo	20.07.14	Toby's Place	-8.62322	31.20044
IPB8	NA	Intloo	20.07.14	Toby's Place	-8.62322	31.20044
IPB9	NA	Intloo	20.07.14	Toby's Place	-8.62322	31.20044
IPC1	F	Peteph	20.07.14	Toby's Place	-8.62322	31.20044
IPC2	NA	Xenspi	20.07.14	Toby's Place	-8.62322	31.20044
IPC3	NA	Neotet	20.07.14	Toby's Place	-8.62322	31.20044
IPC6	F	Ophnas	20.07.14	Toby's Place	-8.62322	31.20044
IPC8	F	Ophnas	21.07.14	Toby's Place	-8.62322	31.20044
IPC9	M	Ophnas	21.07.14	Toby's Place	-8.62322	31.20044
IPD1	M	Ophnas	21.07.14	Toby's Place	-8.62322	31.20044
IPD2	F	Ophnas	21.07.14	Toby's Place	-8.62322	31.20044
IPD3	F	Ophnas	21.07.14	Toby's Place	-8.62322	31.20044
IPD6	F	Lamlem	21.07.14	Toby's Place	-8.62322	31.20044
IPD8	NA	Neosav	21.07.14	Toby's Place	-8.62322	31.20044
IPD9	NA	Neosav	21.07.14	Toby's Place	-8.62322	31.20044
IPE2	NA	Neosav	21.07.14	Toby's Place	-8.62322	31.20044
IPE3	M	Xenbou	21.07.14	Toby's Place	-8.62322	31.20044
IPE4	NA	Lamlem	21.07.14	Toby's Place	-8.62322	31.20044
IPE5	M	Lepatt	21.07.14	Toby's Place	-8.62322	31.20044
IPE6	F	Lepatt	21.07.14	Toby's Place	-8.62322	31.20044
IPE7	F	Xenbou	21.07.14	Toby's Place	-8.62322	31.20044
IPE8	M	Permic	21.07.14	Toby's Place	-8.62322	31.20044
IPE9	NA	Permic	21.07.14	Toby's Place	-8.62322	31.20044
IPF2	F	Intloo	21.07.14	Toby's Place	-8.62322	31.20044
IPF3	M	Intloo	21.07.14	Toby's Place	-8.62322	31.20044
IPF7	M	Neotet	21.07.14	Toby's Place	-8.62322	31.20044
IPG1	NA	Permic	21.07.14	Toby's Place	-8.62322	31.20044
IPG2	NA	Permic	21.07.14	Toby's Place	-8.62322	31.20044
IPG3	F	Neotet	21.07.14	Toby's Place	-8.62322	31.20044
IPG4	F	Xenspi	21.07.14	Toby's Place	-8.62322	31.20044
IPG5	F	Lepelo	21.07.14	Toby's Place	-8.62322	31.20044
IPG7	M	Neofas	21.07.14	Toby's Place	-8.62322	31.20044
IPG8	F	Gnapfe	21.07.14	Toby's Place	-8.62322	31.20044
IPG9	M	Auldew	21.07.14	Toby's Place	-8.62322	31.20044
IPH1	F	Auldew	21.07.14	Toby's Place	-8.62322	31.20044
IPH2	M	Lamcal	21.07.14	Toby's Place	-8.62322	31.20044
IPH3	F	Altcom	21.07.14	Toby's Place	-8.62322	31.20044
IPH4	M	Xenspi	21.07.14	Toby's Place	-8.62322	31.20044
IPH5	M	Auldew	21.07.14	Toby's Place	-8.62322	31.20044
IPH7	F	Lepatt	21.07.14	Toby's Place	-8.62322	31.20044
IPH8	NA	TelteS	21.07.14	Toby's Place	-8.62322	31.20044
IPI1	M	Lamlem	21.07.14	Toby's Place	-8.62322	31.20044
IPI2	NA	Neotet	21.07.14	Toby's Place	-8.62322	31.20044
IPI3	NA	Neotet	21.07.14	Toby's Place	-8.62322	31.20044
IPI4	NA	Neotet	21.07.14	Toby's Place	-8.62322	31.20044
IPI5	NA	Neotet	21.07.14	Toby's Place	-8.62322	31.20044
IPI6	NA	Neotet	21.07.14	Toby's Place	-8.62322	31.20044
IPI7	NA	Neotet	21.07.14	Toby's Place	-8.62322	31.20044
IPI8	NA	Neotet	21.07.14	Toby's Place	-8.62322	31.20044
IQA3	M	Neocau	21.07.14	Toby's Place	-8.62322	31.20044
IQA4	F	Neocau	21.07.14	Toby's Place	-8.62322	31.20044
IQA6	NA	Xenspi	21.07.14	Toby's Place	-8.62322	31.20044
IQA7	M	TelteS	21.07.14	Toby's Place	-8.62322	31.20044
IQA9	F	Neocau	21.07.14	Toby's Place	-8.62322	31.20044
IQB1	F	Neocau	21.07.14	Toby's Place	-8.62322	31.20044
IQB2	F	Neocau	21.07.14	Toby's Place	-8.62322	31.20044
IQB3	F	Neocau	21.07.14	Toby's Place	-8.62322	31.20044
IQB4	M	Neocau	21.07.14	Toby's Place	-8.62322	31.20044
IQB5	M	Neocau	21.07.14	Toby's Place	-8.62322	31.20044
IQB6	F	Haptri	22.07.14	Toby's Place	-8.62322	31.20044
IQB8	M	Hapmic	22.07.14	Toby's Place	-8.62322	31.20044
IQB9	M	Pcybri	22.07.14	Toby's Place	-8.62322	31.20044
IQC1	F	Pcybri	22.07.14	Toby's Place	-8.62322	31.20044
IQC4	M	Permic	22.07.14	Toby's Place	-8.62322	31.20044
IQD3	M	Ophven	22.07.14	Toby's Place	-8.62322	31.20044
IQD5	M	Enamel	22.07.14	Toby's Place	-8.62322	31.20044
IQD6	M	Enamel	22.07.14	Toby's Place	-8.62322	31.20044
IQD7	NA	Lepelo	22.07.14	Toby's Place	-8.62322	31.20044
IQE1	M	Pcybri	22.07.14	Toby's Place	-8.62322	31.20044
IQE2	F	Pcybri	22.07.14	Toby's Place	-8.62322	31.20044
IQE3	M	Pcybri	22.07.14	Toby's Place	-8.62322	31.20044
IQE4	F	Ophven	22.07.14	Toby's Place	-8.62322	31.20044
IQE6	F	Pcybri	22.07.14	Toby's Place	-8.62322	31.20044
IQE7	NA	Pcybri	22.07.14	Toby's Place	-8.62322	31.20044
IQF1	M	Xenbou	22.07.14	Toby's Place	-8.62322	31.20044
IQF2	M	Cypcol	22.07.14	Toby's Place	-8.62322	31.20044
IQF3	M	Cypcol	22.07.14	Toby's Place	-8.62322	31.20044
IQF5	M	Cyafur	22.07.14	Toby's Place	-8.62322	31.20044
IQF6	NA	Chabri	22.07.14	Toby's Place	-8.62322	31.20044
IQF7	NA	Chabri	22.07.14	Toby's Place	-8.62322	31.20044
IQF8	NA	Lepelo	22.07.14	Toby's Place	-8.62322	31.20044
IQF9	M	Ophven	22.07.14	Toby's Place	-8.62322	31.20044
IQG1	M	Ophven	22.07.14	Toby's Place	-8.62322	31.20044
IQG3	M	Ophven	22.07.14	Toby's Place	-8.62322	31.20044
IQG4	M	Ophven	22.07.14	Toby's Place	-8.62322	31.20044
IQG5	F	Ophven	22.07.14	Toby's Place	-8.62322	31.20044
IQG6	F	Ophven	22.07.14	Toby's Place	-8.62322	31.20044
IQG7	F	Ophven	22.07.14	Toby's Place	-8.62322	31.20044
IQG8	M	Gnapfe	22.07.14	Toby's Place	-8.62322	31.20044
IQH2	M	Ophven	22.07.14	Toby's Place	-8.62322	31.20044
IQH3	F	Ophven	22.07.14	Toby's Place	-8.62322	31.20044
IQH4	F	Ophven	22.07.14	Toby's Place	-8.62322	31.20044
IQH6	M	Xenbou	22.07.14	Toby's Place	-8.62322	31.20044
IQH7	F	Enamel	22.07.14	Toby's Place	-8.62322	31.20044
IQH8	F	Auldew	22.07.14	Toby's Place	-8.62322	31.20044
IQH9	M	Gnapfe	22.07.14	Toby's Place	-8.62322	31.20044
IQI1	M	Cyafur	22.07.14	Toby's Place	-8.62322	31.20044
IQI2	M	Lamlem	22.07.14	Toby's Place	-8.62322	31.20044
IQI3	NA	Neofas	22.07.14	Toby's Place	-8.62322	31.20044
IQI4	F	Permic	22.07.14	Toby's Place	-8.62322	31.20044
IQI6	M	Ctehor	22.07.14	Toby's Place	-8.62322	31.20044
IQI7	F	Gnapfe	22.07.14	Toby's Place	-8.62322	31.20044
IQI8	M	Neotet	22.07.14	Toby's Place	-8.62322	31.20044
IQI9	M	Neotet	22.07.14	Toby's Place	-8.62322	31.20044
IRA1	M	Lesper	24.08.14	Chimba	-8.42611	30.45667
IRA2	F	Lesper	24.08.14	Chimba	-8.42611	30.45667
IRA3	F	Neofur	24.08.14	Chimba	-8.42611	30.45667
IRA4	M	Neofur	24.08.14	Chimba	-8.42611	30.45667
IRA5	M	Neofur	24.08.14	Chimba	-8.42611	30.45667
IRA6	F	Neofur	24.08.14	Chimba	-8.42611	30.45667
IRA7	M	Neofur	24.08.14	Chimba	-8.42611	30.45667
IRA8	F	Pscple	24.08.14	Chimba	-8.42611	30.45667
IRA9	M	Petfam	24.08.14	Chimba	-8.42611	30.45667
IRB1	M	Petfam	24.08.14	Chimba	-8.42611	30.45667
IRB2	F	Julreg	24.08.14	Chimba	-8.42611	30.45667
IRB3	NA	Julreg	24.08.14	Chimba	-8.42611	30.45667

ID	Sex	SpeciesID	CollectionDate	CollectionLocation	latitude	longitude
IRB4	NA	Julreg	24.08.14	Chimba	-8.42611	30.45667
IRB5	NA	Julreg	24.08.14	Chimba	-8.42611	30.45667
IRB6	NA	Julreg	24.08.14	Chimba	-8.42611	30.45667
IRB7	NA	Julreg	24.08.14	Chimba	-8.42611	30.45667
IRB8	M	Julreg	24.08.14	Chimba	-8.42611	30.45667
IRB9	NA	Telvit	24.08.14	Chimba	-8.42611	30.45667
IRC1	NA	Telvit	24.08.14	Chimba	-8.42611	30.45667
IRC2	NA	Telvit	24.08.14	Chimba	-8.42611	30.45667
IRC4	M	Juldic	24.08.14	Chimba	-8.42611	30.45667
IRC5	F	Juldic	24.08.14	Chimba	-8.42611	30.45667
IRC6	M	Juldic	24.08.14	Chimba	-8.42611	30.45667
IRC7	M	Juldic	24.08.14	Chimba	-8.42611	30.45667
IRC8	NA	Juldic	24.08.14	Chimba	-8.42611	30.45667
IRC9	M	Juldic	24.08.14	Chimba	-8.42611	30.45667
IRD1	M	Juldic	24.08.14	Chimba	-8.42611	30.45667
IRD2	NA	Xchhec	25.08.14	Ndole Fishermen	-8.47669	30.45567
IRD3	NA	Xchhec	25.08.14	Ndole Fishermen	-8.47669	30.45567
IRD4	F	Gralem	25.08.14	Ndole Fishermen	-8.47669	30.45567
IRD5	M	Lepcun	25.08.14	Ndole Fishermen	-8.47669	30.45567
IRD6	NA	Lepcun	25.08.14	Ndole Fishermen	-8.47669	30.45567
IRD7	M	Ectdes	25.08.14	Ndole bay harbor	-8.47614	30.44933
IRD8	F	Ectdes	25.08.14	Ndole bay harbor	-8.47614	30.44933
IRD9	M	Xensin	25.08.14	Ndole bay harbor	-8.47614	30.44933
IRE1	F	Xensin	25.08.14	Ndole bay harbor	-8.47614	30.44933
IRE2	M	Xensin	25.08.14	Ndole bay harbor	-8.47614	30.44933
IRE3	F	Xensin	25.08.14	Ndole bay harbor	-8.47614	30.44933
IRE5	M	Ectdes	25.08.14	Ndole bay harbor	-8.47614	30.44933
IRE6	F	Ectdes	25.08.14	Ndole bay harbor	-8.47614	30.44933
IRE7	M	Ectdes	25.08.14	Ndole bay harbor	-8.47614	30.44933
IRE8	F	Ectdes	25.08.14	Ndole bay harbor	-8.47614	30.44933
IRE9	F	Ectdes	25.08.14	Ndole bay harbor	-8.47614	30.44933
IRF1	F	Ectdes	25.08.14	Ndole bay harbor	-8.47614	30.44933
IRF2	F	Ectdes	25.08.14	Ndole bay harbor	-8.47614	30.44933
IRF3	F	Ectdes	25.08.14	Ndole bay harbor	-8.47614	30.44933
IRF4	M	Ectdes	25.08.14	Ndole bay harbor	-8.47614	30.44933
IRF5	F	Ectdes	25.08.14	Ndole bay harbor	-8.47614	30.44933
IRF6	M	Neomul	25.08.14	Chibwensolo	-8.44278	30.45472
IRF8	F	Neomul	25.08.14	Chibwensolo	-8.44278	30.45472
IRG1	NA	Neomul	25.08.14	Chibwensolo	-8.44278	30.45472
IRG2	NA	Neomul	25.08.14	Chibwensolo	-8.44278	30.45472
IRG3	NA	Neomul	25.08.14	Chibwensolo	-8.44278	30.45472
IRG4	NA	Neomul	25.08.14	Chibwensolo	-8.44278	30.45472
IRG5	NA	Neomul	25.08.14	Chibwensolo	-8.44278	30.45472
IRG6	NA	Neomul	25.08.14	Chibwensolo	-8.44278	30.45472
IRG7	NA	Neomul	25.08.14	Chibwensolo	-8.44278	30.45472
IRG8	NA	Neomul	25.08.14	Chibwensolo	-8.44278	30.45472
IRG9	NA	Neomul	25.08.14	Chibwensolo	-8.44278	30.45472
IRH1	NA	Neomul	25.08.14	Chibwensolo	-8.44278	30.45472
IRH2	M	Altshe	25.08.14	Chibwensolo	-8.44278	30.45472
IRH4	F	Altshe	25.08.14	Chibwensolo	-8.44278	30.45472
IRH6	F	Altshe	25.08.14	Chibwensolo	-8.44278	30.45472
IRH7	M	Altshe	25.08.14	Chibwensolo	-8.44278	30.45472
IRH8	F	Altshe	25.08.14	Chibwensolo	-8.44278	30.45472
IRH9	NA	Altshe	25.08.14	Chibwensolo	-8.44278	30.45472
IRI1	NA	Altshe	25.08.14	Chibwensolo	-8.44278	30.45472
IRI2	NA	Altshe	25.08.14	Chibwensolo	-8.44278	30.45472
IRI3	NA	Altshe	25.08.14	Chibwensolo	-8.44278	30.45472
IRI5	NA	Altshe	25.08.14	Chibwensolo	-8.44278	30.45472
IRI6	NA	Altshe	25.08.14	Chibwensolo	-8.44278	30.45472
IRI7	NA	Altshe	25.08.14	Chibwensolo	-8.44278	30.45472
IRI8	M	Telshe	25.08.14	Chibwensolo	-8.44278	30.45472
IRI9	F	Telshe	25.08.14	Chibwensolo	-8.44278	30.45472
ISA1	M	Tremar	22.07.14	Toby's Place	-8.62322	31.20044
ISA3	F	Tremar	22.07.14	Toby's Place	-8.62322	31.20044
ISA6	M	Neopul	23.07.14	Toby's Place	-8.62322	31.20044
ISA8	M	Neosav	23.07.14	Toby's Place	-8.62322	31.20044
ISB1	M	Altcom	23.07.14	Toby's Place	-8.62322	31.20044
ISB3	F	Neopul	23.07.14	Toby's Place	-8.62322	31.20044
ISB7	M	Julorn	23.07.14	Toby's Place	-8.62322	31.20044
ISC1	F	Julorn	23.07.14	Toby's Place	-8.62322	31.20044
ISC9	F	Altcom	23.07.14	Toby's Place	-8.62322	31.20044
ISD4	NA	Lamlem	23.07.14	Toby's Place	-8.62322	31.20044
ISD5	NA	Neopul	23.07.14	Toby's Place	-8.62322	31.20044
ISD6	NA	Xenfla	23.07.14	Toby's Place	-8.62322	31.20044
ISD7	NA	Xenfla	23.07.14	Toby's Place	-8.62322	31.20044
ISD8	M	Loblab	23.07.14	Toby's Place	-8.62322	31.20044
ISE1	NA	Lepelo	23.07.14	Toby's Place	-8.62322	31.20044
ISE2	M	Pscple	23.07.14	Toby's Place	-8.62322	31.20044
ISE3	F	Pscple	23.07.14	Toby's Place	-8.62322	31.20044
ISE4	F	Pscple	23.07.14	Toby's Place	-8.62322	31.20044
ISE5	F	Loblab	23.07.14	Toby's Place	-8.62322	31.20044
ISE7	NA	Altcom	23.07.14	Toby's Place	-8.62322	31.20044
ISE8	NA	Altcom	23.07.14	Toby's Place	-8.62322	31.20044
ISF1	NA	Neopul	23.07.14	Toby's Place	-8.62322	31.20044
ISF4	F	Cyafur	23.07.14	Toby's Place	-8.62322	31.20044
ISF5	M	Cyafur	23.07.14	Toby's Place	-8.62322	31.20044
ISF6	NA	Lamlem	23.07.14	Toby's Place	-8.62322	31.20044
ISF7	NA	Lepatt	23.07.14	Toby's Place	-8.62322	31.20044
ISF8	NA	Neopul	23.07.14	Toby's Place	-8.62322	31.20044
ISF9	NA	Neopul	23.07.14	Toby's Place	-8.62322	31.20044
ISG4	NA	Neofas	23.07.14	Toby's Place	-8.62322	31.20044
ISG5	NA	Neocau	23.07.14	Toby's Place	-8.62322	31.20044
ISG6	NA	Neocau	23.07.14	Toby's Place	-8.62322	31.20044
ISG7	NA	Neocau	23.07.14	Toby's Place	-8.62322	31.20044
ISG8	NA	Neocau	23.07.14	Toby's Place	-8.62322	31.20044
ISH1	NA	Lepelo	23.07.14	Toby's Place	-8.62322	31.20044
ISH2	NA	Lepelo	23.07.14	Toby's Place	-8.62322	31.20044
ISH3	NA	Lepelo	23.07.14	Toby's Place	-8.62322	31.20044
ISH4	NA	Lepelo	23.07.14	Toby's Place	-8.62322	31.20044
ISH5	NA	Gnapfe	23.07.14	Toby's Place	-8.62322	31.20044
ISH6	NA	Gnapfe	23.07.14	Toby's Place	-8.62322	31.20044
ISH7	NA	Neopul	23.07.14	Toby's Place	-8.62322	31.20044
ISH8	NA	Neopul	23.07.14	Toby's Place	-8.62322	31.20044
ISI1	NA	Varmoo	23.07.14	Toby's Place	-8.62322	31.20044
ISI2	M	Cyplep	24.07.14	Toby's Place	-8.62322	31.20044
ISI6	F	Cyplep	24.07.14	Toby's Place	-8.62322	31.20044

ID	Sex	SpeciesID	CollectionDate	CollectionLocation	latitude	longitude
ITA4	F	Gnaper	24.07.14	Chipwa Fishermen	-8.60617	31.18611
ITA6	F	Lchsta	24.07.14	Chipwa Fishermen	-8.60617	31.18611
ITB1	F	Lchaur	24.07.14	Chipwa Fishermen	-8.60617	31.18611
ITB3	F	Lchabe	24.07.14	Chipwa Fishermen	-8.60617	31.18611
ITB4	M	Lchabe	24.07.14	Chipwa Fishermen	-8.60617	31.18611
ITB5	NA	Lchsta	24.07.14	Chipwa Fishermen	-8.60617	31.18611
ITB6	NA	Lchsta	24.07.14	Chipwa Fishermen	-8.60617	31.18611
ITB7	NA	Lchsta	24.07.14	Chipwa Fishermen	-8.60617	31.18611
ITB8	NA	Lchsta	24.07.14	Chipwa Fishermen	-8.60617	31.18611
ITB9	NA	Lchabe	24.07.14	Chipwa Fishermen	-8.60617	31.18611
ITC1	M	Batgra	24.07.14	Chipwa Fishermen	-8.60617	31.18611
ITC2	M	Lchsta	24.07.14	Chipwa Fishermen	-8.60617	31.18611
ITC3	F	Cyplep	24.07.14	Chipwa Fishermen	-8.60617	31.18611
ITC4	F	Cyplep	24.07.14	Chipwa Fishermen	-8.60617	31.18611
ITC5	M	Cyplep	24.07.14	Chipwa Fishermen	-8.60617	31.18611
ITC6	M	Cyplep	24.07.14	Chipwa Fishermen	-8.60617	31.18611
ITC7	M	Cyplep	24.07.14	Chipwa Fishermen	-8.60617	31.18611
ITD4	NA	Cypcol	24.07.14	Toby's Place	-8.62322	31.20044
ITD5	NA	Batgra	24.07.14	Chipwa Fishermen	-8.60617	31.18611
ITD6	NA	Batgra	24.07.14	Chipwa Fishermen	-8.60617	31.18611
ITD7	M	Batvit	24.07.14	Chipwa Fishermen	-8.60617	31.18611
ITD8	F	Pcybri	24.07.14	Chipwa Fishermen	-8.60617	31.18611
ITD9	NA	Pcybri	24.07.14	Chipwa Fishermen	-8.60617	31.18611
ITE1	M	Pcybri	24.07.14	Chipwa Fishermen	-8.60617	31.18611
ITE2	M	Pcybri	24.07.14	Chipwa Fishermen	-8.60617	31.18611
ITE3	F	Pcybri	24.07.14	Chipwa Fishermen	-8.60617	31.18611
ITE4	NA	Batleo	24.07.14	Chipwa Fishermen	-8.60617	31.18611
ITE6	F	Cyplep	24.07.14	Chipwa Fishermen	-8.60617	31.18611
ITE7	F	Cyplep	24.07.14	Chipwa Fishermen	-8.60617	31.18611
ITE8	M	Cyplep	24.07.14	Chipwa Fishermen	-8.60617	31.18611
ITE9	M	Cyplep	24.07.14	Chipwa Fishermen	-8.60617	31.18611
ITF1	NA	Cyplep	24.07.14	Chipwa Fishermen	-8.60617	31.18611
ITF2	NA	Batleo	24.07.14	Chipwa Fishermen	-8.60617	31.18611
ITF3	M	Batvit	24.07.14	Chipwa Fishermen	-8.60617	31.18611
ITF5	M	Cypcol	24.07.14	Toby's Place	-8.62322	31.20044
ITF6	NA	Cypcol	24.07.14	Toby's Place	-8.62322	31.20044
ITF7	NA	Cypcol	24.07.14	Toby's Place	-8.62322	31.20044
ITF8	NA	Batvit	24.07.14	Chipwa Fishermen	-8.60617	31.18611
ITF9	M	Xenbou	24.07.14	Chipwa Fishermen	-8.60617	31.18611
ITG1	NA	Petpol	24.07.14	Chipwa Fishermen	-8.60617	31.18611
ITG2	F	Neochr	24.07.14	Chipwa Fishermen	-8.60617	31.18611
ITG3	M	Hapmic	24.07.14	Chipwa Fishermen	-8.60617	31.18611
ITG4	M	Hapmic	24.07.14	Chipwa Fishermen	-8.60617	31.18611
ITG5	M	Hapmic	24.07.14	Chipwa Fishermen	-8.60617	31.18611
ITG6	M	Hapmic	24.07.14	Chipwa Fishermen	-8.60617	31.18611
ITG7	F	Auldew	24.07.14	Toby's Place	-8.62322	31.20044
ITG8	NA	Petpol	24.07.14	Toby's Place	-8.62322	31.20044
ITG9	NA	Petpol	24.07.14	Toby's Place	-8.62322	31.20044
ITH3	M	Batfas	24.07.14	Chipwa Fishermen	-8.60617	31.18611
ITH6	NA	Boumic	24.07.14	Chipwa Fishermen	-8.60617	31.18611
ITH7	NA	Boumic	24.07.14	Chipwa Fishermen	-8.60617	31.18611
ITH8	NA	Batfas	24.07.14	Chipwa Fishermen	-8.60617	31.18611
ITI2	M	Trenig	24.07.14	Chipwa Fishermen	-8.60617	31.18611
IUA8	F	Trenig	25.07.14	Toby's Place	-8.62322	31.20044
IUA9	F	Trenig	25.07.14	Toby's Place	-8.62322	31.20044
IUB1	F	Trenig	25.07.14	Toby's Place	-8.62322	31.20044
IUB2	F	Trenig	25.07.14	Toby's Place	-8.62322	31.20044
IUB3	F	Trenig	25.07.14	Toby's Place	-8.62322	31.20044
IUB4	F	Trenig	25.07.14	Toby's Place	-8.62322	31.20044
IUB5	F	Trenig	25.07.14	Toby's Place	-8.62322	31.20044
IUC2	M	Tremar	25.07.14	Toby's Place	-8.62322	31.20044
IUC3	M	Tremar	25.07.14	Toby's Place	-8.62322	31.20044
IUC6	F	Tremar	25.07.14	Toby's Place	-8.62322	31.20044
IUC7	F	Tremar	25.07.14	Toby's Place	-8.62322	31.20044
IUD2	F	Tremar	25.07.14	Toby's Place	-8.62322	31.20044
IUD3	M	Tremar	25.07.14	Toby's Place	-8.62322	31.20044
IUD4	F	Tremac	25.07.14	Toby's Place	-8.62322	31.20044
IUD5	F	Tremac	25.07.14	Toby's Place	-8.62322	31.20044
IUD6	F	Tremac	25.07.14	Toby's Place	-8.62322	31.20044
IUD8	M	Tremac	25.07.14	Toby's Place	-8.62322	31.20044
IUD9	F	Tremac	25.07.14	Toby's Place	-8.62322	31.20044
IUE1	M	Tremac	25.07.14	Toby's Place	-8.62322	31.20044
IUE2	M	Tremac	25.07.14	Toby's Place	-8.62322	31.20044
IUE5	M	Trenig	25.07.14	Toby's Place	-8.62322	31.20044
IUE7	M	Tresti	25.07.14	Toby's Place	-8.62322	31.20044
IUF7	M	Xensim	25.07.14	Toby's Place	-8.62322	31.20044
IUF8	F	Xensim	25.07.14	Toby's Place	-8.62322	31.20044
IUG8	F	Xensim	25.07.14	Toby's Place	-8.62322	31.20044
IUG9	NA	Gralem	25.07.14	Toby's Place	-8.62322	31.20044
IUH1	M	Cyafur	25.07.14	Toby's Place	-8.62322	31.20044
IUH2	M	Cyafur	25.07.14	Toby's Place	-8.62322	31.20044
IUH3	M	Cunlon	25.07.14	Isanga	-8.65456	31.19183
IUH4	M	Neofas	25.07.14	Isanga	-8.65456	31.19183
IUH5	M	Batgra	25.07.14	Chipwa Fishermen	-8.60617	31.18611
IUH6	M	Batgra	25.07.14	Chipwa Fishermen	-8.60617	31.18611
IUH7	F	Batgra	25.07.14	Toby's Place	-8.62322	31.20044
IUH8	F	Batgra	25.07.14	Toby's Place	-8.62322	31.20044
IUH9	M	Batgra	25.07.14	Toby's Place	-8.62322	31.20044
IUI1	M	Regcal	25.07.14	Chipwa Fishermen	-8.60617	31.18611
IUI3	M	Regcal	26.07.14	Chipwa Fishermen	-8.60617	31.18611
IUI4	F	Regcal	26.07.14	Chipwa Fishermen	-8.60617	31.18611
IUI5	M	Gnaper	27.07.14	Chipwa Fishermen	-8.60617	31.18611
IUI7	M	Xchhec	27.07.14	Chipwa Fishermen	-8.60617	31.18611
IUI8	F	Batgra	27.07.14	Chipwa Fishermen	-8.60617	31.18611
IVA1	NA	Telshe	25.08.14	Chibwensolo	-8.44278	30.45472
IVA2	NA	Telshe	25.08.14	Chibwensolo	-8.44278	30.45472
IVA3	NA	Telshe	25.08.14	Chibwensolo	-8.44278	30.45472
IVA4	NA	Telshe	25.08.14	Chibwensolo	-8.44278	30.45472
IVA5	NA	Telshe	25.08.14	Chibwensolo	-8.44278	30.45472
IVA6	NA	Telshe	25.08.14	Chibwensolo	-8.44278	30.45472
IVA7	NA	Telshe	25.08.14	Chibwensolo	-8.44278	30.45472
IVA8	NA	Telshe	25.08.14	Chibwensolo	-8.44278	30.45472
IVA9	NA	Telshe	25.08.14	Chibwensolo	-8.44278	30.45472
IVB1	M	Enamel	25.08.14	Ntingila	-8.48139	30.46139
IVB2	M	Enamel	25.08.14	Ntingila	-8.48139	30.46139
IVB4	M	Xenbat	25.08.14	Ntingila	-8.48139	30.46139

ID	Sex	SpeciesID	CollectionDate	CollectionLocation	latitude	longitude
IVB5	F	Xenbat	25.08.14	Ntingila	-8.48139	30.46139
IVB6	M	Xenbat	25.08.14	Ntingila	-8.48139	30.46139
IVB7	M	Xenbat	25.08.14	Ntingila	-8.48139	30.46139
IVB8	NA	Xenbat	25.08.14	Ntingila	-8.48139	30.46139
IVB9	NA	Xenbat	25.08.14	Ntingila	-8.48139	30.46139
IVC1	M	Xenbat	25.08.14	Ntingila	-8.48139	30.46139
IVC2	NA	Xenbat	25.08.14	Ntingila	-8.48139	30.46139
IVC4	F	Xenbat	25.08.14	Ntingila	-8.48139	30.46139
IVC7	NA	Xenbat	25.08.14	Ntingila	-8.48139	30.46139
IVC8	NA	Lepcun	25.08.14	Ntingila	-8.48139	30.46139
IVC9	NA	Lepcun	25.08.14	Ntingila	-8.48139	30.46139
IVD1	NA	Lepcun	25.08.14	Ntingila	-8.48139	30.46139
IVD2	NA	Lepcun	25.08.14	Ntingila	-8.48139	30.46139
IVD3	NA	Lepcun	25.08.14	Ntingila	-8.48139	30.46139
IVD5	NA	Julreg	25.08.14	Ntingila	-8.48139	30.46139
IVD6	NA	Julreg	25.08.14	Ntingila	-8.48139	30.46139
IVD8	NA	Juldic	25.08.14	Ntingila	-8.48139	30.46139
IVD9	NA	Juldic	25.08.14	Ntingila	-8.48139	30.46139
IVE1	NA	Juldic	25.08.14	Ntingila	-8.48139	30.46139
IVE2	NA	Juldic	25.08.14	Ntingila	-8.48139	30.46139
IVE3	NA	Juldic	25.08.14	Ntingila	-8.48139	30.46139
IVE5	NA	LamorS	25.08.14	Ntingila	-8.48139	30.46139
IVE6	NA	LamorS	25.08.14	Ntingila	-8.48139	30.46139
IVE7	NA	LamorS	25.08.14	Ntingila	-8.48139	30.46139
IVE8	M	Neocra	26.08.14	Katete	-8.33878	30.50794
IVF1	F	Neocra	26.08.14	Katete	-8.33878	30.50794
IVF4	M	Xenpap	26.08.14	Katete 3	-8.33778	30.51111
IVF5	F	Xenpap	26.08.14	Katete 3	-8.33778	30.51111
IVF7	M	Neocra	26.08.14	Katete 2	-8.32806	30.52667
IVF8	NA	Neocra	26.08.14	Katete 2	-8.32806	30.52667
IVF9	NA	Neocra	26.08.14	Katete 2	-8.32806	30.52667
IVG1	M	Neocra	26.08.14	Katete 2	-8.32806	30.52667
IVG2	M	Neocra	26.08.14	Katete 2	-8.32806	30.52667
IVG3	NA	Neocra	26.08.14	Katete 2	-8.32806	30.52667
IVG4	M	Neocra	26.08.14	Katete 2	-8.32806	30.52667
IVG5	NA	Neocra	26.08.14	Katete 2	-8.32806	30.52667
IVG6	NA	Neocra	26.08.14	Katete 2	-8.32806	30.52667
IVG7	F	Neocra	26.08.14	Katete 2	-8.32806	30.52667
IVG8	NA	Loblab	26.08.14	Katete 2	-8.32806	30.52667
IVG9	NA	Loblab	26.08.14	Katete 2	-8.32806	30.52667
IVH1	M	Neopro	26.08.14	Katete 2	-8.32806	30.52667
IVH2	F	Neopro	26.08.14	Katete 2	-8.32806	30.52667
IVH3	NA	Neopro	26.08.14	Katete 2	-8.32806	30.52667
IVH5	F	Xenpap	26.08.14	Katete 3	-8.33778	30.51111
IVH6	NA	Xenpap	26.08.14	Katete 3	-8.33778	30.51111
IVH7	F	Xenpap	26.08.14	Katete 3	-8.33778	30.51111
IVH8	NA	Xenpap	26.08.14	Katete 3	-8.33778	30.51111
IVH9	NA	Xenpap	26.08.14	Katete 3	-8.33778	30.51111
IVI1	NA	Xenpap	26.08.14	Katete 3	-8.33778	30.51111
IVI2	NA	Xenpap	26.08.14	Katete 3	-8.33778	30.51111
IVI3	NA	Xenpap	26.08.14	Katete 3	-8.33778	30.51111
IVI4	NA	Xenpap	26.08.14	Katete 3	-8.33778	30.51111
IVI5	NA	Xenpap	26.08.14	Katete 3	-8.33778	30.51111
IVI8	NA	Mdcrot	26.08.14	Katete 2	-8.32806	30.52667
IVI9	NA	Mdcrot	26.08.14	Katete 2	-8.32806	30.52667
IWA1	NA	Mdcrot	26.08.14	Katete 2	-8.32806	30.52667
IWA2	NA	Mdcrot	26.08.14	Katete 2	-8.32806	30.52667
IWA3	NA	Mdcrot	26.08.14	Katete 2	-8.32806	30.52667
IWA4	NA	Mdcrot	26.08.14	Katete 2	-8.32806	30.52667
IWA5	M	Neobue	26.08.14	Katete 3	-8.33778	30.51111
IWA8	M	Neoobs	26.08.14	Katete 2	-8.32806	30.52667
IWA9	M	Neoobs	26.08.14	Katete 2	-8.32806	30.52667
IWB1	M	Neoobs	26.08.14	Katete 2	-8.32806	30.52667
IWB2	F	Neoobs	26.08.14	Katete 2	-8.32806	30.52667
IWB3	NA	Plestr	26.08.14	Katete 3	-8.33778	30.51111
IWB5	M	Pethor	26.08.14	Katete 3	-8.33778	30.51111
IWB6	F	Pethor	26.08.14	Katete 3	-8.33778	30.51111
IWB7	F	Pethor	26.08.14	Katete 3	-8.33778	30.51111
IWB8	F	Pethor	26.08.14	Katete 3	-8.33778	30.51111
IWB9	F	Pethor	26.08.14	Katete 3	-8.33778	30.51111
IWC1	F	Pethor	26.08.14	Katete 3	-8.33778	30.51111
IWC2	F	Pethor	26.08.14	Katete 3	-8.33778	30.51111
IWC4	NA	Neofur	26.08.14	Katete 2	-8.32806	30.52667
IWC5	NA	Neofur	26.08.14	Katete 2	-8.32806	30.52667
IWC7	NA	Gnapfe	26.08.14	Katete 3	-8.33778	30.51111
IWC9	M	Pettre	26.08.14	Katete 2	-8.32806	30.52667
IWD1	F	Pettre	26.08.14	Katete 2	-8.32806	30.52667
IWD2	F	Pettre	26.08.14	Katete 2	-8.32806	30.52667
IWD3	F	Pettre	26.08.14	Katete 2	-8.32806	30.52667
IWD4	F	Pettre	26.08.14	Katete 2	-8.32806	30.52667
IWD5	M	Lamsig	28.08.14	Chimba	-8.42611	30.45667
IWD6	F	Lamsig	28.08.14	Chimba	-8.42611	30.45667
IWD7	M	Cunlon	27.08.14	Ntingila	-8.48139	30.46139
IWD8	F	Cunlon	27.08.14	Ntingila	-8.48139	30.46139
IWE1	M	Cunlon	27.08.14	Ntingila	-8.48139	30.46139
IWE2	M	Cunlon	27.08.14	Ntingila	-8.48139	30.46139
IWE3	M	Cunlon	27.08.14	Ntingila	-8.48139	30.46139
IWE4	M	Cunlon	27.08.14	Ntingila	-8.48139	30.46139
IWE5	F	Cunlon	27.08.14	Ntingila	-8.48139	30.46139
IWE6	F	Cunlon	27.08.14	Ntingila	-8.48139	30.46139
IWE7	F	Cunlon	27.08.14	Ntingila	-8.48139	30.46139
IWE8	F	Cunlon	27.08.14	Ntingila	-8.48139	30.46139
IWE9	F	Cunlon	27.08.14	Ntingila	-8.48139	30.46139
IWF1	NA	Lchaur	27.08.14	Ntingila	-8.48139	30.46139
IWF2	NA	Lchaur	27.08.14	Ntingila	-8.48139	30.46139
IWF3	NA	Lchaur	28.08.14	Ndole Fishermen	-8.47669	30.45567
IWF4	M	Lamsig	28.08.14	Chimba	-8.42611	30.45667
IWF5	M	Lamsig	28.08.14	Chimba	-8.42611	30.45667
IWF6	M	Lamsig	28.08.14	Chimba	-8.42611	30.45667
IWF7	M	Lamsig	28.08.14	Chimba	-8.42611	30.45667
IWF8	M	Lamsig	28.08.14	Chimba	-8.42611	30.45667
IWF9	M	Lamsig	28.08.14	Chimba	-8.42611	30.45667
IWG2	F	Lamsig	28.08.14	Chimba	-8.42611	30.45667
IWG3	F	Lamsig	28.08.14	Chimba	-8.42611	30.45667
IWG6	NA	Gralem	28.08.14	Ndole Fishermen	-8.47669	30.45567
IWG7	NA	Lepcun	28.08.14	Ndole Fishermen	-8.47669	30.45567
IWG8	NA	Gnapfe	28.08.14	Chimba village	-8.42139	30.45722
IWG9	NA	Gnapfe	28.08.14	Chimba village	-8.42139	30.45722
IWH1	NA	Gnapfe	28.08.14	Chimba village	-8.42139	30.45722
IWH2	F	Psccur	28.08.14	Chimba village	-8.42139	30.45722
IWH3	F	Psccur	28.08.14	Chimba village	-8.42139	30.45722
IWH4	M	Pscple	28.08.14	Chimba village	-8.42139	30.45722
IWH5	F	Pscple	28.08.14	Chimba village	-8.42139	30.45722
IWH6	NA	Pettre	28.08.14	Chimba village	-8.42139	30.45722
IWH7	NA	Pettre	28.08.14	Chimba village	-8.42139	30.45722
IWH8	NA	Pettre	28.08.14	Chimba village	-8.42139	30.45722
IWH9	NA	Pettre	28.08.14	Chimba village	-8.42139	30.45722
IWI1	NA	Pettre	28.08.14	Chimba village	-8.42139	30.45722
IWI4	M	Lamsig	29.08.14	Kabyolwe	-8.56917	30.75056
IWI5	F	Lamsig	29.08.14	Kabyolwe	-8.56917	30.75056
IWI6	F	Petfas	29.08.14	Kabyolwe	-8.56917	30.75056
IWI7	F	Trioto	29.08.14	Kabyolwe	-8.56917	30.75056
IWI8	M	Trioto	29.08.14	Kabyolwe	-8.56917	30.75056
IXA3	M	Treuni	27.07.14	Chipwa Fishermen	-8.60617	31.18611
IXA4	M	Perecc	27.07.14	Chipwa Fishermen	-8.60617	31.18611
IXA5	F	Batmin	27.07.14	Chipwa Fishermen	-8.60617	31.18611
IXA6	F	Treuni	27.07.14	Chipwa Fishermen	-8.60617	31.18611
IXB5	F	Gwcbel	27.07.14	Chipwa Fishermen	-8.60617	31.18611
IXB6	M	Lchsta	27.07.14	Chipwa Fishermen	-8.60617	31.18611
IXB8	M	Benmel	27.07.14	Chipwa Fishermen	-8.60617	31.18611
IXB9	M	Xencau	27.07.14	Chipwa Fishermen	-8.60617	31.18611
IXC1	F	Xencau	27.07.14	Chipwa Fishermen	-8.60617	31.18611
IXC2	M	Hemste	27.07.14	Chipwa Fishermen	-8.60617	31.18611
IXC3	F	Hemste	27.07.14	Chipwa Fishermen	-8.60617	31.18611
IXC5	M	Hemste	27.07.14	Chipwa Fishermen	-8.60617	31.18611
IXC6	M	Hemste	27.07.14	Chipwa Fishermen	-8.60617	31.18611
IXC7	M	Hemste	27.07.14	Chipwa Fishermen	-8.60617	31.18611
IXC8	M	Hemste	27.07.14	Chipwa Fishermen	-8.60617	31.18611
IXC9	M	HemstZ	27.07.14	Chipwa Fishermen	-8.60617	31.18611
IXD5	NA	Gnaper	27.07.14	Chipwa Fishermen	-8.60617	31.18611
IXD6	NA	Gnaper	27.07.14	Chipwa Fishermen	-8.60617	31.18611
IXD7	NA	Gnaper	27.07.14	Chipwa Fishermen	-8.60617	31.18611
IXD8	NA	Gnaper	27.07.14	Chipwa Fishermen	-8.60617	31.18611
IXD9	NA	Gnaper	27.07.14	Chipwa Fishermen	-8.60617	31.18611
IXE1	NA	Gnaper	27.07.14	Chipwa Fishermen	-8.60617	31.18611
IXE2	NA	Gnaper	27.07.14	Chipwa Fishermen	-8.60617	31.18611
IXE3	NA	Gnaper	27.07.14	Chipwa Fishermen	-8.60617	31.18611
IXE4	NA	Gnaper	27.07.14	Chipwa Fishermen	-8.60617	31.18611
IXE5	M	Tremac	27.07.14	Chipwa Fishermen	-8.60617	31.18611
IXE6	M	Tremac	27.07.14	Chipwa Fishermen	-8.60617	31.18611
IXE8	M	Tremac	27.07.14	Chipwa Fishermen	-8.60617	31.18611
IXE9	F	Treuni	27.07.14	Chipwa Fishermen	-8.60617	31.18611
IXF1	NA	Treuni	27.07.14	Chipwa Fishermen	-8.60617	31.18611
IXF2	M	Treuni	27.07.14	Chipwa Fishermen	-8.60617	31.18611
IXF3	M	Treuni	27.07.14	Chipwa Fishermen	-8.60617	31.18611
IXF4	F	XenniS	27.07.14	Chipwa Fishermen	-8.60617	31.18611
IXF5	M	Treuni	27.07.14	Chipwa Fishermen	-8.60617	31.18611
IXF6	F	Treuni	27.07.14	Chipwa Fishermen	-8.60617	31.18611
IXF7	NA	Treuni	27.07.14	Chipwa Fishermen	-8.60617	31.18611
IXF9	NA	Treuni	27.07.14	Chipwa Fishermen	-8.60617	31.18611
IXG1	M	Treuni	27.07.14	Chipwa Fishermen	-8.60617	31.18611
IXG2	NA	Batgra	27.07.14	Chipwa Fishermen	-8.60617	31.18611
IXG3	NA	Batgra	27.07.14	Chipwa Fishermen	-8.60617	31.18611
IXG4	NA	Xencau	27.07.14	Chipwa Fishermen	-8.60617	31.18611
IXG5	NA	Xencau	27.07.14	Chipwa Fishermen	-8.60617	31.18611
IXG6	NA	Benmel	27.07.14	Chipwa Fishermen	-8.60617	31.18611
IXG7	NA	Gwcchr	27.07.14	Chipwa Fishermen	-8.60617	31.18611
IXG8	NA	Lchsta	27.07.14	Chipwa Fishermen	-8.60617	31.18611
IXG9	NA	Lchsta	27.07.14	Chipwa Fishermen	-8.60617	31.18611
IXH1	NA	Lchsta	27.07.14	Chipwa Fishermen	-8.60617	31.18611
IXH2	NA	Lchsta	27.07.14	Chipwa Fishermen	-8.60617	31.18611
IXH3	NA	Lchsta	27.07.14	Chipwa Fishermen	-8.60617	31.18611
IXH4	NA	Lchsta	27.07.14	Chipwa Fishermen	-8.60617	31.18611
IXH5	NA	Gwcbel	27.07.14	Chipwa Fishermen	-8.60617	31.18611
IXH6	NA	Gwcbel	27.07.14	Chipwa Fishermen	-8.60617	31.18611
IXH7	NA	Gwcbel	27.07.14	Chipwa Fishermen	-8.60617	31.18611
IXH8	NA	Gwcbel	27.07.14	Chipwa Fishermen	-8.60617	31.18611
IXI1	M	Gwcbel	28.07.14	Chipwa Fishermen	-8.60617	31.18611
IXI2	F	Gwcbel	28.07.14	Chipwa Fishermen	-8.60617	31.18611
IXI3	NA	Benmel	28.07.14	Chipwa Fishermen	-8.60617	31.18611
IXI4	NA	Benmel	28.07.14	Chipwa Fishermen	-8.60617	31.18611
IXI5	NA	Benmel	28.07.14	Chipwa Fishermen	-8.60617	31.18611
IXI6	NA	Benmel	28.07.14	Chipwa Fishermen	-8.60617	31.18611
IXI7	NA	Benmel	28.07.14	Chipwa Fishermen	-8.60617	31.18611
IXI8	NA	Benmel	28.07.14	Chipwa Fishermen	-8.60617	31.18611
IYA4	F	Neosav	29.07.14	Toby's Place	-8.62322	31.20044
IYA5	M	Peteph	29.07.14	Toby's Place	-8.62322	31.20044
IYA6	F	Petfam	29.07.14	Toby's Place	-8.62322	31.20044
IYA7	M	Petfam	29.07.14	Toby's Place	-8.62322	31.20044
IYA8	F	Cteben	29.07.14	Chipwa Fishermen	-8.60617	31.18611
IYA9	NA	Neochr	29.07.14	Toby's Place	-8.62322	31.20044
IYB1	NA	Neochr	29.07.14	Toby's Place	-8.62322	31.20044
IYB2	NA	Neosav	29.07.14	Toby's Place	-8.62322	31.20044
IYB3	M	Neosav	29.07.14	Toby's Place	-8.62322	31.20044
IYB4	F	Regcal	29.07.14	Chipwa Fishermen	-8.60617	31.18611
IYB5	NA	Varmoo	29.07.14	Toby's Place	-8.62322	31.20044
IYB6	NA	Varmoo	29.07.14	Toby's Place	-8.62322	31.20044
IYB7	M	Neochr	29.07.14	Toby's Place	-8.62322	31.20044
IYB8	NA	Neochr	29.07.14	Toby's Place	-8.62322	31.20044
IYB9	NA	Loblab	29.07.14	Toby's Place	-8.62322	31.20044
IYC1	NA	Simdia	29.07.14	Toby's Place	-8.62322	31.20044
IYC2	NA	Varmoo	29.07.14	Toby's Place	-8.62322	31.20044
IYC3	NA	Varmoo	29.07.14	Toby's Place	-8.62322	31.20044
IYC4	NA	Varmoo	29.07.14	Toby's Place	-8.62322	31.20044
IYC5	NA	Chabri	29.07.14	Toby's Place	-8.62322	31.20044
IYC6	NA	Chabri	29.07.14	Toby's Place	-8.62322	31.20044
IYC7	NA	Varmoo	29.07.14	Toby's Place	-8.62322	31.20044
IYC8	NA	Varmoo	29.07.14	Toby's Place	-8.62322	31.20044
IYC9	NA	Altcom	29.07.14	Toby's Place	-8.62322	31.20044
IYD1	M	Petpol	29.07.14	Toby's Place	-8.62322	31.20044
IYD2	F	Petpol	29.07.14	Toby's Place	-8.62322	31.20044
IYD3	F	Cyafur	29.07.14	Toby's Place	-8.62322	31.20044

ID	Sex	SpeciesID	CollectionDate	CollectionLocation	latitude	longitude
IYD4	M	Petpol	29.07.14	Toby's Place	-8.62322	31.20044
IYD5	F	Petpol	29.07.14	Toby's Place	-8.62322	31.20044
IYD7	NA	Chabri	29.07.14	Toby's Place	-8.62322	31.20044
IYD8	NA	Altcom	29.07.14	Toby's Place	-8.62322	31.20044
IYE2	NA	Loblab	29.07.14	Toby's Place	-8.62322	31.20044
IYE3	M	Psccur	29.07.14	Toby's Place	-8.62322	31.20044
IYE5	NA	Intloo	29.07.14	Toby's Place	-8.62322	31.20044
IYE7	NA	Altcom	29.07.14	Toby's Place	-8.62322	31.20044
IYE8	NA	Altcom	29.07.14	Toby's Place	-8.62322	31.20044
IYE9	NA	Petpol	29.07.14	Toby's Place	-8.62322	31.20044
IYF1	M	Neochr	29.07.14	Toby's Place	-8.62322	31.20044
IYF2	M	Neosav	29.07.14	Toby's Place	-8.62322	31.20044
IYF4	NA	Petfam	29.07.14	Toby's Place	-8.62322	31.20044
IYF5	NA	Neosav	29.07.14	Toby's Place	-8.62322	31.20044
IYF6	NA	Neochr	29.07.14	Toby's Place	-8.62322	31.20044
IYF7	NA	Intloo	29.07.14	Toby's Place	-8.62322	31.20044
IYF8	NA	Intloo	29.07.14	Toby's Place	-8.62322	31.20044
IYF9	M	Loblab	29.07.14	Toby's Place	-8.62322	31.20044
IYG1	NA	Simdia	29.07.14	Toby's Place	-8.62322	31.20044
IYG2	F	Loblab	29.07.14	Toby's Place	-8.62322	31.20044
IYG3	F	Loblab	29.07.14	Toby's Place	-8.62322	31.20044
IYG4	M	Psccur	29.07.14	Toby's Place	-8.62322	31.20044
IYG5	F	Petpol	29.07.14	Toby's Place	-8.62322	31.20044
IYG6	M	Petfam	29.07.14	Toby's Place	-8.62322	31.20044
IYG7	NA	Neofas	29.07.14	Toby's Place	-8.62322	31.20044
IYG8	NA	Intloo	29.07.14	Toby's Place	-8.62322	31.20044
IYG9	NA	Intloo	29.07.14	Toby's Place	-8.62322	31.20044
IYH5	NA	Auldew	29.07.14	Toby's Place	-8.62322	31.20044
IYH6	NA	TelteS	29.07.14	Toby's Place	-8.62322	31.20044
IYH7	NA	Neochr	29.07.14	Toby's Place	-8.62322	31.20044
IYH8	NA	Varmoo	29.07.14	Toby's Place	-8.62322	31.20044
IYH9	NA	Neosav	29.07.14	Toby's Place	-8.62322	31.20044
IYI1	NA	Auldew	29.07.14	Toby's Place	-8.62322	31.20044
IYI2	NA	Auldew	29.07.14	Toby's Place	-8.62322	31.20044
IYI3	NA	Xenspi	29.07.14	Toby's Place	-8.62322	31.20044
IYI4	NA	Xenspi	29.07.14	Toby's Place	-8.62322	31.20044
IYI5	NA	Xenspi	29.07.14	Toby's Place	-8.62322	31.20044
IYI6	NA	Auldew	29.07.14	Toby's Place	-8.62322	31.20044
IYI7	NA	Xenspi	29.07.14	Toby's Place	-8.62322	31.20044
IYI8	NA	Neochr	29.07.14	Toby's Place	-8.62322	31.20044
IZA1	M	Astbur	28.07.14	Kalambo Lake / Chipwa	-8.60174	31.18701
IZA2	F	Benmel	28.07.14	Chipwa Fishermen	-8.60617	31.18611
IZA4	F	Benmel	28.07.14	Chipwa Fishermen	-8.60617	31.18611
IZA5	NA	HemstZ	28.07.14	Chipwa Fishermen	-8.60617	31.18611
IZA6	F	Lchaur	28.07.14	Chipwa Fishermen	-8.60617	31.18611
IZA8	F	Plemul	28.07.14	Chipwa Fishermen	-8.60617	31.18611
IZA9	M	Plemul	28.07.14	Chipwa Fishermen	-8.60617	31.18611
IZB2	M	Perecc	28.07.14	Chipwa Fishermen	-8.60617	31.18611
IZB4	NA	Perecc	28.07.14	Chipwa Fishermen	-8.60617	31.18611
IZB5	NA	Regcal	28.07.14	Chipwa Fishermen	-8.60617	31.18611
IZB6	NA	Boumic	28.07.14	Chipwa Fishermen	-8.60617	31.18611
IZB8	M	Xchhec	28.07.14	Chipwa Fishermen	-8.60617	31.18611
IZB9	M	Xchhec	28.07.14	Chipwa Fishermen	-8.60617	31.18611
IZC1	M	Xchhec	28.07.14	Chipwa Fishermen	-8.60617	31.18611
IZC2	M	Xchhec	28.07.14	Chipwa Fishermen	-8.60617	31.18611
IZC3	NA	Xencau	28.07.14	Chipwa Fishermen	-8.60617	31.18611
IZC5	F	Astbur	28.07.14	Kalambo Lake / Chipwa	-8.60174	31.18701
IZC7	M	XenniS	28.07.14	Chipwa Fishermen	-8.60617	31.18611
IZC9	NA	Gwcbel	28.07.14	Chipwa Fishermen	-8.60617	31.18611
IZD1	NA	Gwcbel	28.07.14	Chipwa Fishermen	-8.60617	31.18611
IZD2	NA	Gwcbel	28.07.14	Chipwa Fishermen	-8.60617	31.18611
IZD3	NA	Gwcbel	28.07.14	Chipwa Fishermen	-8.60617	31.18611
IZD4	M	Batfas	28.07.14	Chipwa Fishermen	-8.60617	31.18611
IZE1	M	Tresti	28.07.14	Chipwa Fishermen	-8.60617	31.18611
IZE4	M	Gwcchr	28.07.14	Chipwa Fishermen	-8.60617	31.18611
IZF1	F	Gwcchr	28.07.14	Chipwa Fishermen	-8.60617	31.18611
IZF2	NA	Gwcchr	28.07.14	Chipwa Fishermen	-8.60617	31.18611
IZF3	NA	Gwcchr	28.07.14	Chipwa Fishermen	-8.60617	31.18611
IZF4	NA	Gwcchr	28.07.14	Chipwa Fishermen	-8.60617	31.18611
IZF9	M	Tresti	28.07.14	Chipwa Fishermen	-8.60617	31.18611
IZG1	M	Tresti	28.07.14	Chipwa Fishermen	-8.60617	31.18611
IZG2	M	Tresti	28.07.14	Chipwa Fishermen	-8.60617	31.18611
IZG3	M	Tresti	28.07.14	Chipwa Fishermen	-8.60617	31.18611
IZG4	M	Tresti	28.07.14	Chipwa Fishermen	-8.60617	31.18611
IZG5	M	Tresti	28.07.14	Chipwa Fishermen	-8.60617	31.18611
IZG6	NA	TeldhS	28.07.14	Kalambo Lake / Chipwa	-8.60174	31.18701
IZG7	NA	TeldhS	28.07.14	Kalambo Lake / Chipwa	-8.60174	31.18701
IZG8	NA	TeldhS	28.07.14	Kalambo Lake / Chipwa	-8.60174	31.18701
IZG9	NA	TeldhS	28.07.14	Kalambo Lake / Chipwa	-8.60174	31.18701
IZH1	NA	TeldhS	28.07.14	Kalambo Lake / Chipwa	-8.60174	31.18701
IZH2	NA	TeldhS	28.07.14	Kalambo Lake / Chipwa	-8.60174	31.18701
IZH3	NA	TeldhS	28.07.14	Chipwa Fishermen	-8.60617	31.18611
IZH4	NA	TeldhS	28.07.14	Chipwa Fishermen	-8.60617	31.18611
IZH5	NA	TeldhS	28.07.14	Kalambo Lake / Chipwa	-8.60174	31.18701
IZH6	NA	TeldhS	28.07.14	Kalambo Lake / Chipwa	-8.60174	31.18701
IZH7	M	Erecya	29.07.14	Toby's Place	-8.62322	31.20044
IZI3	F	Erecya	29.07.14	Toby's Place	-8.62322	31.20044
IZI7	M	Lamlem	29.07.14	Toby's Place	-8.62322	31.20044
IZI8	M	Neochr	29.07.14	Toby's Place	-8.62322	31.20044
JAA1	F	Xencau	29.07.14	Chipwa Fishermen	-8.60617	31.18611
JAA2	NA	Xencau	29.07.14	Chipwa Fishermen	-8.60617	31.18611
JAA3	NA	Xencau	29.07.14	Chipwa Fishermen	-8.60617	31.18611
JAA4	NA	Xencau	29.07.14	Chipwa Fishermen	-8.60617	31.18611
JAB1	F	Lamcal	30.07.14	Toby's Place	-8.62322	31.20044
JAB6	M	Oretan	30.07.14	Chipwa Fishermen	-8.60617	31.18611
JAB7	M	Baicen	30.07.14	Chipwa Fishermen	-8.60617	31.18611
JAB8	F	Baicen	30.07.14	Chipwa Fishermen	-8.60617	31.18611
JAB9	M	Lamcal	30.07.14	Toby's Place	-8.62322	31.20044
JAC2	M	Tremac	30.07.14	Chipwa Fishermen	-8.60617	31.18611
JAC4	NA	Plemul	30.07.14	Chipwa Fishermen	-8.60617	31.18611
JAC5	NA	Gnaper	30.07.14	Chipwa Fishermen	-8.60617	31.18611
JAC7	F	Oretan	30.07.14	Chipwa Fishermen	-8.60617	31.18611
JAC8	NA	Xchhec	30.07.14	Chipwa Fishermen	-8.60617	31.18611
JAC9	NA	Hapmic	30.07.14	Toby's Place	-8.62322	31.20044
JAD1	NA	Xencau	30.07.14	Toby's Place	-8.62322	31.20044
JAD2	NA	Lchaur	30.07.14	Chipwa Fishermen	-8.60617	31.18611
JAD3	NA	Lchabe	30.07.14	Chipwa Fishermen	-8.60617	31.18611
JAD4	F	Simdia	30.07.14	Toby's Place	-8.62322	31.20044
JAD5	NA	TelteS	30.07.14	Toby's Place	-8.62322	31.20044
JAD6	NA	Xenspi	30.07.14	Toby's Place	-8.62322	31.20044
JAD7	F	Permic	30.07.14	Toby's Place	-8.62322	31.20044
JAD8	NA	Permic	30.07.14	Toby's Place	-8.62322	31.20044
JAD9	M	Ctehor	30.07.14	Toby's Place	-8.62322	31.20044
JAE1	F	Petfas	30.07.14	Toby's Place	-8.62322	31.20044
JAE2	F	Simdia	30.07.14	Toby's Place	-8.62322	31.20044
JAE3	NA	Neofas	30.07.14	Toby's Place	-8.62322	31.20044
JAE7	F	Boumic	31.07.14	Chipwa Fishermen	-8.60617	31.18611
JAE9	F	Baicen	31.07.14	Chipwa Fishermen	-8.60617	31.18611
JAF5	M	Lchaur	31.07.14	Chipwa Fishermen	-8.60617	31.18611
JAF7	M	Xenfla	31.07.14	Toby's Place	-8.62322	31.20044
JAF9	F	Xenfla	31.07.14	Toby's Place	-8.62322	31.20044
JAG2	M	Tylpol	31.07.14	Chipwa Fishermen	-8.60617	31.18611
JAG3	M	Baicen	31.07.14	Chipwa Fishermen	-8.60617	31.18611
JAG4	M	Regcal	31.07.14	Chipwa Fishermen	-8.60617	31.18611
JAG6	M	Xenbou	31.07.14	Toby's Place	-8.62322	31.20044
JAG7	M	Xenbou	31.07.14	Toby's Place	-8.62322	31.20044
JAG8	F	Xenbou	31.07.14	Toby's Place	-8.62322	31.20044
JAG9	M	Xenbou	31.07.14	Toby's Place	-8.62322	31.20044
JAH2	F	Xenbou	31.07.14	Toby's Place	-8.62322	31.20044
JAH3	F	Xenbou	31.07.14	Toby's Place	-8.62322	31.20044
JAH5	F	Tylpol	31.07.14	Chipwa Fishermen	-8.60617	31.18611
JAH6	M	Regcal	31.07.14	Chipwa Fishermen	-8.60617	31.18611
JAH7	F	Xchhec	31.07.14	Chipwa Fishermen	-8.60617	31.18611
JAH9	NA	Neopul	31.07.14	Toby's Place	-8.62322	31.20044
JAI1	NA	Neopul	31.07.14	Toby's Place	-8.62322	31.20044
JAI2	NA	Neopul	31.07.14	Toby's Place	-8.62322	31.20044
JAI3	NA	Neopul	31.07.14	Toby's Place	-8.62322	31.20044
JAI5	M	Lchabe	31.07.14	Chipwa Fishermen	-8.60617	31.18611
JAI6	M	Lchabe	31.07.14	Chipwa Fishermen	-8.60617	31.18611
JAI7	F	Lchabe	31.07.14	Chipwa Fishermen	-8.60617	31.18611
JAI8	F	Batvit	31.07.14	Chipwa Fishermen	-8.60617	31.18611
JAI9	F	Lamlem	31.07.14	Toby's Place	-8.62322	31.20044
JBA1	M	Neobif	30.08.14	Cape Chaitika Fishermen	-8.56889	30.79706
JBA2	M	Cphgib	30.08.14	Cape Chaitika Fishermen	-8.56889	30.79706
JBA3	M	Cphgib	30.08.14	Cape Chaitika Fishermen	-8.56889	30.79706
JBA4	F	Cphgib	30.08.14	Cape Chaitika Fishermen	-8.56889	30.79706
JBA5	NA	Cphgib	30.08.14	Cape Chaitika Fishermen	-8.56889	30.79706
JBA7	M	Telbra	30.08.14	Kabyolwe	-8.56917	30.75056
JBA8	M	Telbra	30.08.14	Kabyolwe	-8.56917	30.75056
JBA9	M	Plestr	30.08.14	Kabyolwe	-8.56917	30.75056
JBB1	F	Trioto	30.08.14	Kabyolwe	-8.56917	30.75056
JBB2	M	Trioto	30.08.14	Kabyolwe	-8.56917	30.75056
JBB3	M	Trioto	30.08.14	Kabyolwe	-8.56917	30.75056
JBB6	M	Lepken	30.08.14	Misepa	-8.58889	30.80306
JBB7	M	Lepken	30.08.14	Misepa	-8.58889	30.80306
JBB8	F	Lepken	30.08.14	Misepa	-8.58889	30.80306
JBB9	NA	Petfas	30.08.14	Misepa	-8.58889	30.80306
JBC1	F	Psccur	30.08.14	Misepa	-8.58889	30.80306
JBC2	M	Psccur	30.08.14	Misepa	-8.58889	30.80306
JBC3	F	Psccur	30.08.14	Misepa	-8.58889	30.80306
JBC4	F	Gralem	31.08.14	Chitweshiba	-8.59583	30.80750
JBC5	M	Gralem	31.08.14	Chitweshiba	-8.59583	30.80750
JBC6	M	Gralem	31.08.14	Chitweshiba	-8.59583	30.80750
JBC7	M	Telbra	31.08.14	Chitweshiba	-8.59583	30.80750
JBC8	M	Telbra	31.08.14	Chitweshiba	-8.59583	30.80750
JBC9	M	Telbra	31.08.14	Chitweshiba	-8.59583	30.80750
JBD2	NA	Pscple	31.08.14	Chitweshiba	-8.59583	30.80750
JBD3	NA	Pscple	31.08.14	Chitweshiba	-8.59583	30.80750
JBD4	M	Petfas	31.08.14	Chitweshiba	-8.59583	30.80750
JBD5	M	Telvit	31.08.14	Chitweshiba	-8.59583	30.80750
JBD6	F	Telvit	31.08.14	Chitweshiba	-8.59583	30.80750
JBD7	NA	Telvit	31.08.14	Chitweshiba	-8.59583	30.80750
JBD8	NA	Telvit	31.08.14	Chitweshiba	-8.59583	30.80750
JBD9	NA	Telvit	31.08.14	Chitweshiba	-8.59583	30.80750
JBE1	NA	Telvit	31.08.14	Chitweshiba	-8.59583	30.80750
JBE2	NA	Telvit	31.08.14	Chitweshiba	-8.59583	30.80750
JBE3	NA	Telvit	31.08.14	Chitweshiba	-8.59583	30.80750
JBE5	M	Leppro	31.08.14	Chitweshiba	-8.59583	30.80750
JBE6	M	Mdcrot	31.08.14	Nakaku	-8.64344	30.87281
JBE7	F	Mdcrot	31.08.14	Nakaku	-8.64344	30.87281
JBE8	M	Telbra	31.08.14	Nakaku	-8.64344	30.87281
JBE9	F	Telbra	31.08.14	Nakaku	-8.64344	30.87281
JBF2	NA	Mdcrot	31.08.14	Nakaku	-8.64344	30.87281
JBF3	NA	Mdcrot	31.08.14	Nakaku	-8.64344	30.87281
JBF4	NA	Mdcrot	31.08.14	Nakaku	-8.64344	30.87281
JBF5	NA	Mdcrot	31.08.14	Nakaku	-8.64344	30.87281
JBF6	NA	Limdar	31.08.14	Nakaku	-8.64344	30.87281
JBF8	F	Pethor	01.09.14	Kanfonki	-8.70278	30.92250
JBF9	F	Pethor	01.09.14	Kanfonki	-8.70278	30.92250
JBG1	NA	Cphgib	01.09.14	Kanfonki	-8.70278	30.92250
JBG3	M	Batmin	01.09.14	Chezi Fishermen	-8.77889	31.00694
JBG4	M	Lchabe	01.09.14	Chezi Fishermen	-8.77889	31.00694
JBG5	M	Lchabe	01.09.14	Chezi Fishermen	-8.77889	31.00694
JBG6	M	Lamlap	01.09.14	Kombe	-8.79389	31.01583
JBG7	M	Lamlap	01.09.14	Kombe	-8.79389	31.01583
JBG8	M	Lamlap	01.09.14	Kombe	-8.79389	31.01583
JBH1	M	Lamlap	01.09.14	Kombe	-8.79389	31.01583
JBH2	M	Lamlap	01.09.14	Kombe	-8.79389	31.01583
JBH3	F	Lamlap	01.09.14	Kombe	-8.79389	31.01583
JBH4	M	Tromoo	02.09.14	Mbita Island W	-8.75333	31.08631
JBH5	F	Tromoo	02.09.14	Mbita Island W	-8.75333	31.08631
JBH6	M	Tromoo	02.09.14	Mbita Island W	-8.75333	31.08631
JBH7	M	Tromoo	02.09.14	Mbita Island W	-8.75333	31.08631
JBH9	NA	Tromoo	02.09.14	Mbita Island W	-8.75333	31.08631
JBI1	NA	Tromoo	02.09.14	Mbita Island W	-8.75333	31.08631
JBI2	NA	Julorn	02.09.14	Mbita Island W	-8.75333	31.08631
JBI3	NA	Julorn	02.09.14	Mbita Island W	-8.75333	31.08631
JBI4	NA	Julorn	02.09.14	Mbita Island W	-8.75333	31.08631
JBI5	NA	Julorn	02.09.14	Mbita Island W	-8.75333	31.08631
JBI6	NA	Julorn	02.09.14	Mbita Island W	-8.75333	31.08631
JBI7	NA	Boumic	02.09.14	Mbita Island W	-8.75333	31.08631
JBI8	NA	Boumic	02.09.14	Mbita Island W	-8.75333	31.08631

ID	Sex	SpeciesID	CollectionDate	CollectionLocation	latitude	longitude
JCA1	NA	Lchaur	31.07.14	Chipwa Fishermen	-8.60617	31.18611
JCA2	M	Psccur	31.07.14	Toby's Place	-8.62322	31.20044
JCA5	NA	Xenfla	31.07.14	Toby's Place	-8.62322	31.20044
JCA6	NA	Xenfla	31.07.14	Toby's Place	-8.62322	31.20044
JCA7	NA	Xenfla	31.07.14	Toby's Place	-8.62322	31.20044
JCA8	NA	Xenfla	31.07.14	Toby's Place	-8.62322	31.20044
JCA9	NA	Xenfla	31.07.14	Toby's Place	-8.62322	31.20044
JCB1	NA	Xenfla	31.07.14	Toby's Place	-8.62322	31.20044
JCB2	NA	Xenfla	31.07.14	Toby's Place	-8.62322	31.20044
JCB3	NA	Xenfla	31.07.14	Toby's Place	-8.62322	31.20044
JCB5	F	Batvit	31.07.14	Chipwa Fishermen	-8.60617	31.18611
JCB6	NA	Gwcchr	31.07.14	Chipwa Fishermen	-8.60617	31.18611
JCB7	NA	Lamlem	31.07.14	Toby's Place	-8.62322	31.20044
JCB8	M	Enamel	31.07.14	Toby's Place	-8.62322	31.20044
JCB9	M	Enamel	31.07.14	Toby's Place	-8.62322	31.20044
JCC1	M	Enamel	31.07.14	Toby's Place	-8.62322	31.20044
JCC2	M	Enamel	31.07.14	Toby's Place	-8.62322	31.20044
JCC3	M	Enamel	31.07.14	Toby's Place	-8.62322	31.20044
JCC6	M	Baicen	31.07.14	Chipwa Fishermen	-8.60617	31.18611
JCC7	M	Baicen	31.07.14	Chipwa Fishermen	-8.60617	31.18611
JCC8	M	Baicen	31.07.14	Chipwa Fishermen	-8.60617	31.18611
JCC9	F	Baicen	31.07.14	Chipwa Fishermen	-8.60617	31.18611
JCD1	NA	Baicen	31.07.14	Chipwa Fishermen	-8.60617	31.18611
JCD3	M?	Regcal	31.07.14	Chipwa Fishermen	-8.60617	31.18611
JCD4	M	Regcal	31.07.14	Chipwa Fishermen	-8.60617	31.18611
JCD5	M	Regcal	31.07.14	Chipwa Fishermen	-8.60617	31.18611
JCD6	M	Benmel	31.07.14	Chipwa Fishermen	-8.60617	31.18611
JCD7	M	Benmel	31.07.14	Chipwa Fishermen	-8.60617	31.18611
JCD8	NA	Lchabe	31.07.14	Chipwa Fishermen	-8.60617	31.18611
JCD9	NA	Lchaur	31.07.14	Chipwa Fishermen	-8.60617	31.18611
JCE1	NA	Lchaur	31.07.14	Chipwa Fishermen	-8.60617	31.18611
JCE2	NA	Xencau	31.07.14	Chipwa Fishermen	-8.60617	31.18611
JCE3	NA	Xencau	31.07.14	Chipwa Fishermen	-8.60617	31.18611
JCE4	NA	Gwcchr	31.07.14	Chipwa Fishermen	-8.60617	31.18611
JCE6	NA	Gwcchr	31.07.14	Chipwa Fishermen	-8.60617	31.18611
JCE7	NA	Gwcchr	31.07.14	Chipwa Fishermen	-8.60617	31.18611
JCE8	NA	Gwcchr	31.07.14	Chipwa Fishermen	-8.60617	31.18611
JCE9	M	Tylpol	31.07.14	Chipwa Fishermen	-8.60617	31.18611
JCF1	M	Oretan	31.07.14	Chipwa Fishermen	-8.60617	31.18611
JCF2	M	Boumic	01.08.14	Chipwa Fishermen	-8.60617	31.18611
JCF4	NA	Oretan	01.08.14	Chipwa Fishermen	-8.60617	31.18611
JCF5	NA	Oretan	01.08.14	Chipwa Fishermen	-8.60617	31.18611
JCF6	NA	Calmac	01.08.14	Toby's Place	-8.62322	31.20044
JCF7	NA	Calmac	01.08.14	Toby's Place	-8.62322	31.20044
JCF8	M	Calmac	01.08.14	Toby's Place	-8.62322	31.20044
JCF9	NA	Julom	01.08.14	Toby's Place	-8.62322	31.20044
JCG1	NA	Julom	01.08.14	Toby's Place	-8.62322	31.20044
JCG2	NA	Peteph	01.08.14	Toby's Place	-8.62322	31.20044
JCG3	NA	Peteph	01.08.14	Toby's Place	-8.62322	31.20044
JCG4	NA	Peteph	01.08.14	Toby's Place	-8.62322	31.20044
JCG5	NA	Peteph	01.08.14	Toby's Place	-8.62322	31.20044
JCG6	NA	Peteph	01.08.14	Toby's Place	-8.62322	31.20044
JCG7	NA	Peteph	01.08.14	Toby's Place	-8.62322	31.20044
JCG8	NA	Peteph	01.08.14	Toby's Place	-8.62322	31.20044
JCG9	NA	Petfam	01.08.14	Toby's Place	-8.62322	31.20044
JCH1	NA	Petfam	01.08.14	Toby's Place	-8.62322	31.20044
JCH2	NA	Petfam	01.08.14	Toby's Place	-8.62322	31.20044
JCH4	NA	Petfam	01.08.14	Toby's Place	-8.62322	31.20044
JCH5	M	Calmac	01.08.14	Toby's Place	-8.62322	31.20044
JCH6	NA	Simdia	01.08.14	Toby's Place	-8.62322	31.20044
JCH7	NA	Peteph	01.08.14	Toby's Place	-8.62322	31.20044
JCH8	M	Calmac	01.08.14	Toby's Place	-8.62322	31.20044
JCH9	M	Calmac	01.08.14	Toby's Place	-8.62322	31.20044
JCI1	F	Calmac	01.08.14	Toby's Place	-8.62322	31.20044
JCI2	NA	Julom	01.08.14	Toby's Place	-8.62322	31.20044
JCI3	NA	Julom	01.08.14	Toby's Place	-8.62322	31.20044
JCI4	NA	Calmac	01.08.14	Toby's Place	-8.62322	31.20044
JCI5	M	Calmac	01.08.14	Toby's Place	-8.62322	31.20044
JCI6	F	Calmac	01.08.14	Toby's Place	-8.62322	31.20044
JCI7	NA	Peteph	01.08.14	Toby's Place	-8.62322	31.20044
JCI8	NA	Petfam	01.08.14	Toby's Place	-8.62322	31.20044
JDA1	F	Erecya	01.08.14	Toby's Place	-8.62322	31.20044
JDA2	F	Erecya	01.08.14	Toby's Place	-8.62322	31.20044
JDA3	F	Erecya	01.08.14	Toby's Place	-8.62322	31.20044
JDA4	M	Erecya	01.08.14	Toby's Place	-8.62322	31.20044
JDA5	F	Erecya	01.08.14	Toby's Place	-8.62322	31.20044
JDA6	M	Erecya	01.08.14	Toby's Place	-8.62322	31.20044
JDA7	M	Erecya	01.08.14	Toby's Place	-8.62322	31.20044
JDA8	M	Erecya	01.08.14	Toby's Place	-8.62322	31.20044
JDA9	F	Erecya	01.08.14	Toby's Place	-8.62322	31.20044
JDB1	F	Erecya	01.08.14	Toby's Place	-8.62322	31.20044
JDB2	M	Ctehor	01.08.14	Toby's Place	-8.62322	31.20044
JDB4	M	Oretan	01.08.14	Toby's Place	-8.62322	31.20044
JDB5	M	Ctehor	01.08.14	Toby's Place	-8.62322	31.20044
JDB6	M	Ctehor	01.08.14	Toby's Place	-8.62322	31.20044
JDB7	M	Simdia	01.08.14	Toby's Place	-8.62322	31.20044
JDB8	F	Simdia	01.08.14	Toby's Place	-8.62322	31.20044
JDB9	F	Simdia	01.08.14	Toby's Place	-8.62322	31.20044
JDC1	NA	Simdia	01.08.14	Toby's Place	-8.62322	31.20044
JDC2	F	Simdia	01.08.14	Toby's Place	-8.62322	31.20044
JDC3	NA	Ctehor	01.08.14	Toby's Place	-8.62322	31.20044
JDC4	F	Neochr	01.08.14	Toby's Place	-8.62322	31.20044
JDC7	NA	Neomod	01.08.14	Toby's Place	-8.62322	31.20044
JDC8	NA	Ctehor	01.08.14	Toby's Place	-8.62322	31.20044
JDC9	NA	Asplep	01.08.14	Toby's Place	-8.62322	31.20044
JDD2	NA	Psccur	01.08.14	Toby's Place	-8.62322	31.20044
JDD6	NA	Julom	01.08.14	Toby's Place	-8.62322	31.20044
JDD7	M	Gralem	01.08.14	Toby's Place	-8.62322	31.20044
JDD8	F	Gralem	01.08.14	Toby's Place	-8.62322	31.20044
JDD9	NA	Ctehor	01.08.14	Toby's Place	-8.62322	31.20044
JDE1	NA	Ctehor	01.08.14	Toby's Place	-8.62322	31.20044
JDE3	M	Bathor	02.08.14	Chipwa Fishermen	-8.60617	31.18611
JDE4	M?	Bathor	02.08.14	Chipwa Fishermen	-8.60617	31.18611
JDE6	M	Batvit	14.08.14	Katoto	-8.80611	31.02667
JDE7	F	Batvit	14.08.14	Katoto	-8.80611	31.02667
JDE8	NA	Lepatt	14.08.14	Katoto	-8.80611	31.02667
JDE9	NA	Lepatt	14.08.14	Katoto	-8.80611	31.02667
JDF1	NA	Lchabe	14.08.14	Katoto	-8.80611	31.02667
JDF2	NA	Boumic	14.08.14	Katoto	-8.80611	31.02667
JDF3	M	Neomee	14.08.14	Katoto	-8.80611	31.02667
JDF4	F	Neomee	14.08.14	Katoto	-8.80611	31.02667
JDF5	M	LamorS	14.08.14	Katoto	-8.80611	31.02667
JDF7	F	Neomee	14.08.14	Katoto	-8.80611	31.02667
JDF8	NA	Neomee	14.08.14	Katoto	-8.80611	31.02667
JDF9	M	Neomee	14.08.14	Katoto	-8.80611	31.02667
JDG1	F	Neomee	14.08.14	Katoto	-8.80611	31.02667
JDG2	NA	Neomee	14.08.14	Katoto	-8.80611	31.02667
JDG4	F	LamorS	14.08.14	Katoto	-8.80611	31.02667
JDG6	NA	Neomee	14.08.14	Katoto	-8.80611	31.02667
JDG7	NA	Neomee	14.08.14	Katoto	-8.80611	31.02667
JDG8	NA	Neomee	14.08.14	Katoto	-8.80611	31.02667
JDG9	NA	Neomee	14.08.14	Katoto	-8.80611	31.02667
JDH1	F	Neomee	14.08.14	Katoto	-8.80611	31.02667
JDH4	M	LamorS	14.08.14	Katoto	-8.80611	31.02667
JDH5	F	LamorS	14.08.14	Katoto	-8.80611	31.02667
JDH6	F	LamorS	14.08.14	Katoto	-8.80611	31.02667
JDH7	F	Lamlap	14.08.14	Katoto	-8.80611	31.02667
JDH8	F	Lamlap	14.08.14	Katoto	-8.80611	31.02667
JDI1	F	Lamlap	14.08.14	Katoto	-8.80611	31.02667
JDI2	M	Lamlap	14.08.14	Katoto	-8.80611	31.02667
JDI4	M	Plepar	15.08.14	Katoto	-8.80611	31.02667
JDI6	M	Lepatt	15.08.14	Katoto	-8.80611	31.02667
JDI7	M	Lepatt	15.08.14	Katoto	-8.80611	31.02667
JDI8	M	Lepatt	15.08.14	Katoto	-8.80611	31.02667
JDI9	F	Lepatt	15.08.14	Katoto	-8.80611	31.02667
JEA2	M	Hapmic	20.08.14	Chitweshiba	-8.59583	30.80750
JEA3	F	Hapmic	20.08.14	Chitweshiba	-8.59583	30.80750
JEA4	NA	Lamcal	20.08.14	Chitweshiba	-8.59583	30.80750
JEA5	NA	Lamcal	20.08.14	Chitweshiba	-8.59583	30.80750
JEA6	NA	Lamcal	20.08.14	Chitweshiba	-8.59583	30.80750
JEA7	NA	Lamcal	20.08.14	Chitweshiba	-8.59583	30.80750
JEA8	NA	Cphgib	20.08.14	Misepa	-8.58889	30.80306
JEA9	NA	Cphgib	20.08.14	Misepa	-8.58889	30.80306
JEB1	NA	Cphgib	20.08.14	Misepa	-8.58889	30.80306
JEB2	M	Cyppav	20.08.14	Misepa	-8.58889	30.80306
JEB4	F	Cyppav	20.08.14	Misepa	-8.58889	30.80306
JEB6	M	Cyppav	20.08.14	Misepa	-8.58889	30.80306
JEB7	M	Cyppav	20.08.14	Misepa	-8.58889	30.80306
JEB8	M	Cyppav	20.08.14	Misepa	-8.58889	30.80306
JEB9	F	Cyppav	20.08.14	Misepa	-8.58889	30.80306
JEC1	F	Cyppav	20.08.14	Misepa	-8.58889	30.80306
JEC2	M	Cyppav	20.08.14	Misepa	-8.58889	30.80306
JEC3	M	Cyppav	20.08.14	Misepa	-8.58889	30.80306
JEC4	M	Cyppav	20.08.14	Misepa	-8.58889	30.80306
JEC5	M	Cyppav	20.08.14	Misepa	-8.58889	30.80306
JEC6	M	Cyppav	20.08.14	Chitweshiba	-8.59583	30.80750
JEC7	M	Cypcol	20.08.14	Chitweshiba	-8.59583	30.80750
JEC8	M	Cypcol	20.08.14	Chitweshiba	-8.59583	30.80750
JEC9	F	Cypcol	20.08.14	Chitweshiba	-8.59583	30.80750
JED1	F	Cypcol	20.08.14	Chitweshiba	-8.59583	30.80750
JED2	F	Cypcol	20.08.14	Chitweshiba	-8.59583	30.80750
JED3	M	Leppro	20.08.14	Chitweshiba	-8.59583	30.80750
JED4	M	NeoveS	20.08.14	Chitweshiba	-8.59583	30.80750
JED5	F	NeoveS	20.08.14	Chitweshiba	-8.59583	30.80750
JED6	M	Cphgib	21.08.14	Mibwebwe	-8.56500	30.76111
JED7	M	Hapmic	21.08.14	Mibwebwe	-8.56500	30.76111
JED8	F	Hapmic	21.08.14	Mibwebwe	-8.56500	30.76111
JED9	M	Hapmic	21.08.14	Mibwebwe	-8.56500	30.76111
JEE1	M	Lepken	21.08.14	Mibwebwe	-8.56500	30.76111
JEE2	M	LamorS	21.08.14	Kabyolwe	-8.56917	30.75056
JEE3	F	Lamcal	21.08.14	Mibwebwe	-8.56500	30.76111
JEE4	F	Lamcal	21.08.14	Mibwebwe	-8.56500	30.76111
JEE5	F	Lamcal	21.08.14	Mibwebwe	-8.56500	30.76111
JEE6	F	Lamcal	21.08.14	Mibwebwe	-8.56500	30.76111
JEF1	M	Pleela	21.08.14	Kabyolwe Fishermen	-8.56769	30.75219
JEF4	NA	Batmin	22.08.14	Kasenga West Fishermen	-8.56669	30.75644
JEF5	NA	Batmin	22.08.14	Kasenga West Fishermen	-8.56669	30.75644
JEF6	NA	Batmin	22.08.14	Kasenga West Fishermen	-8.56669	30.75644
JEF7	NA	Batmin	22.08.14	Kasenga West Fishermen	-8.56669	30.75644
JEF8	NA	Batmin	22.08.14	Kasenga West Fishermen	-8.56669	30.75644
JEF9	NA	Batmin	22.08.14	Kasenga West Fishermen	-8.56669	30.75644
JEG2	NA	Batmin	22.08.14	Kasenga West Fishermen	-8.56669	30.75644
JEG4	NA	Batfas	22.08.14	Kasenga West Fishermen	-8.56669	30.75644
JEG5	F	Trioto	22.08.14	Kabyolwe	-8.56917	30.75056
JEG6	M	Trioto	22.08.14	Kabyolwe	-8.56917	30.75056
JEG7	F	Trioto	22.08.14	Kabyolwe	-8.56917	30.75056
JEH2	NA	Lchaur	22.08.14	Kabyolwe	-8.56917	30.75056
JEH4	NA	Telbra	22.08.14	Kabyolwe	-8.56917	30.75056
JEH5	NA	Telbra	22.08.14	Kabyolwe	-8.56917	30.75056
JEH6	NA	LamorS	22.08.14	Kabyolwe	-8.56917	30.75056
JEH7	NA	Lamoce	22.08.14	Kabyolwe	-8.56917	30.75056
JEH8	M	Pscple	22.08.14	Kabyolwe	-8.56917	30.75056
JEH9	NA	Loblab	22.08.14	Kabyolwe	-8.56917	30.75056
JEI1	NA	Neofas	22.08.14	Kabyolwe	-8.56917	30.75056
JEI2	M	Neofas	22.08.14	Kabyolwe	-8.56917	30.75056
JEI3	M	Neofas	22.08.14	Kabyolwe	-8.56917	30.75056
JEI4	M	Neobue	23.08.14	Kachese	-8.49053	30.47750
JEI5	F	Neobue	23.08.14	Kachese	-8.49053	30.47750
JEI6	M	Neofur	23.08.14	Kachese	-8.49053	30.47750
JEI8	F	Neofur	23.08.14	Kachese	-8.49053	30.47750
JEI9	F	Neofur	23.08.14	Kachese	-8.49053	30.47750
JUA1	M	Pscbab	05.01.15	Kitaza south	-3.62569	29.34239
JUA2	M	Pscbab	05.01.15	Kitaza south	-3.62569	29.34239
JUA3	M	Pscbab	05.01.15	Kitaza south	-3.62569	29.34239
JUA4	F	Pscbab	05.01.15	Kitaza south	-3.62569	29.34239
JUA5	M	Pscbab	05.01.15	Kitaza south	-3.62569	29.34239
JUA6	F	Pscbab	05.01.15	Kitaza south	-3.62569	29.34239
JUA9	M	Pscbab	05.01.15	Kitaza south	-3.62569	29.34239
JUB1	F	Pscbab	05.01.15	Kitaza south	-3.62569	29.34239
JUB2	F	Pscbab	05.01.15	Kitaza south	-3.62569	29.34239
JUB3	F	Pscbab	05.01.15	Kitaza south	-3.62569	29.34239
JUB4	F	Pscbab	05.01.15	Kitaza south	-3.62569	29.34239

ID	Sex	SpeciesID	CollectionDate	CollectionLocation	latitude	longitude
JUB5	M	Pscbab	05.01.15	Kitaza south	-3.62569	29.34239
JUB6	M	Spaery	05.01.15	Kitaza south	-3.62569	29.34239
JUB7	F	Spaery	05.01.15	Kitaza south	-3.62569	29.34239
JUC1	M	Spaery	05.01.15	Kitaza south	-3.62569	29.34239
JUC2	F	Spaery	05.01.15	Kitaza south	-3.62569	29.34239
JUC3	M	Spaery	05.01.15	Kitaza south	-3.62569	29.34239
JUC4	M	Spaery	05.01.15	Kitaza south	-3.62569	29.34239
JUC5	M	Spaery	05.01.15	Kitaza south	-3.62569	29.34239
JUC6	F	Spaery	05.01.15	Kitaza south	-3.62569	29.34239
JUC7	M	Spaery	05.01.15	Kitaza south	-3.62569	29.34239
JUC8	M	Spaery	05.01.15	Kitaza south	-3.62569	29.34239
JUC9	F	Spaery	05.01.15	Kitaza south	-3.62569	29.34239
JUD1	F	Spaery	05.01.15	Kitaza south	-3.62569	29.34239
JUD4	M	TeldhN	05.01.15	Kitaza south	-3.62569	29.34239
JUD5	F	TeldhN	05.01.15	Kitaza south	-3.62569	29.34239
JUD7	NA	TeldhN	05.01.15	Kitaza south	-3.62569	29.34239
JUD8	NA	TeldhN	05.01.15	Kitaza south	-3.62569	29.34239
JUE5	NA	TeldhN	05.01.15	Kitaza south	-3.62569	29.34239
JUE6	NA	TeldhN	05.01.15	Kitaza south	-3.62569	29.34239
JUE7	NA	TeldhN	05.01.15	Kitaza south	-3.62569	29.34239
JUF5	NA	TeldhN	05.01.15	Kitaza south	-3.62569	29.34239
JUF6	NA	TeldhN	05.01.15	Kitaza south	-3.62569	29.34239
JUF7	NA	TeldhN	05.01.15	Kitaza south	-3.62569	29.34239
JUF8	NA	TeldhN	05.01.15	Kitaza south	-3.62569	29.34239
JUH5	M	Neobri	06.01.15	Nyaruhongoka	-3.69158	29.32369
JUH6	M	Neobri	06.01.15	Nyaruhongoka	-3.69158	29.32369
JUH7	F	Neobri	06.01.15	Nyaruhongoka	-3.69158	29.32369
JUH8	F	Neobri	06.01.15	Nyaruhongoka	-3.69158	29.32369
JUH9	F	Neobri	06.01.15	Nyaruhongoka	-3.69158	29.32369
JUI1	M	Neobri	06.01.15	Nyaruhongoka	-3.69158	29.32369
JUI2	F	Neobri	06.01.15	Nyaruhongoka	-3.69158	29.32369
JUI3	F	Neobri	06.01.15	Nyaruhongoka	-3.69158	29.32369
JUI4	M	Neobri	06.01.15	Nyaruhongoka	-3.69158	29.32369
JUI5	M	Neobri	06.01.15	Nyaruhongoka	-3.69158	29.32369
JUI7	M	Neobri	06.01.15	Nyaruhongoka	-3.69158	29.32369
JUI8	M	Neobri	06.01.15	Nyaruhongoka	-3.69158	29.32369
JVA2	M	Neomon	06.01.15	Nyaruhongoka	-3.69158	29.32369
JVA5	M	Neomon	06.01.15	Nyaruhongoka	-3.69158	29.32369
JVA6	F	Neomon	06.01.15	Nyaruhongoka	-3.69158	29.32369
JVA9	M	Neomon	06.01.15	Nyaruhongoka	-3.69158	29.32369
JVB1	M	Neomon	06.01.15	Nyaruhongoka	-3.69158	29.32369
JVB2	F	Neomon	06.01.15	Nyaruhongoka	-3.69158	29.32369
JVB3	F	Neomon	06.01.15	Nyaruhongoka	-3.69158	29.32369
JVB4	M	Neomon	06.01.15	Nyaruhongoka	-3.69158	29.32369
JVB5	F	Neomon	06.01.15	Nyaruhongoka	-3.69158	29.32369
JVB6	F	Neomon	06.01.15	Nyaruhongoka	-3.69158	29.32369
JVB7	M	Neomon	06.01.15	Nyaruhongoka	-3.69158	29.32369
JVB8	F	Neomon	06.01.15	Nyaruhongoka	-3.69158	29.32369
JVC3	F	Tronig	06.01.15	Nyaruhongoka	-3.69158	29.32369
JVC4	NA	Tronig	06.01.15	Nyaruhongoka	-3.69158	29.32369
JVC5	F	Tronig	06.01.15	Nyaruhongoka	-3.69158	29.32369
JVC6	NA	Tronig	06.01.15	Nyaruhongoka	-3.69158	29.32369
JVC7	NA	Tronig	06.01.15	Nyaruhongoka	-3.69158	29.32369
JVC8	NA	Tronig	06.01.15	Nyaruhongoka	-3.69158	29.32369
JVC9	M	Tronig	06.01.15	Nyaruhongoka	-3.69158	29.32369
JVD1	NA	Tronig	06.01.15	Nyaruhongoka	-3.69158	29.32369
JVD2	NA	Tronig	06.01.15	Nyaruhongoka	-3.69158	29.32369
JVD3	NA	Tronig	06.01.15	Nyaruhongoka	-3.69158	29.32369
JVD5	NA	Tronig	06.01.15	Nyaruhongoka	-3.69158	29.32369
JVD6	NA	Tronig	06.01.15	Nyaruhongoka	-3.69158	29.32369
JVE1	M	Cypmic	07.01.15	Nyaruhongoka 2	-3.69861	29.32008
JVE2	M	Cypmic	07.01.15	Nyaruhongoka 2	-3.69861	29.32008
JVE4	M	Cypmic	07.01.15	Nyaruhongoka 2	-3.69861	29.32008
JVE6	M	Cypmic	07.01.15	Nyaruhongoka 2	-3.69861	29.32008
JVE7	M	Cypmic	07.01.15	Nyaruhongoka 2	-3.69861	29.32008
JVE9	M	Cypmic	07.01.15	Nyaruhongoka 2	-3.69861	29.32008
JVF1	M	Cypmic	07.01.15	Nyaruhongoka 2	-3.69861	29.32008
JVF2	F	Cypmic	07.01.15	Nyaruhongoka 2	-3.69861	29.32008
JVF3	M	Cypmic	07.01.15	Nyaruhongoka 2	-3.69861	29.32008
JVF5	M	Cypmic	07.01.15	Nyaruhongoka 2	-3.69861	29.32008
JVF6	M	Neofal	07.01.15	Nyaruhongoka 2	-3.69861	29.32008
JVF7	F	Neofal	07.01.15	Nyaruhongoka 2	-3.69861	29.32008
JVG1	NA	Lessta	07.01.15	Nyaruhongoka 2	-3.69861	29.32008
JVG2	NA	Lessta	07.01.15	Nyaruhongoka 2	-3.69861	29.32008
JVG3	NA	Lessta	07.01.15	Nyaruhongoka 2	-3.69861	29.32008
JVG4	NA	Lessta	07.01.15	Nyaruhongoka 2	-3.69861	29.32008
JVG5	NA	Lessta	07.01.15	Nyaruhongoka 2	-3.69861	29.32008
JVG6	NA	Lessta	07.01.15	Nyaruhongoka 2	-3.69861	29.32008
JVG7	NA	Lessta	07.01.15	Nyaruhongoka 2	-3.69861	29.32008
JVG8	NA	Lessta	07.01.15	Nyaruhongoka 2	-3.69861	29.32008
JVG9	NA	Lessta	07.01.15	Nyaruhongoka 2	-3.69861	29.32008
JVH1	NA	Lessta	07.01.15	Nyaruhongoka 2	-3.69861	29.32008
JVH2	F	Lessta	07.01.15	Nyaruhongoka 2	-3.69861	29.32008
JVH3	M	Lessta	07.01.15	Nyaruhongoka 2	-3.69861	29.32008
JVH4	M	Xenoch	07.01.15	Mireille fishermen	-3.40336	29.35925
JVH5	M	Xenoch	07.01.15	Mireille fishermen	-3.40336	29.35925
JVH6	M	Xenoch	07.01.15	Mireille fishermen	-3.40336	29.35925
JVH7	M	Xenoch	07.01.15	Mireille fishermen	-3.40336	29.35925
JVH9	M	Xenoch	07.01.15	Mireille fishermen	-3.40336	29.35925
JVI1	M	Xenoch	07.01.15	Mireille fishermen	-3.40336	29.35925
JVI3	M	Xenoch	07.01.15	Mireille fishermen	-3.40336	29.35925
JVI4	F	Xenoch	07.01.15	Mireille fishermen	-3.40336	29.35925
JVI5	F	Xenoch	07.01.15	Mireille fishermen	-3.40336	29.35925
JVI6	F	Xenoch	07.01.15	Mireille fishermen	-3.40336	29.35925
JVI7	F	Xenoch	07.01.15	Mireille fishermen	-3.40336	29.35925
JVI8	F	Xenoch	07.01.15	Mireille fishermen	-3.40336	29.35925
JVI9	M	Telbri	07.01.15	Nyaruhongoka 2	-3.69861	29.32008
JWA1	M	Julunt	NA	Kieso (Heinz)	NA	NA
JWA2	F	Julunt	NA	Kieso (Heinz)	NA	NA
JWA3	M	LamorC	NA	Tembwe DRC	-7.23972	30.11944
JWA4	F	LamorC	NA	Tembwe DRC	-7.23972	30.11944
JWA5	M	Neovar	NA	Tembwe DRC	-7.23972	30.11944
JWA6	F	Neovar	NA	Tembwe DRC	-7.23972	30.11944
JWA7	M	Neopec	NA	Tembwe DRC	-7.23972	30.11944
JWA8	M	Lammel	NA	Kalubamba DRC	-7.37944	30.18972
JWA9	F	Lammel	NA	Kalubamba DRC	-7.37944	30.18972

ID	Sex	SpeciesID	CollectionDate	CollectionLocation	latitude	longitude
JWC8	M	Tellon	NA	Longola	-7.48194	30.21778
JWC9	F	Tellon	NA	Longola	-7.48194	30.21778
JWD1	M	Pcytem	NA	Tembwe DRC	-7.23972	30.11944
JWD2	F	Pcytem	NA	Tembwe DRC	-7.23972	30.11944
JWD3	NA	Etingu	NA	Cameroon: Mafue River / Ngut	5.33781	9.41739
JWD4	NA	Etrcan	NA	India	NA	NA
JWD5	M	Parpol	NA	Madagaskar: Andapa	NA	NA
JWD7	NA	Andbis	NA	Peru	NA	NA
JWD8	M	Bujvit	NA	Paraguay	NA	NA
JWD9	M	Apidip	NA	Venezuela	NA	NA
JWE1	M	Ampzal	NA	Lake Apoyo	11.93286	-86.05425
JWE2	M	Aussci	NA	Uruguay	NA	NA
JWE3	NA	Hetbut	NA	Liberia	NA	NA
JWE4	M	Bencon	NA	Cameroon: Muyuka	4.27828	9.40408
JWE5	NA	Copbak	NA	Cameroon: Lake Bermin	5.15669	9.63636
JWE6	M	Copren	NA	Toby's Place	-8.62322	31.20044
JWE7	M	Gobeth	NA	Cameroon: Cross / Mamfe	5.76586	9.31067
JWE8	M	Steult	NA	Inga DRC	-5.51328	13.62514
JWE9	M	Hchelo	NA	Cameroon: Ayatto	4.14986	9.52422
JWF1	J	Htcmul	NA	Cameroon: Boumba	3.22003	14.92017
JWF2	J	Pelmar	NA	Cameroon: Cross / Mamfe	5.76586	9.31067
JWF3	M	Phaacu	NA	Mambova / Zambezi	-17.74336	25.17378
JWF4	J	Sarcar	NA	Mambova / Zambezi	-17.74336	25.17378
JWF5	M	Sermac	NA	Mukambi / Kafue	-14.97844	25.99317
JWF6	F	Lamtig	NA	DRC: Congo river	NA	NA
JWF7	M	Tilspa	NA	Lake Chila Outflow	-8.83574	31.38040
JWF8	M	Thobra	NA	Lac Fwa	-5.72875	23.35058
JWF9	F	Tilbre	NA	West-Africa	NA	NA
JWG1	M	Psephi	NA	Mbulu	-8.85725	31.36467
JWG2	M	Ctepol	NA	DRC	NA	NA
JWG3	M	Hplvan	NA	Ruaha	-7.80822	36.89656
JWG4	M	Troann	NA	Mukamba	-6.94750	29.71194
JWG5	F	Troann	NA	Mukamba	-6.94750	29.71194
JWG8	F	Neohel	12.10.15	Kamakonde DRC	-7.87361	30.30389
JWG9	M	Neohel	12.10.15	Kamakonde DRC	-7.87361	30.30389
JWH1	F	Neogra	12.10.15	Kalo DRC	-7.79528	30.26639
JWH2	M	Neogra	12.10.15	Kalo DRC	-7.79528	30.26639
JWH3	M	Neomar	12.10.15	Kafitilila DRC	-7.71522	30.23414
JWH4	F	Neomar	12.10.15	Kafitilila DRC	-7.71522	30.23414
JWH5	F	Neooli	12.10.15	Kyeso DRC	-6.81667	29.61472
JWH6	M	Neooli	12.10.15	Kyeso DRC	-6.81667	29.61472
JWH9	NA	NeoleL	12.10.15	Luhanga (Graz)	-3.49953	29.13992
JWI2	M	Neolon	09.10.15	Kapamba (Mireille)	-7.63028	30.19556
JWI3	F	Neolon	09.10.15	Kapamba (Mireille)	-7.63028	30.19556
JWI4	M	Peltae	NA	Moliwe	NA	NA
JWI5	F	Peltae	NA	Moliwe	NA	NA
JWI6	F	Neopec	NA	NA	NA	NA
JXA1	NA	Telbri	07.01.15	Nyaruhongoka 2	-3.69861	29.32008
JXA2	NA	Telbri	07.01.15	Nyaruhongoka 2	-3.69861	29.32008
JXA3	NA	Telbri	07.01.15	Nyaruhongoka 2	-3.69861	29.32008
JXA4	F	Telbri	07.01.15	Nyaruhongoka 2	-3.69861	29.32008
JXA5	M	Telbri	07.01.15	Nyaruhongoka 2	-3.69861	29.32008
JXA6	M	Telbri	07.01.15	Nyaruhongoka 2	-3.69861	29.32008
JXA8	M	Telbri	07.01.15	Nyaruhongoka 2	-3.69861	29.32008
JXA9	M	Telbri	07.01.15	Nyaruhongoka 2	-3.69861	29.32008
JXB2	M	Telbri	07.01.15	Nyaruhongoka 2	-3.69861	29.32008
JXB3	M	Telbri	07.01.15	Nyaruhongoka 2	-3.69861	29.32008
JXB4	M	Telbri	07.01.15	Nyaruhongoka 2	-3.69861	29.32008
JXB5	M	JulmaN	07.01.15	Nyaruhongoka 2	-3.69861	29.32008
JXB6	NA	JulmaN	07.01.15	Nyaruhongoka 2	-3.69861	29.32008
JXB7	NA	JulmaN	07.01.15	Nyaruhongoka 2	-3.69861	29.32008
JXB8	NA	JulmaN	07.01.15	Nyaruhongoka 2	-3.69861	29.32008
JXB9	NA	JulmaN	07.01.15	Nyaruhongoka 2	-3.69861	29.32008
JXC1	F	JulmaN	07.01.15	Nyaruhongoka 2	-3.69861	29.32008
JXC2	NA	JulmaN	07.01.15	Nyaruhongoka 2	-3.69861	29.32008
JXC3	NA	JulmaN	07.01.15	Nyaruhongoka 2	-3.69861	29.32008
JXC4	NA	JulmaN	07.01.15	Nyaruhongoka 2	-3.69861	29.32008
JXC6	NA	JulmaN	07.01.15	Nyaruhongoka 2	-3.69861	29.32008
JXC7	NA	JulmaN	07.01.15	Nyaruhongoka 2	-3.69861	29.32008
JXC9	NA	JulmaN	07.01.15	Nyaruhongoka 2	-3.69861	29.32008
JXD2	F	Petpol	07.01.15	Nyaruhongoka 2	-3.69861	29.32008
JXD4	M	Neofal	08.01.15	Nyaruhongoka 2	-3.69861	29.32008
JXD5	NA	Neofal	08.01.15	Nyaruhongoka 2	-3.69861	29.32008
JXD6	NA	Neofal	08.01.15	Nyaruhongoka 2	-3.69861	29.32008
JXD7	F	Neofal	08.01.15	Nyaruhongoka 2	-3.69861	29.32008
JXD8	NA	Neofal	08.01.15	Nyaruhongoka 2	-3.69861	29.32008
JXD9	NA	Neofal	08.01.15	Nyaruhongoka 2	-3.69861	29.32008
JXE1	NA	Neofal	08.01.15	Nyaruhongoka 2	-3.69861	29.32008
JXE3	NA	Neofal	08.01.15	Nyaruhongoka 2	-3.69861	29.32008
JXE4	NA	Neofal	08.01.15	Nyaruhongoka 2	-3.69861	29.32008
JXE5	NA	Neofal	08.01.15	Nyaruhongoka 2	-3.69861	29.32008
JXE7	NA	Neosav	08.01.15	Nyaruhongoka 2	-3.69861	29.32008
JXE9	M	Eremar	08.01.15	Nyaruhongoka 2	-3.69861	29.32008
JXF1	F	Eremar	08.01.15	Nyaruhongoka 2	-3.69861	29.32008
JXF2	F	Eremar	08.01.15	Nyaruhongoka 2	-3.69861	29.32008
JXF3	F	Eremar	08.01.15	Nyaruhongoka 2	-3.69861	29.32008
JXF4	F	Eremar	08.01.15	Nyaruhongoka 2	-3.69861	29.32008
JXF5	F	Eremar	08.01.15	Nyaruhongoka 2	-3.69861	29.32008
JXF6	M	Eremar	08.01.15	Nyaruhongoka 2	-3.69861	29.32008
JXF7	F	Eremar	08.01.15	Nyaruhongoka 2	-3.69861	29.32008
JXF9	M	Eremar	08.01.15	Nyaruhongoka 2	-3.69861	29.32008
JXG1	F	Eremar	08.01.15	Nyaruhongoka 2	-3.69861	29.32008
JXG3	M	Eremar	08.01.15	Nyaruhongoka 2	-3.69861	29.32008
JXG4	F	Eremar	08.01.15	Nyaruhongoka 2	-3.69861	29.32008
JXG5	M	Lamkun	08.01.15	Nyaruhongoka 2	-3.69861	29.32008
JXG6	M	Lamkun	08.01.15	Nyaruhongoka 2	-3.69861	29.32008
JXG7	M	Lamkun	08.01.15	Nyaruhongoka 2	-3.69861	29.32008
JXG8	M	Lamkun	08.01.15	Nyaruhongoka 2	-3.69861	29.32008
JXG9	M	Lamkun	08.01.15	Nyaruhongoka 2	-3.69861	29.32008
JXH1	F	Lamkun	08.01.15	Nyaruhongoka 2	-3.69861	29.32008
JXH2	F	Lamkun	08.01.15	Nyaruhongoka 2	-3.69861	29.32008
JXH3	F	Lamkun	08.01.15	Nyaruhongoka 2	-3.69861	29.32008
JXH4	F	Petort	08.01.15	Nyaruhongoka 2	-3.69861	29.32008
JXH5	M	Petort	08.01.15	Nyaruhongoka 2	-3.69861	29.32008
JXH6	M	Petort	08.01.15	Nyaruhongoka 2	-3.69861	29.32008
JXH7	NA	Petort	08.01.15	Nyaruhongoka 2	-3.69861	29.32008

ID	Sex	SpeciesID	CollectionDate	CollectionLocation	latitude	longitude
JXI1	NA	Petfam	08.01.15	Nyaruhongoka 2	-3.69861	29.32008
JXI2	M	PcybrN	09.01.15	Nyaruhongoka 2	-3.69861	29.32008
JXI4	F	PcybrN	09.01.15	Nyaruhongoka 2	-3.69861	29.32008
JXI7	M	PcybrN	09.01.15	Nyaruhongoka 2	-3.69861	29.32008
JXI8	M	PcybrN	09.01.15	Nyaruhongoka 2	-3.69861	29.32008
JXI9	M	PcybrN	09.01.15	Nyaruhongoka 2	-3.69861	29.32008
JYA1	M	PcybrN	09.01.15	Nyaruhongoka 2	-3.69861	29.32008
JYA2	M	PcybrN	09.01.15	Nyaruhongoka 2	-3.69861	29.32008
JYA3	F	PcybrN	09.01.15	Nyaruhongoka 2	-3.69861	29.32008
JYA4	F	PcybrN	09.01.15	Nyaruhongoka 2	-3.69861	29.32008
JYA5	F	PcybrN	09.01.15	Nyaruhongoka 2	-3.69861	29.32008
JYA6	F	PcybrN	09.01.15	Nyaruhongoka 2	-3.69861	29.32008
JYA7	F	PcybrN	09.01.15	Nyaruhongoka 2	-3.69861	29.32008
JYC1	M	Neofur	09.01.15	Nyaruhongoka 2	-3.69861	29.32008
JYC2	F	Ophnas	09.01.15	Nyaruhongoka 2	-3.69861	29.32008
JYD1	NA	Altcom	09.01.15	Nyaruhongoka 2	-3.69861	29.32008
JYD2	NA	Altcom	07.01.15	Nyaruhongoka 2	-3.69861	29.32008
JYD3	M	Hplsta	10.01.15	Bujumbura Creek	-3.39192	29.34942
JYD5	F	Astbur	10.01.15	Bujumbura Creek	-3.39192	29.34942
JYF4	NA	Cphfr5	10.01.15	Nyaruhongoka 2	-3.69861	29.32008
JYF5	F	Cphfr5	10.01.15	Nyaruhongoka 2	-3.69861	29.32008
JYF6	NA	Batfas	10.01.15	Nyaruhongoka 2	-3.69861	29.32008
JYF7	M	Ophpar	11.01.15	Nyanza Lac	-4.24078	29.55011
JYF8	M	Ophpar	11.01.15	Nyanza Lac	-4.24078	29.55011
JYF9	M	Ophpar	11.01.15	Nyanza Lac	-4.24078	29.55011
JYG2	M	Ophpar	11.01.15	Nyanza Lac	-4.24078	29.55011
JYG3	M	Ophpar	11.01.15	Nyanza Lac	-4.24078	29.55011
JYG4	M	Ophpar	11.01.15	Nyanza Lac	-4.24078	29.55011
JYG5	F	Ophpar	11.01.15	Nyanza Lac	-4.24078	29.55011
JYG6	M	Ophpar	11.01.15	Nyanza Lac	-4.24078	29.55011
JYG7	M	Ophpar	11.01.15	Nyanza Lac	-4.24078	29.55011
JYG8	M	Ophpar	11.01.15	Nyanza Lac	-4.24078	29.55011
JYG9	F	Ophpar	11.01.15	Nyanza Lac	-4.24078	29.55011
JYH1	F	Ophpar	11.01.15	Nyanza Lac	-4.24078	29.55011
JYH3	M	Tanirs	11.01.15	Nyanza Lac	-4.24078	29.55011
JYH4	M	Tanirs	11.01.15	Nyanza Lac	-4.24078	29.55011
JYH5	M	Tanirs	11.01.15	Nyanza Lac	-4.24078	29.55011
JYH6	F	Tanirs	11.01.15	Nyanza Lac	-4.24078	29.55011
JYH7	F	Tanirs	11.01.15	Nyanza Lac	-4.24078	29.55011
JYH8	M	Tanirs	11.01.15	Nyanza Lac	-4.24078	29.55011
JYH9	M	Tanirs	11.01.15	Nyanza Lac	-4.24078	29.55011
JYI1	F	Tanirs	11.01.15	Nyanza Lac	-4.24078	29.55011
JYI3	F	Tanirs	11.01.15	Nyanza Lac	-4.24078	29.55011
JYI4	M	Tanirs	11.01.15	Nyanza Lac	-4.24078	29.55011
JYI5	M	Tanirs	11.01.15	Nyanza Lac	-4.24078	29.55011
JYI6	M	Tanirs	11.01.15	Nyanza Lac	-4.24078	29.55011
JYI8	M	Trobri	11.01.15	Nyanza Lac	-4.24078	29.55011
JYI9	NA	Trobri	11.01.15	Nyanza Lac	-4.24078	29.55011
JZA1	NA	Trobri	11.01.15	Nyanza Lac	-4.24078	29.55011
JZA2	NA	Trobri	11.01.15	Nyanza Lac	-4.24078	29.55011
JZA3	F	Trobri	11.01.15	Nyanza Lac	-4.24078	29.55011
JZA4	NA	Trobri	11.01.15	Nyanza Lac	-4.24078	29.55011
JZA5	NA	Trobri	11.01.15	Nyanza Lac	-4.24078	29.55011
JZA6	NA	Trobri	11.01.15	Nyanza Lac	-4.24078	29.55011
JZA8	NA	Trobri	11.01.15	Nyanza Lac	-4.24078	29.55011
JZA9	NA	Trobri	11.01.15	Nyanza Lac	-4.24078	29.55011
JZB1	NA	Trobri	11.01.15	Nyanza Lac	-4.24078	29.55011
JZB2	NA	Trobri	11.01.15	Nyanza Lac	-4.24078	29.55011
JZB4	M	Spamar	11.01.15	Nyanza Lac	-4.24078	29.55011
JZB5	M	Spamar	11.01.15	Nyanza Lac	-4.24078	29.55011
JZB6	M	Spamar	11.01.15	Nyanza Lac	-4.24078	29.55011
JZB7	M	Spamar	11.01.15	Nyanza Lac	-4.24078	29.55011
JZB8	M	Spamar	11.01.15	Nyanza Lac	-4.24078	29.55011
JZB9	F	Spamar	11.01.15	Nyanza Lac	-4.24078	29.55011
JZC1	M	Spamar	11.01.15	Nyanza Lac	-4.24078	29.55011
JZC2	F	Spamar	11.01.15	Nyanza Lac	-4.24078	29.55011
JZC4	F	Spamar	11.01.15	Nyanza Lac	-4.24078	29.55011
JZC5	F	Spamar	11.01.15	Nyanza Lac	-4.24078	29.55011
JZC6	F	Spamar	11.01.15	Nyanza Lac	-4.24078	29.55011
JZC8	NA	Petort	10.01.15	Nyaruhongoka 2	-3.69861	29.32008
JZC9	NA	Petort	10.01.15	Nyaruhongoka 2	-3.69861	29.32008
JZD1	NA	Petort	10.01.15	Nyaruhongoka 2	-3.69861	29.32008
JZD2	NA	Petort	10.01.15	Nyaruhongoka 2	-3.69861	29.32008
JZD3	F	Spamar	11.01.15	Nyanza Lac	-4.24078	29.55011
JZD4	NA	Neotoa	11.01.15	Nyanza Lac	-4.24078	29.55011
JZD5	M	Neotoa	11.01.15	Nyanza Lac	-4.24078	29.55011
JZD6	F	Neotoa	11.01.15	Nyanza Lac	-4.24078	29.55011
JZD7	M	Lamkun	10.01.15	Nyaruhongoka 2	-3.69861	29.32008
JZD8	M	Lamkun	10.01.15	Nyaruhongoka 2	-3.69861	29.32008
JZD9	M	Lamkun	10.01.15	Nyaruhongoka 2	-3.69861	29.32008
JZE1	F	Lamkun	10.01.15	Nyaruhongoka 2	-3.69861	29.32008
JZE2	M	Calple	12.01.15	Bujumbura fishmarket	-3.34783	29.29778
JZE4	F	Calple	12.01.15	Bujumbura fishmarket	-3.34783	29.29778
JZE6	M	Xenom	12.01.15	Bujumbura fishmarket	-3.34783	29.29778
JZE8	F	Xenom	12.01.15	Bujumbura fishmarket	-3.34783	29.29778
JZF1	M	Neople	12.01.15	Bujumbura fishmarket	-3.34783	29.29778
JZF2	F	Neople	12.01.15	Bujumbura fishmarket	-3.34783	29.29778
JZF3	M	Lamom	12.01.15	Bujumbura fishmarket	-3.34783	29.29778
JZF4	F	Lamom	12.01.15	Bujumbura fishmarket	-3.34783	29.29778
JZF5	M	Calple	12.01.15	Bujumbura fishmarket	-3.34783	29.29778
JZF6	M	Calple	12.01.15	Bujumbura fishmarket	-3.34783	29.29778
JZF7	M	Calple	12.01.15	Bujumbura fishmarket	-3.34783	29.29778
JZF8	M	Calple	12.01.15	Bujumbura fishmarket	-3.34783	29.29778
JZF9	M	Calple	12.01.15	Bujumbura fishmarket	-3.34783	29.29778
JZG1	M	Calple	12.01.15	Bujumbura fishmarket	-3.34783	29.29778
JZG2	F	Calple	12.01.15	Bujumbura fishmarket	-3.34783	29.29778
JZG3	F	Calple	12.01.15	Bujumbura fishmarket	-3.34783	29.29778
JZG4	F	Calple	12.01.15	Bujumbura fishmarket	-3.34783	29.29778
JZG5	F	Calple	12.01.15	Bujumbura fishmarket	-3.34783	29.29778
JZG6	M	Xenlon	12.01.15	Bujumbura fishmarket	-3.34783	29.29778
JZG7	F	Xenlon	12.01.15	Bujumbura fishmarket	-3.34783	29.29778
JZG8	NA	Neople	12.01.15	Bujumbura fishmarket	-3.34783	29.29778
JZG9	NA	Neople	12.01.15	Bujumbura fishmarket	-3.34783	29.29778
JZH1	NA	Neople	12.01.15	Bujumbura fishmarket	-3.34783	29.29778
JZH2	M	Calmel	12.01.15	Bujumbura fishmarket	-3.34783	29.29778
JZH3	F	Calmel	12.01.15	Bujumbura fishmarket	-3.34783	29.29778

ID	Sex	SpeciesID	CollectionDate	CollectionLocation	latitude	longitude
JZI1	M	Xenom	12.01.15	Bujumbura fishmarket	-3.34783	29.29778
JZI2	M	Xenom	12.01.15	Bujumbura fishmarket	-3.34783	29.29778
JZI3	M	Xenom	12.01.15	Bujumbura fishmarket	-3.34783	29.29778
JZI4	F	Xenom	12.01.15	Bujumbura fishmarket	-3.34783	29.29778
JZI5	F	Xenom	12.01.15	Bujumbura fishmarket	-3.34783	29.29778
JZI6	F	Xenom	12.01.15	Bujumbura fishmarket	-3.34783	29.29778
JZI7	F	Xenom	12.01.15	Bujumbura fishmarket	-3.34783	29.29778
JZI8	F	Xenom	12.01.15	Bujumbura fishmarket	-3.34783	29.29778
JZI9	F	Xenom	12.01.15	Bujumbura fishmarket	-3.34783	29.29778
KAA1	F	Xenom	12.01.15	Bujumbura fishmarket	-3.34783	29.29778
KAA2	NA	Lchaur	12.01.15	Bujumbura fishmarket	-3.34783	29.29778
KAA5	NA	Lamom	12.01.15	Bujumbura fishmarket	-3.34783	29.29778
KAA6	NA	Lamom	12.01.15	Bujumbura fishmarket	-3.34783	29.29778
KAA7	NA	Lamom	12.01.15	Bujumbura fishmarket	-3.34783	29.29778
KAA8	NA	Lamom	12.01.15	Bujumbura fishmarket	-3.34783	29.29778
KAA9	NA	Lamom	12.01.15	Bujumbura fishmarket	-3.34783	29.29778
KAC4	F	Cphfr5	12.01.15	Nyaruhongoka 2	-3.69861	29.32008
KAC5	F	Cphfr5	12.01.15	Nyaruhongoka 2	-3.69861	29.32008
KAC6	NA	Neotoa	11.01.15	Nyanza Lac	-4.24078	29.55011
KAC7	NA	Neotoa	11.01.15	Nyanza Lac	-4.24078	29.55011
KAC8	NA	Neotoa	11.01.15	Nyanza Lac	-4.24078	29.55011
KAC9	NA	Neotoa	11.01.15	Nyanza Lac	-4.24078	29.55011
KAD1	NA	Neofur	12.01.15	Nyaruhongoka 2	-3.69861	29.32008
KAD2	M	Leppro	12.01.15	Nyaruhongoka 2	-3.69861	29.32008
KAD3	F	Cphfr5	12.01.15	Nyaruhongoka 2	-3.69861	29.32008
KAD4	F	NeoveB	14.01.15	Nyaruhongoka 2	-3.69861	29.32008
KAD5	F	NeoveB	14.01.15	Nyaruhongoka 2	-3.69861	29.32008
KAD6	M	Batmin	14.01.15	Bujumbura fishmarket	-3.34783	29.29778
KAD8	M	Cphfr5	14.01.15	Nyaruhongoka 2	-3.69861	29.32008
KAD9	M	Cphfr5	14.01.15	Nyaruhongoka 2	-3.69861	29.32008
KAE1	F	Batleo	14.01.15	Bujumbura fishmarket	-3.34783	29.29778
KAE3	M	Trespn	14.01.15	Bujumbura fishmarket	-3.34783	29.29778
KAE4	M	Ctehor	14.01.15	Nyaruhongoka 2	-3.69861	29.32008
KAE5	NA	Lepelo	14.01.15	Nyaruhongoka 2	-3.69861	29.32008
KAE6	NA	Xenbou	14.01.15	Nyaruhongoka 2	-3.69861	29.32008
KAE8	M	Arcstr	14.01.15	Rusizi 2 (Gatumba)	-3.33789	29.27383
KAF1	M	Carsch	15.01.15	Bujumbura fishmarket	-3.34783	29.29778
KAF2	F	Carsch	15.01.15	Bujumbura fishmarket	-3.34783	29.29778
KAF3	M	Calmel	15.01.15	Bujumbura fishmarket	-3.34783	29.29778
KAF4	F	Calmel	15.01.15	Bujumbura fishmarket	-3.34783	29.29778
KAF5	M	Xenlon	15.01.15	Bujumbura fishmarket	-3.34783	29.29778
KAF6	F	Xenlon	15.01.15	Bujumbura fishmarket	-3.34783	29.29778
KAG3	M	Cphfr5	15.01.15	Nyaruhongoka 2	-3.69861	29.32008
KAG4	M	Ophnas	15.01.15	Nyaruhongoka 2	-3.69861	29.32008
KAG6	NA	Permic	15.01.15	Nyaruhongoka 2	-3.69861	29.32008
KAG7	M	NeoveB	15.01.15	Nyaruhongoka 2	-3.69861	29.32008
KAG8	F	NeoveB	15.01.15	Nyaruhongoka 2	-3.69861	29.32008
KAG9	F	NeoveB	15.01.15	Nyaruhongoka 2	-3.69861	29.32008
KAH2	M	Xenlon	15.01.15	Bujumbura fishmarket	-3.34783	29.29778
KAH3	M	Xenlon	15.01.15	Bujumbura fishmarket	-3.34783	29.29778
KAH4	M	Xenlon	15.01.15	Bujumbura fishmarket	-3.34783	29.29778
KAH5	M	Xenlon	15.01.15	Bujumbura fishmarket	-3.34783	29.29778
KAH6	F	Xenlon	15.01.15	Bujumbura fishmarket	-3.34783	29.29778
KAH7	F	Xenlon	15.01.15	Bujumbura fishmarket	-3.34783	29.29778
KAH8	F	Xenlon	15.01.15	Bujumbura fishmarket	-3.34783	29.29778
KAH9	M	Xenlon	15.01.15	Bujumbura fishmarket	-3.34783	29.29778
KAI4	F	Calmel	15.01.15	Bujumbura fishmarket	-3.34783	29.29778
KAI5	M	Calmel	15.01.15	Bujumbura fishmarket	-3.34783	29.29778
KAI6	M	Calmel	15.01.15	Bujumbura fishmarket	-3.34783	29.29778
KAI7	M	Calmel	15.01.15	Bujumbura fishmarket	-3.34783	29.29778
KAI8	NA	Calmel	15.01.15	Bujumbura fishmarket	-3.34783	29.29778
KAI9	NA	Trioto	15.01.15	Bujumbura fishmarket	-3.34783	29.29778
KCA1	NA	Trioto	15.01.15	Bujumbura fishmarket	-3.34783	29.29778
KCA2	NA	Tylpol	15.01.15	Bujumbura fishmarket	-3.34783	29.29778
KCA3	NA	Tylpol	15.01.15	Bujumbura fishmarket	-3.34783	29.29778
KCA4	M	Carsch	15.01.15	Bujumbura fishmarket	-3.34783	29.29778
KCA5	M	Carsch	15.01.15	Bujumbura fishmarket	-3.34783	29.29778
KCA6	F	Carsch	15.01.15	Bujumbura fishmarket	-3.34783	29.29778
KCA7	F	Carsch	15.01.15	Bujumbura fishmarket	-3.34783	29.29778
KCA8	F	Carsch	15.01.15	Bujumbura fishmarket	-3.34783	29.29778
KCA9	F	Carsch	15.01.15	Bujumbura fishmarket	-3.34783	29.29778
KCB1	F	Carsch	15.01.15	Bujumbura fishmarket	-3.34783	29.29778
KCB2	F	Carsch	15.01.15	Bujumbura fishmarket	-3.34783	29.29778
KCB3	F	Carsch	15.01.15	Bujumbura fishmarket	-3.34783	29.29778
KCB4	F	Carsch	15.01.15	Bujumbura fishmarket	-3.34783	29.29778
KCB8	NA	Batleo	15.01.15	Bujumbura fishmarket	-3.34783	29.29778
KCB9	NA	Batleo	15.01.15	Bujumbura fishmarket	-3.34783	29.29778
KCC1	NA	Batleo	15.01.15	Bujumbura fishmarket	-3.34783	29.29778
KCC2	NA	Batleo	15.01.15	Bujumbura fishmarket	-3.34783	29.29778
KCC5	NA	Batleo	15.01.15	Bujumbura fishmarket	-3.34783	29.29778
KCC7	NA	Batleo	15.01.15	Bujumbura fishmarket	-3.34783	29.29778
KCC9	NA	Neotoa	16.01.15	Nyanza Lac	-4.24078	29.55011
KCD1	NA	Neotoa	16.01.15	Nyanza Lac	-4.24078	29.55011
KCD2	NA	Neotoa	16.01.15	Nyanza Lac	-4.24078	29.55011
KCD3	NA	Neotoa	16.01.15	Nyanza Lac	-4.24078	29.55011
KCD4	NA	Lamom	16.01.15	Nyanza Lac	-4.24078	29.55011
KCD6	M	Neobou	16.01.15	Nyanza Lac	-4.24078	29.55011
KCD7	NA	Neobou	16.01.15	Nyanza Lac	-4.24078	29.55011
KCD8	NA	Neobou	16.01.15	Nyanza Lac	-4.24078	29.55011
KCE1	F	Neobou	16.01.15	Nyanza Lac	-4.24078	29.55011
KCE2	NA	Neotoa	16.01.15	Nyanza Lac	-4.24078	29.55011
KCE3	NA	Calmel	16.01.15	Nyanza Lac	-4.24078	29.55011
KCE4	NA	Calmel	16.01.15	Nyanza Lac	-4.24078	29.55011
KCE5	F	Neobou	16.01.15	Nyanza Lac	-4.24078	29.55011
KCE7	M	Pscmar	16.01.15	Nyanza Lac	-4.24078	29.55011
KCE9	F	Pscmar	16.01.15	Nyanza Lac	-4.24078	29.55011
KCF1	NA	Pscmar	16.01.15	Nyanza Lac	-4.24078	29.55011
KCF2	NA	Pscmar	16.01.15	Nyanza Lac	-4.24078	29.55011
KCF3	F	Pscmar	16.01.15	Nyanza Lac	-4.24078	29.55011
KCF4	NA	Pscmar	16.01.15	Nyanza Lac	-4.24078	29.55011
KCF5	NA	Pscmar	16.01.15	Nyanza Lac	-4.24078	29.55011
KCF6	NA	Pscmar	16.01.15	Nyanza Lac	-4.24078	29.55011
KCF8	NA	Pscmar	16.01.15	Nyanza Lac	-4.24078	29.55011
KCF9	NA	Pscmar	16.01.15	Nyanza Lac	-4.24078	29.55011
KCG1	NA	Pscmar	16.01.15	Nyanza Lac	-4.24078	29.55011
KCG2	M	Lamspe	16.01.15	Nyanza Lac	-4.24078	29.55011

ID	Sex	SpeciesID	CollectionDate	CollectionLocation	latitude	longitude
KCG3	F	Lamspe	16.01.15	Nyanza Lac	-4.24078	29.55011
KCG4	M	Lamspe	16.01.15	Nyanza Lac	-4.24078	29.55011
KCG5	NA	Lamspe	16.01.15	Nyanza Lac	-4.24078	29.55011
KCG6	NA	Lamspe	16.01.15	Nyanza Lac	-4.24078	29.55011
KCG7	NA	Lamspe	16.01.15	Nyanza Lac	-4.24078	29.55011
KCG8	NA	Lamspe	16.01.15	Nyanza Lac	-4.24078	29.55011
KCG9	NA	Lamspe	16.01.15	Nyanza Lac	-4.24078	29.55011
KCH1	NA	Lamspe	16.01.15	Nyanza Lac	-4.24078	29.55011
KCH2	NA	Lamspe	16.01.15	Nyanza Lac	-4.24078	29.55011
KCH5	NA	NeobrM	16.01.15	Nyanza Lac	-4.24078	29.55011
KCH6	NA	NeobrM	16.01.15	Nyanza Lac	-4.24078	29.55011
KCH7	NA	NeobrM	16.01.15	Nyanza Lac	-4.24078	29.55011
KCH8	NA	NeobrM	16.01.15	Nyanza Lac	-4.24078	29.55011
KCH9	NA	NeobrM	16.01.15	Nyanza Lac	-4.24078	29.55011
KCI1	NA	NeobrM	16.01.15	Nyanza Lac	-4.24078	29.55011
KCI2	NA	NeobrM	16.01.15	Nyanza Lac	-4.24078	29.55011
KCI3	NA	NeobrM	16.01.15	Nyanza Lac	-4.24078	29.55011
KCI4	NA	NeobrM	16.01.15	Nyanza Lac	-4.24078	29.55011
KCI5	NA	NeobrM	16.01.15	Nyanza Lac	-4.24078	29.55011
KCI6	M	NeobrM	16.01.15	Nyanza Lac	-4.24078	29.55011
KCI7	F	NeobrM	16.01.15	Nyanza Lac	-4.24078	29.55011
KDC6	M	Ortmaz	18.01.15	Mazimoero	-3.88472	30.19775
KDF2	F	Cphfr5	22.01.15	Nyaruhongoka 2	-3.69861	29.32008
KDF3	M	NeoveB	22.01.15	Nyaruhongoka 2	-3.69861	29.32008
KDF4	F	NeoveB	22.01.15	Nyaruhongoka 2	-3.69861	29.32008
KDF5	F	NeoveB	22.01.15	Nyaruhongoka 2	-3.69861	29.32008
KDF6	M	Petort	22.01.15	Nyaruhongoka 2	-3.69861	29.32008
KDF7	NA	Neople	22.01.15	Bujumbura fishmarket	-3.34783	29.29778
KDF8	NA	Petort	22.01.15	Nyanza Lac	-4.24078	29.55011
KDF9	M	Cphfr5	24.01.15	Nyaruhongoka 2	-3.69861	29.32008
KDG1	M	Cphfr5	24.01.15	Nyaruhongoka 2	-3.69861	29.32008
KDG2	F	Cphfr5	24.01.15	Nyaruhongoka 2	-3.69861	29.32008
KDG3	F	Cypmic	24.01.15	Nyaruhongoka 2	-3.69861	29.32008
KDG4	NA	Cypmic	24.01.15	Nyaruhongoka 2	-3.69861	29.32008
KEA1	F	Petkas	24.06.15	Kaku	-4.89639	29.61167
KEA2	F	Petkas	24.06.15	Kaku	-4.89639	29.61167
KEA3	M	Petkas	24.06.15	Kaku	-4.89639	29.61167
KEA4	F	Petkas	24.06.15	Kaku	-4.89639	29.61167
KEA5	M	Petkas	24.06.15	Kaku	-4.89639	29.61167
KEA6	M	Petkas	24.06.15	Kaku	-4.89639	29.61167
KEA7	M	Petkas	24.06.15	Kaku	-4.89639	29.61167
KEA9	M	Petkas	24.06.15	Kaku	-4.89639	29.61167
KEB1	M	Petkas	24.06.15	Kaku	-4.89639	29.61167
KEB2	M	Petkas	24.06.15	Kaku	-4.89639	29.61167
KEB3	M	Petkas	24.06.15	Kaku	-4.89639	29.61167
KEB4	M	Petkas	24.06.15	Kaku	-4.89639	29.61167
KEB7	M	Neoleu	25.06.15	Cape Kabogo	-5.46083	29.74750
KEB8	F	Leppro	25.06.15	Cape Kabogo	-5.46083	29.74750
KEB9	F	Leppro	25.06.15	Cape Kabogo	-5.46083	29.74750
KEC1	M	Neosim	25.06.15	Cape Kabogo	-5.46083	29.74750
KEC2	F	Neosim	25.06.15	Cape Kabogo	-5.46083	29.74750
KEC3	NA	Neosim	25.06.15	Cape Kabogo	-5.46083	29.74750
KEC4	NA	Neosim	25.06.15	Cape Kabogo	-5.46083	29.74750
KEC5	NA	Neosim	25.06.15	Cape Kabogo	-5.46083	29.74750
KEC8	NA	Neosim	25.06.15	Cape Kabogo	-5.46083	29.74750
KEC9	NA	Neosim	25.06.15	Cape Kabogo	-5.46083	29.74750
KED1	NA	Neosim	25.06.15	Cape Kabogo	-5.46083	29.74750
KED2	NA	Neosim	25.06.15	Cape Kabogo	-5.46083	29.74750
KED3	NA	Neosim	25.06.15	Cape Kabogo	-5.46083	29.74750
KED4	NA	Neosim	25.06.15	Cape Kabogo	-5.46083	29.74750
KED5	NA	Neosim	25.06.15	Cape Kabogo	-5.46083	29.74750
KED6	M	Trolun	25.06.15	Cape Kabogo	-5.46083	29.74750
KED7	F	Trolun	25.06.15	Cape Kabogo	-5.46083	29.74750
KED8	M	Trolun	25.06.15	Cape Kabogo	-5.46083	29.74750
KED9	F	Trolun	25.06.15	Cape Kabogo	-5.46083	29.74750
KEE1	F	Trolun	25.06.15	Cape Kabogo	-5.46083	29.74750
KEE2	F	Trolun	25.06.15	Cape Kabogo	-5.46083	29.74750
KEE3	M	Trolun	25.06.15	Cape Kabogo	-5.46083	29.74750
KEE4	F	Trolun	25.06.15	Cape Kabogo	-5.46083	29.74750
KEE5	M	Trolun	25.06.15	Cape Kabogo	-5.46083	29.74750
KEE6	M	Trolun	25.06.15	Cape Kabogo	-5.46083	29.74750
KEE7	M	Trolun	25.06.15	Cape Kabogo	-5.46083	29.74750
KEE8	NA	Batvit	26.06.15	Kabogo fishermen	-5.68306	29.76992
KEE9	M	Chando	26.06.15	Katumbi	-6.00861	29.76083
KEF1	F	Chando	26.06.15	Katumbi	-6.00861	29.76083
KEF2	M	Troluk	26.06.15	Katumbi	-6.00861	29.76083
KEF3	F	Troluk	26.06.15	Katumbi	-6.00861	29.76083
KEF4	F	Chando	26.06.15	Katumbi	-6.00861	29.76083
KEF5	M	Chando	26.06.15	Katumbi	-6.00861	29.76083
KEF6	M	Chando	26.06.15	Katumbi	-6.00861	29.76083
KEF7	F	Chando	26.06.15	Katumbi	-6.00861	29.76083
KEF8	F	Chando	26.06.15	Katumbi	-6.00861	29.76083
KEF9	M	Chando	26.06.15	Katumbi	-6.00861	29.76083
KEG1	F	Chando	26.06.15	Katumbi	-6.00861	29.76083
KEG2	F	Chando	26.06.15	Katumbi	-6.00861	29.76083
KEG3	F	Chando	26.06.15	Katumbi	-6.00861	29.76083
KEG4	F	Chando	26.06.15	Katumbi	-6.00861	29.76083
KEG5	F	Troluk	26.06.15	Katumbi	-6.00861	29.76083
KEG6	M	Troluk	26.06.15	Katumbi	-6.00861	29.76083
KEG7	M	Troluk	26.06.15	Katumbi	-6.00861	29.76083
KEG8	F	Troluk	26.06.15	Katumbi	-6.00861	29.76083
KEG9	F	Troluk	26.06.15	Katumbi	-6.00861	29.76083
KEH1	M?	XenspN	26.06.15	Katumbi	-6.00861	29.76083
KEH2	M?	XenspN	26.06.15	Katumbi	-6.00861	29.76083
KEH3	M	Neoleu	27.06.15	Bulu Point	-6.01611	29.74639
KEH4	M	Neoleu	27.06.15	Bulu Point	-6.01611	29.74639
KEH5	M	Neoleu	27.06.15	Bulu Point	-6.01611	29.74639
KEH8	NA	Neoleu	27.06.15	Bulu Point	-6.01611	29.74639
KEH9	M	Plepar	27.06.15	Bulu Point	-6.01611	29.74639
KEI1	M	Plepar	27.06.15	Bulu Point	-6.01611	29.74639
KEI2	F	Troluk	27.06.15	Bulu Point	-6.01611	29.74639
KEI5	M	Troluk	27.06.15	Karilani Island	-6.02056	29.74250
KEI6	F	Troluk	27.06.15	Karilani Island	-6.02056	29.74250
KEI7	F	Troluk	27.06.15	Karilani Island	-6.02056	29.74250
KEI8	F	Troluk	27.06.15	Karilani Island	-6.02056	29.74250
KEI9	M	Plepar	27.06.15	Karilani Island	-6.02056	29.74250

ID	Sex	SpeciesID	CollectionDate	CollectionLocation	latitude	longitude
KFA1	M	Cypdwj	20.06.15	Cave Kigoma	-4.88694	29.61583
KFA2	M	Cypdwj	20.06.15	Cave Kigoma	-4.88694	29.61583
KFA3	M	Cypdwj	20.06.15	Cave Kigoma	-4.88694	29.61583
KFA4	M	Cypdwj	20.06.15	Cave Kigoma	-4.88694	29.61583
KFA5	M	Cypdwj	20.06.15	Cave Kigoma	-4.88694	29.61583
KFA6	F	Cypdwj	20.06.15	Cave Kigoma	-4.88694	29.61583
KFA7	M	Cypdwj	20.06.15	Cave Kigoma	-4.88694	29.61583
KFA9	F	Cypdwj	20.06.15	Cave Kigoma	-4.88694	29.61583
KFB2	F	Cypdwj	20.06.15	Cave Kigoma	-4.88694	29.61583
KFB3	F	Cypdwj	20.06.15	Cave Kigoma	-4.88694	29.61583
KFB4	F	Cypdwj	20.06.15	Cave Kigoma	-4.88694	29.61583
KFB5	F	Cypdwj	20.06.15	Cave Kigoma	-4.88694	29.61583
KFD2	F	Neowal	20.06.15	Tembo Rock	-4.88694	29.61250
KFD4	M	Neowal	20.06.15	Tembo Rock	-4.88694	29.61250
KFD6	M	Neowal	20.06.15	Tembo Rock	-4.88694	29.61250
KFD7	M	Neowal	20.06.15	Tembo Rock	-4.88694	29.61250
KFD8	M	Neowal	20.06.15	Tembo Rock	-4.88694	29.61250
KFD9	M	Neowal	20.06.15	Tembo Rock	-4.88694	29.61250
KFE1	M	Neowal	20.06.15	Tembo Rock	-4.88694	29.61250
KFE2	M	Neowal	20.06.15	Tembo Rock	-4.88694	29.61250
KFE3	F	Neowal	20.06.15	Tembo Rock	-4.88694	29.61250
KFE4	F	Neowal	20.06.15	Tembo Rock	-4.88694	29.61250
KFE5	F	Neowal	20.06.15	Tembo Rock	-4.88694	29.61250
KFE6	F	Neowal	20.06.15	Tembo Rock	-4.88694	29.61250
KFE8	M	Pscmrg	20.06.15	Tembo Rock	-4.88694	29.61250
KFF1	F	Pscmrg	20.06.15	Tembo Rock	-4.88694	29.61250
KFF2	M	Pscmrg	20.06.15	Tembo Rock	-4.88694	29.61250
KFF3	M	Pscmrg	20.06.15	Tembo Rock	-4.88694	29.61250
KFF4	F	JulreK	21.06.15	Kaku	-4.89639	29.61167
KFH4	M	Neotre	21.06.15	Kaku	-4.89639	29.61167
KFH5	F	Neotre	21.06.15	Kaku	-4.89639	29.61167
KFH7	F	Neotre	21.06.15	Kaku	-4.89639	29.61167
KFH8	F	Neotre	21.06.15	Kaku	-4.89639	29.61167
KFH9	F	Neotre	21.06.15	Kaku	-4.89639	29.61167
KFI2	F	Neotre	21.06.15	Kaku	-4.89639	29.61167
KFI3	F	Neotre	21.06.15	Kaku	-4.89639	29.61167
KFI4	M	Neotre	21.06.15	Kaku	-4.89639	29.61167
KFI5	M	Neotre	21.06.15	Kaku	-4.89639	29.61167
KFI6	M	Neotre	21.06.15	Kaku	-4.89639	29.61167
KFI7	F	Neotre	21.06.15	Kaku	-4.89639	29.61167
KFI8	M	Neotre	21.06.15	Kaku	-4.89639	29.61167
KFI9	F	JulreK	21.06.15	Kaku	-4.89639	29.61167
KHA4	M	Trodub	21.06.15	Kaku	-4.89639	29.61167
KHA5	F	Trodub	21.06.15	Kaku	-4.89639	29.61167
KHA6	F	Trodub	21.06.15	Kaku	-4.89639	29.61167
KHA7	M	Neochi	22.06.15	Mwamahunga	-4.91194	29.59833
KHA9	F	Neochi	22.06.15	Mwamahunga	-4.91194	29.59833
KHB2	F	Neochi	22.06.15	Mwamahunga	-4.91194	29.59833
KHB3	F	Neochi	22.06.15	Mwamahunga	-4.91194	29.59833
KHB4	M	Neochi	22.06.15	Mwamahunga	-4.91194	29.59833
KHB5	F	Neochi	22.06.15	Mwamahunga	-4.91194	29.59833
KHB6	F	Neochi	22.06.15	Mwamahunga	-4.91194	29.59833
KHB7	M	Neochi	22.06.15	Mwamahunga	-4.91194	29.59833
KHB8	M	Neochi	22.06.15	Mwamahunga	-4.91194	29.59833
KHB9	M	Neochi	22.06.15	Mwamahunga	-4.91194	29.59833
KHC1	F	Neochi	22.06.15	Mwamahunga	-4.91194	29.59833
KHC2	F	Neochi	22.06.15	Mwamahunga	-4.91194	29.59833
KHC3	F	JulreK	22.06.15	Mwamahunga	-4.91194	29.59833
KHC4	M	EctspN	22.06.15	Mwamahunga	-4.91194	29.59833
KHC5	F	EctspN	22.06.15	Mwamahunga	-4.91194	29.59833
KHC8	M	EctspN	22.06.15	Mwamahunga	-4.91194	29.59833
KHC9	M	EctspN	22.06.15	Mwamahunga	-4.91194	29.59833
KHD1	F	EctspN	22.06.15	Mwamahunga	-4.91194	29.59833
KHD2	F	EctspN	22.06.15	Mwamahunga	-4.91194	29.59833
KHD3	F	EctspN	22.06.15	Mwamahunga	-4.91194	29.59833
KHD4	F	EctspN	22.06.15	Mwamahunga	-4.91194	29.59833
KHD5	M	EctspN	22.06.15	Mwamahunga	-4.91194	29.59833
KHD6	F	EctspN	22.06.15	Mwamahunga	-4.91194	29.59833
KHD7	F	EctspN	22.06.15	Mwamahunga	-4.91194	29.59833
KHD8	F	EctspN	22.06.15	Mwamahunga	-4.91194	29.59833
KHD9	F	Trodub	22.06.15	Mwamahunga	-4.91194	29.59833
KHE1	M	Trodub	22.06.15	Mwamahunga	-4.91194	29.59833
KHE2	F	Trodub	22.06.15	Mwamahunga	-4.91194	29.59833
KHE3	F	Pscmrg	22.06.15	Mwamahunga	-4.91194	29.59833
KHE4	M	Pscmrg	22.06.15	Mwamahunga	-4.91194	29.59833
KHE5	M	Pscmrg	22.06.15	Mwamahunga	-4.91194	29.59833
KHE6	M	JulreK	23.06.15	Nondwa Point	-4.86417	29.60722
KHE7	F	JulreK	23.06.15	Nondwa Point	-4.86417	29.60722
KHE8	F	JulreK	23.06.15	Nondwa Point	-4.86417	29.60722
KHE9	F	JulreK	23.06.15	Nondwa Point	-4.86417	29.60722
KHF1	F	JulreK	23.06.15	Nondwa Point	-4.86417	29.60722
KHF2	F	JulreK	23.06.15	Nondwa Point	-4.86417	29.60722
KHF3	F	JulreK	23.06.15	Nondwa Point	-4.86417	29.60722
KHF6	F	Trodub	23.06.15	Nondwa Point	-4.86417	29.60722
KHF7	F	Trodub	23.06.15	Nondwa Point	-4.86417	29.60722
KHF8	F	Trodub	23.06.15	Nondwa Point	-4.86417	29.60722
KHF9	M	Trodub	23.06.15	Nondwa Point	-4.86417	29.60722
KHG1	M	Trodub	23.06.15	Nondwa Point	-4.86417	29.60722
KHG2	M	Calmel	23.06.15	George's Place	-4.88500	29.62083
KHG3	NA	Pscmrg	23.06.15	George's Place	-4.88500	29.62083
KHG4	NA	Pscmrg	23.06.15	George's Place	-4.88500	29.62083
KHI1	M	Cphfro	23.06.15	Nondwa Point	-4.86417	29.60722
KHI2	M	Cphfro	23.06.15	Nondwa Point	-4.86417	29.60722
KHI3	F	JulreK	24.06.15	Kaku	-4.89639	29.61167
KHI4	M	JulreK	24.06.15	Kaku	-4.89639	29.61167
KHI5	M	Lamspe	24.06.15	Kaku	-4.89639	29.61167
KHI6	M	Lamspe	24.06.15	Kaku	-4.89639	29.61167
KHI7	F	Trodub	24.06.15	Kaku	-4.89639	29.61167
KYA1	M	Neonig	10.07.15	Nondwa Point	-4.86417	29.60722
KYA2	M	Neonig	10.07.15	Nondwa Point	-4.86417	29.60722
KYA3	M	Neonig	11.07.15	Kananiye	-4.79417	29.59944
KYA4	M	Neonig	11.07.15	Kananiye	-4.79417	29.59944
KYA5	F	Neonig	11.07.15	Kananiye	-4.79417	29.59944
KYA6	F	Neonig	11.07.15	Kananiye	-4.79417	29.59944
KYA7	F	Neonig	11.07.15	Kananiye	-4.79417	29.59944
KYA8	M	Neonig	11.07.15	Kananiye	-4.79417	29.59944

ID	Sex	SpeciesID	CollectionDate	CollectionLocation	latitude	longitude
KYA9	M	Neonig	11.07.15	Kananiye	-4.79417	29.59944
KYB1	F	Neonig	11.07.15	Kananiye	-4.79417	29.59944
KYB2	M	Telbif	12.07.15	Nondwa Point	-4.86417	29.60722
KYB3	M	Telbif	12.07.15	Nondwa Point	-4.86417	29.60722
KYB4	F	Cphfro	12.07.15	Nondwa Point	-4.86417	29.60722
KYB5	F	Cphfro	12.07.15	Nondwa Point	-4.86417	29.60722
KYB6	F	Cphfro	12.07.15	Nondwa Point	-4.86417	29.60722
KYB7	M	Telbif	12.07.15	Nondwa Point	-4.86417	29.60722
KYB8	F	Telbif	12.07.15	Nondwa Point	-4.86417	29.60722
KYB9	M	Neobou	13.07.15	Ujiji Fishmarket	-4.90442	29.66911
KYC2	M	Neobou	13.07.15	Ujiji Fishmarket	-4.90442	29.66911
KYC3	M	Neobou	13.07.15	Ujiji Fishmarket	-4.90442	29.66911
KYC4	M	Neobou	13.07.15	Ujiji Fishmarket	-4.90442	29.66911
KYC5	M	Neobou	13.07.15	Ujiji Fishmarket	-4.90442	29.66911
KYC6	M	Neobou	13.07.15	Ujiji Fishmarket	-4.90442	29.66911
KYC7	M	Neobou	13.07.15	Ujiji Fishmarket	-4.90442	29.66911
KYC8	F	Batfas	13.07.15	Ujiji Fishmarket	-4.90442	29.66911
KYC9	F	Batfas	13.07.15	Ujiji Fishmarket	-4.90442	29.66911
KYD1	M	Batfas	13.07.15	Ujiji Fishmarket	-4.90442	29.66911
KYE2	M	Ortred	16.07.15	Malagarasi 2 (Uvinza)	-5.10944	30.39361
KYE7	M	Ortuvi	16.07.15	Malagarasi 2 (Uvinza)	-5.10944	30.39361
KYG1	M	Astpal	16.07.15	Malagarasi 2 (Uvinza)	-5.10944	30.39361
KYH4	F	Oremal	17.07.15	Malagarasi 2 (Uvinza)	-5.10944	30.39361
LBA1	F	JulmaS	31.07.15	Toby's Place	-8.62322	31.20044
LBA2	F	JulmaS	31.07.15	Toby's Place	-8.62322	31.20044
LBA3	F	JulmaS	31.07.15	Toby's Place	-8.62322	31.20044
LBA4	F	JulmaS	31.07.15	Toby's Place	-8.62322	31.20044
LBA5	M	JulmaS	31.07.15	Toby's Place	-8.62322	31.20044
LBA6	F	Neocyl	01.08.15	Toby's Place	-8.62322	31.20044
LBA7	M	JulmaS	01.08.15	Toby's Place	-8.62322	31.20044
LBA8	F	JulmaS	01.08.15	Toby's Place	-8.62322	31.20044
LBA9	F	Pleela	01.08.15	Chipwa Fishermen	-8.60617	31.18611
LBB2	F	Batleo	01.08.15	Chipwa Fishermen	-8.60617	31.18611
LBB3	M	Batvit	01.08.15	Chipwa Fishermen	-8.60617	31.18611
LBB4	F	Batvit	01.08.15	Chipwa Fishermen	-8.60617	31.18611
LBB5	M	Hemste	01.08.15	Chipwa Fishermen	-8.60617	31.18611
LBB6	F	Hemste	01.08.15	Chipwa Fishermen	-8.60617	31.18611
LBB7	F	Hemste	01.08.15	Chipwa Fishermen	-8.60617	31.18611
LBC1	F	Tremac	01.08.15	Chipwa Fishermen	-8.60617	31.18611
LBC2	F	Xensim	01.08.15	Chipwa Fishermen	-8.60617	31.18611
LBC3	NA	Xchhec	01.08.15	Chipwa Fishermen	-8.60617	31.18611
LBC4	NA	Perecc	01.08.15	Chipwa Fishermen	-8.60617	31.18611
LBC5	M	Neocyl	02.08.15	Toby's Place	-8.62322	31.20044
LBC6	M	Neocyl	02.08.15	Toby's Place	-8.62322	31.20044
LBC7	F	Neocyl	02.08.15	Toby's Place	-8.62322	31.20044
LBC8	M	Neocyl	02.08.15	Toby's Place	-8.62322	31.20044
LBC9	M	Neocyl	02.08.15	Toby's Place	-8.62322	31.20044
LBD1	F	JulmaS	02.08.15	Toby's Place	-8.62322	31.20044
LBD2	F	Neocyl	02.08.15	Toby's Place	-8.62322	31.20044
LBD3	M	Batvit	02.08.15	Chipwa Fishermen	-8.60617	31.18611
LBD4	M	Xchhec	02.08.15	Chipwa Fishermen	-8.60617	31.18611
LBD5	F	Hemste	02.08.15	Chipwa Fishermen	-8.60617	31.18611
LBD6	F	Hemste	02.08.15	Chipwa Fishermen	-8.60617	31.18611
LBD8	M	Tremar	02.08.15	Chipwa Fishermen	-8.60617	31.18611
LBD9	M	Trenig	02.08.15	Chipwa Fishermen	-8.60617	31.18611
LBE1	F	Trenig	02.08.15	Chipwa Fishermen	-8.60617	31.18611
LBE2	M	Xensim	02.08.15	Chipwa Fishermen	-8.60617	31.18611
LBE3	M	Xensim	02.08.15	Chipwa Fishermen	-8.60617	31.18611
LBE4	M	Xensim	02.08.15	Chipwa Fishermen	-8.60617	31.18611
LBE5	M	Xensim	02.08.15	Chipwa Fishermen	-8.60617	31.18611
LBE6	M	Xensim	02.08.15	Chipwa Fishermen	-8.60617	31.18611
LBE9	F	Xensim	02.08.15	Chipwa Fishermen	-8.60617	31.18611
LBF1	F	Xensim	02.08.15	Chipwa Fishermen	-8.60617	31.18611
LBF2	F	Xensim	02.08.15	Chipwa Fishermen	-8.60617	31.18611
LBF3	M	JulmaS	03.08.15	Toby's Place	-8.62322	31.20044
LBF4	F	Baicen	04.08.15	Chipwa Fishermen	-8.60617	31.18611
LBF5	M	Baicen	04.08.15	Chipwa Fishermen	-8.60617	31.18611
LBF6	F	Plemul	04.08.15	Chipwa Fishermen	-8.60617	31.18611
LBF7	F	TeldhS	04.08.15	Lunzua Lake / Kapata	-8.74920	31.17274
LBF8	M	TeldhS	04.08.15	Lunzua Lake / Kapata	-8.74920	31.17274
LBF9	M	Neopro	29.07.15	Mpulungu Fishmarket	-8.76047	31.11219
LBG1	F	Neopro	29.07.15	Mpulungu Fishmarket	-8.76047	31.11219
LBG2	M	Perecc	04.08.15	Chipwa Fishermen	-8.60617	31.18611
LBG3	M	XenniS	06.08.15	Chituta	-8.72361	31.15000
LBG4	M	XenniS	06.08.15	Chituta	-8.72361	31.15000
LBG5	M	XenniS	06.08.15	Chituta	-8.72361	31.15000
LBG6	F	XenniS	06.08.15	Chituta	-8.72361	31.15000
LBG7	F	XenniS	06.08.15	Chituta	-8.72361	31.15000
LBG8	M	XenniS	06.08.15	Chituta	-8.72361	31.15000
LBH1	M	XenniS	06.08.15	Chituta	-8.72361	31.15000
LBH2	F	XenniS	06.08.15	Chituta	-8.72361	31.15000
LBH3	M	XenniS	06.08.15	Chituta	-8.72361	31.15000
LBI5	M	Cypzon	06.08.15	Chituta	-8.72361	31.15000
LBI6	F	Cypzon	06.08.15	Chituta	-8.72361	31.15000
LBI7	M	Cypzon	06.08.15	Chituta	-8.72361	31.15000
LBI8	M	Cypzon	06.08.15	Chituta	-8.72361	31.15000
LBI9	M	Cypzon	06.08.15	Chituta	-8.72361	31.15000
LCA1	M	Neolou	01.07.15	Kalila Nkwasi	-6.26056	29.73667
LCA2	F	Neolou	01.07.15	Kalila Nkwasi	-6.26056	29.73667
LCA3	M	Neolou	01.07.15	Kalila Nkwasi	-6.26056	29.73667
LCA4	M	Neolou	01.07.15	Kalila Nkwasi	-6.26056	29.73667
LCA5	M	Neolou	01.07.15	Kalila Nkwasi	-6.26056	29.73667
LCA6	M	Neolou	01.07.15	Kalila Nkwasi	-6.26056	29.73667
LCA7	M	Neolou	01.07.15	Kalila Nkwasi	-6.26056	29.73667
LCA8	M	Neolou	01.07.15	Kalila Nkwasi	-6.26056	29.73667
LCA9	M	Neolou	01.07.15	Kalila Nkwasi	-6.26056	29.73667
LCB1	F	Neolou	01.07.15	Kalila Nkwasi	-6.26056	29.73667
LCB2	M	Neolou	01.07.15	Kalila Nkwasi	-6.26056	29.73667
LCB3	NA	Neolou	01.07.15	Kalila Nkwasi	-6.26056	29.73667
LCB4	M	NeogrM	01.07.15	Kalila Nkwasi	-6.26056	29.73667
LCB5	F	NeofaM	01.07.15	Kalila Nkwasi	-6.26056	29.73667
LCB6	M	NeofaM	01.07.15	Kalila Nkwasi	-6.26056	29.73667
LCB7	M	NeofaM	01.07.15	Kalila Nkwasi	-6.26056	29.73667
LCB8	M	NeofaM	01.07.15	Kalila Nkwasi	-6.26056	29.73667
LCB9	M	NeogrM	01.07.15	Kalila Nkwasi	-6.26056	29.73667
LCC1	M	NeofaM	01.07.15	Kalila Nkwasi	-6.26056	29.73667

ID	Sex	SpeciesID	CollectionDate	CollectionLocation	latitude	longitude
LCC2	M	NeofaM	01.07.15	Kalila Nkwasi	-6.26056	29.73667
LCC3	F	NeogrM	01.07.15	Kalila Nkwasi	-6.26056	29.73667
LCC4	M	NeofaM	01.07.15	Kalila Nkwasi	-6.26056	29.73667
LCC5	F	NeofaM	01.07.15	Kalila Nkwasi	-6.26056	29.73667
LCC6	F	NeogrM	01.07.15	Kalila Nkwasi	-6.26056	29.73667
LCC7	M	NeogrM	01.07.15	Kalila Nkwasi	-6.26056	29.73667
LCC8	F	NeogrM	01.07.15	Kalila Nkwasi	-6.26056	29.73667
LCC9	F	NeogrM	01.07.15	Kalila Nkwasi	-6.26056	29.73667
LCD1	M	Petred	01.07.15	Kalila Nkwasi	-6.26056	29.73667
LCD2	M	Petred	01.07.15	Kalila Nkwasi	-6.26056	29.73667
LCD3	M	Petred	01.07.15	Kalila Nkwasi	-6.26056	29.73667
LCD4	M	Petred	01.07.15	Kalila Nkwasi	-6.26056	29.73667
LCD5	F	Petred	01.07.15	Kalila Nkwasi	-6.26056	29.73667
LCD6	M	Batfer	02.07.15	Nganja	-6.17333	29.74028
LCD7	F	Batfer	02.07.15	Nganja	-6.17333	29.74028
LCD8	M	Batfer	02.07.15	Nganja	-6.17333	29.74028
LCD9	F	Batfer	02.07.15	Nganja	-6.17333	29.74028
LCE1	M	Batfer	02.07.15	Nganja	-6.17333	29.74028
LCE2	F	Batfer	02.07.15	Nganja	-6.17333	29.74028
LCE3	F	Batfer	02.07.15	Nganja	-6.17333	29.74028
LCE4	F	Batfer	02.07.15	Nganja	-6.17333	29.74028
LCE5	M	Batfer	02.07.15	Nganja	-6.17333	29.74028
LCE6	NA	Batfer	02.07.15	Nganja	-6.17333	29.74028
LCE7	F	Petred	02.07.15	Nganja	-6.17333	29.74028
LCE8	F	Petred	02.07.15	Nganja	-6.17333	29.74028
LCE9	M	Petred	02.07.15	Nganja	-6.17333	29.74028
LCF1	M	Trokir	02.07.15	Nganja	-6.17333	29.74028
LCF2	M	Trokir	02.07.15	Nganja	-6.17333	29.74028
LCF3	F	Trokir	02.07.15	Nganja	-6.17333	29.74028
LCF4	F	Trokir	02.07.15	Nganja	-6.17333	29.74028
LCF5	M	Trokir	02.07.15	Nganja	-6.17333	29.74028
LCF6	M	Petmos	02.07.15	Nganja	-6.17333	29.74028
LCF7	M	Petmos	02.07.15	Nganja	-6.17333	29.74028
LCF8	F	Petmos	02.07.15	Nganja	-6.17333	29.74028
LCF9	F	Petmos	02.07.15	Nganja	-6.17333	29.74028
LCG1	M	Petmos	02.07.15	Nganja	-6.17333	29.74028
LCG2	F	Petmos	02.07.15	Nganja	-6.17333	29.74028
LCG3	F	Petmos	02.07.15	Nganja	-6.17333	29.74028
LCG4	F	Petmos	02.07.15	Nganja	-6.17333	29.74028
LCG5	F	Petmos	02.07.15	Nganja	-6.17333	29.74028
LCG6	F	Petmos	02.07.15	Nganja	-6.17333	29.74028
LCG7	F	Leppro	04.07.15	Storo 1	-6.01000	29.75861
LCH5	M	Plemul	05.07.15	Mugambo Fishermen	-5.97608	29.83944
LCH6	M	Plemul	05.07.15	Mugambo Fishermen	-5.97608	29.83944
LCH7	M	Plemul	05.07.15	Mugambo Fishermen	-5.97608	29.83944
LCH8	M	Trolun	07.07.15	Kabogo 2	-5.47694	29.76000
LCI9	F	Leppro	07.07.15	Cape Kabogo	-5.46083	29.74750
LDA1	M	Cypzon	06.08.15	Chituta	-8.72361	31.15000
LDA2	F	Cypzon	06.08.15	Chituta	-8.72361	31.15000
LDA3	F	Cypzon	06.08.15	Chituta	-8.72361	31.15000
LDA4	M	Petmac	06.08.15	Chituta	-8.72361	31.15000
LDA5	M	Petmac	06.08.15	Chituta	-8.72361	31.15000
LDA6	M	Petmac	06.08.15	Chituta	-8.72361	31.15000
LDA7	M	Bentri	07.08.15	Chipwa Fishermen	-8.60617	31.18611
LDA8	M	Bentri	07.08.15	Chipwa Fishermen	-8.60617	31.18611
LDA9	F	Bentri	07.08.15	Chipwa Fishermen	-8.60617	31.18611
LDB2	M	Bentri	07.08.15	Chipwa Fishermen	-8.60617	31.18611
LDB3	M	Bentri	07.08.15	Chipwa Fishermen	-8.60617	31.18611
LDB4	M	Bentri	07.08.15	Chipwa Fishermen	-8.60617	31.18611
LDB5	M	Bentri	07.08.15	Chipwa Fishermen	-8.60617	31.18611
LDB6	M	Bentri	07.08.15	Chipwa Fishermen	-8.60617	31.18611
LDB7	M	Bentri	07.08.15	Chipwa Fishermen	-8.60617	31.18611
LDB8	F	Bentri	07.08.15	Chipwa Fishermen	-8.60617	31.18611
LDB9	F	Neopro	07.08.15	Toby's Place	-8.62322	31.20044
LDC1	F	Neopro	07.08.15	Toby's Place	-8.62322	31.20044
LDC2	M	Neopro	07.08.15	Toby's Place	-8.62322	31.20044
LDC3	M	Petmac	08.08.15	Isanga	-8.65456	31.19183
LDC4	M	Petmac	08.08.15	Isanga	-8.65456	31.19183
LDC5	M	Petmac	08.08.15	Isanga	-8.65456	31.19183
LDC6	M	Petgia	12.08.15	Fulwe	-7.95500	30.82250
LDC7	M	Petgia	12.08.15	Fulwe	-7.95500	30.82250
LDC8	M	Petgia	12.08.15	Fulwe	-7.95500	30.82250
LDC9	M	Petgia	12.08.15	Fulwe	-7.95500	30.82250
LDD1	M	Lepmim	12.08.15	Fulwe	-7.95500	30.82250
LDD2	M	Lepmim	12.08.15	Fulwe	-7.95500	30.82250
LDD3	M	Lepmim	12.08.15	Fulwe	-7.95500	30.82250
LDD4	M	Lepmim	12.08.15	Fulwe	-7.95500	30.82250
LDD5	M	Lepmim	12.08.15	Fulwe	-7.95500	30.82250
LDD6	F	Lepmim	12.08.15	Fulwe	-7.95500	30.82250
LDD7	M	Chacya	12.08.15	Fulwe	-7.95500	30.82250
LDD8	M	Chacya	12.08.15	Fulwe	-7.95500	30.82250
LDD9	F	Chabif	12.08.15	Fulwe	-7.95500	30.82250
LDE1	M	Chabif	12.08.15	Fulwe	-7.95500	30.82250
LDE2	F	Chabif	12.08.15	Fulwe	-7.95500	30.82250
LDE3	M	Petkip	12.08.15	Fulwe	-7.95500	30.82250
LDE4	F	Petkip	12.08.15	Fulwe	-7.95500	30.82250
LDE5	F	Petkip	12.08.15	Fulwe	-7.95500	30.82250
LDE6	F	Petkip	12.08.15	Fulwe	-7.95500	30.82250
LDE7	M	Petkip	12.08.15	Fulwe	-7.95500	30.82250
LDE8	F	Chacya	13.08.15	Twiyu	-7.58194	30.62833
LDE9	M	Neocyg	13.08.15	Twiyu	-7.58194	30.62833
LDF1	F	Neotim	13.08.15	Twiyu	-7.58194	30.62833
LDF2	F	Neotim	13.08.15	Twiyu	-7.58194	30.62833
LDF3	M	Neotim	13.08.15	Twiyu	-7.58194	30.62833
LDF4	F	NeofuU	13.08.15	Twiyu	-7.58194	30.62833
LDF5	M	NeofuU	13.08.15	Twiyu	-7.58194	30.62833
LDF6	F	NeofuU	13.08.15	Twiyu	-7.58194	30.62833
LDF7	M	NeofuU	13.08.15	Twiyu	-7.58194	30.62833
LDF8	F	NeofuU	13.08.15	Twiyu	-7.58194	30.62833
LDF9	F	NeofuU	13.08.15	Twiyu	-7.58194	30.62833
LDG1	F	NeofuU	13.08.15	Twiyu	-7.58194	30.62833
LDG2	M	NeocaK	13.08.15	Twiyu	-7.58194	30.62833
LDG3	F	NeocaK	13.08.15	Twiyu	-7.58194	30.62833
LDG4	F	NeocaK	13.08.15	Twiyu	-7.58194	30.62833
LDG5	F	NeocaK	13.08.15	Twiyu	-7.58194	30.62833
LDG6	M	NeocaK	13.08.15	Twiyu	-7.58194	30.62833

ID	Sex	SpeciesID	CollectionDate	CollectionLocation	latitude	longitude
LDG7	F	NeocaK	13.08.15	Twiyu	-7.58194	30.62833
LDG8	F	NeocaK	13.08.15	Twiyu	-7.58194	30.62833
LDG9	M	NeocaK	13.08.15	Twiyu	-7.58194	30.62833
LDH1	F	NeocaK	13.08.15	Twiyu	-7.58194	30.62833
LDH2	M	NeocaK	13.08.15	Twiyu	-7.58194	30.62833
LDH3	M	Lepmim	13.08.15	Twiyu	-7.58194	30.62833
LDH4	F	Chabif	13.08.15	Twiyu	-7.58194	30.62833
LDH5	M	Chabif	13.08.15	Twiyu	-7.58194	30.62833
LDH6	M	Chabif	13.08.15	Twiyu	-7.58194	30.62833
LDH7	M	Chabif	13.08.15	Twiyu	-7.58194	30.62833
LDH8	F	Petkip	13.08.15	Twiyu	-7.58194	30.62833
LDH9	F	Chabif	14.08.15	Korongwe	-7.13694	30.50778
LDI1	F	Chabif	14.08.15	Korongwe	-7.13694	30.50778
LDI2	M	Chabif	14.08.15	Korongwe	-7.13694	30.50778
LDI3	F	Neocyg	14.08.15	Korongwe	-7.13694	30.50778
LDI4	M	Julmrk	14.08.15	Korongwe	-7.13694	30.50778
LDI5	M	Trompi	14.08.15	Korongwe	-7.13694	30.50778
LDI6	M	Trompi	14.08.15	Korongwe	-7.13694	30.50778
LDI7	F	Trompi	14.08.15	Korongwe	-7.13694	30.50778
LDI8	F	Trompi	14.08.15	Korongwe	-7.13694	30.50778
LDI9	F	Trompi	14.08.15	Korongwe	-7.13694	30.50778
LEA1	M	Plepar	27.06.15	Karilani Island	-6.02056	29.74250
LEA2	M	Plepar	27.06.15	Karilani Island	-6.02056	29.74250
LEA3	M	XenspN	27.06.15	Karilani Island	-6.02056	29.74250
LEA4	F	XenspN	27.06.15	Karilani Island	-6.02056	29.74250
LEA5	M?	XenspN	27.06.15	Karilani Island	-6.02056	29.74250
LEA6	F?	XenspN	27.06.15	Karilani Island	-6.02056	29.74250
LEA7	F?	XenspN	27.06.15	Karilani Island	-6.02056	29.74250
LEA8	M?	XenspN	27.06.15	Karilani Island	-6.02056	29.74250
LEA9	M?	XenspN	27.06.15	Karilani Island	-6.02056	29.74250
LEB1	F?	XenspN	27.06.15	Karilani Island	-6.02056	29.74250
LEB2	F?	XenspN	27.06.15	Karilani Island	-6.02056	29.74250
LEB3	M?	XenspN	27.06.15	Karilani Island	-6.02056	29.74250
LEC6	NA	Plepar	27.06.15	Karilani Island	-6.02056	29.74250
LEC7	F	Plepar	28.06.15	Bulu Fishermen	-6.01797	29.73881
LEC8	F	Plepar	28.06.15	Bulu Fishermen	-6.01797	29.73881
LEC9	M	Neoleu	28.06.15	Bulu Point	-6.01611	29.74639
LED1	M	Neoleu	28.06.15	Bulu Point	-6.01611	29.74639
LED3	M	Neoleu	28.06.15	Bulu Point	-6.01611	29.74639
LED4	M	Telbif	29.06.15	Storo bay	-6.01694	29.74944
LED5	M	Telbif	29.06.15	Storo bay	-6.01694	29.74944
LED6	M	Telbif	29.06.15	Storo bay	-6.01694	29.74944
LED7	M	Telbif	29.06.15	Storo bay	-6.01694	29.74944
LED8	M	Telbif	29.06.15	Storo bay	-6.01694	29.74944
LEE1	F	Neoleu	29.06.15	Bulu Point	-6.01611	29.74639
LEE4	NA	Telbif	30.06.15	Storo bay	-6.01694	29.74944
LEE5	NA	Telbif	30.06.15	Storo bay	-6.01694	29.74944
LEE6	NA	Telbif	30.06.15	Storo bay	-6.01694	29.74944
LEE7	NA	Leppro	30.06.15	Storo bay	-6.01694	29.74944
LEE8	M	Neoleu	01.07.15	Kalila Nkwasi	-6.26056	29.73667
LEE9	F	Neoleu	01.07.15	Kalila Nkwasi	-6.26056	29.73667
LEF1	F	Neoleu	01.07.15	Kalila Nkwasi	-6.26056	29.73667
LEF2	M	BenhoM	02.07.15	Nganja	-6.17333	29.74028
LEF3	M	Trokir	02.07.15	Nganja	-6.17333	29.74028
LEF4	M	Trokir	02.07.15	Nganja	-6.17333	29.74028
LEF5	F	Trokir	02.07.15	Nganja	-6.17333	29.74028
LEF6	M	Trokir	02.07.15	Nganja	-6.17333	29.74028
LEF7	F	Trokir	02.07.15	Nganja	-6.17333	29.74028
LEF8	M	Tropol	05.07.15	Storo 1	-6.01000	29.75861
LEF9	F	Tropol	05.07.15	Storo 1	-6.01000	29.75861
LEG1	M	Tropol	05.07.15	Storo 1	-6.01000	29.75861
LEG2	F	Tropol	05.07.15	Storo 1	-6.01000	29.75861
LEG3	F	Tropol	05.07.15	Storo 1	-6.01000	29.75861
LEG4	F	Tropol	05.07.15	Storo 1	-6.01000	29.75861
LEG5	F	Tropol	05.07.15	Storo 1	-6.01000	29.75861
LEG6	F	Tropol	05.07.15	Storo 1	-6.01000	29.75861
LEG7	F	Tropol	05.07.15	Storo 1	-6.01000	29.75861
LEG8	F	Tropol	05.07.15	Storo 1	-6.01000	29.75861
LEG9	M	Tropol	05.07.15	Storo 1	-6.01000	29.75861
LEH1	F	Tropol	05.07.15	Storo 1	-6.01000	29.75861
LEH2	M	Neodev	08.07.15	Malagarasi 1 (Kigoma)	-5.21194	29.84222
LEI1	F	Pscmrg	10.07.15	Kalalangabo	-4.84361	29.60944
LEI2	F	Pscmrg	10.07.15	Kalalangabo	-4.84361	29.60944
LEI3	F	Pscmrg	10.07.15	Kalalangabo	-4.84361	29.60944
LEI5	M	Cphfro	10.07.15	Kalalangabo	-4.84361	29.60944
LEI6	F	Cphfro	10.07.15	Nondwa Point	-4.86417	29.60722
LEI7	F	Cphfro	10.07.15	Nondwa Point	-4.86417	29.60722
LEI8	F	Cphfro	10.07.15	Nondwa Point	-4.86417	29.60722
LEI9	M	Cphfro	10.07.15	Nondwa Point	-4.86417	29.60722
LFA1	M	Trompi	14.08.15	Korongwe	-7.13694	30.50778
LFA2	F	Trompi	14.08.15	Korongwe	-7.13694	30.50778
LFA3	F	Trompi	14.08.15	Korongwe	-7.13694	30.50778
LFA4	M	Trompi	14.08.15	Korongwe	-7.13694	30.50778
LFA5	M	Trompi	14.08.15	Korongwe	-7.13694	30.50778
LFA6	M	Petiko	14.08.15	Korongwe	-7.13694	30.50778
LFA7	M	Petiko	14.08.15	Korongwe	-7.13694	30.50778
LFA8	F	Petiko	14.08.15	Korongwe	-7.13694	30.50778
LFA9	F	Petiko	14.08.15	Korongwe	-7.13694	30.50778
LFB1	F	Petiko	14.08.15	Msalaba	-7.11667	30.49778
LFB2	M	Petiko	14.08.15	Msalaba	-7.11667	30.49778
LFB3	F	Petiko	14.08.15	Msalaba	-7.11667	30.49778
LFB4	F	Petiko	14.08.15	Msalaba	-7.11667	30.49778
LFB5	M	Petiko	14.08.15	Msalaba	-7.11667	30.49778
LFB6	M	Petiko	14.08.15	Msalaba	-7.11667	30.49778
LFB7	M	Neoese	14.08.15	Msalaba	-7.11667	30.49778
LFB8	M	Neoese	14.08.15	Msalaba	-7.11667	30.49778
LFB9	F	Neoese	14.08.15	Msalaba	-7.11667	30.49778
LFC1	F	Neoese	14.08.15	Msalaba	-7.11667	30.49778
LFC2	F	Neoese	14.08.15	Msalaba	-7.11667	30.49778
LFC3	F	Neoese	14.08.15	Msalaba	-7.11667	30.49778
LFC4	M	Neoese	14.08.15	Msalaba	-7.11667	30.49778
LFC5	M	Neoese	14.08.15	Msalaba	-7.11667	30.49778
LFC6	M	Neoese	14.08.15	Msalaba	-7.11667	30.49778
LFC7	M	Neoese	14.08.15	Msalaba	-7.11667	30.49778
LFC8	M	Neocyg	14.08.15	Msalaba	-7.11667	30.49778
LFC9	M	Trezeb	15.08.15	Korongwe	-7.13694	30.50778

ID	Sex	SpeciesID	CollectionDate	CollectionLocation	latitude	longitude
LFD2	M	Neocyg	15.08.15	Korongwe	-7.13694	30.50778
LFD3	M	Neocyg	15.08.15	Korongwe	-7.13694	30.50778
LFD4	F	Neocyg	15.08.15	Korongwe	-7.13694	30.50778
LFD5	M	Neocyg	15.08.15	Korongwe	-7.13694	30.50778
LFD6	F	Neocyg	15.08.15	Korongwe	-7.13694	30.50778
LFD7	M	Neocyg	15.08.15	Korongwe	-7.13694	30.50778
LFD8	F	Neocyg	15.08.15	Korongwe	-7.13694	30.50778
LFE4	F	Trezeb	15.08.15	Korongwe	-7.13694	30.50778
LFE5	F	Trezeb	15.08.15	Korongwe	-7.13694	30.50778
LFE6	F	Trezeb	15.08.15	Korongwe	-7.13694	30.50778
LFE7	F	Trezeb	15.08.15	Korongwe	-7.13694	30.50778
LFE8	F	Trezeb	15.08.15	Korongwe	-7.13694	30.50778
LFE9	F	Trezeb	15.08.15	Korongwe	-7.13694	30.50778
LFF2	F	Trezeb	15.08.15	Korongwe	-7.13694	30.50778
LFF3	F	Trezeb	15.08.15	Korongwe	-7.13694	30.50778
LFF5	M	Trezeb	15.08.15	Korongwe	-7.13694	30.50778
LFF6	F	Julmrk	15.08.15	Korongwe	-7.13694	30.50778
LFF7	M	Lepkam	16.08.15	Kamamba Island	-7.39750	30.55417
LFF8	F	Lepkam	16.08.15	Kamamba Island	-7.39750	30.55417
LFF9	M	Lepkam	16.08.15	Kamamba Island	-7.39750	30.55417
LFG1	F	Lepkam	16.08.15	Kamamba Island	-7.39750	30.55417
LFG2	F	Lepkam	16.08.15	Kamamba Island	-7.39750	30.55417
LFG3	F	Lepkam	16.08.15	Kamamba Island	-7.39750	30.55417
LFG4	M	Lepkam	16.08.15	Kamamba Island	-7.39750	30.55417
LFG5	M	Lepkam	16.08.15	Kamamba Island	-7.39750	30.55417
LFG6	F	Lepkam	16.08.15	Kamamba Island	-7.39750	30.55417
LFG7	M	Lepkam	16.08.15	Kamamba Island	-7.39750	30.55417
LFG8	M	Julmrk	16.08.15	Kamamba Island	-7.39750	30.55417
LFG9	M	Julmrk	16.08.15	Kamamba Island	-7.39750	30.55417
LFH1	F	Julmrk	16.08.15	Kamamba Island	-7.39750	30.55417
LFH2	F	Julmrk	16.08.15	Kamamba Island	-7.39750	30.55417
LFH3	M	Julmrk	16.08.15	Kamamba Island	-7.39750	30.55417
LFH4	M	Julmrk	16.08.15	Kamamba Island	-7.39750	30.55417
LFH5	M	Julmrk	16.08.15	Kamamba Island	-7.39750	30.55417
LFH6	M	Pettex	17.08.15	Nkondwe	-7.37889	30.54611
LFH7	M	Pettex	17.08.15	Nkondwe	-7.37889	30.54611
LFH8	F	Julmrk	17.08.15	Nkondwe	-7.37889	30.54611
LFH9	F	TrobrK	17.08.15	Nkondwe	-7.37889	30.54611
LFI1	M	TrobrK	17.08.15	Nkondwe	-7.37889	30.54611
LFI2	M	Pettex	17.08.15	Nkondwe	-7.37889	30.54611
LFI3	M	Pettex	17.08.15	Nkondwe	-7.37889	30.54611
LFI4	M	Ophboo	17.08.15	Nkondwe	-7.37889	30.54611
LFI5	M	Ophboo	17.08.15	Nkondwe	-7.37889	30.54611
LFI6	F	Ophboo	17.08.15	Nkondwe	-7.37889	30.54611
LFI7	F	Ophboo	17.08.15	Nkondwe	-7.37889	30.54611
LFI8	M	Ophboo	17.08.15	Nkondwe	-7.37889	30.54611
LFI9	M	Ophboo	17.08.15	Nkondwe	-7.37889	30.54611
LGA1	M	Ophboo	17.08.15	Nkondwe	-7.37889	30.54611
LGA2	M	Ophboo	17.08.15	Nkondwe	-7.37889	30.54611
LGA3	F	Ophboo	17.08.15	Nkondwe	-7.37889	30.54611
LGA4	F	Ophboo	17.08.15	Nkondwe	-7.37889	30.54611
LGA5	M	TrobrK	17.08.15	Nkondwe	-7.37889	30.54611
LGA6	F	TrobrK	17.08.15	Nkondwe	-7.37889	30.54611
LGA7	F	TrobrK	17.08.15	Nkondwe	-7.37889	30.54611
LGA8	F	TrobrK	17.08.15	Nkondwe	-7.37889	30.54611
LGA9	F	TrobrK	17.08.15	Nkondwe	-7.37889	30.54611
LGB1	M	TrobrK	17.08.15	Nkondwe	-7.37889	30.54611
LGB2	M	TrobrK	17.08.15	Nkondwe	-7.37889	30.54611
LGB3	F	TrobrK	17.08.15	Nkondwe	-7.37889	30.54611
LGB4	F	Petkip	17.08.15	Nkondwe	-7.37889	30.54611
LGB5	M	Petrai	17.08.15	Nkondwe	-7.37889	30.54611
LGB6	M	Petrai	17.08.15	Nkondwe	-7.37889	30.54611
LGB7	M	Petrai	17.08.15	Nkondwe	-7.37889	30.54611
LGB8	F	Petrai	17.08.15	Nkondwe	-7.37889	30.54611
LGB9	M	Petrai	17.08.15	Nkondwe	-7.37889	30.54611
LGC1	M	Petrai	17.08.15	Nkondwe	-7.37889	30.54611
LGC2	F	Petrai	17.08.15	Nkondwe	-7.37889	30.54611
LGC3	M	Petrai	17.08.15	Nkondwe	-7.37889	30.54611
LGC4	M	Petrai	17.08.15	Nkondwe	-7.37889	30.54611
LGC5	F	Petrai	17.08.15	Nkondwe	-7.37889	30.54611
LGC7	M	Chacya	18.08.15	Mvuna Island	-7.44417	30.54389
LGC8	M	Chacya	18.08.15	Mvuna Island	-7.44417	30.54389
LGC9	F	Leppro	18.08.15	Mvuna Island	-7.44417	30.54389
LGD1	F	Leppro	18.08.15	Mvuna Island	-7.44417	30.54389
LGD2	M	Petkip	18.08.15	Mvuna Island	-7.44417	30.54389
LGD3	F	Petkip	18.08.15	Mvuna Island	-7.44417	30.54389
LGD4	M	Petkip	18.08.15	Mvuna Island	-7.44417	30.54389
LGD5	M	Lepmim	18.08.15	Mvuna Island	-7.44417	30.54389
LGD7	F	Oretan	18.08.15	Mvuna Island	-7.44417	30.54389
LGD8	F	Oretan	18.08.15	Mvuna Island	-7.44417	30.54389
LGD9	F	Oretan	18.08.15	Mvuna Island	-7.44417	30.54389
LGE2	M	Neotim	19.08.15	Ulwile Musi Point	-7.47889	30.57639
LGE3	F	Neotim	19.08.15	Ulwile Musi Point	-7.47889	30.57639
LGE4	F	Neotim	19.08.15	Ulwile Musi Point	-7.47889	30.57639
LGE5	F	Neotim	19.08.15	Ulwile Musi Point	-7.47889	30.57639
LGE6	F	Neotim	19.08.15	Ulwile Musi Point	-7.47889	30.57639
LGE7	F	Neotim	19.08.15	Ulwile Musi Point	-7.47889	30.57639
LGE8	F	Neotim	19.08.15	Ulwile Musi Point	-7.47889	30.57639
LGE9	NA	NeofuU	19.08.15	Ulwile Musi Point	-7.47889	30.57639
LGF1	M	NeofuU	19.08.15	Ulwile Musi Point	-7.47889	30.57639
LGF2	F	NeofuU	19.08.15	Ulwile Musi Point	-7.47889	30.57639
LGG4	M	Lepmim	19.08.15	Twiyu	-7.58194	30.62833
LGG5	M	Chacya	19.08.15	Twiyu	-7.58194	30.62833
LGG6	M	Chacya	19.08.15	Twiyu	-7.58194	30.62833
LGG7	F	Chacya	19.08.15	Twiyu	-7.58194	30.62833
LGG8	F	Chacya	19.08.15	Twiyu	-7.58194	30.62833
LGG9	F	Chacya	19.08.15	Twiyu	-7.58194	30.62833
LGH1	M	Ophwhi	19.08.15	Twiyu	-7.58194	30.62833
LGH2	M	Ophwhi	19.08.15	Twiyu	-7.58194	30.62833
LGH3	F	Ophwhi	19.08.15	Twiyu	-7.58194	30.62833
LGH4	M	Ophwhi	19.08.15	Twiyu	-7.58194	30.62833
LGH5	M	Ophwhi	19.08.15	Twiyu	-7.58194	30.62833
LGH6	M	Ophwhi	19.08.15	Twiyu	-7.58194	30.62833
LGH7	M	Ophwhi	19.08.15	Twiyu	-7.58194	30.62833
LGH8	M	Neopet	19.08.15	Twiyu	-7.58194	30.62833
LGH9	M	Neopet	19.08.15	Twiyu	-7.58194	30.62833

ID	Sex	SpeciesID	CollectionDate	CollectionLocation	latitude	longitude
LGI1	F	Neopet	19.08.15	Twiyu	-7.58194	30.62833
LGI2	F	Neopet	19.08.15	Twiyu	-7.58194	30.62833
LGI3	M	Neopet	19.08.15	Twiyu	-7.58194	30.62833
LGI4	F	Neopet	19.08.15	Twiyu	-7.58194	30.62833
LGI5	M	Neopet	19.08.15	Twiyu	-7.58194	30.62833
LGI6	F	Neopet	19.08.15	Twiyu	-7.58194	30.62833
LGI7	F	Neopet	19.08.15	Twiyu	-7.58194	30.62833
LGI8	M	Neopet	19.08.15	Twiyu	-7.58194	30.62833
LGI9	M	LepmeK	19.08.15	Twiyu	-7.58194	30.62833
LHA1	M	LepmeK	19.08.15	Twiyu	-7.58194	30.62833
LHA2	F	LepmeK	19.08.15	Twiyu	-7.58194	30.62833
LHA3	M	LepmeK	19.08.15	Twiyu	-7.58194	30.62833
LHA4	M	LepmeK	19.08.15	Twiyu	-7.58194	30.62833
LHA5	M	LepmeK	19.08.15	Twiyu	-7.58194	30.62833
LHA6	M	LepmeK	19.08.15	Twiyu	-7.58194	30.62833
LHA7	M	LepmeK	19.08.15	Twiyu	-7.58194	30.62833
LHA8	M	LepmeK	19.08.15	Twiyu	-7.58194	30.62833
LHA9	M	LepmeK	19.08.15	Twiyu	-7.58194	30.62833
LHB1	M	Pettex	20.08.15	Twiyu	-7.58194	30.62833
LHB2	M	Pettex	20.08.15	Twiyu	-7.58194	30.62833
LHB3	F	Pettex	20.08.15	Twiyu	-7.58194	30.62833
LHB4	M	Pettex	20.08.15	Twiyu	-7.58194	30.62833
LHB5	F	Pettex	20.08.15	Twiyu	-7.58194	30.62833
LHB6	M	Pettex	20.08.15	Twiyu	-7.58194	30.62833
LHB7	F	Ophwhi	20.08.15	Twiyu	-7.58194	30.62833
LHB8	M	Ophwhi	20.08.15	Twiyu	-7.58194	30.62833
LHB9	M	Ophwhi	20.08.15	Twiyu	-7.58194	30.62833
LHC1	M	TeldhT	20.08.15	Twiyu	-7.58194	30.62833
LHC2	M	TeldhT	20.08.15	Twiyu	-7.58194	30.62833
LHC3	M	TeldhT	20.08.15	Twiyu	-7.58194	30.62833
LHC4	M	TeldhT	20.08.15	Twiyu	-7.58194	30.62833
LHC5	M	TeldhT	20.08.15	Twiyu	-7.58194	30.62833
LHC6	M	TeldhT	20.08.15	Twiyu	-7.58194	30.62833
LHC7	M	TeldhT	20.08.15	Twiyu	-7.58194	30.62833
LHC8	M	TeldhT	20.08.15	Twiyu	-7.58194	30.62833
LHC9	M	TeldhT	20.08.15	Twiyu	-7.58194	30.62833
LHD1	M	TeldhT	20.08.15	Twiyu	-7.58194	30.62833
LHD2	F	Petgia	21.08.15	Fulwe	-7.95500	30.82250
LHD3	M	Petgia	21.08.15	Fulwe	-7.95500	30.82250
LHD4	F	Petgia	21.08.15	Fulwe	-7.95500	30.82250
LHD5	F	Petgia	21.08.15	Fulwe	-7.95500	30.82250
LHD6	F	Petgia	21.08.15	Fulwe	-7.95500	30.82250
LHD7	F	Petgia	21.08.15	Fulwe	-7.95500	30.82250
LHD8	M	Oretan	21.08.15	Fulwe	-7.95500	30.82250
LHD9	M	Tromor	21.08.15	Wapembwe	-7.94667	30.83761
LHE1	M	Tromor	21.08.15	Wapembwe	-7.94667	30.83761
LHE2	M	Tromor	21.08.15	Wapembwe	-7.94667	30.83761
LHE3	F	Tromor	21.08.15	Wapembwe	-7.94667	30.83761
LHE4	F	Tromor	21.08.15	Wapembwe	-7.94667	30.83761
LHE5	M	Tromor	21.08.15	Wapembwe	-7.94667	30.83761
LHE6	F	Tromor	21.08.15	Wapembwe	-7.94667	30.83761
LHE7	M	Tromor	21.08.15	Wapembwe	-7.94667	30.83761
LHE8	M	Tromor	21.08.15	Wapembwe	-7.94667	30.83761
LHE9	F	Tromor	21.08.15	Wapembwe	-7.94667	30.83761
LHF2	F	TeldhT	20.08.15	Twiyu	-7.58194	30.62833
LHF3	M	Tylpol	22.08.15	Malasa Island	-8.21194	30.94639
LHF4	F	Neobif	22.08.15	Malasa Island	-8.21194	30.94639
LHF5	M	Neobif	22.08.15	Malasa Island	-8.21194	30.94639
LHF6	M	Neobif	22.08.15	Malasa Island	-8.21194	30.94639
LHF7	F	Neobif	22.08.15	Malasa Island	-8.21194	30.94639
LHF8	M	Neobif	22.08.15	Malasa Island	-8.21194	30.94639
LHF9	M	Neobif	22.08.15	Malasa Island	-8.21194	30.94639
LHG1	M	Neobif	22.08.15	Malasa Island	-8.21194	30.94639
LHG2	F	Neobif	22.08.15	Malasa Island	-8.21194	30.94639
LHG3	M	Neobif	22.08.15	Malasa Island	-8.21194	30.94639
LHG4	M	Mdcten	23.08.15	Malasa Bay	-8.20944	30.96278
LHG6	F	Mdcten	23.08.15	Malasa Bay	-8.20944	30.96278
LHG8	M	Mdcten	23.08.15	Malasa Bay	-8.20944	30.96278
LHG9	M	Mdcten	23.08.15	Malasa Bay	-8.20944	30.96278
LHH1	F	Mdcten	23.08.15	Malasa Bay	-8.20944	30.96278
LHH2	M	Mdcten	23.08.15	Malasa Bay	-8.20944	30.96278
LHH3	F	Mdcten	23.08.15	Malasa Bay	-8.20944	30.96278
LHH4	M	Mdcten	23.08.15	Malasa Bay	-8.20944	30.96278
LHH5	F	Mdcten	23.08.15	Malasa Bay	-8.20944	30.96278
LHH6	M	Mdcten	23.08.15	Malasa Bay	-8.20944	30.96278
LHH7	M	Mdcten	23.08.15	Malasa Bay	-8.20944	30.96278
LHH8	F	Mdcten	23.08.15	Malasa Bay	-8.20944	30.96278
LHH9	M	Neopro	25.08.15	Toby's Place	-8.62322	31.20044
LHI1	M	Neopro	25.08.15	Toby's Place	-8.62322	31.20044
LHI2	F	Neopro	25.08.15	Toby's Place	-8.62322	31.20044
LHI3	M	Perecc	25.08.15	Chipwa Fishermen	-8.60617	31.18611
LHI4	M	Pleela	25.08.15	Chipwa Fishermen	-8.60617	31.18611
LHI5	M	Pleela	25.08.15	Chipwa Fishermen	-8.60617	31.18611
LHI6	F	Pleela	25.08.15	Chipwa Fishermen	-8.60617	31.18611
LHI7	F	Pleela	25.08.15	Chipwa Fishermen	-8.60617	31.18611
LIA1	F	Pleela	25.08.15	Chipwa Fishermen	-8.60617	31.18611
LIA2	F	Pleela	25.08.15	Chipwa Fishermen	-8.60617	31.18611
LIA3	M	Pleela	25.08.15	Chipwa Fishermen	-8.60617	31.18611
LIA4	M	Pleela	25.08.15	Chipwa Fishermen	-8.60617	31.18611
LIA5	M	Batmin	25.08.15	Chipwa Fishermen	-8.60617	31.18611
LIA6	F	Plemul	26.08.15	Mpulungu Fishmarket	-8.76047	31.11219
LIA7	F?	Perecc	26.08.15	Mpulungu Fishmarket	-8.76047	31.11219
LIA8	M	Perecc	26.08.15	Mpulungu Fishmarket	-8.76047	31.11219
LIA9	M	Perecc	26.08.15	Mpulungu Fishmarket	-8.76047	31.11219
LIB1	M	Perecc	26.08.15	Mpulungu Fishmarket	-8.76047	31.11219
LIB2	M	Perecc	26.08.15	Mpulungu Fishmarket	-8.76047	31.11219
LIB3	M	Oretan	26.08.15	Mpulungu Fishmarket	-8.76047	31.11219
LIB4	F	Oretan	26.08.15	Mpulungu Fishmarket	-8.76047	31.11219
LIB5	NA	Oretan	26.08.15	Mpulungu Fishmarket	-8.76047	31.11219
LIC8	M	Tylpol	02.09.15	Mpulungu Fishmarket	-8.76047	31.11219
LIC9	M	Tylpol	02.09.15	Mpulungu Fishmarket	-8.76047	31.11219
LID1	M	Tylpol	02.09.15	Mpulungu Fishmarket	-8.76047	31.11219
LJA1	F	Tylpol	04.11.15	Mpulungu Fishmarket	-8.76047	31.11219
LJA7	M	Tchdha	06.11.15	Chituta	-8.72361	31.15000
LJA8	F	Tchdha	06.11.15	Chituta	-8.72361	31.15000
LJA9	M	Tchdha	06.11.15	Chituta	-8.72361	31.15000
LJB1	F	Petmac	06.11.15	Chituta	-8.72361	31.15000
LJB2	F	Petmac	06.11.15	Chituta	-8.72361	31.15000
LJB3	F	Petmac	06.11.15	Chituta	-8.72361	31.15000
LJB4	M	Xensin	12.11.15	Ndole bay harbor	-8.47614	30.44933
LJB5	M	Xensin	12.11.15	Ndole bay harbor	-8.47614	30.44933
LJB6	M	Xensin	12.11.15	Ndole bay harbor	-8.47614	30.44933
LJB7	M	Xensin	12.11.15	Ndole bay harbor	-8.47614	30.44933
LJB8	F	Xensin	12.11.15	Ndole bay harbor	-8.47614	30.44933
LJB9	F	Xensin	12.11.15	Ndole bay harbor	-8.47614	30.44933
LJC1	F	Plemul	14.11.15	Chipwa Fishermen	-8.60617	31.18611
LJC2	F	Jultra	23.11.15	Pemba DRC	-3.61086	29.15069
LJC3	M	Neonve	NA	NA	NA	NA
LJC5	F	HemstZ	NA	Mpulungu Fishmarket	-8.76047	31.11219
LJC6	NA	Trecap	NA	NA	NA	NA
LJC7	NA	Trecap	NA	NA	NA	NA
LJC8	NA	Trecap	NA	NA	NA	NA
LJC9	NA	Neocan	NA	Wonzye Point	-8.72472	31.13306
LJD1	NA	Neocan	NA	Wonzye Point	-8.72472	31.13306
LJD2	M	Astfla	NA	NA	NA	NA
LJD3	M	Neospl	NA	Kasu	-7.31667	30.15000
LJE8	M	Hplkil	NA	Wami river	NA	NA
LNE7	NA	Perecc	22.08.16	Toby's Place	-8.62322	31.20044
LNF5	NA	Varmoo	22.08.16	Toby's Place	-8.62322	31.20044
LNF6	NA	Peteph	22.08.16	Toby's Place	-8.62322	31.20044
LNH3	F	Xchhec	23.08.16	Chipwa Fishermen	-8.60617	31.18611
LNH7	NA	Batvit	23.08.16	Chipwa Fishermen	-8.60617	31.18611
LNH9	M	Batvit	23.08.16	Chipwa Fishermen	-8.60617	31.18611
LOE1	M	XenorS	26.08.16	Chipwa Fishermen	-8.60617	31.18611
LPA4	M	Telvit	23.08.16	Toby's Place	-8.62322	31.20044
MOB4	F	Xennas	30.08.16	Chituta	-8.72361	31.15000
MOD4	NA	Bathor	01.09.16	Mpulungu Fishmarket	-8.76047	31.11219
MOD7	F	Cypkan	02.09.16	Kanfonki	-8.70278	30.92250
MOD8	F	Cypkan	02.09.16	Kanfonki	-8.70278	30.92250
MOD9	M	Cypkan	02.09.16	Kanfonki	-8.70278	30.92250
MOE1	M	Cypkan	02.09.16	Kanfonki	-8.70278	30.92250
MOE2	NA	NeoveS	03.09.16	Kabwensolo	-8.60972	30.82917
MOE5	M	NeoveS	04.09.16	Misepa	-8.58889	30.80306
MOE6	M	NeoveS	04.09.16	Misepa	-8.58889	30.80306
MOE7	M	NeoveS	04.09.16	Misepa	-8.58889	30.80306
MOE8	F	NeoveS	04.09.16	Misepa	-8.58889	30.80306
MOH3	F	Trored	06.09.16	Chimba	-8.42611	30.45667
MPB2	M	Telshe	07.09.16	Chibwensolo	-8.44278	30.45472
MPD8	F	Lepnka	09.09.16	Kachese	-8.49053	30.47750
MUA4	M	Ophhet	08.08.16	Pemba DRC	-3.61086	29.15069
OME9	NA	Petred	02.02.17	Nganja	-6.17333	29.74028
OMF6	M	BenhoM	04.02.17	Kalila Nkwasi	-6.26056	29.73667
OMF7	M	BenhoM	04.02.17	Kalila Nkwasi	-6.26056	29.73667
OMF8	M	BenhoM	04.02.17	Kalila Nkwasi	-6.26056	29.73667
OMF9	M	BenhoM	04.02.17	Kalila Nkwasi	-6.26056	29.73667
OMG1	F	BenhoM	04.02.17	Kalila Nkwasi	-6.26056	29.73667
OMG2	F	BenhoM	04.02.17	Kalila Nkwasi	-6.26056	29.73667
OMG3	F	BenhoM	04.02.17	Kalila Nkwasi	-6.26056	29.73667
OMG4	F	BenhoM	04.02.17	Kalila Nkwasi	-6.26056	29.73667
OMG5	M	BenhoM	04.02.17	Kalila Nkwasi	-6.26056	29.73667
OMG6	F	Petred	04.02.17	Kalila Nkwasi	-6.26056	29.73667
OMH3	M	NeogrM	04.02.17	Kalila Nkwasi	-6.26056	29.73667
OMH4	M	NeogrM	04.02.17	Kalila Nkwasi	-6.26056	29.73667
OMH5	M	NeogrM	04.02.17	Kalila Nkwasi	-6.26056	29.73667
OMH6	F	NeogrM	04.02.17	Kalila Nkwasi	-6.26056	29.73667
OMH7	M	NeofaM	04.02.17	Kalila Nkwasi	-6.26056	29.73667
OMH8	F	NeofaM	04.02.17	Kalila Nkwasi	-6.26056	29.73667
OMH9	F	NeofaM	04.02.17	Kalila Nkwasi	-6.26056	29.73667
OMI1	M	NeofaM	04.02.17	Kalila Nkwasi	-6.26056	29.73667
ONE7	M	Lamom	21.01.17	Kalalangabo	-4.84361	29.60944
ONE8	M	Lamom	21.01.17	Kalalangabo	-4.84361	29.60944
ONE9	M	Lamom	21.01.17	Kalalangabo	-4.84361	29.60944
ONF1	M	Lamom	21.01.17	Kalalangabo	-4.84361	29.60944
Z03	M	Punmac	NA	NA	NA	NA
Z05	M	Sthloh	NA	NA	NA	NA
Z06	F	Sthloh	NA	NA	NA	NA
Z07	M	Sthste	NA	NA	NA	NA
Z09	M	Stopin	NA	NA	NA	NA
Z17	M	Sthcar	NA	NA	NA	NA

Chapter 3

A functional trade-off between trophic adaptation and parental care predicts sexual dimorphism in cichlid fish

Fabrizia Ronco*, Marius Roesti* & Walter Salzburger*

Proceedings of the Royal Society B (2019)

PROCEEDINGS B

royalsocietypublishing.org/journal/rspb

Research

Cite this article: Ronco F, Roesti M, Salzburger W. 2019 A functional trade-off between trophic adaptation and parental care predicts sexual dimorphism in cichlid fish. *Proc. R. Soc. B* **286**: 20191050. http://dx.doi.org/10.1098/rspb.2019.1050

Received: 7 May 2019
Accepted: 30 July 2019

Subject Category:
Evolution

Subject Areas:
evolution, ecology

Keywords:
Lake Tanganyika, mouthbrooding, trophic morphology, gill rakers

Authors for correspondence:
Fabrizia Ronco
e-mail: fabrizia.ronco@unibas.ch
Marius Roesti
e-mail: marius.roesti@iee.unibe.ch
Walter Salzburger
e-mail: walter.salzburger@unibas.ch

All authors contributed equally to this study (shared authorship).

Electronic supplementary material is available online at https://dx.doi.org/10.6084/m9.figshare.c.4606802.

THE ROYAL SOCIETY PUBLISHING

A functional trade-off between trophic adaptation and parental care predicts sexual dimorphism in cichlid fish

Fabrizia Ronco[1], Marius Roesti[1,2,3] and Walter Salzburger[1]

[1]Zoological Institute, University of Basel, Vesalgasse 1, 4051 Basel, Switzerland
[2]Department of Zoology, University of British Columbia, 6270 University Boulevard, Vancouver, British Columbia, Canada V6T1Z4
[3]Institute of Ecology and Evolution, University of Bern, Bern 3012, Switzerland

MR, 0000-0002-7408-4804; WS, 0000-0002-9988-1674

Although sexual dimorphism is widespread in nature, its evolutionary causes often remain elusive. Here we report a case where a sex-specific conflicting functional demand related to parental care, but not to sexual selection, explains sexual dimorphism in a primarily trophic structure, the gill rakers of cichlid fishes. More specifically, we examined gill raker length in a representative set of cichlid fish species from Lake Tanganyika featuring three different parental care strategies: (i) uni-parental mouthbrooding, whereby only one parental sex incubates the eggs in the buccal cavity; (ii) bi-parental mouthbrooding, whereby both parents participate in mouthbrooding; and (iii) nest guarding without any mouthbrooding involved. As predicted from these different parental care strategies, we find sexual dimorphism in gill raker length to be present only in uni-parental mouthbrooders, but not in bi-parental mouthbrooders nor in nest guarders. Moreover, variation in the extent of sexual dimorphism among uni-parental mouthbrooders appears to be related to trophic ecology. Overall, we present a previously unrecognized scenario for the evolution of sexual dimorphism that is not related to sexual selection or initial niche divergence between sexes. Instead, sexual dimorphism in gill raker length in uni-parental mouthbrooding cichlid fish appears to be the consequence of a sex-specific functional trade-off between a trophic function present in both sexes and a reproductive function present only in the brooding sex.

1. Introduction

Sexual dimorphism—that is, the different appearance of males and females within a species—is a prevalent phenomenon in animals [1,2]. However, the evolutionary processes leading to sexual dimorphism remain poorly understood in many instances [1,3]. Traits that differ between the sexes of a species can, in principle, be categorized into primary, secondary and ecological sex traits [4,5]. Primary sex traits are required functionally for reproduction and relate to organs that are specific to one sex (gonads and copulatory organs). By contrast, secondary and ecological sex traits have no direct function in reproduction and often involve modifications of characters that are shared between sexes, yet are selected towards divergent optima, thus resulting in an inter-sexual conflict [3]. Dimorphism in secondary sex traits is typically driven by sexual selection [4,5], as is the case for ornaments involved in inter-sexual selection (mate choice) or weaponry used in intra-sexual combats (mate competition) [5]. Ecological sex traits, on the other hand, are characteristics that differ between males and females as a consequence of initial ecological niche divergence between the sexes, but not due to sexual selection.

From a theoretical point of view, several models have been developed to explain purely ecology-caused sexual dimorphism [6]. Yet empirical evidence

for ecological sex traits remains scarce [7,8]. A major difficulty is to distinguish between cause and consequence, that is, whether sexual dimorphism is indeed primarily ecologically caused, or whether niche divergence between males and females is the consequence of an initially non-ecological sexual dimorphism [1]. In the latter case, sexual dimorphism in an ecological trait can be the consequence of selective forces that are not primarily related to sexual or ecological selection and that are therefore not covered by available theoretical models [1]. For example, a structure involved in food uptake and/or processing (i.e. a trophic trait) of a species could have an additional function in a reproductive behaviour without sexual selection acting on the focal trait, such as in nest-building or defending offspring [1]. A trait with such a dual function—each of which is likely to have a distinct trait optimum (a trophic and a reproductive one)—is expected to experience a trade-off (figure 1). The realized trait values should thus lie somewhere in-between the two optima (figure 1*b*). If the presence of a conflicting function in such a trait is restricted to only one of the two sexes, the resulting trade-off will be sex-specific too, potentially leading to sexual dimorphism (figure 1*c*). In such a case, the realized trait values are expected to be near the trophic optimum in one sex, while they should be shifted away from the trophic optimum towards the optimum of the conflicting (reproductive) function in the sex experiencing the trade-off. This shift in trophic morphology may subsequently result in divergent niche use between the sexes.

The gill rakers of cichlid fishes from East African Lake Tanganyika provide a rare opportunity to test, in a comparative framework, for a sex-specific trade-off related to brood care—but not to sexual selection—in an otherwise trophic trait. This is because of the important role of gill rakers (i.e. spine-like, bony protrusions of the branchial gill arches in fishes) in food uptake and handling of particles within the buccal cavity [9], the potential involvement of gill rakers in brood care in many cichlids and the different brood care strategies found among the closely related cichlids from Lake Tanganyika. More specifically, one particular feature of gill rakers, gill raker length, has been shown to be strongly associated with trophic ecology in many fish [10–14], including cichlids [15,16], a pattern we here corroborate for gill raker length across 65 Tanganyikan cichlid species (figure 2*a*).

All Tanganyikan cichlids provide intensive parental brood care, either in the form of bi-parental mouthbrooding (both sexes participate in parental care), uni-parental mouthbrooding (only one sex—in the case of Tanganyikan cichlids the female—participates in parental care) or substrate spawning with nest guarding (parental care does not involve any form of mouthbrooding) [17]. Mouthbrooding species incubate their brood in the buccal cavity until the eggs' yolk sac is used up and the fry becomes free-swimming. During this entire period, which in Tanganyikan cichlids lasts between 6 and 30 days, the fertilized eggs—and later also the growing larvae—are in close physical contact with the gill rakers (figure 2*b*) and are regularly 'churned' inside the buccal cavity, probably to facilitate their ventilation and cleaning [18,19]. Gill rakers in mouthbrooding cichlids are thus expected to not only function in the uptake and handling of food particles, but also in the retention and handling of the eggs and larvae in the buccal cavity. Indeed, changes in head morphology have previously been associated with mouthbrooding [16–20], and sexual dimorphism in gill raker length has been reported for *Astatotilapia burtoni*, a uni-parental mouthbrooding cichlid from the Lake Tanganyika basin [15]. Taken together, mouthbrooding emerges as a promising candidate for an additional and probably conflicting functional demand of gill rakers.

In this study, we hypothesized that breeding mode can predict sexual dimorphism in gill raker length in Lake Tanganyika cichlids, whereby the three different breeding modes exemplify the three scenarios illustrated in figure 1. (i) In non-mouthbrooders, gill rakers are expected to have evolved relatively unconstrained towards the trophic trait optimum in both sexes (figure 1*a*). (ii) In bi-parental mouthbrooders, gill raker morphology should be influenced by both feeding and parental care (mouthbrooding). These two functions are unlikely to have identical trait optima, but the optimum resulting from the trade-off should be the same for both sexes (figure 1*b*). (iii) In uni-parental mouthbrooders, the functional trade-off between feeding and parental care should only occur in the mouthbrooding sex (females), whereas gill raker morphology in the non-mouthbrooding sex (males) should be selected towards the trophic optimum (figure 1*c*). Sexual dimorphism in gill raker length should thus occur exclusively in uni-parental mouthbrooders, but not in bi-parental mouthbrooders nor in non-mouthbrooding substrate brooders. The direction of the sexual dimorphism in uni-parental mouthbrooders is, however, hardly predictable as it should depend on the relative position of the two conflicting trait optima with respect to each other, which may well be species-specific. Finally, we hypothesized that trophic ecology determines the strength of the conflict (i.e. how divergent the two conflicting optima are) as a result of different trait optima in different trophic niches. To test these hypotheses, we examined a representative set of cichlid species for sexual dimorphism in gill raker length and tested for an association with breeding mode and trophic ecology.

2. Material and methods

(a) Sampling

Samples were collected between 2014 and 2017 during several field trips to the southern part of Lake Tanganyika, under the research permits number 005937 (F.R.) and 004273 (W.S.) issued by the Republic of Zambia. Combined with available data on gill raker length from additional Tanganyikan cichlid species [16], the final dataset covered 65 species, well representing the phylogenetic (13 out of 16 tribes [21]), eco-morphological and behavioural (breeding modes) diversity of the species-flock of cichlid fishes in Lake Tanganyika (see electronic supplementary material for detailed information on the sampling procedure and electronic supplementary material, table S1 for sample sizes).

(b) Stable isotopes

We assessed the trophic ecology of all species by quantifying stable isotope signatures of carbon (C) and nitrogen (N) in typically 10 specimens per species ($n = 661$). The ratios between the rare isotopes ^{13}C to ^{12}C ($\delta^{13}C$) and ^{15}N to ^{14}N ($\delta^{15}N$) inform about two major components of aquatic ecology, the benthic–pelagic ($\delta^{13}C$) and trophic ($\delta^{15}N$) position within an ecosystem [22]. This method has previously been applied to Tanganyikan cichlids and was compared to stomach content data [21], permitting an interpretation of food types. In this study, we analysed dried muscle tissue (from the epaxialis between the head and the dorsal fin) with a Flash 2000 elemental analyser coupled to

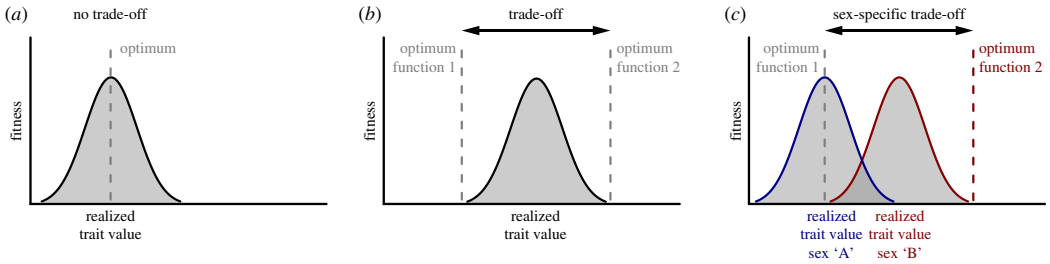

Figure 1. Proposed scenario for how two conflicting functions of the same trait can result in sexual dimorphism. (*a*) No trade-off, single function: the trait value is selected towards a single functional optimum resulting in an overlap between the optimal and the realized trait value. (*b*) Trade-off between two conflicting functions of the trait (two divergent functional optima): selection is likely to favour an intermediate phenotype (solid line), deviating from both functional trait optima (dashed lines). (*c*) Sex-specific trade-off between two conflicting functions, with a single functional optimum for one sex (sex 'A') and two conflicting optima for the other sex (sex 'B'): different selective outcomes are expected. In sex 'A', the trait is selected towards the functional optimum '1'. Hence, the realized trait value for sex 'A' (blue line) is likely to overlap with the optimum (although genetic constrains could lead to a deviation; not shown). In sex 'B', however, the trade-off between the two conflicting functional optima (dashed lines) is likely to result in intermediate realized trait values (red line). (Online version in colour.)

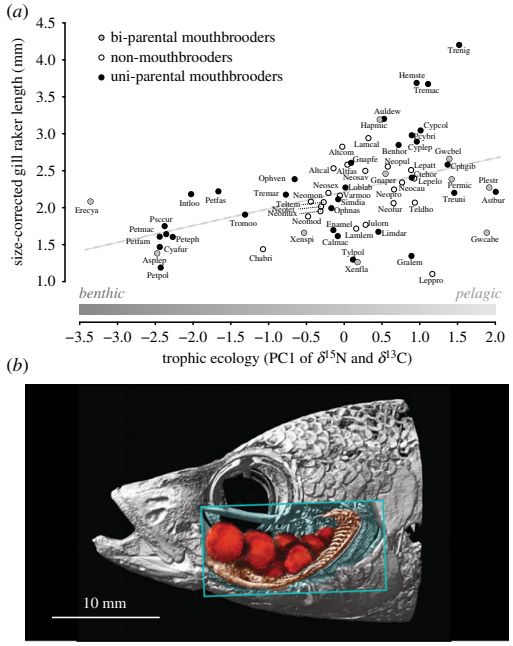

Figure 2. Gill rakers in Lake Tanganyika cichlids and their association with trophic ecology. (*a*) Phenotype–environment correlation between size-corrected gill raker length and trophic ecology (PC1 scores of stable isotope data). Longer gill rakers are associated with pelagic feeding, and shorter gill rakers with benthic feeding. This benthic–pelagic feeding trajectory is indicated above the *x*-axis (see electronic supplementary material, figure S1*a*). Data points represent species means and are shaded according to the breeding mode of the species (see electronic supplementary material, table S1 for full species names). (*b*) CT scan of a mouthbrooding *Paracyprichromis* sp. female (see electronic supplementary material for details on scanning and processing). Parts of the skull were virtually removed (box), revealing the developing eggs in the buccal cavity (highlighted in red) and the gill raker apparatus (highlighted in brown). (Online version in colour.)

a Delta V Plus continuous-flow isotope ratio mass spectrometer (IRMS) via a Conflo IV interface (Thermo Fisher Scientific, Bremen, Germany) in the SLU-Lab at the University of Basel (data have been deposited on the Dryad Digital Repository: https://doi.org/10.5061/dryad.fm4707v [23]). We then used a principal component analysis (PCA) to integrate over the δ^{15}N and δ^{13}C stable isotope ratios to obtain a univariate metric for trophic ecology.

(c) Gill raker morphology

We measured gill raker length under a binocular (Leica MZ7$_5$) as described previously [10,16]. Measurements were taken by two investigators on blinded samples (F.R., M.R.) and recorded by a third investigator (W.S.). Measurements were converted to millimetre scale and averaged across the three gill rakers measured per specimen (i.e. the second, third and fourth raker on the first branchial gill arch). To avoid a potential investigator bias, samples were assigned randomly to one of the two investigators. We measured gill raker length in 508 specimens (38 species). In combination with data from Muschick *et al.* [16], we obtained a dataset comprising 935 specimens and 65 species (data have been deposited on the Dryad Digital Repository: https://doi.org/10.5061/dryad.fm4707v [23]). Gill raker length was strongly correlated with body size (standard length = SL; Pearson's $r = 0.68$, $p < 0.001$), and thus, size corrected prior to further analysis. Size correction was done specifically for each analysis (see below).

(d) Phenotype–environment correlation

To investigate how gill raker length is associated with trophic ecology, we size-corrected gill raker length of each specimen using residuals from a common linear model applied across all specimens from all 65 species (with gill raker length as response variable and SL as explanatory variable; $R^2 = 0.46$, $p < 0.001$). We then added the value of the largest residual to restore positive values in the initial measuring unit (mm). The species mean of these size-independent values and the PC1 scores of stable isotope data were used to test for a phenotype–environment correlation using a linear model and Pearson's *r* statistics. Statistical significance was assessed using 10 000 random permutations of the observed species means over the stable isotope PC1 scores [24]. All *p*-values and 95% confidence intervals in this paper were obtained through analogous resampling procedures, except for analyses accounting for phylogenetic relationships. To account for phylogenetic dependence of the species, we applied a 'phylogenetic generalized least squares' fit using the R package *caper* [25]. For all analyses incorporating phylogenetic relationships, we used the phylogenetic hypothesis from Colombo *et al.* [26] and pruned it to the set of taxa present in our datasets. One species (*Petrochromis ephippium*) was not represented in the phylogenetic tree and was therefore omitted from these analyses.

(e) Sexual dimorphism

To test for sexual dimorphism in gill raker length in non-, bi- and uni-parental mouthbrooders, we focused on a subset of species ($n = 20$) for which sex information was available. Here, size correction of gill raker length was performed separately for each species, using species-specific linear models, maximizing comparability between the sexes. We then tested for a difference in the length of male and female gill rakers within each species, and whether the grand-mean per breeding mode deviated from zero. We further evaluated whether the *extent* of the dimorphism irrespective of directionality (i.e. the *absolute* difference of female minus male gill raker length per species) differed among the breeding modes by calculating *F*-statistics across the three groups (ANOVA), followed by pairwise comparisons of the breeding modes. To account for phylogenetic dependence of the species, we applied a phylogenetic ANOVA using the function phylANOVA from the R package *phytools* [27].

Finally, we tested for an association between the extent of sexual dimorphism and trophic ecology (PC1 scores of stable isotope data) within uni-parental mouthbrooders. Based on a Davies test [28], which tests for a breakpoint in a linear relationship between two variables, we fitted a segmented regression model [28]. Note that the reported *p*-values for the Davies test were not obtained through permutation, but were taken directly from the output of the davies.test function as implemented in the R package *segmented* [28]. To validate the results in a phylogenetic framework, we used the estimated breakpoint in PC1 scores from the segmented regression model as a threshold to assign the uni-parental mouthbrooders into two trophic groups and tested for a difference in the extent of sexual dimorphism between these groups using a phylogenetic ANOVA. All graphing and statistical analyses were conducted in R [29].

3. Results

(a) Gill raker length is associated with trophic ecology

A PCA of the stable isotope ratios of nitrogen (δ^{15}N) and carbon (δ^{13}C) was used to reduce dimensionality of the two components of trophic ecology. This allowed working with a univariate proxy for trophic ecology. PC1 explained 77.3% of the total variation in the stable isotope data, and was loaded negatively for δ^{13}C (−0.71) and positively for δ^{15}N (0.71) (electronic supplementary material, figure S1*a*). Higher PC1 scores thus reflected pelagic feeding (e.g. on zooplankton and/or fish fry) and a relatively high position in the food chain (hereafter simply referred to as 'pelagic'), whereas benthic/littoral species with a mainly algivorous feeding lifestyle and a lower trophic position had lower PC1 scores (hereafter simply called 'benthic'). Gill raker length was positively associated with trophic ecology across the 65 species (Pearson's $r = 0.46$, $p < 0.001$; $R^2 = 0.20$, $p < 0.001$), with shorter gill rakers in benthic and longer gill rakers in pelagic species (figure 2*a*; electronic supplementary material, figure S1*b*). This result held true after accounting for phylogenetic dependence of the trait values ($R^2 = 0.14$, $p = 0.002$, $\lambda = 0.43$).

(b) Sexual dimorphism is predicted by breeding mode and trophic ecology

Sexual dimorphism in size-corrected gill raker length was pronounced in uni-parental mouthbrooders, and reached statistical significance ($p < 0.05$) in three out of nine species (see electronic supplementary material, table S2*a*). By contrast, none of the bi-parental mouthbrooding species, nor any substrate brooding species, showed evidence for sexual dimorphism (figure 3*a*).

The grand mean per breeding mode of the difference between male and female gill raker length did not deviate from zero in any of the three breeding modes (see electronic supplementary material, table S2*b*). However, uni-parental species showed a strongly increased variation in sexual dimorphism compared to bi-parental mouthbrooders and non-mouthbrooders (figure 3*a*). The *absolute* difference in gill raker length between the sexes revealed a significantly greater extent of sexual dimorphism in uni-parental mouthbrooders compared to bi-parental and non-mouthbrooding species in an ordinary ANOVA ($F = 6.19$, $p = 0.007$) (figure 3*b*; electronic supplementary material, table S2*c*,*d*). When accounting for phylogenetic dependence, only uni-parental and bi-parental mouthbrooders showed a difference in the extent of sexual dimorphism ($p = 0.022$).

Finally, we focused on the association between the extent of sexual dimorphism and trophic ecology within uni-parental mouthbrooders. We found a statistically supported breakpoint in the linear relationship between sexual dimorphism and trophic ecology ($p = 0.04$). The fitted segmented model estimated a breakpoint at a PC1 score of 0.34, with PC1 scores higher than 0.34 showing a strong positive association with the extent of sexual dimorphism (figure 4; electronic supplementary material, table S3). When using this estimated breakpoint to assign the species into two trophic groups and accounting for phylogenetic dependence, the species with higher PC1 scores showed a distinctly greater extent of sexual dimorphism than the species with PC1 scores below the threshold ($F = 22.8$, $p = 0.004$).

4. Discussion

In this study, we addressed the question of whether a conflicting (sex-specific) functional demand linked to parental care can explain sexual dimorphism in an otherwise trophic trait. To this end, we investigated gill raker length in a set of cichlid fish species from Lake Tanganyika covering three different breeding modes and a variety of trophic ecologies (figure 2*a*).

Gill rakers are an important structure for uptake and handling of food in the buccal cavity in fish [9], and the length of gill rakers is generally associated with different trophic ecologies: pelagic species feeding on small and mobile prey commonly have longer gill rakers, while benthic species feeding on larger and immobile prey (or *aufwuchs*) have shorter gill rakers [10–16]. Here we corroborate this phenotype–environment correlation in an extensive dataset covering 65 cichlid species from Lake Tanganyika, representing the morphological, ecological and phylogenetic diversity of the lake's cichlid assemblage: we find an association between gill raker length and trophic ecology (as approximated by the PC1 of stable isotope data), with longer gill rakers in cichlids with more pelagic stable isotope signatures, and shorter gill rakers in species with more benthic signatures (figure 2*a*). Based on a previous study linking stable isotope signatures with stomach content analysis in Tanganyika cichlids [21], we conclude that pelagic stable isotope signatures usually correspond to invertebrate/zooplankton/small fish feeders, whereas species with benthic signatures predominantly feed on algae and plants. Note, however, that also predatory species feeding on large fish show pelagic

royalsocietypublishing.org/journal/rspb Proc. R. Soc. B 286: 20191050

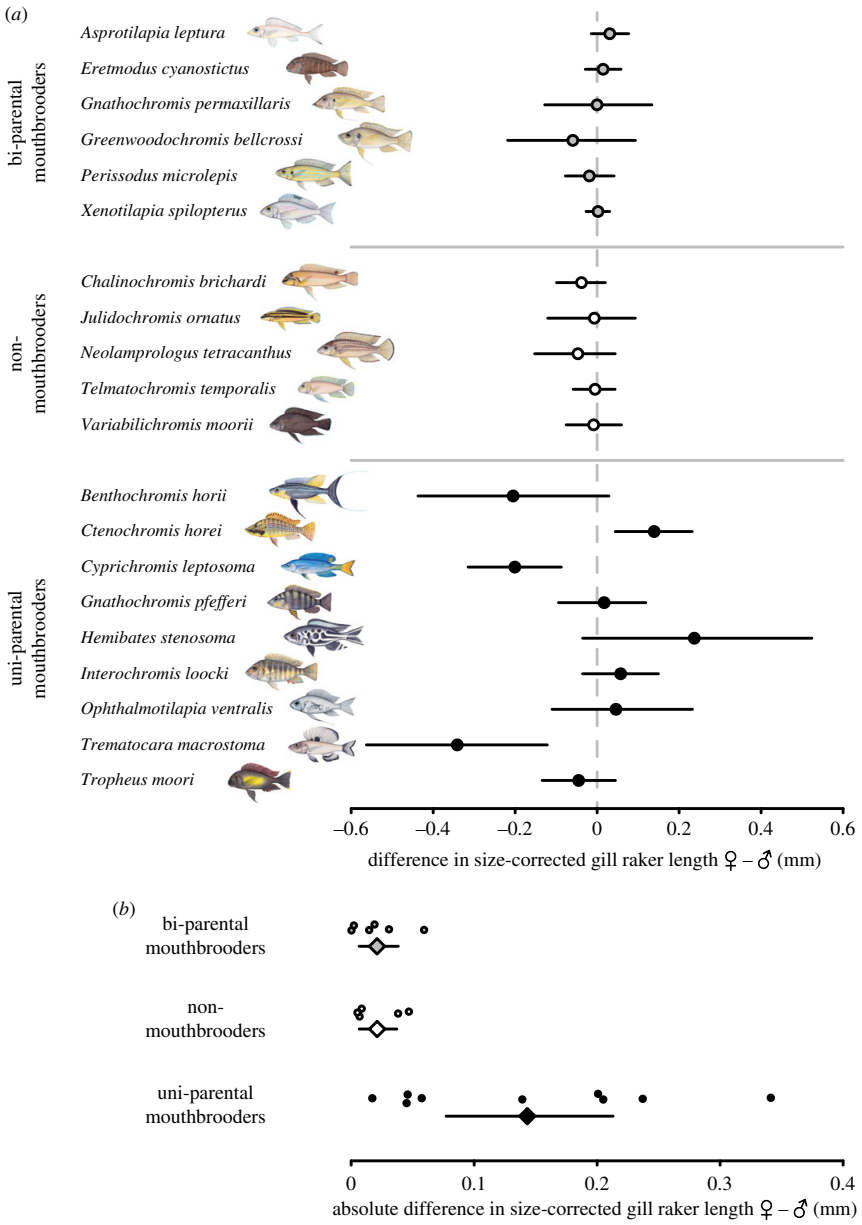

Figure 3. Sexual dimorphism in gill raker length. (*a*) Female minus male size-corrected gill raker length per species shows pronounced sexual dimorphism in uni-parental mouthbrooders compared to bi-parental and non-mouthbrooding species. (*b*) Extent of sexual dimorphism, calculated by the *absolute* difference of female minus male size-corrected gill raker length (circles are species means and squares are grand-means per breeding mode). Uni-parental mouthbrooders show an increased extent of sexual dimorphism compared to bi-parental and non-mouthbrooding species (nest guarders). All error bars represent 95% confidence intervals of the means; see electronic supplementary material, tables S1 and S2 for sample sizes and *p*-values. (Online version in colour.)

signatures, but have rather short gill rakers (see e.g. *Lepidiolamprologus profondicula*; 'Leppro'; figure 2*a*).

We hypothesized that gill raker length is also relevant for mouthbrooding, thus resulting in a conflicting functional demand of gill raker morphology in addition to food update and handling (figure 1*b*). Mouthbrooding is a particular form of parental care and widespread among cichlid fishes, where it occurs in a uni-parental (maternal or paternal) or bi-parental mode. Mouthbrooding is a costly trait [30] and has been reported to induce morphological changes including an enlargement of the head or the buccal cavity [20,31–33], or a reduction in gill size [34]. Gill raker length has, however, not yet been examined in the context of mouthbrooding. This is surprising given that gill rakers are expected to be functionally involved in mouthbrooding, either directly via the active handling of the eggs or larvae [18], or indirectly through the close physical contact between gill rakers and the offspring (figure 2*b*).

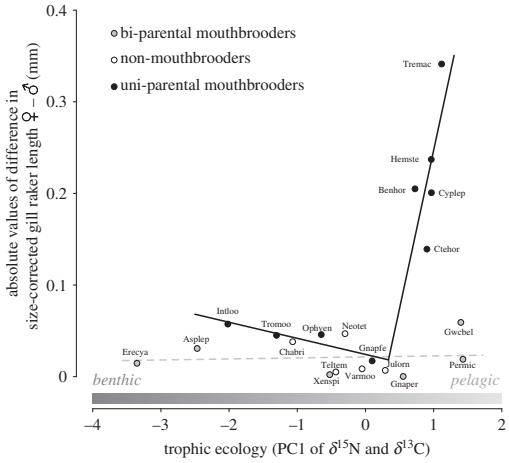

Figure 4. Association between the extent of sexual dimorphism and trophic ecology: in uni-parental mouthbrooders, the linear association between the extent of sexual dimorphism (i.e. absolute difference in size-corrected gill raker length between females and males) and trophic ecology shows a breakpoint at a trophic PC1 score of 0.34. For species above this threshold, PC1 scores and sexual dimorphism correlate strongly and positively. The solid line represents the result of a segmented regression model fitted for uni-parental mouthbrooders. As no differences were found between bi-parental mouthbrooders and non-mouthbrooders, the two groups were pooled in a linear model (dashed grey line). Note that the five uni-parental mouthbrooding species with the largest sexual dimorphism belong to five different tribes (see electronic supplementary material, figure S1*c*). The benthic–pelagic feeding trajectory represented by PC1 scores is indicated above the *x*-axis (see electronic supplementary material, figure S1*a*).

Under the assumption that gill rakers experience different selective regimes among the three breeding modes (bi-parental mouthbrooding, uni-parental mouthbrooding and non-mouthbrooding) due to their dual function in both feeding and breeding, we predicted sexual dimorphism to be present exclusively in uni-parental mouthbrooders (figure 1). We examined 20 Tanganyikan cichlid species and investigated how well breeding mode and/or feeding ecology can explain sexual dimorphism. Indeed, we found males and females of non- and bi-parental mouthbrooding species not to differ in gill raker length. By contrast, several of the uni-parental mouthbrooding species were sexually dimorphic in gill raker length, varying in extent and direction (figure 3*a*). The overall difference between non- and bi-parental mouthbrooders relative to uni-parental mouthbrooders became particularly evident when comparing the *absolute* extent of sexual dimorphism (i.e. sexual dimorphism irrespective of its direction) among breeding modes (figure 3*b*). When accounting for phylogeny, the difference between uni-parental and bi-parental mouthbrooders in the extent of sexual dimorphism was confirmed, but not so for non-mouthbrooders. This is hardly surprising, given the monophyly of the vast majority of non-mouthbrooding cichlids in Lake Tanganyika (the Lamprologini, which make up 50% of all species in that lake; see electronic supplementary material, figure S1*c*), thus reducing statistical power in comparisons involving non-mouthbrooders. Nevertheless, the difference in the extent of sexual dimorphism between uni-parental and bi-parental mouthbrooders supported the idea that breeding mode can partially predict the presence or absence of sexual dimorphism in gill raker length.

How can the variation in the extent and direction of sexual dimorphism *within* uni-parental mouthbrooders be explained? Under the assumption of a trade-off between a trophic versus reproductive function of gill rakers, both the extent and the directionality of the sexual dimorphism should depend on the relative position of the two optima in relation to one another (figure 1). Clearly, the association of gill raker length and trophic ecology across the 65 cichlid species suggests species-specific optima for gill raker length (figure 2*a*). Although the factors determining optimal gill raker length for mouthbrooding are unknown, life-history traits such as clutch and egg size or breeding duration are likely to be relevant. Unfortunately, data on life-history traits are too scarce (and/or too vague) to allow testing for an association with gill raker length. Nevertheless, clutch size emerges as a promising candidate trait to explain variation in the direction of sexual dimorphism among uni-parental mouthbrooders (see electronic supplementary material, figure S2*a*). On the other hand, since life-history traits differ among cichlid species [35], the reproductive optimum of gill raker length is expected to be species-specific too. This is further corroborated by the difference in the *directionality* of sexual dimorphism in gill raker length among uni-parental mouthbrooders with respect to actual gill raker length (electronic supplementary material, figure S2*b*). Thus, the finding that some uni-parental mouthbrooders show a female-biased dimorphism (longer gill rakers in females), while others show a male-biased dimorphism, is likely to reflect variation in the relative position of the conflicting trait optima.

Likewise, the absence of any sexual dimorphism in some of the uni-parental mouthbrooders might be the result of overlapping trait optima for the two functional demands. Species with extreme trophic ecologies may be expected to generally experience stronger deviations between the trophic and reproductive optima than species with intermediate trophic ecologies. Additionally, variation in the extent of sexual dimorphism among uni-parental mouthbrooders might be the result of similarly strong selection towards the optimum for mouthbrooding in all species, but varying selection regimes with respect to the optimal trait value for feeding, depending on the trophic ecology of a species. For example, if gill raker morphology is of particular importance for efficient food uptake and handling in a species (as in pelagic suction feeders [11]), the selective pressures acting antagonistically are expected to be strong and a dimorphism is more likely to be expressed. On the other hand, in species where the gill rakers are less important for feeding (as in benthic algivores), sexually antagonistic selection would be unbalanced, resulting in a less pronounced or no sexual dimorphism. Accordingly, in both cases, the differences in the extent of sexual dimorphism in uni-parental mouthbrooders are expected to depend on the trophic ecology of the species. We tested this prediction and found uni-parental mouthbrooding species to show an association between the (absolute) extent of sexual dimorphism and trophic ecology. This association was not linear along the entire trophic continuum, but rather increased rapidly after a certain breakpoint (figure 4). This implies that whether or not a sexual dimorphism in gill raker length occurs depends on both the breeding mode and the trophic ecology of a species, with breeding

mode determining the potential for a sex-specific functional conflict, and trophic ecology determining the strength of the conflict.

With the data at hand, we cannot formally test for the strength of selection acting on gill raker length, nor can we directly measure the optima in trait value for feeding versus mouthbrooding. Hence, we cannot disentangle cases where the strength of the conflict depends on how balanced the selective pressures are that act on the two optima, on how divergent the two optima are, nor a combination of both. Nevertheless, our findings provide empirical evidence for the scenario that a sex-specific functional conflict due to parental care by only one sex of a species explains sexual dimorphism in a trait.

The finding of sexual dimorphism to be present exclusively in uni-parental mouthbrooders largely contradicts predictions from popular models of ecology-caused sexual dimorphism: if inter-sexual competition for resources were the trigger for sexual dimorphism [6], one would expect sexual dimorphism to occur mainly in species forming pair bonds and sharing feeding and breeding territories [36]. In our study system, this applies primarily to bi-parental mouthbrooders and non-mouthbrooders (bi-parental nest guarders), but not to uni-parental mouthbrooders. Other ecological models for sexual dimorphism, such as the 'bimodal niche model' [6] (two alternative optima in trait value exist, followed by disruptive selection between the sexes) or the 'dimorphic niche model' [6] (intrinsic differences between males and females in energetic needs lead to niche divergence between the sexes), would also not predict sexual dimorphism to occur exclusively in uni-parental mouthbrooders. Moreover, most models of ecology-caused sexual dimorphism assume niche divergence between the sexes. However, such a difference in niche use between males and females is not evident from our stable isotope data (electronic supplementary material, figure S3).

Unlike most studies investigating causes of sexual dimorphism in relation to ecology [7,8,37,38], we can largely exclude the possibility that sexual selection has directly driven or reinforced the observed sexual dimorphism. This is because gill rakers are cryptic to the outer appearance of a fish and thus highly unlikely to serve as a signal in mate choice or mate competition. One could of course argue that sexual selection initially contributed to the evolution of sex-specific roles in breeding behaviour, but here we refer to sexual selection acting directly on the focal trait. Taken together, sexual dimorphism in our study system is unlikely to be explained by sexual selection or initial niche divergence between the sexes, thus providing a novel view on the evolution of sexual dimorphism in nature.

Although our study provides an explanation why gill raker length differs between the sexes in some cichlid species, but not in others, it remains an open question how sexual dimorphism in this trait is achieved developmentally. Variation in gill raker length has been shown to have a largely genetic basis in threespine stickleback [39,40], and a common garden experiment with divergent *A. burtoni* cichlid ecotypes revealed both a genetic and a plastic component in gill raker length variation [15]. What remains to be tested is the degree to which sexual dimorphism in gill raker length of cichlids is genetically based or is the result of a plastic response to mouthbrooding. It would further be interesting to investigate other components of the cichlids' trophic morphology with respect to sexual dimorphism and parental care.

In conclusion, our study establishes an overall phenotype–environment association between gill raker length and trophic ecology across 65 Tanganyikan cichlid species, and reveals that gill raker morphology is influenced by mouthbrooding. As a consequence, the presence and extent of sexual dimorphism in gill raker length is predicted by both the breeding mode and the trophic ecology of a species. Sexual dimorphism in gill raker length of uni-parental mouthbrooding cichlids is unlikely to be explained by sexual selection or initial niche divergence between the sexes, but instead is caused by a sex-specific trade-off between two conflicting functional demands of the same trait, one related to trophic adaptation and one to parental care.

Data accessibility. Data available from the Dryad Digital Repository: https://doi.org/10.5061/dryad.fm4707v [23].

Authors' contributions. M.R. conceived the study, with all authors making later contributions to the study design. F.R. and W.S. collected the samples new to this study in the field. All authors contributed to measuring gill rakers. F.R. obtained stable isotope data, analysed and visualized the data with input from M.R. and W.S. F.R. drafted the manuscript, with all authors contributing to the writing of the final paper.

Competing interests. We declare we have no competing interests.

Funding. This study was funded by European Research Council (ERC, Consolidator Grant 'CICHLID~X') to W.S., and grants from the Swiss National Science Foundation to M.R. (P2BSP3_161931, 300PA_174344) and W.S. (156405).

Acknowledgements. We would like to thank Adrian Indermaur, Athimed El Taher, Ann-Christin Honnen, Lukas Widmer, Elia Heule and Anna Boila for their help in the field, and Ansgar Kahmen, Victor Evrard and Anna Boila for their assistance with stable isotope data collection. We further thank Daniel Berner for statistical advice, Hanna Kokko and Hugo Gante for valuable discussions, Lukas Schärer for helpful comments on the manuscript, Julie Himes for fish illustrations in figure 3*a*, as well as Peter Wainwright and three anonymous reviewers for helpful comments that improved this manuscript.

References

1. Shine R. 1989 Ecological causes for the evolution of sexual dimorphism : a review of the evidence. *Q. Rev. Biol.* **64**, 419–461. (doi:10.1086/416458)
2. Williams TM, Carroll SB. 2009 Genetic and molecular insights into the development and evolution of sexual dimorphism. *Nat. Rev. Genet.* **10**, 797–804. (doi:10.1038/nrg2687)
3. Cox RM, Calsbeek R. 2009 Sexually antagonistic selection, sexual dimorphism, and the resolution of intralocus sexual conflict. *Am. Nat.* **173**, 176–187. (doi:10.1086/595841)
4. Darwin CR. 1871 *The descent of man and selection in relation to sex*. London, UK: John Murray.
5. Andersson M. 1994 *Sexual selection*. Princeton, NJ: Princeton University Press.
6. Slatkin M. 1984 Ecological causes of sexual dimorphism. *Evolution* **38**, 622–630. (doi:10.1111/j.1558-5646.1984.tb00327.x)
7. Temeles EJ, Pan IL, Brennan JL, Horwitt JN. 2000 Evidence for ecological causation of sexual dimorphism in a hummingbird. *Science* **289**, 441–443. (doi:10.1126/science.289.5478.441)

8. Cooper IA. 2010 Ecology of sexual dimorphism and clinal variation of coloration in a damselfly. *Am. Nat.* **176**, 566–572. (doi:10.1086/656491)
9. Sanderson SL, Cheer AY, Goodrich JS, Graziano JD, Callan WT. 2001 Crossflow filtration in suspension-feeding fishes. *Nature* **412**, 439–441. (doi:10.1038/35086574)
10. Berner D, Adams DC, Grandchamp A-C, Hendry AP. 2008 Natural selection drives patterns of lake-stream divergence in stickleback foraging morphology. *J. Evol. Biol.* **21**, 1653–1665. (doi:10.1111/j.1420-9101.2008.01583.x)
11. Robinson BW. 2000 Trade offs in habitat-specific foraging efficiency and the nascent adaptive divergence of sticklebacks in lakes. *Behaviour* **137**, 865–888. (doi:10.1163/156853900502501)
12. Schluter D, McPhail JD. 1992 Ecological character displacement and speciation in sticklebacks. *Am. Nat.* **140**, 85–108. (doi:10.1086/285404)
13. Amundsen P, Bøhn T, Våga GH. 2004 Gill raker morphology and feeding ecology of two sympatric morphs of European whitefish (*Coregonus lavaretus*). *Ann. Zool. Fennici* **41**, 291–300.
14. Østbye K, Amundsen P, Bernatchez L, Klemetsen A, Knudsen R, Kristoffersen R, Naesje TF, Hindar K. 2006 Parallel evolution of ecomorphological traits in the European whitefish *Coregonus lavaretus* (L.) species complex during postglacial times. *Mol. Ecol.* **15**, 3983–4001. (doi:10.1111/j.1365-294X.2006.03062.x)
15. Theis A, Ronco F, Indermaur A, Salzburger W, Egger B. 2014 Adaptive divergence between lake and stream populations of an East African cichlid fish. *Mol. Ecol.* **23**, 5304–5322. (doi:10.1111/mec.12939)
16. Muschick M, Nosil P, Roesti M, Dittmann MT, Harmon L, Salzburger W. 2014 Testing the stages model in the adaptive radiation of cichlid fishes in East African Lake Tanganyika. *Proc. R. Soc. B* **281**, 20140605. (doi:10.1098/rspb.2014.0605)
17. Goodwin NB, Balshine-Earn S, Reynolds JD. 1998 Evolutionary transitions in parental care in cichlid fish. *Proc. R. Soc. Lond. B* **265**, 2265–2272. (doi:10.1098/rspb.1998.0569)
18. Oppenheimer JR. 1970 Mouthbreeding in fishes. *Anim. Behav.* **18**, 493–503. (doi:10.1016/0003-3472(70)90045-X)
19. Fryer G, Iles TD. 1972 *The cichlid fishes of the great lakes of Africa*. Neptune City, NJ: TFH Publications.
20. Tkint T, Verheyen E, De Kegel B, Helsen P, Adriaens D. 2012 Dealing with food and eggs in mouthbrooding cichlids: structural and functional trade-offs in fitness related traits. *PLoS ONE* **7**, e31117. (doi:10.1371/journal.pone.0031117)
21. Muschick M, Indermaur A, Salzburger W. 2012 Convergent evolution within an adaptive radiation of cichlid fishes. *Curr. Biol.* **22**, 2362–2368. (doi:10.1016/j.cub.2012.10.048)
22. Post DM. 2002 Using stable isotopes to estimate trophic position: models, methods, and assumptions. *Ecology* **83**, 703–718. (doi:10.2307/3071875)
23. Ronco F, Roesti M, Salzburger W. 2019 Data from: A functional trade-off between trophic adaptation and parental care predicts sexual dimorphism in cichlid fish. Dryad Digital Repository. (doi:10.5061/dryad.fm4707v)
24. Manly BFJ. 2007 *Randomization, bootstrap and Monte Carlo methods in biology*, 3rd edn. Boca Raton, FL: Chapman & Hall.
25. Orme D. 2018 The caper package: comparative analysis of phylogenetics and evolution in R. R package version 5.
26. Colombo M, Indermaur A, Meyer BS, Salzburger W. 2016 Habitat use and its implications to functional morphology: niche partitioning and the evolution of locomotory morphology in Lake Tanganyikan cichlids (Perciformes: Cichlidae). *Biol. J. Linn. Soc.* **118**, 536–550. (doi:10.1111/bij.12754)
27. Revell LJ. 2012 phytools: an R package for phylogenetic comparative biology (and other things). *Methods Ecol. Evol.* **3**, 217–223. (doi:10.1111/j.2041-210X.2011.00169.x)
28. Muggeo VMR. 2008 segmented: an R package to fit regression models with broken-line relationships. *R News* **8**, 20–25.
29. Team RDC. 2017 *R: a language and environment for statistical computing*. Vienna, Austria: R Foundation for Statistical Computing.
30. Keller IS, Bayer T, Salzburger W, Roth O. 2018 Effects of parental care on resource allocation into immune defense and buccal microbiota in mouthbrooding cichlid fishes. *Evolution* **72**, 1109–1123. (doi:10.1111/evo.13452)
31. Okuda N, Miyazaki M, Yanagisawa Y. 2002 Sexual difference in buccal morphology of the paternal mouthbrooding cardinalfish *Apogon doederleini*. *Zool. Sci.* **19**, 801–807. (doi:10.2108/zsj.19.801)
32. Van Wassenbergh S, Potes NZ, Adriaens D. 2015 Hydrodynamic drag constrains head enlargement for mouthbrooding in cichlids. *J. R. Soc. Interface* **12**, 20150461. (doi:10.1098/rsif.2015.0461)
33. Barnett A, Bellwood DR. 2005 Sexual dimorphism in the buccal cavity of paternal mouthbrooding cardinalfishes (Pisces: Apogonidae). *Mar. Biol.* **148**, 205–212. (doi:10.1007/s00227-005-0052-z)
34. O'Connor CM, Reardon EE, Chapman LJ. 2012 Shorter gills in mouth-brooding females of the cichlid pseudocrenilabrus multicolor. *Copeia* **2012**, 382–388. (doi:10.1643/CG-10-130)
35. Duponchelle F, Paradis E, Ribbink AJ, Turner GF. 2008 Parallel life history evolution in mouthbrooding cichlids from the African Great Lakes. *Proc. Natl Acad. Sci. USA* **105**, 15 475–15 480. (doi:10.1073/pnas.0802343105)
36. Reynolds JD, Harvey PH. 1994 Sexual selection and the evolution of sex differences. In *The differences between the sexes* (eds RV Short, E Balaban), pp. 53–70. Cambridge, UK: Cambridge University Press.
37. Weimerskirch H, Le Corre M, Gadenne H, Pinaud D, Kato A, Ropert-Coudert Y, Bost CA. 2009 Relationship between reversed sexual dimorphism, breeding investment and foraging ecology in a pelagic seabird, the masked booby. *Oecologia* **161**, 637–649. (doi:10.1007/s00442-009-1397-7)
38. Stuart-Fox D, Moussalli A. 2007 Sex-specific ecomorphological variation and the evolution of sexual dimorphism in dwarf chameleons (*Bradypodion* spp.). *J. Evol. Biol.* **20**, 1073–1081. (doi:10.1111/j.1420-9101.2007.01295.x)
39. Glazer AM, Killingbeck EE, Mitros T, Rokhsar DS, Miller CT. 2015 Genome assembly improvement and mapping convergently evolved skeletal traits in sticklebacks with genotyping-by-sequencing. *G3* **5**, 1463–1472. (doi:10.1534/g3.115.017905)
40. Berner D, Moser D, Roesti M, Buescher H, Salzburger W. 2014 Genetic architecture of skeletal evolution in European lake and stream stickleback. *Evolution* **68**, 1–14. (doi:10.1111/evo.12390)

Chapter 3 | Supplementary Material

Supplementary Information

A functional trade-off between trophic adaptation and parental care predicts sexual dimorphism in cichlid fish

Fabrizia Ronco[1*], Marius Roesti[1,2*] & Walter Salzburger[1*]

[1] Zoological Institute, University of Basel, Vesalgasse 1, 4051 Basel, Switzerland
[2] Department of Zoology, University of British Columbia, 6270 University Boulevard, Vancouver, BC V6T1Z4, Canada
[3] Current address: Institute of Ecology and Evolution, University of Bern, 3012, Switzerland

* All authors contributed equally to this work

Authors for correspondence:
Fabrizia Ronco
e-mail: fabrizia.ronco@unibas.ch
Marius Roesti
e-mail: marius.roesti@iee.unibe.ch
Walter Salzburger
e-mail: walter.salzburger@unibas.ch

Sampling procedure

Fish were caught using gill nets while snorkeling or scuba diving, or bought from local fishermen. After euthanasia with clove oil, specimens were measured (standard length = SL) and the sex was determined whenever possible. For subsequent morphological measurements, the entire gill apparatus was extracted and stored in 96% EtOH. For the stable isotope analysis, entire specimens were fixed in 10% formalin for 4 days, rinsed with water and transferred to 70% EtOH.

CT-scanning (figure 2*b*)

The mouthbrooding female (*Paracyprichromis* sp.) was euthanised on ice, fixed in 10% formalin and then gradually transferred to 100% EtOH. To increase contrast of the surface of the developing eggs in the buccal cavity, the mouth was rinsed repeatedly with 5% Lugol's iodine (I3K). CT-scanning of the head region was carried out on a Bruker Skyscan 1174v2, at 50kV, 800µA using a 0.25mm Aluminium filter and 4500ms exposure time. Voxel size was 29.8µm with 600 projections. Reconstruction was performed using NRecon (Version: 1.6.10.2), post-processing and visualisation was done in CTvox (Version: 3.3). Eggs and gill rakers were afterwards highlighted on the image using Adobe Photoshop (CC 2017).

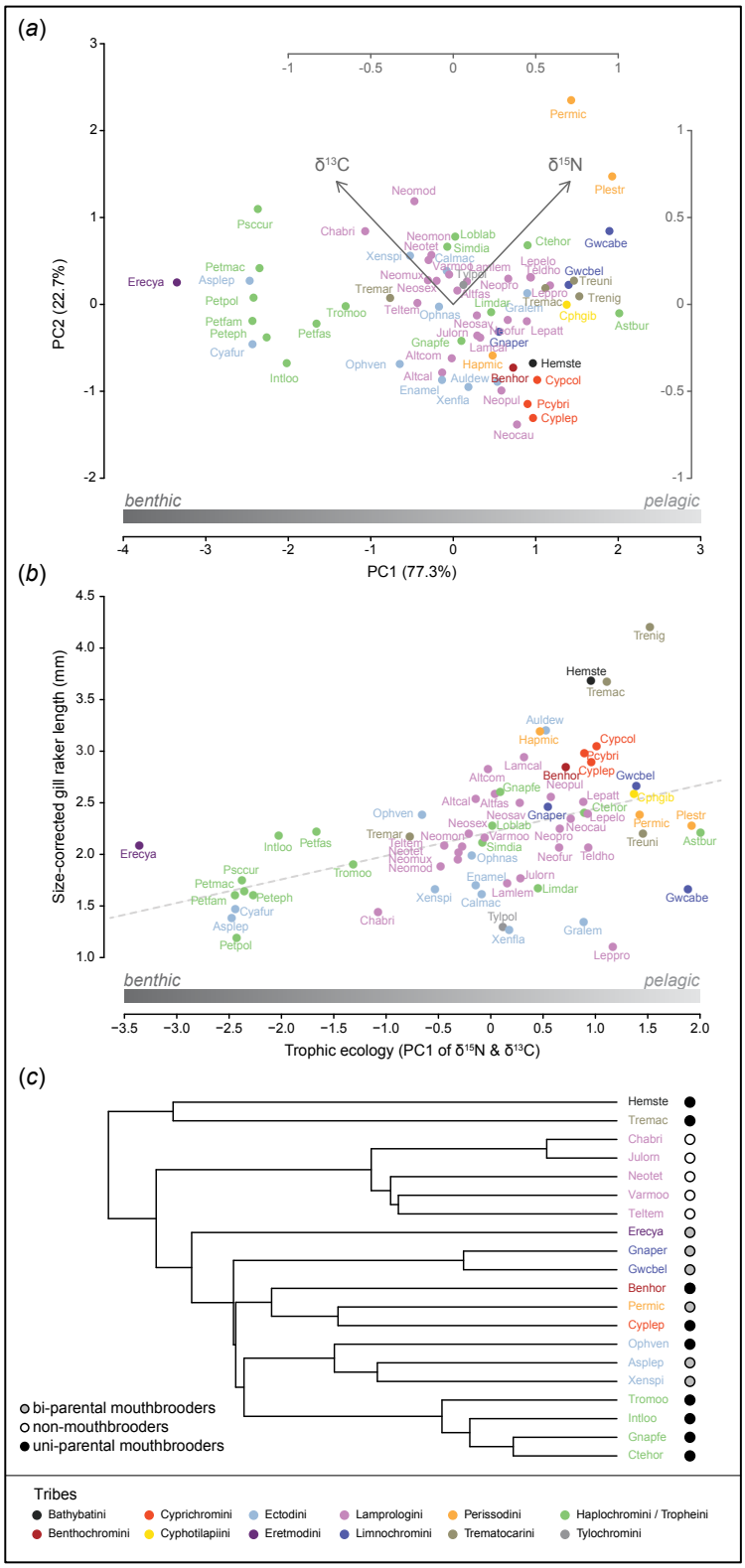

Figure S1: Trophic ecology of 65 Tanganyikan cichlid species, its correlation with gill raker morphology, and the distribution of the different breeding modes across the phylogeny (See supplementary table S1 for full species names): *(a)* A scaled Principal Component Analysis (PCA) of stable isotope measurements ($\delta^{15}N$ and $\delta^{13}C$, species means) was used to infer the major axis of variation across two major components of aquatic ecology: the benthic-pelagic ($\delta^{13}C$) and trophic ($\delta^{15}N$) position. We used PC1-scores (equally loaded with two components ($\delta^{15}N$: 0.71, $\delta^{13}C$: -0.71)) in downstream analyses as a univariate proxy for trophic ecology. *(b)* Phenotype-environment correlation between gill raker length and trophic ecology across 65 Tanganyikan cichlid species. Gill raker length (species mean) is positively associated with PC1-scores of stable isotope data. *(c)* The phylogenetic structure of the three different breeding modes.

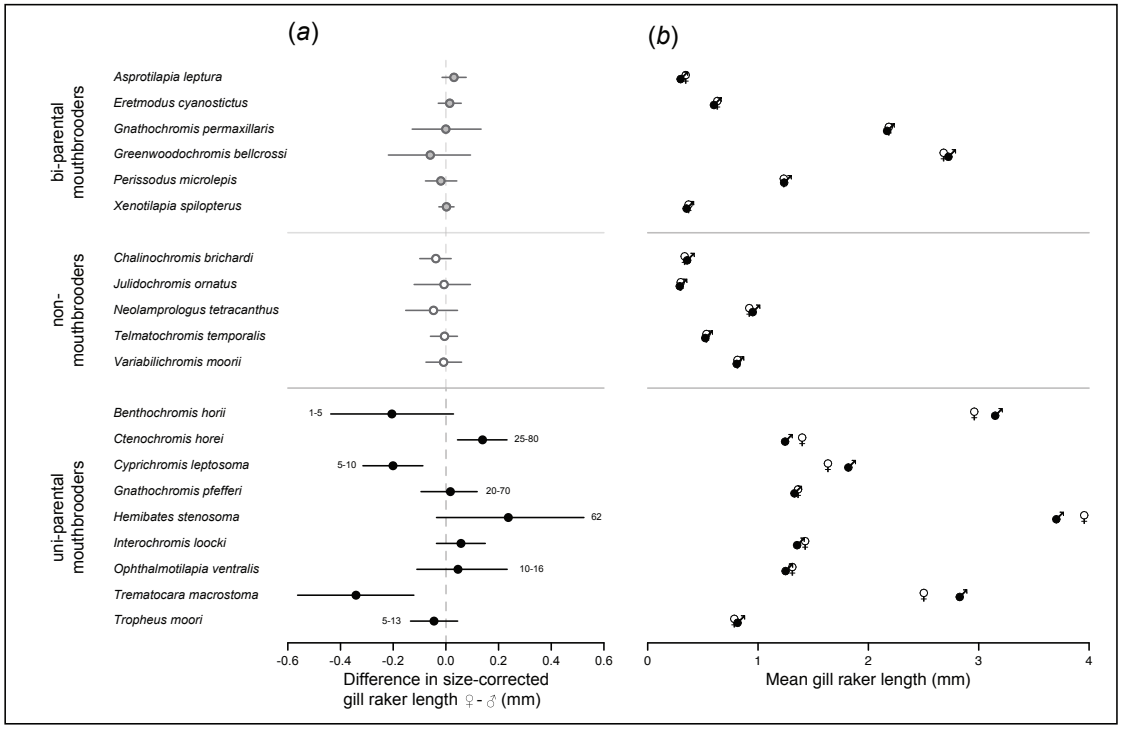

Figure S2: Sexual dimorphism in gill raker lengths. *(a)* Mean gill raker length for either sex of each species, illustrating the extent and the direction of sexual dimorphism with respect to the actual gill raker length. The realized trait value in females (mouthbrooding sex) in respect to males does not show a shift in trait values towards a certain gill raker length across all species (optimum), suggesting more than one optimum for mouthbrooding. *(b)* Difference in size-corrected gill raker length for each species. Numbers next to the data points indicate clutch size [1].

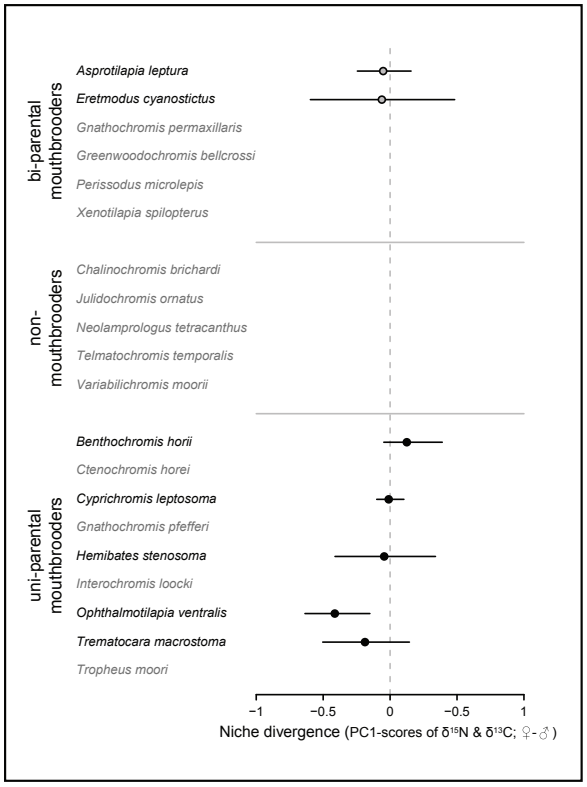

Figure S3: Niche divergence between males and females: Difference in PC1-scores ($\delta^{15}N$ and $\delta^{13}C$ stable isotope signatures) between the sexes showed no evidence for niche divergence between males and females in uni-parental mouthbrooders that are sexually dimorphic in gill raker morphology. Due to missing sex information in the stable isotope data only a subset of species was tested with a very reduced sample size per species (see supplementary table S1). Note that in *Ophthalmotilapia ventrails*, the only species with divergent niche use, males and females differ in habitat preference: While males are territorial in the shallows, females school in deeper waters. Therefore, it is not surprising that the sexes differ in their stable isotope signatures (especially in $\delta^{13}C$).

Table S1: Overview of all 65 Tanganyika cichlid species investigated in this study, including information on taxonomy (species and tribes), breeding mode, and sample sizes. Number of gill raker measurements taken from Muschick et al. [2] are given in brackets.

species information				gill raker measurements					stable isotope analysis			comments	food type (data from [1])
species abb.	full name	tribe	breeding mode	N_{males}	$N_{females}$	N_{total} newly aquired for this study	N_{total} taken from [2]	N_{total} total	N_{males}	$N_{females}$	N_{total}		
Altcal	*Altolamprologus calvus*	Lamprologini	non-mouthbrooder (substrate brooder)	0	1	0	(+1)	1	3	NA	10		
Altcom	*Altolamprologus compressiceps*	Lamprologini	non-mouthbrooder (substrate brooder)	2	1	3	(+11)	14	NA	1	10		
Asplep	*Asprotilapia leptura*	Ectodini	bi-parental mouthbrooder	14	15	27	(+8)	35	4	5	10	tested for sexual dimorphism	aufwuchs
Astbur	*Astatotilapia burtoni*	Haplochromini	uni-parental mouthbrooder (maternal)	6	2	0	(+10)	10	4	3	10		
Auldew	*Aulonocranus dewindti*	Ectodini	uni-parental mouthbrooder (maternal)	1	NA	1	(+11)	12	2	3	10		
Benhor	*Benthochromis horii*	Benthochromini	uni-parental mouthbrooder (maternal)	14	7	19	(+3)	22	6	4	10	tested for sex dimorphism	zooplankton
Calmac	*Callochromis macrops*	Ectodini	uni-parental mouthbrooder (maternal)	1	NA	0	(+10)	10	5	2	10		
Chabri	*Chalinochromis brichardi*	Lamprologini	non-mouthbrooder (substrate brooder)	5	5	9	(+4)	13	3	1	10	tested for sex dimorphism	picks sponges & inverebrates
Cphgib	*Cyphotilapia gibberosa*	Cyphotilapiini	uni-parental mouthbrooder (maternal)	2	4	0	(+8)	8	4	1	10		
Ctehor	*Ctenochromis horei*	Tropheini	uni-parental mouthbrooder (maternal)	16	16	30	(+10)	40	6	NA	10	tested for sex dimorphism	picks tiny shrimps & sift worms from sand
Cyafur	*Cyathopharynx furcifer*	Ectodini	uni-parental mouthbrooder (maternal)	4	NA	0	(+9)	9	6	4	10		
Cypcol	*Cyprichromis coloratus*	Cyprichromini	uni-parental mouthbrooder (maternal)	2	1	3		3	5	2	10		
Cyplep	*Cyprichromis leptosoma*	Cyprichromini	uni-parental mouthbrooder (maternal)	17	15	31	(+11)	42	5	4	10	tested for sexual dimorphism	zooplankton
Enamel	*Enantiopus melanogenys*	Ectodini	uni-parental mouthbrooder (maternal)	1	5	0	(+7)	7	9	1	10		
Erecya	*Eretmodus cyanostictus*	Eretmodini	bi-parental mouthbrooder	15	15	30	(+9)	39	4	6	10	tested for sexual dimorphism	filamentous algae
Gnaper	*Gnathochromis permaxillaris*	Limnochromini	bi-parental mouthbrooder	19	16	35		35	NA	NA	10	tested for sexual dimorphism	sucks tiny invertebras from muddy bottom
Gnapfe	*Gnathochromis pfefferi*	Tropheini	uni-parental mouthbrooder (maternal)	7	12	18	(+8)	26	2	2	10	tested for sexual dimorphism	picks shrimps form the substrate
Gralem	*Grammatotria lemairii*	Ectodini	uni-parental mouthbrooder (maternal)	NA	1	0	(+4)	4	3	2	10		
Gwcabe	*Greenwoodochromis abeelei*	Limnochromini	bi-parental mouthbrooder	2	6	8		8	4	1	10		
Gwcbel	*Greenwoodochromis bellcrossi*	Limnochromini	bi-parental mouthbrooder	15	7	22		22	1	1	10	tested for sexual dimorphism	small fish or shrimps (speculative)
Hapmic	*Haplotaxodon microlepis*	Perissodini	bi-parental mouthbrooder	1	2	0	(+15)	15	7	2	10		
Hemste	*Hemibates stenosoma*	Bathybatini	uni-parental mouthbrooder (maternal)	13	11	25		25	6	4	10	tested for sexual dimorphism	small fish
Intloo	*Interochromis loocki*	Tropheini	uni-parental mouthbrooder (maternal)	17	15	31	(+10)	41	1	2	10	tested for sexual dimorphism	diatoms & cyanobacteria
Julorn	*Julidochromis ornatus*	Lamprologini	non-mouthbrooder (substrate brooder)	5	3	7	(+8)	15	NA	NA	10	tested for sexual dimorphism	picks sponges & inverebrates
Lamcal	*Lamprologus callipterus*	Lamprologini	non-mouthbrooder (substrate brooder)	5	NA	3	(+12)	15	1	4	10		
Lamlem	*Lamprologus lemairii*	Lamprologini	non-mouthbrooder (substrate brooder)	1	NA	1	(+5)	6	3	2	10		
Lepatt	*Lepidiolamprologus attenuatus*	Lamprologini	non-mouthbrooder (substrate brooder)	NA	NA	0	(+10)	10	4	3	10		
Lepelo	*Lepidiolamprologus elongatus*	Lamprologini	non-mouthbrooder (substrate brooder)	NA	1	0	(+10)	10	1	1	10		
Leppro	*Lepidiolamprologus profundicola*	Lamprologini	non-mouthbrooder (substrate brooder)	2	2	0	(+5)	5	3	6	10		
Limdar	*Limnotilapia dardennii*	Tropheini	uni-parental mouthbrooder (maternal)	NA	2	2	(+8)	10	3	5	10		
Loblab	*Lobochilotes labiatus*	Tropheini	uni-parental mouthbrooder (maternal)	NA	3	0	(+15)	15	1	2	10		
Neocau	*Neolamprologus caudopunctatus*	Lamprologini	non-mouthbrooder (substrate brooder)	1	5	5	(+10)	15	2	4	10		
Neofas	*Neolamprologus fasciatus*	Lamprologini	non-mouthbrooder (substrate brooder)	5	1	5	(+10)	15	5	NA	10		
Neofur	*Neolamprologus furcifer*	Lamprologini	non-mouthbrooder (substrate brooder)	NA	NA	0	(+1)	1	4	3	10		
Neomod	*Neolamprologus modestus*	Lamprologini	non-mouthbrooder (substrate brooder)	3	NA	3	(+9)	12	6	1	10		
Neomon	*Neolamprologus mondabu*	Lamprologini	non-mouthbrooder (substrate brooder)	NA	NA	0	(+4)	4	5	5	10		
Neomux	*Neolamprologus mustax*	Lamprologini	non-mouthbrooder (substrate brooder)	NA	NA	0	(+2)	2	4	3	10		
Neopro	*Neolamprologus prochilus*	Lamprologini	non-mouthbrooder (substrate brooder)	NA	NA	0	(+1)	1	4	4	10		
Neopul	*Neolamprologus pulcher*	Lamprologini	non-mouthbrooder (substrate brooder)	2	NA	2	(+11)	13	NA	NA	10		
Neosav	*Neolamprologus savoryi*	Lamprologini	non-mouthbrooder (substrate brooder)	2	NA	1	(+11)	12	3	NA	10		
Neosex	*Neolamprologus sexfasciatus*	Lamprologini	non-mouthbrooder (substrate brooder)	NA	2	0	(+8)	8	5	2	10		
Neotet	*Neolamprologus tetracanthus*	Lamprologini	non-mouthbrooder (substrate brooder)	5	4	8	(+6)	14	2	NA	10	tested for sexual dimorphism	snails
Ophnas	*Ophthalmotilapia nasuta*	Ectodini	uni-parental mouthbrooder (maternal)	NA	2	0	(+5)	5	5	5	10		
Ophven	*Ophthalmotilapia ventralis*	Ectodini	uni-parental mouthbrooder (maternal)	16	12	27	(+11)	38	5	5	10	tested for sexual dimorphism	phytoplankton & aufwuchs
Pcybri	*Paracyprichromis brieni*	Cyprichromini	uni-parental mouthbrooder (maternal)	1	NA	1	(+5)	6	4	4	10		
Permic	*Perissodus microlepis*	Perissodini	bi-parental mouthbrooder	15	21	30	(+10)	40	1	1	10	tested for sexual dimorphism	fish scales
Peteph	*Petrochromis ephippium*	Tropheini	uni-parental mouthbrooder (maternal)	NA	1	0	(+5)	5	NA	NA	10		
Petfam	*Petrochromis famula*	Tropheini	uni-parental mouthbrooder (maternal)	NA	3	0	(+10)	10	3	NA	10		
Petfas	*Petrochromis fasciolatus*	Tropheini	uni-parental mouthbrooder (maternal)	1	0	1		1	3	3	10		
Petmac	*Petrochromis macrognathus*	Tropheini	uni-parental mouthbrooder (maternal)	NA	2	0	(+10)	10	6	3	10		
Petpol	*Petrochromis polyodon*	Tropheini	uni-parental mouthbrooder (maternal)	2	NA	0	(+7)	7	2	4	10		
Plestr	*Plecodus straeleni*	Perissodini	bi-parental mouthbrooder	NA	2	0	(+10)	10	6	2	10		
Psccur	*Pseudosimochromis curvifrons*	Tropheini	uni-parental mouthbrooder (maternal)	3	2	0	(+10)	10	5	4	10		
Simdia	*Simochromis diagramma*	Tropheini	uni-parental mouthbrooder (maternal)	NA	2	0	(+10)	10	1	5	10		
Teldho	*Telmatochromis dhonti*	Lamprologini	non-mouthbrooder (substrate brooder)	3	0	3		3	NA	NA	10		
Teltem	*Telmatochromis temporalis*	Lamprologini	non-mouthbrooder (substrate brooder)	5	4	9	(+4)	13	6	NA	10	tested for sexual dimorphism	filamentous algea, plankton
Tremac	*Trematocara macrostoma*	Trematocarini	uni-parental mouthbrooder (maternal)	8	7	15		15	6	4	10	tested for sexual dimorphism	fish or zooplankton (speculative)
Tremar	*Trematocara marginatum*	Trematocarini	uni-parental mouthbrooder (maternal)	0	1	1		1	7	5	12		
Trenig	*Trematocara nigrifrons*	Trematocarini	uni-parental mouthbrooder (maternal)	0	12	12		12	5	15	20		
Treuni	*Trematocara unimaculatum*	Trematocarini	uni-parental mouthbrooder (maternal)	7	3	10		10	4	2	9		
Tromoo	*Tropheus moorii*	Tropheini	uni-parental mouthbrooder (maternal)	15	16	30	(+10)	40	2	NA	10	tested for sexual dimorphism	filamentous algea
Tylpol	*Tylochromis polylepis*	Tylochromini	uni-parental mouthbrooder (maternal)	NA	NA	0	(+3)	3	6	2	10		
Varmoo	*Variabilichromis moorii*	Lamprologini	non-mouthbrooder (substrate brooder)	6	9	9	(+10)	19	NA	NA	10	tested for sexual dimorphism	filamentous algea, diatoms, ostracods
Xenfla	*Xenotilapia flavipinnis*	Ectodini	bi-parental mouthbrooder	1	1	0	(+7)	7	NA	NA	10		
Xenspi	*Xenotilapia spilopterus*	Ectodini	bi-parental mouthbrooder	17	15	31	(+5)	36	1	1	10	tested for sexual dimorphism	insect larvea, rarely zooplankton
Total	***65 species***	***13 tribes***	***3 breeding modes***	***305***	***295***	***508***	***(+427)***	***935***	***224***	***161***	***661***	***20 species***	

Table S2: Summary tables of tests for sexual dimorphism in 20 cichlid species, and for the association between sexual dimorphism and breeding mode. Statistically significant p-values ($p < 0.05$) are highlighted in bold. *(a)* Testing for a difference in mean size-corrected gill raker length between females and males within each species. *(b)* Testing mean dimorphism per breeding mode for deviation from zero. *(c)* ANOVA statistics on mean absolute dimorphism among the breeding modes. *(d)* Pairwise comparisons of absolute difference in mean sexual dimorphism in gill raker length among breeding modes.

(*a*)

breeding mode	species	difference f-m	CI_{min}	CI_{max}	*p*-value
bi-parental mouthbrooders	*Asprotilapia leptura*	0.031	-0.014	0.077	0.208
	Eretmodus cyanostictus	0.015	-0.029	0.058	0.535
	Gnathochromis permaxillaris	0.000	-0.128	0.134	0.998
	Greenwoodochromis bellcrossi	-0.059	-0.218	0.093	0.476
	Perissodus microlepis	-0.019	-0.077	0.041	0.571
	Xenotilapia spilopterus	0.002	-0.027	0.031	0.895
non-mouthbrooders	*Chalinochromis brichardi*	-0.038	-0.099	0.020	0.276
	Julidochromis ornatus	-0.007	-0.120	0.093	0.889
	Neolamprologus tetracanthus	-0.047	-0.152	0.044	0.391
	Telmatochromis temporalis	-0.005	-0.059	0.044	0.853
	Variabilichromis moorii	-0.009	-0.076	0.060	0.828
uni-parental mouthbrooders	*Benthochromis horii*	-0.205	-0.437	0.029	0.126
	Ctenochromis horei	0.139	0.044	0.232	***0.006***
	Cyprichromis leptosoma	-0.201	-0.315	-0.087	***0.003***
	Gnathochromis pfefferi	0.017	-0.094	0.119	0.758
	Hemibates stenosoma	0.237	-0.035	0.524	0.111
	Interochromis loocki	0.057	-0.036	0.150	0.252
	Ophthalmotilapia ventralis	0.046	-0.110	0.233	0.611
	Trematocara macrostoma	-0.341	-0.563	-0.122	***0.014***
	Tropheus moori	-0.045	-0.134	0.045	0.34

(*b*)

breeding mode	$mean_{mode}$	CI_{min}	CI_{max}	*p*-value
bi-parental mouthbrooders	-0.005	-0.029	0.015	0.722
non-mouthbrooders	-0.021	-0.037	-0.006	0.068
uni-parental mouthbrooders	-0.033	-0.152	0.079	0.617

(*c*)

model	F-statistics	*p*-value lm()	*p-value phylANOVA()*
abs(dimorphism) ~ mode	F = 6.19	***0.007***	**0.17**

(*d*)

comparison	mean difference	*p*-value lm()	*p-value phylANOVA()*
difference abs(**UNI**) *vs.* abs(**BI**)	0.122	***0.015***	***0.031***
difference abs(**UNI**) *vs.* abs(**NON**)	0.122	***0.022***	0.172
difference abs(**NON**) *vs.* abs(**BI**)	<0.001	0.995	1.000

Table S3: Summary of the break-point model fitted to investigate the association between sexual dimorphism in gill raker length with trophic ecology within uni-parental mouthbrooders. Statistically significant p-values ($p < 0.05$) are highlighted in bold.

model	lm()				davies.test()	segmented.lm()			phylANOVA()	
	R^2	adjusted R^2	F-statistics	*p* -value	*p* -value	R^2	breakpoint	adjusted R^2	t-statistics	*p* -value
$dimorph_{UNI}$ ~ $PC1_{UNI}$	0.56	0.50	8.92	***0.020***	***0.044***	0.87	0.344	0.796	-	-
$dimorph_{UNI(PC1<0.34)}$ *vs.* $dimorph_{UNI(PC1>0.34)}$	-	-	-	-	-	-	-	-	4.8	***0.001***

References

1. Konings A. 2015 Tanganyika Cichlids in their natural habitat. 3th Editio. El Paso: Cichlid Press.
2. Muschick M, Nosil P, Roesti M, Dittmann MT, Harmon L, Salzburger W. 2014 Testing the stages model in the adaptive radiation of cichlid fishes in East African Lake Tanganyika. Proc. R. Soc. B Biol. Sci. 281, 20140605–20140605. (doi:10.1098/rspb.2014.0605)

Part II | Side Projects

Chapter 4

Adaptive divergence between lake and stream populations of an East African cichlid fish

Anya Theis*, **Fabrizia Ronco***, Adrian Indermaur, Walter Salzburger & Bernd Egger

Molecular Ecology (2014)

This project was partly conducted during my master thesis and partly in the early phase of my PhD. I contributed to the study design, fieldwork, data collection, conducting the experiment, data analysis and writing of the manuscript.

MOLECULAR ECOLOGY

Molecular Ecology (2014) **23**, 5304–5322 doi: 10.1111/mec.12939

Adaptive divergence between lake and stream populations of an East African cichlid fish

ANYA THEIS,[1] FABRIZIA RONCO,[1] ADRIAN INDERMAUR, WALTER SALZBURGER and BERND EGGER

Zoological Institute, University of Basel, Vesalgasse 1, 4051 Basel, Switzerland

Abstract

Divergent natural selection acting in different habitats may build up barriers to gene flow and initiate speciation. This speciation continuum can range from weak or no divergence to strong genetic differentiation between populations. Here, we focus on the early phases of adaptive divergence in the East African cichlid fish *Astatotilapia burtoni*, which occurs in both Lake Tanganyika (LT) and inflowing rivers. We first assessed the population structure and morphological differences in *A. burtoni* from southern LT. We then focused on four lake–stream systems and quantified body shape, ecologically relevant traits (gill raker and lower pharyngeal jaw) as well as stomach contents. Our study revealed the presence of several divergent lake–stream populations that rest at different stages of the speciation continuum, but show the same morphological and ecological trajectories along the lake–stream gradient. Lake fish have higher bodies, a more superior mouth position, longer gill rakers and more slender pharyngeal jaws, and they show a plant/algae and zooplankton-biased diet, whereas stream fish feed more on snails, insects and plant seeds. A test for reproductive isolation between closely related lake and stream populations did not detect population-assortative mating. Analyses of F1 offspring reared under common garden conditions indicate that the detected differences in body shape and gill raker length do not constitute pure plastic responses to different environmental conditions, but also have a genetic basis. Taken together, the *A. burtoni* lake–stream system constitutes a new model to study the factors that enhance and constrain progress towards speciation in cichlid fishes.

Keywords: adaptive divergence, *Astatotilapia burtoni*, East African cichlid fishes, Lake Tanganyika, lake–stream system, speciation continuum

Received 29 July 2014; revision received 19 September 2014; accepted 22 September 2014

Introduction

Different environmental conditions constitute a major source of divergent natural selection between populations (reviewed in Schluter 2000; Nosil 2012). Adaptation to divergent habitats may ultimately lead to speciation, for example when reproductive isolation builds up as by-product of adaptive divergence ('ecological speciation'), or when different mutations become fixed in geographically separated populations adapting to similar environments ('mutation-order speciation') (Rundle & Nosil 2005; Schluter 2009). Both scenarios imply that speciation is a gradual process, which is evidenced by empirical data demonstrating substantial variation in the level of divergence between adjacent populations, even along environmental clines that are free of geographical barriers (Hendry *et al.* 2000; Schluter 2000; Rundle & Nosil 2005; Butlin *et al.* 2008; Mallet 2008; Berner *et al.* 2009; Nosil *et al.* 2009). This so-called speciation continuum can range from weak or no divergence between populations to strong genetic differentiation between what might then be novel pairs of sister species (Hendry *et al.* 2009; Nosil *et al.* 2009). What determines the strength of divergence between populations remains poorly understood, though.

Correspondence: Walter Salzburger and Bernd Egger, Fax: +41 61 267 0301; E-mails: walter.salzburger@unibas.ch and bernd.egger@unibas.ch

[1]These authors contributed equally to this work.

Adaptive divergence has mainly been studied in settings involving populations that differ in their degree of reproductive isolation, such as in stick insects (Nosil & Sandoval 2008), mosquitofish (Langerhans *et al.* 2007) or *Heliconius* butterflies (Mallet & Dasmahapatra 2012). Important model systems in fishes are three-spine sticklebacks and salmonids, which often occur along discrete environmental gradients such as marine–freshwater and/or lake–stream habitats (e.g. Hendry *et al.* 2000; Berner *et al.* 2008; Jones *et al.* 2012; Roesti *et al.* 2012). Stickleback lake–stream populations, for example, differ with regard to resource use and are morphologically distinct, with limnetic-foraging lake forms typically displaying shallower bodies and more and longer gill rakers than the benthic-foraging stream types (Schluter & McPhail 1992; Berner *et al.* 2008). The extent of divergence between lake and stream population pairs depends on the strength of divergent selection, on the level of gene flow and on the time since divergence (Hendry & Taylor 2004; Berner *et al.* 2010; Roesti *et al.* 2012; Hendry *et al.* 2013; Lucek *et al.* 2013). Studies in sticklebacks and salmonids also uncovered that diversification may proceed rapidly (see e.g. Hendry *et al.* 2007). In the sockeye salmon (*Oncorhynchus nerka*), for example, it took about a dozen of generations only until reproductive isolation occurred between two adjacent beach and stream populations that diverged after an introduction event (Hendry *et al.* 2000). However, ecological divergence might also fail to generate the evolution of reproductive isolation barriers (Raeymaekers *et al.* 2010).

In this study, we focus on the early phases of adaptive divergence in a prime model system for evolutionary biology, the East African cichlid fishes (see e.g. Kocher 2004; Salzburger 2009; Santos & Salzburger 2012). More specifically, we examine eco-morphological and genetic divergence in *Astatotilapia burtoni* (Günther 1894), which occurs both in East African Lake Tanganyika (LT) and inflowing rivers. Although *A. burtoni* is one of the most important cichlid model species in various fields of research including developmental biology, neurobiology, genetics and genomics, and behavioural biology (see e.g. Wickler 1962; Robison *et al.* 2001; Hofmann 2003; Lang *et al.* 2006; Salzburger *et al.* 2008; Baldo *et al.* 2011; Theis *et al.* 2012; Santos *et al.* 2014) and represents one of the five cichlid species whose genome has recently been sequenced (Brawand *et al.* 2014), surprisingly little is known about its ecology, phylogeographic distribution, population structure or genetic and phenotypic diversity in the wild.

Taxonomically, *A. burtoni* belongs to the Haplochromini, the most species-rich group of cichlids. Within the haplochromines, *A. burtoni* is nested in the derived 'modern' clade (as defined in Salzburger *et al.* 2005), the members of which are characterized by a pronounced sexual colour dimorphism with typically brightly coloured males and inconspicuous females, a polygynandrous mating system with maternal mouthbrooding, as well as egg-spots on the anal fin of males. The vast majority of haplochromines is endemic to a specific lake or river system, respectively, and specialized to certain habitat types therein. Only very few cichlid species exist that commonly occur in both truly riverine and lacustrine habitats. *Astatotilapia burtoni* is such a habitat generalist, inhabiting the shallow zones of LT as well as rivers and streams surrounding LT (Fernald & Hirata 1977; De Vos *et al.* 2001; Kullander & Roberts 2011), and thus represents an ideal species to study adaptive divergence across an environmental gradient in cichlid fishes.

So far, adaptive divergence in cichlids has mainly been investigated within lakes, for example along depth or habitat gradients (see e.g. Barluenga *et al.* 2006; Seehausen *et al.* 2008). In our study, we targeted divergence along a lake–stream environmental gradient to test whether similar mechanisms are involved in divergence along this habitat gradient as in other groups of fishes. To this end, we first established phylogeographic relationships and assessed the population structure in *A. burtoni* from the southern part of the LT drainage using mtDNA and microsatellite markers. Second, we examined morphological differences between these populations by analysing body shape, a complex quantitative trait encompassing morphological variation associated with multiple ecological factors (Webb 1984). We then focused on four lake–stream systems in detail. In addition to the body shape and population-genetic analyses, we quantified several ecologically relevant traits in these replicate lake–stream population groups, including the gill raker apparatus, which is known to respond to distinct feeding modes in fishes. The number and length of gill rakers have been identified as key elements influencing prey capture and handling in stickleback (Bentzen & McPhail 1984; Lavin & McPhail 1986; Schluter 1993, 1995; Robinson 2000). Furthermore, we examined the pharyngeal jaw apparatus, a highly diverse trait in cichlids linked to trophic diversification (Galis & Drucker 1996; Hulsey *et al.* 2006; Muschick *et al.* 2012), and used stomach content analysis as a proxy for divergent selection acting on foraging morphology. We then tested whether there were associations between shifts in resource use and trophic morphology along the lake–stream gradient that might reflect ecologically based adaptive divergence (Berner *et al.* 2009; Harrod *et al.* 2010). Finally, we conducted a mating experiment to test for reproductive isolation among a lake and stream populations. Additionally, offspring from this common garden setting was used to

evaluate levels of phenotypic plasticity in adaptive traits such as body shape and gill raker morphology.

Materials and methods

Study populations and sampling

Sampling of *A. burtoni* was carried out between February 2010 and July 2013 in the southern basin of LT and in inflowing rivers and streams, with a particular emphasis on four river systems, the Kalambo River, the Chitili Creek, the Lunzua River and the Lufubu River (Figs 1A and 2A) (see Appendix S1, Supporting information for a detailed description of these river systems). Specimens were collected using hook and line fishing, minnow traps and gill nets under the permission of the LT Research Unit, Department of Fisheries, Republic of Zambia. In total, we sampled 22 populations (several of these multiple times), resulting in a data set comprising 1425 individuals (see Tables S1 and S2A, Supporting information for details). Specimens were anaesthetized using clove oil (2–3 drops clove oil per litre water) and photographed in a standardized manner for morphometric analyses; a fin clip was taken and stored in ethanol (96%) for a DNA sample; specimens for gill raker measurements, pharyngeal jaw and stomach content analyses were preserved in ethanol (96%).

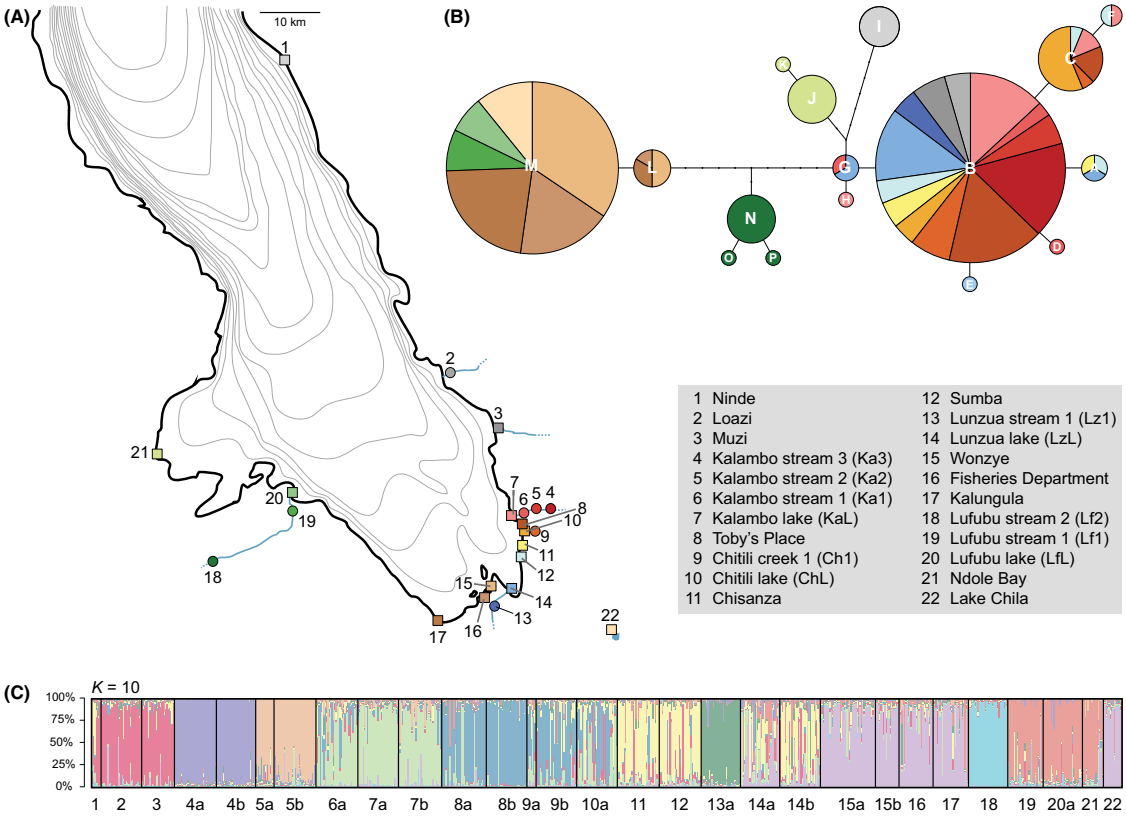

Fig. 1 Sampling locations and genetic differentiation among all populations revealed by microsatellite and mtDNA analyses. (A) The 22 sampling localities indicated by numbers on the southern part of LT (squares represent lake and circles stream populations; bathymetric lines are placed at every 100 m water depth, after Coulter 1991). Names of localities are listed in the grey box. (B) Haplotype genealogy based on mtDNA showing the 16 haplotypes (A–P) and the deep split between eastern (populations 2–14; haplotypes A–H) and western (populations 15–17, 19–20; haplotypes L and M) populations. Each colour represents a locality, which correspond to the colours on the map. (C) Structure plot based on nine microsatellite loci for all populations: the 29 population samples from 22 localities (names in the grey box; 'a' and 'b' refer to different sampling years, note that not all sampling years were analysed) group in 10 genetic clusters ($K = 10$; colours representing these clusters are decoupled from the population colours in the map). LT, Lake Tanganyika.

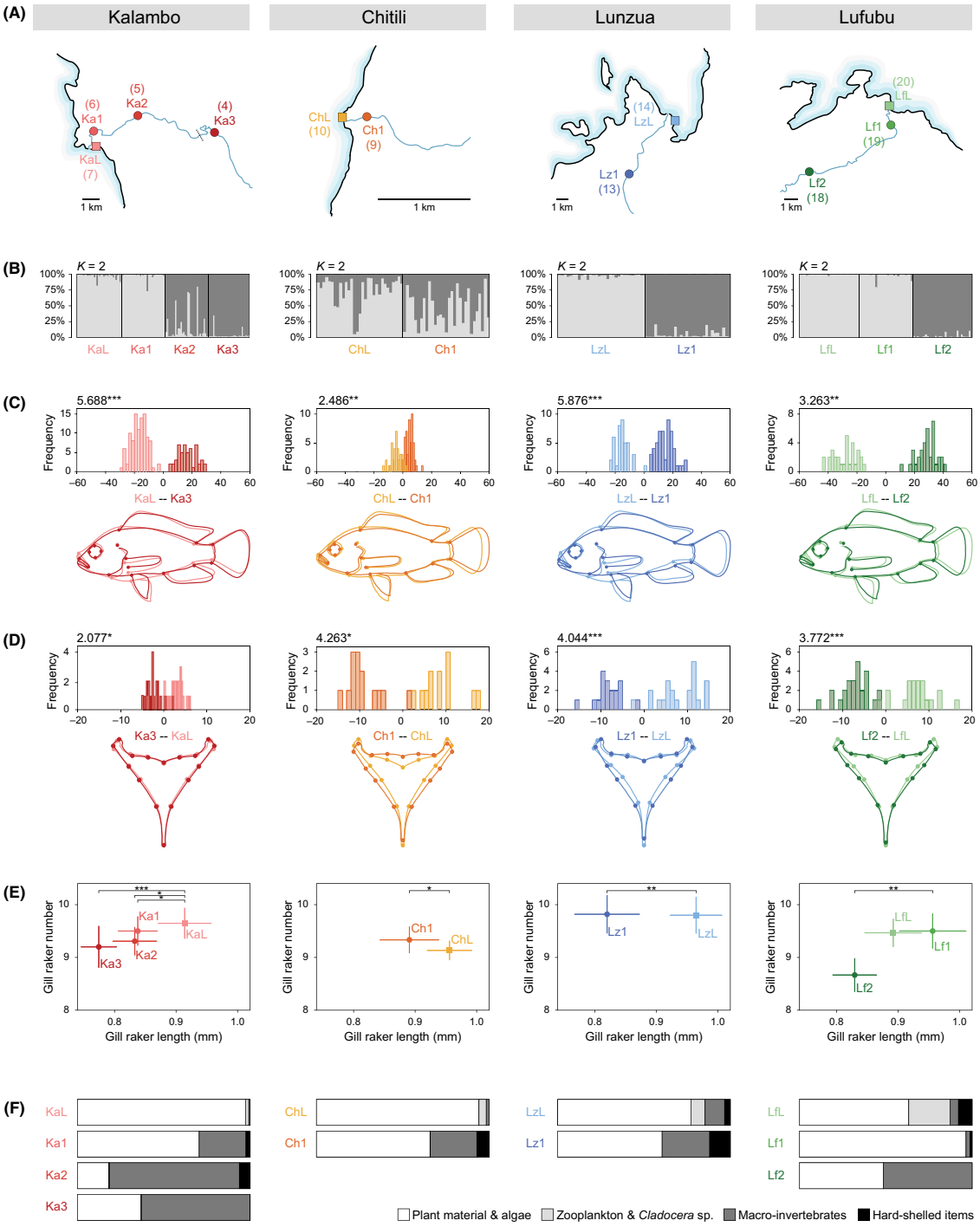

Fig. 2 Divergence between lake and stream habitats in four systems. (A) Maps showing sampling localities for each lake–stream system (see grey box in Fig. 1 for full names of localities). (B) Structure plots for each lake–stream system (shades of grey represent different genetic clusters; K = number of genetic clusters). (C) Discriminant scores of body shape comparisons and corresponding landmark shifts from the discriminant function analyses (DFA) between the lake population and the most upstream population for each lake–stream system show that lake fish generally have a deeper body and a more superior mouth position compared with stream fish. DF differences are always increased threefold in the outlines, which are drawn for illustration purposes only. DFA results are indicated with Mahalanobis distances on top of the DF score plots. (D) Discriminant scores of lower pharyngeal jaw (LPJ) shape comparisons and corresponding landmark shifts from the DFA between the lake population and the most upstream population for each lake–stream system show that lake fish generally have a slender and more elongated LPJ compared with stream fish. (E) Differences in size corrected male gill raker length and number between populations within each lake–stream system. Error bars represent 95% confidence intervals of the means. Lake fish generally have longer gill rakers compared with stream fish (Table S6, Supporting information). (F) Averaged proportions of the different stomach content categories for each population. Generally, lake fish feed more on softer and smaller food particles, whereas stream populations feed more on hard-shelled and larger food items. Significance levels: $*P < 0.05$, $**P < 0.01$ and $***P < 0.0001$.

Water current measurements

Surface water current and microhabitat current (measured directly where the fish were sighted) were determined at 10 sampling sites in July 2013. The flow regime differs between dry and wet season; however, relative differences between sampling sites are likely to be consistent. Surface current was estimated by measuring the time a float (0.5 L plastic bottle filled with 0.25 L water) travelled 10 m downstream. Measurements were taken five times at each site, and the velocity was calculated from the average of these measurements. For microhabitat current, we determined the relative level of water motion in lake and stream habitats as a proxy. To this end, we used Life Savers candies (wint-o-green flavour, individually wrapped variety; $N = 5$) to measure the relative rate of dissolution (which is directly related to water current), following the method described by Koehl & Alberte (1988). Life Savers were either tied to plants or were hand-held into the underwater habitat using a stick and line and left to dissolve for 6 min. Additionally, a baseline dissolution rate was determined by placing a candy in a bucket filled with water from the respective site (no current) for 6 min. We determined the weight of each candy before and after treatment (dried at ambient temperature for at least 2 h) to calculate the mass (g) lost relative to the baseline.

Genetics

Total DNA was extracted from fin clips preserved in ethanol applying a proteinase K digestion followed by either a high-salt (Bruford *et al.* 1998) or a MagnaPure extraction using a robotic device (MagnaPure LC; Roche Diagnostics), following the manufacturer's protocol (Roche, Switzerland). We first determined the DNA sequence of a 369-bp segment of the mitochondrial control region for 5–40 samples per location (total $N = 359$, Table S1, Supporting information) using published primers (Kocher *et al.* 1989; Salzburger *et al.* 2002). The PCR fragments of the control region were purified using ExoSAP-IT (USB), directly sequenced with the BigDye sequencing chemistry (Applied Biosystems) and analysed on an ABI 3130*xl* genetic analyzer (Applied Biosystems). Mitochondrial DNA sequences were aligned using CODONCODE ALIGNER (v.3.5; CodonCode Corporation). A maximum-likelihood analysis, using the GTR + G + I as suggested by JMODELTEST (Posada 2008), was carried out in PAUP*4.0b10 (Swofford 2002) to construct an unrooted mitochondrial haplotype genealogy following the method described in Salzburger *et al.* (2011).

A total of 786 individuals (Table S1, Supporting information) were genotyped at the following nine microsatellite loci: Ppun5, Ppun7, Ppun21 (Taylor *et al.* 2002), UNH130, UNH989 (Lee & Kocher 1996), Abur82 (Sanetra *et al.* 2009), HchiST46, HchiST68 (Maeda *et al.* 2009) and Pzeb3 (Van Oppen *et al.* 1997). Fragment size calling was carried out on an ABI 3130*xl* genetic analyzer (Applied Biosystems) in comparison with the LIZ 500(−250) internal size standard. Genotypes were determined manually using PEAK SCANNER (v.1.0; Applied Biosystems). Microsatellite scoring data were examined and rounded to valid integers using TANDEM (Matschiner & Salzburger 2009). The microsatellite data were used to calculate population pairwise F_{ST} values in ARLEQUIN (v.3.5.1.2; Schneider *et al.* 1999) and D_{EST} (Jost 2008) using the package DEMETICS (Gerlach *et al.* 2010) in R (v.3.1.0; R Development Core Team 2014). STRUCTURE (v.2.3.3; Pritchard *et al.* 2000) was then used to infer population structure. First, all 29 populations (22 localities, seven of which were sampled twice in different years) were run in a joint analysis (Markov chain Monte Carlo simulations were run for 500 000 replications, burn in = 50 000, admixture and correlated allele frequency options). Ten replicated simulations were performed for $K = 1$–16, and the most likely number of genetic clusters was inferred using the ΔK method (Evanno *et al.* 2005) implemented in the software HARVESTER (Earl & von Holdt 2012). Then, each lake–stream system

was analysed separately using the same parameters as described above and K = 1–10 for Kalambo, K = 1–6 for Lufubu, Chitili and Lunzua.

To test for isolation by distance, we conducted a simple Mantel test in R (package ecodist, Goslee & Urban 2007) using the genetic distance (pairwise F_{ST} values) and the geographic distance in metres between sites measured along the shoreline on Google Earth. For this analysis, only populations from the LT shoreline were used (N_{pop} = 13) and all riverine populations (2, 4–6, 9, 13, 18, 19; see Fig. 1) and the population from Lake Chila (22) were excluded.

Body shape

The photographs of 791 individuals (Table S1, Supporting information) were used for geometric morphometric analyses by recording the coordinates of 17 homologous landmarks (Fig. S1A, Supporting information; for details see Muschick *et al.* 2012) using TPSDIG2 (v.2.11; Rohlf 2008). The x and y coordinates were transferred to the program MORPHOJ (v.1.05f; Klingenberg 2011) and superimposed with a Procrustes generalized least squares fit (GLSF) algorithm to remove all nonshape variation (Rohlf & Slice 1990). Additionally, the data were corrected for allometric size effects using the residuals of the regression of shape on centroid size for further analyses. Canonical variate analyses (CVA; Mardia *et al.* 1979) were used to assess shape variation when several populations were compared, and discriminant function analyses (DFA) were performed for comparisons between two populations only (i.e. within some lake–stream systems). The mean shape distances of CV and DF analyses were obtained using permutation tests (10 000 permutations). Although males and females show strong body shape differences, the pooled data revealed the same results as the separate analyses for each sex (data not shown), presumably because intersexual within-population differences are smaller than intrasexual differences among populations (Fig. S2, Supporting information). Therefore, both sexes were combined in the analyses presented.

In a first step, we conducted a CVA for 20 populations and another one for the 11 shoreline populations only to test whether the clustering in morphospace shows signs of isolation by distance. Further tests for morphological isolation by distance were conducted with a simple Mantel test in the ecodist package in R using the morphological (Mahalanobis) and the geographic distance (measured in metres along the shoreline). In a second step, the lake–stream populations were tested within each system as well as in a combined data set.

Finally, we also performed a CVA focusing on the mouth position (landmarks 1, 2, 7 and 12, capturing mouth angle; Fig. S1A, Supporting information). We only used male individuals here, as this trait shows a much stronger sexual dimorphism compared with, for example, body shape.

Gill raker morphology

Following Berner *et al.* (2008), we counted gill raker number and measured the length of the 2nd, 3rd and 4th gill raker of the right first branchial arch and calculated the mean for each of 281 individuals collected from the four lake–stream systems (Table S1, Supporting information). As average gill raker length correlated positively with standard length (SL) in both sexes (males: regression, $R^2 = 0.8432$, $P < 0.0001$; females: regression, $R^2 = 0.5477$, $P < 0.0001$), mean gill raker length was regressed to SL for size correction. The individual residuals from the common within-group slope were then added to the expected gill raker length at grand mean SL (male = 0.879 mm, female = 0.783 mm) to maintain the original measurement unit. These values represent a size-independent gill raker length and were used for the comparisons between populations within each lake–stream system separately applying an ANOVA. For the Kalambo and Lufubu systems, for which we had more than two populations, a TukeyHSD was performed to adjust for multiple testing. Male (N = 155) and female (N = 126) data were analysed separately because size corrected gill raker length differed between the sexes (gill rakers are longer in females; ANOVA using size corrected values, P = 0.0095), and the sex ratios differed among populations. As we obtained similar results for males and females, we present the results of male data only. All statistical analyses were conducted in R.

Lower pharyngeal jaw morphology

Geometric morphometric analyses were applied on 224 lower pharyngeal jaw bones (LPJ) from the four lake–stream systems (Table S1, Supporting information). Pictures of the cleaned jaws were generated using an office scanner (EPSON perfection V30/V300, resolution: 4800 dpi) with a ruler on every scan to maintain size information. Following Muschick *et al.* (2012), x and y coordinates of eight homologous landmarks and 20 semilandmarks plus the image scales were acquired in TPSDIG2. After a sliding process with TPSRELW (Rohlf 2007), we reduced the initial data set to 16 landmarks consisting of eight true landmarks and eight semilandmarks (Fig. S1C, Supporting information; for details see Muschick *et al.* 2012). The symmetric components of the procrustes-aligned coordinates (GLSF algorithm) were then regressed against centroid size to correct for

allometry. The residuals of the regression were used to perform DFA for each lake–stream system by comparing each lake population with the geographically most distant stream population. Further, we conducted several CVAs comparing multiple populations within each system and over all populations of the lake–stream systems. The significance levels of the obtained mean shape distances were computed using permutation tests (10 000 permutations). As we found smaller intersexual within-population differences in LPJ shape than intrasexual differences among populations (Fig. S2, Supporting information), all analyses were conducted with pooled sexes. Statistical analyses of the morphometric data were performed in MorphoJ.

Stomach and gut content

To investigate whether the populations differ with respect to food resource use, we inspected gut and stomach contents. To this end, the intestines of 102 male individuals (Table S1, Supporting information) were opened under a binocular (LEICA, $MZ7_5$) and the content was separated into the following five categories: plant material and algae, sand, macro-invertebrates (insects and insect larvae), hard-shelled items (mollusc shells and plant seeds), and zooplankton and micro-invertebrates (mainly small shrimps of the LT endemic genus *Limnocaridina*, cladocerans and copepods). The volume (in %) of each category was determined by comparison with serial volume units. For the illustration of the proportions of food items only, the category 'sand' was excluded.

Testing for associations between genetic differentiation, morphometric traits and environment

Partial Mantel tests were applied to compare pairwise differences of morphometric traits (Mahalanobis distances for body shape, mouth position and LPJ, metric measurements for gill rakers) from lake–stream populations with the corresponding F_{ST} values, while correcting for geographic distances. In a second step, the influences of several environmental parameters (microhabitat current, proportion of hard-shelled food items and proportion of macro-invertebrates) and geographic distance on the same morphometric differences were analysed with a multiple regression on distance matrices (MRM). MRM is an extension of the partial Mantel analysis and allows multiple regression of the response matrix on any number of explanatory matrices (Lichtstein 2007). Of 10 000 permutations were performed, as recommended by Jackson & Somers (1989). All analyses were performed using the package ecodist in R. Note that we had to exclude Lf1 in these analyses due to the lack of environmental data.

Testing for reproductive isolation and trait plasticity

We evaluated reproductive isolation among lake and stream *A. burtoni* populations in triadic mating trials. The common garden setting of this pond experiment also allowed us to test for plasticity in body shape and gill raker morphology in F1 offspring.

The experiment was carried out between July 2013 and January 2014 in five concrete ponds at Kalambo Lodge, Zambia. Experimental ponds (dimensions: 3.2 × 1.4 × 0.5 m) were stocked with seven females and four males each from two stream populations (Ka3 and Lz1) and one lake population (KaL). Wild-caught adults were photographed and fin-clipped before starting the experiment. Males were selected for size to achieve a similar size distribution among the three populations within each pond. Concrete ponds were supplied with lake water; fish were fed with commercial flake food two times a day.

After a period of six months, we collected and fin-clipped all offspring plus all remaining adult fish (55 out of 165 initially introduced) from the ponds. Fish weighting more than 1 g were photographed and measured. We then genotyped all putative parental individuals and 593 offspring (i.e. all free living juveniles plus 5 individuals from each brood within a females' mouth) at five microsatellite loci (Ppun5, Ppun7, Ppun21, UNH130 and Abur82), following the methods described above. Parentage was inferred using the software CERVUS (Kalinowski *et al.* 2007), with no mismatch allowed. Offspring that were assigned to the same mother and father were combined as a single mating event, except if they belonged to different size classes (free-swimming young vs. wrigglers). In case of the detection of more than one father in broods collected from mouthbrooding females, these were treated as two mating events. Multiple paternity in *A. burtoni* has been detected previously in mate choice experiments under laboratory conditions in ~7% of genotyped broods (Theis *et al.* 2012).

We then used F1-offspring to test for a heritable component of body shape ($N = 130$) and gill raker ($N = 132$) morphology. F1 individuals were categorized as offspring resulting from the following mating combinations: KaL-KaL, Ka3-Ka3, Lz1-Lz1, Ka3-Lz1, KaL-Ka3 and KaL-Lz1 (Table S2B, Supporting information). Body shape was analysed using the same methods as described above. Due to low sample size in some of the crosses, we reduced the number of landmarks to 6 (landmarks 1, 2, 8, 12, 14 and 15; Fig. S1A, Supporting information). We first conducted CVAs for the three interpopulation crosses (KaL-Ka3, KaL-Lz1, Lz1-Ka3) and their corresponding within-population crosses (KaL-KaL, Ka3-Ka3, Lz1-Lz1) separately to test

whether (i) within-population crosses are differentiated and (ii) whether interpopulation crosses show intermediate body shape with respect to within-population crosses. Additionally, within-population F1 offspring were analysed in a CVA together with their corresponding wild-type populations to detect plastic shifts in body shape induced by the common garden setup. Moreover, we conducted a CVA to compare body shape of introduced specimens before and after the experiment, to test for plastic responses in adults. Gill raker length and number of F1 offspring were measured and analysed using the same methods as described above for wild populations. Mean gill raker length correlated positively with SL ($R^2 = 0.58$, $P < 0.0001$) and was corrected for body size. As with body shape, the three interpopulation crosses (KaL-Ka3, KaL-Lz1 and Lz1-Ka3) and their corresponding within-population crosses (KaL-KaL, Ka3-Ka3 and Lz1-Lz1) were first analysed separately. Then, within-population crosses were compared with their corresponding wild-type populations after applying a common size correction.

Results

Water current measurements

Water current was generally stronger at upstream localities, with the exception of Kalambo (water current was stronger at Ka2 than Ka3; see Table 1A for values and Appendix S1, Supporting information for habitat descriptions). As surface and microhabitat current are significantly correlated ($R^2 = 0.6155$, $P = 0.0072$), we used only microhabitat current for further analyses.

Genetics

Sequencing of the mitochondrial control region of 359 specimens revealed the presence of 16 haplotypes. The haplotype genealogy (Fig. 1B) indicates a deep split between the eastern (1–14, haplotypes A–I) and the western (15–17, 19–20, haplotypes L and M) populations. Moreover, the most upstream Lufubu population (18) comprises three haplotypes (N–P), which are clearly distinct from all other lineages. The haplotypes found at the western shoreline of LT at Ndole Bay (21, haplotypes J and K) group with the ones from the northernmost population at the eastern shoreline of LT at Ninde (1, haplotype I). The Lake Chila fish (22) contain the major mtDNA haplotype of the western haplotype lineage (haplotype M).

The analysis of nine microsatellite loci revealed moderate to strong differentiation between populations, even within lake–stream systems (Table S3A, Supporting information for population pairwise F_{ST} and D_{EST}). F_{ST} and D_{EST} values are highly congruent, and P-values (F_{ST}) and confidence intervals (D_{EST}) indicate significant differentiation between most population pairs except for some geographically adjacent populations (15 and 16 for both F_{ST} and D_{EST}, 16 and 17 for F_{ST} but not D_{EST}) and some of the populations sampled twice in two different years (4a and 4b, 7a and 7b, 15a and 15b). Based on F_{ST} and D_{EST} values, population 22 (Lake Chila) and 16 (Fisheries Department, LT) are not significantly differentiated.

Bayesian clustering with STRUCTURE of the entire data set resulted in a most likely number of $K = 10$ (Fig. 1C). The three Tanzanian populations (1–3) cluster together, despite rather large geographic distances between them.

Table 1 Microhabitat current as well as stomach and gut content information. (A) Microhabitat current (represented by dissolution rate in mg/s) at the localities from the lake–stream systems with 95% confidence intervals in brackets. (B) Average values with corresponding 95% confidence intervals in brackets for the proportions of the different stomach content categories (plant and algae, zooplankton, sand, macro-invertebrates, and hard-shelled items)

A		B					
Locality	Microhabitat current: dissolution rate (mg/s)	Population	Plants and algae	Zooplankton	Sand	Macro-invertebrates	Hard-shelled items
KaL	0.032 (±0.039)	KaL (N = 10)	0.954 (±0.036)	0.018 (±0.015)	0.020 (±0.037)	0.008 (±0.006)	0 (±0)
Ka1	0.280 (±0.356)	Ka1 (N = 10)	0.605 (±0.120)	0 (±0)	0.148 (±0.070)	0.228 (±0.095)	0.019 (±0.017)
Ka2	4.842 (±0.986)	Ka2 (N = 10)	0.179 (±0.090)	0.001 (±0.002)	0.009 (±0.018)	0.749 (±0.102)	0.061 (±0.031)
Ka3	2.962 (±0.888)	Ka3 (N = 10)	0.359 (±0.098)	0.004 (±0.005)	0.018 (±0.017)	0.618 (±0.105)	0.001 (±0.001)
ChL	1.029 (±0.223)	ChL (N = 5)	0.877 (±0.101)	0.039 (±0.021)	0.069 (±0.094)	0.015 (±0.010)	0 (±0)
Ch1	4.311 (±0.542)	Ch1 (N = 10)	0.613 (±0.148)	0.001 (±0.001)	0.064 (±0.046)	0.253 (±0.138)	0.069 (±0.053)
LzL	0.094 (±0.096)	LzL (N = 10)	0.565 (±0.226)	0.027 (±0.034)	0.313 (±0.227)	0.087 (±0.096)	0.008 (±0.009)
Lz1	2.749 (±0.685)	Lz1 (N = 10)	0.441 (±0.091)	0 (±0)	0.259 (±0.121)	0.224 (±0.099)	0.076 (±0.036)
LfL	0.693 (±0.604)	LfL (N = 10)	0.628 (±0.233)	0.240 (±0.257)	0.007 (±0.007)	0.047 (±0.061)	0.077 (±0.081)
Lf1	n/a	Lf1 (N = 7)	0.935 (±0.039)	0 (±0)	0.031 (±0.026)	0.023 (±0.031)	0.011 (±0.011)
Lf2	4.261 (±0.763)	Lf2 (N = 10)	0.433 (±0.164)	0.001 (±0.002)	0.117 (±0.053)	0.450 (±0.156)	0 (±0)

Along the Zambian shoreline, several 'pure lacustrine populations', that is populations not being adjacent to a river, cluster together, even when being separated by large sandy bays (16 and 17, separated by Mbete Bay; 12 and 14, separated by Chituta Bay). The population from Lake Chila (22) belongs to the same genotypic cluster as populations 15, 16 and 17 from LT. Specimens from the same population but sampled in different years always cluster together (indicated by 'a' and 'b' in Fig. 1C).

There was a strong pattern of isolation by distance for populations sampled along the shoreline (Mantel-$R = 0.5539$, $P = 0.0164$).

The separate STRUCTURE analyses for each of the four lake–stream systems are depicted in Fig. 2B. The most likely number of genetic clusters was $K = 2$ for all systems (Fig. S3, Supporting information). Note, however, that it is not possible to infer ΔK for $K = 1$.

Body shape

The CVA of body shape of the 20 sampled populations revealed a significant differentiation between all populations (Fig. S4A; Table S3B, Supporting information). The main body shape changes are described by canonical variate 1 (CV1, accounting for 32% of the variance), which shows a change in body depth, mouth position as well as in head size, and CV2 (accounting for 17% of the variance) describing additional changes in caudal peduncle and eye size.

No pattern of isolation by distance was detected regarding body shape for populations sampled along the shoreline (Mantel-$R = 0.2116$, $P = 0.1415$). The CVA plot of all shoreline populations (Fig. S4B, Supporting information) does not show closer positions in morphospace of more closely located populations, but rather indicates stronger clustering of pure lacustrine populations (of LT and Lake Chila) compared with the more scattered shoreline populations that are adjacent to streams.

When analysing each lake–stream system separately, and comparing each lake population with the most distinct corresponding stream population, it becomes apparent that lake fish generally have a deeper body and a more superior mouth position compared with stream fish. This body shape change, together with clearly partitioned discriminant scores, was found in the systems Kalambo (KaL and Ka3), Lunzua (LzL and Lz1) and Lufubu (LfL and Lf2). The lake and river populations of the Chitili system (ChL and Ch1) showed an overlap of the discriminant scores of the DFA and therefore smaller but still significant changes in body shape (Fig. 2C).

The pattern is more complex when body shape is compared within the river systems for which more than two populations have been sampled (Kalambo and Lufubu River). Three of the four Kalambo populations (KaL, Ka1 and Ka3) show a continuous shift from lake towards more upstream populations, with lake fish having a deeper body and a more superior mouth. The remaining Kalambo population (Ka2) clustered separately (Fig. S5A; Table S4A, Supporting information). The two downstream populations of the Lufubu system (LfL and Lf1) displayed a similar differentiation in body shape compared with the distinct upstream population (Lf2), again in the form of a more superior mouth position (Fig. S5A; Table S4B, Supporting information).

All populations of the lake–stream systems together show little congruence in CV1–CV2 morphospace occupation and only the populations from the two lake populations of the similar rivers Kalambo and Lunzua clustered together (KaL and LzL in Fig. 3A) and one of the Kalambo populations overlapped substantially with the first two Lufubu populations (Ka2, LfL and Lf1 in Fig. 3A). The body shape changes, however, followed similar trajectories between river and lake populations throughout all systems, as evidenced by similar unidirectional shifts in CV1 (illustrated by a bar in Fig. 3A). In all four river systems, lake fish had deeper bodies and a more superior mouth along CV1 (accounting for 45% of the variance in the CVA) (Fig. 3A and Table S5A, Supporting information).

Gill raker morphology

ANOVA detected significant differences in gill raker length between male lake and stream fish in all populations, with generally longer gill rakers in lake populations and raker length decreasing with increasing geographic distance from the lake (Fig. 2E; Table S6, Supporting information). In more detail, the lake population from the Kalambo system (KaL) showed significantly longer gill rakers compared with each of the stream populations (Ka1, Ka2 and Ka3), which did not differ significantly among each other. In the Chitili and the Lunzua system, we found a significant difference between the lake and stream populations. In Lufubu, the lake population (LfL) showed no differences in raker length compared with the first upstream population (Lf1), but gill rakers of Lf1 fish were longer compared with the most upstream population (Lf2). However, gill raker number did not differ between lake and stream fish in any of the four lake–stream systems. The results for females, which showed the same trend of longer gill rakers in lake populations compared with stream populations, are shown in Fig. S5C and Table S6 (Supporting information).

Lower pharyngeal jaw morphology

We also detected differentiation between lake and stream fish in the morphology of the LPJ (Fig. 2D). For

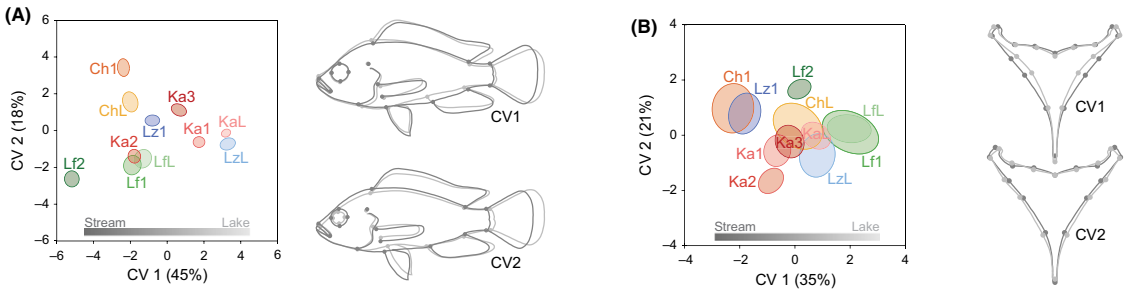

Fig. 3 Body shape and lower pharyngeal jaw (LPJ) shape differentiations of all populations from the lake–stream systems. Canonical variate analyses (CVA) plots illustrate the distribution of the populations on CV1 and CV2 (ellipses represent the 95% confidence intervals of the means) and the shifts are represented in the outline drawings (outlines are always drawn for illustration purposes only, from dark to light grey with increasing values, scaling factor 10 by default; abbreviations of locality names are defined in the grey box in Fig. 1). (A) Shifts in body shape between each lake population and their corresponding stream populations are unidirectional on the axis of CV1 (represented with the bar), indicating that lake fish have deeper bodies and a more superior mouth (Table S5A, Supporting information). (B) For LPJ morphometrics, all lake populations cluster together and show unidirectional shifts along CV1 towards their corresponding stream populations. Lake fish generally have slender and more elongated LPJ compared with stream fish (Table S5B, Supporting information).

each system, we compared the lake population to the stream population with the largest geographic distance to the lake. The Kalambo lake (KaL) and the most upstream population (Ka3) showed a minor overlap in discriminant scores and only a small but still significant difference in LPJ shape, with broader LPJ in stream fish compared with lake fish. In the Chitili, Lunzua and Lufubu systems, we found similar, yet more pronounced shifts in LPJ width. In the Chitili system, an additional shift towards a more convex posterior curve and shorter posterolateral horns in stream fish was detected. Although the underlying shape changes differed among the systems, there was a consistent shift in width of the jaws with broader LPJ in stream fish compared with lake fish.

The system specific CVA of the Kalambo River populations showed a continuous increase in LPJ width and an increasing angle of the posterolateral horns from the lake population (KaL) to the first and the second upstream populations (Ka1 and Ka2). The fourth Kalambo population (Ka3) clustered with the first upstream population (Ka1). In the Lufubu system, we found a considerable overlap in CV1 and CV2 of the lake population (LfL) and the adjacent stream population (Lf1), but a distinct LPJ shape in the furthermost upstream population (Lf2) having broader and shorter LPJ (Fig. S5B; Table S4C,D, Supporting information).

The CVA with all 11 lake–stream populations included showed a significant difference (based on Mahalanobis distances) in LPJ shape among all populations except between LfL and Lf1 (Fig. 3B; Table S5B, Supporting information). CV1 (accounting for 35% of the variance) represented mainly a change in broadness and length of the LPJ, whereas CV2 (accounting for 21% of the variance) described an additional change in angle of the posterolateral horns. In the CV1–CV2 morphospace, all lake populations clustered together, indicating similar LPJ shapes in the lake populations. All systems show a shift in LPJ shape along CV1 with broader and shorter LPJ in stream fish compared with lake fish (illustrated by a bar in Fig. 3B). Along CV2, the lake populations showed a consistent shift in angle of the posterolateral horns (except for the Kalambo system, where the shift was in the opposite direction).

Stomach and gut content

Stomach and gut content analyses revealed that *A. burtoni* is a generalist, feeding on a mixed diet composed of plant material, algae, insects, insect larvae, molluscs and planktonic components (Fig. 2F). The diet composition differed between lake and stream habitats, whereby lake fish feed more on softer and smaller food particles (plants and algae, zooplankton) and stream fish more on hard-shelled and bigger prey items (mollusc shells, plant seeds, insects and insect larvae).

In all four systems, we found a plant, algae and zooplankton-biased diet in lake fish and a parallel increase in the proportion of macro-invertebrates with increasing distance to the lake (Table 1B). In addition, the proportion of hard-shelled food items was generally higher in river populations, except for the Lufubu lake population, where a considerable proportion of hard-shelled food items has been found.

Testing for associations between genetic differentiation, morphometric traits and environment

The partial Mantel tests revealed that none of the morphometric trait differences correlated with genetic distance (F_{ST} values; Table 2A). Genetic differentiation at neutral markers therefore does not seem to be the determining factor for the observed differences among the lake and stream populations. The MRM including environmental parameters showed that the differences rather arise by the effect of environmental conditions: body shape was significantly influenced by both geographic distance and by water current. Mouth position correlated with current and was also influenced by feeding (proportion of macro-invertebrates). While gill raker length correlated with the proportion of macro-invertebrates, LPJ shape tends to be influenced by feeding on hard-shelled food items and correlated with microhabitat current (Table 2B).

Testing for reproductive isolation and trait plasticity

A total of 55 (of 165 initially introduced) wild-caught adult individuals and 593 F1 offspring were recovered from the experimental ponds. Loss of individuals was most likely due to aggressive and territorial behaviour of males. At the time the experiment was terminated, at least one female per population had survived in each pond, and in three of five ponds, at least one male per population had survived (Table S2A, Supporting information). Parentage analyses revealed that across the five ponds, all possible mating combinations occurred, but were not evenly distributed among the replicates (see Appendix S2, Supporting information for details). A qualitative inspection of the data indicated no assortative mating with respect to population but revealed that only 2–5 males reproduced per pond. Further, reproducing males were predominantly large males based on SL measurements taken at the beginning and at the end of the experiment. In *A. burtoni*, size and dominance are positively correlated (Fernö 1987), and dominant males are much more likely to reproduce. Accordingly, the observed pattern is likely a result of biased mating with respect to male size and dominance. This is also supported by comparing our observed data with a simulation assuming random mating with respect to population, but an increased mating probability of large males (see Appendix S2, Supporting information for details).

The morphometric analyses in F1 offspring revealed that while purebred (i.e. intrapopulation crosses) differed among each other in body shape in CV1 (accounting for 62–88% of the variance), between-population crosses were intermediate (Figs 4A and S6; Table S7A, Supporting information). A CVA including F1 offspring and wild populations demonstrates shifts in body shape under common garden conditions and a closer clustering of within-population crosses as compared to the corresponding wild populations (Fig. S7A; Table S8A, Supporting information). Interestingly, the body shape of introduced adult specimens also converged during the experimental period, with the stream populations (Ka3 & Lz1) becoming more like the lake population (KaL) (Fig. S7B; Table S8B, Supporting information). (Note that the experimental set-up in ponds resembles more the lake situation.)

Gill rakers were significantly longer in within-lake population offspring compared with within-stream population offspring, and intermediate in the interpopulation crosses (Fig. 4B; Table S7B, Supporting information). No difference in gill raker number was detected. Within-population offspring from the common garden experiment show a shift towards longer gill rakers compared with the corresponding wild populations (Fig. S7C; Table S8C, Supporting information).

Discussion

Phylogeography and population structure of Astatotilapia burtoni in southern LT

Overall, our study revealed an unexpectedly high degree of genetic and morphological diversity and

Table 2 Testing for associations between genetic differentiation, morphometric traits, and environment. (A) Genetic distances (F_{ST}) were correlated with morphological distances (Mahalanobis) using a partial Mantel test including geographic distance as a correction factor. (B) Combined multiple regression on distance matrices (MRM) between morphological and ecological distances

A Morphometric trait	Genetic distance (F_{ST})	B Morphometric trait	Microhabitat current	Hard-shelled items	Macro-invertebrates	Geographic distance
Overall body shape	0.268 (Mantel- R = 0.133)	Overall body shape	0.0042**	0.2717	0.4323	0.0253*
Mouth position	0.825 (Mantel- R = −0.226)	Mouth position	0.0157*	0.1793	0.0175*	0.8627
Gill raker length	0.496 (Mantel- R = −0.005)	Gill raker length	0.4182	0.4504	0.0373*	0.2270
LPJ shape	0.762 (Mantel- R = −0.186)	LPJ shape	0.0219*	0.0587	0.4712	0.3425

LPJ, lower pharyngeal jaw.
Significance levels: *P < 0.05 and **P < 0.01.

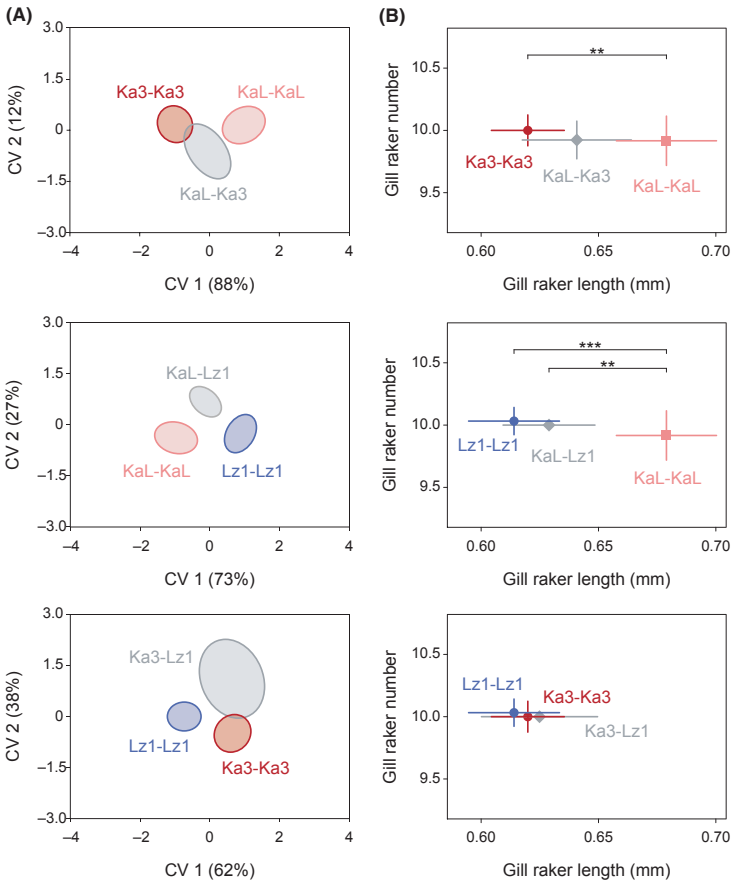

Fig. 4 Body shape (A) and gill raker comparisons (B) of each interpopulation cross with the corresponding within-population crosses from the pond experiment (Fig. S6, Supporting information for corresponding CV outlines and Table S7, Supporting information for distance and significance values).

extensive population structure in *A. burtoni* from southern LT (Figs 1, 2 and S4A, Supporting information). Notably, we identified two main mtDNA control region haplotype lineages in *A. burtoni* that are separated by 10 mutations (Fig. 1B). The genetic diversity in *A. burtoni* is thus similar to, or even exceeds the diversity observed in the same marker in the entire haplochromine cichlid assemblage of Lake Victoria (Verheyen *et al.* 2003). It has long been recognized that substantial differences exist in inter- and intraspecific genetic variation in mtDNA within different East African cichlid radiations and that the degree of differentiation reflects the respective age of a lineage rather than morphological disparity (Sturmbauer & Meyer 1992). The great diversity in mtDNA in *A. burtoni*, even across small geographic scales, thus suggests a deep coalescence time and, consequently, the presence of this species in the study area over long time periods. This is in line with a previous multispecies study that detected deep coalescence times in the only analysed *A. burtoni* population (collected in the area of our Ka3 site) based on microsatellite markers (Elmer *et al.* 2009).

The data at hand indicate that while mtDNA clearly separates the populations into an eastern (1–14) and a western clade (15–20; with the exception of population 21, see below) (Fig. 1B), such a clear-cut barrier to gene flow is not evident in the nuclear DNA markers (Fig. 1C): The population assignment tests with STRUCTURE suggest some gene exchange between populations 14 and 15, and the pairwise differences in F_{ST} and D_{EST} between populations 14 and 15 are among the smallest detected (nevertheless significant), fitting the isolation-by-distance scenario among the lacustrine populations. Similarly, while population 21 is clearly distinct in its mtDNA from the geographically nearest populations 19 and 20 (Fig. 1B), some level of gene flow between these populations is indicated based on the nuclear DNA markers (Fig. 1C). Such a pattern could be explained by male-biased dispersal along the shoreline of LT (Stiver *et al.* 2007). Male-biased dispersal and the preference

for shallow, sandy habitats would also explain why—in contrast to lake cichlids occurring in the rocky shoreline habitat of LT (e.g. Koblmüller *et al.* 2011)—long stretches of sandy shorelines do not seem to act as strong barriers to gene flow in *A. burtoni* (see e.g. 1–3, 12 and 14, 16 and 17, 20 and 21).

Recent migration along the shoreline cannot, however, explain the distribution of the main mtDNA haplotype lineages in *A. burtoni* (i.e. the clear-cut separation into an eastern and a western haplotype clade and the distinctiveness of populations 18 and 21). The bathymetry of the southern LT basin together with periodically occurring and climatically induced fluctuations in the lake level of LT (see e.g. Sturmbauer *et al.* 2001, 2005; Koblmüller *et al.* 2011) might provide one explanation for the overall structure of the mtDNA haplotype genealogy (Fig. 1B). The deep split between the eastern and the western haplotype lineages could, for example, be directly related to an underwater ridge in exactly the area between populations 14 and 15 (see fig. 1 of Koblmüller *et al.* 2011), which might have acted as migration barrier at times of low lake level stands, especially for a species associated to rivers, estuaries and shallow waters such as *A. burtoni*. Low lake level might also permit migration across what is at present two opposite shorelines of LT (see e.g. Sturmbauer *et al.* 2001; Baric *et al.* 2003), thus explaining the close relationship between population 21 from the western (Zambian/Congolese) part of LT to the eastern (Tanzanian) populations 1–3.

The close relatedness of the Lake Chila population (22) to populations sampled around Mpulungu (15–17), and especially to population 16 (Table S3A, Supporting information), is somewhat puzzling. Lake Chila is a small and shallow lake about 20 km southeast of LT, and connected to LT through a small outflow draining into LT near Sumba (population 12). However, there is no faunistic association between Lake Chila and LT, except for *A. burtoni*, and we could only detect elements of a fish fauna in Lake Chila, which is otherwise typical for the Chambeshi, Zambesi and the Zambian/Congo watersheds (*Serranochromis angusticeps*, *S. robustus*, *S. thumbergi*, *Pseudocrenilabrus* cf. *philander* and *Tilapia sparmanii*) (Skelton 1993). As Lake Chila's *A. burtoni* are genetically indistinguishable from population 16, yet distinct from population 12, and because there are reports of a recent stocking of this small lake (L. Makasa, Fisheries Department Mpulungu, personal cummunication), a human-induced translocation is the likely source of the current Lake Chila *A. burtoni* stock (despite records of the presence of *A. burtoni* in that lake more than 50 years ago as evidenced by a collection by M. Poll from 1949 deposited in the Royal Museum for Central Africa in Tervuren, Belgium).

In summary, we show that *A. burtoni* occurs along a lake–stream environmental gradient in southern LT and that several lake–stream systems have been colonized independently. One of these systems, the Lufubu, is genetically very distinct from the other three (Kalambo, Chitili and Lunzua), especially with respect to mtDNA. However, we can, at present, not infer the precise colonization history of *A. burtoni* in southern LT. In particular, we cannot assess whether any of the surveyed river populations is the source of *A. burtoni* in the area or whether all the river systems have been colonized from LT. A more thorough analysis including a denser sampling across a much larger geographic area would be necessary to fully understand the phylogeographic history and population structure of *A. burtoni*.

Adaptive divergence between lake and stream habitats in Astatotilapia burtoni

Integrative studies of fish species that occur along an environmental gradient have provided important insights into speciation (Hendry *et al.* 2000; Seehausen *et al.* 2008; Berner *et al.* 2009; Roesti *et al.* 2012). Our survey of *A. burtoni* in the southern part of LT reveals that this species occurs along a lake–stream environmental gradient and is present, in high abundance, in every suitable habitat ranging from truly lacustrine environments to river estuaries, larger rivers and small creeks draining into LT (Figs 1A and 2A). Importantly, we show that populations inhabiting the same environment tend to be morphologically similar, irrespective of their genetic background (Figs 2, 3 and S4B, Supporting information). For example, among populations sampled within LT, there is a closer morphological resemblance between the truly lacustrine populations (i.e. the populations away from any river) and between the populations near river estuaries (Fig. S4B, Supporting information). Interestingly, the only sampled lacustrine *A. burtoni* population outside from LT (from Lake Chila) clusters closely in morphospace with the truly lacustrine populations from LT (Fig. S4B, Supporting information) (note, however, that this resemblance might also be due to recent introduction; see above). In addition, while there is a strong signal of isolation by distance with respect to genetics along the shoreline of LT, this is not the case for body morphology, suggesting that similar environmental pressures, but not relatedness, mediate the emergence of similar body shapes in *A. burtoni*.

This pattern becomes even more evident when comparing the body shape between lake and stream populations from the four lake–stream systems studied in detail. Generally, we find that lake fish exhibit deeper

bodies and a more superior mouth compared with stream fish (Figs 2C and 3A) and that mouth position is correlated with feeding mode (Table 2B). In addition, we detected a significant correlation between body shape and water current (Table 2B), which is in line with adaptations to different flow rates as predicted by hydrodynamic theory (Webb 1984). However, these changes in morphology only partially agree with those found in other lake–stream systems in fishes. In sockeye salmon, for example, beach residents, too, have deeper bodies compared with their riverine counterparts (Hendry *et al.* 2000). In Canadian three-spine stickleback, on the other hand, lake fish tend to have more slender bodies compared with stream fish due to shifts in feeding modes (e.g. Schluter & McPhail 1992; Berner *et al.* 2008, 2010; Ravinet *et al.* 2013).

In addition to the body shape differences, we also detected significant shifts in trophic morphology across the lake–stream transition in *A. burtoni* (Fig. 2D,E and 3B). The morphological trajectory of the gill raker apparatus along this habitat gradient resembles that in other groups of fishes. Just as in sticklebacks (Berner *et al.* 2008; Ravinet *et al.* 2013), gill rakers are shorter in *A. burtoni* stream fish compared with lake fish. Gill rakers are an important trophic trait in fishes, and believed to function as a cross-flow filter to concentrate particles inside the oral cavity and to transport particles towards the oesophagus (Sanderson *et al.* 2001). In stickleback and other fishes, divergence in gill raker morphology is driven by differential prey resource use (e.g. Bentzen & McPhail 1984; Robinson & Wilson 1994; Skulason & Smith 1995; Berner *et al.* 2008). Likewise, in *A. burtoni*, shorter gill rakers are associated with the consumption of larger food items and longer gill rakers with smaller food particles. However, there were no significant differences in gill raker numbers between lake and stream populations. Divergence in gill raker length accompanied by stasis in gill raker number has also been found in European stickleback lake–stream population pairs, which was explained by the insufficient time for divergence and differences in the genetic architecture compared with Canadian lake–stream populations (Berner *et al.* 2010). While our population-genetic analyses based on mtDNA suggest a deep coalescence time among the major haplotype lineages in *A. burtoni*, little is known about the timing of splitting events among the studied lake–stream populations. Generally, gill raker number varies considerably among LT cichlid species (M. Rösti, personal observation), but it may be less prone to environmentally induced phenotypic variation than other morphological traits such as gill raker length and the LPJ (Lindsey 1981). We also detected sexual dimorphism in gill raker length, with females having longer gill rakers compared with males. In addition, there appears to be a sexual dimorphism in head shape, with females showing more slender yet larger heads (Fig. S1B, Supporting information). Both might be explained by functional differences due to the female mouthbrooding behaviour characteristic for haplochromines.

Trophic divergence between *A. burtoni* lake–stream populations is also evident from differences in LPJ morphology between habitats. The morphology of the oral and pharyngeal jaws is highly diverse in cichlids (Fryer & Iles 1972; Liem 1973; Salzburger 2009; Muschick *et al.* 2012) and related to functional feeding ecology (Liem 1980; Muschick *et al.* 2012, 2014). Experimentally induced, plastic changes in cichlid pharyngeal jaws have been shown to be due to the mode of feeding rather than differences in nutritional composition. For example, Nicaraguan Midas cichlids (*Amphilophus citrinellus*) fed on whole snails developed heavier and more hypertrophied LPJs compared with individuals fed on either crushed whole snails or snail bodies without shells (Muschick *et al.* 2011). Similar shifts in LPJ morphology along with different resource use are known from natural cichlid populations (Meyer 1990; Hulsey *et al.* 2008). In line with these studies, the broader and shorter LPJs of *A. burtoni* stream fish compared with lake fish may pose an adaptation to the shift in diet towards harder food items such as seeds, snails and other hard-shelled invertebrates found in stomachs of stream populations (Fig. 2F; Table 1B). In our analyses, we found that LPJ morphology tends to correlate with the proportion of hard-shelled food items, but there is also a correlation between LPJ and water current (Table 2B). This latter correlation could be due to the method used to infer LPJ shape, which might be influenced by more general shifts in head morphology across the lake–stream gradient.

Phenotypic plasticity constitutes an alternative outcome to speciation in the face of divergent selection (West-Eberhard 2005; Pfennig *et al.* 2010). The generalist species *A. burtoni* dwells in many different habitats, which could result in the evolution of highly plastic populations expressing a variety of phenotypes. On the other hand, speciation could also be initiated via plastic responses to novel environments followed by genetic assimilation (e.g. Waddington 1942; West-Eberhard 2003). Our common garden experiment demonstrated that both plastic and genetic components influence body shape and gill raker length in *A. burtoni*. The F1 offspring from the within-population matings generally show significant differentiation with respect to both body shape and gill raker length, and interpopulation crosses generally display intermediate phenotypes. This pattern, together with the conserved higher body shape and shorter gill rakers of the lake population offspring

(KaL-KaL), compared with the within-stream population crosses speaks for a genetic component underlying trait differentiation (Fig. 4). However, shifts in F1 offspring in both traits under common garden conditions compared with wild populations indicate that trait plasticity also contributes to the detected differences (Fig. S7, Supporting information). Whether these patterns also hold with regard to LPJ morphology and to what extent plasticity and heritability contribute to the detected differences in body shape and trophic traits remains to be tested in future experiments.

We did not find any evidence for assortative mating with regard to population in our mating experiment. All possible mating combinations occurred, and male dominance effects seemed to determine the observed mating patterns (Appendix S2, Supporting information). The absence of reproductive barriers in spite of strong genetic and morphological differentiation has also been reported from lake and stream stickleback (Raeymaekers *et al.* 2010). However, a transplant experiment later indicated that selection against immigrants, together with various other factors, might be contributing to reproductive isolation in this system (Räsänen & Hendry 2014). Similarly, we cannot rule out that barriers, which we did not detect in our experiment, could contribute to reproductive isolation among lake and stream populations. In *A. burtoni*, with its lek-like polygynandrous mating system, only dominant males gain access to territories as well as (several) females and are therefore able to reproduce (Fernald & Hirata 1977). Although no bias in dominance among populations was evident from our data, possible male aggression biases (and probably undetected female preferences) should be tested under more controlled conditions in the future (see Theis *et al.* 2012). As a next step, it would be interesting to test whether the genetically most distinct populations, for example Lf2 vs. KaL, are reproductively isolated.

Evidence for (ecological) speciation is often inferred via a positive correlation between the levels of (adaptive) divergence in phenotypic traits and the levels of neutral genetic differentiation between populations, when controlled for geographic distance ('isolation by adaptation', Nosil 2012). In *A. burtoni*, we did not find correlations between any morphological trait measured and F_{ST} values (Table 2A). This gene-flow approach based on neutral markers does have several caveats, though (see Nosil 2012), and a lack of signal does not necessarily exclude the possibility of (ecological) speciation. Due to the geographic isolation of some populations (e.g. populations located above waterfalls or geographically very distant populations), differentiation at neutral loci might occur without barriers to gene flow caused by divergent selection in *A. burtoni*, resulting in a failure to detect isolation by adaptation. Note that there was also no pattern of isolation by distance detectable if only lake–stream populations were included in the analysis, as opposed to the pattern detected along the shoreline (see above). However, lake and stream populations from the four lake–stream systems (and populations within systems) appear to rest at different stages of the speciation continuum. In the Chitili system, for example, the lake and stream populations are geographically close, genetically admixed and also less differentiated in body shape and gill rakers compared with the pairwise comparisons from the Kalambo, Lunzua and Lufubu systems shown in Fig. 2. Although there are several outliers in our data (e.g. relatively pronounced LPJ differentiation within the Chitili system compared with very little LPJ differences between the clearly genetically distinct populations KaL and Ka3), lake and stream populations belonging to distinct genetic clusters generally show more differentiation in morphological traits (Fig. 2).

Taken together, our study revealed the presence of multiple divergent lake–stream populations in the southern LT drainage. Phenotypic divergence between populations from the four independent lake–stream systems follows similar trajectories: Divergence in body shape is associated with different flow regimes in lake and stream habitats, whereas shifts in trophic structures are linked to differential resource use. We did not detect a signal for isolation by adaptation; however, more powerful genetic data such as genome scans may clarify the interplay between levels of gene flow and phenotypic divergence in these systems. A first test for reproductive isolation among the more closely related lake and stream populations did not reveal any population-assortative mating patterns. Importantly, analyses of F1 offspring reared under common garden conditions indicate that the detected trait differences among *A. burtoni* populations do not reflect pure plastic responses to different environmental conditions, but that these differences also have a genetic basis.

The *A. burtoni* lake–stream system constitutes a valuable model to study the factors that enhance and constrain progress towards speciation, and offers the unique possibility to contrast replicated lake–stream population pairs at different stages along the speciation continuum in cichlids. In addition, it allows evaluating parallelism across different species, that is lake–stream pairs of stickleback and cichlids. Characterizing potential reproductive barriers and the role of plasticity in phenotypic divergence in more detail, together with studies on genomic differentiation, promises to contribute to understanding the process of speciation in natural populations.

Acknowledgements

We would like to thank our helpers in the field, J. Bachmann, A. Böhne, T. Bosia, V. Campos, M. Colombo, M. Dittmann, S. Egger, Y. Klaefiger, J. De Maddalena, N. Merdas, D. Moser, M. Roesti, O. Roth, L. Schild, J. Weber, M. Zubler; H. H. Büscher and G. Tembo and his crew for their logistic support in Africa, respectively; the Lake Tanganyika Research Unit, Department of Fisheries, Republic of Zambia, for research permits. We further thank M. Muschick and M. Colombo for help in morphometric analyses, B. Meyer for help in population-genetic analyses, D. Berner and J. Raeymaekers for contributing to statistical analyses, L. Schärer for valuable suggestions, A. Bieri and S. Fischer for help with LPJ preparations and N. Rose and H. Bichsel for help with stomach content analysis. We further thank D. Berner and C. L. Peichel for valuable comments and feedback from Axios Review (axiosreview.org) on a previous version of this manuscript. This study was supported by grants from the Freiwillige Akademische Gesellschaft Basel (FAG) to AI and AT, the Swiss Academy of Sciences (SCNAT) to AI, FR and AT, the Basler Stiftung für experimentelle Zoologie to BE, FR and AT, the Swiss Zoological Society (SZS) to AT and the European Research Council (ERC, Starting Grant 'INTERGEN-ADAPT' and Consolidator Grant 'CICHLID~X'), the University of Basel and the Swiss National Science Foundation (SNF, grant 3100A0_138224) to WS.

References

Baldo L, Santos ME, Salzburger W (2011) Comparative transcriptomics of Eastern African cichlid fishes shows signs of positive selection and a large contribution of untranslated regions to genetic diversity. *Genome Biology and Evolution*, **3**, 443–455.

Baric S, Salzburger W, Sturmbauer C (2003) Phylogeography and evolution of the *Tanganyikan cichlid* genus *Tropheus* based upon mitochondrial DNA sequences. *Journal of Molecular Evolution*, **56**, 54–68.

Barluenga M, Stoelting KN, Salzburger W, Muschick M, Meyer A (2006) Sympatric speciation in Nicaraguan crater lake cichlid fish. *Nature*, **436**, 719–723.

Bentzen P, McPhail JD (1984) Ecology and evolution of sympatric sticklebacks (*Gasterosteus*) – specialization for alternative trophic niches in the Enos Lake species pair. *Canadian Journal of Zoology – Revue Canadienne De Zoologie*, **62**, 2280–2286.

Berner D, Adams DC, Grandchamp AC, Hendry AP (2008) Natural selection drives patterns of lake-stream divergence in stickleback foraging morphology. *Journal of Evolutionary Biology*, **21**, 1653–1665.

Berner D, Grandchamp AC, Hendry AP (2009) Variable progress toward ecological speciation in parapatry: stickleback across eight lake-stream transitions. *Evolution*, **63**, 1740–1753.

Berner D, Roesti M, Hendry AP, Salzburger W (2010) Constraints on speciation suggested by comparing lake-stream stickleback divergence across two continents. *Molecular Ecology*, **19**, 4963–4978.

Brawand D, Wagner CE, Li YI *et al.* (2014) The genomic substrate for adaptive radiation in African cichlid fish. *Nature*, **513**, 375–381.

Bruford MW, Hanotte O, Brookfield JFY, Burke T (1998) Multilocus and single-locus DNA fingerprinting. In: *Molecular Analysis of Populations* (ed. Hozel AR), pp. 283–336. Oxford University Press, New York, New York.

Butlin RK, Galindo J, Grahame JW (2008) Sympatric, parapatric or allopatric: the most important way to classify speciation? *Philosophical Transactions of the Royal Society B-Biological Sciences*, **363**, 2997–3007.

Coulter GW (1991) *Lake Tanganyika and its Life*. Oxford University Press, Oxford.

De Vos L, Seegers L, Taverne L, Thys van den Audenaerde D (2001) L'ichtyofaune du basin de la Malagarasi (Système du Lac Tanganyika): une synthèse de la connaissance actuelle. *Annales, Musée Royal de l'Afrique Centrale, Sciences Zoologiques*, **285**, 117–152.

Earl DA, von Holdt BM (2012) Structure Harvester: a website and program for visualizing Structure output and implementing the Evanno method. *Conservation Genetics Resources*, **4**, 359–361.

Elmer KR, Reggio C, Wirth T, Verheyen E, Salzburger W, Meyer A (2009) Pleistocene desiccation in East Africa bottlenecked but did not extirpate the adaptive radiation of Lake Victoria haplochromine cichlid fishes. *Proceedings of the National Academy of Sciences USA*, **106**, 13404–13409.

Evanno G, Regnaut S, Goudet J (2005) Detecting the number of clusters of individuals using the software Structure: a simulation study. *Molecular Ecology*, **14**, 2611–2620.

Fernald RD, Hirata NR (1977) Field study of *Haplochromis burtoni* – quantitative behavioral observations. *Animal Behaviour*, **25**, 964–975.

Fernö A (1987) Aggressive behavior between territorial cichlids (*Astatotilapia burtoni*) in relation to rank and territorial stability. *Behaviour*, **103**, 241–258.

Fryer G, Iles T (1972) *The Cichlid Fishes of the Great Lakes of Africa: Their Biology and Evolution*. Oliver & Boyd, Edinburgh.

Galis F, Drucker EG (1996) Pharyngeal biting mechanics in centrarchid and cichlid fishes: insights into a key evolutionary innovation. *Journal of Evolutionary Biology*, **9**, 641–670.

Gerlach G, Jueterbock A, Kraemer P, Deppermann J, Harmand P (2010) Calculations of population differentiation based on G(ST) and D: forget G(ST) but not all of statistics!. *Molecular Ecology*, **19**, 3845–3852.

Goslee SC, Urban DL (2007) The ecodist package for dissimilarity-based analysis of ecological data. *Journal of Statistical Software*, **22**, 1–19.

Günther ACLG (1894) Descriptions of the reptiles and fishes collected by Mr. E. Coode-Hore on Lake Tanganyika. *Proceedings of the Zoological Society of London, B*, **1893**, 628–632.

Harrod C, Mallela J, Kahilainen KK (2010) Phenotype-environment correlations in a putative whitefish adaptive radiation. *The Journal of Animal Ecology*, **79**, 1057–1068.

Hendry AP, Taylor EB (2004) How much of the variation in adaptive divergence can be explained by gene flow? – an evaluation using lake-stream stickleback pairs. *Evolution*, **58**, 2319–2331.

Hendry AP, Wenburg JK, Bentzen P, Volk EC, Quinn TP (2000) Rapid evolution of reproductive isolation in the wild: evidence from introduced salmon. *Science*, **290**, 516–519.

Hendry AP, Nosil P, Rieseberg LH (2007) The speed of ecological speciation. *Functional Ecology*, **21**, 455–464.

Hendry AP, Bolnick DI, Berner D, Peichel CL (2009) Along the speciation continuum in sticklebacks. *Journal of Fish Biology*, **75**, 2000–2036.

Hendry AP, Peichel CL, Matthews B, Boughman JW, Nosil P (2013) Stickleback research: the now and the next. *Evolutionary Ecology Research*, **15**, 111–141.

Hofmann HA (2003) Functional genomics of neural and behavioral plasticity. *Journal of Neurobiology*, **54**, 272–282.

Hulsey CD, García de León FJ, Rodiles-Hernández R (2006) Micro- and macroevolutionary decoupling of cichid jaws: a test of Liem's key innovation hypothesis. *Evolution*, **60**, 2096–2109.

Hulsey CD, Roberts RJ, Lin ASP, Guldberg R, Streelman JT (2008) Convergence in a mechanically complex phenotype: detecting structural adaptations for crushing in cichlid fish. *Evolution*, **62**, 1587–1599.

Jackson DA, Somers KM (1989) Are probability estimates from the permutation model of Mantel's test stable? *Canadian Journal of Zoology*, **67**, 766–769.

Jones FC, Grabherr MG, Chan YF *et al.* (2012) The genomic basis of adaptive evolution in threespine sticklebacks. *Nature*, **484**, 55–61.

Jost L (2008) G(ST) and its relatives do not measure differentiation. *Molecular Ecology*, **17**, 4015–4026.

Kalinowski ST, Taper ML, Marshall TC (2007) Revising how the computer program CERVUS accommodates genotyping error increases success in paternity assignment. *Molecular Ecology*, **16**, 1099–1106.

Klingenberg CP (2011) MorphoJ: an integrated software package for geometric morphometrics. *Molecular Ecology Resources*, **11**, 353–357.

Koblmüller S, Salzburger W, Obermüller B, Eigner E, Sturmbauer C, Sefc KM. (2011) Separated by sand, fused by dropping water: habitat barriers and fluctuating water levels steer the evolution of rock-dwelling cichlid populations in Lake Tanganyika. *Molecular Ecology*, **20**, 2272–2290.

Kocher TD (2004) Adaptive evolution and explosive speciation: the cichlid fish model. *Nature Reviews Genetics*, **5**, 288–298.

Kocher TD, Thomas WK, Meyer A *et al.* (1989) Dynamics of mitochondrial DNA evolution in animals: amplification and sequencing with conserved primers. *Proceedings of the National Academy of Sciences of the USA*, **86**, 6196–6200.

Koehl MAR, Alberte RS (1988) Flow, flapping, and photosynthesis of *Nereocystis leutkeana*: a functional comparison of undulate and flat blade morphologies. *Marine Biology*, **99**, 435–444.

Kullander SO, Roberts TR (2011) Out of Lake Tanganyika: endemic lake fishes inhabit rapids of the Lukuga River. *Ichthyological Exploration of Freshwaters*, **22**, 355–376.

Lang M, Miyake T, Braasch I *et al.* (2006) A BAC library of the East African haplochromine cichlid fish *Astatotilapia burtoni*. *Journal of Experimental Zoology Part B-Molecular and Developmental Evolution*, **306**, 35–44.

Langerhans RB, Gifford ME, Joseph EO (2007) Ecological speciation in *Gambusia* fishes. *Evolution*, **61**, 2056–2074.

Lavin PA, McPhail JD (1986) Adaptive divergence of trophic phenotype among freshwater populations of the threespine stickleback (*Gasterosteus aculeatus*). *Canadian Journal of Fisheries and Aquatic Sciences*, **43**, 2455–2463.

Lee WJ, Kocher TD (1996) Microsatellite DNA markers for genetic mapping in *Oreochromis niloticus*. *Journal of Fish Biology*, **49**, 387–397.

Lichtstein JW (2007) Multiple regression on distance matrices: a multivariate spatial analysis tool. *Plant Ecology*, **188**, 117–131.

Liem KF (1973) Evolutionary strategies and morphological innovations: cichlid pharyngeal jaws. *Systematic Zoology*, **22**, 425–441.

Liem KF (1980) Adaptive significance of intra- and interspecific differences in the feeding repertoires of cichlid fishes. *American Zoologist*, **20**, 295–314.

Lindsey CC (1981) Stocks are chameleons: plasticity in gill rakers of coregonid fishes. *Canadian Journal of Fisheries and Aquatic Sciences*, **38**, 1497–1506.

Lucek K, Sivasundar A, Roy D, Seehausen O (2013) Repeated and predictable patterns of ecotypic differentiation during a biological invasion: lake-stream divergence in parapatric Swiss stickleback. *Journal of Evolutionary Biology*, **26**, 2691–2709.

Maeda K, Takeda M, Kamiya K *et al.* (2009) Population structure of two closely related pelagic cichlids in Lake Victoria, *Haplochromis pyrrhocephalus* and *H. laparogramma*. *Gene*, **441**, 67–73.

Mallet J (2008) Hybridization, ecological races and the nature of species: empirical evidence for the ease of speciation. *Philosophical Transactions of the Royal Society B-Biological Sciences*, **363**, 2971–2986.

Mallet J, Dasmahapatra KK (2012) Hybrid zones and the speciation continuum in *Heliconius* butterflies. *Molecular Ecology*, **21**, 5643–5645.

Mardia KV, Kent J, Bibby J (1979) *Multivariate Analysis*. Academic Press, New York, New York.

Matschiner M, Salzburger W (2009) TANDEM: integrating automated allele binning into genetics and genomics workflows. *Bioinformatics*, **25**, 1982–1983.

Meyer A (1990) Ecological and evolutionary consequences of the trophic polymorphism in *Cichlasoma citrinellum* (Pisces: Cichlidae). *Biological Journal of the Linnean Society*, **39**, 279–299.

Muschick M, Barluenga M, Salzburger W, Meyer A (2011) Adaptive phenotypic plasticity in the Midas cichlid fish pharyngeal jaw and its relevance in adaptive radiation. *BMC Evolutionary Biology*, **11**, 116.

Muschick M, Indermaur A, Salzburger W (2012) Convergent evolution within an adaptive radiation of cichlid fishes. *Current Biology*, **22**, 2362–2368.

Muschick M, Nosil P, Roesti M, Dittmann MT, Harmon L, Salzburger W (2014) Testing the stage model in the adaptive radiation of cichlid fishes in East African Lake Tanganyika. *Proceedings of the Royal Society B*, **281**, 20140605. doi: 10.1098/rspb.2014.0605.

Nosil P (2012) *Ecological Speciation*. Oxford University Press, Oxford.

Nosil P, Sandoval CP (2008) Ecological niche dimensionality and the evolutionary diversification of stick insects. *PLoS ONE*, **3**, e1907.

Nosil P, Harmon LJ, Seehausen O (2009) Ecological explanations for (incomplete) speciation. *Trends in Ecology & Evolution*, **24**, 145–156.

Pfennig DW, Wund MA, Snell-Rood EC, Cruickshank T, Schlichting CD, Moczek AP (2010) Phenotypic plasticity's impacts on diversification and speciation. *Trends in Ecology & Evolution*, **25**, 459–467.

Posada D (2008) jModelTest: phylogenetic model averaging. *Molecular Biology and Evolution*, **25**, 1253–1256.

Pritchard JK, Stephens M, Donnelly P (2000) Inference of population structure using multilocus genotype data. *Genetics*, **155**, 945–959.

R Core Team (2014) *R: A Language and Environment for Statistical Computing*. R Foundation for Statistical Computing, Vienna. ISBN 3-900051-07-0. Available from http://www.R-project.org/.

Raeymaekers JAM, Boisjoly M, Delaire L, Berner D, Räsänen K, Hendry AP (2010) Testing for mating isolation between ecotypes: laboratory experiments with lake, stream and hybrid stickleback. *Journal of Evolutionary Biology*, **23**, 2694–2708.

Räsänen K, Hendry AP (2014) Asymmetric reproductive barriers and mosaic reproductive isolation: insights from Misty lake-stream stickleback. *Ecology and Evolution*, **4**, 166–1175.

Ravinet M, Prodohl PA, Harrod C (2013) Parallel and nonparallel ecological, morphological and genetic divergence in lake-stream stickleback from a single catchment. *Journal of Evolutionary Biology*, **26**, 186–204.

Robinson BW (2000) Trade offs in habitat-specific foraging efficiency and the nascent adaptive divergence of sticklebacks in lakes. *Behaviour*, **137**, 865–888.

Robinson BW, Wilson DS (1994) Character release and displacement in fishes: a neglected literature. *The American Naturalist*, **144**, 596–627.

Robison RR, White RB, Illing N *et al*. (2001) Gonadotropin-releasing hormone receptor in the teleost *Haplochromis burtoni*: structure, location, and function. *Endocrinology*, **142**, 1737–1743.

Roesti M, Hendry AP, Salzburger W, Berner D (2012) Genome divergence during evolutionary diversification as revealed in replicate lake-stream stickleback population pairs. *Molecular Ecology*, **21**, 2852–2862.

Rohlf FJ (2007) *TPSRELW, Version 2.11*. Department of Ecology and Evolution, State University of New York at Stony Brook. Available from http://life.bio.sunysb.edu/morrph/.

Rohlf FJ (2008) *TPSDIG, Version 2.11*. Department of Ecology and Evolution, State University of New York at Stony Brook. Available from http://life.bio.sunysb.edu/morph/.

Rohlf FJ, Slice DE (1990) Extensions of the Procrustes method for the optimal superimposition of landmarks. *Systematic Zoology*, **39**, 40–59.

Rundle HD, Nosil P (2005) Ecological speciation. *Ecology Letters*, **8**, 336–352.

Salzburger W (2009) The interaction of sexually and naturally selected traits in the adaptive radiations of cichlid fishes. *Molecular Ecology*, **18**, 169–185.

Salzburger W, Meyer A, Baric S, Verheyen E, Sturmbauer C (2002) Phylogeny of the Lake Tanganyika Cichlid species flock and its relationship to the Central and East African Haplochromine Cichlid fish faunas. *Systematic Biology*, **51**, 113–135.

Salzburger W, Mack T, Verheyen E, Meyer A (2005) Out of Tanganyika: genesis, explosive speciation, key-innovations and phylogeography of the haplochromine cichlid fishes. *BMC Evolutionary Biology*, **5**, 17.

Salzburger W, Renn SCP, Steinke D, Braasch I, Hofmann H, Meyer A (2008) Annotation of expressed sequence tags for the East African cichlid fish *Astatotilapia burtoni* and evolutionary analyses of cichlid ORFs. *BMC Genomics*, **9**, 96.

Salzburger W, Ewing GB, von Haeseler A (2011) The performance of phylogenetic algorithms in estimating haplotype genealogies with migration. *Molecular Ecology*, **20**, 1952–1963.

Sanderson SL, Cheer AY, Goodrich JS, Graziano JD, Callan WT (2001) Crossflow filtration in suspension-feeding fishes. *Nature*, **412**, 439–441.

Sanetra M, Henning F, Fukamachi S, Meyer A (2009) A microsatellite-based genetic linkage map of the cichlid fish, *Astatotilapia burtoni* (Teleostei): a comparison of genomic architectures among rapidly speciating cichlids. *Genetics*, **182**, 387–397.

Santos ME, Salzburger W (2012) Evolution. How cichlids diversify. *Science*, **338**, 619–621.

Santos ME, Braasch I, Boileau N *et al*. (2014) The evolution of cichlid fish egg-spots is linked with a *cis*-regulatory change. *Nature Communications*, **5**, 5149. doi: 10.1038/ncomms6149.

Schluter D (1993) Adaptive radiation in sticklebacks: size, shape, and habitat use efficiency. *Ecology*, **74**, 699–709.

Schluter D (1995) Adaptive radiation in sticklebacks: trade-offs in feeding performance and growth. *Ecology*, **76**, 82–90.

Schluter D (2000) Ecological character displacement in adaptive radiation. *The American Naturalist*, **156**, S4–S16.

Schluter D (2009) Evidence for ecological speciation and its alternative. *Science*, **323**, 737–741.

Schluter D, McPhail JD (1992) Ecological character displacement and speciation in sticklebacks. *The American Naturalist*, **140**, 85–108.

Schneider S, Roessli D, Excoffier L (1999) *Arlequin, Version 2.0: A Software for Genetic Data Analysis*. Genetics and Biometry Laboratory, University of Geneva, Geneva.

Seehausen O, Terai Y, Magalhaes IS *et al*. (2008) Speciation through sensory drive in cichlid fish. *Nature*, **455**, 620–626.

Skelton P (1993) *A Complete Guide to the Freshwater Fishes of Southern Africa*. Southern Book Publishers, Halfway House.

Skulason S, Smith TB (1995) Resource polymorphisms in vertebrates. *Trends in Ecology & Evolution*, **10**, 366–370.

Stiver KA, Desjardins JK, Fitzpatrick JL, Neff JS, Quinn JS, Balshine S (2007) Evidence for size and sex-specific dispersal in a cooperatively breeding cichlid fish. *Molecular Ecology*, **16**, 2974–2984.

Sturmbauer C, Meyer A (1992) Genetic divergence, speciation and morphological stasis in a lineage of African cichlid fishes. *Nature*, **358**, 578–581.

Sturmbauer C, Baric S, Salzburger W, Rüber L (2001) Lake level fluctuations synchronize genetic divergences of cichlid fishes in African lakes. *Molecular Biology and Evolution*, **18**, 144–154.

Sturmbauer C, Koblmüller S, Sefc KM, Duftner N (2005) Phylogeographic history of the genus *Tropheus*, a lineage of rock-dwelling cichlid fishes endemic to Lake Tanganyika. *Hydrobiologia*, **542**, 335–366.

Swofford DL (2002) *PAUP*. Phylogenetic Analysis Using Parsimony (*and Other Methods)*. Sinauer Associates, Sunderland, Massachusetts.

Taylor MI, Meardon F, Turner G, Seehausen O, Mrosso HDJ, Rico C (2002) Characterization of tetranucleotide microsatellite loci in a Lake Victorian, haplochromine cichlid fish: a *Pundamilia pundamilia* × *Pundamilia nyererei* hybrid. *Molecular Ecology Notes*, **2**, 443–445.

Theis A, Salzburger W, Egger B (2012) The function of anal fin egg-spots in the cichlid fish *Astatotilapia burtoni*. *PLoS ONE*, **7**, e29878.

Van Oppen MJH, Rico C, Deutsch JC, Turner GF, Hewitt GM (1997) Isolation and characterization of microsatellite loci in the cichlid fish *Pseudotropheus zebra*. *Molecular Ecology*, **6**, 387–388.

Verheyen E, Salzburger W, Snoeks J, Meyer A (2003) Origin of the superflock of cichlid fishes from Lake Victoria, East Africa. *Science*, **300**, 325–329.

Waddington CH (1942) Canalisation of development and the inheritance of acquired characters. *Nature*, **150**, 563–565.

Webb P (1984) Body form, locomotion and foraging in aquatic vertebrates. *American Zoologist*, **24**, 107–120.

West-Eberhard MJ (2003) *Developmental Plasticity and Evolution*. Oxford University Press, New York, New York.

West-Eberhard MJ (2005) Phenotypic accommodation: adaptive innovation due to developmental plasticity. *Journal of Experimental Zoology. Part B, Molecular and Developmental Evolution*, **304B**, 610–618.

Wickler W (1962) Egg-dummies as natural releasers in mouthbreeding cichlids. *Nature*, **194**, 1092–1093.

B.E., W.S., A.T. and F.R. designed the study; B.E., W.S., A.T. and F.R. wrote the manuscript. B.E. produced and analysed the population-genetic data, A.T. produced and analysed body shape data and conducted mantel test and MRM statistics, F.R. produced and analysed data on gill rakers, LPJs, stomach contents and paternity. All authors participated in sampling, were involved in the experimental design of the pond experiment and provided input on the manuscript.

Data accessibility

Mitochondrial DNA sequences: GenBank accessions KM508103–KM508461.

mtDNA sequence alignment, microsatellite genotypes, morphological data, stomach and gut content data, environmental data and common garden experiment data: Dryad doi:10.5061/dryad.pp0q1.

Supporting information

Additional supporting information may be found in the online version of this article.

Fig. S1 Landmark positions for body shape and LPJ analyses and sex differences in head shape.

Fig. S2 Comparison of intersexual within-population differences and intrasexual differences among populations in morphometric traits (body shape and LPJ).

Fig. S3 Mean likelihood (L(K) ± SD) over 10 STRUCTURE runs assuming K clusters (left); ΔK statistic (right).

Fig. S4 Body shape differentiation among the 20 sampled populations and among the 11 shoreline populations only.

Fig. S5 Body shape and LPJ shape differentiation within systems with more than two populations and gill raker length and number in females.

Fig. S6 Outlines to illustrate the body shape changes in F1 individuals of the pond experiment.

Fig. S7 Plasticity in body shape and gill raker length.

Table S1 Sample size details for each analysis with information about sampling year and geographic coordinates for each locality.

Table S2 Sample size details and result summary of the pond experiment.

Table S3 Pairwise genetic and morphometric (body shape) distances between populations.

Table S4 Pairwise morphometric (body shape and LPJ) distances within systems with more than two populations.

Table S5 Pairwise morphometric (body shape and LPJ) distances of all populations from the lake-stream systems.

Table S6 *P*-values for within system gill raker length comparisons for males and females.

Table S7 Pairwise morphometric (body shape and LPJ) distances between F1 crosses

Table S8 Pairwise morphometric (body shape) distances and *P*-values of gill raker comparisons among different groups of the pond experiment.

Table S9 Microsatellite diversity in populations of *Astatotilapia burtoni*.

Table S10 Genetic diversity of mtDNA sequences.

Appendix S1 Description of river systems.

Appendix S2 Pond experiment—Simulation.

Chapter 4 | Supplementary Material

Appendix S1: Description of river systems

Kalambo

The catchment of the Kalambo River is located mainly in Tanzania, with a small portion in Zambia. The lake population of the Kalambo system (KaL) was collected at Chipwa village, close to the Kalambo River mouth at the border between Zambia and Tanzania (Fig. A1A, Fig. 1A and Fig. 2A). The habitat at Chipwa is characterized by mainly sandy bottom with bulrush (*Typha* spp.) vegetation and a maximum depth of 1.5 m. The first riverine population (Ka1) was sampled 1500 m upstream from KaL, within a slowly flowing, maximally 3 m deep water and vegetation comprising mainly hippo grass (*Vossia cuspidata*). The second upstream population (Ka2) originates from predominantly rocky habitat with a maximum depth of 1 m. The third upstream population (Ka3) is separated from downstream populations by the Kalambo Falls – with a drop of more than 200 m the second-tallest waterfall in Africa. Compared to Ka2 there is less water current at Ka3, fewer rocks but more vegetation (predominantly reeds and hippo grass).

Chitili

The Chitili Creek is a very small yet permanent stream flowing through Chitili village, and is therefore greatly affected by human activities including agriculture (Fig. A1B). The corresponding lake population (ChL) dwells in a heterogeneous shallow (max. 0.6 m) habitat with rock and sand bottom covered with aquatic plants and hippo grass belts. At the relatively close upstream sampling site, the creek is narrow, shallow (max. 0.3 m deep) and densely vegetated.

Lunzua

Although the Lunzua catchment is almost three times smaller in area than that of the Kalambo, both catchments are comparable with regard to slope angles, water discharge rates and drainage densities (Sichingabula 1999; Kakogonzo *et al.* 2000). The habitat of the Lunzua lake population (LzL) is similar to KaL, with mostly sandy bottom, bulrush vegetation and relatively shallow waters (max. 0.6 m depth) (Fig. A1C). A 3 m tall waterfall close to the river mouth and several rapids separate the lake population from the upstream riverine population (Lz1). The habitat at Lz1 consists mainly of sand and mud bottom, the water depth was around 0.5 m.

Lufubu

The Lufubu River is the largest tributary of southern LT (Langenberg *et al*. 2003). The sampling site at the river mouth (LfL) is shallow (0.3 – 2 m), densely vegetated with papyrus (*Cyperus papyrus*), hippo grass and balsa wood trees (*Aeshynomene elaphroxylon*) (Fig. A1D). The first upstream population (Lf1) was sampled at a location with very similar habitat conditions to LfL with very slowly flowing water. The upstream population (Lf2) was collected more than 30 km upstream the estuary, with habitat comprising pebbles and submerged vegetation and fast flowing waters (max. depth 0.5 m).

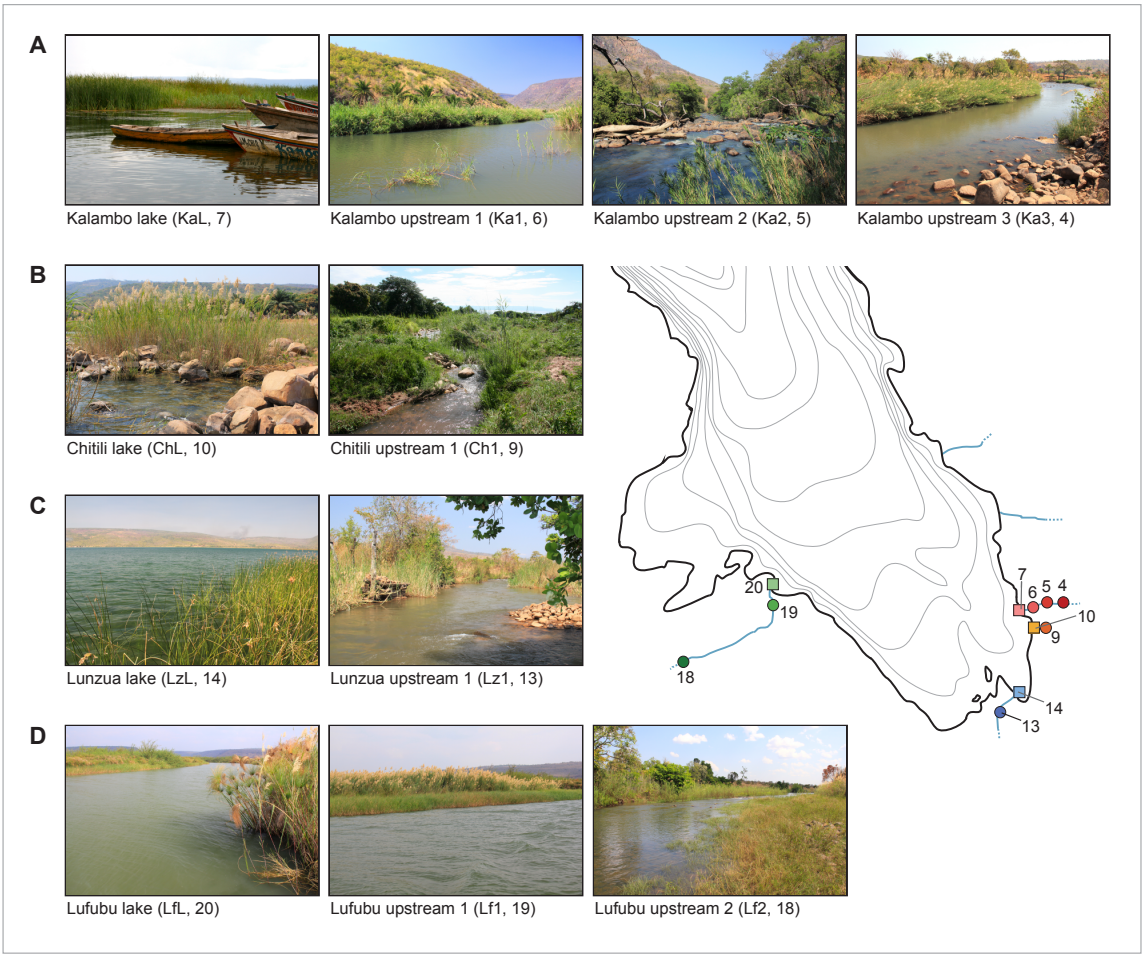

Fig. A1 Map of the southern part of LT (altered from Fig. 1A) showing the populations of the four lake-stream systems with corresponding habitat photographs. (A) The four Kalambo populations, (B) the two populations from the Chitili Creek, (C) the two Lunzua populations and (D) the three populations from the large Lufubu River.

References

Kakogozo B, Kahindo N, Mwenyemaile B, Drieu O (2000) Etude Hydrologique du Bassin Nord-Ouest du Lac Tanganyika (R. D. Congo). *Pollution Control and Other Measures to Protect Biodiversity in Lake Tanganyika*, UNDP/GEF/RAF/92/G32. 44p.

Langenberg V, Nyamushahu S, Roijackers R, Koelmans A (2003) External nutrient sources for Lake Tanganyika. *Journal of Great Lakes Research*, **29**, 169–180.

Sichingabula H (1999) Analysis and results of discharge and sediment monitoring activities in the Southern Lake Tanganyika basin, Zambia. *Pollution Control and Other Measures to Protect Biodiversity in Lake Tanganyika*, UNDP/GEF, RAF/92/G32, Technical Report No: 4.

Appendix S2: Pond experiment– Simulation

To test whether biased mating with respect to body size might explain the observed pattern, we simulated the experiment under the conditions of random mating with an increased mating probability, however, for large males. The simulations were conducted for each pond separately, with the observed number of male and female survivors per pond and reproductively active individuals (based on the paternity analyses, Table S2A). The frequencies for all 9 possible mating combinations were simulated for the observed number of mating events per pond (Table S2A) with 1'000 iterations. We tested 43'910 models with different mating probabilities for four dominant males per pond: for the two largest males at the starting point of the experiment (accounting for dominance in the early phase) and at the end point of the experiment (accounting for dominance in the late phase). We assigned dominance for two males per phase (early and late) to include possible dynamics in dominance ranks. The models covered a range from 1- to 20-fold mating probabilities for the four dominant males. Females were sampled randomly with equal probabilities in each model. To find the best fitted model we calculated the absolute deviation of the observed data form each of the iterations per model (Δ_{SIM}). Then the sum of the mean Δ_{SIM} (SUM_{Δ}) over all ponds was calculated. Therefore the model with the smallest SUM_{Δ} represents the model, which fits the observed data best. The macro for the simulations was written in R.

Comparing the SUM_{Δ} of the 43'910 models revealed that the model assuming random mating (without dominance) shows the highest SUM_{Δ} whereas several models accounting for biased mating with respect to size fit the observed data very well (Fig. A2). Generally, the model improves with increasing probability for the largest male to mate at the end point of the experiment. Further, SUM_{Δ} decreases with increasing mating probability for the largest male at the starting point of the experiment, achieving an optimum when the probability to mate is 10- to 12-fold higher for the largest, i.e. dominant male(s). If the mating probabilities for the two largest males (starting point and end point) increase, SUM_{Δ} decreases asymptotically resulting in several well fitting models. Thereby an increasing mating probability for the second largest male in the late phase does not substantially contribute to an improvement of the model. However the model improves with 4- to 6-fold higher mating probability for the second largest male in the early phase.

Comparing the best-fitting models with the observed data revealed that the observed frequencies of all mating combinations overlap with the 95% confidence limits of the simulated model (1'000 iterations) in all 5 ponds (Fig. A3). This suggests that the model assumptions of an increased mating probability for the largest males (10- to 12-fold higher for males in the early phase and 15- to 20-fold higher in the late phase of the experiment), plus a 4- to 6-fold higher probability for the second largest males in the early phase, explain best the observed frequencies of mating combinations. The lower mating probability for the dominant male in the early phase in combination with an increased probability for the second largest males might reflect an unstable dominance status and relatively early changes in dominance ranks. The observed aggressive territorial fights within the first two weeks (which led to high mortality in the early phase of the experiment) also support this.

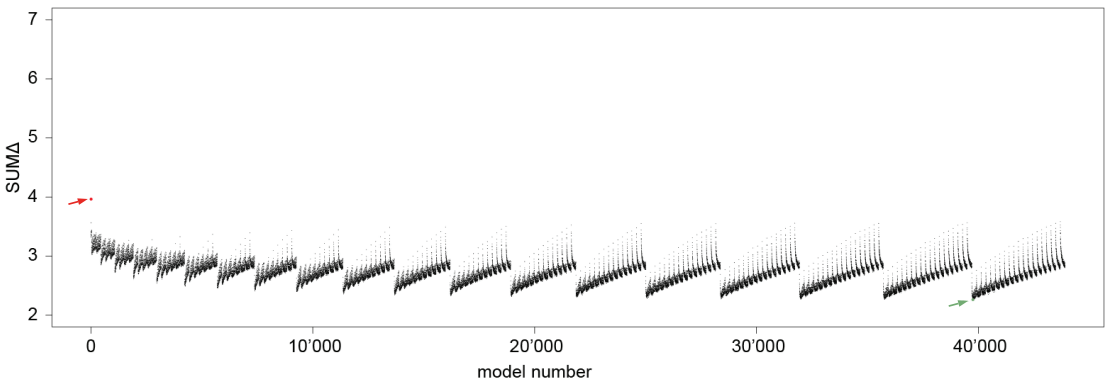

Fig. A2 SUM_{Δ} of the 43'910 models tested. The different combinations of mating probabilities (from 1- to 20-fold) for the four dominant males sorted by increasing mating probabilities for (*i*) the largest male at the end point of the experiment, (*ii*) the largest male at the starting point of the experiment, (iii) the second largest males at the end point and (*iiii*) the second largest males at the starting point of the experiment. The model without assigning any dominance to the males is marked in red and the best fitting model (lowest SUM_{Δ}) in green.

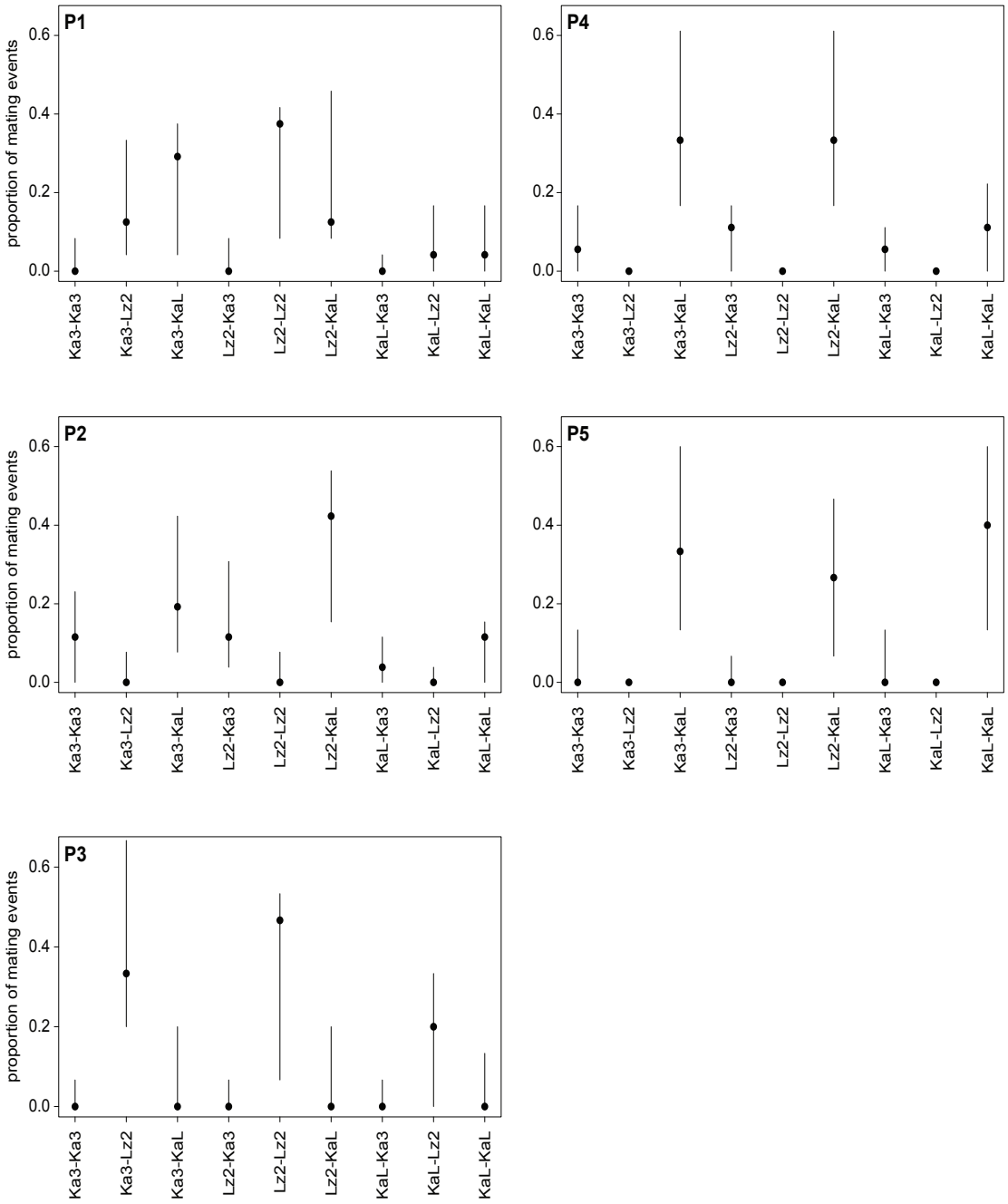

Fig. A3 Observed frequencies of mating combinations per replicate (filled circles) and simulated mating combinations with 1‘000 iterations (bars show the 95% confidence limits) using the best fitting model (green arrow in Fig. A2) with following mating probabilities: 10-folded and 5-folded mating probabilities for the largest and the second largest males at the starting point of the experiment and 20- and 1-folded probabilities for the largest and the second largest males at the end point of the experiment.

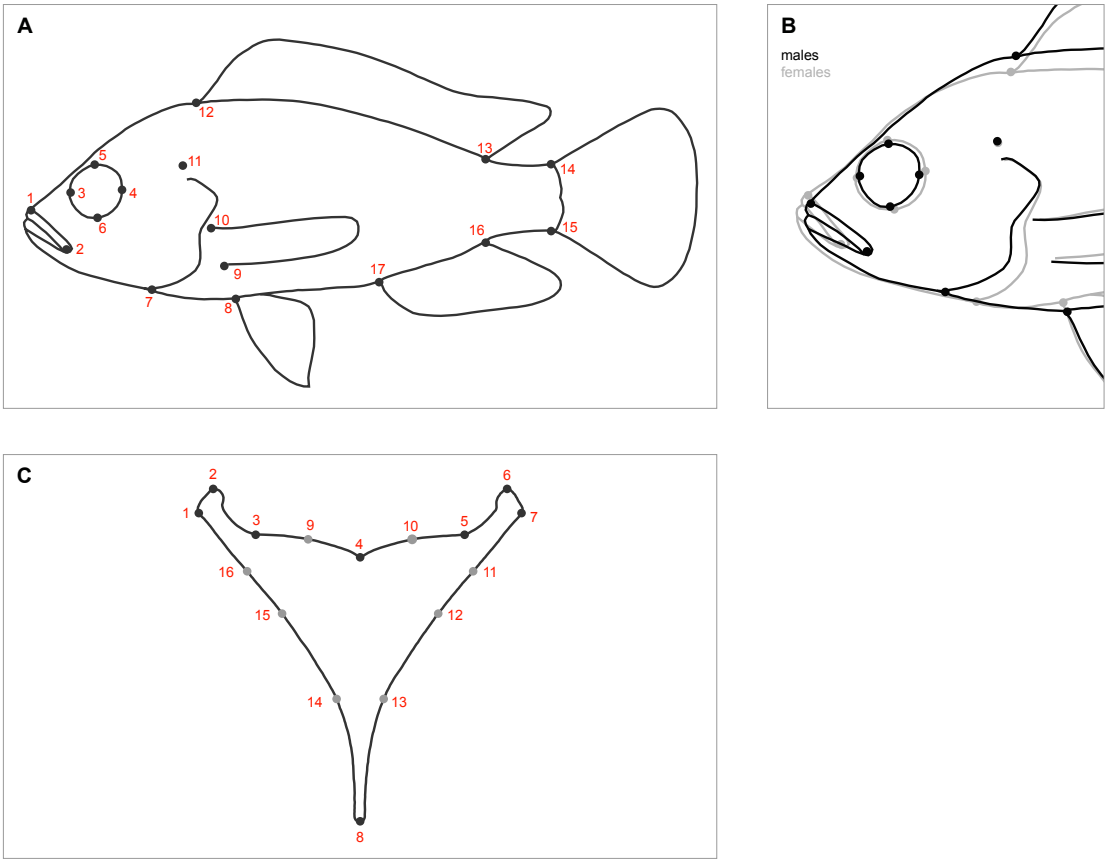

Fig. S1 Landmark positions for body shape and LPJ analyses and sex differences in head shape. (A) All 17 landmarks were used for body shape analyses comparing the wild populations, whereas only the 6 landmarks 1, 2, 8, 12, 14 and 15 were used for comparisons of the body shape of adults and F1 offspring of the pond experiment and only the four landmarks 1, 2, 7 and 12 were included in the mouth position analysis. (B) Only the landmarks describing head shape (1-8, 11 and 12) were used to compare head morphology of males (black outline) and females (grey outline). A DFA showed that females generally have more slender, but longer heads (DF differences are increased tenfold in the outlines). (C) True (black) and semi-landmarks (grey), which were included in the comparisons of the LPJ shape.

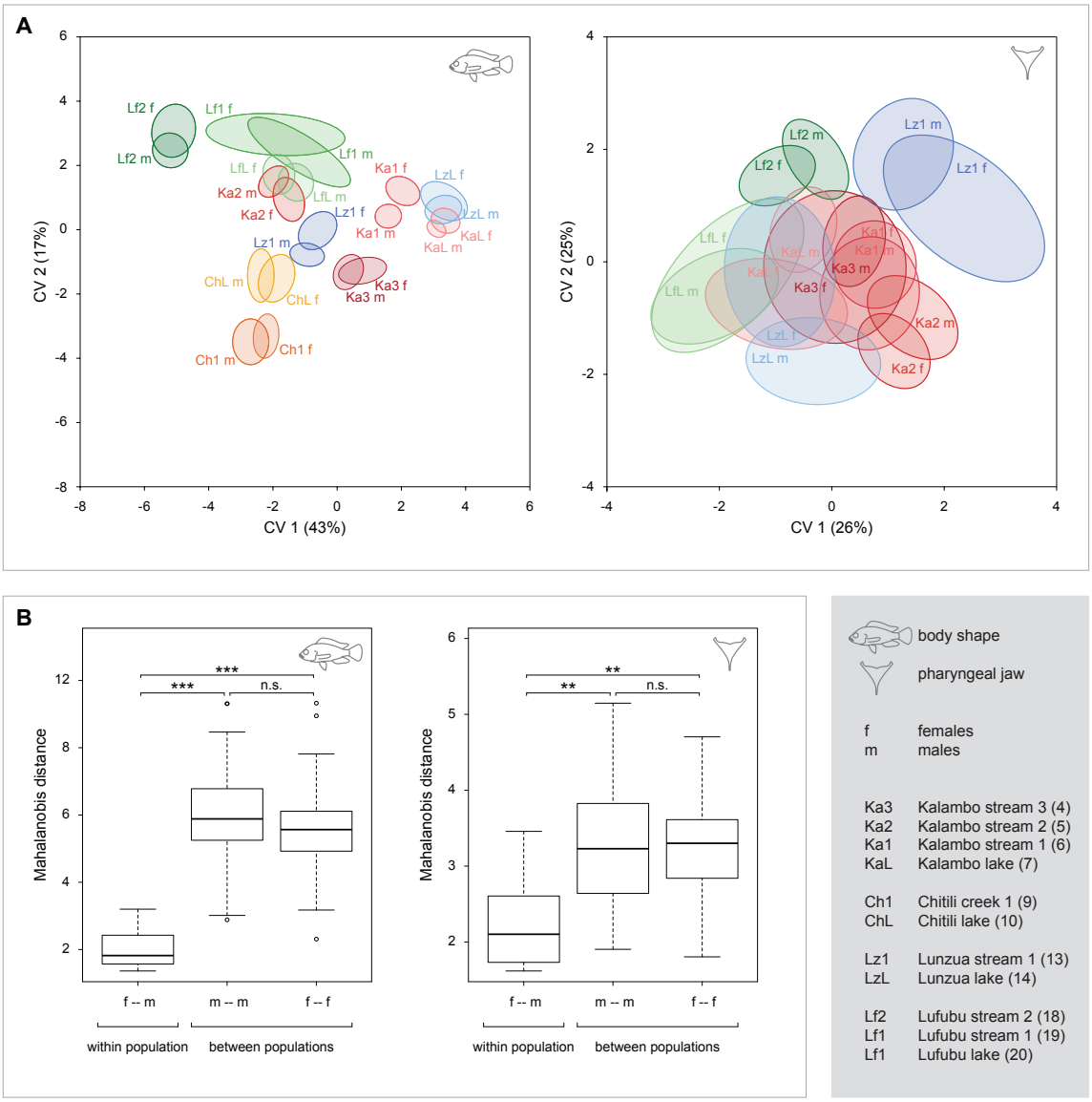

Fig. S2 Comparison of inter-sexual within population differences and intra-sexual differences among populations in morphometric traits (body shape and LPJ). (A) CVA plots show strong population specific overlap of male and female body, as well as in LPJ shape (ellipses represent the 95% confidence intervals of the means). The Chitili system was excluded for LPJ shape since sample size was low in females (Table S1). (B) ANOVAs with additional TukeyHSD show significantly smaller Mahalanobis distances in inter-sexual comparisons within populations, compared to intra-sexual comparisons among populations for body shape as well as for LPJ shape. Significance levels: $P < 0.05$*, $P < 0.01$** and $P < 0.0001$***.

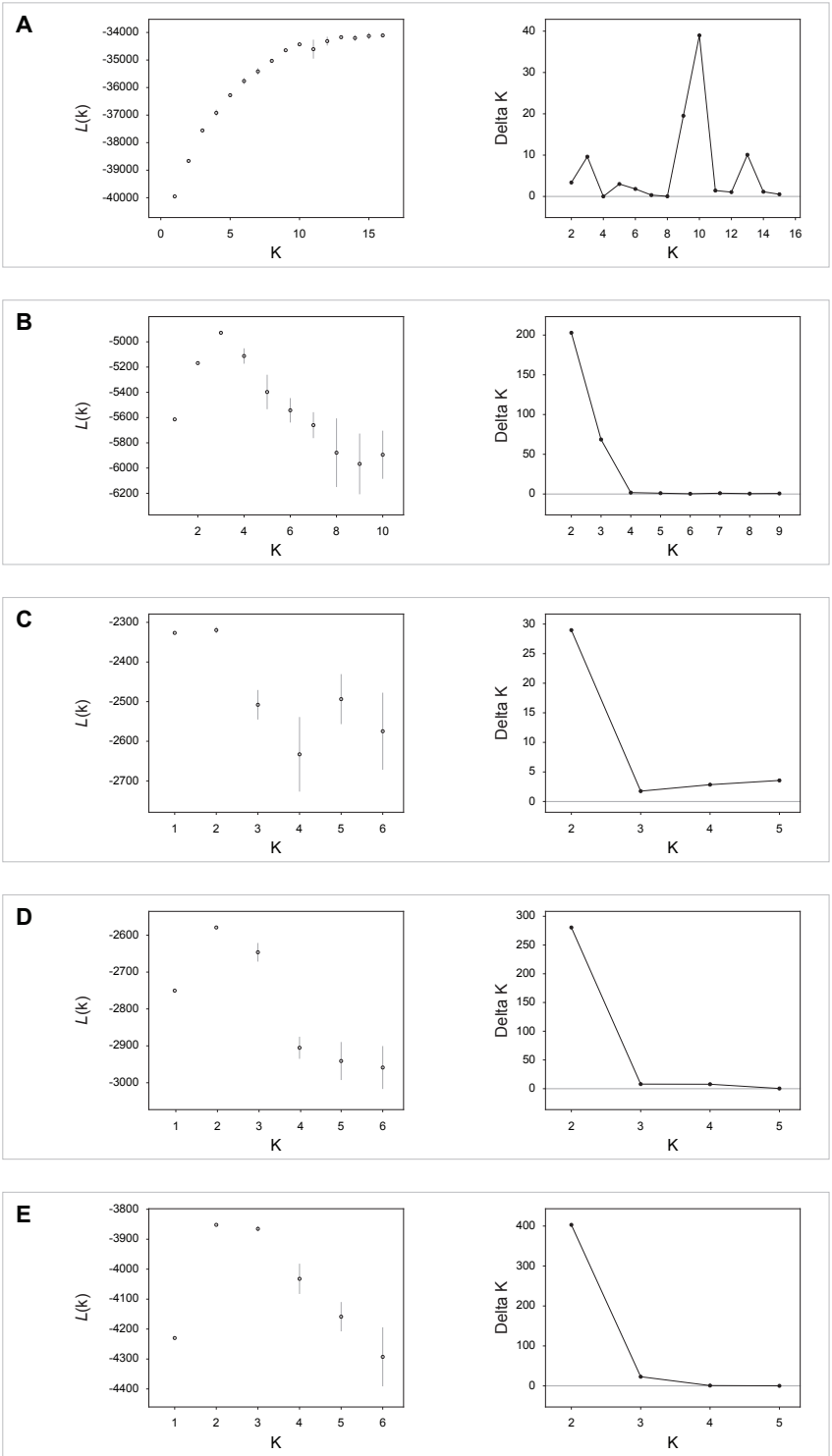

Fig. S3 Mean likelihood (L(*K*) ± SD) over 10 STRUCTURE runs assuming *K* clusters (left); Δ*K* statistic (right); (A) full data, (B) samples from the Kalambo river, (C) samples from the Chitili creek, (D) samples from the Lunzua river, (E) samples from the Lufubu river.

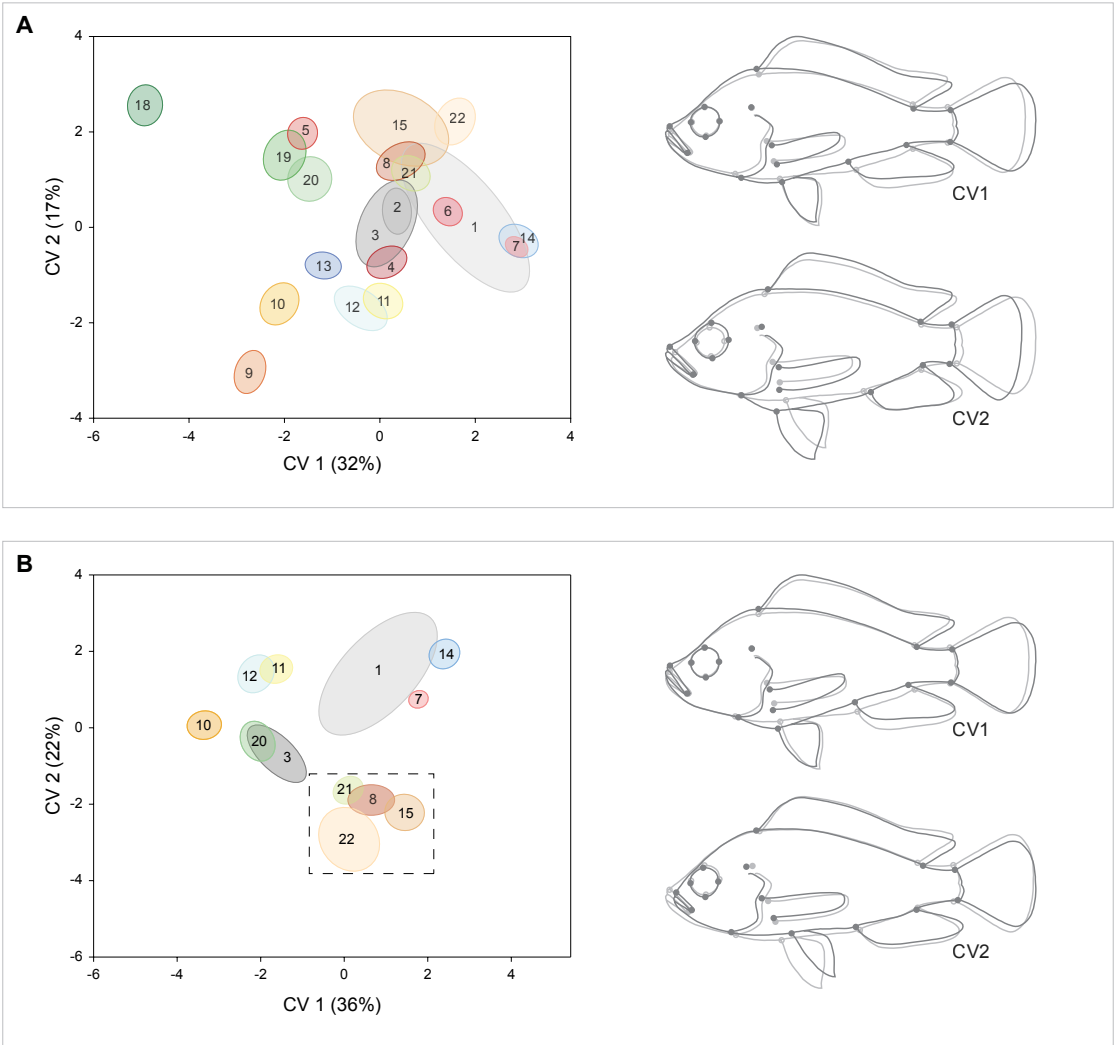

1 Ninde	6 Kalambo stream 1 (Ka1)	11 Chisanza	18 Lufubu stream 2 (Lf2)
2 Loazi	7 Kalambo lake (KaL)	12 Sumba	19 Lufubu stream 1 (Lf1)
3 Muzi	8 Toby's Place	13 Lunzua stream 1 (Lz1)	20 Lufubu lake (LfL)
4 Kalambo stream 3 (Ka3)	9 Chitili creek 1 (Ch1)	14 Lunzua lake (LzL)	21 Ndole Bay
5 Kalambo stream 2 (Ka2)	10 Chitili lake (ChL)	15 Wonzye	22 Lake Chila

Fig. S4 Body shape differentiation among the 20 sampled populations and among the 11 shoreline populations only (ellipses represent the 95% confidence intervals of the means). (A) Overall body shape differentiation among 20 populations (numbers and colors of the populations correspond with Fig. 1). The most extreme shape changes of the first two CVs are illustrated by landmark shifts (from grey to black with increasing values) (Table S3B). (B) CVA plot for the first two CVs and corresponding landmark shifts for the shoreline populations only. The clustering of populations in the morpho-space indicates stronger clustering of pure lacustrine populations (framed with a dashed line) compared to the other, more scattered shoreline populations, which are adjacent to streams.

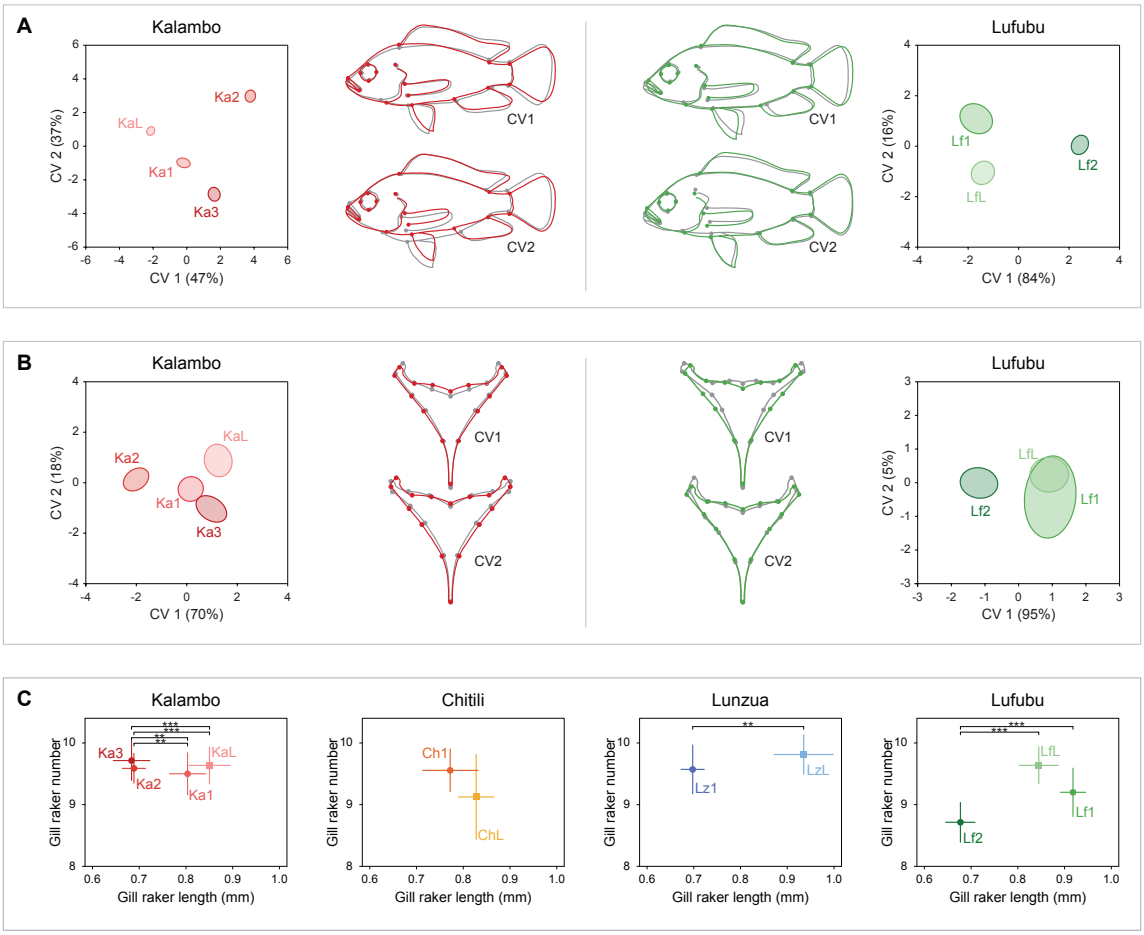

Fig. S5 Body shape and LPJ shape differentiation within systems with more than two populations and gill raker length and number in females. (A) Body shape differentiation separately for the four Kalambo populations (ellipses represent the 95% confidence intervals of the means, outlines from colored to grey with increasing CV-values, Table S4A) as well for the three Lufubu populations (Table S4B). (B) LPJ shape differentiation for the four Kalambo populations separately (Table S4C) as well for the three Lufubu populations (Table S4D). (C) Differences in size corrected female gill raker lengths and number between populations within each lake-stream system (error bars represent 95% confidence intervals of the means) (Table S6). Significance levels: $P < 0.05$*, $P < 0.01$** and $P < 0.0001$***.

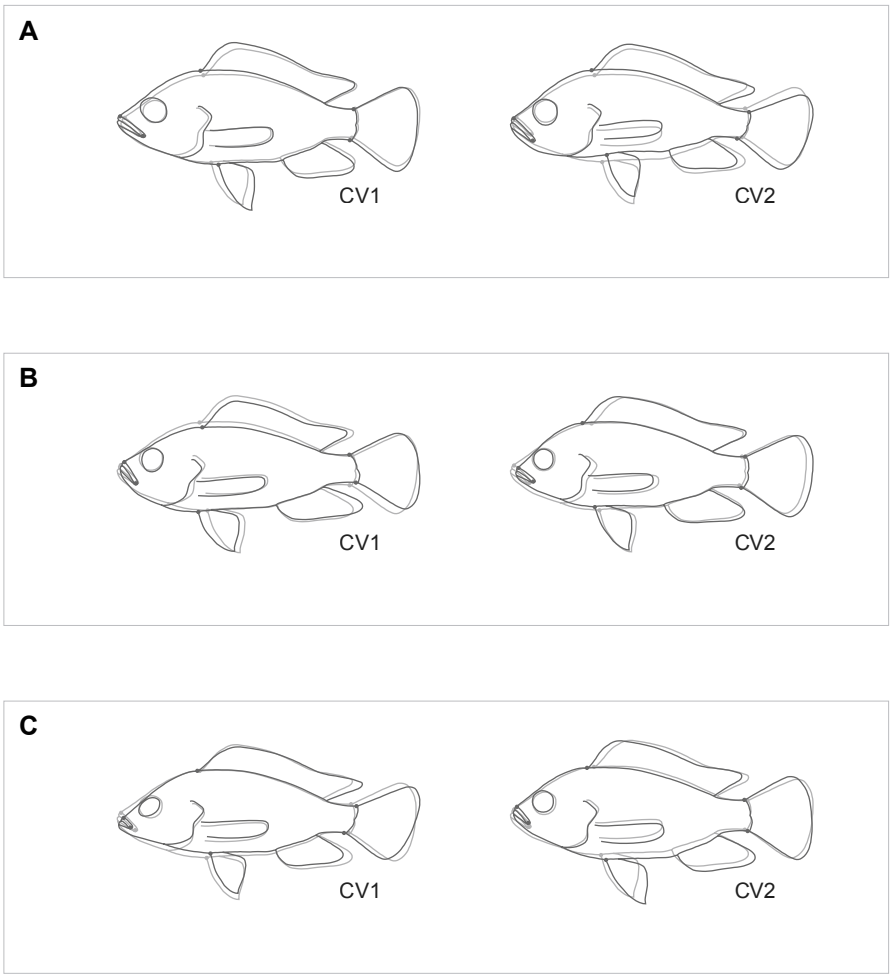

Fig. S6 Outlines to illustrate the body shape changes in F1 individuals of the pond experiment (CVA plots in Fig. 4A; distance values Table S7). From light grey to dark outlines with increasing values, scaling factor ten by default.
(A) KaL-KaL/KaL-Ka3/Ka3-Ka3, (B) KaL-KaL/KaL-Lz1/Lz1-Lz1 and (C) Ka3-Ka3/Ka3-Lz1/Lz1-Lz1.

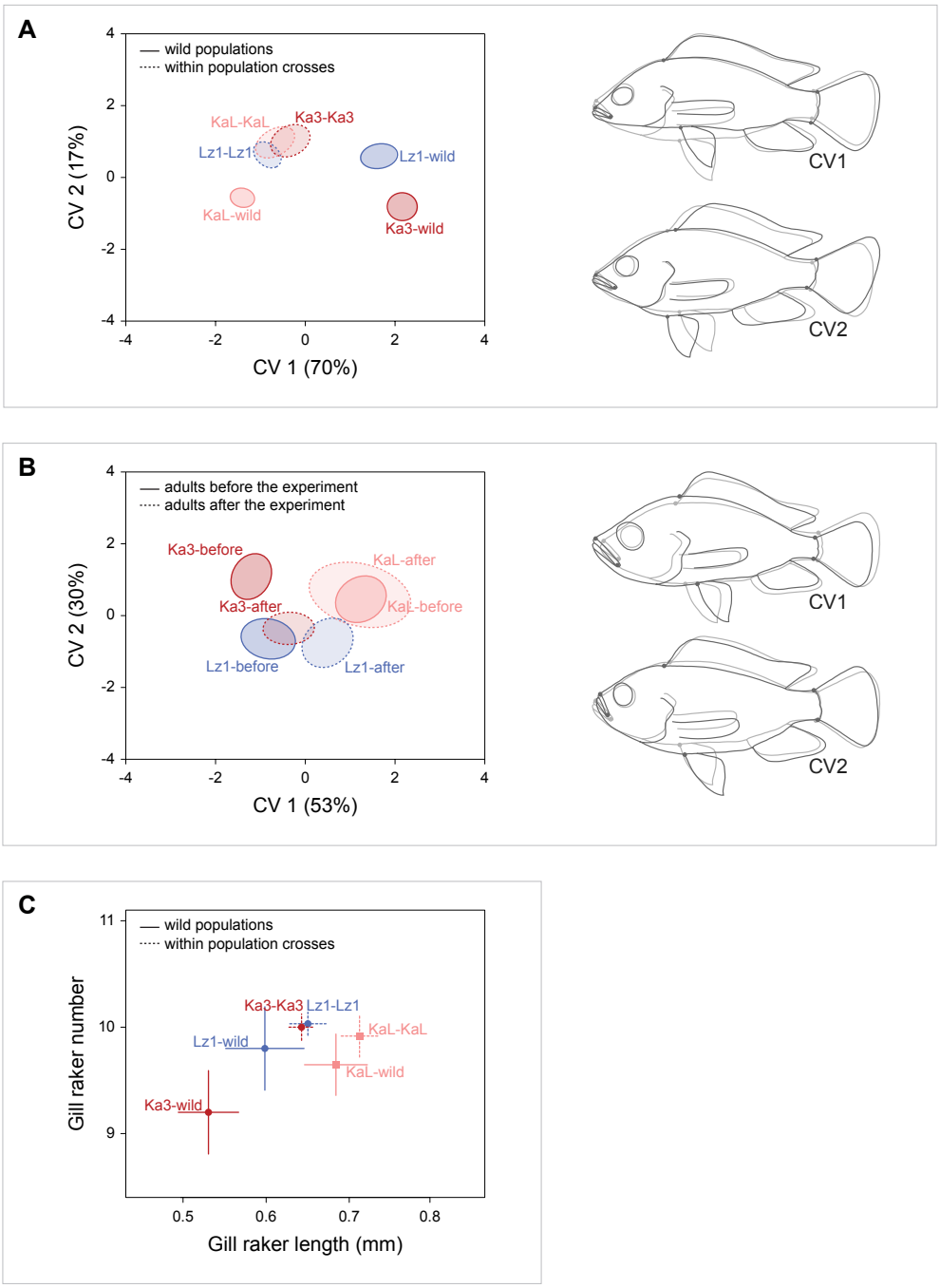

Fig. S7 Plasticity in body shape and gill raker length. (A) CVA of body shape among the within population F1 offspring and their corresponding wild populations. Outlines for illustration purposes only, from light grey to dark outlines with increasing values, scaling factor ten by default. (B) CVA comparing the body shape of surviving adults at the beginning and at the end of the experimental period. (C) Comparison of gill raker length among the within population F1 offspring and their corresponding wild populations. (Table S8)

Table S1 Sample size details for each analysis with information about sampling year and geographic coordinates for each locality (note that some individuals were used for more than one analysis).

	sampling information						body shape analysis				LPJ analysis					gill raker analysis				microsatellite analysis				mtDNA analysis				stomach and gut content analysis			
	population	locality	specification	latitude	longitude	year	total	males	females	juveniles	total	males	females	juveniles	undef. sex	total	males	females	juveniles	total	males	females	juveniles	total	males	females	juveniles	total	males	females	juveniles
	1	Ninde	lake population adjacent to stream	7°40'51.10"S	30°43'20.67"E	2011	7	2	5	0	n/a	n/a	n/a	n/a	n/a	n/a	n/a	n/a	n/a	7	2	5	0	7	2	5	0	n/a	n/a	n/a	n/a
	2	Loazi	lake population adjacent to stream	8°18'49.55"S	31° 2'57.54"E	2011	32	17	15	0	n/a	n/a	n/a	n/a	n/a	n/a	n/a	n/a	n/a	31	16	15	0	7	7	0	0	n/a	n/a	n/a	n/a
	3	Muzi	lake population adjacent to stream	8°23'1.84"S	31° 7'47.15"E	2011	24	12	12	0	n/a	n/a	n/a	n/a	n/a	n/a	n/a	n/a	n/a	25	14	11	0	9	7	2	0	n/a	n/a	n/a	n/a
Kalambo system	4a Ka3	Kalambo stream 3	stream population	8°35'41.59"S	31°14'50.32"E	2010	n/a	n/a	n/a	n/a	20	10	9	1	0	n/a	n/a	n/a	n/a	32	4	10	18	27	4	9	14	n/a	n/a	n/a	n/a
	4b Ka3					2011	52	29	23	0	n/a	n/a	n/a	n/a	n/a	29	15	14	0	30	17	13	0	n/a	n/a	n/a	n/a	10	10	0	0
	5a Ka2	Kalambo stream 2	stream population	8°35'6.24"S	31°12'29.32"E	2011	n/a	n/a	n/a	n/a	14	2	12	0	0	14	2	12	0	14	1	13	0	n/a	n/a	n/a	n/a	n/a	n/a	n/a	n/a
	5b Ka2					2012	38	23	15	0	14	10	4	0	0	16	11	5	0	32	19	12	1	8	6	2	0	10	10	0	0
	6a Ka1	Kalambo stream 1	stream population	8°35'35.23"S	31°11'6.18"E	2011	59	41	18	0	n/a	n/a	n/a	n/a	n/a	n/a	n/a	n/a	n/a	32	17	15	0	6	4	2	0	n/a	n/a	n/a	n/a
	6b Ka1					2012	n/a	n/a	n/a	n/a	25	13	11	0	1	28	14	14	0	n/a	n/a	n/a	n/a	n/a	n/a	n/a	n/a	10	10	0	0
	7a KaL	Kalambo lake	lake population adjacent to stream	8°36'6.27"S	31°11'13.24"E	2010	n/a	n/a	n/a	n/a	n/a	n/a	n/a	n/a	n/a	n/a	n/a	n/a	n/a	31	27	4	0	29	25	4	0	n/a	n/a	n/a	n/a
	7b KaL					2011	102	59	43	0	23	11	8	0	4	25	17	8	0	33	19	14	0	n/a	n/a	n/a	n/a	10	10	0	0
	7c KaL					2012	n/a	n/a	n/a	n/a	3	1	2	0	0	3	0	3	0	n/a	n/a	n/a	n/a	n/a	n/a	n/a	n/a	n/a	n/a	n/a	n/a
	8a	Toby's place	pure lake population	8°37'25.99"S	31°12'2.86"E	2010	n/a	n/a	n/a	n/a	n/a	n/a	n/a	n/a	n/a	n/a	n/a	n/a	n/a	34	16	11	7	30	15	10	5	n/a	n/a	n/a	n/a
	8b					2012	33	19	14	0	n/a	n/a	n/a	n/a	n/a	n/a	n/a	n/a	n/a	31	19	12	0	n/a	n/a	n/a	n/a	n/a	n/a	n/a	n/a
Chitili system	9a Ch1	Chitili creek 1	stream population	8°38'16.91"S	31°12'4.02"E	2010	n/a	n/a	n/a	n/a	n/a	n/a	n/a	n/a	n/a	n/a	n/a	n/a	n/a	7	1	4	2	7	1	4	2	n/a	n/a	n/a	n/a
	9b Ch1					2011	53	24	29	0	n/a	n/a	n/a	n/a	n/a	n/a	n/a	n/a	n/a	31	14	17	0	10	6	4	0	n/a	n/a	n/a	n/a
	9c Ch1					2012	n/a	n/a	n/a	n/a	14	13	1	0	0	24	15	9	0	n/a	n/a	n/a	n/a	n/a	n/a	n/a	n/a	10	10	0	0
	10a ChL	Chitili lake	lake population adjacent to stream	8°38'18.42"S	31°11'55.34"E	2011	38	10	28	0	n/a	n/a	n/a	n/a	n/a	n/a	n/a	n/a	n/a	31	11	20	0	10	6	4	0	n/a	n/a	n/a	n/a
	10b ChL					2012	n/a	n/a	n/a	n/a	12	8	3	0	1	23	15	8	0	n/a	n/a	n/a	n/a	n/a	n/a	n/a	n/a	5	5	0	0
	11	Chisanza	lake population adjacent to stream	8°39'57.39"S	31°11'41.26"E	2011	41	22	19	0	n/a	n/a	n/a	n/a	n/a	n/a	n/a	n/a	n/a	32	19	12	1	9	6	3	0	n/a	n/a	n/a	n/a
	12	Sumba	lake population adjacent to stream	8°40'18.58"S	31°11'33.94"E	2011	33	22	11	0	n/a	n/a	n/a	n/a	n/a	n/a	n/a	n/a	n/a	32	21	11	0	9	6	3	0	n/a	n/a	n/a	n/a
Lunzua system	13a Lz1	Lunzua stream 1	stream population	8°47'23.51"S	31° 8'14.33"E	2011	53	36	17	0	18	11	7	0	0	n/a	n/a	n/a	n/a	30	17	12	1	7	5	2	0	10	10	0	0
	13b Lz1					2012	n/a	n/a	n/a	n/a	n/a	n/a	n/a	n/a	n/a	18	11	7	0	n/a	n/a	n/a	n/a	n/a	n/a	n/a	n/a	n/a	n/a	n/a	n/a
	14a LzL	Lunzua lake	lake population adjacent to stream	8°44'57.13"S	31°10'21.86"E	2010	n/a	n/a	n/a	n/a	n/a	n/a	n/a	n/a	n/a	n/a	n/a	n/a	n/a	30	21	9	0	24	20	4	0	n/a	n/a	n/a	n/a
	14b LzL					2011	40	23	17	0	11	3	8	0	0	16	5	11	0	31	16	15	0	n/a	n/a	n/a	n/a	5	5	0	0
	14c LzL					2012	n/a	n/a	n/a	n/a	11	7	4	0	0	15	10	5	0	n/a	n/a	n/a	n/a	n/a	n/a	n/a	n/a	5	5	0	0
	15a	Wonzye	pure lake population	8°45'1.76"S	31° 7'49.02"E	2010	n/a	n/a	n/a	n/a	n/a	n/a	n/a	n/a	n/a	n/a	n/a	n/a	n/a	42	24	8	10	39	21	8	10	n/a	n/a	n/a	n/a
	15b					2012	36	17	19	0	n/a	n/a	n/a	n/a	n/a	n/a	n/a	n/a	n/a	18	10	8	0	10	6	4	0	n/a	n/a	n/a	n/a
	16	Fisheries Department	pure lake population	8°45'58.52"S	31° 6'23.99"E	2010	n/a	n/a	n/a	n/a	n/a	n/a	n/a	n/a	n/a	n/a	n/a	n/a	n/a	26	15	5	6	24	19	5	0	n/a	n/a	n/a	n/a
	17	Kalungula	lake population adjacent to stream	8°48'33.39"S	31° 7'49.02"E	2010	n/a	n/a	n/a	n/a	n/a	n/a	n/a	n/a	n/a	n/a	n/a	n/a	n/a	27	17	10	0	28	17	10	1	n/a	n/a	n/a	n/a
Lufubu system	18 Lf2	Lufubu stream 2	stream population	8°41'9.37"S	30°33'51.90"E	2012	36	21	15	0	26	14	12	0	0	29	15	14	0	30	15	15	0	13	4	9	0	10	10	0	0
	19 Lf1	Lufubu stream 1	stream population	8°35'49.31"S	30°43'38.96"E	2011	27	21	6	0	12	8	4	0	0	15	10	5	0	27	21	6	0	10	8	2	0	7	7	0	0
	20a LfL	Lufubu lake	lake population adjacent to stream	8°33'36.56"S	30°43'33.79"E	2011	30	24	6	0	14	10	4	0	0	16	11	5	0	30	24	6	0	9	8	1	0	6	6	0	0
	20b LfL					2012	n/a	n/a	n/a	n/a	7	3	4	0	0	10	4	6	0	n/a	n/a	n/a	n/a	n/a	n/a	n/a	n/a	4	4	0	0
	21	Ndole bay	pure lake population	8°28'34.61"S	30°26'57.48"E	2012	45	24	21	0	n/a	n/a	n/a	n/a	n/a	n/a	n/a	n/a	n/a	16	8	8	0	13	5	8	0	n/a	n/a	n/a	n/a
	22	Lake Chila	pure lake population	8°50'8.68"S	31°22'49.44"E	2012	12	4	8	0	n/a	n/a	n/a	n/a	n/a	n/a	n/a	n/a	n/a	14	4	8	2	14	4	8	2	n/a	n/a	n/a	n/a
	total sample size per analysis						**791**	**450**	**341**	**0**	**224**	**124**	**93**	**1**	**6**	**281**	**155**	**126**	**0**	**786**	**429**	**309**	**48**	**359**	**212**	**113**	**34**	**102**	**102**	**0**	**0**

Table S2 Sample size details and result summary of the pond experiment. (A) Number of stocked adult fish per population and information about survival and reproduction. (B) Number of F1 individuals used for body shape and gill raker analyses.

A

pond	original stock males			original stock females			surviving males			surviving females			non-surviving reproducing males			non-surviving reproducing females			reproducing males	reproducing females	genotyped offspring	mating events
	KaL	Ka3	Lz1	KaL	Ka3	Lz1	KaL	Ka3	Lz1	KaL	Ka3	Lz1	KaL	Ka3	Lz1	KaL	Ka3	Lz1				
1	4	4	4	7	7	7	1	1	2	1	3	3	0	0	1	0	0	1	3	8	148	24
2	4	4	4	7	7	7	2	1	1	1	2	5	1	2	0	0	2	1	5	11	160	26
3	4	4	4	7	7	7	1	1	2	1	3	2	0	0	1	0	0	0	2	8	95	15
4	4	4	4	7	7	7	1	0	0	1	4	4	0	1	0	0	0	0	2	9	111	18
5	4	4	4	7	7	7	2	2	0	3	3	2	0	0	0	0	0	0	2	6	79	15
total	**20**	**20**	**20**	**35**	**35**	**35**	**7**	**5**	**5**	**7**	**15**	**16**	**1**	**3**	**2**	**0**	**2**	**2**	**14**	**42**	**593**	**98**

B

F1 juveniles	body shape	gill raker
KaL-KaL	25	25
Ka3-Ka3	24	24
Lz1-Lz1	31	32
KaL-Ka3	13	13
KaL-Lz1	26	26
Ka3-Lz1	11	12
total	130	132

Table S3 Pairwise genetic and morphometric (body size) distances between populations (full names of localities are given in the grey box in Fig. 1 and Table S1). (A) Pairwise genetic differentiation: D_{EST}-values (upper triangular matrix) and F_{ST}-values (lower triangular matrix). Both indices indicate significant differentiation (P values < 0.05) between most populations (non-significant values are underlined). (B) Pairwise body shape differentiation among populations: Procrustes (upper triangular matrix) and Mahalanobis (lower triangular matrix) distances from the CVA (Fig. S4A). All comparisons showed significant body shape differences (P values < 0.05).

A

population	1	2	3	4a	4b	5a	5b	6a	7a	7b	8a	8b	9a	9b	10a	11	12	13a	14a	14b	15a	15b	16	17	18	19	20a	21	22
1		0.5450	0.6476	0.7410	0.7528	0.7166	0.7754	0.5761	0.5899	0.6407	0.6578	0.6486	0.6970	0.6573	0.6161	0.6554	0.6300	0.6773	0.6453	0.6003	0.6412	0.6333	0.6351	0.6578	0.7470	0.6216	0.6655	0.6624	0.6907
2	0.0925		0.3848	0.6392	0.6646	0.6361	0.7401	0.4525	0.4374	0.4860	0.5584	0.5472	0.5172	0.4678	0.3930	0.4036	0.4120	0.5416	0.4667	0.3968	0.4887	0.4827	0.5121	0.4972	0.6498	0.4745	0.4926	0.5976	0.5610
3	0.1118	0.0513		0.6317	0.6486	0.5918	0.6942	0.3512	0.4235	0.4443	0.5425	0.4995	0.4250	0.3380	0.3183	0.4006	0.3507	0.4906	0.3661	0.3507	0.4920	0.4609	0.5078	0.5254	0.6776	0.5332	0.5121	0.6015	0.5262
4a	0.1430	0.1134	0.1126		-0.0087	0.6502	0.5503	0.6848	0.5581	0.5785	0.5677	0.6405	0.5553	0.6398	0.6050	0.5682	0.5981	0.4527	0.4345	0.5110	0.5681	0.6076	0.5490	0.5943	0.6727	0.4306	0.4634	0.6278	0.5313
4b	0.1577	0.1256	0.1236	-0.0018		0.6382	0.5497	0.6898	0.6248	0.6422	0.6422	0.6841	0.6098	0.6267	0.6209	0.5875	0.5832	0.4352	0.4716	0.4965	0.5914	0.6429	0.5820	0.6397	0.6602	0.4656	0.5044	0.6579	0.5555
5a	0.2053	0.1379	0.1350	0.1719	0.1773		0.1128	0.3582	0.4219	0.3503	0.5523	0.5373	0.6257	0.5373	0.4357	0.5269	0.4961	0.6008	0.6377	0.5163	0.6777	0.6678	0.6311	0.5992	0.7017	0.6676	0.6408	0.5476	0.6259
5b	0.2154	0.1707	0.1659	0.1560	0.1613	0.0422		0.5291	0.4378	0.3579	0.5354	0.6415	0.5772	0.6369	0.5614	0.6299	0.6157	0.6668	0.5818	0.6264	0.6384	0.6557	0.5710	0.5932	0.7059	0.6950	0.6743	0.5443	0.5409
6a	0.1039	0.0671	0.0436	0.1309	0.1391	0.0818	0.1398		0.5291	0.1467	0.3445	0.3142	0.3983	0.3149	0.1728	0.3078	0.3022	0.5222	0.4162	0.3323	0.5202	0.5074	0.4909	0.5093	0.6767	0.5084	0.4730	0.4701	0.4930
7a	0.1052	0.0741	0.0727	0.0922	0.1110	0.1045	0.1030	0.0615		-0.0053	0.2640	0.4185	0.2659	0.4136	0.2243	0.3483	0.3616	0.5369	0.2220	0.3715	0.3418	0.3094	0.3311	0.3085	0.6529	0.4233	0.4280	0.3903	0.3756
7b	0.1240	0.0888	0.0821	0.1026	0.1220	0.0993	0.0887	0.0740	0.0006		0.2424	0.4437	0.2318	0.4171	0.2517	0.3967	0.3987	0.6047	0.2631	0.3982	0.3872	0.4222	0.3590	0.3717	0.6343	0.4850	0.4727	0.4230	0.3898
8a	0.1334	0.1011	0.1009	0.1135	0.1357	0.1437	0.1376	0.0915	0.0370	0.0346		0.1788	0.2516	0.3862	0.3416	0.5063	0.5220	0.6175	0.4398	0.5535	0.5639	0.5682	0.5506	0.5464	0.7040	0.4957	0.5201	0.4737	0.5773
8b	0.1496	0.1037	0.0865	0.1542	0.1717	0.1594	0.1958	0.0526	0.1042	0.1176	0.0789		0.4689	0.2878	0.2595	0.4627	0.4957	0.5815	0.5763	0.5227	0.6696	0.6482	0.6495	0.6972	0.7306	0.6498	0.6589	0.6168	0.6790
9a	0.1282	0.0623	0.0373	0.1267	0.1376	0.1088	0.1511	0.0227	0.0714	0.0816	0.0905	0.0450		0.2260	0.2549	0.2184	0.2473	0.4618	0.3573	0.2845	0.4853	0.4388	0.4555	0.5103	0.6709	0.5284	0.5416	0.5376	0.5607
9b	0.1372	0.0788	0.0703	0.0977	0.1154	0.1493	0.1473	0.0819	0.0333	0.0347	0.0442	0.0577	0.0789		0.0952	0.4628	0.3521	0.5596	0.3127	0.4332	0.4381	0.3847	0.3680	0.4434	0.6248	0.4096	0.4208	0.5379	0.3992
10a	0.1408	0.0874	0.0520	0.1480	0.1545	0.1422	0.1878	0.0451	0.1042	0.1151	0.0919	0.0572	0.0674	0.0142		0.3266	0.3269	0.5092	0.4391	0.3709	0.5790	0.5637	0.5762	0.5892	0.6841	0.5251	0.5744	0.6248	0.6055
11	0.1052	0.0538	0.0418	0.0929	0.1003	0.1138	0.1469	0.0379	0.0680	0.0792	0.0938	0.0752	0.0735	0.0463	0.0278		0.0892	0.4358	0.2670	0.1940	0.4398	0.4005	0.4366	0.4242	0.6550	0.4286	0.3965	0.5390	0.4644
12	0.0797	0.0474	0.0340	0.0929	0.0987	0.0987	0.1362	0.0322	0.0586	0.0703	0.0872	0.0765	0.0496	0.0470	0.0289	0.0095		0.3829	0.2465	0.1214	0.3546	0.3484	0.3775	0.3983	0.6399	0.4277	0.3935	0.5134	0.4150
13a	0.1286	0.0957	0.0786	0.1058	0.1097	0.1534	0.1869	0.0818	0.1074	0.1246	0.1375	0.1247	0.1144	0.1004	0.0810	0.0630	0.0520		0.4966	0.3472	0.5844	0.6242	0.5866	0.5359	0.6777	0.5717	0.6258	0.7185	0.5394
14a	0.1013	0.0728	0.0608	0.0618	0.0776	0.1400	0.1254	0.0868	0.0207	0.0228	0.0537	0.1200	0.0330	0.1027	0.0790	0.0513	0.0460	0.0943		0.1211	0.2074	0.1525	0.2331	0.3151	0.6680	0.3023	0.2637	0.4265	0.3091
14b	0.0800	0.0455	0.0313	0.0796	0.0845	0.1014	0.1384	0.0330	0.0630	0.0730	0.0920	0.0751	0.0587	0.0469	0.0289	0.0119	0.0069	0.0453	0.0410		0.3132	0.2815	0.3157	0.3570	0.6836	0.3839	0.3665	0.5661	0.3695
15a	0.1004	0.0633	0.0654	0.0823	0.0913	0.1293	0.1302	0.0857	0.0362	0.0444	0.0764	0.1247	0.0480	0.1050	0.0791	0.0560	0.0474	0.0959	0.0198	0.0432		-0.0202	0.0808	0.1652	0.6550	0.4034	0.3584	0.4657	0.1277
15b	0.0960	0.0566	0.0603	0.0878	0.0998	0.1330	0.1390	0.0822	0.0350	0.0477	0.0769	0.1247	0.0425	0.1022	0.0740	0.0538	0.0426	0.0983	0.0215	0.0396	-0.0021		0.0648	0.2240	0.6696	0.3461	0.3325	0.4295	0.2123
16	0.0943	0.0607	0.0644	0.0843	0.0938	0.1262	0.1218	0.0812	0.0379	0.0480	0.0784	0.1235	0.0398	0.1034	0.0761	0.0576	0.0454	0.0960	0.0250	0.0420	0.0065	0.0020		0.0748	0.6558	0.3653	0.3424	0.4662	0.0575
17	0.1135	0.0689	0.0703	0.0950	0.1074	0.1238	0.1287	0.0876	0.0378	0.0487	0.0771	0.1384	0.0510	0.1095	0.0833	0.0605	0.0503	0.0473	0.0987	0.0318	0.0143	0.0178	0.0054		0.6973	0.3978	0.3745	0.4929	0.1040
18	0.1978	0.1483	0.1541	0.1644	0.1690	0.2100	0.2161	0.1686	0.1471	0.1575	0.1709	0.2147	0.1493	0.1894	0.1664	0.1491	0.1383	0.1394	0.1771	0.1413	0.1270	0.1286	0.1272	0.1364		0.5617	0.6571	0.6803	0.6186
19	0.0853	0.0528	0.0581	0.0713	0.0799	0.1208	0.1345	0.0735	0.0500	0.0606	0.0691	0.1175	0.0415	0.0965	0.0748	0.0491	0.0422	0.0419	0.0966	0.0345	0.0360	0.0292	0.0289	0.0348	0.1021		0.0676	0.3984	0.4382
20a	0.0838	0.0661	0.0766	0.0693	0.0795	0.1396	0.1526	0.0900	0.0583	0.0716	0.0767	0.1278	0.0548	0.1045	0.0910	0.0652	0.0583	0.0556	0.1043	0.0405	0.0527	0.0449	0.0452	0.0508	0.1318	0.0115		0.4544	0.3790
21	0.1505	0.0956	0.0956	0.1143	0.1255	0.1459	0.1379	0.0772	0.0418	0.0603	0.0828	0.1481	0.0809	0.1343	0.1040	0.0822	0.0616	0.0739	0.1364	0.0555	0.0463	0.0504	0.0509	0.0611	0.1485	0.0404	0.0550		0.5562
22	0.1214	0.0745	0.0720	0.0898	0.0982	0.1330	0.1253	0.0862	0.0471	0.0573	0.0894	0.1371	0.0528	0.1137	0.0884	0.0633	0.0506	0.0994	0.0395	0.0502	0.0170	0.0168	0.0047	0.0183	0.1344	0.0620	0.0392	0.0751	

B

population	1	2	3	4b	5b	6a	7b	8b	9b	10a	11	12	13a	14b	15b	18	19	20a	21	22
1		0.0295	0.0404	0.0484	0.0233	0.0511	0.0327	0.0228	0.0420	0.0379	0.0369	0.0457	0.0438	0.0276	0.0316	0.0395	0.0401	0.0319	0.0324	0.0337
2	4.9489		0.0220	0.0320	0.0279	0.0346	0.0225	0.0190	0.0273	0.0188	0.0194	0.0258	0.0269	0.0236	0.0205	0.0290	0.0231	0.0219	0.0223	0.0235
3	5.5377	3.5329		0.0309	0.0398	0.0303	0.0224	0.0337	0.0370	0.0269	0.0275	0.0268	0.0380	0.0331	0.0257	0.0399	0.0332	0.0340	0.0164	0.0252
4b	6.8230	5.1413	5.0948		0.0458	0.0220	0.0252	0.0382	0.0314	0.0300	0.0290	0.0198	0.0238	0.0330	0.0430	0.0473	0.0338	0.0381	0.0326	0.0364
5b	6.0672	4.7985	5.2939	5.3491		0.0537	0.0371	0.0169	0.0350	0.0307	0.0322	0.0426	0.0397	0.0297	0.0304	0.0289	0.0313	0.0258	0.0309	0.0322
6a	5.8194	4.2485	4.5856	3.9140	5.8216		0.0250	0.0433	0.0456	0.0399	0.0379	0.0276	0.0342	0.0373	0.0418	0.0518	0.0402	0.0435	0.0339	0.0349
7b	4.6544	3.9309	4.7515	4.4821	5.9213	3.6119		0.0271	0.0362	0.0290	0.0259	0.0266	0.0319	0.0202	0.0262	0.0423	0.0322	0.0300	0.0178	0.0219
8b	5.0837	3.6133	4.9001	4.8953	3.2746	4.5877	4.1048		0.0323	0.0262	0.0267	0.0343	0.0311	0.0225	0.0214	0.0292	0.0260	0.0210	0.0259	0.0227
9b	7.4268	5.4561	5.8027	5.2976	5.6321	6.4922	6.4594	5.7587		0.0157	0.0207	0.0267	0.0232	0.0344	0.0426	0.0369	0.0295	0.0302	0.0383	0.0405
10a	6.4120	4.3150	4.5920	4.9249	4.8566	5.5860	5.4444	4.8670	2.7773		0.0122	0.0208	0.0246	0.0301	0.0313	0.0275	0.0191	0.0199	0.0275	0.0309
11	5.3302	3.9713	4.4396	5.4390	5.5530	5.2339	4.0371	4.7344	4.6413	3.2506		0.0175	0.0226	0.0237	0.0307	0.0297	0.0185	0.0201	0.0266	0.0330
12	5.3235	4.1567	3.9157	5.0405	5.4377	4.7458	4.4480	4.7718	4.3730	3.1550	2.6681		0.0195	0.0302	0.0370	0.0382	0.0253	0.0309	0.0307	0.0355
13a	5.5699	3.9608	4.9743	4.2981	4.7427	4.7551	5.0274	4.2964	4.2820	4.1919	4.4350	3.7757		0.0279	0.0411	0.0370	0.0266	0.0302	0.0390	0.0384
14b	4.7761	4.7438	5.9381	6.0316	6.3602	5.3310	3.1124	4.8900	7.2722	6.4282	4.6146	5.0731	5.0915		0.0280	0.0366	0.0313	0.0276	0.0266	0.0304
15b	5.9430	4.0590	4.9601	5.8978	4.9754	5.3011	4.3202	3.1856	7.2228	5.9421	5.1375	5.6335	5.6291	5.0148		0.0324	0.0308	0.0271	0.0189	0.0211
18	8.6069	6.8003	7.1742	7.4456	5.6354	7.6059	8.6780	6.9380	7.0098	6.1314	7.5099	7.0728	5.8962	8.8590	7.8515		0.0236	0.0221	0.0355	0.0380
19	7.2622	5.0887	5.7369	5.7504	5.0762	5.5812	6.1696	5.2621	6.2073	4.7727	4.8053	5.2103	5.2406	6.9723	5.7678	5.6799		0.0119	0.0298	0.0312
20a	6.1171	4.7340	5.5192	5.5934	4.9598	5.3450	5.4051	4.8552	5.8256	4.1782	4.1792	4.7464	4.7929	6.1352	5.5719	5.7718	1.9520		0.0277	0.0276
21	5.4945	3.6410	3.4655	4.2158	3.8495	4.1331	3.5529	3.3760	5.7653	4.4868	4.2807	4.3444	4.9261	5.0558	3.5793	6.8204	5.0064	4.6630		0.0200
22	6.1168	5.0319	5.0086	5.6808	4.4431	5.0999	5.0892	3.7617	6.9245	5.5506	5.8239	5.5646	5.7433	6.4322	4.3525	7.5547	5.6727	5.1649	3.7673	

Table S4 Pairwise morphometric (body shape and LPJ) distances within systems with more than two populations. Procrustes (upper triangular matrix) and Mahalanobis (lower triangular matrix) distances from the CVA (Fig. S5A & B) (non-significant values are underlined). (A) Pairwise body shape differentiation among the four Kalambo populations. (B) Pairwise body shape differentiation among the three Lufubu populations. (C) Pairwise LPJ shape differentiation among the four Kalambo populations. (D) Pairwise LPJ shape differentiation among the three Lufubu populations.

A

population	KaL	Ka1	Ka2	Ka3
KaL		0.0251	0.0368	0.0253
Ka1	3.8781		0.0535	0.0220
Ka2	6.3056	6.0287		0.0456
Ka3	5.3659	4.2863	6.3437	

B

population	LfL	Lf1	Lf2
LfL		0.0122	0.0182
Lf1	2.1637		0.0208
Lf2	4.0045	4.2414	

C

population	KaL	Ka1	Ka2	Ka3
KaL		0.0175	0.0217	0.0158
Ka1	1.9260		0.0122	0.0192
Ka2	3.3438	2.4847		0.0257
Ka3	1.9681	1.8445	3.2216	

D

population	LfL	Lf1	Lf2
LfL		0.0064	0.0266
Lf1	0.6663		0.0258
Lf2	2.1046	2.1603	

Table S5 Pairwise morphometric (body shape and LPJ) distances of all populations from the lake-stream systems. Procrustes (upper triangular matrix) and Mahalanobis (lower triangular matrix) distances from the CVA (Fig. 3) (non-significant values are underlined). (A) Pairwise body shape differentiation. (B) Pairwise LPJ shape differentiation.

A

population	Ka3	Ka2	Ka1	KaL	Ch1	ChL	Lz1	LzL	Lf2	Lf1	LfL
Ka3		0.0457	0.0220	0.0253	0.0314	0.0295	0.0238	0.0331	0.0474	0.0341	0.0386
Ka2	5.6679		0.0535	0.0369	0.0349	0.0312	0.0396	0.0296	0.0288	0.0301	0.0243
Ka1	3.9344	5.9029		0.0251	0.0455	0.0393	0.0341	0.0373	0.0518	0.0406	0.0442
KaL	4.5737	6.1411	3.5549		0.0361	0.0288	0.0320	0.0202	0.0423	0.0321	0.0301
Ch1	5.4110	5.8736	6.5003	6.6979		0.0158	0.0231	0.0344	0.0370	0.0291	0.0300
ChL	5.0602	4.9994	5.5704	5.7198	2.7821		0.0242	0.0302	0.0278	0.0182	0.0196
Lz1	4.3098	5.0077	4.6585	5.0996	4.3658	4.2179		0.0279	0.0371	0.0268	0.0307
LzL	6.0366	6.6764	5.2110	3.0927	7.4857	6.6939	5.1698		0.0366	0.0309	0.0273
Lf2	7.7497	5.8296	7.8774	9.0269	7.0925	6.1512	6.0970	9.2435		0.0229	0.0214
Lf1	5.6788	4.9360	5.4026	6.1579	6.0796	4.5449	5.0511	6.9778	5.6664		0.0121
LfL	5.4917	4.7787	5.1340	5.3243	5.6660	3.8408	4.5813	6.0876	5.7561	2.0123	

B

population	Ka3	Ka2	Ka1	KaL	Ch1	ChL	Lz1	LzL	Lf2	Lf1	LfL
Ka3		0.0273	0.0214	0.0160	0.0414	0.0086	0.0277	0.0257	0.0317	0.0287	0.0247
Ka2	2.7659		0.0122	0.0226	0.0260	0.0310	0.0254	0.0202	0.0193	0.0188	0.0212
Ka1	1.8301	2.1889		0.0188	0.0269	0.0256	0.0191	0.0171	0.0193	0.0234	0.0232
KaL	2.0079	2.9577	2.0749		0.0421	0.0162	0.0278	0.0158	0.0255	0.0238	0.0216
Ch1	3.5801	3.4244	3.1368	4.1603		0.0445	0.0280	0.0419	0.0291	0.0377	0.0392
ChL	1.7643	3.2636	2.5246	1.9657	3.6404		0.0296	0.0291	0.0347	0.0318	0.0270
Lz1	2.5159	3.3232	2.2841	2.9991	2.8786	2.8934		0.0313	0.0200	0.0392	0.0388
LzL	2.8324	3.2146	1.9479	2.1601	4.4232	3.1740	3.7602		0.0252	0.0233	0.0239
Lf2	3.0152	3.6780	2.7341	2.4114	3.3427	2.9693	2.9560	3.0189		0.0310	0.0339
Lf1	3.1319	3.5420	3.3800	2.6641	4.5602	3.1829	4.4215	3.2175	3.0839		0.0074
LfL	2.8893	3.6144	3.2140	2.3889	4.4794	2.8310	4.2185	3.0297	3.0012	0.6559	

Table S6 P values for within system gill raker length comparisons for males and females. P values were obtained with an ANOVA and adjusted with a TukeyHSD in systems with more than two populations to correct for multiple testing (Fig. 2E, Fig. S5C).

sex	Kalambo						Chitili	Lunzua	Lufubu		
	KaL-Ka1	KaL-Ka2	KaL-Ka3	Ka1-Ka2	Ka1-Ka3	Ka2-Ka3	ChL-Ch1	LzL-Lz1	LfL-Lf1	LfL-Lf2	Lf1-Lf2
males	0.0211*	0.0149*	< 0.0001***	0.9979	0.0864	0.1407	0.0419*	0.0003**	0.1544	0.1107	0.0017**
females	0.3340	< 0.0001***	< 0.0001***	0.0001**	0.0001**	0.9967	0.1531	0.0001**	0.0840	< 0.0001***	< 0.0001***

Table S7 Pairwise morphometric (body shape and LPJ) distances between F1 crosses. (A) Pairwise morphometric distances described by Procrustes (upper triangular matrix) and Mahalanobis (lower triangular matrix) distances from the CVAs comparing each inter-population cross with the corresponding within population crosses (non-significant values are underlined, for CVA plots see Fig. 4A). (B) P values for pairwise comparisons of gill raker length among all within and inter-population crosses (Fig. 4B).

A

F1 juveniles	KaL-KaL	KaL-Ka3	Ka3-Ka3
KaL-KaL		0.0086	0.0097
KaL-Ka3	1.2961		0.0048
Ka3-Ka3	1.9713	1.2240	

F1 juveniles	KaL-KaL	KaL-Lz1	Lz1-Lz1
KaL-KaL		0.0081	0.0110
KaL-Lz1	1.3536		0.0078
Lz1-Lz1	1.8514	1.3714	

F1 juveniles	Ka3-Ka3	Ka3-Lz1	Lz2-Lz1
Ka3-Ka3		0.0081	0.0079
Ka3-Lz1	1.6021		0.0090
Lz1-Lz1	1.4724	1.7618	

B

F1 juveniles	Ka3-Ka3	Lz1-Lz1	KaL-Ka3	KaL-Lz1	Ka3-Lz1
KaL-KaL	0.00078	0.00004	0.22130	0.00588	0.02763
Ka3-Ka3		0.99788	0.82486	0.98741	0.99975
Lz1-Lz1			0.57282	0.86382	0.98707
KaL-Ka3				0.98122	0.96682
KaL-Lz1					0.99990

Table S8 Pairwise morphometric (body shape) distances and P values of gill raker comparisons among different groups of the pond experiment. Procrustes (upper triangular matrix) and Mahalanobis (lower triangular matrix) distances of the CVA comparing body shape among the within population F1 offspring and their corresponding wild populations (A) and among population of surviving adults at the beginning and at the end of the experimental period (B). (C) Comparison of gill raker length among the within population F1 offspring and their corresponding wild populations. (Fig. S7)

A

F1 and wild populations	KaL-KaL	Ka3-Ka3	Lz1-Lz1	KaL-wild	Ka3-wild	Lz1-wild
KaL-KaL		0.0094	0.0108	0.0119	0.0266	0.0241
Ka3-Ka3	1.5840		0.0080	0.0145	0.0261	0.0225
Lz1-Lz1	1.3126	1.3175		0.0154	0.0309	0.0284
KaL-wild	2.1099	2.0466	1.7501		0.0235	0.0242
Ka3-wild	3.4504	3.2127	3.3877	3.6574		0.0103
Lz1-wild	2.8738	2.2854	2.9527	3.2975	1.9800	

B

parental populations	KaL-before	Ka3-before	Lz1-before	KaL-after	Ka3-after	Lz1-after
KaL-before		0.0215	0.0218	0.0079	0.0134	0.0106
Ka3-before	2.6663		0.0131	0.0196	0.0132	0.0225
Lz1-before	2.4212	1.9504		0.0211	0.0109	0.0184
KaL-after	1.1066	2.5476	2.4792		0.0127	0.0138
Ka3-after	1.9615	1.7624	1.0353	2.0022		0.0119
Lz1-after	1.8311	2.5275	1.7273	1.7073	1.2464	

C

F1 and wild populations	Ka3-Ka3	Lz1-Lz1	KaL-wild	Ka3-wild	Lz1-wild
KaL-KaL	0.00214	0.00401	0.69902	< 0.00001	0.00005
Ka3-Ka3		0.99760	0.30149	< 0.00001	0.42067
Lz1-Lz1			0.47098	< 0.00001	0.20750
KaL-wild				< 0.00001	0.01044
Ka3-wild					0.09142

sampling information			locus									
population	year		Ppun7	Ppun21	UNH130	Abur82	Ppun5	HchiST46	HchiST68	UNH989	Pzeb3	average
Ninde	2011	N_G	7	7	6	3	7	1	7	6	7	5.67
		N_A	6	4	6	3	8	1	3	7	4	4.67
		H_O	0.85714	0.42857	0.83333	0.33333	0.85714	na	0.00000	0.66667	0.42857	0.55
		H_E	0.8022	0.73626	0.87879	0.60000	0.91209	na	0.48352	0.83333	0.57143	0.73
Loazi	2011	N_G	31	31	30	31	27	31	28	28	31	29.78
		N_A	27	20	21	15	24	2	18	22	6	17.22
		H_O	0.93548	0.87097	**0.70000**	0.74194	0.88889	0.12903	0.71429	0.92857	0.70968	0.74
		H_E	0.9413	0.92491	0.92147	0.86409	0.94689	0.12269	0.85390	0.92208	0.71232	0.80
Muzi	2011	N_G	25	25	24	25	25	24	24	24	24	24.44
		N_A	15	14	15	15	15	2	12	18	6	12.44
		H_O	0.96000	0.84000	0.79167	0.76000	0.72000	0.04167	0.79167	**0.66667**	0.58333	0.68
		H_E	0.90531	0.90531	0.91135	0.90776	0.90367	0.04167	0.86968	0.94681	0.64539	0.78
Kalambo stream 3	2010	N_G	32	31	32	32	32	32	32	32	32	31.89
		N_A	9	11	15	7	16	2	6	8	7	9.00
		H_O	0.90625	0.87097	0.87500	0.84375	0.84375	0.46875	0.65625	0.71875	0.75000	0.77
		H_E	0.82192	0.83131	0.88790	0.76290	0.91915	0.44792	0.75694	0.84226	0.80655	0.79
	2011	N_G	30	30	30	30	30	30	30	30	30	30.00
		N_A	11	10	10	7	15	2	4	10	6	8.33
		H_O	0.93333	0.76667	0.76667	0.73333	0.63333	0.43333	0.63333	**0.80000**	0.60000	0.70
		H_E	0.87627	0.79887	0.87175	0.78588	0.89492	0.48079	0.75763	0.82316	0.73446	0.78
Kalambo stream 2	2011	N_G	14	14	13	14	14	1	13	14	14	12.33
		N_A	7	12	10	6	13	1	6	6	6	7.44
		H_O	0.64286	0.71429	0.69231	0.42857	0.71429	na	0.69231	0.64286	0.78571	0.66
		H_E	0.69312	0.79630	0.84308	0.43915	0.92593	na	0.71385	0.72751	0.76720	0.74
	2012	N_G	32	32	32	32	31	32	32	32	32	31.89
		N_A	9	13	9	10	14	2	9	12	6	9.33
		H_O	0.50000	0.56250	0.84375	0.59375	0.74194	0.09375	0.81250	0.78125	0.71875	0.63
		H_E	0.57391	0.62351	0.74504	0.68006	0.84294	0.09077	0.82440	0.76885	0.75198	0.66
Kalambo stream 1	2011	N_G	32	32	32	32	31	32	32	31	32	31.78
		N_A	21	23	23	20	19	3	12	20	6	16.33
		H_O	0.96875	0.90625	0.93750	0.93750	0.83871	0.15625	**0.37500**	0.93548	0.40625	0.72
		H_E	0.91419	0.94643	0.93800	0.94444	0.94289	0.17708	0.76935	0.91962	0.49603	0.78
Kalambo lake	2010	N_G	31	31	30	31	30	30	31	31	31	30.67
		N_A	18	25	22	19	20	3	14	19	5	16.11
		H_O	0.96774	0.93548	0.86667	0.96774	**0.76667**	0.26667	0.54839	1.00000	0.58065	0.77
		H_E	0.91645	0.94342	0.94407	0.93971	0.94068	0.24350	0.80539	0.93178	0.59598	0.81
	2011	N_G	33	33	32	33	33	33	33	33	33	32.89
		N_A	18	21	20	18	22	3	17	20	5	16.00
		H_O	0.87879	0.93939	0.84375	0.87879	0.81818	0.24242	0.81818	0.9697	0.42424	0.76
		H_E	0.87832	0.93706	0.93204	0.91422	0.95058	0.29324	0.86993	0.93986	0.43357	0.79
Toby's place	2010	N_G	34	34	31	33	34	34	34	34	33	33.44
		N_A	13	14	20	14	15	2	11	16	7	12.44
		H_O	0.91176	0.85294	0.93548	0.93939	0.88235	0.05882	0.73529	0.91176	0.54545	0.75
		H_E	0.80114	0.84372	0.88525	0.87925	0.90386	0.11238	0.83055	0.89245	0.52214	0.74
	2012	N_G	31	31	28	31	31	31	31	27	31	30.22
		N_A	11	10	12	13	14	2	4	9	5	8.89
		H_O	0.96774	0.83871	0.82143	0.90323	0.96774	0.03226	0.61290	0.74074	0.48387	0.71
		H_E	0.85405	0.77737	0.80779	0.83765	0.85616	0.03226	0.68324	0.83718	0.45267	0.68
Chitili creek 1	2010	N_G	7	7	7	7	7	1	7	7	6	6.22
		N_A	9	7	9	7	9	1	7	5	4	6.44
		H_O	1.00000	0.71429	0.85714	**0.42857**	1.00000	na	0.85714	1.00000	1.00000	0.86
		H_E	0.94505	0.89011	0.91209	0.85714	0.93407	na	0.85714	0.83516	0.72727	0.87
	2011	N_G	31	31	31	31	31	31	30	29	31	30.67
		N_A	15	17	14	13	16	2	12	12	5	11.78
		H_O	0.90323	0.80645	0.64516	0.80645	0.87097	0.06452	0.70000	0.89655	0.32258	0.67
		H_E	0.87996	0.87943	0.86039	0.85087	0.90164	0.06346	0.85424	0.87719	0.34320	0.72
Chitili lake	2011	N_G	31	31	29	31	31	1	28	30	31	27.00
		N_A	16	13	18	19	19	1	14	14	6	13.33
		H_O	0.87097	0.90323	0.96552	0.83333	0.86667	na	**0.57143**	0.73333	0.41935	0.77
		H_E	0.90375	0.91698	0.92257	0.91808	0.91751	na	0.88636	0.91751	0.46007	0.86
Chisanza	2011	N_G	32	30	30	32	31	32	31	32	32	31.33
		N_A	25	24	19	23	20	2	13	21	10	17.44
		H_O	0.96875	1.00000	**0.63333**	0.81250	0.83871	0.37500	**0.61290**	**0.75000**	0.59375	0.73
		H_E	0.94792	0.95593	0.92712	0.94990	0.91539	0.30952	0.85669	0.92808	0.67560	0.83
Sumba	2011	N_G	32	31	32	32	32	32	32	32	31	31.78
		N_A	27	25	22	23	20	2	14	20	9	18.00
		H_O	0.93750	0.96774	**0.75000**	**0.81250**	0.78125	0.21875	**0.53125**	**0.62500**	0.70968	0.70
		H_E	0.96081	0.95346	0.93204	0.94891	0.93056	0.19792	0.90228	0.92808	0.72343	0.83
		p	0.10437	0.41513	**0.00142**	**0.00379**	**0.01741**	1.00000	**0.00000**	**0.00000**	0.37605	0.21
Lunzua stream 1	2011	N_G	30	30	30	30	30	30	30	30	30	30.00
		N_A	11	13	12	12	13	2	10	9	6	9.78
		H_O	0.83333	0.90000	0.66667	0.66667	**0.60714**	0.23333	**0.60000**	0.70000	0.60000	0.65
		H_E	0.87458	0.85480	0.83446	0.75819	0.86104	0.20960	0.85706	0.82542	0.60791	0.74
Lunzua lake	2010	N_G	30	30	29	30	28	28	30	29	30	29.33
		N_A	24	29	31	26	20	3	18	22	8	20.11
		H_O	0.93333	0.96667	0.89655	0.93333	0.89286	0.42857	**0.63333**	0.93103	0.66667	0.81
		H_E	0.95876	0.96667	0.97217	0.96271	0.94675	0.38247	0.92825	0.95523	0.5887	0.85
	2011	N_G	31	31	31	31	31	31	31	31	31	31.00
		N_A	25	30	27	25	20	3	23	23	8	20.44
		H_O	0.87097	1.00000	**0.74194**	0.80645	0.80645	0.32258	**0.70968**	0.87097	0.67742	0.76
		H_E	0.94553	0.96616	0.96140	0.95928	0.94236	0.32311	0.94342	0.94553	0.68852	0.85
Wonzye	2010	N_G	41	42	42	42	37	42	42	42	42	41.33
		N_A	29	33	30	24	23	3	15	24	10	21.22
		H_O	**0.95122**	**0.95238**	**0.88095**	**0.95238**	**0.86486**	0.38095	**0.61905**	**0.90476**	0.73810	0.80
		H_E	0.95574	0.96644	0.95668	0.95726	0.95002	0.32014	0.82760	0.94894	0.79891	0.85
	2012	N_G	18	18	17	18	15	18	18	18	18	17.56
		N_A	23	23	22	20	12	2	13	19	9	15.89
		H_O	0.94444	0.83333	0.88235	1.00000	0.66667	0.16667	0.83333	0.94444	0.88889	0.80
		H_E	0.96349	0.96508	0.96791	0.96825	0.91264	0.15714	0.82698	0.95714	0.85556	0.84
Fisheries Department	2010	N_G	25	26	24	25.00000	26	26	26	26	26	25.56
		N_A	27	20	24	23	17	3	15	23	11	18.11
		H_O	1.00000	1.00000	0.95833	0.80000	0.80769	0.15385	**0.61538**	**0.76923**	0.84615	0.77
		H_E	0.94694	0.93288	0.96188	0.95020	0.93363	0.14706	0.88612	0.94872	0.84238	0.84
Kalungula	2010	N_G	26	27	26	26	20	27	27	27	27	25.89
		N_A	23	20	18	19	15	3	15	17	10	15.56
		H_O	0.88462	0.92593	0.92308	0.84615	**0.70000**	0.11111	0.62963	**0.70370**	0.70370	0.71
		H_E	0.94344	0.94340	0.92609	0.94118	0.92821	0.10832	0.84696	0.90566	0.82250	0.82
Lufubu stream 2	2012	N_G	30	30	29	30	30	30	30	29	30	29.78
		N_A	9	20	14	17	15	2	6	10	5	10.89
		H_O	0.80000	0.96667	0.79310	0.93333	0.75862	0.03333	0.60000	**0.96552**	**0.30000**	0.68
		H_E	0.71469	0.94407	0.76830	0.90904	0.91712	0.03333	0.60904	0.69752	0.58136	0.69
Lufubu stream 1	2011	N_G	27	27	27	27	24	27	27	27	27	26.67
		N_A	19	28	21	25	21	3	16	21	12	18.44
		H_O	0.88889	0.88889	**0.66667**	0.85185	**0.62500**	0.25926	**0.74074**	0.92593	0.85185	0.74
		H_E	0.95318	0.96995	0.95038	0.94200	0.94592	0.23410	0.92872	0.94829	0.85325	0.86
Lufubu lake	2011	N_G	30	30	30	30	30	30	29	30	30	29.89
		N_A	18	28	22	22	24	4	14	19	13	18.22
		H_O	0.9	0.86667	**0.46667**	0.93333	**0.73333**	0.46667	**0.55172**	**0.83333**	0.86667	0.74
		H_E	0.93616	0.9661	0.86723	0.93164	0.95028	0.45989	0.79492	0.94746	0.83051	0.85
		p	0.08827	0.12133	**0.00008**	0.77188	**0.00048**	0.61206	**0.00000**	**0.00672**	0.33487	0.22
Ndole bay	2012	N_G	16	16	8	16	13	16	16	15	16	14.67
		N_A	15	9	12	7	12	2	7	10	7	9.00
		H_O	1.00000	0.93750	0.87500	0.68750	**0.61538**	0.18750	0.68750	0.53333	0.68750	0.69
		H_E	0.93347	0.88105	0.96667	0.74194	0.93846	0.17540	0.71371	0.85057	0.74395	0.77
Lake Chila	2012	N_G	13	14	13	14	12	1	14	14	14	12.11
		N_A	13	19	15	16	14	1	12	12	8	12.22
		H_O	1.00000	1.00000	0.76923	1.00000	0.75000	na	0.78571	0.71429	0.85714	0.86
		H_E	0.92000	0.96825	0.94154	0.94974	0.94203	na	0.84656	0.88624	0.84656	0.91

Table S9 Microsatellite diversity in populations of *Astatotilapia burtoni*. NG, number of genotypes per locus; NA, number of alleles per locus; HO, obsevered heterozygosity; HE, expected heterozygosity. Deviations from Hardy-Weinberg expectations at a 0.05 significance level after sequential Bonferroni correction are indicated in bold print.

Table S10 Genetic diversity of mtDNA sequences. N, number of sequences per population; H, number of haplotypes; He, gene diversity; π, nucleotide diversity.

population	*N*	*H*	*He*	*π*
Ninde	7	1	0.00000	0.00000
Loazi	7	1	0.00000	0.00000
Muzi	9	1	0.00000	0.00000
Kalambo stream 3	27	1	0.00000	0.00000
Kalambo stream 2	8	1	0.00000	0.00000
Kalambo stream 1	6	3	0.60000	0.00182
Kalambo lake	29	3	0.25400	0.00071
Toby's place	30	2	0.18600	0.00051
Chitili creek 1	17	2	0.44100	0.00120
Chitili lake	10	2	0.55600	0.00151
Chisanza	9	3	0.41700	0.00182
Sumba	9	3	0.58300	0.00227
Lunzua stream 1	7	1	0.00000	0.00000
Lunzua lake	24	4	0.30800	0.00098
Wonzye	49	2	0.08000	0.00022
Fisheries Department	24	1	0.00000	0.00000
Kalungula	28	1	0.00000	0.00000
Lufubu stream 2	13	3	0.41000	0.00119
Lufubu stream 1	10	1	0.00000	0.00000
Lufubu lake	9	1	0.00000	0.00000
Ndole	13	2	0.15400	0.00042
Lake Chila	14	1	0.00000	0.00000

Chapter 5

Variation of anal fin egg-spots along an environmental gradient in a haplochromine cichlid fish

Anya Theis, Olivia Roth, Fabio Cortesi, **Fabrizia Ronco**,
Walter Salzburger & Bernd Egger

Evolution (2017)

I contributed to the field work to collect the raw data for this study.

BRIEF COMMUNICATION

doi:10.1111/evo.13166

Variation of anal fin egg-spots along an environmental gradient in a haplochromine cichlid fish

Anya Theis,[1] Olivia Roth,[2] Fabio Cortesi,[1,3] Fabrizia Ronco,[1] Walter Salzburger,[1,4] and Bernd Egger[1]

[1]*Zoological Institute, University of Basel, Vesalgasse 1, 4051 Basel, Switzerland*

[2]*GEOMAR, Helmholtz Centre for Ocean Research, Evolutionary Ecology of Marine Fishes, Düsternbrooker Weg 20, 24105 Kiel, Germany*

[3]*Queensland Brain Institute, The University of Queensland, Brisbane, Queensland 4072, Australia*

[4]*E-mail: walter.salzburger@unibas.ch*

Received August 12, 2016
Accepted December 8, 2016

Male secondary sexual traits are targets of inter- and/or intrasexual selection, but can vary due to a correlation with life-history traits or as by-product of adaptation to distinct environments. Trade-offs contributing to this variation may comprise conspicuousness toward conspecifics versus inconspicuousness toward predators, or between allocating resources into coloration versus the immune system. Here, we examine variation in expression of a carotenoid-based visual signal, anal-fin egg-spots, along a replicate environmental gradient in the haplochromine cichlid fish *Astatotilapia burtoni*. We quantified egg-spot number, area, and coloration; applied visual models to estimate the trait's conspicuousness when perceived against the surrounding tissue under natural conditions; and used the lymphocyte ratio as a measure for immune activity. We find that (1) males possess larger and more conspicuous egg-spots than females, which is likely explained by their function in sexual selection; (2) riverine fish generally feature fewer but larger and/or more intensely colored egg-spots, which is probably to maintain signal efficiency in intraspecific interactions in long wavelength shifted riverine light conditions; and (3) egg-spot number and relative area correlate with immune defense, suggesting a trade-off in the allocation of carotenoids. Taken together, haplochromine egg-spots feature the potential to adapt to the respective underwater light environment, and are traded off with investment into the immune system.

KEY WORDS: ***Astatotilapia burtoni*, Cichlidae, Lake Tanganyika, male secondary sexual trait, natural selection, sexual selection.**

Male secondary sexual traits constitute what are among the most conspicuous characters in animals and often play a key role in female choice and male–male competition (Darwin 1871; Andersson 1994; Espmark et al. 2000). Signals that aim to attract mating partners and to intimidate rivals are considered "honest" if comprising a handicap and if being costly to display and/or to produce (Zahavi 1975; Iwasa et al. 1991; Iwasa and Pomianowski 1999; but see e.g., Számadó 2011 for other models of honest signaling). According to the "handicap principle", displaying an honest signal should reflect the overall quality of its bearer (Zahavi 1975; Andersson 1994; Rowe and Houle 1996; but see Fisher 1930; Lande 1981; Kirkpatrick and Ryan 1991; Kokko et al. 2006). Importantly, variation in the expression of an honest signal is not expected to be purely under genetic control, but should instead correlate with life-history traits such as age, nutritional status, social status, or parasite load (Kodric-Brown and Brown 1984; van Noordwijk and de Jong 1986; de Jong and van Noordwijk 1992). Further, phenotypic divergence in such signals can emerge as by-product of adaptation to distinct environmental niches (Nosil 2012), since the traits are expected to evolve to a point where viability costs balance out mating advantage (Endler 1978; Jennions et al. 2001). Thus, variation in visual, acoustic, and chemical signals can be affected by a wide array of environmental parameters.

A key component in visual signaling is the conspicuousness of the signal as it influences the perceptibility of the visual

Evolution 71-3: 766–777

signal to the potential receivers such as mates and intraspecific rivals, but also interspecific competitors and, in particular, predators (Endler 1992). High predation pressure is often accompanied by a reduction in conspicuousness of signal expression (Endler 1980; Stuart-Fox and Ord 2004; Schwartz and Hendry 2007), whereas reduced visibility may lead to increased conspicuousness of visual signals, most probably to maintain their function in intraspecific interactions (Marchetti 1993; Zahavi and Zahavi 1997; Keksläinen et al. 2010; Dugas and Franssen 2011). However, especially in aquatic environments, reduced visibility can also decrease conspicuousness of visual signals, for example, when intraspecific receivers reduce their responsiveness to visual signals and/or when investing into this costly trait is maladaptive (e.g., Luyten and Liley 1991; Seehausen et al., 1997, 2008; Boughman 2001; Wong et al. 2007; Maan et al. 2010). Additionally, the size, shape, or coloration of visual displays can be influenced by the physical or chemical properties of habitats (e.g., Hill and Montgomerie 1994; Endler and Houde 1995; Moller 1995; Candolin et al. 2007). In case of carotenoid-based visual signals, for example, the expression might be directly influenced by the accessibility to food resources, since carotenoids cannot be synthesized de novo by animals and thus have to be obtained through their diet (Goodwin 1986). The conspicuousness of carotenoid-based visual signals should therefore reflect the ability to feed successfully on carotenoid-rich food (Hill 1992)—or even more likely—to be an indicator of the bearer's health, since carotenoids are also used as antioxidants in immune responses (Lozano, 1994, 2001; von Schantz et al. 1999; Svensson and Wong 2011; Simons et al. 2012). Consequently, using carotenoids for signaling instead of the immune system is considered to be costly. Under stressful conditions carotenoids may therefore primarily be invested into the immune response or, alternatively, they may be allocated to offspring (Sheldon and Verhulst 1996) or to other life-history traits such as general fitness (Smith et al. 2007) and survival (Pike et al. 2007).

Taken together, visual signals can be shaped by both, sexual selection and a broad range of environmental and physiological factors. Examining the contribution of environmental factors on signal expression in nature is challenging, but has been successfully studied with respect to color patterns in some species (Endler 1980). A promising set-up to study the influence of natural selection on color patterns consists of populations of a species displaying secondary male ornaments that occur, in replication, along a marked environmental gradient. Such a setting can be found in the haplochromine cichlid species *A. burtoni* (Günther 1894), which occurs both in East African Lake Tanganyika and inflowing rivers. This generalist species displays typical haplochromine features such as sexual dimorphism, female mouthbrooding and egg-spots, that is, a characteristic carotenoid-containing visual signal and evolutionary innovation (Goldschmidt and de Visser 1990; Salzburger et al. 2005; Santos et al. 2014). Egg-spots are ovoid markings on the anal fin of haplochromines primarily composed of two types of chromatophores (xanthophores and iridophores) (Salzburger et al. 2007; Santos et al. 2014). In male haplochromines egg-spots consist of a conspicuously colored yellow, orange, or reddish inner circle and a transparent outer ring (Wickler 1962) (Fig. 1A). The function of anal fin egg-spots has initially been attributed to female choice (Wickler 1962; Hert, 1989, 1991; Couldridge 2002) or—more recently in the species examined here—to male–male competition (Theis et al., 2012, 2015). *Astatotilapia burtoni* exhibits a lek-like polygynandrous mating system, with only dominant males gaining access to territories as well as to females (Fernald and Hirata 1977). Moreover, egg-spots appear to play a pivotal role in interactions among males, as they appear to have an intimidating effect in *A. burtoni* (Theis et al. 2012). In both female choice and male–male competition, males are expected to benefit from adapting signal conspicuousness to be effective within their respective environment. Indeed, most haplochromine cichlids from Lake Victoria display fewer but larger and hence, more conspicuous egg-spots in more turbid waters (Goldschmidt 1991). Contrarily, in *Pundamilia pundamilia*, also a haplochromine from Lake Victoria, populations show a trend toward less conspicuous egg-spots with respect to saturation and hue in more turbid waters (Castillo Cajas et al. 2012).

In this study, we focus on the natural variation of egg-spots within and among four lake-stream systems of *A. burtoni*. Each replicate system consists of at least one population sampled from a stream flowing into Lake Tanganyika and one lake population sampled from a lake habitat close to the estuary of the respective stream (Fig. 1B). Note that all lake populations originate from the same lake, Lake Tanganyika, but represent replicates as they show genetic structuring (Theis et al. 2014). Previous work has demonstrated that populations from replicate lake-stream systems show similar adaptations to divergent selection regimes with regard to body shape and trophic morphologies (Theis et al. 2014). Importantly, the detected trait differences among populations do not reflect pure plastic responses to different environmental conditions, but have a substantial genetic component (Theis et al. 2014). Here, we first explored sex-specific differences in egg-spots by comparing egg-spot number, relative average area, relative total area, and coloration inferred from photographs of fish. Due to the proposed function of egg-spots in male–male competition (Theis et al., 2012, 2015), males were expected to display more, larger, and more intensely colored egg-spots compared to females. To ascertain habitat-specific differences, the same egg-spot characteristics were then compared among males of the different lake and stream populations. We hypothesized that egg-spot characteristics from replicate lake-stream systems would follow similar trajectories along this environmental gradient. We then

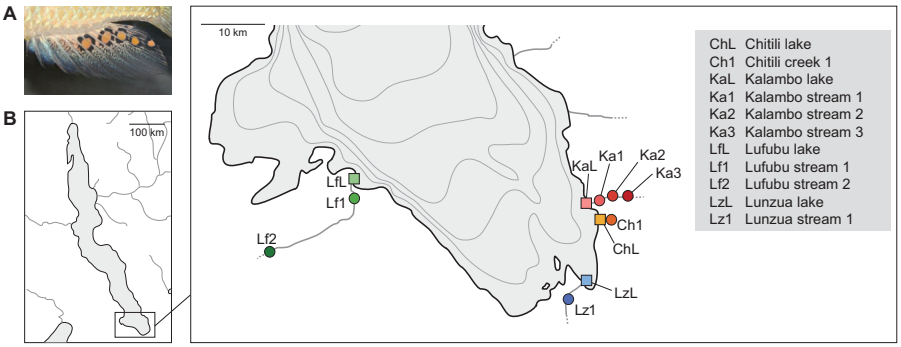

Figure 1. Male secondary sexual trait and populations under investigation. (A) Egg-spots on the anal fin of a male *Astatotilapia burtoni*. (B) Map showing the 11 sampling localities in the southern part of Lake Tanganyika (squares represent lake and circles stream populations; bathymetric lines are placed at every 100 m water depth, after Coulter (1991); full names of populations are listed in the gray box).

examined how the underwater light environment and the status of the immune system affect the conspicuousness of male egg-spots. To this end, we measured immune activity of males and underwater light environments from lake and stream populations and asked whether these factors were associated with divergence in the egg-spot characteristics number, relative average area, relative total area, and coloration based on photographs. Finally, reflectance and irradiance spectrophotometry and theoretical fish visual models were used to determine the color contrast between male egg-spots and the surrounding anal fin tissue under natural ambient light conditions. We hypothesized that males from longer wavelength shifted environments, and/or males experiencing less stress to the immune system, would display the most conspicuous egg-spots.

We found sex- and habitat-specific differences in egg-spots of *A. burtoni.* Males had more elaborate egg-spots compared to females, and are likely to use them as honest signals with the potential to adapt their conspicuousness according to underwater light environment and immune defense. This study provides novel insights into the highly complex interactions between sexual and ecological selection that influence the expression of male secondary visual signals.

Materials and Methods

SAMPLING

Astatotilapia burtoni specimens, underwater ambient light measurements and immunological data were obtained between June 2011 and August 2013 from the Southern part of Lake Tanganyika, Zambia. In total, we sampled at 11 locations from four lake-stream systems (Fig. 1B; for detailed description of these localities see Appendix I in Theis et al. 2014), resulting in a dataset comprising 643 individuals (for detailed information on sample sizes see Table S1). Fish were collected using hook and line fishing, minnow traps or gill nets under the permission of the Lake Tanganyika Research Unit, Department of Fisheries, Republic of Zambia.

EGG-SPOT MEASUREMENTS BASED ON PHOTOGRAPHS

Before taking the photographs, the fish ($n_{\text{females per population}} = 6$–39, $n_{\text{females total}} = 204$; $n_{\text{males per population}} = 10$–55, $n_{\text{males total}} = 300$; for detailed information on sample sizes see Table S1) were anaesthetized with clove oil (2–3 drops per liter water) to reduce stress of handling. Two standardized photographs per individual were taken, one in lateral position to measure body size, and one focusing on the anal fin for subsequent measurements of the egg-spot characteristics (Fig. S1). All images were taken on a gray card to allow for manual white balance. We used digital cameras (Canon EOS 400D, Canon EOS 550D or Nikon D5000) with an external flash (Nikon, Speedlight SB-24).

To assess body size of fish, we recorded 17 homologous landmarks on the full body photographs (for details see Muschick et al. 2012) in the program TPSDIG (version 2.11; Rohlf 2008) followed by a transformation into centroid size in MORPHOJ (version 1.05f; Klingenberg 2011). Centroid size was then used as the representative measure for body size. The photographs were further used to assess egg-spot number, relative average egg-spot area, relative total egg-spot area, and egg-spot coloration. To this end, egg-spot and anal fin areas were measured using the lasso tool in Photoshop (Adobe Photoshop CS3 extended, version 10.0.1). The relative total egg-spot area was defined as the proportion of the anal fin area occupied by the pigmented egg-spot area. The relative average egg-spot area was calculated as the relative total egg-spot area divided by the relative number of egg-spots (a

complete egg-spot was counted as 1 and incomplete egg-spots as 0.5; following Albertson et al. 2014) to avoid artifacts through smaller—still growing egg-spots—typically at the edge of the anal fin.

In addition, egg-spots were assigned to one of six color categories by AT ranging from a faint, barely pigmented to an intense appearance. The color categories (referred to as coloration from here on) therefore describe the conspicuousness of egg-spots based on a combination of hue, saturation, and brightness (representative photographs of the color categories are provided in Fig. S2). Since every specimen displayed more than one egg-spot, an average value was calculated for each individual. Although coloration was defined by a categorical measure, it reflected a continuous variable after calculating the average value across all egg-spots for each specimen.

The differences in egg-spot measurements based on photographs (number, relative average area, relative total area, and coloration) were analyzed in two steps: (1) sex-specific differences of egg-spots in all populations combined and (2) habitat-specific differences of egg-spots among males of lake and stream populations within each system.

To test for differences in egg-spot characteristics between females and males, we conducted sex-specific centering and scaling of the data with respect to centroid size. This was necessary because *A. burtoni* shows pronounced body size dimorphism between males and females (Fernald 1977). Our aim here was to compare average sized females to average sized males (and not same sized females and males). A generalized linear mixed model (GLMM) with Poisson distribution was used in the case of egg-spot number and normal linear mixed models (LME) with ANOVA comparison were used for relative average egg-spot area (square root transformation), relative total egg-spot area, and coloration data. Analyses were conducted using the package LME4 (Bates et al. 2014) in R (version 3.0.3, R Core Team 2014), which was also used for all further statistical analyses. The models included population (separately for each sex) as a random effect and were combined with a random slope (the centered body size) in cases where this improved the model (based on ANOVA comparisons). Additionally to the fixed effect sex, the centered body size and/or the interaction thereof was added if necessary (for details on the models see Table S2A).

Before the habitat-specific differences in the egg-spot characteristics were analyzed in detail, we tested for the biggest differences among populations with regard to egg-spot phenotype in males. To this end, we conducted a principal component analysis (PCA) with the function PRCOMP of the R package STATS for the combined egg-spot characteristics (number, relative average area, relative total area, and coloration). Due to the large sample size, we calculated the mean PC loadings per population for graphical illustration.

Habitat-specific differences of egg-spot characteristics were then analyzed among males of lake populations in comparison to the corresponding stream populations. A generalized linear model (GLM) with Poisson distribution was used in the case of egg-spot number, and normal LM were used for relative average area, relative total area, and coloration (with square transformation) data. Additionally to the fixed effect population, we included body size as a fixed effect if it improved the model (for details on the models see Table S2B). To correct for multiple comparisons, the function GLHT from the package MULTCOMP (Hothorn et al. 2008) with mcp specification (population comparisons within system) was used, with a correction for variance heterogeneity (vcov argument with sandwich function of the package sandwich; Zeileis, 2004, 2006) for egg-spot characteristics number, relative average area, and relative total area, but not for coloration.

EGG-SPOT REFLECTANCE AND THEORETICAL FISH VISUAL MODELS

Theoretical fish visual models (Vorobyev and Osorio 1998; Vorobyev et al. 2001) from the perspective of *A. burtoni* were used to measure the color contrast (color distance; ΔS) between male egg-spots and the surrounding anal fin tissue under natural ambient light conditions. For this purpose, specimens were caught in 2013 from each locality ($n_{\text{males per population}} = 4$–$9$, $n_{\text{males total}} = 45$) except for the populations ChL, Ch1, and Lf1 (for detailed information on sample sizes see Table S1). Immediately upon collection, fish were anaesthetized with clove oil (2–3 drops per liter water) and reflectance spectra of the second egg-spot and the area above the egg-spots on the anal fin of males (see Fig. 1A) were taken in the field using a JAZ Modular Portable Spectrometer (Ocean Optics; wavelength range 300–980 nm) with an integrated, pulsed Xenon lamp module (OCOJAZ-PX) and an OCOWS-1 diffuse reflection standard according to the methods described in Gray et al. (2011). Between four to six reflectance spectra were taken per area and specimen. Spectral files were visually inspected and processed using the R package PAVO (Maia et al. 2013). Wavelengths were interpolated in 1 nm bins over a spectral range from 400 to 750 nm. Spectra from egg-spot and fin measurements were combined and averaged for each individual. To account for the light environment under which egg-spots are viewed, we modeled color discrimination using natural illumination measurements for each population taken from their environment at different water depths (see irradiance measurements as described below; Fig. S3). Whereby, using natural illumination measurements as part of the model, allows us to recreate what egg-spot colors look like in their environment independent of where (natural environment, laboratory, etc.) the spectral reflectance measurements are taken (see e.g. Cortesi et al. 2015).

Astatotilapia burtoni photoreceptors are arranged in a classical mosaic pattern with four double cone receptors surrounding a

single cone (Fernald and Liebman 1980; Fernald 1981). The single cone expresses a short-wavelength sensitive (SWS) "blue" pigment with a peak spectral sensitivity (λ_{max}) at 455 nm, the shorter tuned double cone member expresses a middle-wavelength sensitive (MWS) "green" pigment at 523 nm λ_{max} and the longer tuned double cone member expresses a long-wavelength sensitive (LWS) "red" pigment at 562 nm λ_{max} (Fernald and Liebman 1980). Members of double cones have previously been shown to contribute separately to color discrimination in some fishes (Pignatelli et al. 2010) and we therefore modeled *A. burtoni* as having a trichromatic visual system with a cone photoreceptor ratio of 1:2:2 (SWS:MWS:LWS) and a 0.05 LWS noise threshold for the Weber fraction (ω) (for similar approaches see Boileau et al. 2015; Cortesi et al. 2015). The visual model calculates ΔS within the visual "space" of the fish based on an opponent mechanism, which is limited by the noise of different photoreceptor types (Vorobyev and Osorio 1998; Vorobyev et al. 2001). Similar colors will result in low ΔS values, whereas chromatically contrasting colors will result in high ΔS values with $\Delta S = 1$ as the discrimination threshold (just noticeable difference; JND). We would like to note that we currently do not know how *A. burtoni* processes visual stimuli and that behavioral experiments are needed to comprehend what a change in JND beyond the discrimination threshold of 1 signifies. Similarly, behavioral experiments would be needed to assess whether the discrimination threshold varies depending on direction and position in the visual space. Moreover, due to the difficulty of measuring egg-spots in the field we were restricted in sample size, which did not allow for further statistical analyses. However, it is our best estimator in that the larger ΔS is, the more likely it is that the signal can be distinguished, especially when visual information needs to remain reliable over distance in turbid water conditions.

ASSOCIATION TESTS

Finally, we tested for an association between egg-spot measurements based on photographs and underwater light environments (i.e., orange ratio) as well as immunological parameters. To this end downwelling irradiance was measured for each locality (except Lf1) at the surface and at the following depths: 10, 20, 30, 40, 50, 70, and 100 cm, or to the deepest possible point within the interval. At each depth, we took five measurements using a JAZ modular portable spectrometer (Ocean Optics; wavelength range 300–980 nm) with an OFRM25L05 optical fiber and a CC-3-UV-T cosine corrector attached. Before measurements, an OCOWS-1 diffuse reflection standard was used for relative calibration. All measurements were taken in July 2013 on clear days around noon (between 11:30 and 14:00). Spectral data were inspected and processed using the package PAVO (Maia et al. 2013) in R. Wavelengths were interpolated in 1 nm bins from 400 to 700 nm, and five measurements from each depth level were averaged. As a measure for underwater light environments, irradiance data were transformed into orange ratio values. The orange ratio quantifies the relative transmission of long wavelength light by dividing the integral of 400–550 nm absorbance by the integral of 550–700 nm absorbance (Endler and Houde 1995). This ratio generally increases with depth and increasing turbidity, as short wavelengths are selectively scattered and absorbed (Levring and Fish 1956). For further statistical comparisons among the localities, the average change in orange ratio for each locality was calculated from the deepest available measurement divided by the number of 10 cm depth levels.

As an immunological measurement, the activity of the immune system that can be found under natural environmental conditions was determined in the field. We measured the lymphocyte ratio in the blood (lymphocyte count/(lymphocyte + monocyte counts)) to estimate the proportion of cells of the adaptive immune system. Measurements were taken during the dry season in July 2013 for all lake-stream localities except for ChL, Ch1, and Lf1. Blood samples were taken from the caudal vein ($n_{\text{males per population}} = 6–22$, $n_{\text{males total}} = 94$; for detailed information on sample sizes see Table S1) and directly analyzed with a flow cytometer (BD Accuri C6 Flow Cytometer, Becton and Dickinson, Heidelberg, Germany). Immunological assays were performed according to protocols developed for sticklebacks (Scharsack et al., 2004, 2007a,b) with the modifications reported in Roth et al. (2011) as well as cichlid-specific settings as developed and described in Diepeveen et al. (2013). The distinction of blood cell types (lymphocytes vs. monocytes) was based on differences in their light scatter profiles (FSC, forward scatter, approximation for cell size; SSC, side scatter, approximation for cell complexity).

To test for an association between egg-spot measurements based on photographs, orange ratio, and immune response, each egg-spot characteristic (size-corrected, if necessary) was used as response variable in a multiple regression on distance matrices (MRM) with 10,000 permutations using the R package ECODIST (Goslee and Urban 2007). The explanatory variables in the MRMs were pairwise differences in orange ratio, immune response, and geographic distance. Note that the MRM excluded the populations ChL, Ch1, and Lf1 due to lack of underwater ambient light and/or immunological data. In addition to the global MRMs, we also conducted separate MRMs with each egg-spot characteristic as single response variable and one or two explanatory variables combined.

Results

SEX-SPECIFIC DIFFERENCES IN EGG-SPOTS

Egg-spot number was the only examined egg-spot characteristic that showed no difference between sexes but correlated positively

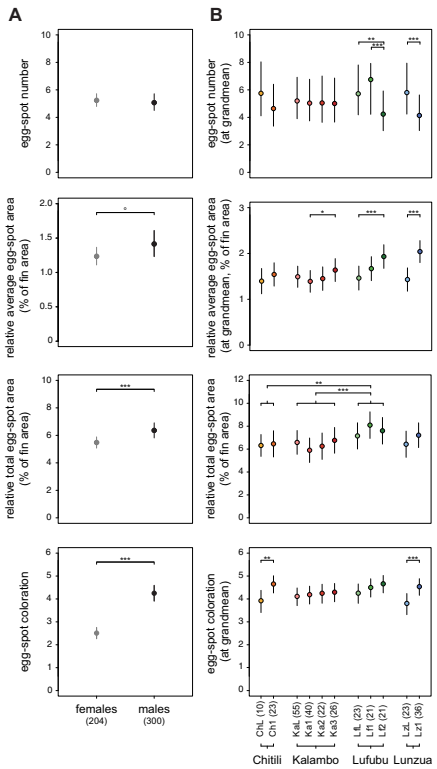

Figure 2. **Differences in the four examined egg-spot characteristics measured based on photographs (number, relative average area, relative total area, and coloration) between all females and males (A) and among males of the populations within the lake-stream systems (B). Full names of populations are listed in the gray box of Figure 1. Significance levels: °$P < 0.1$, *$P < 0.05$, **$P < 0.01$ and ***$P < 0.001$. Corresponding sample sizes are parenthesized. For each system, populations are ordered on the *x*-axis with the lake populations on the left followed by the stream population(s).**

with body size (GLMM: $z_{sex} = -0.52$, $P_{sex} = 0.602$; $z_{CS} = 9.43$, $P_{CS} < 0.0001$) (Fig. 2A). The measurements on egg-spot areas revealed that males tended to have larger average egg-spot areas and a significantly larger total egg-spot area relative to their fin areas compared to females (Fig. 2A). Therefore sex, but not body size improved the model for both egg-spot area characteristics (LME comparison with ANOVA: relative average egg-spot area – $\chi^2_{sex} = 3.4139$, $P_{sex} = 0.0647$; $\chi^2_{CS} = 0.1485$, $P_{CS} = 0.6999$; relative total egg-spot area – $\chi^2_{sex} = 7.5488$, $P_{sex} = 0.0060$; $\chi^2_{CS} = 0.0073$, $P_{CS} = 0.9318$). Male egg-spots showed way more intense coloration, which also increased faster with increasing body size compared to females (LME comparison with ANOVA: $\chi^2_{interaction\ sex:CS} = 8.5799$, $P_{interaction\ sex:CS} = 0.0034$; $\chi^2_{sex} = 41.691$, $P_{sex} < 0.0001$; $\chi^2_{CS} = 11.757$, $P_{CS} = 0.0006$; Fig. 2A) (for graphs showing sex-specific correlations of body size and egg-spot characteristics see Fig. S4A; for sex-specific mean values with corresponding confidence intervals of each egg-spot characteristic see Table S3A).

HABITAT-SPECIFIC DIFFERENCES IN EGG-SPOTS

The PCA revealed a clear separation between lacustrine and riverine populations within the lake-stream systems, except for the four populations of the Kalambo system, which clustered together (Fig. 3A). The other three systems—Chitili, Lufubu, and Lunzua—were separated into lake and stream populations along principal component 1 (PC1, explaining 46% of the variance) and PC2 (explaining 32% of the variance) (for detailed information on proportions of variance and averaged PC loadings see Table S4). Lake populations generally showed greater egg-spot numbers compared to stream populations. Stream populations had a larger relative average egg-spot area and more intense coloration, as well as a larger relative total egg-spot area in the case of Lf1.

The more detailed analyses for each egg-spot characteristic separately showed similar overall trends as the PCA results, but revealed lake-stream system-specific differences. The analysis of egg-spot number among populations within systems revealed that more upstream populations had significantly fewer egg-spots in the rivers Lufubu and Lunzua, but not in Kalambo and Chitili (GLM with correction for multiple comparisons: LfL–Lf2: $z = 3.873$, $P = 0.0011$; Lf1–Lf2: $z = 4.616$, $P < 0.0001$; LzL–Lz1: $z = 5.114$, $P < 0.0001$; only significant values are presented in the text, for all population comparisons within systems see Table S3D and for all population-specific mean values with corresponding confidence intervals for each egg-spot characteristic see Table S3B) (Fig. 2B). The model for egg-spot number also revealed an increase in egg-spot number with increasing body size of the males (GLM: $z = 6.985$, $P < 0.0001$; population-specific correlations of body size and egg-spot characteristics are shown in Fig. S4B).

The relative average egg-spot area increased with larger distance from the lake within the Lufubu and Lunzua systems and between two riverine populations of the Kalambo River (LM with correction for multiple comparisons: Ka1–Ka3: $z = -2.997$, $P = 0.0291$; LfL–Lf2: $z = -4.736$, $P < 0.0001$; LzL–Lz1: $z = -6.470$, $P < 0.0001$) (Fig. 2B; Tables S3B, S3D). With increasing body size of the males the average egg-spots became smaller in relation to fin area (LM: $t = -9.680$, $P < 0.0001$) (Fig. S4B).

Relative total egg-spot area was the only parameter that showed no divergence along the lake-stream gradient (Fig. 2B;

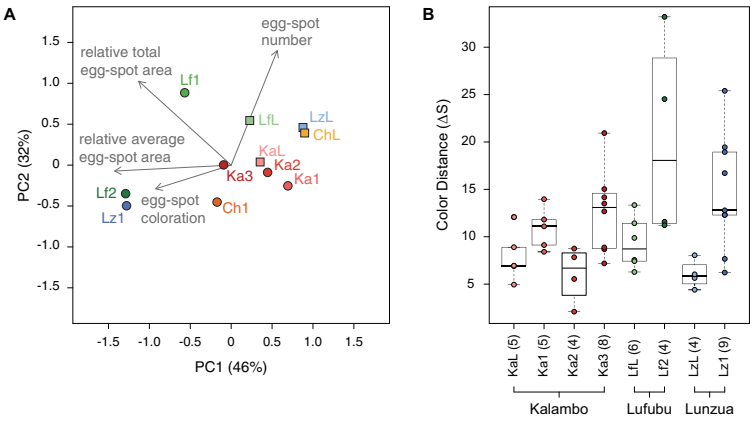

Figure 3. Differences in egg-spot characteristics. (A) PCA-biplot of all populations based on the examined egg-spot characteristics measured from photographs (number, relative average area, relative total area, and coloration). The circles/squares represent the mean for all males per population. Sample sizes are the same as reported in Figure 2B. (B) Chromatic distances between egg-spot and anal fin colors based on theoretical A. burtoni visual models (considering the orange ratio at 30 cm below surface). Sample sizes are parenthesized. For each system, populations are ordered on the *x*-axis with the lake populations on the left followed by the stream population(s).

Tables S3B, S3D). There was a trend of body size improving the model, indicating a correlation between body size and relative total egg-spot area (LM comparison with ANOVA: $F = 2.8532$, $P = 0.0923$). Note, however, that this result was mainly influenced by the riverine Chitili population (Ch1), as without Ch1, the trend did not persist (LM comparison with ANOVA: $F = 0.4716$, $P = 0.4928$). This most probably reflects the data better and therefore body size was excluded as a fixed effect in this case. However, there were differences among systems with respect to this trait, with the Lufubu populations showing a larger relative total egg-spot area compared to the Chitili and Kalambo populations (LM with correction for multiple comparisons: Chitili–Lufubu: $z = 3.378$, $P = 0.0045$; Kalambo–Lufubu: $z = 4.712$, $P < 0.001$; only significant values are presented in the text, for all system comparisons see Table S3E and for system-specific mean values with corresponding confidence intervals see Table S3C) (Fig. 2B).

Based on our color categories, riverine populations showed more intensely colored egg-spots than lake populations in the Chitili and Lunzua systems (LM with correction for multiple comparisons: ChL–Ch1: $z = -3.531$, $P = 0.0050$; LzL–Lz1: $z = -4.889$, $P < 0.0001$) (Fig. 2B; Tables S3B, S3D). Additionally, egg-spot coloration showed a positive correlation with body size (LM: $t = 12.283$, $P < 0.0001$) (Fig. S4B).

The visual models revealed a higher egg-spot to fin contrast (i.e. larger color distance) in riverine populations compared to lake populations (except for the Ka2 population; Fig. 3B). This pattern was consistent when visual models were calculated with underwater ambient light profiles from different depths (i.e. 10 cm, 30 cm, and maximal depth, see Fig. S5).

ASSOCIATION TESTS

The results of the underwater ambient light and immunological parameters are shown in Figure 4. Within systems, the underwater light environment in stream populations was characterized by higher orange ratio values when compared to lake populations (for detailed information on orange ratio values see Table S5; for underwater ambient light spectral curves see Fig. S3). The proportion of lymphocytes showed higher values for stream populations compared to lake populations in the Lufubu and the Lunzua systems, but less variation for the populations from the Kalambo system (Fig. 4).

The MRMs indicated that the examined egg-spot characteristics were influenced to a different extent by the explanatory variables. Relative average egg-spot area and egg-spot number correlated with the proportion of lymphocytes. However, egg-spot coloration correlated with underwater light environment and relative total egg-spot area with geographic distance (Table 1, Table S6).

Discussion

In this study, we examine natural variation in a putative sexually selected trait, anal fin egg-spots, in lake and stream populations

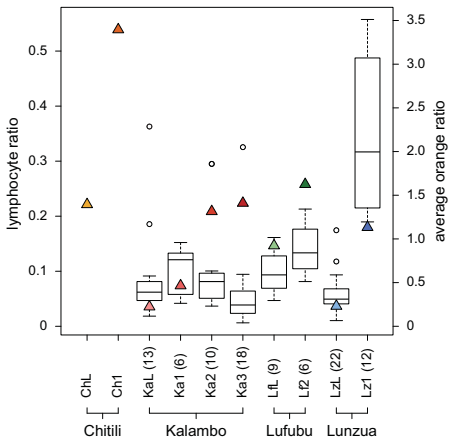

Figure 4. Boxplots of lymphocyte ratios and average orange ratio values (indicated by triangles; average change in orange ratio per 10 cm calculated from the deepest available measurement) per population (note that for the populations ChL and Ch1, no data on lymphocyte ratio were available). For each system, populations are ordered on the *x*-axis with the lake populations on the left followed by the stream population(s).

of the haplochromine cichlid *A. burtoni*. Egg-spots constitute a carotenoid based signal that has been suggested to be an evolutionary innovation of haplochromine cichlids (Goldschmidt and de Visser 1990; Salzburger et al. 2005; Santos et al. 2014).

We first show that egg-spot phenotypes differ substantially between sexes, with females showing smaller and less colored egg-spots compared to the larger and more intensely colored egg-spots of males (Fig. 2A). The increased conspicuousness of egg-spots in males is most probably founded in their function. Egg-spots play an important role in strength assessment of a competitor and elicit an intimidating effect in male combats in *A. burtoni* (Theis et al. 2012), as well as in its congener *A. calliptera* (Theis et al. 2015). Interestingly, in some haplochromine species including *A. burtoni* and *A. calliptera*, also female individuals show egg-spots. To the best of our knowledge, no function for female egg-spots has been reported yet, and, additionally to the reduced area and less conspicuous coloration, female egg-spots also lack the translucent, nonpigmented area around the egg-spots. This translucent ring is likely to enhance contrast of egg-spots in males (Tobler 2006). Reduction or absence of visual signals in females is most probably to decrease energy investment and to reduce conspicuousness toward predators. Alternatively, this might be a corollary of the necessity to invest most of their resources directly into offspring (Trivers 1972). In addition, sexual immune dimorphism could play a role, that is, whereas males increase fitness through mating success, females need to invest more resources in their immune system as they gain fitness through longevity (Rolff 2002) and should benefit from allocating carotenoids to immune responses instead of a costly trait (Lozano, 1994, 2001; Svensson and Wong 2011). The reduced conspicuousness of egg-spots in females due to a reduction in egg-spot area and coloration goes along with a generally more drab body coloration. Interestingly, fin and flank traits seem to be coupled in females of Lake Malawi cichlids, but showed two distinct clusters in males (Brzozowski et al. 2012). This developmental uncoupling might enable males to specifically alter the conspicuousness of the trait in dependence of, for example, status (Brzozowski et al. 2012). Our finding that egg-spots in *A. burtoni* are only reduced in area and coloration, but not in number between males and females, might be the result of a developmental constraint.

Among males within systems, there is a general trend of increasing conspicuousness of egg-spots from lake toward riverine populations, with the latter generally showing fewer, but larger egg-spots with a more intense coloration and a higher egg-spot to fin contrast (Fig. 3A, B). Within systems, this increase in conspicuousness is either connected with a change to more intense egg-spot coloration (Chitili; no data available for egg-spot to fin color distance), larger relative egg-spot area, and higher egg-spot to fin contrast (Lufubu), a combination of all three factors (larger relative average egg-spot area, more intense egg-spot coloration and higher egg-spot to fin contrast; Lunzua) or absent (Kalambo) (Figs. 2B, 3B). Except for the Kalambo system, egg-spots were more conspicuous in areas where predation pressure is presumably lower, that is, the stream localities. *Astatotilapia burtoni* supposedly experiences predation through piscivorous fishes, other aquatic predators (e.g., otters and snakes), and birds (e.g., kingfisher and cormorants), of which only the latter and some piscivorous fishes also chase regularly in upstream riverine localities. It has been shown that in areas with high predation pressure ornamentation and coloration is reduced or cryptic (Endler 1980; Stuart-Fox and Ord 2004). Because predation pressure most probably correlates negatively with orange ratio in our study system, it is difficult to disentangle their relative influences. Egg-spot conspicuousness could be lower in the lake localities because of higher predation pressure, or—maybe more realistically—increased egg-spot conspicuousness in riverine systems could serve to maintain signal transmission in underwater light environments with higher orange ratios (i.e. long wavelength shifted environments).

Turbidity in aquatic systems can either lead to an increase in the conspicuousness of visual signals, most probably to maintain their function (Kekäläinen et al. 2010; Dugas and Franssen 2011), or a decrease in conspicuousness, because intraspecific receivers respond less to visual signals (e.g., Luyten and Liley 1991;

Table 1. Multiple regression on distance matrices (MRM) among pairwise differences in egg-spot characteristics, orange ratio, lymphocyte ratio as well as geographic distance.

Egg-spot characteristic	Orange ratio	Lymphocyte ratio	Geographic distance
Number	0.2336	0.0065	0.0744
Relative average area	0.1069	0.0076	0.1397
Relative total area	0.8409	0.7708	0.0247
Coloration	0.0082	0.1485	0.5281

The egg-spot characteristics number, relative average area, and coloration were corrected for centroid size before the analyses. The reported *P*-values for each parameter (orange ratio, lymphocyte ratio, and geographic distance) result from combined MRMs including those three parameters.

Seehausen et al., 1997, 2008; Wong et al. 2007). Both scenarios have been discussed in the context of egg-spots (Goldschmidt 1991; Castillo Cajas et al. 2012). These two hypotheses are not mutually exclusive, however, given that the expression of visual signals could be linked to the properties of the ambient light environment or, more general, the overall costs and benefits of carrying and producing the signal. With respect to egg-spot divergence, this would suggest a scenario of increasing egg-spot conspicuousness with increasing turbidity, as long as the benefit outbalances the costs. This corresponds to our finding of more intensely colored egg-spots and higher egg-spot to fin contrast in longer wavelength shifted environments, where also predation is expected to be lower. The reduced expression found in other haplochromine species could be due to the high costs involved in maintenance or due to the absorption of reddish signals in very turbid conditions or deep water (e.g., Seehausen et al., 1997, 2008). This could possibly explain the secondary loss of egg-spots in some deep-water lineages of Lake Malawi haplochromines (Salzburger et al. 2005), and the decrease in egg-spot conspicuousness in more turbid water in *P. pundamilia* (Castillo Cajas et al. 2012), as these examined populations occur in much deeper and more turbid habitats compared to our examined *A. burtoni* populations.

The costs involved in producing and maintaining carotenoid-based ornaments are often linked to immune defense. The relative cost of allocating carotenoid pigments to visual signals is likely to increase upon activation of an immune response, which involves carotenoids (Lozano, 1994, 2001; Svensson and Wong 2011). For example, fishes experiencing high levels of stress show reduced immune responses, which may result in a decreased lymphocyte ratio (Ellsaesser and Clem 1986; Witeska 2005). Allocation of carotenoids to the immune response is, in these cases, likely to be beneficial for the immune system. However, if carotenoids are limited or if there is a metabolic constraint for carotenoid conversion, investing in the immune system would likely reduce the conspicuousness of carotenoid based visual signals. In support of this trade-off hypothesis we found that *A. burtoni* populations with a decreased lymphocyte ratio show smaller egg-spots and populations with high lymphocyte ratios possess fewer but larger and more conspicuous egg-spots. (Note, however, that a shift in the lymphocyte ratio could also imply that there are more monocytes present, which are the first line of the immune defense, or fewer lymphocytes, which are indicative of a recovery from a recent infection.)

The relative influence of underwater light environment and immunological parameters seem to vary among egg-spot characteristics. Egg-spot coloration most probably depends on underwater light environment (i.e., orange ratio), whereas egg-spot number and relative average egg-spot area rather correlate with immune defense (Tables 1, S6). In systems showing population-specific differences in relative average egg-spot area (Lufubu and Lunzua), the fewer but larger egg-spots of riverine populations result in the same relative total area as the many smaller egg-spots of lacustrine populations. Relative total egg-spot area was therefore the only parameter, which did not differ among populations within systems and, interestingly, did also not correlate with body size. However, there is an among-system variation in relative total egg-spot area, with populations from Lufubu showing a larger relative total egg-spot area compared to the Chitili and Kalambo systems. We would like to note here that the Lufubu populations are, genetically, the most distinct ones (Theis et al. 2014).

Overall, the association between egg-spot characteristics, environmental, and immunological parameters suggests that the relative total egg-spot area is rather fixed within systems, whereas egg-spot number, relative average egg-spot area, and egg-spot coloration seem to adapt to the respective environment. Likewise, in the guppy *Poecilia reticulata*, the area of the sexually selected orange spots was fixed, but brightness was affected by the environment through scarcity in dietary carotenoids supplied by algae (Grether et al. 1999). However, that carotenoid uptake as such would influence egg-spot conspicuousness is rather unlikely as *A. burtoni* feed mainly on algae, plant material, and macroinvertebrates (Theis et al. 2014), which offer plenty of carotenoids. There might be other factors, however, which were not taken into account here, and that might influence egg-spot characteristics as well, for example, other abiotic environmental factors, special biotic interactions, and/or anthropogenic influences. Further, the

results on the association between egg-spots, underwater light environment and immunological parameters should be taken with caution since correlations of data from the field are vulnerable to contain artifacts and are based on a few populations only. Nevertheless, our findings provide a first insight with respect to possible environmental and immunological factors influencing the egg-spot phenotype. The fact that different egg-spot characteristics may be influenced by variable environmental factors illustrates that several replicates need to be examined to elucidate the causes for variation in such a complex trait. To which degree underwater light environment and/or immune response are involved in shaping egg-spot characteristics needs further examinations under controlled laboratory conditions.

In summary, egg-spots show sex- and habitat-specific differences in the haplochromine cichlid *A. burtoni.* Males possess more conspicuous egg-spots compared to females, and, within populations, larger males have more conspicuous egg-spots than smaller ones, both of which could be explained by their function in sexual selection. Further, males of three out of four examined lake-stream systems show similar shifts in egg-spot divergence, with riverine fish possessing fewer but larger and/or more intensely colored egg-spots compared to fish from the corresponding lake habitats. Moreover, the visual model revealed more conspicuous egg-spots in riverine populations as compared to lake populations. Taken together, egg-spots represent an honest trait, which shows the potential to adapt to differences in signal transmittance, and that is traded off with investment into the immune system. Our findings indicate that the expression of a visual signal to maximize both, survival and reproduction is a complex and sensitive equilibrium, which should always be interpreted in the context of several aspects of both, sexual and ecological selection.

ACKNOWLEDGMENTS

We would like to thank the helpers in the field, Judith Bachmann, Astrid Böhne, Tania Bosia, Vasco Campos, Marco Colombo, Marie Dittmann, Simon Egger, Adrian Indermaur, Isabel Keller, Yuri Klaefiger, Julia De Maddalena, Nina Merdas, Florian Meury, Dario Moser, Marius Roesti, Jakob Weber, and Marisa Zubler; Heinz H. Büscher, Craig Zytkow (Conservation Lake Tanganyika) and Gilbert Tembo and his crew for their logistic support in Zambia; the Lake Tanganyika Research Unit, Department of Fisheries, Republic of Zambia, for research permits; and Axios Review as well as Associate Editor Rafael Rodriguez for valuable feedback on this manuscript. This study was supported by grants from the Freiwillige Akademische Gesellschaft Basel (FAG), the Swiss Academy of Sciences (SCNAT), and the Swiss Zoological Society (SZS) to A.T.; the Volkswagen Stiftung and the German Research foundation (DFG) to O.R.; and the European Research Council (ERC, Starting Grant "INTERGENADAPT" and Consolidator Grant "CICHLID∼X"), the University of Basel and the Swiss National Science Foundation (SNF, grants 3100A0_138224 and 3100A0_156405) to W.S.

DATA ARCHIVING

The doi for our data is: DOI 10.5061/dryad.18j1h.2.

LITERATURE CITED

Albertson, R. C., K. E. Powder, Y. Hu, K. P. Coyle, R. B. Roberts, and K. J. Parsons. 2014. Genetic basis of continuous variation in the levels and modular inheritance of pigmentation in cichlid fishes. Mol. Ecol. 23:5135–5150.

Andersson, M. 1994. Sexual Selection. Princeton Univ. Press, Princeton, NJ.

Bates, D., M. Maechler, B. Bolker, and S. Walker. 2014. lme4: linear mixed-effects models using Eigen and S4. R package version 1.1–7. Available at http://CRAN.R-project.org/package=lme4.

Boileau, N., F. Cortesi, B. Egger, M. Muschick, A. Indermaur, A. Theis, H. H. Büscher, and W. Salzburger. 2015. A complex mode of aggressive mimicry in a scale-eating cichlid fish. Biol. Lett. 11:20150521.

Boughman, J. 2001. Divergent sexual selection enhances reproductive isolation in sticklebacks. Nature 411:944–948.

Brzozowski, F., J. Roscoe, K. Parsons, and C. Albertson. 2012. Sexually dimorphic levels of color trait integration and the resolution of sexual conflict in Lake Malawi cichlids. J. Exp. Zool. B. Mol. Dev. Evol. 318:268–278.

Candolin, U., T. Salesto, and M. Evers. 2007. Changed environmental conditions weaken sexual selection in sticklebacks. J. Evol. Biol. 20:233–239.

Castillo Cajas, R. F., O. M. Selz, E. A. P. Ripmeester, O. Seehausen, and M. E. Maan. 2012. Species-specific relationships between water transparency and male coloration within and between two closely related Lake Victoria cichlid species. Int. J. Evol. Biol. 2012:1–12.

Cortesi, F., W. E. Feeney, M. C. O. Ferrari, P. A. Waldie, G. A. C. Phillips, E. C. McClure, H. N. Sköld, W. Salzburger, N. J. Marshall, and K. L. Cheney. 2015. Phenotypic plasticity confers multiple fitness benefits to a mimic. Curr. Biol. 25:949–954.

Couldridge, V. C. K. 2002. Experimental manipulation of male eggspots demonstrates female preference for one large spot in *Pseudotropheus lombardoi*. J. Fish. Biol. 60:726–730.

Coulter, G. W. 1991. Lake Tanganyika and its life. Oxford Univ. Press, Oxford, U.K.

Darwin, C. R. 1871. The descent of man and selection in relation to sex. John Murray, London, U.K.

de Jong, G., and A. J. Noordwijk. 1992. Acquisition and allocation of resources: genetic (co)variances, selection and life histories. Am. Nat. 39:749–770.

Diepeveen, E. T., O. Roth, and W. Salzburger. 2013. Immune-related functions of the *Hivep* gene family in East African cichlid fishes. G3 (Bethesda). 3:2205–2217.

Dugas, M. B., and N. R. Franssen. 2011. Nuptial coloration of red shiners *(Cyprinella lutrensis)* is more intense in turbid habitats. Naturwissenschaften 98:247–251.

Ellsaesser, C. F., and L. W. Clem. 1986. Hematological and immunological changes in channel catfish stressed by handling and transport. J. Fish. Biol. 28:511–521.

Endler, J. A. 1978. A predator's view of animal color patterns. Pp. 319–364 *in* M. K. Hecht, W. C. Steere, and B. Wallace, eds. Evolutionary biology. Vol. 11. Plenum Press, New York/London.

———. 1980. Natural selection on color patterns in *Poecilia reticulata*. Evolution 34:76–91.

———. 1992. Signals, signal conditions, and the direction of evolution. Am. Nat. 139:125–153.

Endler, J. A., and A. E. Houde. 1995. Geographic variation in female preferences for male traits in *Poecilia reticulata*. Evolution 49:456–468.

Espmark, Y., T. Amundsen, and G. Rosenqvist. 2000. Animal signals: signalling and signal design in animal communication. Tapir Academic Press, Trondheim, Norway.

Fernald, R. D. 1977. Quantitative behavioural observations of *Haplochromis burtoni* under semi-natural conditions. Anim. Behav. 25:643–653.

———. 1981. Chromatic organization of a cichlid fish retina. Vision Res. 21:1749–1753.

Fernald, R. D., and N. R. Hirata. 1977. Field study of *Haplochromis burtoni*: quantitative behavioural observations. Anim. Behav. 25:964–975.

Fernald, R. D., and P. A. Liebman. 1980. Visual receptor pigments in the African cichlid fish, *Haplochromis burtoni*. Vision Res. 20:857–864.

Fisher, R. A. 1930. The genetical theory of natural selection. Clarendon Press, Oxford, U.K.

Goldschmidt, T., and J. de Visser. 1990. On the possible role of egg mimics in speciation. Acta Biotheor. 38:125–134.

Goldschmidt, T. 1991. Egg mimics in haplochromine cichlids (Pisces, Perciformes) from Lake Victoria. Ethology 88:177–190.

Goodwin, T. W. 1986. Metabolism, nutrition, and function of carotenoids. Ann. Rev. Nutr. 6:273–297.

Goslee, S. C., and D. L. Urban. 2007. The ecodist package for dissimilarity-based analysis of ecological data. J. Stat. Softw. 22:1–19.

Gray, S. M., F. L. Hart, M. E. M. Tremblay, T. J. Lisney, and C. W. Hawryshyn. 2011. The effects of handling time, ambient light, and anaesthetic method, on the standardized measurement of fish colouration. Can. J. Fish. Aquat. Sci. 68:330–342.

Grether, G. F, J. Hudon, and D. F. Millie. 1999. Carotenoid limitation of sexual coloration along an environmental gradient in guppies. Proc. R. Soc. B 266:1317–1322.

Günther, A. C. L. G. 1894. Descriptions of the reptiles and fishes collected by Mr. E. Coode-Hore on Lake Tanganyika. Proc. Zool. Soc. Lond. 1893:628–632.

Hert, E. 1989. The function of egg-spots in an African mouth-brooding cichlid fish. Anim. Behav. 37:726–732.

———. 1991. Female choice based on egg-spots in *Pseudotropheus aurora* Burgess 1976, a rock-dwelling cichlid of Lake Malawi, Africa. J. Fish. Biol. 38:951–953.

Hill, G. E. 1992. Proximate basis of variation in carotenoid pigmentation in male house finches. Auk 109:1–12.

Hill, G. E., and R. Montgomerie. 1994. Plumage colour signals nutritional condition in the house finch. Proc. R. Soc. B 258:47–52.

Hothorn, T., F. Bretz, and P. Westfall. 2008. Simultaneous inference in general parametric models. Biom. J. 50:346–363.

Iwasa, Y., and A. Pomianowski. 1999. Good parent and good genes models of handicap evolution. J. Theor. Biol. 200:97–109.

Iwasa, Y., A. Pomianowski, and S. Nee. 1991. The evolution of costly mate preferences. II. The "handicap" principle. Evolution 45:1431–1442.

Jennions, M. D, A. P Moller, and M. Petrie. 2001. Sexually selected traits and adult survival: a meta-analysis. Q. Rev. Biol. 76:3–36.

Kekäläinen, J., H. Huuskonen, V. Kiviniemi, and J. Taskinen. 2010. Visual conditions and habitat shape the coloration of the Eurasian perch (*Perca fluviatilis* L.): a trade-off between camouflage and communication? Biol. J. Linn. Soc. 99:47–59.

Kirkpatrick, M. and M. J. Ryan. 1991. The evolution of mating preferences and the paradox of the lek. Nature 350:33–38.

Klingenberg, C. P. 2011. MorphoJ: an integrated software package for geometric morphometrics. Mol. Ecol. Res. 11:353–357.

Kodric-Brown, A., and J. H. Brown. 1984. Truth in advertising: the kinds of traits favored by sexual selection. Am. Nat. 124:309–323.

Kokko, H., M. D. Jennions, and R. Brooks. 2006. Unifying and testing models of sexual selection. Annu. Rev. Ecol. Syst. 37:43–66.

Lande, R. 1981. Models of speciation by sexual selection on polygenic traits. Proc. Natl. Acad. Sci. U. S. A. 78:3721–3725.

Levring, T., and G. R. Fish. 1956. The penetration of light in some tropical East-African waters. Oikos 7:98–109.

Lozano, G. A. 1994. Carotenoids, parasites, and sexual selection. Oikos 70:309–311.

———. 2001. Carotenoids, immunity, and sexual selection: comparing apples and oranges? Am. Nat. 158:200–203.

Luyten, P. H., and N. R. Liley. 1991. Sexual selection and competitive mating success of males guppies *(Poecilia reticulata)* from four Trinidad populations. Behav. Ecol. Sociobiol. 28:329–336.

Maan, M. E., O. Seehausen, and J. J. M. van Alphen. 2010. Female mating preferences and male coloration covary with water transparency in a Lake Victoria cichlid fish. Biol. J. Linn. Soc. 99:398–406.

Maia, R., C. M. Eliason, P.-P. Bitton, S. M. Doucet, and M. D. Shawkey. 2013. pavo: an R package for the analysis, visualization and organization of spectral data. Methods Ecol. Evol. 4:906–913.

Marchetti, K. 1993. Dark habitats and bright birds illustrate the role of the environment in species divergence. Nature 362:149–152.

Moller, A. P. 1995. Sexual selection in the barn swallow *(Hirundo rustica)*. V. Geographic variation in ornament size. J. Evol. Biol. 8:3–19.

Muschick, M., A. Indermaur, and W. Salzburger. 2012. Convergent evolution within an adaptive radiation of cichlid fishes. Curr. Biol. 22:2362–2368.

Nosil, P. 2012. Ecological Speciation. Oxford Univ. Press, Oxford, UK.

Pignatelli, V., C. Champ, J. Marshall, and M. Vorobyev. 2010. Double cones are used for colour discrimination in the reef fish, *Rhinecanthus aculeatus*. Biol. Lett. 6:537–539.

Pike, T. W., J. D. Blount, B. Bjerkeng, J. Lindström, and N. B. Metcalfe. 2007. Carotenoids, oxidative stress and female mating preference for longer lived males. Proc. R. Soc. B 274:1591–1596.

R Core Team. 2014. R: a language and environment for statistical computing. R Foundation for Statistical Computing, Vienna. Available at http://www.R-project.org/.

Rohlf, F. J. 2008. tpsDIG, Version 2.11. Department of Ecology and Evolution, State University of New York at Stony Brook. Available at http://life.bio.sunysb.edu/morph/.

Rolff, J. 2002. Bateman's principle and immunity. Proc. R. Soc. B 269:867–872.

Roth, O., J. P. Scharsack, I. Keller, and T. B. H. Reusch. 2011. Bateman's principle and immunity in a sex-role reversed pipefish. J. Evol. Biol. 24:1410–1420.

Rowe, L., and D. Houle. 1996. The lek paradox and the capture of genetic variance by condition dependent traits. Proc. R. Soc. London Ser. B 263:1415–21.

Salzburger, W., T. Mack, E. Verheyen, and A. Meyer. 2005. Out of Tanganyika: genesis, explosive speciation, key-innovations and phylogeography of the haplochromine cichlid fishes. BMC Evol. Biol. 5:1–15.

Salzburger, W., I. Braasch, and A. Meyer. 2007. Adaptive sequence evolution in a color gene involved in the formation of the characteristic egg-dummies of male haplochromine cichlid fishes. BMC Biol. 5: 1–13.

Santos, M. E., I. Braasch, N. Boileau, B. S. Meyer, L. Sauteur, A. Böhne, H.-G. Belting, M. Affolter, and W. Salzburger. 2014. The evolution of cichlid fish egg-spots is linked with a *cis*-regulatory change. Nat. Commun. 5:1–11.

Scharsack, J. P., M. Kalbe, R. Derner, J. Kurtz, and M. Milinski. 2004. Modulation of granulocyte responses in three-spined sticklebacks *Gasterosteus aculeatus* infected with the tapeworm *Schistocephalus solidus*. Dis. Aquat. Organ. 59:141–150.

Scharsack, J. P., M. Kalbe, C. Harrod, and G. Rauch. 2007a. Habitat-specific adaptation of immune responses of stickleback *(Gasterosteus aculeatus)* lake and river ecotypes. Proc. Roy. Soc. B 274:1523–1532.

Scharsack, J. P., K. Koch, and K. Hammerschmidt. 2007b. Who is in control of the stickleback immune system: interactions between *Schistocephalus solidus* and its specific vertebrate host. Proc. Roy. Soc. B 274:3151–3158.

Schwartz, A. K, and A. P. Hendry. 2007. A test for the parallel co-evolution of male colour and female preference in Trinidadian guppies (*Poecilia reticulata*). Evol. Ecol. Res. 9:71–90.

Seehausen, O., J. J. M. van Alphen, and F. Witte. 1997. Cichlid fish diversity threatened by eutrophication that curbs sexual selection. Science 277:1808–1811.

Seehausen, O., Y. Terai, I. S. Magalhaes, K. L. Carleton, H. D. J. Mrosse, et al. 2008. Speciation through sensory drive in cichlid fish. Nature 455:620–626.

Sheldon, B. C., and S. Verhulst. 1996. Ecological immunology: costly parasite defences and trade-offs in evolutionary ecology. Trends Ecol. Evol. 11:317–321.

Simons, M. J., A. A. Cohen, and S. Verhulst. 2012. What does carotenoid-dependent coloration tell? Plasma carotenoid level signals immunocompetence and oxidative stress state in birds-A meta-analysis. PLoS One 7:e43088.

Smith, H. G., L. Råberg, T. Ohlsson, M. Granbom, and D. Hasselquist. 2007. Carotenoid and protein supplementation have differential effects on pheasant ornamentation and immunity. J. Evol. Biol. 20:310–319.

Stuart-Fox, D. M., and T. J. Ord. 2004. Sexual selection, natural selection and the evolution of dimorphic coloration and ornamentation in agamid lizards. Proc. Roy. Soc. B 271:2249–2255.

Svensson, P. A., and B. B. M. Wong. 2011. Carotenoid-based signals in behavioural ecology: a review. Behaviour 148:131–189.

Számadó, S. 2011. The cost of honesty and the fallacy of the handicap principle. Anim. Behav. 81:3–10.

Theis, A., W. Salzburger, and B. Egger. 2012. The function of anal fin egg-spots in the cichlid fish *Astatotilapia burtoni*. PLoS One 7:e29878.

Theis, A., F. Ronco, A. Indermaur, W. Salzburger, and B. Egger. 2014. Adaptive divergence between lake and stream populations of an East African cichlid fish. Mol. Ecol. 23:5304–5322.

Theis, A., T. Bosia, T. Roth, W. Salzburger, and B. Egger. 2015. Egg-spot and body size asymmetries influence attack strategies in haplochromine cichlid fishes. Behav. Ecol. 26:1512–1519.

Tobler, M. 2006. The eggspots of cichlids: Evolution through sensory exploitation? Z. Fischkd. 8:39–46.

Trivers, R. L. 1972. Parental investment and sexual selection. Pp. 136–179 *in* B. Campbell, ed. Sexual selection and the descent of man 1871–1971. Aldine Press, Chicago, IL.

van Noordwijk, A. J., and G. de Jong. 1986. Acquisition and allocation of resources: their influence on variation in life history tactics. Am. Nat. 128:137–142.

von Schantz, T., S. Bensch, M. Grahn, D. Hasselquist, H. and Wittzell. 1999. Good genes, oxidative stress and condition-dependent sexual signals. Proc. Roy. Soc. B 266:1–12.

Vorobyev, M., and D. Osorio. 1998. Receptor noise as a determinant of colour thresholds. Proc. Roy. Soc. B 265:351–358.

Vorobyev, M., R. Brandt, D. Peitsch, S. B. Laughlin, and R. Menzel. 2001. Colour thresholds and receptor noise: Behaviour and physiology compared. Vision Res. 41:639–653.

Wickler, W. 1962. 'Egg-dummies' as natural releasers in mouth-breeding cichlids. Nature 194:1092–1093.

Witeska, M. 2005. Stress in fish—hematological and immunological effects of heavy metals. Electron. J. Ichthyol. 1:35–41.

Wong, B. B. M., U. Candolin, and K. Lindström. 2007. Environmental deterioration compromises socially enforced signals of male quality in three-spined sticklebacks. Am. Nat. 170:184–189.

Zahavi, A. 1975. Mate selection—a selection for a handicap. J. Theor. Biol. 53:205–214.

Zahavi, A., and A. Zahavi. 1997. The handicap principle: a missing piece of Darwin's puzzle. Oxford Univ. Press, Oxford, U.K.

Zeileis, A. 2004. Econometric computing with HC and HAC covariance matrix estimators. J. Stat. Softw. 11:1–17.

———. 2006. Object-oriented computation of sandwich estimators. J. Stat. Softw. 16:1–16.

Associate Editor: R. Rodriguez
Handling Editor: M. Noor

Supporting Information

Additional Supporting Information may be found in the online version of this article at the publisher's website:

Table S1. Sample size details for analyses on egg-spot characteristics and lymphocyte ratios (blood measurements), with geographic coordinates for each locality.
Table S2. Linear models to test for differences in egg-spot measurements based on photographs (number, relative average area, relative total area and coloration).
Table S3. Detailed results on sex-, population- and system-specific mean values (with corresponding confidence intervals) of egg-spots and the pairwise comparisons thereof.
Table S4. Results of the principal component analysis (PCA).
Table S5. Orange ratio values for each depth level at the sample locations.
Table S6. Stepwise multiple regression on distance matrices (MRM) among pairwise differences in egg-spot characteristics, orange ratio, lymphocyte ratio as well as geographic distance.
Figure S1. Photographs of a representative male and female individual of *A. burtoni*.
Figure S2. Representative photographs of the six categories used to describe the coloration of egg-spots.
Figure S3. Underwater light environments.
Figure S4. Correlations of body size and the four examined egg-spot characteristics based on photographs.
Figure S5. Color distances resulting from the visual models from different depths.

Chapter 5 | Supplementary Material

Table S1. Sample size details for analyses on egg-spot characteristics and lymphocyte ratios (blood measurements), with geographic coordinates for each locality.

sampling information				egg-spot characteristic measurements				blood measurements
				taken from the photographs			reflectance spectrometry	lymphocyte ratio
population		latitude	longitude	all	females	males	males	males
ChL	Chitli lake	8°38'18.42"S	31°11'55.34"E	37	27	10	NA	NA
Ch1	Chitli creek 1	8°38'16.91"S	31°12'4.02"E	51	28	23	NA	NA
KaL	Kalambo lake	8°36'6.27"S	31°11'13.24"E	94	39	55	5	13
Ka1	Kalambo stream 1	8°35'35.23"S	31°11'6.18"E	53	13	40	5	6
Ka2	Kalambo stream 2	8°35'6.24"S	31°12'29.32"E	37	15	22	4	10
Ka3	Kalambo stream 3	8°35'41.59"S	31°14'50.32"E	49	23	26	8	18
LfL	Lufubu lake	8°33'36.56"S	30°43'33.79"E	29	6	23	6	9
Lf1	Lufubu stream 1	8°35'49.31"S	30°43'38.96"E	27	6	21	NA	NA
Lf2	Lufubu stream 2	8°41'9.37"S	30°33'51.90"E	36	15	21	4	6
LzL	Lunzua lake	8°44'57.13"S	31°10'21.86"E	39	16	23	4	22
Lz1	Lunzua stream 1	8°47'23.51"S	31° 8'14.33"E	52	16	36	9	10
total sample size per method				**504**	204	300	**45**	**94**

Table S2. Linear models to test for differences in egg-spot measurements based on photographs (number, relative average area, relative total area and coloration) between sexes (A) and among populations (males only) (B).

A

egg-spot characteristic	linear model
number	glmer(number ~ sex + centred_centroid_size + (1|sex_specific_population), data=data, family="poisson")
relative average area	lmer(sqrt(relative_average_area) ~ sex + (centred_centroid_size|sex_specific_population), data=data)
relative total area	lmer(relative_total_area ~ sex + (centred_centroid_size|sex_specific_population), data=data)
coloration	lmer(coloration ~ sex + centred_centroid_size + sex:centred_centroid_size + (centred_centroid_size|sex_specific_population), data=data)

B

egg-spot characteristic	linear model
number	glm(number ~ population + centroid_size, data=data, family="poisson")
relative average area	lm(relative_average_area ~ population + centroid_size, data=data)
relative total area	lm(relative_total_area ~ population, data=data)
coloration	lm(coloration^2 ~ population + centroid_size, data=data)

Table S3. Detailed results on sex-, population- and system-specific mean values (with corresponding confidence intervals) of egg-spots and the pairwise comparisons thereof. Mean values with corresponding confidence intervals for each egg-spot measurement based on photographs (number, relative average area, relative total area and coloration) and mean values with corresponding standard deviation and range for body size (standard length and centroid size) for each sex (A) and for the males of each population (B) as well as for relative total area for each system (C). Results of all pairwise comparisons for each egg-spot measurement based on photographs (number, relative average area, relative total area and coloration) between populations within lake-stream systems (D) and for comparisons of total egg-spot area between systems (E). Significance levels: *p < 0.05, **p < 0.01 and ***p < 0.001.

A

sex	egg-spot number			relative average egg-spot area (% of fin area)			relative total egg-spot area (% of fin area)			egg-spot coloration			body size			
													standard length (SL; mm)		centroid size (CS)	
	mean	lower CI	upper CI	mean	lower CI	upper CI	mean	lower CI	upper CI	mean	lower CI	upper CI	mean ± sd	range	mean ± sd	range
females	5.23	4.79	5.72	1.23	1.11	1.37	5.48	5.08	5.88	2.51	2.26	2.76	46.79 ± 7.78	27.80 - 75.40	64.67 ± 10.86	39.88 - 106.20
males	5.07	4.50	5.71	1.41	1.23	1.61	6.36	5.81	6.91	4.25	3.90	4.60	54.81 ± 12.40	33.67 - 106.42	76.14 ± 17.79	45.99 - 148.76

B

population	egg-spot number (at grandmean)			relative average egg-spot area (at grandmean, % of fin area)			relative total egg-spot area (% of fin area)			egg-spot coloration			body size			
													standard length (SL; mm)		centroid size (CS)	
	mean	lower CI	upper CI	mean	lower CI	upper CI	mean	lower CI	upper CI	mean	lower CI	upper CI	mean ± sd	range	mean ± sd	range
ChL	5.75	4.11	8.04	1.40	1.12	1.67	6.32	5.36	7.27	3.92	3.41	4.38	51.98 ± 11.66	40.14 - 75.78	72.22 ± 16.58	55.76 - 107.31
Ch1	4.64	3.36	6.41	1.54	1.29	1.80	6.46	5.31	7.60	4.65	4.26	5.01	54.21 ± 14.26	35.25 - 78.15	75.39 ± 20.04	48.74 - 108.22
KaL	5.19	3.90	6.92	1.49	1.26	1.72	6.58	5.55	7.62	4.11	3.71	4.48	55.13 ± 8.61	42.47 - 78.19	75.87 ± 11.99	58.80 - 108.37
Ka1	5.03	3.74	6.77	1.39	1.15	1.63	5.90	4.83	6.97	4.19	3.78	4.56	53.86 ± 13.59	36.09 - 89.60	74.01 ± 18.99	49.24 - 125.66
Ka2	5.05	3.64	7.01	1.45	1.19	1.71	6.25	5.10	7.41	4.25	3.81	4.64	46.98 ± 5.89	36.53 - 59.20	65.27 ± 8.44	51.08 - 82.71
Ka3	5.01	3.66	6.86	1.64	1.39	1.89	6.76	5.64	7.89	4.30	3.88	4.68	51.59 ± 12.33	33.67 - 89.88	71.22 ± 17.83	45.99 - 128.05
LfL	5.72	4.18	7.81	1.46	1.20	1.72	7.15	6.01	8.30	4.25	3.81	4.65	68.99 ± 14.38	47.17 - 102.20	97.27 ± 21.36	61.41 - 143.66
Lf1	6.75	4.22	7.93	1.67	1.41	1.93	8.09	6.93	9.25	4.50	4.08	4.88	64.32 ± 18.17	44.63 - 106.42	90.40 ± 26.02	61.93 - 148.76
Lf2	4.23	3.03	5.92	1.93	1.67	2.19	7.60	6.44	8.76	4.66	4.27	5.03	52.88 ± 7.57	41.67 - 71.23	74.48 ± 10.99	59.36 - 101.69
LzL	5.80	4.24	7.94	1.43	1.18	1.69	6.43	5.28	7.57	3.80	3.32	4.24	51.56 ± 6.38	41.58 - 67.19	71.56 ± 8.96	57.35 - 93.65
Lz1	4.14	3.04	5.63	2.04	1.80	2.28	7.21	6.13	8.29	4.54	4.16	4.88	52.27 ± 8.44	34.55 - 81.25	72.72 ± 12.18	47.48 - 115.62

C

system	relative total egg-spot area (% of fin area)			body size			
				standard length (SL; mm)		centroid size (CS)	
	mean	lower CI	upper CI	mean ± sd	range	mean ± sd	range
Chitili	6.42	5.88	6.95	53.54 ± 13.39	35.25 - 78.15	74.43 ± 18.86	48.74 - 108.22
Kalambo	6.37	5.78	6.97	52.88 ± 10.90	33.67 - 89.88	72.88 ± 15.28	45.99 - 128.05
Lufubu	7.60	6.95	8.26	62.27 ± 15.45	41.67 - 106.42	87.69 ± 22.33	59.36 - 148.76
Lunzua	6.91	6.24	7.57	52.00 ± 7.65	34.55 - 81.25	72.27 ± 10.97	47.48 - 115.62

D

population comparison	egg-spot number		relative average egg-spot area		relative total egg-spot area		egg-spot coloration	
	z-value	p-value	z-value	p-value	z-value	p-value	z-value	p-value
ChL - Ch1	1.938	0.3793	-1.062	0.9307	-0.235	1.0000	-3.531	0.0050**
KaL - Ka1	0.817	0.9834	1.570	0.6470	2.507	0.1141	-0.633	0.9964
KaL - Ka2	0.759	0.9892	0.509	0.9991	0.963	0.9585	-0.949	0.9616
KaL - Ka3	0.728	0.9916	-1.905	0.4041	-0.624	0.9967	-1.380	0.7787
Ka1 - Ka2	-0.071	1.0000	-0.688	0.9939	-0.974	0.9559	-0.414	0.9998
Ka1 - Ka3	0.111	1.0000	-2.997	0.0291*	-2.781	0.0549	-0.784	0.9869
Ka2 - Ka3	0.161	1.0000	-1.989	0.3492	-1.364	0.7882	-0.299	1.0000
LfL - Lf1	-0.154	1.0000	-2.089	0.2895	-1.677	0.5690	-1.524	0.6818
LfL - Lf2	3.873	0.0011**	-4.736	< 0.001***	-0.832	0.9815	-2.483	0.1214
Lf1 - Lf2	4.616	< 0.001***	-2.274	0.1971	0.820	0.9829	-1.006	0.9479
LzL - Lz1	5.114	< 0.001***	-6.470	< 0.001***	-1.777	0.4961	-4.889	< 0.001***

E

system comparison	relative total egg-spot area	
	z-value	p-value
Chitili - Kalambo	-0.143	0.9989
Chitili - Lufubu	3.378	0.0045**
Chitili - Lunzua	1.457	0.4550
Kalambo - Lufubu	4.712	< 0.001***
Kalambo - Lunzua	2.209	0.1184
Lufubu - Lunzua	-2.195	0.1223

Table S4. Results of the principal component analysis (PCA) testing the differences among males with regard to combined egg-spot characteristics number, relative average area, relative total area and coloration. Indicated are standard deviation, proportion of variance, cumulative variance and the mean of the PC loadings per population.

	PC1	PC2	PC3	PC4
Standard deviation	1.349000	1.123100	0.892800	0.348550
Proportion of Variance	0.455000	0.315300	0.199300	0.030370
Cumulative Proportion	0.455000	0.770300	0.969600	1.000000
ChL	0.898797	0.392387	-0.232222	0.061097
Ch1	-0.172236	-0.451941	0.528927	-0.075866
KaL	0.354268	0.037904	-0.119336	-0.089378
Ka1	0.693357	-0.253529	0.099019	-0.011017
Ka2	0.445778	-0.089104	0.158584	-0.002847
Ka3	-0.092053	0.002139	-0.016620	0.071001
LfL	0.226920	0.544469	0.144157	-0.110003
Lf1	-0.567835	0.884261	0.261697	-0.054627
Lf2	-1.290450	-0.349412	-0.016046	-0.057009
LzL	0.877900	0.459667	-0.414205	0.065597
Lz1	-1.279061	-0.497085	-0.256797	0.224243

Table S5. Orange ratio values for each depth level at the sample locations. The last column describes the average change in orange ratio per 10 cm, which was calculated from the deepest possible measurement (in bold). This average orange ratio was used in the analyses as a representative value for the underwater ambient light at each location.

locality	surface	10 cm	20 cm	30 cm	40 cm	50 cm	70 cm	100 cm	average (per 10 cm)
ChL	3.75	5.86	6.17	6.56	7.17	**7.56**	NA	NA	1.51
Ch1	3.59	6.06	**7.03**	NA	NA	NA	NA	NA	3.51
KaL	2.29	2.46	2.43	2.38	2.51	2.71	3.05	**3.41**	0.34
Ka1	2.82	3.37	3.56	3.77	4.09	4.46	5.30	**8.61**	0.86
Ka2	3.22	3.57	3.86	4.27	4.84	5.43	**10.02**	NA	1.43
Ka3	2.95	3.49	3.94	4.67	5.68	**7.64**	NA	NA	1.53
LfL	3.21	3.45	3.69	4.04	4.44	4.98	6.88	**10.40**	1.04
Lf2	3.02	3.60	4.33	**5.23**	NA	NA	NA	NA	1.74
LzL	2.45	2.57	2.67	2.71	2.78	2.81	2.94	**3.48**	0.35
Lz1	2.90	4.29	4.72	4.99	5.65	**6.25**	NA	NA	1.25

Table S6. Stepwise multiple regression on distance matrices (MRM) among pairwise differences in egg-spot characteristics, orange ratio, lymphocyte ratio as well as geographic distance. The egg-spot characteristics number, relative average area and coloration were corrected on centroid size before the analyses.

model		r^2-value	p-value
number	~ orange ratio + lymphocyte ratio + geographic distance	0.3729	0.0730
	~ orange ratio + lymphocyte ratio	0.2790	0.0580
	~ orange ratio + geographic distance	0.0501	0.5689
	~ lymphocyte ratio + geographic distance	0.3436	0.0417
	~ orange ratio	0.0007	0.8875
	~ lymphocyte ratio	0.2535	0.0102
	~ geographic distance	0.0498	0.1958
relative average area	~ orange ratio + lymphocyte ratio + geographic distance	0.5649	0.0573
	~ orange ratio + lymphocyte ratio	0.5245	0.0151
	~ orange ratio + geographic distance	0.0848	0.4083
	~ lymphocyte ratio + geographic distance	0.5279	0.0540
	~ orange ratio	0.0349	0.4330
	~ lymphocyte ratio	0.4902	0.0103
	~ geographic distance	0.0657	0.1489
relative total area	~ orange ratio + lymphocyte ratio + geographic distance	0.2428	0.1440
	~ orange ratio + lymphocyte ratio	0.0018	0.9789
	~ orange ratio + geographic distance	0.3995	0.0088
	~ lymphocyte ratio + geographic distance	0.2416	0.0688
	~ orange ratio	0.0633	0.2165
	~ lymphocyte ratio	0.0015	0.8887
	~ geographic distance	0.3826	0.0053
coloration	~ orange ratio + lymphocyte ratio + geographic distance	0.4493	0.0535
	~ orange ratio + lymphocyte ratio	0.4208	0.0460
	~ orange ratio + geographic distance	0.1024	0.2625
	~ lymphocyte ratio + geographic distance	0.1024	0.2625
	~ orange ratio	0.1001	0.0803
	~ lymphocyte ratio	0.0817	0.3902
	~ geographic distance	0.0003	0.9209

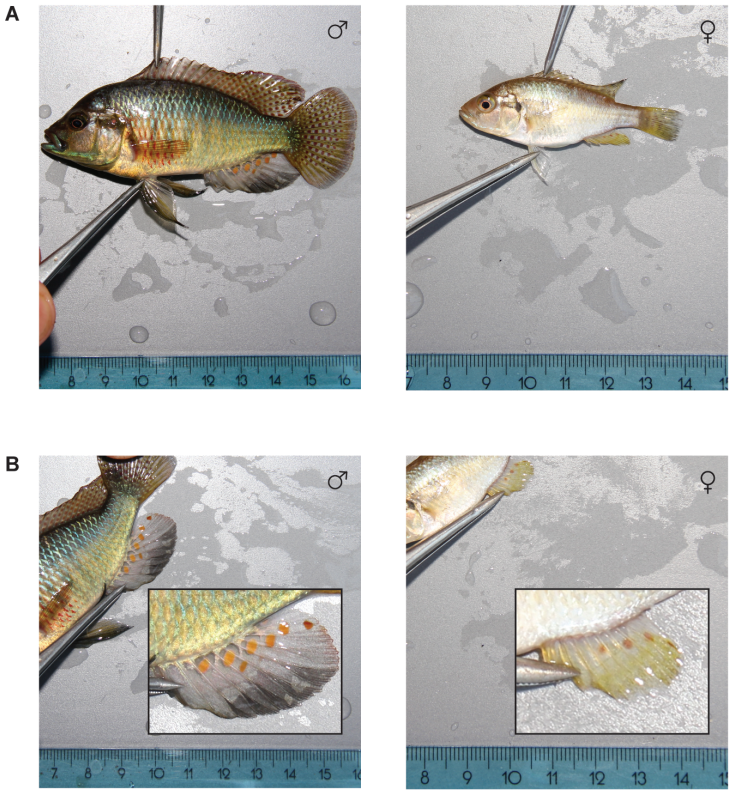

Figure S1. Photographs of a representative male (left side) and female (right side) in lateral position to measure centroid size (A) and focusing on the anal fin for later egg-spot measurements assessing the number, relative average area, relative total area and coloration (B).

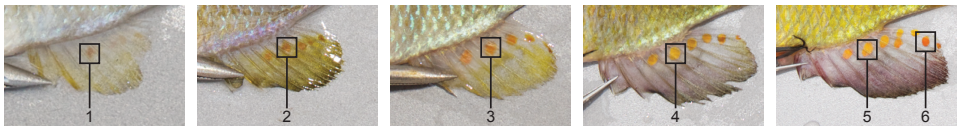

Figure S2. Representative photographs of the six categories used to describe the coloration of egg-spots. The categories ascend with increasing conspicuousness based on a combination of hue, saturation and brightness. 1 dull aggregated pigments; 2 dull egg-spot; 3 intermediate egg-spot; 4 normal egg-spot; 5 bright egg-spot (light orange); 6 bright and more saturated egg-spot (dark orange).

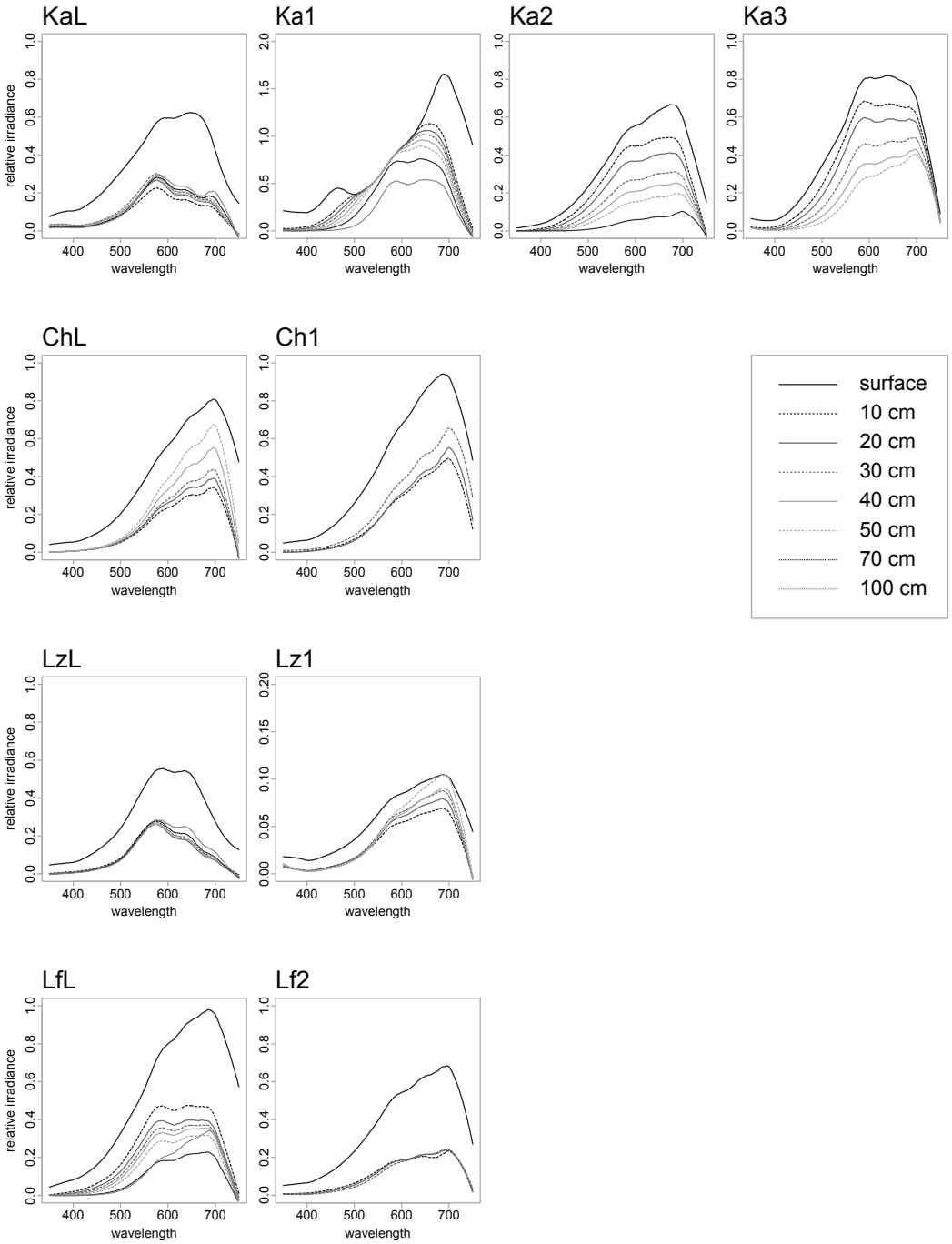

Figure S3. Underwater light environments. In each panel, the curves show underwater ambient light spectra at different depths.

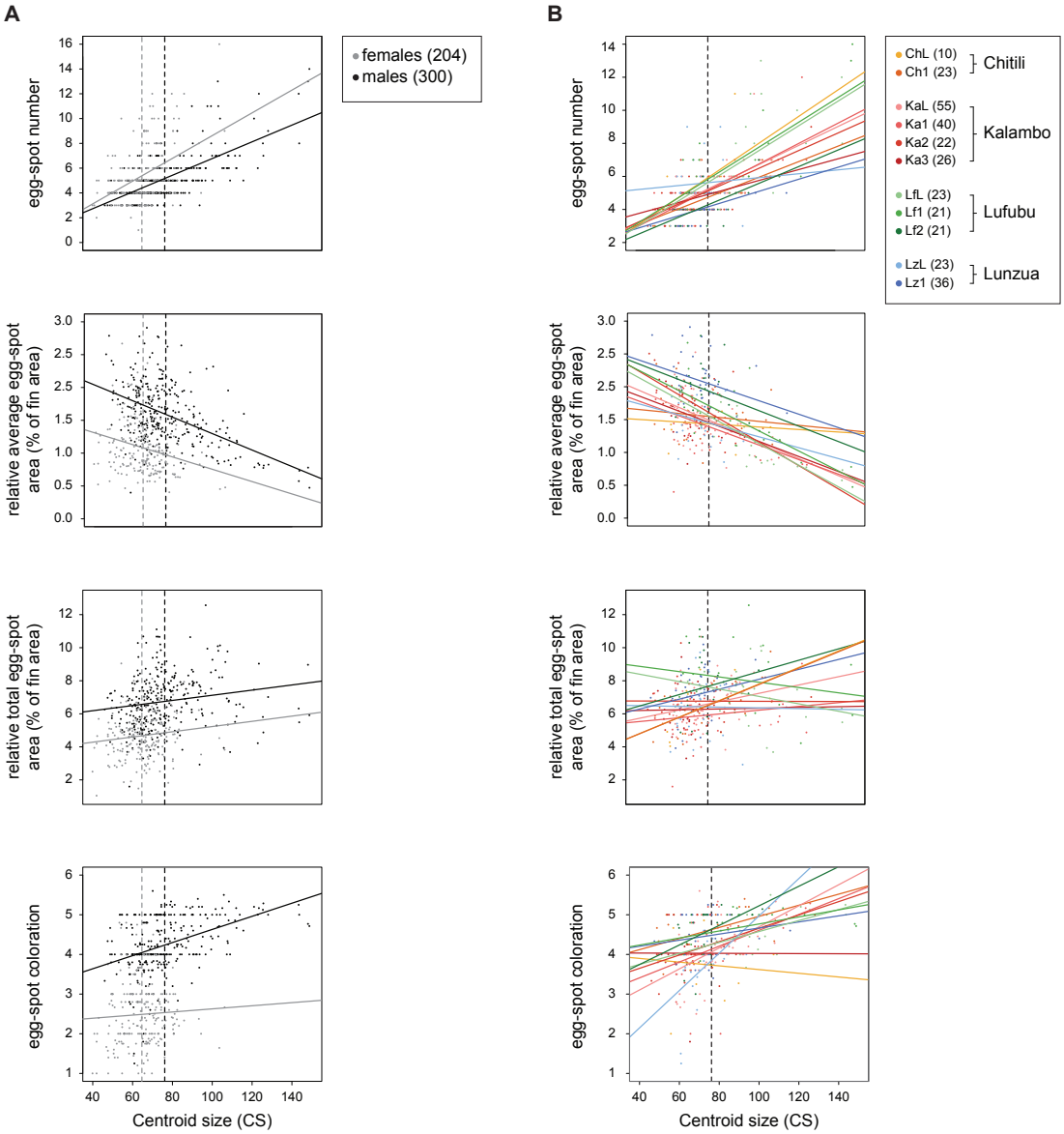

Figure S4. Correlations of body size and the four examined egg-spot characteristics measured based on photographs (number, relative average area, relative total area and coloration) for males and females (A) and for males of the populations of the lake-stream systems. Full names of the populations are listed in the grey box of Fig. 1.
The dashed vertical lines represent the mean value of body size (grey = females, black = males), which were used for the sex-specific centering and scaling of the data to compare males and females (A) and to correct for size in males to compare among populations (as illustrated in Fig. 2B) (B).

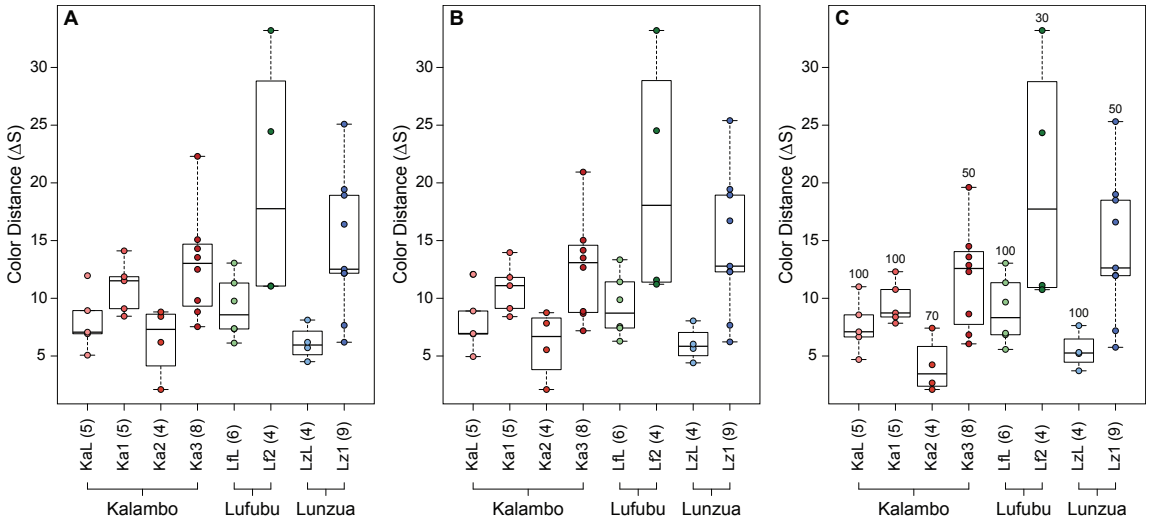

Figure S5. Color distances resulting from the visual models generated for 10 cm below water surface (A), 30 cm below surface (B) and for the deepest measurable depth for each locality (C; the corresponding depth is specified above the boxes). Corresponding sample sizes per population are parenthesized. For each system, populations are ordered on the x-axis with the lake populations on the left followed by the stream population(s).

Chapter 6

Point-Combination Transect (PCT): Incorporation of small underwater cameras to study fish communities

Lukas Widmer, Elia Heule, Marco Colombo, Attila Rueegg, Adrian Indermaur,
Fabrizia Ronco & Walter Salzburger

Methods in Ecology and Evolution (2019)

I contributed to the extensive field work to collect the raw data for this study, provided the taxon list for the image analyses tool and data on body size of all species.

Received: 11 August 2018 | Accepted: 22 January 2019
DOI: 10.1111/2041-210X.13163

RESEARCH ARTICLE

Methods in Ecology and Evolution BRITISH ECOLOGICAL SOCIETY

Point-Combination Transect (PCT): Incorporation of small underwater cameras to study fish communities

Lukas Widmer | Elia Heule | Marco Colombo | Attila Rueegg | Adrian Indermaur | Fabrizia Ronco | Walter Salzburger

Department of Environmental Sciences, Zoological Institute, University of Basel, Basel, Switzerland

Correspondence
Lukas Widmer
Email: widmer.lukas@gmail.com
and
Walter Salzburger
Email: walter.salzburger@unibas.ch

Funding information
H2020 European Research Council, Grant/Award Number: 617585; European Research Council

Handling Editor: Chris Sutherland

Abstract

1. Available underwater visual census (UVC) methods such as line transects or point count observations are widely used to obtain community data of underwater species assemblages, despite their known pit-falls. As interest in the community structure of aquatic life is growing, there is need for more standardized and replicable methods for acquiring underwater census data.
2. Here, we propose a novel approach, Point-Combination Transect (PCT), which makes use of automated image recording by small digital cameras to eliminate observer and identification biases associated with available UVC methods. We conducted a pilot study at Lake Tanganyika, demonstrating the applicability of PCT on a taxonomically and phenotypically highly diverse assemblage of fishes, the Tanganyikan cichlid species-flock.
3. We conducted 17 PCTs consisting of five GoPro cameras each and identified 22,867 individual cichlids belonging to 61 species on the recorded images. These data were then used to evaluate our method and to compare it to traditional line transect studies conducted in close proximity to our study site at Lake Tanganyika.
4. We show that the analysis of the second hour of PCT image recordings (equivalent to 360 images per camera) leads to reliable estimates of the benthic cichlid community composition in Lake Tanganyika according to species accumulation curves, while minimizing the effect of disturbance of the fish through SCUBA divers. We further show that PCT is robust against observer biases and outperforms traditional line transect methods.

KEYWORDS
cichlid fish, community ecology, comparative analysis, diversity, lake tanganyika, monitoring, sampling, underwater visual census

1 | INTRODUCTION

Underwater visual census (UVC) methods such as line transect (Brock, 1954) or point count observation (Samoilys & Carlos, 1992, 2000) are widely applied in ecology and, today, represent a standard approach for the non-invasive assessment of underwater communities, particularly of fish. In order to obtain UVC data the observation is typically performed directly by SCUBA divers (or snorkelers), who

record the presence and abundance of the species under investigation following standardized procedures (Colvocoresses & Acosta, 2007; Dickens, Goatley, Tanner, & Bellwood, 2011; Whitfield et al., 2014). A major drawback of UVC applications involving human observers is that these are subject to a number of biases, which are – depending on the strategy used – difficult or impossible to avoid. For example the presence of the observer can itself have a strong effect on the local fish community by altering fish behaviour (Dickens et al., 2011; Pais & Cabral, 2017). Observer swimming speed and distance to substratum have been reported as additional factors that can influence the observational results of transect studies (Edgar, Barrett, & Morton, 2004). Another potential problem is observer expertise and subjectivity, typically resulting in data skewing towards well-known species (Thompson & Mapstone, 1997; Williams, Walsh, Tissot, & Hallacher, 2006). These problems can largely be overcome using digital imaging technologies that are observer-independent and generate underwater images or video footage that can subsequently be analysed (Pereira, Leal, & de Araújo, 2016). Using digital information has the additional advantage that the raw data can be stored and re-evaluated if desired, thus facilitating repeatability and reproducibility of the results.

The application of camera-based census methods in the aquatic realm is, however, much more challenging than in terrestrial ecosystems. For example aquatic habitats are typically much less accessible, and light penetration and visibility are much lower in water than in air. Cameras for underwater use need to be specifically equipped and protected, which subsequently makes the handling, installation and recovery of cameras more difficult; standard procedures used in census surveys in terrestrial habitats cannot easily be applied underwater (e.g. the use of motion sensors would cause cameras to fire constantly due to water movement and/or suspended particles, whereas the use of artificial or flash light would bias the observations by attracting or scaring off certain individuals). Despite the general difficulties, several camera-based census methods are available to date specifically tailored towards underwater use. The STAVIRO method introduced by Pelletier et al. (2012), for instance, consists of an encased camera revolving about itself on a motor, taking images of a circular area in accordance with the principles of point observations. Although bias by observer presence is reduced or entirely eliminated, the moving object of the STAVIRO apparatus might still alter fish behaviour (Mallet, Wantiez, Lemouellic, Vigliola, & Pelletier, 2014). The often-used Baited-Remote Underwater Video (BRUV) technique involves video surveillance of bait, which is placed in a particular habitat (Lowry, Folpp, Gregson, & Mckenzie, 2011; Unsworth, Peters, McCloskey, & Hinder, 2014). The resulting footage is then used to estimate fish abundance. Although under certain circumstances this might be a valuable approach, it is not suitable for observing a community as a whole, as there is a species-specific bias through the bait used (Wraith, Lynch, Minchinton, Broad, & Davis, 2013).

Here we introduce a novel approach, the Point-Combination Transect (PCT) method (Figure 1a,b), which incorporates elements of conventional UVC line and point transects with digital underwater imaging tools. We demonstrate the wide applicability of PCT by employing it on a rather complex assemblage of fishes, the species flock of cichlid fishes from Lake Tanganyika in East Africa. This fish community is dominated by species that strongly interact with the substrate, exemplified through numerous substrate breeders or algae scrappers; but even highly mobile and pelagic species interact closely with the benthos, for example when predating others or during spawning (Konings, 1998). Our novel approach is based on small, automated digital cameras in underwater housings that are placed on the benthos and aligned along a given distance at a set depth level. The PCT method enables a researcher to observe several spatially close communities simultaneously by automatically recording images in a defined time lapse. Once the cameras are placed, there is no further disturbance by SCUBA divers and no interaction of the camera with its surroundings, including no movement and no visual or audible signalling. We show how with relatively little monetary and timely investment, valuable and robust data on fish community structures can be collected, even at remote places and under demanding field conditions.

2 | MATERIALS AND METHODS

2.1 | Study site

The pilot was conducted at Lake Tanganyika, East Africa. The study site was restricted to the bay off Kalambo Falls Lodge located close to the mouth of Kalambo River (8°37′36″ S, 31°12′2″ E) in northern Zambia (Figure 1c). This bay was chosen for its diversity in habitats present within close proximity and its accessibility from Kalambo Falls Lodge. Furthermore, the bay is subjected to moderate fishing pressure only, primarily targeting non-cichlid fish species. Hence we assumed to observe a relatively undisturbed, local fish community bereft of extensive anthropogenic influences. The study area comprises a diverse set of environments, such as predominantly rock- or sand-covered habitats; areas with an intermediate coverage of the lakebed; or vegetation dominated habitats. PCTs were conducted on a variety of depth levels, ranging from <1 m up to 21 m.

2.2 | Point-Combination Transect settings

The technical equipment for our PCT consisted of GoPro cameras (Hero 3+ Silver Edition, Hero 4+ Silver Edition, © GoPro, Inc.), each equipped with a 16 GB microSD card (ScanDisk) ensuring sufficient storage capacity for high-quality image storage. The protective housing provided by the supplier is waterproof to a depth of 40 m, making additional underwater housing unnecessary. The cameras were mounted in their housing on the supplied stand and fixed to a small rock (approximate dimensions: length = 15 cm, width = 15 cm, height = 5 cm) to provide negative buoyancy, immobility and stability once placed underwater on the lakebed (Figure 1b).

The setup for a PCT consists of five GoPro cameras positioned in a distance of 10 m of each other along a marked cord (total length of the transect: 40 m) (Figure 1a). The length of 40 m for one transect

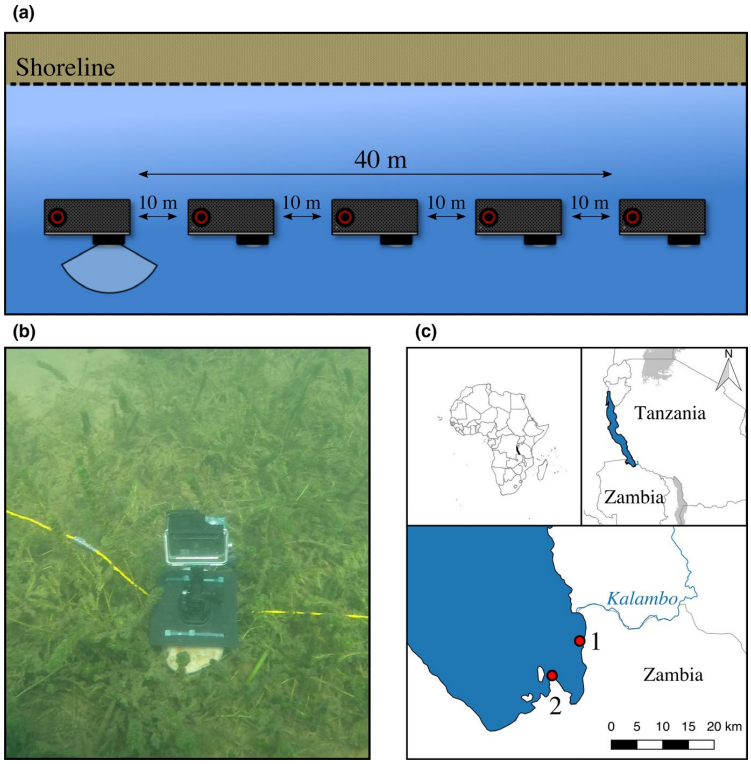

FIGURE 1 (a) Design and set up of a Point-Combination Transect (PCT) as used in the pilot. GoPros face perpendicular away from shoreline. The focal angle of 120° is illustrated for one camera. (b) Underwater image of GoPro placement. (c) Map of sampling locations at Lake Tanganyika in Zambia, Africa: 1 – This study, MetA, and MetC; 2 – MetB (See section 2.4.3 for corresponding comparitive studies)

was chosen to ensure safe placement of two PCTs within the bottom time restrictions for a diver pair as advised by PADI. The deployment of a complete PCT was feasible within 10 to 15 min not considering the time to reach the starting point of the PCT and the return dive. The study area of the pilot was initially classified into major substrate types. Based on these classifications, the SCUBA pairs dove into a substrate type to target a certain depth and started the PCT at a random point. As depth was the main criteria for the starting point within a substrate type, distance between PCTs was directly linked to the slope of the lakebed. The cameras were placed perpendicular to the shoreline facing the open water (or facing the shoreline if depth of camera was 1 m or less; Figure 1a) and immediately turned on after setting up. The exact depth of each camera was determined with a diving computer and recorded on a dive slate.

The cameras were left for roughly three hours at their observation point and images were automatically recorded every 10 s during this entire period. The image recording was set to maximum quality, that is, 4,000 × 3,000 pixels for the GoPro Hero 4+ model and 3,680 × 2,760 pixels for the GoPro Hero 3+. No flash was used and all visual and acoustic signals of the cameras were suppressed to prevent attraction or repulsion of fish. The observational area of one camera was considered a segment of a circle and therefore could be estimated using the radius r and focal angle Θ of the lens. The radius was approximated to 3.0 m (due to visibility limitations and variations among cameras), resulting into an observational area of 5.5 m^2 (based on the focal angle of GoPro cameras of 120°). The deployment of a signalling buoy 2 m from the end of the transect line ensured the secure retrieval of transects. Images were subsequently copied to two separate 1 TB hard drives for storage and backup. Within the framework of the pilot a total of 17 PCTs were conducted during July and August in two consecutive years (2014 and 2015).

2.3 | Image analysis

Prior to any analysis, an image selection based on the last appearance of SCUBA divers on the images was performed to minimize any influence on the local fish assemblage that may have been caused by human presence. Whenever feasible the first 60 min of the recordings were discarded to guarantee observation of an undisturbed community and the second 60 min (360 images) were extracted for visual inspection. Due to shorter battery runtimes or other technical issues, this criterion could not be met for all cameras. In cases where cameras recorded images for less than 120 min, we extracted a frame of 360 images maximizing time to last appearance of a SCUBA diver (Table S1). The selected set of 360 images per camera was transferred onto a server, whereby each image received a unique ID consisting of PCT-, GoPro-, and image number (e.g. 005-21-00130023). The images were processed in a custom-made web platform, linked to a SQL database to provide safe and efficient storage. All 360 images per camera were individually analysed, whereby cichlid specimens were

TABLE 1 Compilation of criteria for specimen selection and identification during image analysis

Species identification and count	
Individual is **IDENTIFIED** and **COUNTED** if the fish is: • fully visible (entire body, head to caudal fin) • facing squarely (body ~ 90°–135°) to camera • a cichlid* • neither omitted/marked as unidentifiable (see criteria below)	
OMITTED completely if: • partially on picture or partially covered by stone or other structures (e.g. vegetation) • body angles more than ~135° from camera	marked as **UNIDENTIFIABLE** if: • body angles less than 135° from camera • clearly a cichlid • passed criteria for omission but contortion or velocity impedes on identification

Note. *Non-Cichlids were selected under the same criteria, no identification was done however.

identified to species level and counted according to a set of predefined criteria (Table 1). Both, adults and juveniles were included in the analysis. In cases where species identification was not reliably possible, the respective specimen was classified into the next higher taxonomic rank (genus or tribe). Our custom-made analysis tool also included a "review" button to highlight questionable specimens for later inspection by a taxonomy expert artificial intelligence.

For habitat characterization individual images from each PCT were overlaid with a 10 × 10 rectangular grid-layer implemented in the web interface. Habitat parameters were visually characterized by first categorizing each rectangle into visible structure (e.g. lakebed, rock formations) or open water. The visible structure was then examined for rock, sand, and vegetation coverage. Every rectangle was assigned a single category corresponding to the most dominant feature within. Topological features such as rock size and frequency were also quantified (Table S2).

2.4 | Data analysis

2.4.1 | Data preparation

Following image analysis, the fish abundance was summarized for every camera. A notorious problem for point observation data is the overestimation of population sizes due to multiple counting of the same individuals (Ward-Paige, Flemming, & Lotze, 2010). To reduce the effect of multiple counting, the maximum number of individuals (MaxN; Merrett, Bagley, Smith, & Creasey, 1994; Wartenberg & Booth, 2015) per species on a single image out of the 360 images was taken as the species count for the given camera. As a comparative measure we calculated the mean per species over 360 images, using only non-zero values. We subjected data of each camera to additional scrutiny by filtering for species that occurred only on three or less images and verified these findings through a second visual inspection of the images in question.

2.4.2 | Method evaluation

To evaluate the robustness of the PCT method, we first computed a species accumulation curve (SAC) in R (R Development Core Team, 2016) using the *specaccum* function from the VEGAN package version 2.4-5 (Oksanen et al., 2018) (10,000 permutations) for each camera. The resulting curves were fitted to a quadratic response plateau model using *nlsfit* implemented in the EASYNLS package version 5.0 (Arnhold, 2017) to evaluate if and after which number of images species richness R reaches a plateau for each of the SACs. The computed SAC data were additionally used to predict species richness for an increased sampling effort of 720 images (two hours of analysis) and to illustrate the theoretical gain in species. The same procedure was applied to the number of cameras within a PCT, for up to 20 cameras. The issue of a possible observer bias was also investigated: First, a comparison of observed species was performed to detect discrepancies in identified species between two observers (LW, EH). Second, an ANOVA was performed to test the difference between the two observers in the raw fish count and species richness data. Finally, we examined possible differences in fish count and species richness data between the first and second hour of recording by comparing 1,000 random sets of 12 images from the first and second hour of recordings, using ANOVAs.

2.4.3 | Comparison to previous studies

In order to assess the power of PCT, we compared the results of our pilot experiment to three traditionally performed transect studies conducted in the close vicinity to our study site (Janzen et al., 2017; Sturmbauer et al., 2008; Takeuchi, Ochi, Kohda, Sinyinza, & Hori, 2010). Hereafter, we will refer to these studies as follows; MetA – Sturmbauer et al. (2008), MetB – Takeuchi et al. (2010), MetC – Janzen et al. (2017). MetA and MetC were completed within a 500 m distance from our study site, whereas MetB monitored an area of 400 m^2 for over 20 years at Kasenga Point (8°43′ S, 31°08′ E), which is located roughly 15 km from our location (see Figure 1c). Due to their close proximity and general setup, these studies seem well suited to evaluate the efficiency of our PCT methodology. All three studies used conventional UVC SCUBA diver line transects as a means to observe and quantify the fish population and species diversity at their respective location. To maximize comparability among the studies, we only considered data from a depth level between 1 to 5 m and rocky habitat (rock coverage >75%) (Table S2). Species richness and the Shannon diversity index were calculated for all studies using the *diversity* function in VEGAN. Variances in observed

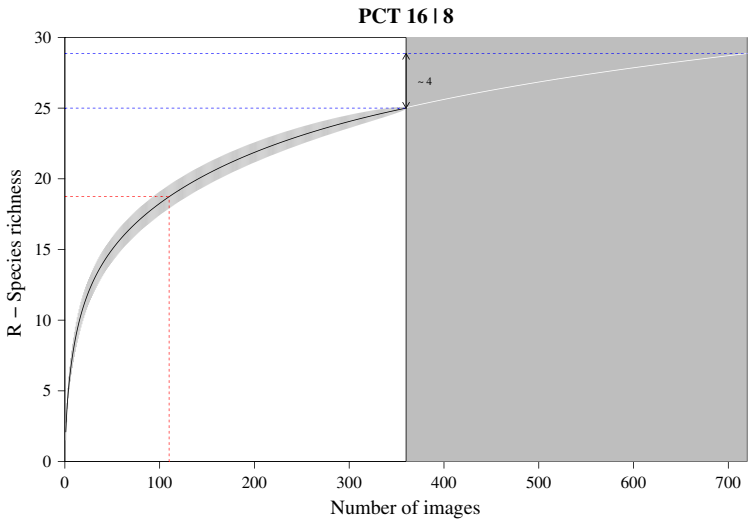

FIGURE 2 Exemplary SAC plot of PCT No 16 and camera No 8. On white background the computed SAC, with indication of reaching 75% of the total species number observed (red dashed line). On grey background the predicted gain in species number, calculated using the Weibull growth model. The theoretical gain in species richness is indicated between the two blue lines (blue dashed line)

fish density among the three studies were compared using a Mann–Whitney *U* test on the count data per species. MetA provided no actual counts for species observed three times or fewer, hence we assumed a value of three for these species in the above-mentioned analyses. As an additional evaluation of the appropriateness of the PCT approach, we tested for a size-dependent observation bias. To this end, we categorized the observed species into two size classes based on their standard length (SL). The mean SL of at least 10 specimens per species, extracted from the Tanganyika cichlid collection at the Zoological Institute of the University of Basel, was used for this comparison.

3 | RESULT

3.1 | Pilot study

The 17 PCTs of this study yielded data from 78 cameras, that is, 28,080 images for the subsequent analysis of the cichlid community at the study site (Exemplary images: Figure S3). The PCTs encompass depths from 1 m to 21 m and three major habitat types: sandy, rocky and intermediate. 17,322 individual fish were identified to species level, 1,566 to genus level and 5,269 fish could not be identified on the images. The MaxN statistics of the raw count data resulted in 3,030 specimens at the species level (2,761 specimens if using the mean), 124 at the genus level and 324 at the tribe level. In total 61 cichlid species were recorded in the 2 years of this pilot on three different habitat types.

3.2 | Method evaluation

The species accumulation curves (SACs) were calculated for 64 cameras (14 cameras were excluded from the analysis due to the small number of species recorded) (Table S4). The SACs of 53 cameras reached the plateau of species richness saturation before 360 images. The resulting image number for saturation was between 107 and 360 with an average of 262 ± 75 images. The remaining 11 SACs would reach the plateau between 362 and 409 images, with an average of 380 ± 16 images. A threshold of 75% of species observation was achieved after 128 ± 50 images for all 64 cameras (Figure 2). The theoretical gain of increased sampling effort in species richness could be computed for 50 cameras and ranged from 0.00 to 4.64 (± 1.19). For the SACs of the PCTs, none displayed a plateau, but on average 75% of species were observed after half of the cameras were analysed (Table S4). Boosting the camera number to 20 per PCT predicted a gain in species richness between 2.04 and 10.03 (± 2.62).

The comparison of 1,000 subsets of 12 images each from the first and second hour of recordings provided no evidence for any significant effect of elevated disturbance in the first hour after installation (Table S5).

The difference in the number of observed species between the two independent observers was non-significant (ANOVA, $F = 0.18$, $p = 0.68$), as was the difference in actual fish counts (ANOVA, $F = 0.13$, $p = 0.72$) (Figure 3). Among the 61 taxonomically assigned species only two differences were registered between the two observers.

3.3 | Comparison to previous studies

Of the 17 PCTs used in this study, five PCTs (8,280 images) were considered for the comparison to previous studies due to the similar depth range (up to 5 m) and habitat structure (rock coverage higher than 75%) (Table S2). Although the five PCTs analysed here covered a much smaller area, we detected more species than MetA or MetC; only in the 20-years census of MetB more species were found (Table 2). The observed density for cichlids was significantly higher

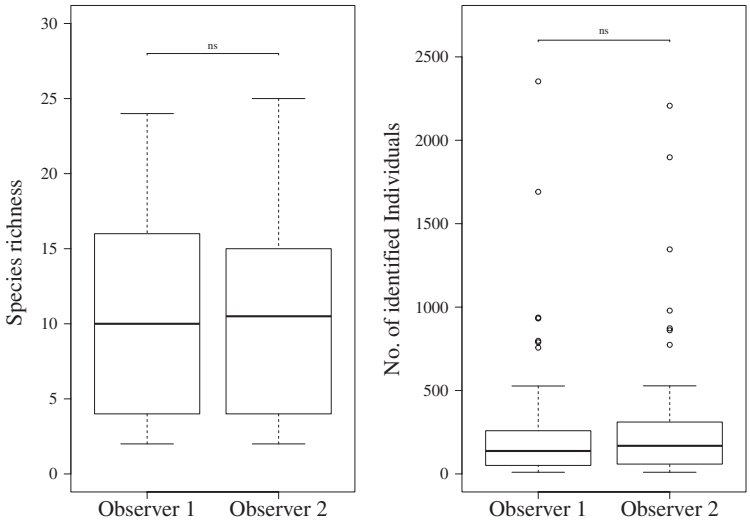

FIGURE 3 Boxplots of the comparison between two independent observers (Observer 1: L.W., Observer 2: E.H.) of 17 PCTs (78 cameras). Comparison of species richness R: ANOVA $p = 0.68$. Total of identified cichlid fish: ANOVA $p = 0.72$

in the present study compared to the three studies based on conventional UVC methods (MetA, Mann–Whitney *U* test, $W = 1{,}347$, $p = 0.00$; MetB, Mann–Whitney *U* test, $W = 1{,}483$, $p = 0.02$; MetC, Mann–Whitney *U* test, $W = 994$, $p = 0.03$) (Figure 4). If considering only species for which four or more individuals were observed, as executed in MetA, species richness is highest with PCT (Table 3). The observed cichlid densities, however, were then only significantly higher compared to MetA (Figure S6). Finally, no significant size bias through more frequent observation of smaller species was observed for PCT (Mann–Whitney *U* test, $W = 186$, $p = 0.44$) (Figure S7).

4 | DISCUSSION

In this study, we present a novel method – PCT – specifically tailored towards the examination of underwater communities, particularly fish. Interest in the community structures of aquatic species assemblages is increasing and is no longer restricted to ecology but gains importance in other fields such as evolutionary and conservation biology (Pillar & Duarte, 2010; Schmidt, White, & Denef, 2016; Yang, Powell, Zhang, & Du, 2012; Yunoki & Velasco, 2016). This increased interest calls for appropriate, standardized, and replicable methodologies to acquire such data.

Our new method involves small, easily available digital cameras (GoPro) that are set in the benthic environment of a water body and record images in a set time-interval to capture the local fish community. Two SCUBA divers set out five cameras along a line of 40 m, record the depth of each camera, and then leave the water to ensure minimal disturbance during observation time. We verified our new method PCT in a pilot study, covering two consecutive field seasons (2014 and 2015), in which we aimed to quantify the cichlid fish community of Lake Tanganyika at Kalambo Falls Lodge. Furthermore we compared the results to studies using conventional UVC line transect approaches, which were conducted in close proximity to our own study site.

In the 17 PCTs performed, a total of 22,867 cichlid fish were identified, of which 17,322 (75.8%) could be assigned to species level (6.8% to genus and 17.4% to the next higher taxonomic rank). In our pilot, we analysed 360 images per camera, a number that appears to be sufficient to capture most of the species present, considering the results from our SAC analysis. For the majority of the cameras we found that reducing the number of analysed images by a 100 would not have impacted the species composition compared with the total of 360 images (Table S4). However, the sampling effort of 360 images seems a good compromise between establishing a robust dataset and the time-consuming image analysis. As a measure to reduce the effect of multiple counting of individuals we used MaxN for each species. This approach is arguably prudent, however, we aimed to illustrate that even conservatively analysed, PCTs are able to outperform conventional methods. MaxN is favoured, as a comparison with the species mean per camera suggests an underestimation of the specimen count by the mean metric (Figure S8). Regarding the number of cameras used within a PCT, an increase would most certainly lead to an increase in observed species richness R as suggested by the SACs of the PCTs. However, extending a PCT in such a manner would not be feasible for all depth levels due to bottom time restrictions and diver safety.

A main advantage of our PCT methodology is the exclusion of different observer-based biases. Our method allows the omission of the first hour of recordings, or rather the maximization of time between beginning of analysis and "last seen diver" (an element added to our approach purposefully to reduce bias introduced by human presence). As we did not find any differences in the species composition for the omitted images and the data used for the analysis, however, it appears to be an excessive restraint. Observer expertise has been discussed in various studies and shown to directly influence

TABLE 2 List of species observed in different studies as count and density data. Density calculations were based on 126.5 m^2 for this study, 400 m^2 for MetA, 180 m^2 for MetB, and 1,200 m^2 for MetC (*: species not occurring at the study location, +: for MetA a count of 3 or less individuals from a particular species)

	This study		MetA		MetB		MetC	
	Count	Density	Count	Density	Count	Density	Count	Density
Altolamprologus compressiceps	9	0.071	5	0.013	2.0	0.005	22	0.018
Aulonocranus dewindti	4	0.032	166	0.415	53.2	0.133	4	0.003
Boulengerochromis microlepis			+					
Callochromis macrops	6	0.047	+				3	0.003
Chalinochromis brichardi	17	0.134	19.5	0.049			86	0.072
Ctenochromis horei	6	0.047	+		1.5	0.004	15	0.013
Cunningtonia longiventralis	2	0.016			0.6	0.002		
Cyathopharyxn foae	2	0.016						
Cyathopharyxn furcifer	3	0.024	75.3	0.188				
Cyprichromis zonatus								
Cyprichromis coloratus								
Cyprichromis leptosoma	14	0.111			5.1	0.013	1	0.001
Eretmodus cyanostictus	18	0.142	50.1	0.125	122.7	0.307	443	0.369
Gnathochromis pfefferi	12	0.095	+		12.2	0.031		
Haplotaxodon microlepis	3	0.024	+		4.6	0.012	2	0.002
Interchromis loocki	5	0.040			14.1	0.035		
Julidochromis marlieri			+					
Julidochromis ornatus	4	0.032	10	0.025	11.7	0.029	97	0.081
Lamprologus callipterus	3	0.024	+		8.1	0.020	22	0.018
Lamprologus lemairii	2	0.016	+		4.4	0.011		
Lepidiolamprologus attenuatus			+		5.0	0.013	4	0.003
Lepidiolamprologus cunningtoni					0.2	0.001		
Lepidiolamprologus elongatus	14	0.111	8	0.020	14.1	0.035	6	0.005
Lepidiolamprologus kendalli								
Lepidiolamprologus mimicus								
Lepidiolamprologus profunidcula					0.7	0.002		
Limnotilapia dardennii	10	0.079	+		12.8	0.032		
Lobochilotes labiatus	20	0.158	22	0.055	18.5	0.046	50	0.042
Neolamprologus fasciatus	29	0.229	+		75.7	0.189	131	0.109
Neolamprologus furcifer			+		1.0	0.003		
*Neolamprologus buescheri**								
Neolamprologus caudopunctatus			+		10.8	0.027	33	0.028

(continued)

TABLE 2 (Continued)

	This study		MetA		MetB		MetC	
	Count	Density	Count	Density	Count	Density	Count	Density
Neolamprologus cylindricus			+		1.9	0.005	4	0.003
Neolamprologus modestus	3	0.024	3.6	0.009			47	0.039
*Neolamprologus mustax**					1.3	0.003		
Neolamprologus obscurus					0.2	0.000		
*Neolamprologus petricola**					1.4	0.004		
Neolamprologus prochilus					0.6	0.001	2	0.002
Neolamprologus pulcher	6	0.047			4.3	0.011	123	0.103
Neolamprologus savoryi	8	0.063			1.1	0.003	34	0.028
Neolamprologus sexfasciatus					4.5	0.011		
Neolamprologus tetracanthus	5	0.040	16.5	0.041	0.2	0.001	122	0.102
Opthalmotilapia nasuta	4	0.032	+					
Opthalmotilapia ventralis	8	0.063	87	0.218	196.8	0.492		
Oreochromis tanganicae			+					
Paracyprichromis brieni					3.4	0.008		
Perissodus microlepis	21	0.166	+		31.4	0.079		
Petrochromis ephippium	7	0.055					41	0.034
Petrochromis famula	4	0.032			4.1	0.010	19	0.016
Petrochromis fasciolatus	8	0.063			12.9	0.032	45	0.038
Petrochromis polyodon	10	0.079			23.3	0.058	19	0.016
*Petrochromis trewavasae**					34.1	0.085		
Plecodus straeleni			+		2.7	0.007		
Pseudosimochromis curvifrons	16	0.126	+		4.6	0.012		
Simochromis diagramma	28	0.221			44.6	0.112	54	0.045
Telmatochromis temporalis	15	0.119	+		12.1	0.030	846	0.705
Telmatochromis vittatus	15	0.119	+		139.7	0.349	160	0.133
Tropheus moorii	56	0.443	108	0.270	151.4	0.379	437	0.364
Tylochromis polylepis			+					
Variabilichromis moorii	42	0.332	255	0.638	367.7	0.919	687	0.573
Xenotilapia boulengeri	5	0.040	+				107	0.089
*Xenotilapia papilio**					3.1	0.008		
Xenotilapia spilopterus	7	0.055	+		37.0	0.093	213	0.178
Total	451		826		1,463.4		3,879	

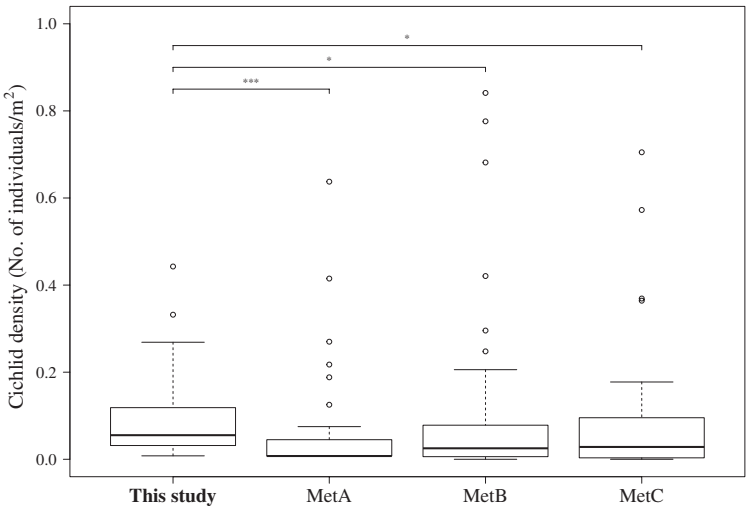

FIGURE 4 Boxplot of comparison among cichlid density for the pilot and the three comparative studies. Densities calculated for each species based on count data and area of observation: This study (125 m^2), MetA (400 m^2), MetB (180 m^2), MetC (1,200 m^2) (***p = 0.00, *p < 0.05)

TABLE 3 Summary table of this study and three studies used for comparison. Area of observation (AoO), species richness (R), species richness for species with 4 or more individuals sighted (R^4) and Shannon-Diversity Index (SI) are shown. For MetB species richness (R) except species that do not occur at location of this study is shown in brackets

Study	AoO	R	R^4	SI
This study	125 m^2	39	32	3.30
Sturmbauer et al. (2008)—MetA	400 m^2	37	12	2.37
Takeuchi et al. (2010)—MetB	180 m^2	46 (41)	30 (29)	2.65
Janzen et al. (2017)—MetC	1,200 m^2	32	28	2.56

count data and identification efforts (Thompson & Mapstone, 1997; Williams et al., 2006). In the case of PCT, the difference between two independent observers proved to be insignificant (Figure 3). In 28,080 images and 61 cichlid species only two individuals were assigned to different species by the two observers. Even count data were the same between the two observers, likely as a result of the highly standardized approach to identify and count the cichlid fishes on the images.

To compare directly with studies done in a similar location we stripped down our data to only five PCTs, which reduced the number of species observed in the full pilot (61 to 39 species, see Section 3.1). In terms of species richness, PCT outperformed the conventional UVC line-transect for both studies done in very close proximity to our study location and is virtually tantamount to the 20-year census done by MetB. This result clearly indicates the power of the PCT in comparison with the conventional UVC line-transect methodology. Taking into account the difference in the area covered with UVC line-transect and PCT this impression is further strengthened: Even though our PCTs covered only a fraction of the area of observation compared to the three comparative studies, they captured as many species as the average of the 20 year-census of MetB and more than double the species of MetA, suggesting that traditional UVC line transect approaches fail to record all species present at study site. The lack of specifications in the comparative studies and the different nature of observations – continuous observation in traditional transects of approximately 12 min (Samoilys & Carlos, 1992) vs. 360 snapshots taken during 60 min (PCT) – made it unreliable to directly compare sampling effort as a function of time of observation. Although time surely must have an effect, we believe that the distinct feature of PCT, the absence of divers during recording, surpasses that effect in regard to the observed species richness. Regarding count data, all comparative studies reported markedly greater numbers. While count data were higher, we would like to stress that they were mainly driven by a few species, such as the shoaling females of ectodini genera *Cyathopharynx* and *Ophthalmotilpia* or densely occurring *Variabilichromis moorii*; it has previously been shown by Pais and Cabral (2017) that abundance of schooling or in this case shoaling fish is usually overestimated in traditional census methods. After taking into account the area covered in the studies, we compared fish densities and again found that PCT outperformed the conventional methods by a fair margin. Furthermore, we believe that even though a GoPro camera only covers a fraction of the area usually covered by conventional UVC dives, we are able to capture the fish community structure in gross detail and in a mostly undisturbed state. As mentioned above, PCT delivers accurate local abundance data of the species community. Using

abundance and standard length (SL), biomass may be approximated, although prior information on SL is necessary as no length measurements can be taken from non-stereo images (as performed on stereo images by Wilson, Graham, Holmes, MacNeil, & Ryan, 2018). An alternative approach could be the measuring of landmarks while setting up PCT to allow researchers to measure individuals *a posteriori*. As this was not the aim of this study, we are unable to provide more detailed information here.

Looking in depth at the species that were observed, we investigated if camera position biased our data to small and benthic species. We did, however, not find any evidence that would support this. When comparing this aspect directly with the other studies and the UVC strip transect, there was no evidence for a significant shift towards small species. The general set up of the PCT does suggest a focus on benthic communities; however, our method is able to capture mobile and pelagic species as well (Figure S9). We thus see the advantage of the observational success not depending on the size or position in the water column of the fish, as illustrated within this study. However, it is advisable to select target species with a certain degree of dependence on the substrate.

To date, several approaches exist to incorporate the use of electronic equipment and therefore reduce a number of biases associated with conventional UVC used for ecological observation of underwater communities. For example TOWed Video (TOWV) is used to monitor communities by recording footage as the cameras are pulled through the habitat (Mallet & Pelletier, 2014). However, regarding observer presence, the use of cameras would not have markedly benefited the quality of the collected data in this instance, as firstly, depending on the depth, heavy surface disturbance has to be considered, and more importantly the moving, baited object pulled through the fish community might selectively attract some fish species over others (Pais & Cabral, 2017; Pereira et al., 2016). Therefore, abundance and species richness data of the habitat in question might not reflect reality. A different approach was introduced in 2012 (STAVIRO; Pelletier et al., 2012) using stationary cameras that rotate to simulate a point transect, presumably eliminating the bias of observer presence. This approach marginally failed to show its superiority to general UVC techniques and might still contain bias through its moving apparatus (Mallet et al., 2014). In contrast, an indication for the inconspicuousness of our outlined methodology (PCT) is that a number of species difficult to monitor could be captured on camera, for example pelagic predators such as *Bathybates fasciatus* and the African tigerfish *Hydrocynus vittatus*, the latter of which was never directly observed in this area (personal observation) in 10 years diving at this location, or the shy cichlid species *Neolamprologus prochilus* that usually remains under rocks and is therefore rarely seen (Konings, 1998).

Considering all approaches using cameras, including PCT, it is important to note that the recording of the underwater image material is the smaller part of data collection, followed by a time intensive period of images analysis. The main advantages of PCT compared to other camera-based approaches are its compact design, its cost effectiveness, its standardized setup and handling, as well as its ability to deliver robust digital data, making PCT well suited for the observation of underwater communities even under difficult field conditions.

ACKNOWLEGEMENTS

We thank Daniel Lüscher and the crew of Kalambo Falls Lodge for the support in logistics, the Lake Tanganyika Research Unit, Department of Fisheries, Republic of Zambia, for research permits, and two anonymous reviewers and the associate editor for valuable suggestions. This study was supported by the European Research Council (ERC, CoG 'CICHLID~X' to W.S.).

AUTHORS' CONTRIBUTIONS

L.W., E.H., M.C. and W.S. conceived and supervised the study, all co-authors conducted the fieldwork, L.W. constructed the image analysis tool and SQL database, L.W. and E.H. processed the images, with A.I. reviewing difficult cases. F.R. provided data on standard length, L.W. analysed the data, and wrote the manuscript with feedback from all co-authors.

DATA ACCCESSIBILTY

All raw count data used in this study including a separate species list are available from the Dryad Digital Repository https://doi.org/10.5061/dryad.1kr7759 (Widmer et al., 2019).

ORCID

Lukas Widmer http://orcid.org/0000-0003-2642-8163

REFERENCES

Arnhold, E. (2017). EASYNLS: Easy nonlinear model. R Package Version 5.0, 1–9. Retrieved from https://cran.r-project.org/package=easynls

Brock, V. E. (1954). A preliminary report on a method of estimating reef fish populations. *The Journal of Wildlife Management*, *18*(3), 297. https://doi.org/10.2307/3797016

Colvocoresses, J., & Acosta, A. (2007). A large-scale field comparison of strip transect and stationary point count methods for conducting length-based underwater visual surveys of reef fish populations. *Fisheries Research*, *85*(1–2), 130–141. https://doi.org/10.1016/j.fishres.2007.01.012

Dickens, L. C., Goatley, C. H. R., Tanner, J. K., & Bellwood, D. R. (2011). Quantifying relative diver effects in underwater visual censuses. *PLoS ONE*, *6*(4), 6–8. https://doi.org/10.1371/journal.pone.0018965

Edgar, G. J., Barrett, N. S., & Morton, A. J. (2004). Biases associated with the use of underwater visual census techniques to quantify the density and size-structure of fish populations. *Journal of Experimental Marine Biology and Ecology*, *308*(2), 269–290. https://doi.org/10.1016/j.jembe.2004.03.004

Janzen, T., Alzate, A., Muschick, M., Maan, M. E., van der Plas, F., & Etienne, R. S. (2017). Community assembly in Lake Tanganyika cichlid fish: Quantifying the contributions of both niche-based and neutral processes. *Ecology and Evolution*, *7*(4), 1057–1067. https://doi.org/10.1002/ece3.2689

Konings, A. (1998). *Tanganyika cichlids in their natural habitat* (3rd ed.). El Paso, TX: Cichlid Press.

Lowry, M., Folpp, H., Gregson, M., & Mckenzie, R. (2011). A comparison of methods for estimating fish assemblages associated with estuarine artificial reefs. *Brazilian Journal of Oceanography*, *59*(Spec. Issue 1), 119–131. https://doi.org/10.1590/S1679-87592011000500014

Mallet, D., & Pelletier, D. (2014). Underwater video techniques for observing coastal marine biodiversity: A review of sixty years of publications (1952-2012). *Fisheries Research*, *154*, 44–62. https://doi.org/10.1016/j.fishres.2014.01.019

Mallet, D., Wantiez, L., Lemouellic, S., Vigliola, L., & Pelletier, D. (2014). Complementarity of rotating video and underwater visual census for assessing species richness, frequency and density of reef fish on coral reef slopes. *PLoS ONE*, *9*(1), e84344. https://doi.org/10.1371/journal.pone.0084344

Merrett, N. R., Bagley, P. M., Smith, A., & Creasey, S. (1994). Scavenging deep demersal fishes of the Porcupine Seabight, north-east Atlantic: Observations by baited camera, trap and trawl. *Journal of the Marine Biological Association of the United Kingdom*, *74*(3), 481–498. https://doi.org/10.1017/S0025315400047615

Oksanen, J., Blanchet, F. G., Kindt, R., Legendre, P., Minchin, P. R., O'hara, R. B., … Oksanen, M. J. (2018). VEGAN: Community ecology package. R Package Version 2. 4-6. https://doi.org/10.1093/molbev/msv334

Pais, M. P., & Cabral, H. N. (2017). Fish behaviour effects on the accuracy and precision of underwater visual census surveys. A virtual ecologist approach using an individual-based model. *Ecological Modelling*, *346*, 58–69. https://doi.org/10.1016/j.ecolmodel.2016.12.011

Pelletier, D., Leleu, K., Mallet, D., Mou-Tham, G., Hervé, G., Boureau, M., & Guilpart, N. (2012). Remote high-definition rotating video enables fast spatial survey of marine underwater macrofauna and habitats. *PLoS ONE*, *7*(2), e30536. https://doi.org/10.1371/journal.pone.0030536

Pereira, P. H. C., Leal, I. C. S., & de Araújo, M. E. (2016). Observer presence may alter the behaviour of reef fishes associated with coral colonies. *Marine Ecology*, *37*(4), 760–769. https://doi.org/10.1111/maec.12345

Pillar, V. D., & Duarte, L. d. S. (2010). A framework for metacommunity analysis of phylogenetic structure. *Ecology Letters*, *13*(5), 587–596. https://doi.org/10.1111/j.1461-0248.2010.01456.x

R Development Core Team. (2016). *R: A language and environment for statistical computing*. Vienna, Austria: R Foundation for Statistical Computing. https://doi.org/10.1038/sj.hdy.6800737

Samoilys, M., & Carlos, G. (1992). *Development of an underwater visual census method for assessing shallow water reef fish stocks in the south west Pacific: Final report*. Queensland: Queensland Dept. of Primary Industries. Retrieved from http://www.worldcat.org/title/development-of-an-underwater-visual-census-method-for-assessing-shallow-water-reef-fish-stocks-in-the-south-west-pacific-final-report/oclc/32021136?referer=di&ht=edition

Samoilys, M. A., & Carlos, G. (2000). Determining methods of underwater visual census for estimating the abundance of coral reef fishes. *Environmental Biology of Fishes*, *57*(3), 289–304. https://doi.org/10.1023/A:1007679109359

Schmidt, M. L., White, J. D., & Denef, V. J. (2016). Phylogenetic conservation of freshwater lake habitat preference varies between abundant bacterioplankton phyla. *Environmental Microbiology*, *18*(4), 1212–1226. https://doi.org/10.1111/1462-2920.13143

Sturmbauer, C., Fuchs, C., Harb, G., Damm, E., Duftner, N., Maderbacher, M., & Koblmüller, S. (2008). Abundance, distribution, and territory areas of rock-dwelling Lake Tanganyika cichlid fish species. *Hydrobiologia*, *615*(1), 57–68. https://doi.org/10.1007/s10750-008-9557-z

Takeuchi, Y., Ochi, H., Kohda, M., Sinyinza, D., & Hori, M. (2010). A 20-year census of a rocky littoral fish community in Lake Tanganyika. *Ecology of Freshwater Fish*, *19*(2), 239–248. https://doi.org/10.1111/j.1600-0633.2010.00408.x

Thompson, A. A., & Mapstone, B. D. (1997). Observer effects and training in underwater visual surveys of reef fishes. *Marine Ecology Progress Series*, *154*, 53–63. https://doi.org/10.3354/meps154053

Unsworth, R. K. F., Peters, J. R., McCloskey, R. M., & Hinder, S. L. (2014). Optimising stereo baited underwater video for sampling fish and invertebrates in temperate coastal habitats. *Estuarine, Coastal and Shelf Science*, *150*(PB), 281–287. https://doi.org/10.1016/j.ecss.2014.03.020

Ward-Paige, C., Flemming, J. M., & Lotze, H. K. (2010). Overestimating fish counts by non-instantaneous visual censuses: Consequences for population and community descriptions. *PLoS ONE*, *5*(7), 1–9. https://doi.org/10.1371/journal.pone.0011722

Wartenberg, R., & Booth, A. J. J. (2015). Video transects are the most appropriate underwater visual census method for surveying high-latitude coral reef fishes in the southwestern Indian Ocean. *Marine Biodiversity*, *45*(4), 633–646. https://doi.org/10.1007/s12526-014-0262-z

Whitfield, P. E., Muñoz, R. C., Buckel, C. A., Degan, B. P., Freshwater, D. W., & Hare, J. A. (2014). Native fish community structure and Indo-Pacific lionfish Pterois volitans densities along a depth-temperature gradient in Onslow Bay, North Carolina, USA. *Marine Ecology Progress Series*, *509*, 241–254. https://doi.org/10.3354/meps10882

Widmer, L., Heule, E., Colombo, M., Rueegg, A., Indermaur, A., Ronco, F., & Salzburger, W. (2019). Data from: Point-Combination Transect (PCT): Incorporation of small underwater cameras to study fish communities. *Dryad Digital Repository*, https://doi.org/10.5061/dryad.1kr7759

Williams, I. D., Walsh, W. J., Tissot, B. N., & Hallacher, L. E. (2006). Impact of observers' experience level on counts of fishes in underwater visual surveys. *Marine Ecology Progress Series*, *310*, 185–191. https://doi.org/10.3354/meps310185

Wilson, S. K., Graham, N. A. J., Holmes, T. H., MacNeil, M. A., & Ryan, N. M. (2018). Visual versus video methods for estimating reef fish biomass. *Ecological Indicators*, *85*(October 2017), 146–152. https://doi.org/10.1016/j.ecolind.2017.10.038

Wraith, J., Lynch, T., Minchinton, T. E., Broad, A., & Davis, A. R. (2013). Bait type affects fish assemblages and feeding guilds observed at baited remote underwater video stations. *Marine Ecology Progress Series*, *477*, 189–199. https://doi.org/10.3354/meps10137

Yang, Z., Powell, J. R., Zhang, C., & Du, G. (2012). The effect of environmental and phylogenetic drivers on community assembly in an alpine meadow community. *Ecology*, *93*(11), 2321–2328. https://doi.org/10.1890/11-2212.1

Yunoki, T., & Velasco, L. T. (2016). Fish metacommunity dynamics in the patchy heterogeneous habitats of varzea lakes, turbid river channels and transparent clear and black water bodies in the Amazonian Lowlands of Bolivia. *Environmental Biology of Fishes*, *99*, 391–408. https://doi.org/10.1007/s10641-016-0481-1

SUPPORTING INFORMATION

Additional supporting information may be found online in the Supporting Information section at the end of the article.

How to cite this article: Widmer L, Heule E, Colombo M, et al. Point-Combination Transect (PCT): Incorporation of small underwater cameras to study fish communities. *Methods Ecol Evol*. 2019;10:891–901. https://doi.org/10.1111/2041-210X.13163

Chapter 6 | Supplementary Material

Table S1: List of placed cameras for each PCT, including start, end, runtime, start of analysis (S_A) and end of analysis (E_A). maxTime indicates where the time to last seen diver was maximised.

PCT	GoPro No	Start (hh:mm)	End (hh:mm)	Runtime (hh:mm)	S_A (hh:mm)	E_A (hh:mm)	maxTime
6	1	10:32	14:39	04:07	11:33	12:32	
6	2	10:40	14:49	04:09	11:42	12:41	
6	3	10:44	14:53	04:09	11:46	12:45	
6	4	10:46	14:52	04:06	11:48	12:47	
7	1	08:07	10:57	02:50	09:09	10:08	
7	2	08:10	10:56	02:46	09:12	10:11	
7	3	08:11	12:04	03:53	09:13	10:12	
7	4	08:16	09:49	01:33	08:28	09:27	✔
7	5	08:18	11:23	03:05	09:20	10:19	
8	1	10:14	12:23	02:09	10:42	11:41	✔
8	2	10:18	12:24	02:06	10:40	11:39	✔
8	3	10:20	12:24	02:04	10:39	11:38	✔
8	4	10:27	12:26	01:59	10:48	11:47	✔
10	6	16:15	17:43	01:28	16:43	17:42	✔
10	7	16:22	17:44	01:22	16:44	17:43	✔
10	8	16:25	17:45	01:20	16:45	17:44	✔
10	9	16:27	17:46	01:19	16:46	17:45	✔
10	10	16:28	17:46	01:18	16:47	17:46	✔
11	11	11:10	12:53	01:43	11:52	12:51	✔
11	12	11:13	15:41	04:28	12:13	13:12	
11	13	11:18	15:58	04:40	12:19	13:18	
11	15	11:24	16:12	04:48	12:25	13:24	
12	6	11:30	14:37	03:07	12:31	13:30	
12	7	11:38	16:22	04:44	12:40	13:39	
12	8	11:42	14:47	03:05	12:43	13:42	
12	9	11:45	15:02	03:17	12:45	13:44	
12	10	11:49	15:15	03:26	12:50	13:49	
13	16	15:43	17:05	01:22	16:05	17:04	✔
13	17	15:50	17:06	01:16	16:07	17:06	✔
13	19	15:53	17:06	01:13	16:06	17:05	✔
13	20	15:54	17:05	01:11	16:05	17:04	✔
14	11	10:11	14:55	04:44	11:13	12:12	
14	13	10:20	15:10	04:50	11:22	12:21	
14	14	10:21	15:12	04:51	11:23	12:22	
14	15	10:23	11:57	01:34	10:57	11:56	✔
15	6	10:31	13:08	02:37	11:32	12:31	
15	7	10:35	12:17	01:42	11:17	12:16	✔
15	8	10:38	14:51	04:13	11:39	12:38	
15	9	10:40	12:31	01:51	11:31	12:30	✔
15	10	10:42	14:48	04:06	11:43	12:42	
16	6	10:25	12:26	02:01	10:35	11:34	✔
16	7	10:29	12:25	01:56	10:39	11:38	✔
16	8	10:32	12:24	01:52	10:42	11:41	✔
16	9	10:35	12:22	01:47	10:45	11:44	✔
16	10	10:38	12:17	01:39	10:48	11:47	✔
17	11	15:51	17:31	01:40	16:30	17:29	✔
17	12	15:50	17:30	01:40	16:29	17:28	✔
17	13	15:53	17:30	01:37	16:28	17:27	✔
17	14	15:53	17:28	01:35	16:26	17:25	✔
17	15	15:55	17:27	01:32	16:26	17:25	✔
18	11	10:48	12:31	01:43	10:58	11:57	✔
18	12	10:50	12:32	01:42	11:00	11:59	✔
18	13	10:54	12:35	01:41	11:04	12:03	✔
18	14	10:54	12:31	01:37	11:04	12:03	✔
18	15	10:55	12:32	01:37	11:04	12:03	✔
19	6	10:32	15:20	04:48	11:33	12:32	
19	7	10:38	15:24	04:46	11:39	12:38	
19	8	10:41	15:21	04:40	11:42	12:41	
19	9	10:42	15:25	04:43	11:43	12:42	
19	10	10:44	15:25	04:41	11:45	12:44	
20	12	12:05	15:13	03:08	13:06	14:05	
20	13	12:09	15:19	03:10	13:10	14:09	
20	14	12:12	15:15	03:03	13:13	14:12	
20	15	12:15	15:15	03:00	13:16	14:15	
21	6	11:55	16:04	04:09	12:56	13:55	
21	7	11:58	16:19	04:21	12:59	13:58	
21	8	12:02	15:48	03:46	13:03	14:02	
21	9	12:04	15:46	03:42	13:05	14:04	
21	10	12:06	15:44	03:38	13:07	14:06	
22	16	10:54	15:26	04:32	11:04	12:03	
22	17	10:58	15:26	04:28	11:08	12:07	
22	18	11:00	15:25	04:25	11:10	12:09	
22	19	11:02	15:23	04:21	11:12	12:11	
22	20	11:05	15:20	04:15	11:15	12:14	
23	12	11:23	16:02	04:39	12:24	13:23	
23	13	11:28	16:14	04:46	12:29	13:28	
23	14	11:29	16:12	04:43	12:30	13:29	
23	15	11:29	16:09	04:40	12:30	13:29	

Table S2: The environmental parameters recorded for cameras of pilot study at Lake Tanganyika, Zambia. Cameras used for comparison between studies are in red font. Rock frequency: the actual count of individual rocks on the examined image. Rock size: Average of estimated rock size according to following categories: 1 = rock size < 1% of image; 2 = rock size < 5% of image; 3 = rock size < 10% of image; 4 = rock size < 25% of image; 5 = rock size > 25% of image.

PCT	GoPro No	Depth (m)	Date	Visible habitat (%)	Sand	Vegetation	Rock	Rock frequenc	Rock size	Habitat type
6	1	17.9	27.07.14	57	0.07	0.00	0.93	5	4	rock
6	2	18.4	27.07.14	38	0.00	0.00	1.00	2	5	rock
6	3	19.7	27.07.14	40	1.00	0.00	0.00	0	0	sand
6	4	20	27.07.14	40	0.98	0.00	0.03	1	1	sand
7	1	11.2	28.07.14	75	0.00	0.00	1.00	5	5	rock
7	2	9.8	28.07.14	42	0.00	0.00	1.00	2	4	rock
7	3	9	28.07.14	34	0.00	0.00	1.00	4	3	rock
7	4	10.5	28.07.14	65	0.02	0.00	0.98	8	4	rock
7	5	12.3	28.07.14	29	0.00	0.00	1.00	2	4	rock
8	1	13.4	29.07.14	9	0.00	0.00	1.00	3	1	rock
8	2	14.7	29.07.14	18	0.00	0.00	1.00	7	2	rock
8	3	14.1	29.07.14	31	0.58	0.00	0.42	3	2	inter
8	4	13.1	29.07.14	15	0.00	0.00	1.00	4	2	rock
10	6	5	30.07.15	50	1.00	0.00	0.00	0	0	sand
10	7	5	30.07.15	47	1.00	0.00	0.00	0	0	sand
10	8	4.9	30.07.15	45	1.00	0.00	0.00	0	0	sand
10	9	5.3	30.07.15	56	1.00	0.00	0.00	0	0	sand
10	10	5.8	30.07.15	60	1.00	0.00	0.00	0	0	sand
11	11	5.2	31.07.15	48	0.25	0.00	0.75	18	1	rock
11	12	5.6	31.07.15	52	0.04	0.00	0.96	50	1	rock
11	13	5.9	31.07.15	44	0.00	0.00	1.00	40	1	rock
11	15	6.2	31.07.15	57	0.16	0.00	0.84	20	2	rock
12	6	9.6	31.07.15	51	0.00	0.00	1.00	45	1	rock
12	7	10.2	31.07.15	54	0.09	0.00	0.91	45	2	rock
12	8	11.4	31.07.15	62	0.00	0.00	1.00	30	3	rock
12	9	11.4	31.07.15	57	0.00	0.00	1.00	16	3	rock
12	10	10.2	31.07.15	53	0.00	0.00	1.00	12	3	rock
13	16	0.5	31.07.15	47	0.00	0.00	1.00	25	2	rock
13	17	0.5	31.07.15	44	0.00	0.00	1.00	20	2	rock
13	19	0.5	31.07.15	34	0.00	0.00	1.00	20	2	rock
13	20	0.5	31.07.15	51	0.00	0.04	0.96	12	3	rock
14	11	5.5	01.08.15	45	1.00	0.00	0.00	0	0	sand
14	13	6.6	01.08.15	50	0.82	0.00	0.18	1	3	sand
14	14	6.5	01.08.15	51	1.00	0.00	0.00	0	0	sand
14	15	6	01.08.15	60	1.00	0.00	0.00	0	0	sand
15	6	10	01.08.15	40	1.00	0.00	0.00	0	0	sand
15	7	10.4	01.08.15	46	1.00	0.00	0.00	0	0	sand
15	8	10.6	01.08.15	40	1.00	0.00	0.00	0	0	sand
15	9	10.4	01.08.15	30	1.00	0.00	0.00	0	0	sand
15	10	10	01.08.15	50	1.00	0.00	0.00	0	0	sand
16	6	5	02.08.15	44	0.00	0.00	1.00	26	3	rock
16	7	5	02.08.15	42	0.00	0.00	1.00	30	2	rock
16	8	5.2	02.08.15	66	0.00	0.00	1.00	40	3	rock
16	9	6	02.08.15	74	0.00	0.00	1.00	30	2	rock
16	10	6.3	02.08.15	40	0.00	0.00	1.00	13	2	rock
17	11	0.5	02.08.15	36	0.00	0.00	1.00	10	3	rock
17	12	0.5	02.08.15	47	0.00	0.00	1.00	35	2	rock
17	13	0.5	02.08.15	50	0.00	0.00	1.00	100	1	rock
17	14	0.5	02.08.15	50	0.00	0.00	1.00	38	2	rock
17	15	0.5	02.08.15	47	0.00	0.00	1.00	9	3	rock
18	11	0.5	02.08.15	57	0.00	0.00	1.00	10	4	rock
18	12	0.5	02.08.15	69	0.00	0.03	0.97	19	3	rock
18	13	0.5	02.08.15	52	0.00	0.06	0.94	17	2	rock
18	14	0.5	02.08.15	62	0.00	0.00	1.00	12	4	rock
18	15	0.5	02.08.15	61	0.00	0.02	0.98	21	3	rock
19	6	15	03.08.15	40	1.00	0.00	0.00	0	0	sand
19	7	15.1	03.08.15	50	1.00	0.00	0.00	0	0	sand
19	8	15.4	03.08.15	57	1.00	0.00	0.00	0	0	sand
19	9	15.8	03.08.15	58	1.00	0.00	0.00	0	0	sand
19	10	16.4	03.08.15	49	1.00	0.00	0.00	0	0	sand
20	12	4.9	03.08.15	50	1.00	0.00	0.00	0	0	sand
20	13	5.3	03.08.15	53	1.00	0.00	0.00	0	0	sand
20	14	5.4	03.08.15	53	1.00	0.00	0.00	0	0	sand
20	15	5.4	03.08.15	50	1.00	0.00	0.00	0	0	sand
21	6	20	05.08.15	46	1.00	0.00	0.00	0	0	sand
21	7	19.9	05.08.15	50	1.00	0.00	0.00	0	0	sand
21	8	19.6	05.08.15	47	1.00	0.00	0.00	0	0	sand
21	9	19.6	05.08.15	40	1.00	0.00	0.00	0	0	sand
21	10	19.8	05.08.15	40	1.00	0.00	0.00	0	0	sand
22	16	10.2	06.08.15	31	0.00	0.00	1.00	3	4	rock
22	17	9.9	06.08.15	42	0.29	0.00	0.71	4	3	inter
22	18	9.7	06.08.15	50	0.00	0.00	1.00	6	3	rock
22	19	10.1	06.08.15	44	0.00	0.00	1.00	2	4	rock
22	20	10.5	06.08.15	41	0.00	0.00	1.00	4	4	rock
23	12	20.9	07.08.15	47	0.00	0.00	1.00	14	3	rock
23	13	20.7	07.08.15	50	0.52	0.00	0.48	15	2	inter
23	14	20	07.08.15	30	0.47	0.00	0.53	4	2	inter
23	15	20	07.08.15	35	0.00	0.00	1.00	9	3	rock

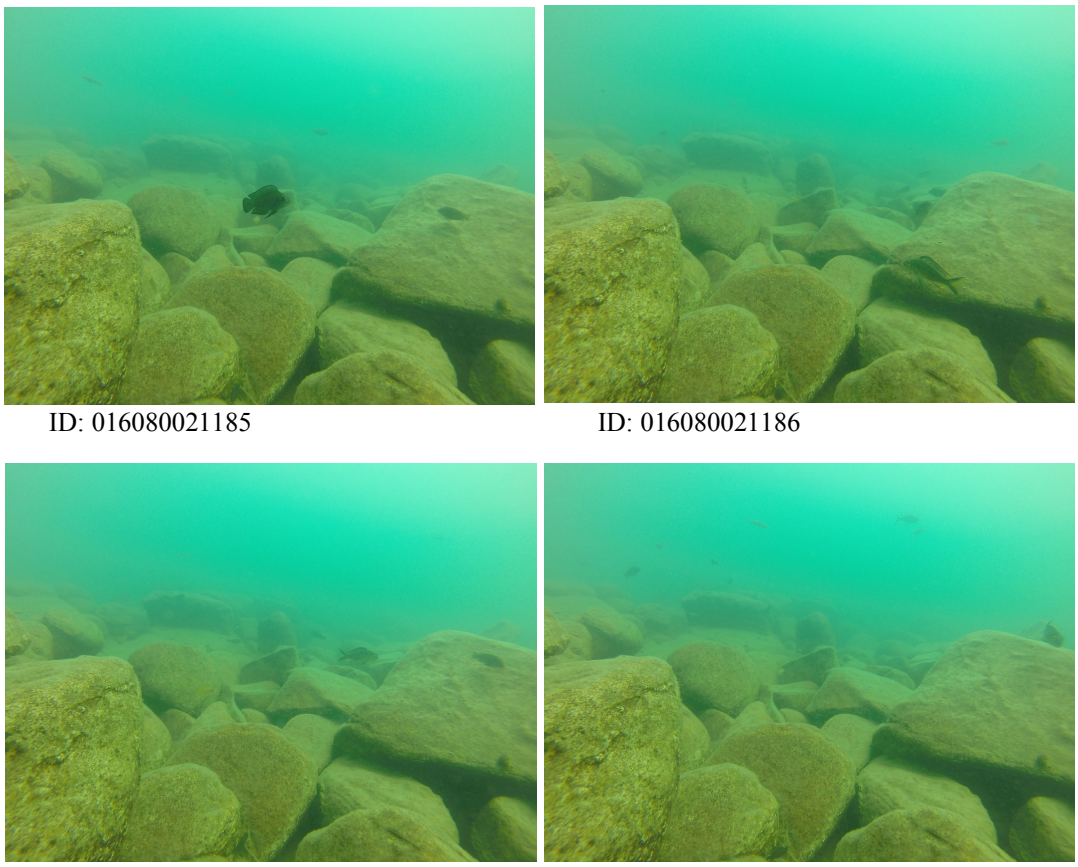

Fig S3: 4 Exemplary images from the collection of 28'080 images used in the pilot. Underneath each image the unique ID consisting of PCT, camera and image number (e.g. 016 - 08 - 0021185)

PCT	Camera No	Observed R	R75	Saturation
6	1	9	102	211.23
6	2	6	194	409.44
6	3	4	83	175.16
6	4	7	144	295.92
7	1	3	244	NA
7	2	12	154	350.31
7	3	8	176	354.60
7	4	10	193	398.58
7	5	2	185	344.74
8	1	10	180	372.35
8	2	13	88	198.13
8	3	17	176	361.86
8	4	13	169	350.42
10	6	NA	NA	NA
10	7	2	270	NA
10	8	NA	NA	NA
10	9	NA	NA	NA
10	10	NA	NA	NA
11	11	19	115	287.78
11	12	20	60	166.78
11	13	21	58	161.80
11	15	14	76	223.44
12	6	21	144	329.97
12	7	22	122	290.60
12	8	28	159	359.19
12	9	22	165	359.89
12	10	19	87	223.28
13	16	19	147	339.92
13	17	17	128	316.52
13	19	18	78	217.63
13	20	16	90	250.83
14	11	NA	NA	NA
14	13	2	182	341.36
14	14	NA	NA	NA
14	15	NA	NA	NA
15	6	NA	NA	NA
15	7	NA	NA	NA
15	8	2	133	267.24
15	9	8	157	312.16
15	10	7	91	199.23
16	6	22	143	320.47
16	7	19	100	249.88
16	8	25	110	284.60
16	9	22	126	382.15
16	10	17	133	278.96
17	11	7	66	180.92
17	12	15	144	324.89
17	13	9	32	119.95
17	14	11	68	171.25
17	15	9	143	321.82
18	11	11	157	378.25
18	12	16	100	263.54
18	13	15	57	147.59
18	14	10	42	115.88
18	15	17	74	244.58
19	6	2	47	106.59
19	7	3	103	216.97
19	8	5	184	350.65
19	9	8	157	314.42
19	10	12	195	388.85
20	12	NA	NA	NA
20	13	NA	NA	NA
20	14	NA	NA	NA
20	15	NA	NA	NA
21	6	NA	NA	NA
21	7	7	54	127.11
21	8	10	87	204.78
21	9	8	144	308.79
21	10	7	103	229.57
22	16	20	133	282.44
22	17	11	164	343.06
22	18	16	113	275.18
22	19	12	73	166.61
22	20	23	156	366.91
23	12	14	172	363.47
23	13	18	128	270.87
23	14	9	175	357.83
23	15	15	173	353.13
6	all	14	3	NA
7	all	18	3	9.83
8	all	22	2	6.12
12	all	33	2	5.04
15	all	9	3	7.17
16	all	34	2	5.79
19	all	15	3	7.29
21	all	13	3	5.77
10	all	1	1	NA
11	all	25	2	4.14
14	all	3	2	NA
17	all	13	2	5.88
18	all	19	2	5.37
20	all	1	1	NA
23	all	23	2	4.03
13	all	20	1	4.21
22	all	28	2	5.36

Table S4: List of species accumulation curves (SAC) for cameras and PCT including observed species richness R. R75 = Number of images/PCT to reach 75% of observed R. Saturation = Number of images/PCT to reach plateau of SAC.

Table S5: 1'000 random subsamples of 12 images, comparing analysed hour (group 2) and images from starting point until selection (group 1). ns = non-significant; s = significant, p-value = p-value at 95% confidence. Tests were performed on raw count data and number of species for subsamples between first and second part and within second part.

	COUNT DATA						SPECIES DATA					
	between group 1 & 2			within group 2			between group 1 & 2			within group 2		
PCT	ns	s	p-value	ns	s	p-value	ns	s	p-value	ns	s	p-value
40 | 28	975	25	0.08	999	1	0.27	989	11	0.13	999	1	0.38
35 | 07	937	63	0.04	800	200	0	990	10	0.14	998	2	0.18

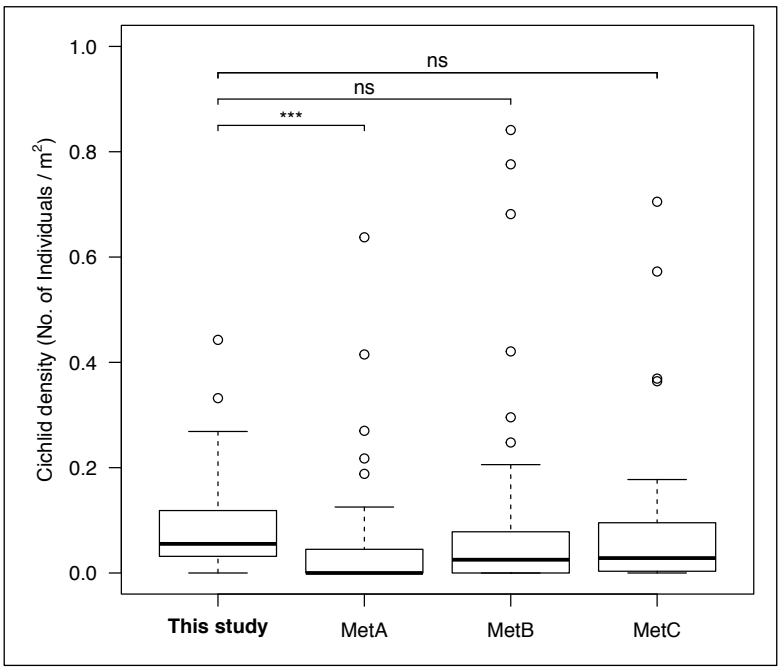

Fig S6: Boxplot of comparison among cichlid density for the pilot and the three comparative studies. Densities calculated for species with 4 or more counts for the area of observation: This study (125 m^2), MetA (400 m^2), MetB (180 m^2), MetC (1'200 m^2) (***: $P < 0.001$, ns: not significant).

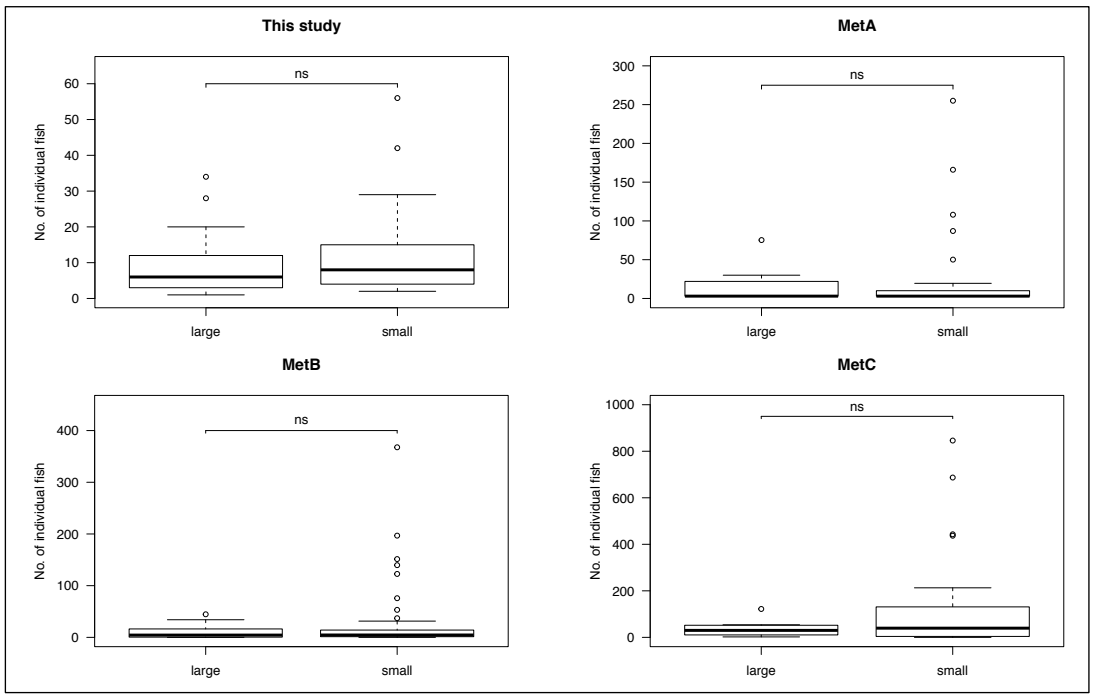

Fig S7: Comparison between the observed number of individuals of large and small cichlid species, presented in separate boxplots for each study. All pairs were tested using Mann-Whitney U test and proved not significant: This study, W = 186, P = 0.44; MetA, W = 182, P = 0.83; MetB, W = 255, P = 0.56; MetC, W = 89, P = 0.56.

A)

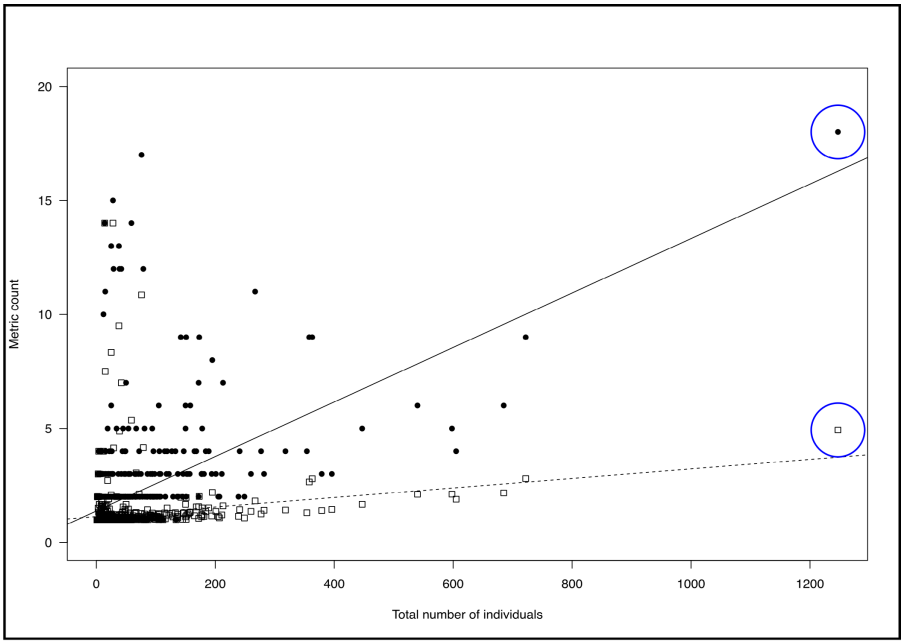

B)

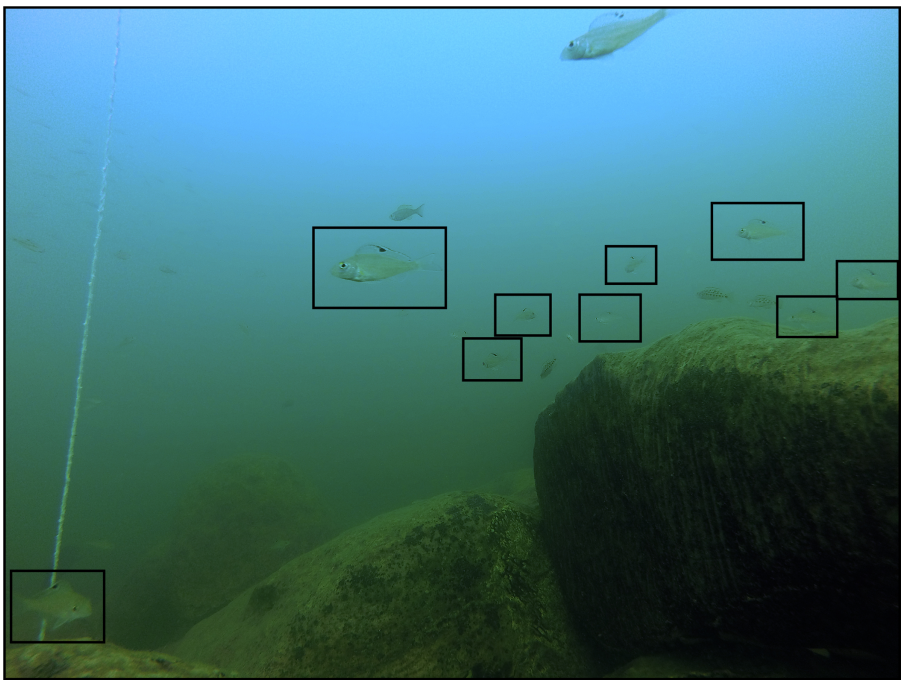

Fig S8: A) The two metrics, MaxN (circles) and mean (squares) against the total number of individuals per species per camera. The mean underestimates more "densely" occurring species at a site, e.g. *Xenotilpia spiloptera* (blue circle), as well as species with only few occurrences (in which the mean value is almost always close to 1). B) Example of an image showing 9 recorded specimens of *X. spiloptera* (squares on the image). The other individuals were discarded on the basis of our "Identification and count protocol" (Table 1). For this species, the mean for the respective camera was calculated at 4.4 specimens (due to fewer sightings on other images). However, a maximum of 18 specimens was observed on one image, suggesting that MaxN more accurately represents the number of individuals present at any given location.

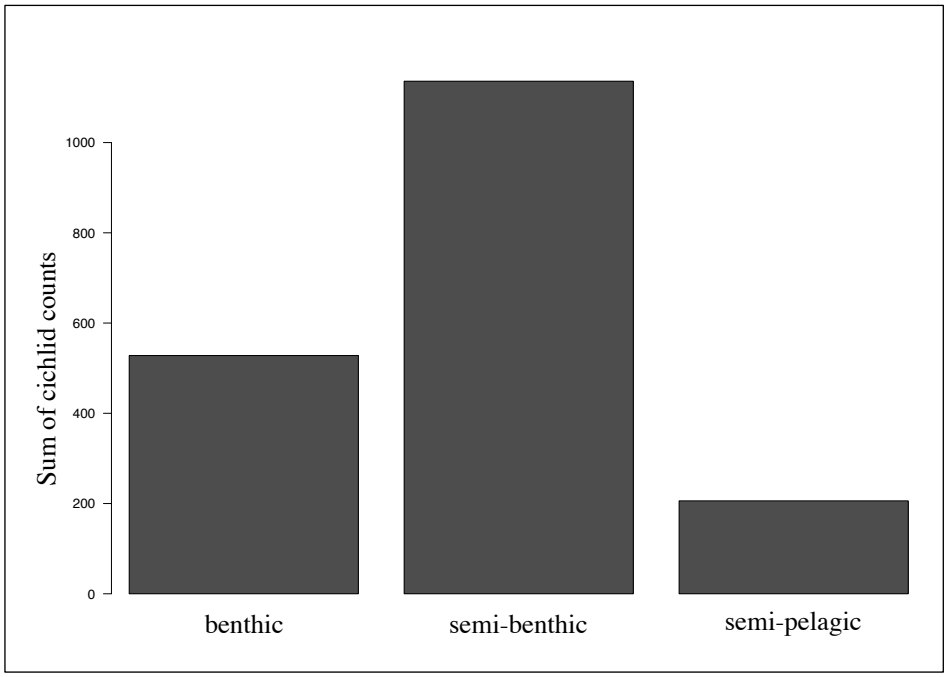

Fig S9: Total sum of 17 PCT fish counts at pilot location. Cichlids divided into three benthic-pelagic categories as defined by Colombo, Indermauer, Meyer & Salzburger (2016).

Chapter 7

Community assembly patterns and niche evolution in the species-flock of cichlid fishes from the East African Lake Tanganyika

Lukas Widmer, Adrian Indermaur, **Fabrizia Ronco,**
Athimed El Taher & Walter Salzburger

Manuscript in preparation

I contributed to the extensive field work to collect the raw data for this study and provided the taxon list for species assignment.

Community assembly patterns and niche evolution in the species-flock of cichlid fishes from the East African Lake Tanganyika

Lukas Widmer[1], Adrian Indermaur[1], Fabrizia Ronco[1], Athimed El Taher[1] & Walter Salzburger[1]

[1] University of Basel, Zoological Institute, Vesalgasse 1, CH-4051 Basel

Abstract

The study of community assemblies is no longer restricted to the field of ecology. In evolutionary biology, for example, the understanding of the factors promoting the co-existence of closely related species might contribute to uncover the processes involved in speciation. In this context, ecological niche modelling is a powerful tool to characterize the ecological niche differences among closely related species and to determine the environmental factors that shape animal communities. Here, we apply a newly developed method, Points-Combination-Transects (PCT), to the cichlid species-flock of Lake Tanganyika, a highly diverse adaptive radiation that formed within an island-like environment within the last ~9-12 million years. On the basis of 314'280 underwater images taken with GoPro cameras along the eastern shore of Lake Tanganyika, we obtained occurrence data and environmental parameters for 141 species of cichlid fishes. Ecological niche modelling revealed substantial differences in niche occupation between some species, but also strong overlap between others. Additional ancestral niche reconstructions and age-range-correlations indicate patterns of niche conservatism not found in other older adaptive radiation, such as the Caribbean Anolis Lizards.

Introduction

Adaptive radiation

Adaptive radiation is the rapid evolution of ecological diversity from a single ancestor into an array of ecologically and morphologically diverse descendants exploiting a variety of environments (Schluter, 2000). Instances of adaptive radiations are well-suited to study niche evolution, as the initial presence of a novel environment (ecological opportunity), among other factors (key innovation, bio-geographical influences, and divergence – convergence patterns), is thought to drive the species diversification of such adaptive radiations (Sturmbauer, 1998; Schluter, 2000; Gavrilets & Losos, 2009; Sturmbauer, Husemann, & Danley, 2011; Salzburger, Bocxlaer, & Cohen, 2014; Salzburger, 2018). Various patterns, such as an increased level of specialisation are associated with adaptive radiations (Schluter, 2000). In respect to the ecological opportunity we

will focus on a few of these patterns, which we might expect to observe based on ecological data (Gavrilets & Losos, 2009): (1) Early burst: A considerable diversification into different habitats is assumed to have taken place at the root of the radiation followed by less niche divergence within the separate lineages, therefore we would observe conserved niches within lineages. (2) Stages in radiation: Here we expect to observe the splitting along several environmental axes at different times, first macrohabitat (e.g. rock / sand in the cichlid radiation of Lake Malawi (Danley & Kocher, 2001)), then microhabitat (e.g. depth) followed further splits less tied environmental axes (e.g. sexual selection (Deutsch, 1997)). (3) Non-allopatric speciation: In this case taxa with small genetic distances show significant niche similarity and co-occurrence that might indicate an absence of a distinctive barrier to promote allopatric speciation.

Ecological Niche and Co-Occurrence Patterns

The study of a species' niche (e.g. fundamental niche as defined by Hutchinson (1957) has received increased attention by evolutionary biologists (Ackerly, Schwilk, & Webb, 2006; Losos, 2008; Wiens et al., 2010; Münkemüller, Boucher, Thuiller, & Lavergne, 2015; Comte, Cucherousset, & Olden, 2016). As the ecological niche that is occupied by a species will have had an apparent influence on the evolution of its morphological, physiological or behaviour traits, the diversification of the niche can be studied to understand the evolution of species diversity (Knouft, Losos, Glor, & Kolbe, 2006). Patterns of niche overlap can give insight in how environmental conditions might have impacted the diversification of species. An example for this are the marsupial mice, the Sminthopsini in Australia, where niche conservatism, the pattern of species retaining ancestral niche characteristics, may have promoted speciation by contributing to the formation of allopatric lineages (García-Navas & Westerman, 2018). The issue, however, is that the ecological niche that we observe is seldom the fundamental niche, but rather the realized niche. We therefore should not solely rely on the information gained through environmental variables, but the community structure and co-occurrence patterns influencing the niche occupancy should be considered as well.

Cichlids

The cichlids fishes of the East African Great Lakes in particular the species-flock of Lake Tanganyika are a prime example of an adaptive radiation (Schluter, 2000; Sturmbauer et al., 2011; Salzburger, 2018). Thus, it is not surprising that there exists a large number of studies focusing on cichlids. However, many studies, especially such that focus on the ecology of cichlids, are based on investigations of a single species (Sturmbauer & Dallinger, 1994; Boileau et al., 2015; Indermaur, Theis, Egger, & Salzburger, 2018), a genus (Egger, Sefc, Makasa, Sturmbauer, & Salzburger, 2012), or regional species assemblies (Sturmbauer et al., 2008; Takeuchi, Ochi, Kohda, Sinyinza, & Hori, 2010; Janzen et al., 2017). In Lake Tanganyika there are approximately 240 endemic cichlid species belonging to 14 different lineages (also called tribes) (Ronco, Indermaur, Büscher, & Salzburger *in revision*), exhibiting a vast diversity in morphology, ecology and behaviour. Due to their popularity with aquarists, descriptive literature on the ecology of many species is available (Konings, 1998; Fermon, Nshombo, Muzumani, & Jonas, 2017). A broad-scale evaluation using standardised methods, however, is lacking to date. The earliest broad-scale reports of the taxonomy of Lake Tanganyika's cichlid fauna, including a discussion about the ecology and diversity of the then known species, was published over a century ago (Boulenger, 1898), the more recent one is still over 60 years old (Poll, 1956). Therefore, an extensive exploration of the cichlid community and their ecological niches seems due. To enable this primary investigation of niche evolution and community assembly patterns within a strong phylogenetic

framework, we make use of a recent and very robust phylogeny based on whole genome sequencing of all Tanganyikan cichlids species (Ronco et al. *in preparation*).

Aim

In this study we examine the extant cichlid species of Lake Tanganyika in respect to their community structure, co-occurrences patterns and ecological niche in a uniquely broad-scale and lake-wide context. We considered the entire cichlid species-flock of ~240 endemic species from the along the coast of Lake Tanganyika (Ronco et al. in revision). Through extensive fieldwork campaigns we collected a comprehensive data set of the occurrence, habitat preferences and distribution of the primarily benthic cichlid fishes in Lake Tanganyika. With the collected data we first explored the community structure and the underlying assembly processes using co-occurrence data. We then constructed ecological niche models for each species and examined, in a phylogenetic context, the patterns of niche diversification within the Lake Tanganyika cichlid assembly.

Methods and Material

Cichlid visual census survey

Census data of cichlid fishes were collected between 2014 and 2017 at 45 locations along the Zambian and Tanzanian coastline of Lake Tanganyika (Fig 1A) (total time in the field: three months); under research permits issued by the Department of Fisheries, Republic of Zambia and Tanzania Commission for Science and Technology (COSTECH). For data collection we used a method we introduced recently, Point-Combination-Transects (PCTs), following the strategy described in Widmer et al. (2019). In short, a PCT consists of five GoPro cameras (Hero 3+ Silver Edition, Hero 4+ Silver Edition, © GoPro, Inc.) in underwater housings, which are placed within the benthic environment in a standardized manner and equally spaced along a transect line of 40 m, and set to record digital images in a time interval of 10 s for a period of approximately 3 h (second hour of recordings was used for analysis, 360 images). Each camera covered an area of approximately 5.5 m^2 (Widmer et al., 2019). The sampling locations were chosen to cover the three sub-basins of Lake Tanganyika and adequately sample the different benthic habitat types in the littoral and sublittoral zone (up to a maximum depth of 40 m). At each location, the target depths for three to four PCTs were defined a priori and assigned to two SCUBA diver pairs. Each pair deployed up to two PCTs per dive; this ensured safe installation and retrieval of PCTs under PADI safety regulations.

At the University of Basel, Switzerland, the resulting images were analysed as described in Widmer et al. (2019). In brief, on each image only specimens that were fully visible and their body facing the camera squarely (~ 90° – 135°) were counted and identified. To minimise the effect of multiple counting of specimens we applied the MaxN count (maximum observed number of specimens per species in a single image of a camera) (Merrett, Bagley, Smith, & Creasey, 1994). Census data was either used in the form of each cameras' MaxN value or as the sum of MaxN values per PCT (five cameras), indicated from hereon as CAM- and PCT-data respectively. All of the following data analysis was performed in R Statistic software (R Development Core Team, 2016), unless stated otherwise.

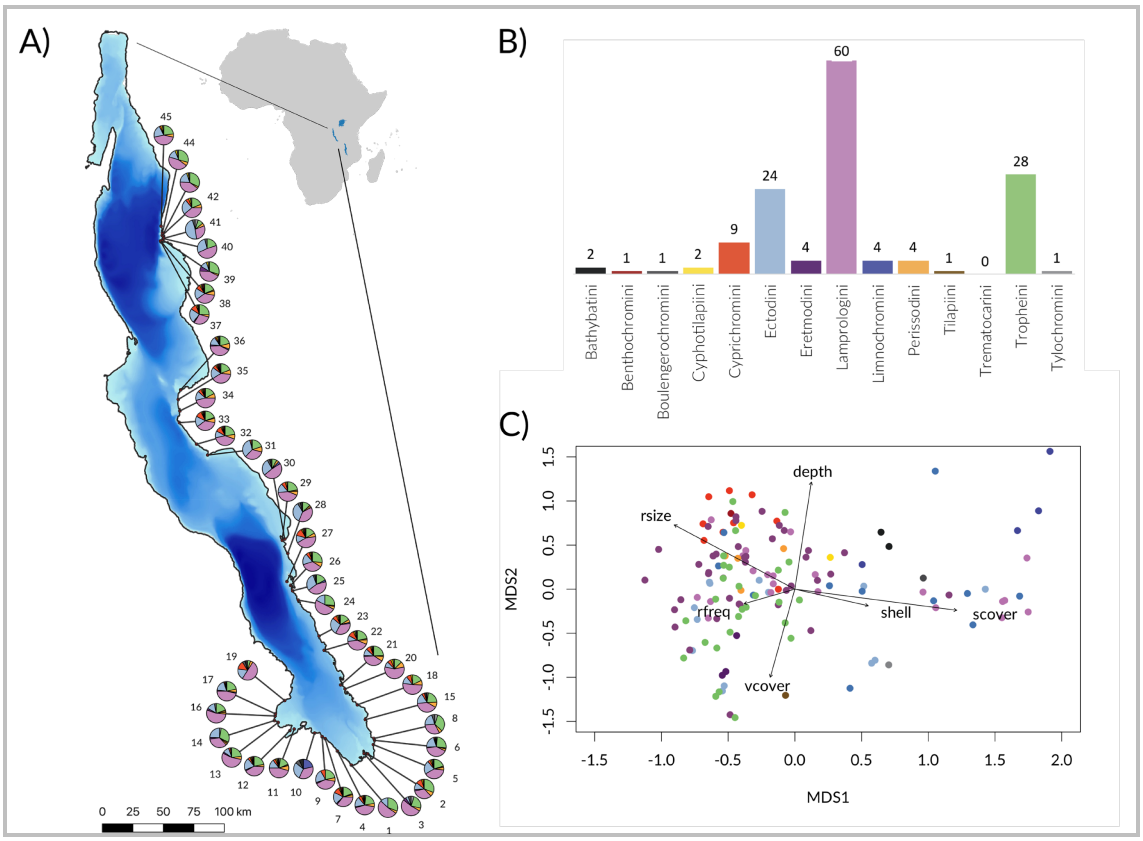

Figure 1: A) Sampling sites along the Zambian and Tanzanian coast of Lake Tanganyika (numbers correspond with list of locations on Table S1, Supplementary Information) with pie charts depicting local species richness per tribe (see color code in 1B). **B)** Bar plot showing the species recorded in this study (number of species per tribe indicated). **C)** Species distribution along environmental gradients based on Multi-Dimension-Scaling (MDS, see Fig S2, Supplementary Information).

Environmental variables

For each camera, a set of environmental parameters was extracted a posteriori from the image material (except depth, which was recorded on site); namely rock-, sand-, shell-, and vegetation cover, rock size and rock frequency (Table S3, Supplementary Information) (Widmer et al., 2019). Furthermore, we included habitat complexity (HC), which was defined as an images' mean standard deviation of its intensity values, applying an approach using images transformed to grey scale (Shumway, Hofmann, & Dobberfuhl, 2007).

Co-Occurrence

Patterns of co-occurrence were analysed using the widely applied C-score (Stone & Roberts, 1990). To enable comparison among species a standard effect size (SES) of the C-Score was calculated as implemented in package ecospat (Di Cola et al., 2017) and transformed to a scale ranging from 0 (no co-occurrence) to 1 (high co-occurrence). In order to distinguish between the different community assembly processes (stochastic 'ST', environmental filtering 'EF' and biotic interactions 'BI'), we applied a method introduced by Kohli et al. (2018). This trait-based approach considers landscape (PCT-data) and local (CAM-data aggregated by PCT and dominant substrate type) co-occurrences to evaluate species co-occurrences in a heterogenous habitat. Hypothesis testing on what process may drive aggregation or segregation of species relies on 'EF' (substrate preference, geographic affinity) and 'BI' (size class, trophic guild) traits, which were defined for each taxon (see trait definitions and species trait list in Table S4, Supplementary Information).

Environmental Niche Quantification

Prior to niche quantification, the environmental variables were screened for collinearity using the variance inflation factor (VIF, threshold of 4) (Hair, Black, Babin, & Anderson, 2014). We did not include rock coverage for niche quantifications analyses, due to high collinearity to sand cover and depth. The remaining variables retained a mean VIF of 2.00 ± 0.86. We applied ecological niche modelling (ENM) to quantify the environmental niches of the extant taxa of Lake Tanganyika's cichlid fauna. Species presence points and environmental data are required for ENM. Species presence data was extracted from our field observations (CAM Data), excluding species with less than 15 observations to ensure the construction of robust models, and environmental data was gathered as described above (see section Environmental variables). The environmental variables of the complete CAM Data set were used as environmental background for ENM calculations. For ENM we used Maxent Java-Version 3.4.0 (Phillips, Anderson, & Schapire, 2006; Phillips & Dudík, 2008), which relies only on presence data for a maximum entropy method and has been shown to perform well with only few occurrence points (Hernandez, Graham, Master, & Albert, 2006; Wisz et al., 2008). We applied the most common approach of cross-validation (k-fold), whereby the species occurrences are equally split into k subsets and the model run k times (k = 4). In the k runs each subset is once excluded during model training and used for model testing instead, thereby all points are used for model training and model testing. Each species' ENM was evaluated using area under the curve method (AUC) (Mason & Graham, 2002). AUC values range from 0.5 (presences can be predicted no better than with a random model) and 1.0 (presences can be predicted perfectly).

Niche overlap and partitioning

The underlying phylogeny was adapted from Ronco et al. (in preparation), which was constructed using whole-genome-sequencing based on 529 cichlid genomes. For all phylogenetic analysis the tree was pruned to contain only tips that corresponded to the list of species observed during this study (Table S4, Supplementary Information).

In order to gather information of niche overlap between species-pairs in respect to the combined set of environmental variables, all variables were coupled with occurrence data to estimate density grids for occupancy for each species, from which we calculated the niche overlap metric Schoener's D (ranging from 0 = no similarity and 1 = high similarity). Further we tested for niche equivalency by pooling occurrence points of a species-pair and randomly splitting this set and compare the obtain overlap D with the true value (100 replicates) (Warren, Glor, & Turelli, 2008). Niche similarity for each species-pair was tested by comparing D for a random subset of occurrences of species B against species A, and vice versa, against actual D (100 replicates) (Warren et al., 2008). Niche overlap, niche equivalency and niche similarity tests were done with functions implemented in ecospat package (Di Cola et al., 2017). To evaluate overlap in singular niche dimensions we estimated D for an environmental axis based on our MaxEnt results. We calculated D using the mean of raw suitability scores from the 4 replicates (see Niche Quantification) with the phyloclim package (Heibl & Calenge, 2018). To evaluate patterns of niche overlap within the adaptive radiation (e.g. conservatism, divergence-convergence), pairwise overlap was correlated with the pairwise genetic distance using Mantel tests. In a further step, we examined how niche overlap behaved over time by conducting an age–range correlation (ARC) test. Prevalent niche conservatism would results in high niche overlap at the tips with a tendency to decrease to time of divergence (Fitzpatrick & Turelli, 2006). The null hypothesis of niche divergence

was tested with 1'000 permutations as implemented in the R package phyloclim by randomizing the overlap matrix.

Niche evolution and disparity

Ancestral niche reconstruction was performed by first complementing our MaxEnt results with environmental data (sensu Evans, Smith, Flynn, & Donoghue, 2009) to obtain the predicted niche occupancy profiles (PNO) of each species per environmental variable. On the basis of an available whole-genome phylogeny (Ronco et al. in preparation) maximum likelihood estimates for each environmental variable at every interior node were calculated assuming Brownian motion (Schluter, Price, Mooers, & Ludwig, 1997), and by randomly resampling 1'000 times from each taxa's PNO, we reconstructed a distribution of environmental tolerance rather than a state (Evans et al., 2009). Using relative disparity through time (DTT) plots (Harmon, Schulte, Larson, & Losos, 2003), based on the mean environmental niche value (obtained through ancestral niche reconstruction), we assessed the distribution of disparity within (diverged niche) vs. among lineages (conserved niche). Niche disparity index (NDI) was computed, with negative values indicating that disparity tends to be distributed among subclades, while positive NDI values would indicate increased subclade disparity (Slater, Price, Santini, & Alfaro, 2010; Colombo, Damerau, Hanel, Salzburger, & Matschiner, 2015). As we are supplied with a robust phylogeny, we refrained from using posterior trees and simulated trait behaviour under BM (replicates 1000). All functions are implemented in phyloclim (Heibl & Calenge, 2018), APE (Paradis, Claude, & Strimmer, 2004) and GEIGER (Harmon, Weir, Brock, Glor, & Challenger, 2008).

Results

In the course of this study we conducted 182 PCTs at 45 different sites at Lake Tanganyika (Fig 1A) covering all substrate types and water depths from 1 to 36.2 m and an area of approximately 4'800 m^2 (Table S5, Supplementary Information). In total, 314'280 images were used for analyses. On these images, we assigned 635'127 cichlid specimens to species level (after applying MaxN: 19'311), 65'730 to genus level and 129'054 to tribe level. The average MaxN per camera was 22 ± 16 specimens with a maximum of 101 and the average species richness per camera was 11 ± 6 with a maximum 31. Only three cameras out of 873 yielded zero observations, one placed in sandy substrate (location 8, see Fig 1A) and the other two in dense vegetation (location 6, see Fig 1A). We captured 141 different cichlid species on camera (94; when excluding those with less than 15 occurrences), and at least one member of each of the 14 tribes (Figure 1B) (Table S4, Supplementary Information), expect Trematocarini, the members of which could only be identified to the genus level. We found that the three most species-rich tribes were also the most abundant ones (MaxN, species level): Lamprologini: 8'531 individuals (44 %), Ectodini: 3'588 individuals (18.6 %), and Tropheini: 3'180 individuals (16.5 %). The most abundant species, however, was from the tribe Cyprichromini, *Paracyprichromis brieni* with 1'667 individuals (8.6 %). When assigning each tribe a category (species-rich: Ectodini, Lamprologini, Tropheini or species-poor: Bathybatini, Benthochromini, Boulengerochromini, Cyphotilapiini, Cyprichromini, Eretmodini, Limnochromini, Perissodini, Tilapiini, Trematocarini, Tylochromini), abundance was not significantly different among the groups (ANOVA, $F = 0.001$, $p = 0.97$).

Over the varying habitats and depths, different tribes and species are dominating (Fig 1C, while the species per tribe ratio is relatively constant among sites (Fig S7, Supplementary Information). The community composition is predominantly structured along two environmental axes, a rock-

sand gradient (ANOSIM-Sand: R = 0.36, p = 0.001) and depth (ANOSIM-Depth: R = 0.48, p = 0.001), explaining 84 % of the dissimilarities in NMDS 1 - and 85 % in NMDS 2 – respectively (Fig S2, Supplementary Information). Along the sand-rock gradient there was positive correlation with species richness (F = 383.6, p < 0.001) and with abundance (F = 123.7, p < 0.001).

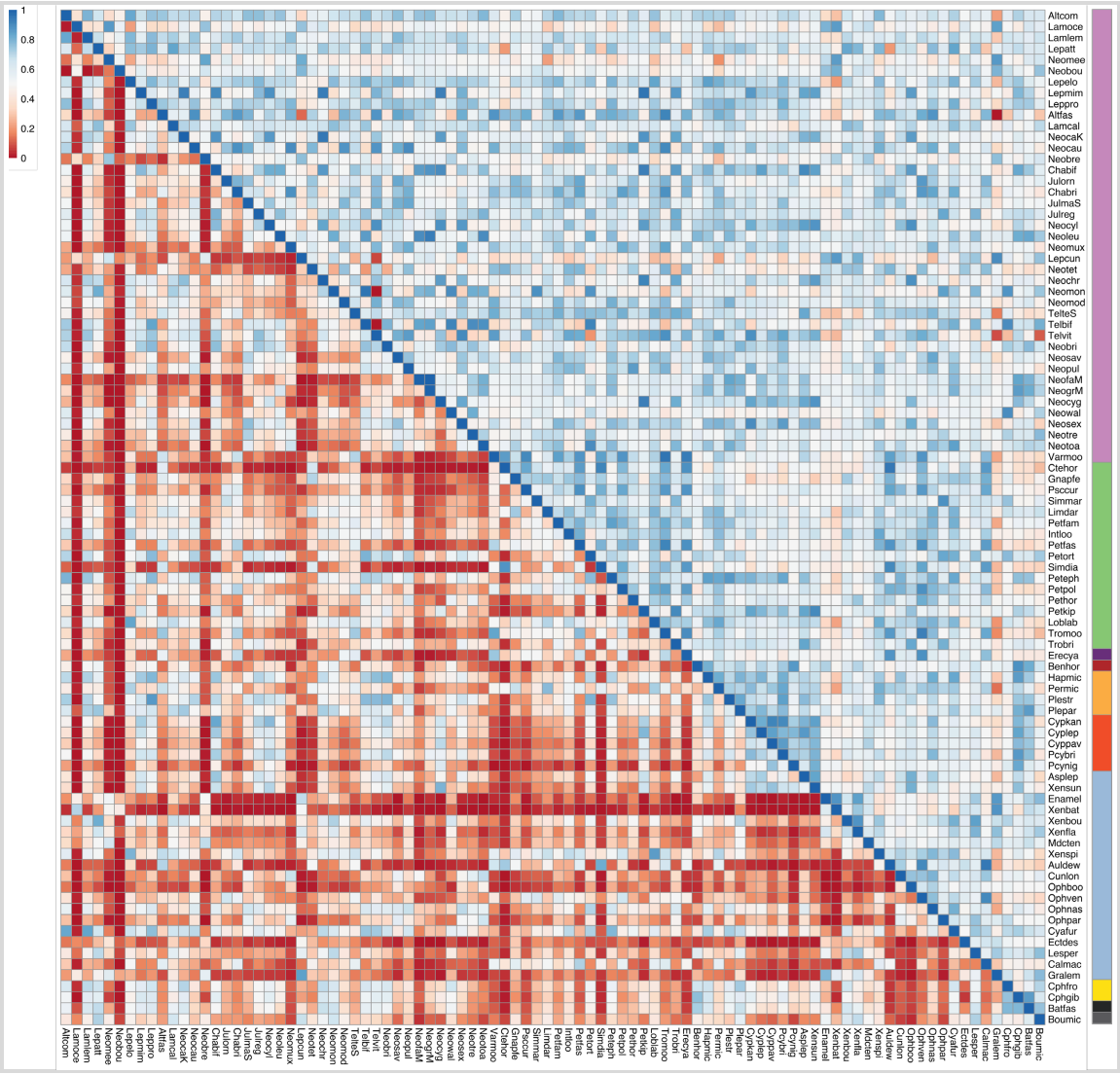

Figure 2: Heatmap of rescaled co-occurrence SES (0 = segregation, 1 = aggregation, upper triangle) and niche overlap Schoener's D (0 = no overlap, 1 = complete overlap, lower triangle). Species are clustered based on their phylogenetic distance, the coloured bar on the right indicating tribe assignment. Clustering based on niche overlap or co-occurrence available in Fig S8-S9, Supplementary Information. Full species names corresponding to 6-letter identifier can be found in Table S4, Supplementary Information.

Co-Occurrence patterns

Out of 4'731 possibly co-occurring species-pairs, 1'722 were identified as non-random, showing either significant aggregation (843 species-pairs) or segregation (879 species-pairs). The species-pair *Lepidiolamprologus elongatus* (Lamprologini) and *Limnotilapia dardennii* (Tropheini) co-occurred most often (No of co-occurrences: 281, SES = -2.38, p = 0.01). The two-stage classification of all connections show the dominant driver of community assembly is environmental filtering (83.7 % of all non-stochastic connections), with only few connections decidedly categorised as biotic interactions (10.0 % negative interactions, 0.1 % positive interactions) (Fig S10, Supplementary Information). We further found a correlation between degree of co-occurrence and genetic distance within the species-flock as a whole (z = 809.0, p < 0.001) (Fig 2), and within Ectodini when analysed tribe-wise (z = 35.12, p = 0.008).

Ecological niche of Lake Tanganyikan cichlids

Based on niche quantification considering all environmental variables, the cichlid community exhibits low (0.00) to high (0.88) niche overlap in Schoener's D (mean D = 0.28 ± 0.20), with only three species-pairs showing significant niche equivalency (mean D = 0.848 ± 0.028, p = 0.03 ± 0.015). Significant niche similarity was found for 314 species-pairs in both directions and for 301 species-pairs in one direction only. Species-pairs from within the same tribe exhibited niche similarity in 64 (both directions) and 63 (one direction) instances with species-pairs from within species-poor tribes more often displaying niche similarity than from within species-rich tribes (W = 0, p = 0.07). The amount of niche overlap between species, from within the same tribe, was significantly higher in species-poor than in species-rich tribes (F = 26.59, p < 0.001). An overall pattern between niche overlap and genetic distance was detectable for all species-pairs (Mantel test, z = 767.95, p < 0.001) (Fig 2) and for Lamprologini (Mantel test, z = 98.91, p = 0.02) (Table S11, Supplementary Information). Moreover, the age range correlation also showed a clear negative correlation for the entire species-flock (F = 0.98, p = 0.04) (Fig 3). We found evidence for a negative relationship between niche overlap and genetic distance within Lamprologini as well (F = 0.99, p = 0.04). Also, niche overlap of three tribes was significantly higher when compared to niche overlap of other species-pairs with the similar genetic distance (Ectodini, w = 59'622, p < 0.001; Cyprichromini, w = 777, p < 0.001; Perissodini, w = 189, p = 0.03).

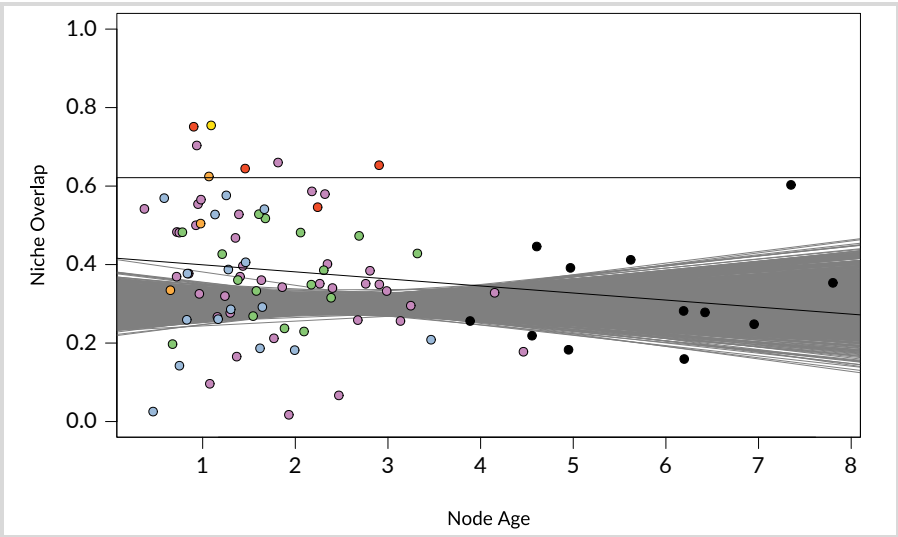

Figure 3: Age–range correlation of niche overlap (Schoener's D) in function of time (Ma). Each dot represents a node within the phylogeny, the nodes are coloured if within one of the 14 tribes.

Our, with MaxEnt computed, ENMs had an average AUC score of 0.81 (SD ± 0.07), indicating rather robust models (Table S12, Supplementary Information). Based on the calculated suitability scores from ENMs, we found a correlation with genetic distance over the entire radiation with all environmental axes, save shell cover (Table 1). Species-poor tribes exhibited no correlation, whereas species-rich tribes showed a correlation along different axes (Ectodini with depth, habitat complexity (HC) and shell cover; Lamprologini with HC, rock frequency and size, and sand and shell cover; Tropheini with sand cover) (Table 1). Age range correlations support the same trends for depth and HC for the entire radiation (Fig S13, Supplementary Information).

Finally, ancestral niche reconstruction showed niche differentiation between environmental axes for the different tribes along depth and rock-sand-gradient, for which we also detected a strong phylogenetic signal ($\lambda_{Depth} = 0.90$, $p_{Depth} < 0.001$; $\lambda_{Rock\text{-}Sand} = 0.93$, $p_{Rock\text{-}Sand} < 0.001$) (Fig 4) (Fig S14 & Table S15, Supplementary Information). Disparity through time analysis show an early increase in disparity for depth and rock-sand-gradient resulting in slightly positive NDI values 0.08 and 0.16 respectively, non of which was significantly different from BM model simulations (Fig S16, Supplementary Information).

Table 1: Results of mantel tests of the correlation between genetic distance and the niche overlap along single environmental axes. HC = habitat complexity, rFreq = rock frequency, rSize = rock size.

		Environmental variable						
		Depth	**HC**	**rFreq**	**rSize**	**Sand**	**Shell**	**Vegetation**
All species	p	*0.001*	*0.001*	*0.012*	*0.017*	*0.002*	0.109	0.051
	z	1785	1179	1815	1870	1968	2644	2589
Cyphotilapiini	p	1.000	1.000	1.000	1.000	1.000	1.000	1.000
	z	0.078	0.066	0.081	0.079	0.085	0.099	0.099
Cyprichromini	p	0.379	0.412	0.249	0.459	0.320	0.646	0.588
	z	1.885	1.756	2.266	2.358	2.506	2.676	2.684
Ectodini	p	*0.013*	*0.035*	0.078	0.128	0.103	*0.036*	0.262
	z	38.61	21.48	37.96	37.23	35.59	61.42	61.40
Lamprologini	p	0.221	*0.020*	*0.006*	*0.015*	*0.013*	*0.011*	0.278
	z	273.54	173.42	231.85	237.69	265.90	340.71	356.72
Perissodini	p	0.547	0.429	0.671	0.563	0.335	0.468	0.678
	z	0.588	0.521	0.597	0.605	0.591	0.667	0.649
Tropheini	p	0.498	0.289	0.136	0.260	*0.010*	0.278	0.130
	z	20.45	16.46	23.00	23.92	26.51	30.41	25.73

Discussion

Here we present a substantial data set based on a non-invasive cichlid visual census survey, which includes information on their environmental preferences along the Zambian and Tanzanian shores of Lake Tanganyika. Data collection was conducted in a standardised manner and provides a unique insight into the littoral and sublittoral community assembly of this most diverse cichlid radiation. The consistently high tribal diversity across the lake, and its sub basins, underlines our balanced sampling efforts (Fig 1). The predominantly endemic cichlids of Lake Tanganyika were the dominating contributor to the local fish community and are found in each of the vast number of diverse habitats within the lake (Konings, 1998; Sturmbauer et al., 2011; Salzburger, 2018). Contemporary studies of evolutionary community ecology are often limited by the fact that only closely related groups are studied, due to sampling and availablility of phylogenetic framework for small groups (Mayfield & Levine, 2010; Clarke, Thomas, & Freckleton, 2017). These factors, however, might hamper the power of studies of niche evolution, as certainly interactions are not

soley restricted to close relatives (Wilcox, Schwartz, & Lowe, 2018). Nevertheless, exclusively examinig cichlids and the structuring of their community shows that they follow general rules of fish assemblies, which are otherwise comprised of many families. Thus, we believe that the focus on the cichlid community only, does not hamper our conclusions. We explored the detailed structure and drivers of the cichlid community and co-occurrence patterns, and assessed the evolution of the ecological niche in a phylogenetic framework.

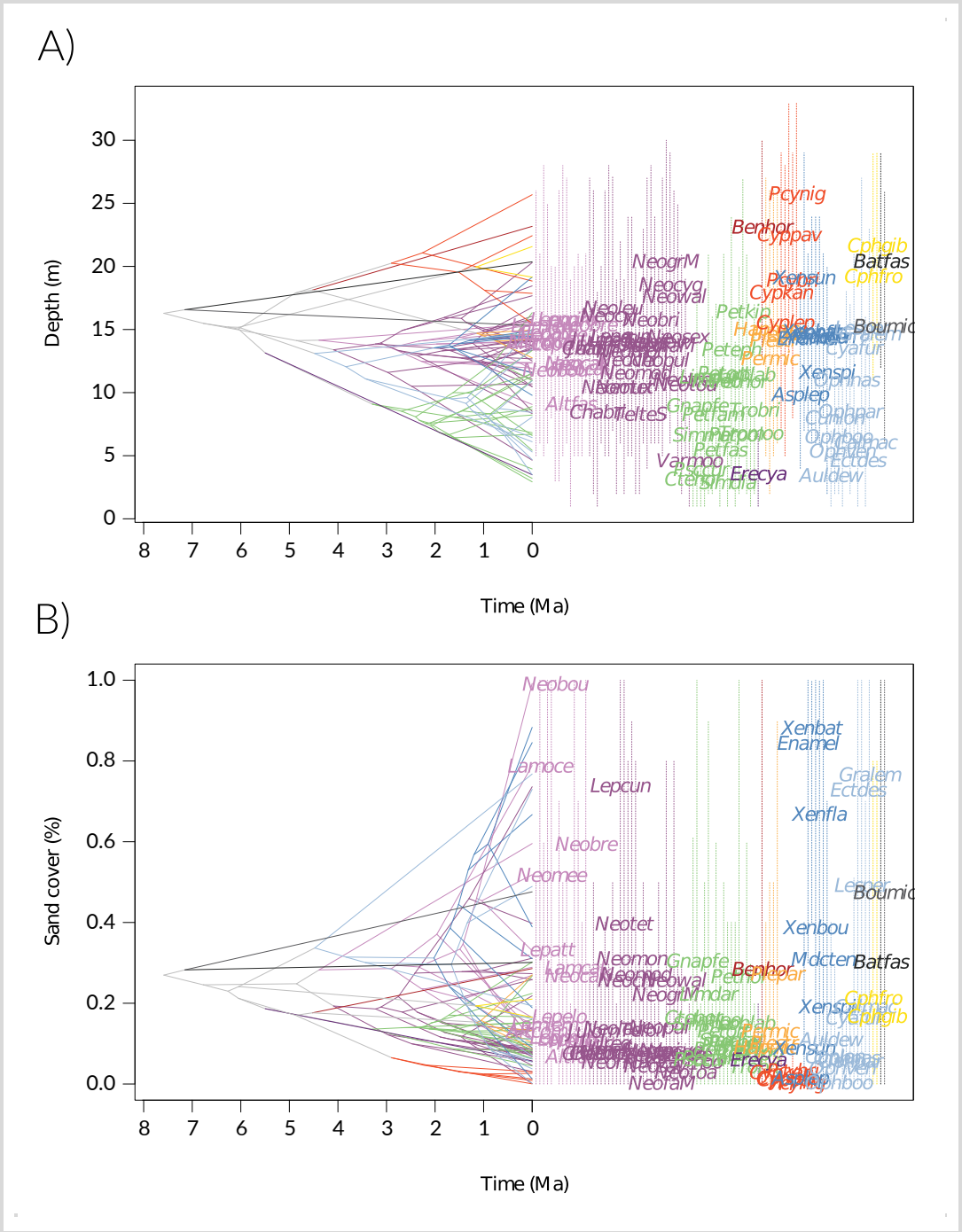

Figure 4: Ancestral niche reconstruction for depth (A) and rock-sand-gradient (B), which exhibited the strongest phylogenetic signal λ > 0.9. The remaining environmental axes showed intermediate to low phylogenetic signal (λ from 0.6 to 0) (see Table S15, Supplementary Information).

Community structure

High tribal diversity was found at all sites, nevertheless there are marked differences in the contribution of each tribe to communities on different substrates and depths. The structuring of the species assemblies along these two environmental gradients, depth and rock-sand, is well documented (Danley & Kocher, 2001). Depth has a strong impact on fish communities in the marine environment (Garrabou, Ballesteros, & Zabala, 2002; Smith & Brown, 2002) and as such it is little surprising to observe a similar effect on the cichlid assembly that inhabits Lake Tanganyika, which is the second deepest fresh water lake in the world (Salzburger et al., 2014). The importance of substrate, in particular the sand-rock gradient, is also expected and its implication on diversification has been reported for the cichlid radiation of Lake Malawi (Danley & Kocher, 2001).

The two-step approach introduced by Kohli et al. (2018) identified the main force influencing co-occurrences to be a stochastic process, with environmental filtering only being second. The importance of environmental filtering is further supported by the highly significant structuring of the community along environmental gradients (Fig S2, Supplementary Information). This is congruous with previous findings on the community assembly of Tanganyikan cichlids in localised study (Janzen et al., 2017). A prevalence of environmental filtering seems a general pattern applying to cichlids communities in Lake Tanganyika on a larger scale. However, we find little evidence for phylogenetic clustering, indicating that the different tribes converged on the habitats with competition among members of different tribes not being of sufficient strength to promote extensive phylogenetic clustering (Vamosi, Heard, Vamosi, & Webb, 2009; Gerhold, Cahill, Winter, Bartish, & Prinzing, 2015). We do, however, observe some clustering and potential niche conservatism within the tribes Tropheini and Cyprichromini (Fig 1C & 2). The negative biotic interactions that were uncovered mostly refer to geographically separated sister taxa (e.g. *Telmatochromis vittatus* and *T. bifrenatus* see Fig 2) or other geographical variants restricted to a particular location. Although the ranges of these taxa often abut, it is difficult to predict if these separations happened due to competition or a geographic barrier that is no longer present. As it was shown for the Tropheini genus Tropheus, relatively small stretches of sand can already function as effective barriers to promote reproductive isolation (Egger et al., 2012).

Ecological Niche

The overall moderate niche overlap within the entire radiation illustrates the high degree of specialisation and the vast diversity in ecological niche space occupied by the cichlids in Lake Tanganyika. This impression is further strengthened by the scarce prevalence of niche similarity among species. Considering the effect of niche-based processes (environmental filtering) in community composition, the weak correlation of relatedness and niche overlap suggests some importance of niche conservatism, supporting the niche-based process of community assembly, as it was found in other adaptive radiations (Danley & Kocher, 2001). Despite a lack of niche similarity between sister taxa, which is arguably a strong indication for niche conservatism (Knouft et al., 2006; Warren et al., 2008), the age range correlation confirmed the weak negative trend indicating a pattern of niche convservatism in the entire cichlid-species flock. The contrasting levels of niche overlap might indicate the varying relevance of niche conversatim for the different tribes. The variation among tribes is further highlighted by the correlations of relatedness to differing environmental axes among the tribes. The observation that not all clades (here tribes) within a radiation feature patterns of niche convservatism is not uncommon (García-Navas & Westerman, 2018); several studies provdied evidence for such asymmetries among species in terms of niche evolution at different scales (geographic and taxonomic) (Blair, Sterling, Dusch, Raxworthy, &

Pearson, 2013; Culumber & Tobler, 2016). Coupled with the results from the ancestral niche reconstruction, wherein a general patterns of narrow niche width of the species-poor tribes (Eretmodini, Limnochromini, Cyphotilapiini, Cyprichromini, Perissodini) along at least either depth or sand-rock emerged further strengthens this impression of variable niche conservatism among tribes. However, for three of these tribes (Eretmodini, Limnochromini, Perissodini) we have a small number of species records only, and therefore cannot weight these results to heavily.

Overall, these varying patterns of niche conservatism among tribes in combination with the importance of niche-based community assembly could suggest that niche evolution and diversification happened along different environmental axes for the different tribes. The history of niche occupation estimated through ancestral niche reconstruction could further indicate that the environmental diversifcation of the Lake Tanganyika cichlid species flock happened in stages.

Acknowledgments

We thank Heinz H. Büscher, the crew of Kalambo Falls Lodge and George Kazumbe and his crew for the support in logistics and fieldwork, the Lake Tanganyika Research Unit, Department of Fisheries, Republic of Zambia and the Tanzania Commission for Science and Technology (COSTECH), for research permits. This study was supported by the European Research Council (ERC, CoG 'CICHLID~X' to WS).

Author's contribution

LW and WS conceived and supervised the study, all co-authors conducted the fieldwork, LW processed the images, analysed the data, and wrote the manuscript with feedback from all co-authors.

Data accessibility

All raw count data used in this study including a separate species list is available from the Dryad Digital

References

Ackerly, D. D., Schwilk, D. W., & Webb, C. O. (2006). Niche evolution and adaptive radiation: Testing the order of trait divergence. Ecology, 87(7 SUPPL.), 50–61. doi:10.1890/0012-9658(2006)87[50:NEAART]2.0.CO;2

Blair, M. E., Sterling, E. J., Dusch, M., Raxworthy, C. J., & Pearson, R. G. (2013). Ecological divergence and speciation between lemur (Eulemur) sister species in Madagascar. Journal of Evolutionary Biology, 26(8), 1790–1801. doi:10.1111/jeb.12179

Boileau, N., Cortesi, F., Egger, B., Muschick, M., Indermaur, A., Theis, A., … Salzburger, W. (2015). A complex mode of aggressive mimicry in a scale-eating cichlid fish. Biology Letters, 11(9), 20150521. doi:10.1098/rsbl.2015.0521

Boulenger, G. A. (1898). Report on the fishes recently obtained by Mr. JES Moore in Lake Tanganyika. Proceedings of the Zoological Society of London, 3.

Clarke, M., Thomas, G. H., & Freckleton, R. P. (2017). Trait Evolution in Adaptive Radiations: Modeling and Measuring Interspecific Competition on Phylogenies. The American Naturalist, 189(2), 121–137. doi:10.1086/689819

Colombo, M., Damerau, M., Hanel, R., Salzburger, W., & Matschiner, M. (2015). Diversity and disparity through time in the adaptive radiation of Antarctic notothenioid fishes. Journal of Evolutionary Biology, 28(2), 376–394. doi:10.1111/jeb.12570

Comte, L., Cucherousset, J., & Olden, J. D. (2016). Global test of Eltonian niche conservatism of nonnative freshwater fish species between their native and introduced ranges. Ecography, (February), 1–9. doi:10.1111/ecog.02007

Culumber, Z. W., & Tobler, M. (2016). Ecological divergence and conservatism: spatiotemporal patterns of niche evolution in a genus of livebearing fishes (Poeciliidae: Xiphophorus). BMC Evolutionary Biology, 16(1), 44. doi:10.1186/s12862-016-0593-4

Danley, P. D., & Kocher, T. D. (2001). Speciation in rapidly diverging systems: Lessons from Lake Malawi. Molecular Ecology, 10(5), 1075–1086. doi:10.1046/j.1365-294X.2001.01283.x

Deutsch, J. C. (1997). Colour diversification in Malawi cichlids: Evidence for adaptation, reinforcement or sexual selection? Biological Journal of the Linnean Society, 62(1), 1–14. doi:10.1006/bijl.1997.0135

Di Cola, V., Broennimann, O., Petitpierre, B., Breiner, F. T., D'Amen, M., Randin, C., … Guisan, A. (2017). ecospat: an R package to support spatial analyses and modeling of species niches and distributions. Ecography, 40(6), 774–787. doi:10.1111/ecog.02671

Egger, B., Sefc, K. M., Makasa, L., Sturmbauer, C., & Salzburger, W. (2012). Introgressive hybridization between color morphs in a population of cichlid fishes twelve years after human-induced secondary admixis. Journal of Heredity, 103(4), 515–522. doi:10.1093/jhered/ess013

Evans, M. E. K., Smith, S. A., Flynn, R. S., & Donoghue, M. J. (2009). Climate, Niche Evolution, and Diversification of the " Bird-Cage " Evening Primroses (Oenothera, Sections Anogra and Kleinia). Am. Nat, 173(173), 0–0. doi:10.1086/595757

Fermon, Y., Nshombo, M., Muzumani, R., & Jonas, B. (2017). Lac Tanganyika – Guide de la faune des poissons de la côte congolaise, d'Ubwari à la Ruzizi. AFC (Association France Cichlid).

Fitzpatrick, B. M., & Turelli, M. (2006). the Geography of Mammalian Speciation: Mixed Signals From Phylogenies and Range Maps. Evolution, 60(3), 601. doi:10.1554/05-453.1

García-Navas, V., & Westerman, M. (2018). Niche conservatism and phylogenetic clustering in a tribe of arid-adapted marsupial mice, the Sminthopsini. Journal of Evolutionary Biology, 31(8), 1204–1215. doi:10.1111/jeb.13297

Garrabou, J., Ballesteros, E., & Zabala, M. (2002). Structure and Dynamics of North-western Mediterranean Rocky Benthic Communities along a Depth Gradient. Estuarine, Coastal and Shelf Science, 55(3), 493–508. doi:10.1006/ecss.2001.0920

Gavrilets, S., & Losos, J. B. (2009). Adaptive radiation: Contrasting theory with data. Science. doi:10.1126/science.1157966

Gerhold, P., Cahill, J. F., Winter, M., Bartish, I. V., & Prinzing, A. (2015). Phylogenetic patterns are not proxies of community assembly mechanisms (they are far better). Functional Ecology, 29(5), 600–614. doi:10.1111/1365-2435.12425

Hair, J. F., Black, W. C., Babin, J. B., & Anderson, R. E. (2014). Multivariate Data Analysis (7th ed.). Pearson Education Limited.

Harmon, L. J., Schulte, J. A., Larson, A., & Losos, J. B. (2003). Tempo and mode of evolutionary radiation in iguanian lizards. Science (New York, N.Y.), 301(5635), 961–4. doi:10.1126/science.1084786

Harmon, L. J., Weir, J. T., Brock, C. D., Glor, R. E., & Challenger, W. (2008). GEIGER: investigating evolutionary radiations. Bioinformatics, 24(1), 129–131. doi:10.1093/bioinformatics/btm538

Heibl, C., & Calenge, C. (2018). R Package 'phyloclim': Integrating Phylogenetics and Climatic Niche Modeling. Cran.

Hernandez, P. A., Graham, C. H., Master, L. L., & Albert, D. L. (2006). The effect of sample size and species characteristics on performance of different species distribution modeling methods. Ecography, 29(5), 773–785. doi:10.1111/j.0906-7590.2006.04700.x

Hutchinson, G. E. (1957). Concluding Remarks. Cold Spring Harbor Symposia on Quantitative Biology, 22, 415–427. doi:10.1101/SQB.1957.022.01.039

Indermaur, A., Theis, A., Egger, B., & Salzburger, W. (2018). Mouth dimorphism in scale-eating cichlid fish from Lake Tanganyika advances individual fitness. Evolution, 72(9), 1962–1969. doi:10.1111/evo.13552

Janzen, T., Alzate, A., Muschick, M., Maan, M. E., van der Plas, F., & Etienne, R. S. (2017). Community assembly in Lake Tanganyika cichlid fish: quantifying the contributions of both niche-based and neutral processes. Ecology and Evolution, 7(4), 1057–1067. doi:10.1002/ece3.2689

Knouft, J. H., Losos, J. B., Glor, R. E., & Kolbe, J. J. (2006). Phylogenetic analysis of the evolution of the niche in lizards of the Anolis sagrei group. Ecology, 87, S29-38.

Kohli, B. A., Terry, R. C., & Rowe, R. J. (2018). A trait-based framework for discerning drivers of species co-occurrence across heterogeneous landscapes. Ecography, 41(12), 1921–1933. doi:10.1111/ecog.03747

Konings, A. (1998). Tanganyika cichlids in their natural habitat (3rd ed.). Cichlid Press, El Paso, USA.

Losos, J. B. (2008). Phylogenetic niche conservatism, phylogenetic signal and the relationship between phylogenetic relatedness and ecological similarity among species. Ecology Letters. doi:10.1111/j.1461-0248.2008.01229.x

Mason, S. J., & Graham, N. E. (2002). Areas beneath the relative operating characteristics (ROC) and relative operating levels (ROL) curves: Statistical significance and interpretation. Quarterly Journal of the Royal Meteorological Society, 128(584), 2145–2166. doi:10.1256/003590002320603584

Mayfield, M. M., & Levine, J. M. (2010). Opposing effects of competitive exclusion on the phylogenetic structure of communities. Ecology Letters, 13(9), 1085–1093. doi:10.1111/j.1461-0248.2010.01509.x

Merrett, N. R., Bagley, P. M., Smith, A., & Creasey, S. (1994). Scavenging Deep Demersal Fishes of the Porcupine Seabight, North-East Atlantic: Observations by Baited Camera, Trap and Trawl. Journal of the Marine Biological Association of the United Kingdom, 74(3), 481–498. doi:10.1017/S0025315400047615

Münkemüller, T., Boucher, F. C., Thuiller, W., & Lavergne, S. (2015). Phylogenetic niche conservatism - common pitfalls and ways forward. Functional Ecology, 29(5), 627–639. doi:10.1111/1365-2435.12388

Paradis, E., Claude, J., & Strimmer, K. (2004). APE: Analyses of Phylogenetics and Evolution in R language. Bioinformatics, 20(2), 289–290. doi:10.1093/bioinformatics/btg412

Phillips, S. J., Anderson, R. P., & Schapire, R. E. (2006). Maximum entropy modeling of species geographic distributions. Ecological Modelling, 190(3–4), 231–259. doi:10.1016/J.ECOLMODEL.2005.03.026

Phillips, S. J., & Dudík, M. (2008). Modeling of species distribution with Maxent: new extensions and a comprehensive evalutation. Ecograpy, 31(December 2007), 161–175. doi:10.1111/j.2007.0906-7590.05203.x

Poll, M. (1956). Exploration Hydrobiologique Du Lac Tanganyika (1946-1947) Volume III fascicule 5B: Poissons Cichlidae (Vol. 3). doi:10.2307/1439430

R Development Core Team. (2016). R: A Language and Environment for Statistical Computing. R Foundation for Statistical Computing Vienna Austria. doi:10.1038/sj.hdy.6800737

Ronco, F., Indermaur, A., Büscher, H. H., & Salzburger, W. (in press). The taxonomic diversity of the cichlid fish fauna of Lake Tanganyika. Journal of Great Lakes Research, (SIAL special issue).

Salzburger, W. (2018). Understanding explosive diversification through cichlid fish genomics. Nature Reviews Genetics. doi:10.1038/s41576-018-0043-9

Salzburger, W., Bocxlaer, B. Van, & Cohen, A. S. (2014). Ecology and Evolution of the African Great Lakes and Their Faunas. Annual Review of Ecology, Evolution and Systematics. doi:10.1146/annurev-ecolsys-120213-091804

Schluter, D. (2000). The Ecology of Adaptive Radiation. Oxford Series in Ecology and Evolution. doi:10.2307/3558417

Schluter, D., Price, T., Mooers, A. O., & Ludwig, D. (1997). Likelihood of Ancestor States in Adaptive Radiation. Evolution, 51(6), 1699–1711.

Shumway, C. A., Hofmann, H. A., & Dobberfuhl, A. P. (2007). Quantifying habitat complexity in aquatic ecosystems. Freshwater Biology, 52(6), 1065–1076. doi:10.1111/j.1365-2427.2007.01754.x

Slater, G. J., Price, S. A., Santini, F., & Alfaro, M. E. (2010). Diversity versus disparity and the radiation of modern cetaceans. Proceedings. Biological Sciences, 277(1697), 3097–104. doi:10.1098/rspb.2010.0408

Smith, K. F., & Brown, J. H. (2002). Patterns of diversity, depth range and body size among pelagic fishes along a gradient of depth. Global Ecology and Biogeography, 11(4), 313–322. doi:10.1046/j.1466-822X.2002.00286.x

Stone, L., & Roberts, A. (1990). The checkerboard score and species distributions. Oecologia, 85(1), 74–79. doi:10.1007/BF00317345

Sturmbauer, C. (1998). Explosive speciation in cichlid fishes of the African Great Lakes: a dynamic model of adaptive radiation. Journal of Fish Biology, 53(sa), 18–36. doi:10.1111/j.1095-8649.1998.tb01015.x

Sturmbauer, C., & Dallinger, R. (1994). Diurnal Variation of Spacing and Foraging Behaviour in Tropheus Moorii (Cichlidae) in Lake Tanganyika, Eastern Africa. Netherlands Journal of Zoology, 45(3–4), 386–401. doi:10.1163/156854295X00375

Sturmbauer, C., Fuchs, C., Harb, G., Damm, E., Duftner, N., Maderbacher, M., … Koblmüller, S. (2008). Abundance, distribution, and territory areas of rock-dwelling Lake Tanganyika cichlid fish species. Hydrobiologia, 615(1), 57–68. doi:10.1007/s10750-008-9557-z

Sturmbauer, C., Husemann, M., & Danley, P. D. (2011). Explosive Speciation and Adaptive Radiation of East African Cichlid Fishes. In Biodiversity Hotspots (pp. 333–362). Berlin, Heidelberg: Springer Berlin Heidelberg. doi:10.1007/978-3-642-20992-5_18

Takeuchi, Y., Ochi, H., Kohda, M., Sinyinza, D., & Hori, M. (2010). A 20-year census of a rocky littoral fish community in Lake Tanganyika. Ecology of Freshwater Fish, 19(2), 239–248. doi:10.1111/j.1600-0633.2010.00408.x

Vamosi, S. M., Heard, S. B., Vamosi, J. C., & Webb, C. O. (2009). Emerging patterns in the comparative analysis of phylogenetic community structure. Molecular Ecology, 18(4), 572–592. doi:10.1111/j.1365-294X.2008.04001.x

Warren, D. L., Glor, R. E., & Turelli, M. (2008). Environmental niche equivalency versus conservatism: Quantitative approaches to niche evolution. Evolution, 62(11), 2868–2883. doi:10.1111/j.1558-5646.2008.00482.x

Widmer, L., Heule, E., Colombo, M., Rueegg, A., Indermaur, A., Ronco, F., & Salzburger, W. (2019). Point-Combination Transect (PCT): Incorporation of small underwater cameras to study fish communities. Methods in Ecology and Evolution, 2019(August 2018), 1–11. doi:10.1111/2041-210X.13163

Wiens, J. J., Ackerly, D. D., Allen, A. P., Anacker, B. L., Buckley, L. B., Cornell, H. V., … Stephens, P. R. (2010). Niche conservatism as an emerging principle in ecology and conservation biology. Ecology Letters, 13(10), 1310–1324. doi:10.1111/j.1461-0248.2010.01515.x

Wilcox, T. M., Schwartz, M. K., & Lowe, W. H. (2018). Evolutionary Community Ecology: Time to Think Outside the (Taxonomic) Box. Trends in Ecology and Evolution. doi:10.1016/j.tree.2018.01.014

Wisz, M. S., Hijmans, R. J., Li, J., Peterson, A. T., Graham, C. H., Guisan, A., … Zimmermann, N. E. (2008). Effects of sample size on the performance of species distribution models. Diversity and Distributions, 14(5), 763–773. doi:10.1111/j.1472-4642.2008.00482.x

Chapter 7 | Supplementary Material

Table S1: List of locations where PCTs were placed during fieldwork including GPS coordinates, date and number of PCT conducted at location. Numbers (No.) correspond to map in Figure 1 of main article.

No.	Location	Country	Latitude	Longitude	Year	PCTs
1	Mbete	Zambia	-8.806111	31.026667	15.08.14	1
2	Chituta	Zambia	-8.723611	31.15	30.08.16	5
3	Mwina Point	Zambia	-8.721944	31.122222	01.09.16	2
4	Kanfonki	Zambia	-8.702778	30.9225	02.09.16	5
5	Isanga	Zambia	-8.654556	31.191833	23.08.16	3
6	Toby	Zambia	-8.623032	31.20044	29.07.14	18
7	Kabwensolo	Zambia	-8.609722	30.829167	03.09.16	4
8	Lukes Beach	Zambia	-8.609056	31.195944	28.08.16	3
9	Chitweshiba	Zambia	-8.595833	30.8075	04.09.16	3
10	Kabyolwe	Zambia	-8.569167	30.750556	05.09.16	2
11	Nkondwe	Tanzania	-8.550833	30.566222	20.08.17	4
12	Sumbu	Zambia	-8.539777	30.597869	11.09.16	5
13	Kachese	Zambia	-8.490528	30.4775	09.09.16	3
14	Ndole	Zambia	-8.476139	30.449333	10.09.16	5
15	Chilesa	Tanzania	-8.469611	31.13075	12.08.17	3
16	Chibwensolo	Zambia	-8.442778	30.454722	07.09.16	3
17	Chimba	Zambia	-8.426111	30.456667	06.09.16	3
18	Szamasi	Tanzania	-8.359361	31.0715	25.08.17	4
19	Katete 2	Zambia	-8.328056	30.526667	08.09.16	3
20	Kasola Island	Tanzania	-8.241944	30.978889	13.08.17	4
21	Malasa Island	Tanzania	-8.211944	30.946389	24.08.17	4
22	Fulwe	Tanzania	-7.955	30.8225	23.08.17	4
23	Liuli	Tanzania	-7.849111	30.784806	14.08.17	4
24	Twiyu	Tanzania	-7.581944	30.628333	22.08.17	4
25	Tanganyika village	Tanzania	-7.512583	30.586056	15.08.17	4
26	Ulwile 5	Tanzania	-7.474194	30.571222	21.08.17	4
27	Mvuna	Tanzania	-7.444167	30.543889	16.08.17	4
28	Kasowo	Tanzania	-7.234194	30.549583	19.08.17	4
29	Korongwe	Tanzania	-7.136944	30.507778	17.08.17	3
30	Utinta	Tanzania	-7.128056	30.527278	18.08.17	3
31	Sibwesa Rocks	Tanzania	-6.50275	29.948417	07.02.17	4
32	Msilambula Rocks	Tanzania	-6.421667	29.866111	08.02.17	4
33	Kalila Nkwasi	Tanzania	-6.260556	29.736667	04.02.17	4
34	Nganja	Tanzania	-6.173333	29.740278	02.02.17	4
35	Myako	Tanzania	-6.088	29.727944	05.02.17	4
36	Bulu Point	Tanzania	-6.016111	29.746389	06.02.17	3
37	Mwamahunga	Tanzania	-4.911944	29.598333	27.01.17	5
38	Mwamawimbi	Tanzania	-4.905	29.595556	23.01.17	3
39	Kaku	Tanzania	-4.896389	29.611667	26.01.17	7
40	Cave Kigoma	Tanzania	-4.886944	29.615833	10.02.17	3
41	Georges Place	Tanzania	-4.885	29.620833	19.01.17	3
42	Nondwa Point	Tanzania	-4.864167	29.607222	18.01.17	3
43	Nondwa Bay	Tanzania	-4.864111	29.609639	24.01.17	4
44	Kalalangabo	Tanzania	-4.843611	29.609444	21.01.17	4
45	Kananiye	Tanzania	-4.794167	29.599444	28.01.17	6

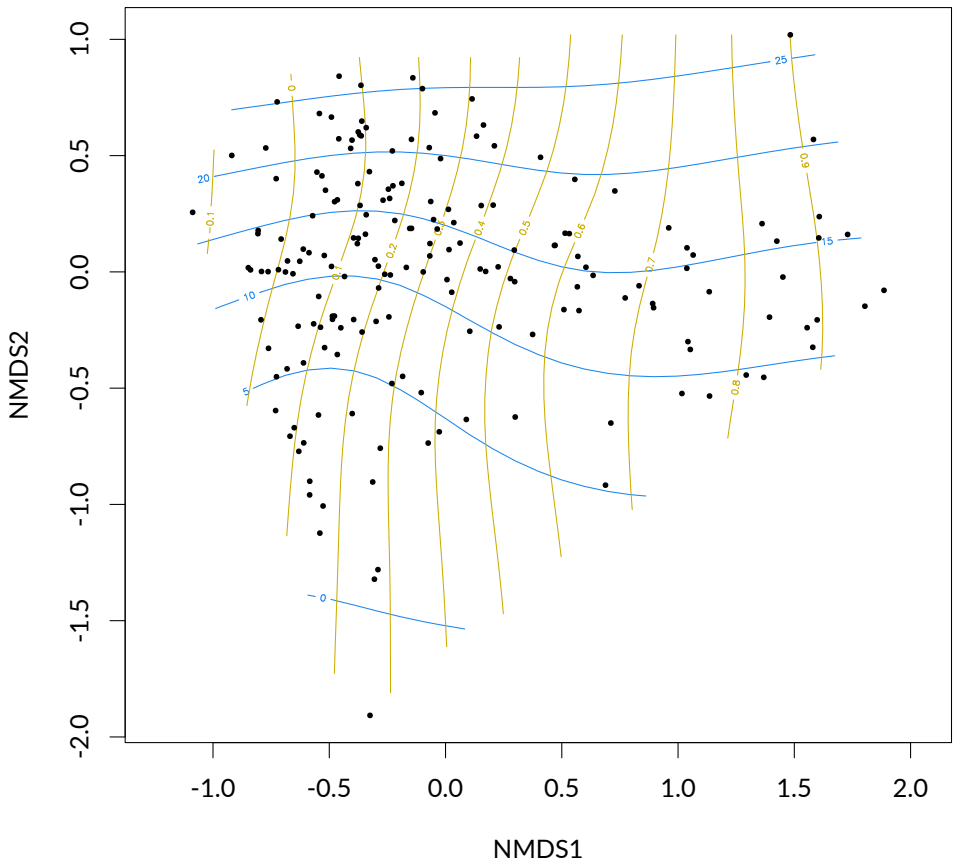

Figure S2: Multidimensional scaling (MDS) was performed based on PCT-data. Wisconsin standardisation was applied before using Euclidean distance to determine dissimilarities between communities. Analysis was performed using metaMDS of R package vegan (Oksanen et al., 2018).

Table S3: List of environmental variables that were recorded and considered for ecological niche quantification (expect 'rock').

Name	Description	Unit	Observed range	Obtained trough
rock	Rock proportion of substrate	%	0.0 – 1.0	Image Analysis
sand	Sand proportion of substrate	%	0.0 – 1.0	Image Analysis
veg	Vegetation coverage of substrate	%	0.0 – 1.0	Image Analysis
shell	Shell coverage of substrate	%	0.0 – 1.0	Image Analysis
depth	Depth	m	0.5 – 36.2	Dive Computer
rfreq	Rock frequency	-	0 - 157	Image Analysis
rsize	Rock size	-	0 - 5	Image Analysis
HC	Habitat complexity (Z-score)		-1.8 – 4.7	Sensu Shumway et al.

Table S4: List of species observed during this study, including traits for co-occurrence analysis. Biotic Interaction 'BI' traits: TL (trophic level), SL (standard length in cm), SiC (size class; small = 2 – 12 cm, medium = 12 - 18 cm, large = 18 – 30 cm); Environmental filtering 'EF' traits: Depth (weighted mean of depth in m), Rock (weighted mean of rock cover in %), SuC (substrate category; sand = 0 – 1/3 rock cover, inter = 1/3 – 2/3 rock cover, rock = 2/3 – 1 rock cover), EW (East-West affinity, EW = both), NS (North-South affinity, NS = both).

			'BI'-traits			'EF'-traits				
ID	**Species**	**Tribe**	**TL**	**SL**	**SiC**	**Depth**	**Rock**	**SuC**	**EW**	**NS**
Altcal	Altolamprologus calvus	Lamprologini	carnivore	7.6	small	13.0	0.9	rock	EW	S
Altcom	Altolamprologus compressiceps	Lamprologini	carnivore	8.1	small	14.2	0.9	rock	EW	NS
Altfas	Altolamprologus fasciatus	Lamprologini	carnivore	7.5	small	8.7	0.9	rock	EW	NS
Altshe	Altolamprologus sp. 'shell'	Lamprologini	carnivore	3.6	small	15.3	0.1	sand	W	S
Asplep	Asprotilapia leptura	Ectodini	omnivore	8.3	small	9.2	1.0	rock	EW	NS
Astbur	Astatotilapia burtoni	Tropheini	omnivore	5.9	small	1.0	0.0	sand	EW	S
Auldew	Aulonocranus dewindti	Ectodini	omnivore	7.4	small	3.2	0.7	rock	EW	NS
Batfas	Bathybates fasciatus	Bathybatini	piscivore	18.8	large	20.4	0.6	inter	EW	NS
Batfer	Bathybates ferox	Bathybatini	piscivore	13.4	medium	13.0	0.0	sand	E	N
Benhor	Benthochromis horii	Benthochromini	omnivore	14.3	medium	24.5	0.7	rock	EW	NS
Boumic	Boulengerochromis microlepis	Boulengerochromini	piscivore	40.3	NA	15.1	0.4	inter	EW	NS
Calmac	Callochromis macrops	Ectodini	carnivore	8.9	small	7.9	0.7	rock	EW	NS
Calple	Callochromis pleurospilus	Ectodini	carnivore	6.3	small	1.5	0.4	inter	E	NS
Chabif	Chalinochromis bifrenatus	Lamprologini	omnivore	9.4	small	13.2	0.9	rock	E	NS
Chabri	Chalinochromis brichardi	Lamprologini	omnivore	8.0	small	8.8	0.9	rock	EW	NS
Chacya	Chalinochromis cyanophleps	Lamprologini	omnivore	11.7	small	14.7	1.0	rock	E	S
Cphfro	Cyphotilapia frontosa	Cyphotilapiini	piscivore	12.7	medium	19.6	0.8	rock	E	N
Cphgib	Cyphotilapia gibberosa	Cyphotilapiini	piscivore	11.7	small	21.8	0.8	rock	EW	NS
Ctehor	Ctenochromis horei	Tropheini	omnivore	8.0	small	2.9	0.4	inter	EW	NS
Cunlon	Cunningtonia longiventralis	Ectodini	herbivore	9.3	small	8.6	0.9	rock	E	NS
Cyafur	Cyathopharynx furcifer	Ectodini	omnivore	10.9	small	12.9	0.8	rock	EW	NS
Cypcol	Cyprichromis coloratus	Cyprichromini	omnivore	8.8	small	18.6	0.9	rock	E	S
Cypdwj	Cyprichromis sp. 'dwarf jumbo'	Cyprichromini	omnivore	7.7	small	19.5	1.0	rock	E	N
Cypkan	Cyprichromis sp. 'kanfonki'	Cyprichromini	omnivore	8.7	small	17.9	1.0	rock	EW	S
Cyplep	Cyprichromis leptosoma	Cyprichromini	omnivore	7.3	small	15.2	1.0	rock	EW	NS
Cypmic	Cyprichromis microlepidotus	Cyprichromini	omnivore	8.0	small	20.3	1.0	rock	E	N
Cyppav	Cyprichromis pavo	Cyprichromini	omnivore	9.5	small	23.5	1.0	rock	EW	NS
Cypzon	Cyprichromis zonatus	Cyprichromini	omnivore	7.6	small	21.6	1.0	rock	E	NS
Ectdes	Ectodus descampsii	Ectodini	omnivore	7.4	small	4.5	0.2	sand	EW	NS
Enamel	Enantiopus melanogenys	Ectodini	carnivore	10.6	small	14.2	0.1	sand	E	NS
Erecya	Eretmodus cyanostictus	Eretmodini	herbivore	5.6	small	3.3	0.8	rock	EW	S
Eremar	Eretmodus marksmithi	Eretmodini	herbivore	5.1	small	3.6	0.9	rock	E	N
Gnaper	Gnathochromis permaxillaris	Limnochromini	omnivore	12.2	medium	21.0	0.5	inter	E	NS
Gnapfe	Gnathochromis pfefferi	Tropheini	omnivore	8.4	small	8.4	0.5	inter	EW	NS
Gralem	Grammatotria lemairii	Ectodini	omnivore	16.9	medium	13.5	0.1	sand	EW	NS
Hapmic	Haplotaxodon microlepis	Perissodini	piscivore	12.7	medium	14.3	0.9	rock	EW	NS
Intloo	Interochromis loocki	Tropheini	omnivore	9.4	small	10.7	0.8	rock	EW	NS
Juldic	Julidochromis dickfeldi	Lamprologini	omnivore	6.9	small	7.0	0.9	rock	W	S
JulmaS	Julidochromis sp. 'marlieri south'	Lamprologini	omnivore	7.7	small	14.1	0.9	rock	EW	NS
Julorn	Julidochromis ornatus	Lamprologini	omnivore	6.6	small	11.9	0.9	rock	EW	S
Julreg	Julidochromis regani	Lamprologini	omnivore	6.7	small	13.7	0.9	rock	EW	NS
Lamcal	Lamprologus callipterus	Lamprologini	carnivore	7.6	small	12.4	0.6	inter	EW	NS
Lamlem	Lamprologus lemairii	Lamprologini	piscivore	10.9	small	15.2	0.8	rock	EW	NS
Lamoce	Lamprologus ocellatus	Lamprologini	carnivore	3.8	small	14.4	0.0	sand	EW	S
Lamorn	Lamprologus ornatipinnis	Lamprologini	carnivore	4.4	small	20.5	0.0	sand	EW	NS
Lamsig	Lamprologus signatus	Lamprologini	omnivore	3.7	small	24.0	0.0	sand	W	S
Lchaur	Limnochromis auritus	Limnochromini	carnivore	10.7	small	21.8	0.0	sand	EW	S
Lepatt	Lepidiolamprologus attenuatus	Lamprologini	piscivore	9.4	small	15.5	0.5	inter	EW	NS
Lepcun	Lepidiolamprologus cunningtoni	Lamprologini	piscivore	14.7	medium	14.2	0.1	sand	EW	NS
Lepelo	Lepidiolamprologus elongatus	Lamprologini	piscivore	11.6	small	13.5	0.8	rock	EW	NS
Lepken	Lepidiolamprologus kendalli	Lamprologini	piscivore	10.1	small	23.7	0.9	rock	EW	S
Lepmim	Lepidiolamprologus mimicus	Lamprologini	piscivore	13.1	medium	15.3	0.9	rock	EW	NS
Leppro	Lepidiolamprologus profundicola	Lamprologini	piscivore	15.0	medium	14.7	0.9	rock	EW	NS
Lesper	Lestradea perspicax	Ectodini	omnivore	8.6	small	13.1	0.3	sand	EW	NS
Limdar	Limnotilapia dardennii	Tropheini	omnivore	14.8	medium	12.4	0.7	rock	EW	NS
Loblab	Lobochilotes labiatus	Tropheini	carnivore	11.2	small	11.2	0.8	rock	EW	NS
Mdcten	Microdontochromis tenuidentata	Ectodini	omnivore	6.5	small	14.0	0.5	inter	EW	NS
Neobou	Neolamprologus boulengeri	Lamprologini	carnivore	5.6	small	10.4	0.0	sand	E	N
Neobre	Neolamprologus brevis	Lamprologini	omnivore	4.2	small	13.9	0.0	sand	EW	NS
Neobri	Neolamprologus brichardi	Lamprologini	omnivore	6.2	small	14.9	0.9	rock	EW	NS
Neobue	Neolamprologus buescheri	Lamprologini	carnivore	5.9	small	22.8	0.9	rock	EW	S
NeocaK	Neolamprologus sp. 'caudopunctatus kipili'	Lamprologini	omnivore	6.8	small	10.9	0.6	inter	E	S
Neocal	Neolamprologus calliurus	Lamprologini	omnivore	5.9	small	18.4	0.7	rock	EW	S
Neocau	Neolamprologus caudopunctatus	Lamprologini	omnivore	5.1	small	12.4	0.9	rock	EW	S
Neochi	Neolamprologus chitamwebwai	Lamprologini	omnivore	6.0	small	19.2	0.9	rock	E	N
Neochr	Neolamprologus christyi	Lamprologini	carnivore	8.3	small	11.8	0.7	rock	E	S
Neocyg	Neolamprologus sp. 'cygnus'	Lamprologini	omnivore	6.7	small	20.0	0.9	rock	E	S
Neocyl	Neolamprologus cylindricus	Lamprologini	carnivore	7.5	small	16.0	0.9	rock	E	S

→ Table continuous on the next page

				'BI'-traits			'EF'-traits			
ID	Species	Tribe	TL	SL	SiC	Depth	Rock	SuC	EW	NS
Neoese	Neolamprologus sp. 'eseki'	Lamprologini	carnivore	7.6	small	9.0	0.7	rock	E	S
Neofal	Neolamprologus falcicula	Lamprologini	omnivore	5.7	small	16.6	1.0	rock	E	NS
NeofaM	Neolamprologus sp. 'falcicula mahale'	Lamprologini	omnivore	5.4	small	13.1	1.0	rock	E	N
Neofur	Neolamprologus furcifer	Lamprologini	carnivore	8.3	small	15.0	0.9	rock	E	NS
NeogrM	Neolamprologus sp. 'gracilis tanzania'	Lamprologini	omnivore	5.7	small	22.7	0.7	rock	E	N
Neoleu	Neolamprologus longior	Lamprologini	carnivore	7.1	small	17.6	0.9	rock	E	N
Neolou	Neolamprologus leloupi	Lamprologini	carnivore	4.6	small	18.1	0.7	rock	E	N
Neomee	Neolamprologus meeli	Lamprologini	carnivore	5.1	small	14.0	0.0	sand	EW	NS
Neomod	Neolamprologus modestus	Lamprologini	carnivore	8.2	small	10.5	0.7	rock	EW	NS
Neomon	Neolamprologus mondabu	Lamprologini	carnivore	5.8	small	12.6	0.7	rock	E	N
Neomul	Neolamprologus multifasciatus	Lamprologini	omnivore	2.3	small	14.9	0.0	sand	EW	S
Neomux	Neolamprologus mustax	Lamprologini	carnivore	6.4	small	9.6	0.9	rock	W	S
Neonig	Neolamprologus niger	Lamprologini	carnivore	4.7	small	7.8	1.0	rock	E	N
Neoobs	Neolamprologus obscurus	Lamprologini	carnivore	5.7	small	17.2	0.9	rock	W	S
Neopro	Neolamprologus prochilus	Lamprologini	carnivore	7.8	small	17.7	0.9	rock	EW	S
Neopul	Neolamprologus pulcher	Lamprologini	carnivore	5.8	small	11.1	0.9	rock	EW	S
Neosav	Neolamprologus savoryi	Lamprologini	carnivore	5.8	small	15.1	1.0	rock	EW	NS
Neosex	Neolamprologus sexfasciatus	Lamprologini	carnivore	9.1	small	14.5	0.9	rock	EW	S
Neotet	Neolamprologus tetracanthus	Lamprologini	carnivore	8.4	small	10.5	0.4	inter	EW	NS
Neotoa	Neolamprologus toae	Lamprologini	carnivore	7.6	small	10.3	1.0	rock	E	N
Neotre	Neolamprologus tretocephalus	Lamprologini	carnivore	7.5	small	11.0	1.0	rock	E	N
Neowal	Neolamprologus walteri	Lamprologini	omnivore	4.9	small	16.3	0.8	rock	E	N
Ophboo	Ophthalmotilapia boops	Ectodini	herbivore	9.0	small	6.0	1.0	rock	E	S
Ophnas	Ophthalmotilapia nasuta	Ectodini	herbivore	9.1	small	10.4	0.9	rock	EW	NS
Ophpar	Ophthalmotilapia paranasuta	Ectodini	herbivore	8.4	small	9.1	1.0	rock	E	N
Ophven	Ophthalmotilapia ventralis	Ectodini	omnivore	7.6	small	5.3	0.9	rock	EW	NS
Ophwhi	Ophthalmotilapia sp. 'white cap'	Ectodini	herbivore	9.3	small	3.3	1.0	rock	E	N
Oretan	Oreochromis tanganicae	Tilapiini	herbivore	18.1	large	5.4	0.4	inter	EW	NS
Pcybri	Paracyprichromis sp. 'brieni south'	Cyprichromini	herbivore	8.0	small	20.7	0.9	rock	EW	NS
Pcynig	Paracyprichromis nigripinnis	Cyprichromini	herbivore	5.9	small	28.6	1.0	rock	EW	NS
Permic	Perissodus microlepis	Perissodini	scales	8.1	small	12.5	0.8	rock	EW	NS
Peteph	Petrochromis ephippium	Tropheini	herbivore	10.1	small	12.8	0.9	rock	EW	NS
Petfam	Petrochromis famula	Tropheini	omnivore	9.3	small	8.3	0.9	rock	EW	NS
Petfas	Petrochromis fasciolatus	Tropheini	omnivore	9.5	small	5.9	0.8	rock	EW	NS
Petgia	Petrochromis sp. 'giant'	Tropheini	herbivore	19.7	large	13.8	1.0	rock	E	S
Pethor	Petrochromis horii	Tropheini	herbivore	9.0	small	10.9	0.7	rock	EW	S
Petkas	Petrochromis sp. 'kazumbae'	Tropheini	herbivore	12.3	medium	6.5	0.9	rock	E	N
Petkip	Petrochromis sp. 'kipili brown'	Tropheini	herbivore	13.4	medium	15.7	0.9	rock	E	S
Petort	Petrochromis orthognathus	Tropheini	herbivore	9.3	small	10.9	0.9	rock	E	NS
Petpol	Petrochromis polyodon	Tropheini	omnivore	12.8	medium	5.9	0.9	rock	EW	NS
Petrai	Petrochromis sp. 'macrognathus rainbow'	Tropheini	herbivore	16.5	medium	8.5	0.9	rock	E	S
Petred	Petrochromis sp. 'red'	Tropheini	herbivore	15.0	medium	18.1	0.7	rock	E	N
Pettex	Petrochromis polyodon sp. 'texas'	Tropheini	herbivore	17.9	medium	5.7	0.9	rock	E	NS
Pettre	Petrochromis trewavasae	Tropheini	herbivore	11.2	small	5.2	1.0	rock	W	S
Plepar	Plecodus paradoxus	Perissodini	scales	14.1	medium	13.8	0.7	rock	EW	NS
Plestr	Plecodus straeleni	Perissodini	scales	8.1	small	14.3	0.9	rock	EW	NS
Psccur	Pseudosimochromis curvifrons	Tropheini	omnivore	8.4	small	3.5	0.9	rock	EW	S
Regcal	Reganochromis calliurus	Limnochromini	carnivore	10.2	small	24.8	0.0	sand	W	S
Simbab	Simochromis babaulti	Tropheini	omnivore	6.4	small	2.5	0.6	inter	EW	NS
Simdia	Simochromis diagramma	Tropheini	omnivore	8.0	small	2.6	0.6	inter	EW	NS
Simmar	Simochromis marginatus	Tropheini	herbivore	7.2	small	6.1	0.8	rock	E	N
Spaery	Spathodus erythrodon	Eretmodini	omnivore	4.8	small	1.0	1.0	rock	E	N
Tanirs	Tanganicodus irsacae	Eretmodini	omnivore	5.0	small	1.0	1.0	rock	E	N
Telbif	Telmatochromis bifrenatus	Lamprologini	herbivore	3.2	small	12.4	0.9	rock	E	N
TeldhS	Telmatochromis dhonti	Lamprologini	herbivore	6.2	small	2.3	0.0	sand	EW	NS
TelteS	Telmatochromis temporalis	Lamprologini	herbivore	5.8	small	8.0	0.8	rock	EW	NS
Telvit	Telmatochromis vittatus	Lamprologini	herbivore	4.8	small	13.8	0.8	rock	EW	S
Trioto	Triglachromis otostigma	Limnochromini	herbivore	6.9	small	24.2	0.0	sand	W	S
Trobri	Tropheus brichardi	Tropheini	herbivore	6.9	small	7.5	0.9	rock	E	NS
Trodub	Tropheus duboisi	Tropheini	herbivore	8.7	small	9.4	0.9	rock	E	N
Trokir	Tropheus sp. 'kirschfleck'	Tropheini	herbivore	8.3	small	6.7	1.0	rock	E	N
Tromoo	Tropheus moorii	Tropheini	omnivore	8.0	small	5.9	0.9	rock	EW	NS
Tropol	Tropheus polli	Tropheini	herbivore	9.0	small	7.0	1.0	rock	E	N
Tylpol	Tylochromis polylepis	Tylochromini	carnivore	17.3	medium	7.1	0.1	sand	EW	NS
Varmoo	Variabilichromis moorii	Lamprologini	carnivore	6.2	small	3.8	0.9	rock	EW	S
Xenbat	Xenotilapia bathyphila	Ectodini	carnivore	7.6	small	14.6	0.0	sand	EW	NS
Xenbou	Xenotilapia boulengeri	Ectodini	carnivore	10.0	small	12.8	0.5	inter	EW	NS
Xencau	Xenotilapia caudafasciata	Ectodini	carnivore	9.7	small	25.2	0.3	inter	EW	S
Xenfla	Xenotilapia flavipinnis	Ectodini	carnivore	6.9	small	13.6	0.3	sand	EW	NS
Xenoch	Xenotilapia ochrogenys	Ectodini	carnivore	6.9	small	5.4	0.0	sand	E	N
Xensin	Xenotilapia singularis	Ectodini	carnivore	9.1	small	3.4	0.3	sand	EW	S
Xenspi	Xenotilapia spilopterus	Ectodini	carnivore	6.6	small	10.8	0.8	rock	EW	NS
Xensun	Xenotilapia sp. 'papilio sunflower'	Ectodini	carnivore	6.2	small	18.8	0.9	rock	EW	S

Table S5: List of 182 PCTs with their respective location and camera, including environmental variables. Rock frequency: the actual count of individual rocks on the examined image. Rock size: Average of estimated rock size according to following categories: 1 = rock size < 1% of image; 2 = rock size < 5% of image; 3 = rock size < 10% of image; 4 = rock size < 25% of image; 5 = rock size > 25% of image.

				Substrate cover (0 – 1)				Rock		
PCT	Cam	Location	Depth	Sand	Vegetation	Rock	Shell	Frequency	Size	HC
26	1	Mbete	5	0.2	0	0.8	0	7	3	1.4
26	3	Mbete	5	0	0	0.8	0.2	11	3	1.8
26	4	Mbete	5	0.1	0	0.8	0.1	30	2	1.5
27	1	Kanfonki	5	0	0	1	0	7	3	-0.2
27	3	Kanfonki	5	0	0	0	0	0	0	0.2
27	4	Kanfonki	5	0	0	1	0	2	3	0.4
27	5	Kanfonki	5	0	0	1	0	10	2	0.2
28	1	Kabwensolo	5	0	0.8	0.2	0	5	2	3
28	2	Kabwensolo	5	0	1	0	0	0	0	4.8
28	4	Kabwensolo	5	0	0.7	0.3	0	14	2	3.1
28	5	Kabwensolo	5	0	0.1	0.9	0	28	2	3.5
29	13	Toby	5	0.1	0.5	0.4	0	5	3	2
29	14	Toby	5	0	0	1	0	13	3	1.4
29	15	Toby	5	0	0	1	0	12	3	1.4
29	16	Toby	5	0	0	1	0	22	2	0.6
29	17	Toby	5	0	0	1	0	27	2	0.3
30	10	Toby	1	0	1	0	0	0	0	1.2
30	12	Toby	1	0	0	1	0	5	2	2.4
30	8	Toby	1	0.3	0.7	0	0	0	0	-0.2
30	9	Toby	1	0.9	0.1	0	0	2	2	-1.4
31	26	Toby	15.5	1	0	0	0	0	0	-0.1
31	27	Toby	14.9	1	0	0	0	0	0	0
31	28	Toby	14.8	1	0	0	0	0	0	-0.9
31	29	Toby	14.7	0.8	0	0.2	0	7	2	-0.6
31	30	Toby	15.2	0.6	0	0.4	0	4	2	0.1
32	11	Toby	10.1	1	0	0	0	0	0	-1.3
32	12	Toby	10.5	0.6	0	0.4	0	10	2	-1.5
32	21	Toby	10.5	0	0	1	0	11	2	0.2
32	23	Toby	10.7	0	0	1	0	8	3	-0.4
32	25	Toby	10.1	0	0	1	0	8	2	-0.1
34	26	Isanga	18.8	0.2	0	0.8	0	12	2	0.3
34	27	Isanga	18.6	0.1	0	0.9	0	8	2	1.2
34	28	Isanga	18.4	0.7	0	0.3	0	13	2	0
34	29	Isanga	18.4	0.3	0	0.7	0	7	3	0.8
34	30	Isanga	18.1	0.1	0	0.9	0	5	2	0.8
35	10	Isanga	14.4	0	0	1	0	12	3	0.9
35	17	Isanga	13.8	0.3	0	0.7	0	20	2	0.4
35	7	Isanga	14.4	0	0	1	0	10	3	0.3
35	8	Isanga	14.3	0	0	1	0	5	2	0.4
35	9	Isanga	14.9	0	0	1	0	5	3	2.2
36	11	Isanga	8.3	0	0	1	0	6	2	0.3
36	12	Isanga	8.6	0	0	1	0	11	3	0
36	13	Isanga	7.5	0	0	1	0	4	2	0.4
36	14	Isanga	7.7	0	0	1	0	2	3	0.3
36	15	Isanga	7.7	0	0	1	0	6	3	-0.3
37	10	Toby	5.4	0	0	1	0	27	2	0.1
37	6	Toby	5.7	0	0	1	0	12	3	0.8
37	7	Toby	4.9	0	0.1	0.9	0	18	3	1.5
37	8	Toby	4.7	0	0.1	0.9	0	15	3	1.3
37	9	Toby	5	0	0	1	0	24	2	1.3
38	11	Toby	6	0.1	0.1	0.8	0	17	2	1.1
38	12	Toby	6	1	0	0	0	1	1	-1
38	13	Toby	6	1	0	0	0	0	0	-0.4
38	14	Toby	6.5	1	0	0	0	0	0	-0.2
38	15	Toby	7.5	1	0	0	0	0	0	-0.5
39	21	Toby	6	0.1	0.1	0.7	0	17	2	2.5
39	22	Toby	6	1	0	0	0	1	1	1.3
39	23	Toby	6	1	0	0	0	0	0	0.9
39	24	Toby	6.5	1	0	0	0	0	0	0.3
39	25	Toby	7.5	1	0	0	0	0	0	0.1
40	26	Toby	5.7	0	0	1	0	13	3	1.4
40	27	Toby	4.9	0	0	1	0	13	3	2.8
40	28	Toby	4.7	0	0	1	0	13	3	2.2
40	29	Toby	5	0	0	1	0	23	2	1
40	30	Toby	5.4	0	0	1	0	26	2	0.7
41	11	Toby	15.4	0	0	1	0	17	2	0.5
41	12	Toby	15.7	0.3	0	0.7	0	17	2	0.8
41	13	Toby	15.7	0.1	0	0.9	0	10	3	1.9
41	14	Toby	15.1	0.2	0	0.8	0	12	2	1.5
41	15	Toby	15	0	0	1	0	18	2	1.4
42	10	Toby	1	0	0.2	0.8	0	9	2	2.1
42	6	Toby	1	0	0.3	0.7	0	17	2	0.8
42	7	Toby	1	0	0	1	0	10	3	1.9
42	8	Toby	1	0	0.1	1	0	9	3	2.8
42	9	Toby	1	0	0.2	0.8	0	7	3	3.4
43	11	Toby	19.6	1	0	0	0	0	0	-0.8
43	12	Toby	19.9	1	0	0	0	0	0	-1
43	13	Toby	20	1	0	0	0	0	0	-1.2
43	14	Toby	20.3	1	0	0	0	0	0	-0.9
43	15	Toby	20.5	1	0	0	0	0	0	-0.9
44	11	Toby	3.2	0	0.8	0.2	0	8	2	0.9
44	12	Toby	3.2	0	1	0	0	0	0	0.1
44	13	Toby	3	0	0.9	0.1	0	2	1	-0.5
44	14	Toby	2.7	0	1	0	0	0	0	1.2
44	15	Toby	3.3	0	1	0	0	0	0	0.7
45	17	Lukes Beach	12.8	1	0	0	0	0	0	-0.6
45	26	Lukes Beach	13	1	0	0	0	0	0	-0.9
45	27	Lukes Beach	13.1	1	0	0	0	0	0	-0.3
45	28	Lukes Beach	13.2	1	0	0	0	0	0	-0.4
45	29	Lukes Beach	13	1	0	0	0	0	0	-0.6
46	22	Lukes Beach	1	0.3	0.7	0	0	0	0	-0.4
46	23	Lukes Beach	1	0.3	0.7	0	0	0	0	-0.6
46	24	Lukes Beach	1	0.2	0.7	0	0	1	2	-0.8
46	25	Lukes Beach	1	1	0	0	0	0	0	-1.3
47	10	Lukes Beach	7.3	1	0	0	0	0	0	-0.5
47	6	Lukes Beach	7	1	0	0	0	0	0	0.3
47	7	Lukes Beach	7.3	1	0	0	0	0	0	0
47	8	Lukes Beach	7.4	1	0	0	0	0	0	-0.3
47	9	Lukes Beach	7.6	1	0	0	0	0	0	-0.6

→ Table continuous on the next page

				Substrate cover (0 – 1)				Rock		
PCT	Cam	Location	Depth	Sand	Vegetation	Rock	Shell	Frequency	Size	HC
48	22	Chituta	29.5	0	0	1	0	3	3	0
48	23	Chituta	29.5	0	0	1	0	4	3	0.5
48	24	Chituta	29.1	0	0	1	0	1	3	0.5
48	25	Chituta	29.3	0	0	1	0	5	3	0.4
49	26	Chituta	20.4	0	0	1	0	10	2	1.2
49	27	Chituta	20.9	0	0	1	0	11	2	1
49	28	Chituta	21.4	0	0	1	0	11	3	1.3
49	29	Chituta	20.8	0	0	1	0	10	3	1.5
49	30	Chituta	21	0	0	1	0	8	3	2
50	10	Chituta	1	0	0	1	0	38	2	-0.1
50	6	Chituta	1	0.1	0	0.9	0	7	3	0
50	7	Chituta	1	0	0	1	0	45	2	-1.1
50	8	Chituta	1	0	0	1	0	10	4	-0.5
50	9	Chituta	1	0	0	1	0	15	3	0.5
51	10	Chituta	27.2	0	0	1	0	13	3	0.1
51	6	Chituta	25.7	0	0	1	0	3	3	0.2
51	8	Chituta	26.5	0	0	1	0	7	2	0.2
51	9	Chituta	26.9	0	0	1	0	11	2	0.5
52	26	Chituta	14.8	0	0	1	0	12	3	1.1
52	27	Chituta	15.4	0	0	1	0	9	2	0.2
52	28	Chituta	15.5	0	0	1	0	7	2	0.8
52	29	Chituta	15.2	0	0	1	0	4	3	0.4
52	30	Chituta	15.7	0	0	1	0	12	2	0.8
53	26	Mwina Point	14.6	0	0	0	1	0	0	1.2
53	27	Mwina Point	14.8	0	0	0	1	0	0	1.1
53	28	Mwina Point	14.9	0	0	0	1	0	0	0.7
53	29	Mwina Point	15.2	0	0	0	1	0	0	1.1
53	30	Mwina Point	15.3	0.4	0	0	0.6	0	0	0.6
54	10	Mwina Point	14.1	0	0	0.1	0.9	7	1	1.2
54	6	Mwina Point	12.4	0	0	0.3	0.7	18	2	0.8
54	7	Mwina Point	12.7	0	0	0	1	6	1	0.5
54	8	Mwina Point	13.1	0	0	0.7	0.3	40	1	0.7
54	9	Mwina Point	13.7	0	0	1	0	30	2	1.4
55	17	Kanfonki	5.9	0	0	1	0	40	1	-1.4
55	22	Kanfonki	5.5	0	0.1	0.9	0	40	1	-0.9
55	23	Kanfonki	5.2	0	0	1	0	40	1	-0.3
55	24	Kanfonki	5	0	0	1	0	40	1	-0.2
55	25	Kanfonki	5.2	0	0	1	0	40	1	-0.6
56	11	Kanfonki	12.8	0.9	0	0.1	0	2	2	-0.6
56	13	Kanfonki	12.8	1	0	0	0	0	0	-0.4
56	14	Kanfonki	12.8	0.9	0	0.1	0	8	1	0
56	21	Kanfonki	13.2	1	0	0	0	0	0	-0.3
57	10	Kanfonki	20.8	0.9	0	0.1	0	4	2	0
57	6	Kanfonki	23.9	0	0	1	0	1	4	1.1
57	7	Kanfonki	24.1	1	0	0	0	1	1	0.6
57	8	Kanfonki	22.6	0.9	0	0.1	0	2	2	0.4
57	9	Kanfonki	21.6	0.5	0	0.5	0	6	1	0.6
58	26	Kanfonki	17.3	0	0	1	0	25	3	0.5
58	27	Kanfonki	18	0	0	1	0	17	3	0.7
58	28	Kanfonki	18.2	0	0	1	0	6	2	1.2
58	29	Kanfonki	19.2	0	0	1	0	6	3	1.5
58	30	Kanfonki	18.4	0	0	1	0	19	3	0.2
59	12	Kabwensolo	9.2	0	0	1	0	10	4	0.3
59	13	Kabwensolo	9.1	0	0	1	0	5	3	-0.7
59	14	Kabwensolo	7.8	0	0	1	0	5	3	-0.5
59	17	Kabwensolo	8	0	0	1	0	9	3	-0.5
59	21	Kabwensolo	7.6	0	0	1	0	6	4	-0.9
60	10	Kabwensolo	29.7	0	0	1	0	20	3	1.3
60	6	Kabwensolo	33.3	0	0	1	0	14	3	2.1
60	7	Kabwensolo	33.2	0	0	1	0	4	4	2.1
60	8	Kabwensolo	33.2	0	0	1	0	7	3	1.4
60	9	Kabwensolo	30	0	0	1	0	1	5	2
61	26	Kabwensolo	18.1	0.8	0	0.2	0	7	2	-1
61	27	Kabwensolo	18.3	0.7	0	0.3	0	5	2	-1.2
61	28	Kabwensolo	17.5	0	0	1	0	16	3	-0.2
61	29	Kabwensolo	17.5	0	0	1	0	8	4	0.7
61	30	Kabwensolo	17.1	0	0	1	0	9	3	-0.1
62	26	Chitweshiba	22.3	0	0	1	0	11	2	1
62	27	Chitweshiba	19.3	0	0	1	0	4	2	1
62	28	Chitweshiba	18.8	0	0	1	0	6	2	0.6
62	29	Chitweshiba	17.4	0	0	1	0	19	2	0.5
62	30	Chitweshiba	17.9	0.7	0	0.3	0	5	1	0.2
63	21	Chitweshiba	6.8	0	0	1	0	8	3	-0.7
63	22	Chitweshiba	5.8	0.5	0	0.5	0	23	2	-0.8
63	23	Chitweshiba	6.5	0.4	0	0.6	0	26	2	-0.8
63	24	Chitweshiba	7	0.2	0	0.8	0	30	1	-1.1
63	25	Chitweshiba	7.4	0	0	1	0	12	3	-0.8
64	10	Chitweshiba	12.4	0	0	1	0	10	3	0.5
64	6	Chitweshiba	12.3	0.2	0	0.8	0	7	2	0.6
64	7	Chitweshiba	11.7	0	0	1	0	23	2	0.4
64	8	Chitweshiba	12.8	0.2	0	0.8	0	30	2	0.5
64	9	Chitweshiba	12.2	0	0	1	0	38	2	0.1
65	11	Kabvolwe	24.8	1	0	0	0	0	0	0.4
65	12	Kabvolwe	24.2	1	0	0	0	0	0	0.3
65	13	Kabvolwe	24.2	1	0	0	0	0	0	0.4
65	14	Kabvolwe	24	1	0	0	0	0	0	0.4
65	17	Kabvolwe	23.8	1	0	0	0	0	0	0.8
66	21	Kabvolwe	14.8	1	0	0	0	0	0	0.6
66	22	Kabvolwe	13	1	0	0	0	0	0	0.2
66	23	Kabvolwe	12.5	1	0	0	0	0	0	0.1
66	24	Kabvolwe	11.9	1	0	0	0	0	0	0
66	25	Kabvolwe	11.2	1	0	0	0	0	0	0.4
67	16	Chimba	7.6	0	0	1	0	7	4	0.5
67	26	Chimba	8.1	0.8	0	0.2	0	3	2	-1.2
67	27	Chimba	8	0.5	0	0.5	0	7	2	-0.7
67	29	Chimba	7.1	0	0	1	0	24	2	-0.7
67	30	Chimba	8	0	0	1	0	15	3	-0.5
68	21	Chimba	17.5	0.1	0	0.9	0	12	3	0
68	22	Chimba	18	0.8	0	0	0.2	0	0	0.1
68	23	Chimba	18	0.9	0	0	0.1	0	0	0.1
68	24	Chimba	18	1	0	0	0	0	0	-0.2
68	25	Chimba	17.9	0.9	0	0	0.2	0	0	0
69	10	Chimba	24.7	1	0	0	0	0	0	-0.6
69	6	Chimba	22	0.8	0	0	0.2	0	0	0
69	7	Chimba	22.7	1	0	0	0	0	0	-0.3
69	8	Chimba	23.7	1	0	0	0	0	0	-0.5
69	9	Chimba	24.4	1	0	0	0	0	0	-0.4
70	27	Chibwensolo	15.9	0	0	0	1	0	0	1.2
70	29	Chibwensolo	16.3	0.1	0	0	1	0	0	0.9
70	30	Chibwensolo	16.7	0	0	0	1	0	0	0.9
70	7	Chibwensolo	15.7	0	0	0	1	0	0	0.6
71	21	Chibwensolo	13.5	0.1	0	0	0.9	0	0	0.6

→ Table continuous on the next page

				Substrate cover (0 – 1)				Rock		
PCT	Cam	Location	Depth	Sand	Vegetation	Rock	Shell	Frequency	Size	HC
71	23	Chibwensolo	13.5	0.2	0	0	0.8	0	0	-0.1
71	24	Chibwensolo	13.5	0.3	0	0	0.7	0	0	-0.5
71	25	Chibwensolo	13.5	0.2	0	0	0.8	0	0	0
71	6	Chibwensolo	13.5	0.4	0	0	0.6	0	0	-0.4
72	12	Chibwensolo	3.9	0	0.3	0.7	0	6	3	-0.5
72	13	Chibwensolo	3.7	0.7	0	0.3	0	13	2	-0.6
72	14	Chibwensolo	3.5	0	0.5	0.5	0	12	2	-0.4
72	17	Chibwensolo	3.1	0	0.6	0.4	0	8	2	-0.9
73	10	Katete 2	21.1	1	0	0	0	0	0	-1.5
73	6	Katete 2	20.8	1	0	0	0	0	0	-1.7
73	7	Katete 2	21	1	0	0	0	0	0	-1.5
73	8	Katete 2	21.4	1	0	0	0	0	0	-1.7
73	9	Katete 2	21.2	1	0	0	0	0	0	-1.7
74	11	Katete 2	12.2	1	0	0	0	0	0	-0.8
74	12	Katete 2	12	1	0	0	0	0	0	-1.2
74	13	Katete 2	11.5	1	0	0	0	0	0	-1.2
74	14	Katete 2	11.5	1	0	0	0	0	0	-1.2
74	16	Katete 2	12.2	1	0	0	0	0	0	-1.4
75	27	Katete 2	36.2	0	0	1	0	23	1	0.6
75	29	Katete 2	34.1	0.2	0	0.8	0	35	1	0
75	30	Katete 2	35.5	0	0	0	0	0	0	1
76	21	Kachese	5	0	0	1	0	21	2	0
76	22	Kachese	5.2	0	0	1	0	32	1	-0.8
76	23	Kachese	5.4	0	0	1	0	4	3	-0.8
76	24	Kachese	4.8	0	0	1	0	7	4	0.4
76	25	Kachese	5.3	0	0	1	0	5	3	-0.7
77	17	Kachese	24.3	0.3	0	0.7	0	7	2	-0.3
77	26	Kachese	24.1	0.5	0	0.5	0	5	2	-0.6
77	27	Kachese	24.6	0.4	0	0.6	0	9	3	0.6
77	29	Kachese	24.3	0	0	1	0	14	2	0
77	30	Kachese	24.2	0.3	0	0.7	0	15	2	-0.1
78	11	Kachese	15.2	0	0	1	0	40	2	0.3
78	12	Kachese	15.5	0	0	1	0	8	3	1.1
78	13	Kachese	15.5	0	0	1	0	3	3	0.4
78	14	Kachese	15.6	0	0	1	0	26	2	0.6
79	10	Ndole	5.2	1	0	0	0	0	0	-1.4
79	6	Ndole	7.4	1	0	0	0	0	0	-1
79	7	Ndole	6	1	0	0	0	0	0	-1.4
79	8	Ndole	5.4	1	0	0	0	0	0	-1.8
79	9	Ndole	5.1	1	0	0	0	0	0	-1.8
80	11	Ndole	1	0	1	0	0	0	0	2.6
80	12	Ndole	1	0	1	0	0	0	0	0.8
80	13	Ndole	1	0	1	0	0	0	0	0.3
80	14	Ndole	1	0	1	0	0	0	0	0.8
80	16	Ndole	1	0	0.9	0.1	0	1	2	-0.1
81	17	Ndole	11.3	0.7	0	0	0.3	0	0	-0.8
81	26	Ndole	11.6	0.5	0	0	0.5	0	0	-0.4
81	27	Ndole	11.5	0.4	0	0	0.6	0	0	-0.3
81	29	Ndole	11.7	0.5	0	0	0.5	0	0	0
81	30	Ndole	11.9	0.4	0	0	0.6	0	0	-0.2
82	21	Ndole	1.5	0.5	0	0.5	0	14	2	-0.8
82	22	Ndole	1.5	0.3	0	0.8	0	10	3	0.3
82	23	Ndole	1.5	0	0	1	0	12	3	0.6
82	24	Ndole	1.5	0.4	0	0.6	0	0	0	0.3
82	25	Ndole	1.5	0	0	1	0	4	4	1.2
83	10	Sumbu	16.2	0.3	0	0	0.7	0	0	0.7
83	6	Sumbu	13.8	0	0	1	0	6	5	1.6
83	7	Sumbu	14.9	0.5	0	0.6	0	2	3	0
83	8	Sumbu	14.6	0	0	1	0	0	0	0
83	9	Sumbu	15.8	1	0	0	0	0	0	-0.1
84	11	Sumbu	16.2	0.2	0	0	0.8	0	0	-0.7
84	12	Sumbu	16.8	0.7	0	0	0.3	0	0	0.1
84	13	Sumbu	17.8	0	0	0	1	0	0	-0.3
84	14	Sumbu	19.8	0.6	0	0	0.4	0	0	-0.1
84	16	Sumbu	20.2	0	0	0	1	0	0	-0.4
85	17	Sumbu	18.3	0.8	0	0	0.2	0	0	-0.4
85	26	Sumbu	15	0	0	1	0	6	4	1.5
85	27	Sumbu	16.9	0.6	0	0.4	0	2	3	-0.5
85	29	Sumbu	17.3	1	0	0	0	0	0	0
85	30	Sumbu	18	1	0	0	0	0	0	-0.6
86	21	Sumbu	15.4	0	0	1	0	6	3	0.5
86	22	Sumbu	16.2	0	0	1	0	5	3	0.9
86	23	Sumbu	16.6	0	0	1	0	1	4	1
86	24	Sumbu	16.8	0	0	1	0	6	3	1
86	25	Sumbu	16.7	0	0	1	0	12	2	0.9
87	17	Sumbu	23.3	0.3	0	0.7	0	14	2	0.3
87	26	Sumbu	23.4	0	0	1	0	8	3	0.8
87	27	Sumbu	22.9	0	0	1	0	9	3	0
87	29	Sumbu	22.8	0	0	1	0	7	3	0.6
87	30	Sumbu	21.5	0.7	0	0.3	0	11	2	0
88	10	Ndole	1.5	0.2	0.1	0.6	0	1	4	0
88	6	Ndole	1.5	0.4	0	0.6	0	5	3	-1.1
88	7	Ndole	1.5	0.3	0	0.7	0	6	3	-0.8
88	8	Ndole	1.5	0.4	0	0.6	0	6	2	-1.2
88	9	Ndole	1.5	0	0.1	0.9	0	7	4	-0.4
89	21	Toby	1	0.4	0.6	0	0	0	0	0.3
89	22	Toby	1	0	1	0	0	0	0	3.8
89	23	Toby	1	0	1	0	0	0	0	2
89	24	Toby	1	0.2	0.8	0	0	0	0	0.6
89	25	Toby	1	0.9	0	0.1	0	5	1	-1
90	26	Toby	1	0.9	0	0	0	1	1	-0.2
90	27	Toby	1	0	0.9	0.1	0	1	3	2.4
90	28	Toby	1	0	1	0	0	0	0	3.4
90	29	Toby	1	0	1	0	0	0	0	2.8
90	30	Toby	1	0.7	0.3	0	0	0	0	2.1
91	21	Toby	1	0	0.3	0.7	0	8	2	2.5
91	22	Toby	1	0	0.3	0.7	0	3	2	2.8
91	23	Toby	1	0	0.2	0.8	0	21	1	1.7
91	24	Toby	1	0.1	0.3	0.6	0	6	2	1.7
91	25	Toby	1	0	0.1	0.9	0	23	1	1.2
92	11	Kaku	17.3	0.9	0	0.1	0	3	1	-0.3
92	12	Kaku	17.6	0.9	0	0.1	0	4	1	-0.1
92	13	Kaku	18.1	0.5	0	0.5	0	12	2	-0.5
92	14	Kaku	18.1	0.2	0	0.8	0	3	3	0.5
92	15	Kaku	18.4	0.8	0	0.3	0	4	2	-0.2
93	21	Kaku	6.7	0.5	0	0.5	0	6	5	-1.2
93	22	Kaku	7	0	0	1	0	20	2	-1.1
93	23	Kaku	7.1	0	0	1	0	27	5	-0.3
93	24	Kaku	7.1	0	0	1	0	1	5	-1
93	25	Kaku	7.2	0.1	0	0.9	0	6	5	-0.3
94	26	Kaku	12.6	0	0	1	0	12	2	-0.5
94	27	Kaku	12.8	0	0	1	0	14	2	-1.2

→ Table continuous on the next page

				Substrate cover (0 – 1)				Rock		
PCT	Cam	Location	Depth	Sand	Vegetation	Rock	Shell	Frequency	Size	HC
94	28	Kaku	13.2	0	0	1	0	17	2	-0.4
94	29	Kaku	15.9	0.1	0	0.9	0	15	2	-0.8
94	30	Kaku	16.2	0.1	0	0.9	0	17	2	-0.2
95	26	Nondwa Point	18.1	0	0	1	0	1	5	1
95	27	Nondwa Point	18.6	0	0	1	0	1	5	1.2
95	28	Nondwa Point	19.3	0	0	1	0	6	5	1
95	29	Nondwa Point	19.7	0.1	0	0.9	0	21	2	1.1
96	11	Nondwa Point	6.6	0	0	1	0	1	5	0.3
96	12	Nondwa Point	6.4	0	0	1	0	1	5	-0.1
96	13	Nondwa Point	8.6	0	0	1	0	1	5	0.6
96	14	Nondwa Point	8.6	0	0	1	0	3	5	0.2
96	15	Nondwa Point	8.4	0	0	1	0	1	5	2.2
97	22	Nondwa Point	16.6	0.5	0	0.5	0	3	5	0.2
97	23	Nondwa Point	16.8	0.5	0	0.5	0	2	3	0.8
97	24	Nondwa Point	16.5	0.5	0	0.5	0	1	5	-0.8
97	25	Nondwa Point	15.3	0	0	1	0	1	5	1.4
98	26	Georges Place	10.9	1	0	0	0	0	0	-0.6
98	27	Georges Place	11	1	0	0	0	0	0	-1
98	28	Georges Place	11	1	0	0	0	0	0	-0.8
98	29	Georges Place	10.9	1	0	0	0	0	0	-0.6
98	30	Georges Place	11	1	0	0	0	0	0	-0.7
99	21	Georges Place	2	1	0	0	0	0	0	-1.5
99	22	Georges Place	1.8	1	0	0	0	0	0	-1.4
99	23	Georges Place	1.7	1	0	0	0	0	0	-1.1
99	24	Georges Place	1.6	1	0	0	0	0	0	-1.5
99	25	Georges Place	1.4	1	0	0	0	0	0	-1.5
100	11	Georges Place	5.4	1	0	0	0	0	0	-1.2
100	12	Georges Place	5.7	1	0	0	0	0	0	-0.7
100	13	Georges Place	6	1	0	0	0	0	0	-1.6
100	14	Georges Place	5.7	1	0	0	0	0	0	-1.5
100	15	Georges Place	5.6	1	0	0	0	0	0	-1.3
101	21	Mwamahunga	6.4	0	0	1	0	16	3	-0.3
101	22	Mwamahunga	5.3	0	0	1	0	5	4	-0.3
101	23	Mwamahunga	5.9	0	0	1	0	3	5	0.3
101	24	Mwamahunga	7	0	0	1	0	4	4	0.1
101	25	Mwamahunga	5	0	0	1	0	12	3	-0.5
102	28	Mwamahunga	18.8	0.8	0	0.2	0	6	2	-1.7
102	29	Mwamahunga	18.5	0.7	0	0.3	0	3	2	-0.3
102	30	Mwamahunga	19.1	0.3	0	0.7	0	14	2	-0.3
103	11	Mwamahunga	29.5	0	0	1	0	17	2	1.3
103	12	Mwamahunga	30.1	0	0	1	0	5	2	0.9
103	13	Mwamahunga	31.1	0	0	1	0	23	2	0.8
103	14	Mwamahunga	32.7	0	0	1	0	7	2	0.9
103	15	Mwamahunga	31.3	0	0	1	0	7	2	0.8
104	21	Kalalangabo	18.4	1	0	0	0	0	0	-1.1
104	22	Kalalangabo	19	1	0	0	0	0	0	-0.9
104	23	Kalalangabo	19	1	0	0	0	0	0	-0.9
104	24	Kalalangabo	18.9	1	0	0	0	0	0	-0.9
104	25	Kalalangabo	18.8	1	0	0	0	0	0	-1.3
105	26	Kalalangabo	12.2	1	0	0	0	0	0	-1.8
105	27	Kalalangabo	11.9	1	0	0	0	0	0	-1.2
105	28	Kalalangabo	12.1	1	0	0	0	0	0	-1.1
105	29	Kalalangabo	12.2	1	0	0	0	0	0	-1.4
105	30	Kalalangabo	12.6	0.4	0	0.6	0	5	2	-0.7
106	11	Kalalangabo	12.5	0	0	1	0	2	5	-1
106	12	Kalalangabo	13.6	0	0	1	0	1	5	-0.7
106	13	Kalalangabo	13.2	0	0	1	0	10	3	-0.9
106	14	Kalalangabo	12.8	0	0	1	0	1	5	-1.5
106	15	Kalalangabo	12.6	0	0	1	0	1	5	-1.1
107	10	Kalalangabo	1	0.1	0	0.9	0	100	1	-1.1
107	6	Kalalangabo	1	0	0	1	0	66	1	-1
108	11	Mwamawimbi	26.4	0.1	0	0.9	0	10	3	0.4
108	12	Mwamawimbi	26.4	0	0	1	0	8	3	-0.1
108	14	Mwamawimbi	27.1	0	0	1	0	39	2	-0.1
108	15	Mwamawimbi	25.9	0	0	1	0	13	3	1
109	26	Mwamawimbi	17.8	1	0	0	0	0	0	-1.3
109	27	Mwamawimbi	17.3	0.7	0	0.3	0	2	3	-1.5
109	28	Mwamawimbi	17.4	1	0	0	0	0	0	-1.5
109	29	Mwamawimbi	17.5	0.6	0	0.4	0	5	3	-1.1
109	30	Mwamawimbi	17.8	1	0	0	0	0	0	-1.6
110	22	Mwamawimbi	5.5	0	0	1	0	14	3	-0.5
110	23	Mwamawimbi	5.9	0.7	0	0.3	0	6	3	-0.9
110	24	Mwamawimbi	6.4	0.7	0	0.3	0	6	3	-0.7
110	25	Mwamawimbi	5.4	0.6	0	0.4	0	8	3	-0.5
111	16	Nondwa Bay	10.6	0	0	1	0	2	4	-1
111	21	Nondwa Bay	9.4	0.1	0	0.9	0	5	3	-1.2
111	23	Nondwa Bay	9.6	0	0	1	0	3	5	-1.2
111	24	Nondwa Bay	8.9	0	0	1	0	2	5	-0.8
111	25	Nondwa Bay	9.2	0	0	1	0	4	5	-0.7
112	10	Nondwa Bay	1	0	0.1	0.9	0	120	1	-1.2
112	6	Nondwa Bay	1	0	1	0	0	0	0	-0.2
112	7	Nondwa Bay	1	0	1	0	0	1	1	0.2
112	8	Nondwa Bay	1	0	1	0	0	0	0	-0.6
112	9	Nondwa Bay	1	0	0	1	0	75	2	-0.8
113	11	Nondwa Bay	17	0.3	0	0.7	0	13	2	-0.1
113	12	Nondwa Bay	16.2	0.1	0	0.9	0	24	2	0
113	13	Nondwa Bay	15.9	0.2	0	0.8	0	6	2	-0.1
113	14	Nondwa Bay	16.2	0.1	0	0.9	0	14	2	-0.2
113	15	Nondwa Bay	16.4	0.1	0	0.9	0	11	3	0.1
114	26	Nondwa Bay	12.2	0	0	1	0	8	2	0.5
114	27	Nondwa Bay	11.8	0	0	1	0	70	2	0.1
114	28	Nondwa Bay	11.8	0	0	1	0	46	2	0.2
114	29	Nondwa Bay	12.2	0.1	0	0.9	0	19	2	0.8
114	30	Nondwa Bay	12.4	0	0	1	0	45	1	0
115	10	Kananive	15.8	0	0	1	0	40	1	-0.9
115	6	Kananive	15.8	0	0	1	0	4	3	-0.9
115	7	Kananive	15.4	0.8	0.1	0.1	0	6	2	-1
115	8	Kananive	15.5	0.1	0	0.9	0	9	3	-0.5
115	9	Kananive	15	1	0	0	0	9	1	-1
116	21	Kananive	7.5	0.3	0	0.7	0	45	1	-1.2
116	22	Kananive	8.8	0.4	0	0.6	0	21	2	-0.9
116	23	Kananive	9.1	0	0	1	0	90	1	-1
116	24	Kananive	9.9	0.7	0	0.3	0	11	2	-1.1
116	25	Kananive	9.4	0.9	0	0.1	0	1	2	-0.9
117	11	Kananive	27.2	0	0	1	0	5	3	0.1
117	12	Kananive	25.8	0.1	0	0.9	0	36	2	-0.4
117	13	Kananive	26.3	1	0	0	0	0	0	-0.7
117	14	Kananive	27	0.7	0	0.3	0	1	2	-0.1
117	15	Kananive	26.9	0.8	0	0.2	0	7	2	-0.6
118	21	Kaku	10.2	0.2	0	0.8	0	11	3	-1
118	22	Kaku	11	0.5	0	0.5	0	37	1	-1.2
118	23	Kaku	11.2	0	0	1	0	39	2	-1.1

→ Table continuous on the next page

				Substrate cover (0 – 1)				Rock		
PCT	Cam	Location	Depth	Sand	Vegetation	Rock	Shell	Frequency	Size	HC
118	24	Kaku	10.6	0	0	1	0	60	2	-1.3
118	25	Kaku	10.3	0	0	1	0	5	3	-1.2
119	26	Kaku	15.6	0.9	0	0.1	0	10	2	-1.2
119	27	Kaku	16	1	0	0	0	0	0	-1.1
119	28	Kaku	16.2	0.3	0	0.7	0	10	2	-0.1
119	29	Kaku	16.2	0.1	0	0.9	0	14	2	-0.2
119	30	Kaku	16.6	0.5	0	0.5	0	10	2	-0.6
120	10	Kaku	17.1	0	0	1	0	6	2	-0.4
120	6	Kaku	19.9	0.8	0	0.3	0	7	2	-0.1
120	7	Kaku	19.6	0	0	1	0	12	2	0.2
120	8	Kaku	18.9	0	0	1	0	13	3	0.3
120	9	Kaku	18.1	0.5	0	0.5	0	11	2	-0.3
121	11	Kaku	1	0	0	1	0	140	1	-0.9
121	12	Kaku	1	0	0	1	0	140	1	-0.8
121	13	Kaku	1	0	0	1	0	140	1	-0.2
121	14	Kaku	1	0	0	1	0	140	1	0
121	15	Kaku	1	0	0	1	0	140	1	-1.2
122	21	Mwamahunga	2.1	0.3	0	0.7	0	12	3	0.2
122	22	Mwamahunga	1.9	0.4	0	0.6	0	40	3	0.1
122	23	Mwamahunga	1.5	0	0	1	0	50	2	-0.5
122	24	Mwamahunga	1.7	0	0	1	0	17	3	0.8
122	25	Mwamahunga	1.5	0.2	0	0.8	0	16	4	1.1
123	26	Mwamahunga	2.7	1	0	0	0	0	0	0.4
123	27	Mwamahunga	2.7	1	0	0	0	0	0	0.5
123	28	Mwamahunga	2.8	1	0	0	0	0	0	0.6
123	29	Mwamahunga	2.8	1	0	0	0	0	0	0.7
123	30	Mwamahunga	2.9	1	0	0	0	0	0	0.7
124	21	Kananive	11.3	1	0	0	0	0	0	-1.6
124	22	Kananive	11.7	1	0	0	0	0	0	-1.4
124	23	Kananive	12	1	0	0	0	0	0	-1.6
124	24	Kananive	12.2	1	0	0	0	0	0	-1.1
124	25	Kananive	12.2	1	0	0	0	0	0	-1.5
125	11	Kananive	7.7	0.9	0	0.1	0	1	2	-0.9
125	12	Kananive	7.7	1	0	0	0	0	0	-1
125	14	Kananive	7.2	1	0	0	0	0	0	-1
125	15	Kananive	7	1	0	0	0	0	0	-0.9
126	10	Kananive	21	0	0	1	0	6	3	0.4
126	6	Kananive	20.4	0.5	0	0.5	0	19	2	-0.9
126	7	Kananive	20.8	0.2	0	0.8	0	23	2	-0.7
126	8	Kananive	20	0.3	0	0.7	0	20	2	-1.1
126	9	Kananive	20.7	0	0	1	0	33	1	-0.4
127	11	Ngania	26	0	0	1	0	3	3	0.6
127	12	Ngania	25.7	0.1	0	0.9	0	8	3	1.1
127	13	Ngania	25.8	1	0	0	0	0	0	-1.6
127	14	Ngania	26.2	0.9	0	0.1	0	5	1	-0.7
127	15	Ngania	26.5	1	0	0	0	0	0	-0.8
128	10	Ngania	15.9	1	0	0	0	0	0	-0.9
128	6	Ngania	16.1	0.1	0	0.9	0	1	5	-0.3
128	7	Ngania	16.9	0	0	1	0	9	3	0.4
128	8	Ngania	15.4	0	0	1	0	1	5	-0.9
128	9	Ngania	16.7	1	0	0	0	0	0	-1
129	21	Ngania	21	0	0	0	0	0	0	0.8
129	22	Ngania	20.2	0.1	0	0.9	0	3	2	-0.3
129	23	Ngania	19.6	0	0	1	0	4	3	0.9
129	24	Ngania	21	1	0	0	0	0	0	-1.4
129	25	Ngania	20.2	0.2	0	0.8	0	10	2	0.6
130	26	Ngania	7.8	0.4	0	0.6	0	6	3	-1
130	27	Ngania	6.9	0	0	1	0	4	3	0.7
130	28	Ngania	6.5	0.2	0	0.8	0	10	3	1
130	29	Ngania	6.5	0	0	1	0	25	3	0.1
130	30	Ngania	6.1	0	0	1	0	22	3	0
131	10	Kalila Nkwasi	18	0	0	1	0	15	3	-0.1
131	6	Kalila Nkwasi	19.7	0.7	0	0.3	0	1	4	-0.5
131	7	Kalila Nkwasi	20.7	0	0	1	0	9	3	1.3
131	8	Kalila Nkwasi	20.4	0	0	1	0	13	2	1
131	9	Kalila Nkwasi	19	0	0	1	0	6	3	0.4
132	21	Kalila Nkwasi	11.7	0	0	1	0	22	3	-1.1
132	22	Kalila Nkwasi	12.3	0	0	1	0	7	3	-0.4
132	23	Kalila Nkwasi	13.1	0	0	1	0	11	3	-0.1
132	24	Kalila Nkwasi	11.6	0	0	1	0	6	3	-0.5
132	25	Kalila Nkwasi	12.6	0	0	1	0	2	2	0.3
133	11	Kalila Nkwasi	29	0.5	0	0.5	0	16	2	-0.4
133	12	Kalila Nkwasi	28.2	0.2	0	0.8	0	15	3	-0.2
133	13	Kalila Nkwasi	28.6	0.3	0	0.7	0	9	2	0.4
133	14	Kalila Nkwasi	29	0.7	0	0.3	0	14	1	0.4
133	15	Kalila Nkwasi	28.4	0.8	0	0.2	0	6	1	-0.2
134	26	Kalila Nkwasi	4.8	0	0	1	0	8	4	0
134	27	Kalila Nkwasi	4	0	0	1	0	9	5	0.2
134	28	Kalila Nkwasi	3.5	0	0	1	0	20	3	-1.2
134	29	Kalila Nkwasi	3.7	0	0	1	0	12	4	-1.3
134	30	Kalila Nkwasi	3.7	0	0	1	0	19	3	-0.9
135	21	Myako	16.4	0.7	0	0.3	0	3	2	-1.3
135	22	Myako	16.6	1	0	0	0	0	0	-1.4
135	23	Myako	16.9	1	0	0	0	0	0	-1.2
135	24	Myako	16.5	0.9	0	0.1	0	1	2	-1.4
135	25	Myako	15.2	1	0	0	0	0	0	-0.8
136	11	Myako	11.8	1	0	0	0	0	0	-0.4
136	12	Myako	11.9	1	0	0	0	0	0	-0.4
136	13	Myako	10.8	1	0	0	0	0	0	-0.7
136	14	Myako	9.2	0.3	0	0.7	0	10	2	-0.9
136	15	Myako	10.4	1	0	0	0	0	0	-1.1
137	10	Myako	5.6	0.3	0	0.7	0	24	1	-0.8
137	6	Myako	5.8	0	0	1	0	35	2	-1
137	7	Myako	5.8	0	0	1	0	50	2	-1.3
137	8	Myako	5.9	0	0	1	0	50	2	-1.3
137	9	Myako	5.7	0.8	0	0.2	0	7	1	-1.4
138	26	Myako	27	0	0	1	0	2	4	0.5
138	27	Myako	28.6	0.5	0	0.5	0	5	4	0.1
138	28	Myako	29.3	0	0	1	0	65	2	1.3
138	29	Myako	31.1	0.9	0	0.1	0	4	2	-1
138	30	Myako	31.8	0.8	0	0.2	0	14	1	-0.7
139	11	Bulu Point	13.4	0	0	1	0	10	2	0.3
139	12	Bulu Point	13.4	0	0	1	0	12	2	0.4
139	13	Bulu Point	11.9	0	0	1	0	9	3	0.7
139	14	Bulu Point	12.8	0	0	1	0	28	2	-0.6
139	15	Bulu Point	12.5	0.2	0	0.8	0	5	3	0.4
140	26	Bulu Point	19.6	0.3	0	0.7	0	8	3	0.8
140	27	Bulu Point	19.5	0.1	0	0.9	0	28	2	0.7
140	28	Bulu Point	19.6	0.1	0	0.9	0	32	2	-0.5
140	29	Bulu Point	19.9	0	0	1	0	10	2	0.9
140	30	Bulu Point	19.1	0	0	1	0	12	3	0.5
141	6	Bulu Point	6.7	0	0	1	0	40	2	-0.7

→ Table continuous on the next page

				Substrate cover (0 – 1)				Rock		
PCT	Cam	Location	Depth	Sand	Vegetation	Rock	Shell	Frequency	Size	HC
141	7	Bulu Point	6.5	0	0	1	0	21	2	-0.9
141	8	Bulu Point	6.8	0	0	1	0	39	2	-1.2
141	9	Bulu Point	6.9	0	0	1	0	16	2	-0.7
142	11	Sibwesa Rocks	15.8	0.1	0	0	0.9	0	0	0.1
142	12	Sibwesa Rocks	15.8	0	0	0	1	0	0	0.5
142	13	Sibwesa Rocks	16	0	0	0	1	0	0	0.4
142	15	Sibwesa Rocks	16.4	0	0	0	1	0	0	0.7
143	6	Sibwesa Rocks	4.3	0	0	1	0	8	4	1.5
143	7	Sibwesa Rocks	3.1	0	0	1	0	19	3	-1
143	8	Sibwesa Rocks	2.8	0	0	1	0	19	3	3.4
143	9	Sibwesa Rocks	1.8	0	0	1	0	9	3	-0.8
144	21	Sibwesa Rocks	7.9	0	0	0	1	0	0	0.6
144	22	Sibwesa Rocks	8.2	0	0	0	1	0	0	-0.2
144	23	Sibwesa Rocks	8.4	0	0	0	1	0	0	-0.4
144	24	Sibwesa Rocks	8.5	0	0	0	1	0	0	-0.5
144	25	Sibwesa Rocks	9.1	0.1	0	0	0.9	0	0	-0.5
145	26	Sibwesa Rocks	7.3	0.2	0	0.4	0.4	2	5	-0.4
145	27	Sibwesa Rocks	5.8	0	0	1	0	19	3	0.2
145	28	Sibwesa Rocks	7.2	0.3	0	0.7	0	13	4	-0.8
145	29	Sibwesa Rocks	6.9	0.9	0	0.1	0	1	2	-0.3
145	30	Sibwesa Rocks	7.3	0.5	0	0.5	0	4	4	0.1
146	10	Msilambula Rocks	6.4	0	0	1	0	18	3	-0.8
146	6	Msilambula Rocks	7.7	0	0	1	0	10	3	-0.8
146	8	Msilambula Rocks	6.2	0	0	1	0	8	3	-0.5
146	9	Msilambula Rocks	6.3	0	0	1	0	11	4	-0.5
147	11	Msilambula Rocks	12.4	0	0	1	0	6	2	-0.4
147	12	Msilambula Rocks	12.6	0	0	1	0	13	2	-0.6
147	13	Msilambula Rocks	13	0	0	1	0	5	3	-0.7
147	14	Msilambula Rocks	12.9	0	0	1	0	7	2	0
147	15	Msilambula Rocks	13	0	0	1	0	6	2	-0.1
148	22	Msilambula Rocks	17.6	0	0	1	0	6	4	0.8
148	23	Msilambula Rocks	18.8	0	0	1	0	12	3	-0.2
148	24	Msilambula Rocks	19.4	0	0	1	0	10	3	1
148	25	Msilambula Rocks	17.9	0	0	1	0	6	2	0.4
149	26	Msilambula Rocks	25.5	0	0	1	0	8	3	0.5
149	27	Msilambula Rocks	25.4	0.8	0	0.2	0	4	2	0.3
149	28	Msilambula Rocks	24.5	0.8	0	0.2	0	2	2	-0.1
149	29	Msilambula Rocks	24	0.2	0	0.8	0	16	3	0.9
149	30	Msilambula Rocks	22.5	0	0	1	0	5	3	0.9
150	26	Cave Kigoma	17	0.2	0	0.8	0	14	2	-0.2
150	27	Cave Kigoma	17	0.9	0	0.1	0	7	2	-0.9
150	28	Cave Kigoma	17.2	1	0	0	0	1	1	-1.1
150	29	Cave Kigoma	17.7	1	0	0	0	1	1	-1.1
150	30	Cave Kigoma	17.4	0.9	0	0.1	0	3	2	-0.9
151	10	Cave Kigoma	16	1	0	0	0	0	0	-0.9
151	6	Cave Kigoma	15.6	1	0	0	0	0	0	-1
151	7	Cave Kigoma	16	1	0	0	0	1	2	-1
151	8	Cave Kigoma	16.3	1	0	0	0	0	0	-0.9
151	9	Cave Kigoma	15.8	1	0	0	0	0	0	-1.1
152	11	Cave Kigoma	6.8	0	0	1	0	1	5	-1.6
152	12	Cave Kigoma	6.9	0	0	1	0	5	5	-1.4
152	13	Cave Kigoma	6.9	0	0	1	0	1	5	-1.5
152	14	Cave Kigoma	6.7	0	0	1	0	1	5	-1.2
152	15	Cave Kigoma	7.4	0.4	0	0.7	0	3	5	-1.4
153	19	Toby	15.4	0.1	0	0.9	0	16	2	-0.2
153	20	Toby	13.9	0.8	0	0.2	0	5	2	-1.2
153	26	Toby	14.3	0	0	1	0	26	2	-0.4
153	28	Toby	14	0.5	0	0.5	0	7	2	-1.1
153	29	Toby	16.5	0.1	0	0.9	0	27	2	-0.1
154	16	Toby	10.5	0	0	1	0	15	2	0.4
154	17	Toby	11.6	0.1	0	0.9	0	21	2	-0.1
154	18	Toby	10.2	0	0	1	0	16	3	-0.3
154	27	Toby	10.2	0	0	1	0	18	3	0.2
154	30	Toby	9.9	0.2	0	0.8	0	5	3	-0.3
155	21	Toby	1.5	0	0.1	0.9	0	24	2	1.3
155	22	Toby	1.5	0	0.2	0.8	0	36	1	0.5
155	23	Toby	1.5	0	0	1	0	29	2	0.3
155	24	Toby	1.5	0	0	1	0	8	3	-0.4
155	25	Toby	1.5	0	0	1	0	74	1	0.4
156	21	Chilesa	18.5	0.5	0	0.5	0	8	3	0
156	22	Chilesa	18.9	0.1	0	0.9	0	7	3	1
156	23	Chilesa	19	0.2	0	0.8	0	20	2	0.6
156	24	Chilesa	19.5	0.4	0	0.7	0	14	2	0.6
156	25	Chilesa	19.1	0.1	0	0.9	0	13	2	0.9
157	11	Chilesa	12.3	0	0	1	0	21	3	1
157	13	Chilesa	12.1	0.2	0	0.8	0	13	2	0.1
157	14	Chilesa	12.3	0.1	0	0.9	0	10	2	0.3
157	15	Chilesa	12.5	0	0	1	0	14	3	0.5
158	16	Chilesa	7.7	0.5	0	0.5	0	15	2	-1.1
158	17	Chilesa	7.2	0.6	0	0.4	0	13	2	-1
158	18	Chilesa	7.5	0.2	0	0.8	0	14	2	-1.2
158	19	Chilesa	7.2	0.1	0	0.9	0	19	2	-1.6
159	21	Kasola Island	20.6	0	0	1	0	9	2	0.9
159	22	Kasola Island	19.9	0	0	1	0	45	1	0.6
159	23	Kasola Island	20.7	0.5	0	0.5	0	9	2	-0.1
159	24	Kasola Island	20.6	0.1	0	0.9	0	26	2	-0.1
159	25	Kasola Island	19.5	0	0	1	0	8	2	0.8
160	16	Kasola Island	12.4	0	0	1	0	1	2	1
160	17	Kasola Island	12.3	0	0	1	0	65	1	1.4
160	18	Kasola Island	12.7	0	0	1	0	2	2	1.8
160	19	Kasola Island	12.7	0	0	1	0	6	2	0.9
160	20	Kasola Island	12.5	0	0	1	0	5	3	1
161	26	Kasola Island	29.5	0.3	0	0.7	0	3	3	0.7
161	27	Kasola Island	30.1	0	0	1	0	39	2	-0.3
161	28	Kasola Island	30.8	0.1	0	0.9	0	15	2	-0.2
161	29	Kasola Island	29.5	0	0	1	0	14	2	0.1
161	30	Kasola Island	27.9	0	0	1	0	8	3	0.2
162	10	Kasola Island	4.8	0	0	1	0	9	4	0.9
162	11	Kasola Island	4.7	0	0	1	0	16	3	0.4
162	13	Kasola Island	4.8	0	0	1	0	9	2	0.5
162	14	Kasola Island	4.6	0	0	1	0	11	3	1.5
162	15	Kasola Island	4.9	0	0	1	0	23	3	0.2
163	16	Liuli	15.2	1	0	0	0	0	0	-1.2
163	17	Liuli	15	1	0	0	0	0	0	-1.4
163	18	Liuli	15.1	1	0	0	0	0	0	-1.7
163	19	Liuli	16.4	0.6	0	0.4	0	1	5	0
163	20	Liuli	15.4	0.8	0	0.2	0	1	4	-0.9
164	26	Liuli	11	0.9	0	0.1	0	1	2	-1.4
164	27	Liuli	10.7	1	0	0	0	0	0	-0.9
164	29	Liuli	10.6	1	0	0	0	0	0	-1.4
164	30	Liuli	10.6	1	0	0	0	0	0	-1.3
165	21	Liuli	4.9	0	0	1	0	14	3	-0.1

→ Table continuous on the next page

				Substrate cover (0 – 1)				Rock		
PCT	Cam	Location	Depth	Sand	Vegetation	Rock	Shell	Frequency	Size	HC
165	22	Liuli	5.5	0	0	1	0	1	2	0.1
165	23	Liuli	5.2	0	0	1	0	2	5	-0.4
165	24	Liuli	5.3	0	0	1	0	2	4	-0.3
165	25	Liuli	5.3	0	0	1	0	1	5	-0.7
166	10	Liuli	21	1	0	0	0	0	0	-0.3
166	11	Liuli	21.9	1	0	0	0	0	0	-0.7
166	13	Liuli	22.7	1	0	0	0	0	0	-0.6
166	14	Liuli	22.5	0.8	0	0.2	0	1	4	-0.8
166	15	Liuli	22.8	0.9	0	0.1	0	1	2	-1
167	21	Tanganyika village	20.3	0.9	0	0.1	0	1	3	0
167	22	Tanganyika village	20.2	1	0	0	0	0	0	-0.6
167	23	Tanganyika village	20.3	1	0	0	0	0	0	-0.6
167	24	Tanganyika village	20.5	1	0	0	0	0	0	0.1
167	25	Tanganyika village	20.5	1	0	0	0	0	0	0
168	16	Tanganyika village	5.7	0	0	1	0	2	5	-0.7
168	17	Tanganyika village	4.9	0	0	1	0	1	4	0.1
168	18	Tanganyika village	5.6	0.1	0	0.8	0	4	3	-0.2
168	19	Tanganyika village	4.8	0	0	1	0	2	5	-0.3
168	20	Tanganyika village	5.7	0	0	1	0	1	2	1.7
169	11	Tanganyika village	9.1	0	0	1	0	2	5	-1.5
169	13	Tanganyika village	10	0.5	0	0.4	0.1	4	3	-1.2
169	14	Tanganyika village	11.2	0	0	1	0	1	5	-1
169	15	Tanganyika village	11.4	1	0	0	0	0	0	-1.3
170	26	Tanganyika village	13.7	1	0	0	0.1	0	0	-0.9
170	27	Tanganyika village	13.7	1	0	0	0	0	0	-1
170	28	Tanganyika village	12.5	0.1	0	0.1	0.8	1	3	-1
170	29	Tanganyika village	13.3	1	0	0	0	0	0	-1.1
170	30	Tanganyika village	13.1	0.7	0	0.2	0.1	1	4	-0.9
171	10	Myuna	18.8	0.4	0	0.6	0	1	5	-0.4
171	11	Myuna	19.1	0	0	1	0	8	4	0.3
171	13	Myuna	19.7	0.1	0	0.9	0	15	3	0.5
171	14	Myuna	19.7	0	0	1	0	7	4	1.9
171	15	Myuna	20.7	0	0	1	0	5	4	1.8
172	16	Myuna	12.7	0	0	1	0	5	4	0.9
172	17	Myuna	13.6	0	0	1	0	7	4	2.1
172	18	Myuna	13.5	0.5	0	0.5	0	11	3	-0.9
172	19	Myuna	11.5	0	0	1	0	5	4	0.1
172	20	Myuna	12	0.3	0	0.7	0	4	3	-0.3
173	21	Myuna	28.6	0	0	1	0	16	3	1.1
173	22	Myuna	27.9	0	0	1	0	8	4	2.2
173	23	Myuna	27.2	0	0	1	0	2	5	0
173	24	Myuna	28.5	0.3	0	0.7	0	5	4	-0.1
173	25	Myuna	27.3	0	0	1	0	10	3	2.1
174	26	Myuna	7.3	0	0	1	0	7	4	0.9
174	27	Myuna	7.5	0	0	1	0	10	3	-0.2
174	28	Myuna	7.2	0	0	1	0	4	4	-0.7
174	29	Myuna	5.3	0	0	1	0	12	3	-0.8
174	30	Myuna	6.1	0	0	1	0	10	3	0
175	16	Korongwe	12.1	0	0	1	0	3	4	1.3
175	17	Korongwe	11.3	0	0	1	0	3	4	0.4
175	18	Korongwe	10.9	0	0	1	0	1	5	0.1
175	19	Korongwe	12.6	0	0	1	0	4	5	1
175	20	Korongwe	15.1	0	0	1	0	3	4	1.7
176	10	Korongwe	5.1	0	0	1	0	1	5	0
176	11	Korongwe	6.9	0	0	1	0	5	4	1.4
176	13	Korongwe	7	0	0	1	0	3	3	0.5
176	14	Korongwe	4.4	0	0	1	0	3	5	0.5
176	15	Korongwe	3.7	0	0	1	0	5	4	0.3
177	26	Korongwe	22.5	0	0	1	0	2	5	1
177	27	Korongwe	22.9	0	0	1	0	6	4	-0.1
177	29	Korongwe	26.1	0.3	0	0.7	0	3	5	0.8
177	30	Korongwe	26.7	0	0	1	0	3	5	2.3
178	27	Utinta	10.3	0.1	0	0	0.9	0	0	-0.2
178	28	Utinta	10.1	0	0	0	1	0	0	-0.7
178	29	Utinta	10.1	0.2	0	0	0.8	0	0	-0.5
178	30	Utinta	10.3	0	0	0	1	0	0	0
179	16	Utinta	5	0.8	0	0.2	0	2	3	-1.5
179	17	Utinta	5.1	1	0	0	0	0	0	-1.6
179	18	Utinta	4.9	1	0	0	0	0	0	-1.5
179	19	Utinta	5.4	1	0	0	0	0	0	-1.7
179	20	Utinta	5.3	1	0	0	0	0	0	-1.1
180	21	Utinta	14.9	0	0	0	1	0	0	0.6
180	22	Utinta	14.9	0	0	0	1	0	0	0.3
180	23	Utinta	14.9	0	0	0	1	0	0	0.3
180	24	Utinta	14.9	0.5	0	0	0.5	0	0	0.1
180	25	Utinta	14.9	0.5	0	0	0.5	0	0	-0.2
181	10	Kasowo	1.8	0.3	0	0.7	0	25	2	-0.7
181	11	Kasowo	1.3	0.1	0	0.9	0	157	1	-0.9
181	13	Kasowo	1.3	0.4	0	0.6	0	32	2	-0.3
181	14	Kasowo	1.3	0	0	1	0	31	2	-0.6
181	15	Kasowo	1.6	0.5	0	0.5	0	16	2	-1.1
182	26	Kasowo	6	1	0	0	0	0	0	-1.4
182	27	Kasowo	6.1	1	0	0	0	0	0	-1.5
182	28	Kasowo	6.2	1	0	0	0	0	0	-1.7
182	29	Kasowo	6.3	1	0	0	0	0	0	-1.5
182	30	Kasowo	6.3	1	0	0	0	0	0	-1.6
183	16	Kasowo	17.9	1	0	0	0	0	0	-0.8
183	17	Kasowo	17.8	1	0	0	0	0	0	-0.4
183	18	Kasowo	18	1	0	0	0	0	0	-0.6
183	19	Kasowo	18.1	1	0	0	0	0	0	-0.6
183	20	Kasowo	18.4	1	0	0	0	0	0	-0.6
184	21	Kasowo	9.9	1	0	0	0	0	0	-0.8
184	22	Kasowo	9.5	1	0	0	0	0	0	-0.9
184	23	Kasowo	9.5	1	0	0	0	0	0	-1.2
184	24	Kasowo	9.5	1	0	0	0	0	0	-1.1
184	25	Kasowo	9.2	1	0	0	0	0	0	-1
185	21	Nkondwe	10.7	0	0	1	0	10	3	0.8
185	22	Nkondwe	11.1	0	0	0.3	0.7	8	2	0.9
185	23	Nkondwe	11.1	0.3	0	0.7	0.1	14	3	-0.2
185	24	Nkondwe	10.2	0	0	1	0	10	4	0.8
186	10	Nkondwe	15.4	0.1	0	0.9	0	2	4	0.1
186	11	Nkondwe	15.3	0.4	0	0.6	0	8	3	-0.4
186	13	Nkondwe	15.5	0	0	0.8	0.2	6	3	0.5
186	14	Nkondwe	15.4	0	0	1	0	36	2	-0.3
186	15	Nkondwe	15.5	0.2	0	0.7	0.1	6	3	0.2
187	26	Nkondwe	1.9	0.1	0	0.9	0	34	2	-0.9
187	27	Nkondwe	2.2	0.1	0	0.9	0	30	2	-0.6
187	28	Nkondwe	2.3	0.2	0	0.8	0	38	2	0.3
187	29	Nkondwe	2.1	0	0	1	0	19	2	-0.9
187	30	Nkondwe	2.1	0	0	1	0	32	3	0.9
188	16	Nkondwe	25.9	0.4	0	0.6	0	11	2	1.2
188	17	Nkondwe	25	0.8	0	0.2	0	6	2	0.5

→ Table continuous on the next page

				Substrate cover (0 – 1)				Rock		
PCT	Cam	Location	Depth	Sand	Vegetation	Rock	Shell	Frequency	Size	HC
188	18	Nkondwe	25.1	0	0	0	1	1	1	0.8
188	19	Nkondwe	25.1	0.8	0	0.2	0	4	2	0.7
188	20	Nkondwe	23.9	0	0	1	0	3	3	0.9
189	10	Ulwile 5	10.5	0	0	1	0	11	3	0
189	11	Ulwile 5	12.7	0.7	0	0.3	0	2	3	-0.6
189	13	Ulwile 5	11.8	0.7	0	0.3	0	6	2	-1.1
189	14	Ulwile 5	11.5	0	0	1	0	1	5	-1
189	15	Ulwile 5	12.2	1	0	0	0	0	0	-1.3
190	21	Ulwile 5	16.3	0.5	0	0.5	0	2	4	-0.4
190	22	Ulwile 5	16.2	1	0	0	0	0	0	-0.9
190	23	Ulwile 5	15.6	0.5	0	0.5	0	8	4	0.3
190	24	Ulwile 5	15.5	0.8	0	0.2	0	1	3	-0.1
190	25	Ulwile 5	17.1	0.3	0	0.7	0	2	4	0
191	16	Ulwile 5	6.5	0.5	0	0.5	0	4	3	0.3
191	17	Ulwile 5	5.8	0	0	1	0	3	5	-0.5
191	18	Ulwile 5	5.2	0	0	1	0	7	4	-0.4
191	19	Ulwile 5	6.1	0	0	1	0	10	4	0
192	26	Ulwile 5	26	0	0	1	0	14	4	0.9
192	27	Ulwile 5	24.6	0	0	1	0	11	3	1.7
192	28	Ulwile 5	25.1	0	0	1	0	3	3	1.6
192	29	Ulwile 5	24.6	0	0	1	0	5	3	1.7
192	30	Ulwile 5	24.5	0	0	1	0	7	3	0.9
193	21	Twivu	12	0	0	1	0	3	4	0.7
193	22	Twivu	9.3	0	0	1	0	2	4	0.5
193	23	Twivu	9	0	0	1	0	1	5	-0.9
193	24	Twivu	10.9	0.6	0	0.4	0	2	3	-0.6
193	25	Twivu	8.1	0	0	1	0	2	4	-0.6
194	26	Twivu	18.3	1	0	0	0	0	0	-1.1
194	27	Twivu	18.2	1	0	0	0	0	0	-1.3
194	28	Twivu	18.1	1	0	0	0	0	0	-1
194	29	Twivu	18.4	1	0	0	0	0	0	-0.7
194	30	Twivu	18.1	1	0	0	0	0	0	-1
195	10	Twivu	3.3	0	1	0	0	0	0	1.3
195	11	Twivu	4.2	0.6	0.4	0	0	0	0	-0.3
195	13	Twivu	4.8	0.2	0.8	0	0	0	0	-0.7
195	14	Twivu	6	1	0	0	0	0	0	-0.6
195	15	Twivu	6.7	1	0	0	0	0	0	-0.9
196	16	Twivu	22.9	0	0	1	0	4	5	2.1
196	17	Twivu	22.7	0.2	0	0.8	0	3	5	1.2
196	18	Twivu	23.4	0	0	1	0	5	5	1.5
196	19	Twivu	24.5	0	0	1	0	2	5	0.6
196	20	Twivu	26	0.7	0	0.3	0	4	2	-0.6
197	21	Fulwe	14.6	0	0	1	0	2	4	0.7
197	22	Fulwe	14.2	0	0	1	0	5	4	1.2
197	23	Fulwe	13.8	0	0	1	0	4	4	1.5
197	24	Fulwe	13.7	0	0	1	0	6	4	1.6
197	25	Fulwe	15.4	0	0	1	0	8	3	1.5
198	10	Fulwe	8.2	0	0	1	0	2	5	1.3
198	11	Fulwe	7.5	0	0	1	0	4	4	1.2
198	13	Fulwe	8.1	0	0	1	0	2	4	-0.6
198	14	Fulwe	7	0	0	1	0	1	5	0.1
198	15	Fulwe	8.1	0	0	1	0	2	5	0.9
199	26	Fulwe	28.3	0	0	1	0	14	2	2.1
199	27	Fulwe	28.3	0	0	1	0	16	2	2.2
199	28	Fulwe	28.5	0	0	1	0	6	4	2.2
199	29	Fulwe	27.7	0	0	1	0	23	2	1.7
199	30	Fulwe	28	0.9	0	0.1	0	1	2	0.6
200	16	Fulwe	17.9	0	0	1	0	22	2	1.1
200	17	Fulwe	17.9	0	0	1	0	28	2	1.2
200	18	Fulwe	17.3	0	0	1	0	8	3	1.2
200	19	Fulwe	17.7	0	0	1	0	16	2	1.2
200	20	Fulwe	19.1	0	0	1	0	9	3	1.5
201	10	Malasa Island	10.4	0	0	1	0	7	3	-1
201	11	Malasa Island	10	0	0	1	0	11	2	-1
201	13	Malasa Island	10.5	0	0	1	0	5	2	-0.3
201	14	Malasa Island	9.9	0	0	1	0	12	2	-0.7
201	15	Malasa Island	10.7	0	0	1	0	5	3	-0.9
202	16	Malasa Island	1.6	0	0	1	0	102	1	-0.4
202	17	Malasa Island	1.5	0	0	1	0	44	2	0.6
202	18	Malasa Island	1.6	0	0	1	0	18	3	0.1
202	19	Malasa Island	1.7	0.1	0	0.9	0	41	2	1.3
202	20	Malasa Island	1.5	0	0	1	0	21	2	0.3
203	26	Malasa Island	28.1	0	0	1	0	15	2	-0.3
203	27	Malasa Island	28.1	0.2	0	0.8	0	29	2	0
203	28	Malasa Island	28.2	0	0	1	0	14	2	0.4
203	29	Malasa Island	28.5	0.1	0	0.9	0.1	14	2	0.7
203	30	Malasa Island	28.2	0.1	0	0.9	0	21	2	-0.3
204	21	Malasa Island	16.9	0	0	1	0	29	2	-0.5
204	22	Malasa Island	17.5	0	0	1	0	13	2	-0.6
204	23	Malasa Island	17.3	0	0	1	0	22	2	-0.6
204	24	Malasa Island	17.1	0.1	0	0.9	0	6	2	0
204	25	Malasa Island	16.9	0	0	1	0	13	2	-0.2
205	10	Szamasi	16.8	0	0	1	0	6	2	1.1
205	11	Szamasi	16.9	0	0	1	0	13	3	0.6
205	13	Szamasi	16.6	0	0	1	0	8	2	0.9
205	14	Szamasi	16.2	0	0	1	0	10	3	1.3
205	15	Szamasi	15.4	0	0	1	0	7	3	0.8
206	26	Szamasi	27.8	0	0	1	0	8	3	1
206	28	Szamasi	27.8	0	0	1	0	8	3	0.1
206	29	Szamasi	27.2	0	0	1	0	12	3	1
206	30	Szamasi	26.7	0	0	1	0	8	3	0.9
206	8	Szamasi	27.9	0.1	0	0.9	0	10	3	1
207	16	Szamasi	11.6	0	0	0	0	0	0	0.9
207	17	Szamasi	11.4	0	0	1	0	3	2	0.9
207	18	Szamasi	12	0	0	1	0	8	2	1
207	19	Szamasi	11.2	0	0	1	0	4	2	1.1
207	20	Szamasi	11.2	0	0	1	0	7	3	1.1
208	21	Szamasi	6.6	0	0	1	0	12	3	0.8
208	22	Szamasi	7.3	0	0	1	0	2	3	1.3
208	23	Szamasi	6.6	0	0	0	0	0	0	1.6
208	24	Szamasi	6.5	0	0	1	0	3	3	0.6
208	25	Szamasi	6.4	0	0	1	0	11	3	2.2

Table S6: List of different habitat types with a camera count along the depth gradient (in 5 m steps) with the dominant (most abundant) species in that habitat (irrespective of depth, colour-coded for tribe). Definition shows what parameters were considered to assign type.

Habitat (Definition)	**Count** (cameras) over depth (m)								**Top 5 species**	
	0	5	10	15	20	25	30	35		
Vegetation (veg > 75%)	15	9	-	-	-	-	-	-	*Ctenochromis horii*	28
									Aulonocranus dewindti	23
									Perissodus microlepis	19
									Limnotilapia dardennii	18
									Simochromis diagramma	18
Rock (rock > 75%)	45	108	82	93	59	38	30	6	*Paracyprichromis brieni*	1'551
									Neolamprologus brichardi	649
									Limnotilapia dardennii	640
									Lepidiolamprologus elongatus	574
									Lamprologus callipterus	408
Intermediate (rock < 75% & sand < 75%)	22	21	21	32	22	9	6	-	*Lamprologus callipterus*	203
									Xenotilapia boulengeri	188
									Limnotilapia dardennii	161
									Lepidiolamprologus attenuates	159
									Neolamprologus walteri	104
Sand (sand > 75%)	9	41	44	48	47	23	4	-	*Grammatotria lemairii*	280
									Xenotilapia batiyphylus	201
									Xenotilapia flavipinnis	187
									Limnotilapia dardennii	181
									Lepidiolamprologus attenuates	168
Shell (shell > 75%)	-	-	9	22	2	1	-	-	*Neolamprologus multifasciatus*	67
									Neolamprologus brevis	51
									Neolamprologus meeli	48
									Lamprologus callipterus	43
									Grammatotria lemairii	39

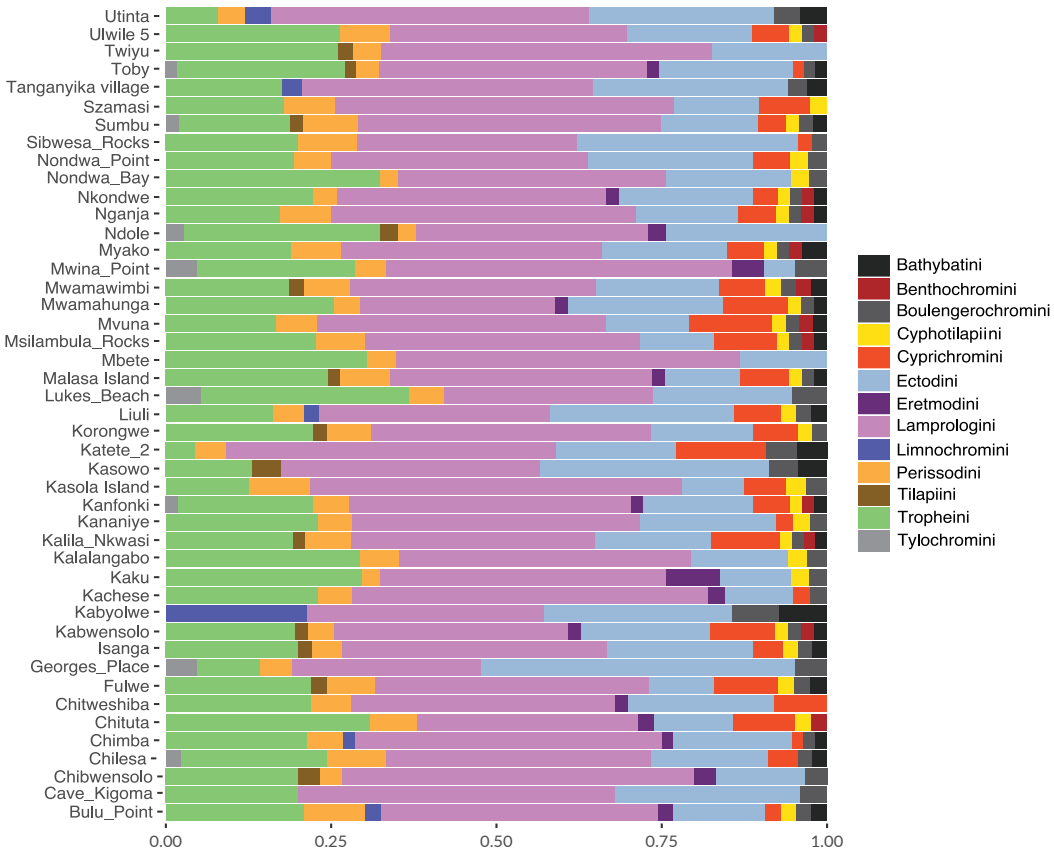

Figure S7: Proportional contribution of tribes to the species richness at the sampling sites at Lake Tanganyika.

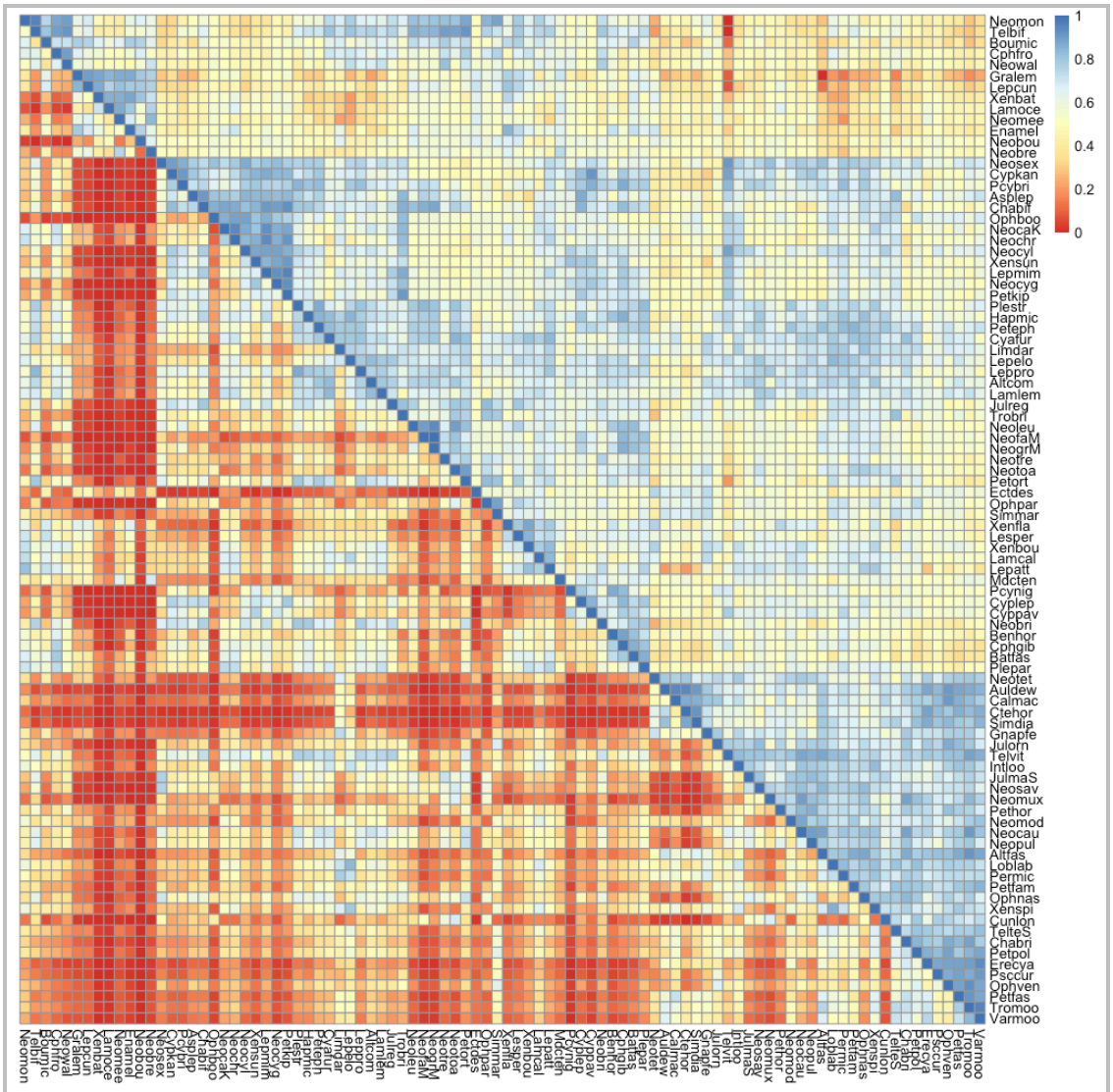

Figure S8: Heatmap of rescaled co-occurrence SES (0 = segregation, 1 = aggregation, upper triangle) and niche overlap D (0 = no overlap, 1 = complete overlap, lower triangle). Species are clustered based on their co-occurrence.

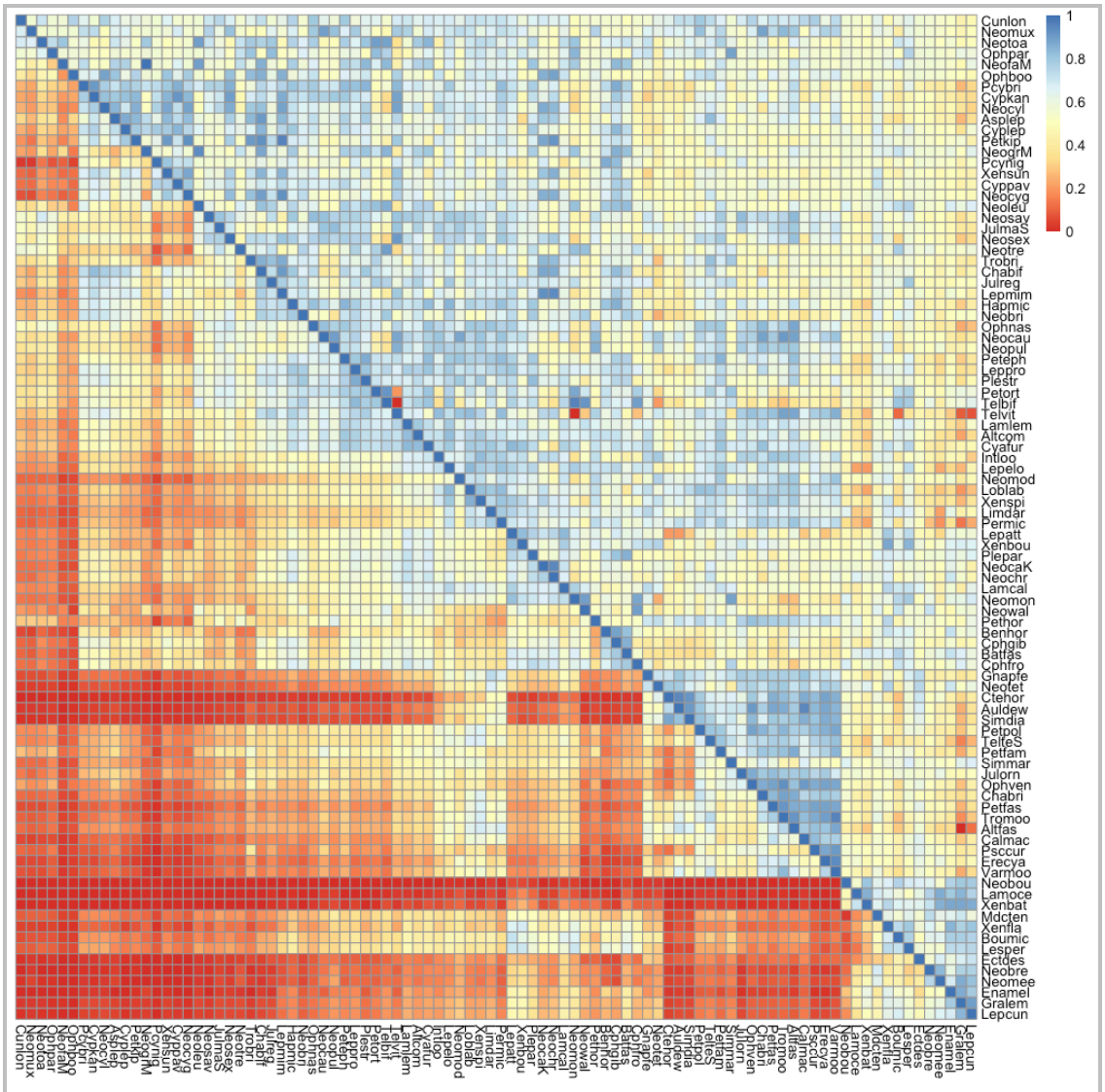

Figure S9: Heatmap of rescaled co-occurrence SES (0 = segregation, 1 = aggregation, upper triangle) and niche overlap D (0 = no overlap, 1 = complete overlap, lower triangle). Species are clustered based on their niche overlap D.

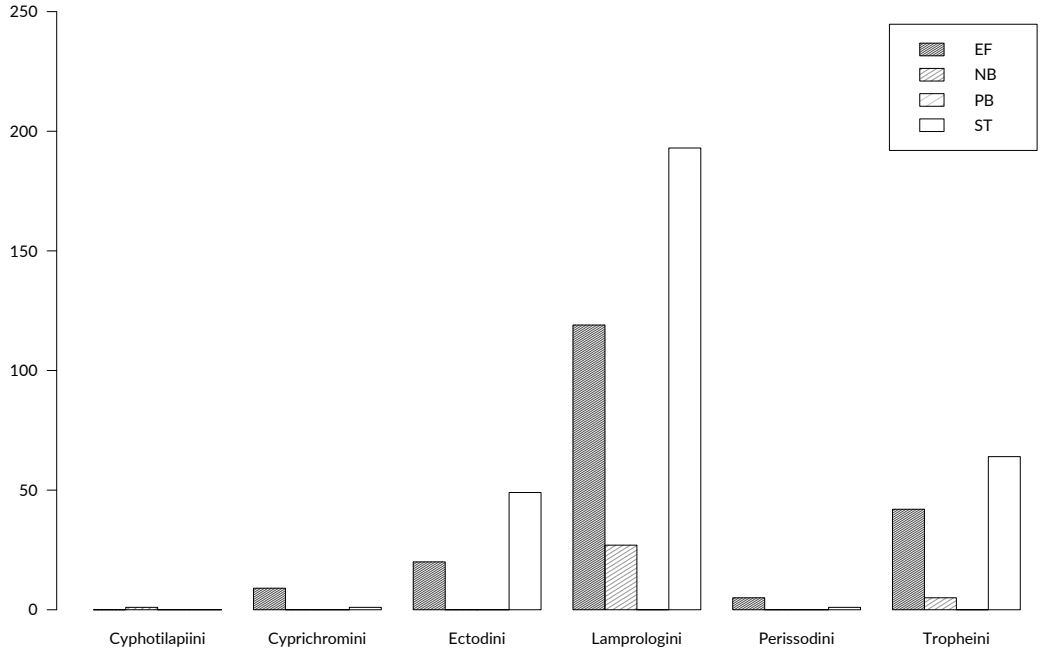

Figure S10: Results of co-occurrences analysis by 2-step approach of Kohli et al. (2018). Barplot of the process likely responsible for co-occurrence patterns of species-pairs from within the same tribe. EF = Environmental filtering, NB = Negative biotic interaction, PB = Positive biotic interaction, ST = Stochastic processes.

Table S11: Result of tribe-wise mantel tests of niche overlap D and relatedness.

	Cyphotilapiini	Cyprichromini	Ectodini	Lamprologini	Perissodini
p-value	1.00	0.32	0.09	*0.02*	0.92
z-statistic	0.01	1.21	12.90	*98.91*	0.13

Table S12: List of mean Area Under Curve (AUC) values of the four replicates of ENM of each species with more than 15 occurrence points. Values for features as default by MaxEnt.

Species ID	AUC	Linear	Categorical	Threshold	Hinge
Altcom	0.748	0.05	0.25	1	0.5
Altfas	0.786	0.05	0.25	1	0.5
Asplep	0.86575	0.20475	0.25	1.5425	0.5
Auldew	0.8935	0.1425	0.25	1.325	0.5
Batfas	0.77925	0.14925	0.25	1.3475	0.5
Benhor	0.86525	0.586	0.321	1.85	0.5
Boumic	0.70175	0.05	0.25	1	0.5
Calmac	0.8385	0.207	0.25	1.55	0.5
Chabif	0.82775	0.156	0.25	1.37	0.5
Chabri	0.82525	0.139	0.25	1.31	0.5
Cphfro	0.81275	0.22175	0.25	1.6025	0.5
Cphgib	0.85025	0.1325	0.25	1.115	0.5
Ctehor	0.9085	0.17075	0.25	1.4225	0.5
Cunlon	0.8405	0.714	0.429	1.88	0.5
Cyafur	0.75725	0.05	0.25	1	0.5
Cypkan	0.83325	0.113	0.25	1.22	0.5
Cyplep	0.847	0.24775	0.25	1.6925	0.5
Cyppav	0.90575	0.423	0.25	1.79	0.5
Ectdes	0.9305	0.61825	0.348	1.8575	0.5
Enamel	0.87425	0.2025	0.25	1.535	0.5
Erecya	0.91775	0.2285	0.25	1.625	0.5
Gnapfe	0.71825	0.05	0.25	1	0.5
Gralem	0.8305	0.05	0.25	1	0.5
Hapmic	0.7545	0.05	0.25	1	0.5
Intloo	0.78925	0.1535	0.25	1.145	0.5
JulmaS	0.8505	0.3945	0.25	1.775	0.5
Julorn	0.735	0.65	0.375	1.865	0.5
Julreg	0.76575	0.21825	0.25	1.5875	0.5
Lamcal	0.664	0.05	0.25	1	0.5
Lamlem	0.74175	0.113	0.25	1.22	0.5
Lamoce	0.906	0.24775	0.25	1.6925	0.5
Lepatt	0.6895	0.05	0.25	1	0.5
Lepcun	0.83625	0.1105	0.25	1.085	0.5
Lepelo	0.663	0.05	0.25	1	0.5
Lepmim	0.789	0.19675	0.25	1.5125	0.5
Leppro	0.76575	0.08425	0.25	1.0475	0.5
Lesper	0.71925	0.2005	0.25	1.5275	0.5
Limdar	0.63325	0.05	0.25	1	0.5
Loblab	0.699	0.05	0.25	1	0.5
Mdcten	0.763	0.5215	0.268	1.835	0.5
Neobou	0.922	0.49525	0.25	1.8275	0.5
Neobre	0.8895	0.46675	0.25	1.8125	0.5
Neobri	0.767	0.113	0.25	1.22	0.5
NeocaK	0.80425	0.40875	0.25	1.7825	0.5
Neocau	0.80825	0.21375	0.25	1.5725	0.5
Neochr	0.776	0.20925	0.25	1.5575	0.5
Neocyg	0.82625	0.714	0.429	1.88	0.5
Neocyl	0.80025	0.1855	0.25	1.475	0.5
NeofaM	0.859	0.714	0.429	1.88	0.5
NeogrM	0.77775	0.74625	0.45525	1.8875	0.5
Neoleu	0.817	0.586	0.321	1.85	0.5
Neomee	0.91675	0.22	0.25	1.595	0.5
Neomod	0.77825	0.1945	0.25	1.505	0.5
Neomon	0.77275	0.057	0.25	1.01	0.5
Neomux	0.83425	0.65	0.375	1.865	0.5
Neopul	0.817	0.19225	0.25	1.4975	0.5
Neosav	0.82375	0.1795	0.25	1.4525	0.5
Neosex	0.793	0.19	0.25	1.49	0.5
Neotet	0.74275	0.05	0.25	1	0.5
Neotoa	0.82475	0.586	0.321	1.85	0.5
Neotre	0.79725	0.714	0.429	1.88	0.5
Neowal	0.867	0.22175	0.25	1.6025	0.5
Ophboo	0.92475	0.714	0.429	1.88	0.5
Ophnas	0.81775	0.073	0.25	1.0325	0.5
Ophpar	0.82425	0.61825	0.348	1.8575	0.5
Ophven	0.882	0.21375	0.25	1.5725	0.5
Oretan	0.848	0.308	0.25	1.73	0.5
Pcybri	0.84325	0.05	0.25	1	0.5
Pcynig	0.93675	0.714	0.429	1.88	0.5
Permic	0.6685	0.05	0.25	1	0.5
Peteph	0.76125	0.05	0.25	1	0.5
Petfam	0.84575	0.13775	0.25	1.1225	0.5
Petfas	0.8645	0.1345	0.25	1.295	0.5
Pethor	0.6845	0.68175	0.402	1.8725	0.5
Petkip	0.86675	0.38	0.25	1.7675	0.5
Petort	0.7855	0.23525	0.25	1.6475	0.5
Petpol	0.83125	0.19125	0.25	1.1975	0.5
Plepar	0.684	0.293	0.25	1.7225	0.5
Plestr	0.7605	0.17075	0.25	1.4225	0.5
Psccur	0.89925	0.46675	0.25	1.8125	0.5
Simdia	0.9015	0.16625	0.25	1.4075	0.5
Simmar	0.8305	0.68175	0.402	1.8725	0.5
Telbif	0.807	0.05	0.25	1	0.5
TelteS	0.79225	0.05	0.25	1	0.5
Telvit	0.7405	0.05	0.25	1	0.5
Trobri	0.83725	0.18775	0.25	1.4825	0.5
Tromoo	0.838	0.05	0.25	1	0.5
Tylpol	0.871	0.43725	0.25	1.7975	0.5
Varmoo	0.9015	0.16	0.25	1.385	0.5
Xenbat	0.88925	0.1515	0.25	1.355	0.5
Xenbou	0.73425	0.05	0.25	1	0.5
Xenfla	0.80875	0.14825	0.25	1.1375	0.5
Xenspi	0.7235	0.05	0.25	1	0.5
Xensun	0.86275	0.2395	0.25	1.6625	0.5

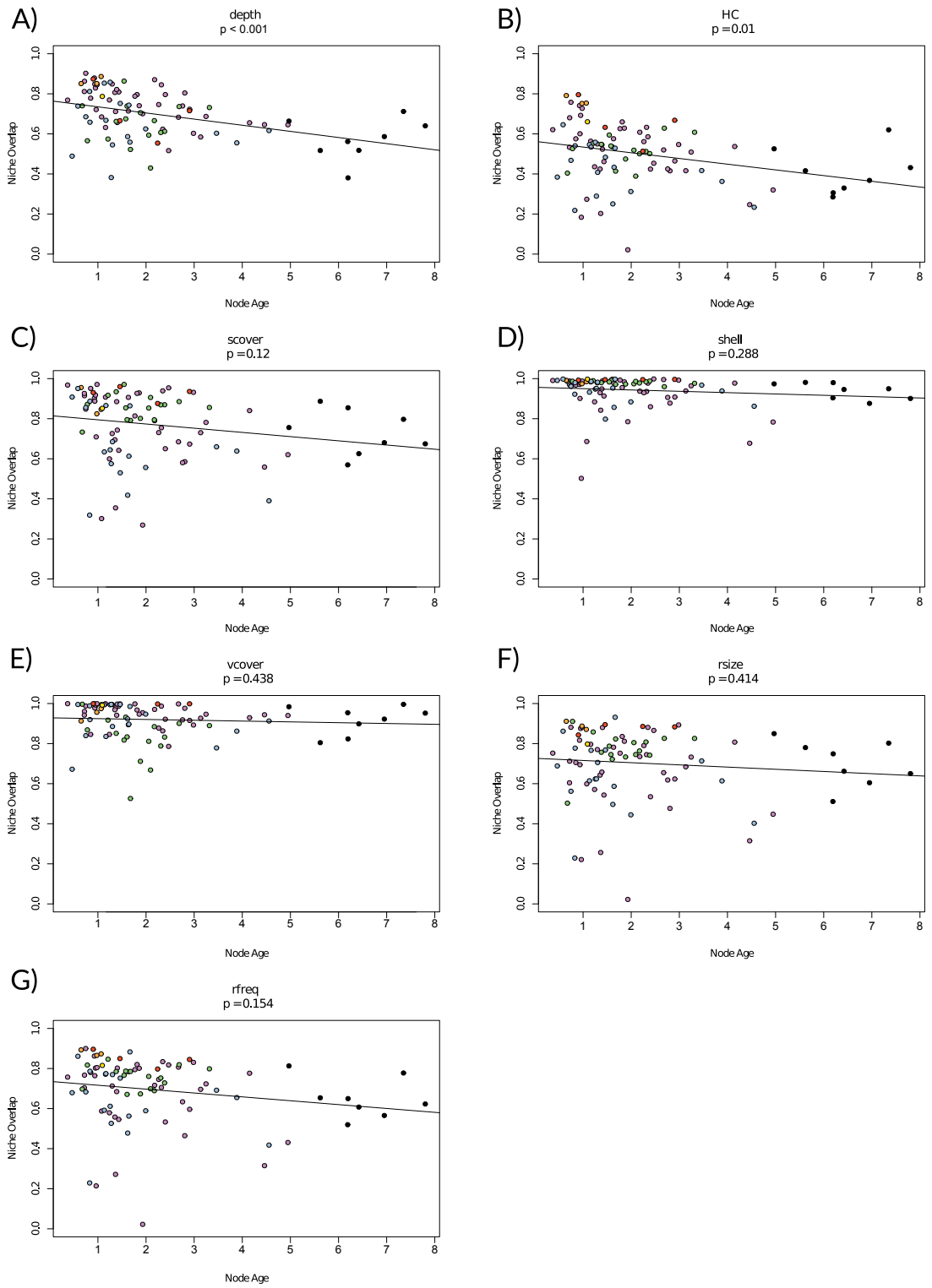

Figure S13A-G: Age-range-correlations between all species and overlap in single environmental axes, p-value is indicated below the identifier of the environmental variables (nodes are coloured if all tips belong to single tribe).

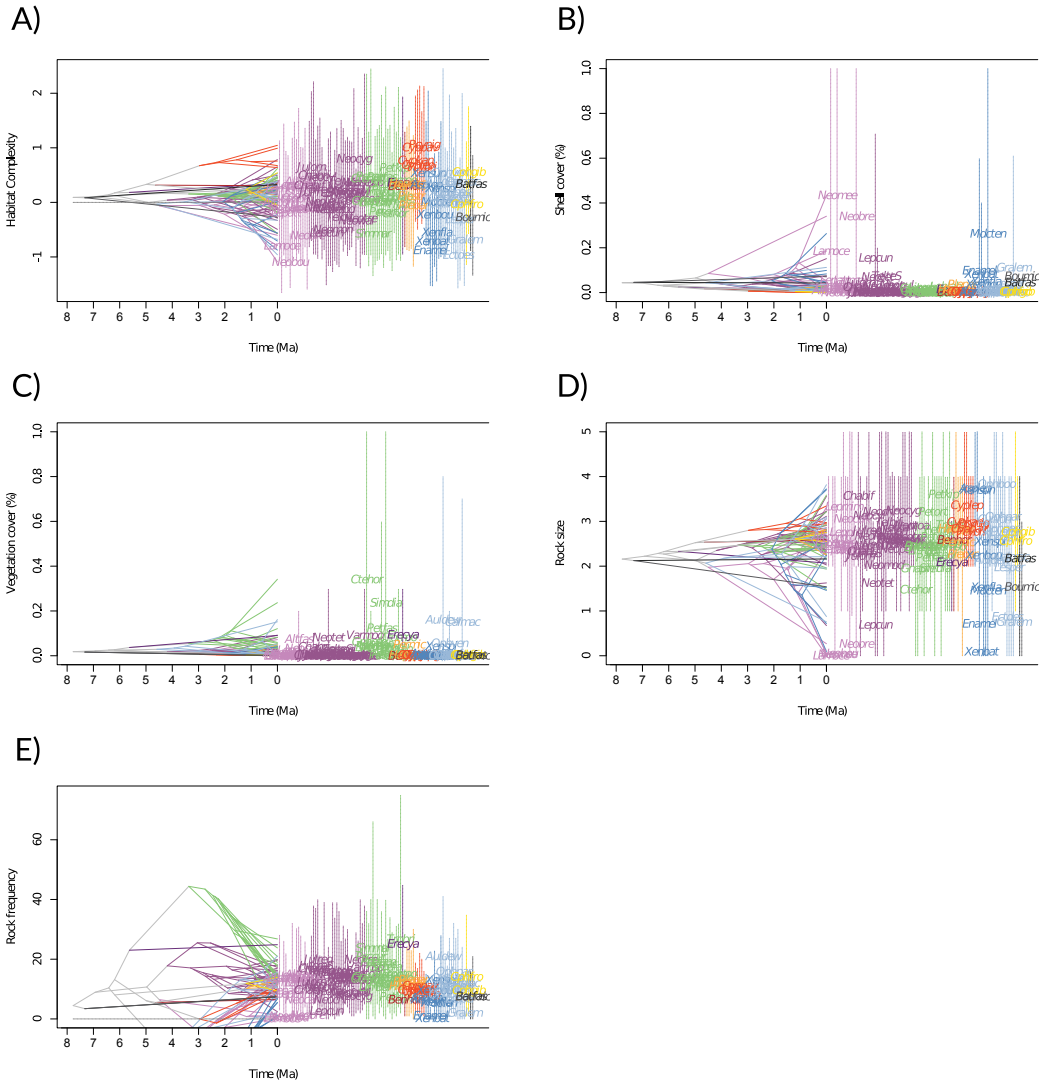

Figure S14A-E: Ancestral niche reconstruction based on maximum likelihood estimates for each environmental variable at every interior node were calculated assuming Brownian motion and by randomly resampling 1'000 times from each taxa's PNO.

Table S15: Phylogenetic signal of the entire cichlid species-flock of Lake Tanganyika for environmental variables; HC = Habitat complexity, rFreq = rock frequency, rSize = rock size.

	Depth	HC	Sand	Shell	Vegetation	rFreq	rSize
Pagel's λ	0.905	0.522	0.928	0.166	0.187	0.603	0.000
p-value	0.000	0.005	0.001	0.286	0.037	0.000	1.000

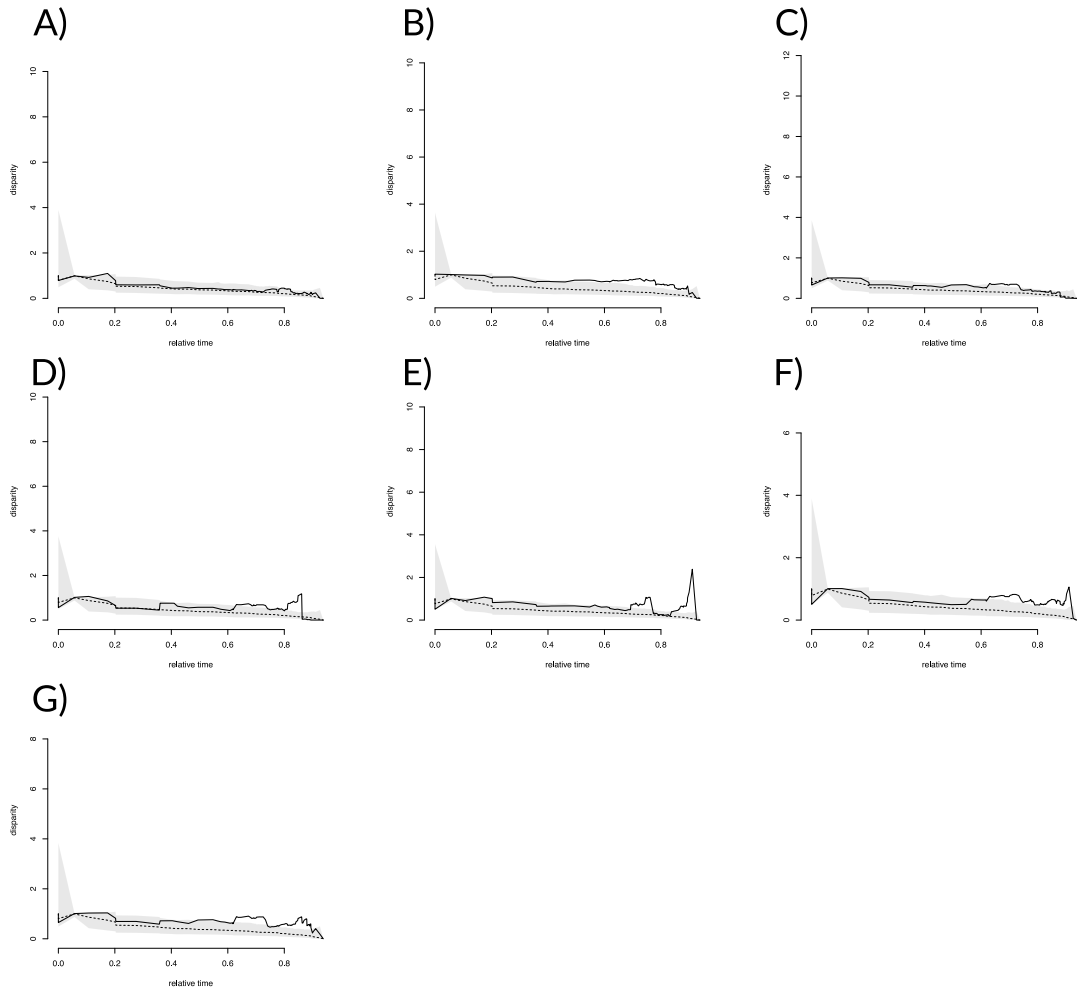

Figure S16: Disparity-through-time plots for different environment variables (simulation of trait behaviour under BM - replicates 1000), A) Depth, NDI = 0.08; B) Habitat complexity, NDI = 0.29; C) Sand cover, NDI = 0.16; D) Shell cover, NDI = 0.15; E) Vegetation cover, NDI = 0.25; F) rock frequency, NDI = 0.21; G) rock size, NDI = 026

Chapter 8

Dynamics of sex chromosome evolution in a rapid radiation of cichlid fish

Athimed El Taher, **Fabrizia Ronco**, Michael Matschiner,
Walter Salzburger & Astrid Böhne

manuscript under review; Science Advances

I contributed to sample collection, lab work and developing and scripting of part of the analyses.

Dynamics of sex chromosome evolution in a rapid radiation of cichlid fish

Athimed El Taher[1], Fabrizia Ronco[1], Michael Matschiner[1,2,3], Walter Salzburger[1] and Astrid Böhne[1,4*]

[1] Zoological Institute, Department of Environmental Sciences, University of Basel, Basel, Switzerland
[2] Department of Palaeontology and Museum, University of Zurich, Zurich, Switzerland.
[3] Centre for Ecological and Evolutionary Synthesis (CEES), Department of Biosciences, University of Oslo, Oslo, Norway.
[4] Center for Molecular Biodiversity Research, Zoological Research Museum Alexander Koenig, Bonn, Germany

[*] e-mail: a.boehne@leibniz-zfmk.de

Sex is a fundamental trait of eukaryotes that is determined, depending on the species, by different environmental and genetic factors[1], including various types and constellations of sex chromosomes with differing degrees of differentiation[2]. Tempo and mode of sex chromosome evolution and its interplay with organismal diversification remain largely elusive, however. Here, we examined the dynamics of sex chromosome evolution in an archetypal example of adaptive radiation, the cichlid fishes of African Lake Tanganyika. Through the inspection of male and female genomes of 244 Tanganyikan cichlid species and the analysis of transcriptomes from 74 of those, we identified sex chromosomal signatures in 90 species, involving 11 different chromosomes. We demonstrate that, taken as a whole, the Tanganyikan cichlids show the by far highest rates of sex chromosome turnover and heterogamety transitions known to date in animals[3]. That the recruitments of chromosomes as sex chromosomes is not at random and that some chromosomes have repeatedly and convergently emerged as new sex chromosomes in Tanganyikan cichlids, provides empirical support for the limited options hypothesis[4] of sex chromosome evolution.

Sex chromosomes – referred to as Z and W in female and X and Y in male heterogametic sex determination (SD) systems – define through their properties and constellations the sex of an individual[5]. The evolutionary trajectories of sex chromosomes differ from those of autosomes: Due to the restriction of one of the two sex chromosomes to one sex (W to females in ZW, Y to males in XY SD systems), their sex-specific inheritance (e.g., XY-fathers pass on their X exclusively to daughters and their Y to sons), and their reduced levels of recombination, sex chromosomes accumulate mutations more rapidly, potentially leading to accelerated functional evolution[6,7]. Sex chromosome constellations can be altered relatively quickly by changes in heterogamety[8] as well as by turnovers (i.e., changes of the actual chromosome pair in use as sex chromosome[3]) caused by a new sex-determining mutation on a previously autosomal locus[9], by translocation of the ancestral sex-determining gene (e.g.[10]), or through sex chromosome-autosome fusions[11]. SD mechanisms as well as sex chromosome evolutionary trajectories vary substantially across vertebrates. In mammals and birds, the same strongly differentiated (heteromorphic) sex chromosomes are shared across the entire class ([1] but see [12]). In amphibians, reptiles, and fish, frequent turnover events and continued

recombination have led to many different and mostly non-degenerated (homomorphic) sex chromosomes (e.g.[3,13]). Despite their fundamental role in development and reproduction, little is known about the dynamics of sex chromosome evolution – especially over short evolutionary timescales.

Here, we examine sex chromosome evolution in an archetypal example of rapid organismal diversification, the adaptive radiation of cichlid fishes in African Lake Tanganyika[14] (LT). Available data from about 30 African cichlid species suggest that sex chromosomes are not conserved with both simple and polygenic sex determination systems being known from different cichlid species; that certain chromosomes have repeatedly been recruited as sex chromosomes; and that sexual antagonism can drive sex chromosome turnovers[15-17]. However, as of yet, no inclusive analysis of sex chromosome evolution exists for a large-scale (cichlid) adaptive radiation. We investigate patterns of sex chromosome evolution using genomic information from 244 Tanganyikan cichlid species[14,18,19] and reconstruct sex chromosome turnover events as well as changes in heterogametic status, and compare sex chromosome dynamics in cichlids with that in other ray-finned fishes.

Sex chromosome evolution

To identify sex chromosomes in LT cichlids, we investigated male and female genomes of 244 species[18] as well as transcriptomes of 74 species[19] for sex-differentiated regions applying four complementary approaches: genome-wide association study (GWAS), identification of sex-patterned SNPs, allele frequency difference tests, and sex-specific sequence subtraction. That way, we detected sex chromosome signatures in 90 species (Figs. 1 and 2; Supplementary Table 1). Within eight of the 13 sub-lineages ('tribes') of the cichlid radiation in LT, several species had the same SD system (chromosomal region and heterogametic type); however, we did not find a SD system that was shared among species of different tribes. In 17 species, we identified species-specific sex chromosomes (i.e., not shared with any other species; Fig. 1).

We found sex chromosome signatures on 11 out of the 23 reference linkage groups (LGs) of the Nile tilapia genome assembly (*Oreochromis niloticus*, the common out-group to all investigated LT cichlid species), and on 8 of these LGs, such signatures were found in species belonging to different tribes (Fig. 2a). This distribution of sex chromosome signatures differs from a random one (Extended Data Fig. 1) and is compatible with the hypothesis that certain chromosomes are more likely to become sex chromosomes than others[3,4]. There was no correlation between the size of a LG, the number of genes on a LG, or the number of known sex-candidate genes on a LG and the frequency at which a LG appeared as sex chromosome in LT cichlids (Extended Data Fig. 1).

In 66 species (73.3% of the 90 species with a sex chromosomal signal), the sex chromosome signatures were compatible with an XY SD system (Fig. 2b). That male heterogamety occurs more frequently than female heterogamety is a common pattern in fish[20], and compatible with models of speciation driven by sexual selection and sex-ratio distortion in cichlids that predict higher probabilities for the maintenance of male heterogamety[21].

Next, to determine when particular sex chromosomes emerged and to trace heterogamety transitions in the course of the cichlid adaptive radiation in LT, we performed ancestral state reconstructions along a time-calibrated species tree[18]. We identified 29 sex chromosome turnovers in the radiation, translating into an estimated rate of 0.16 turnovers per Myr (Fig. 1, Extended Data Fig. 2). On average, we hence expect one sex chromosome turnover event between two species that diverged ~3.1 Ma. This rate is eight times higher than the one that we separately calculated for ricefishes, a model fish group known for its dynamic sex chromosome evolution[22] (Adrianichthyidae;

0.02 per Myr; Extended Data Fig. 3, 19 species investigated, see Methods), and eight times higher than the rate published for true frogs (Ranidae; 0.02 per Myr), which was considered as being the hitherto fastest sex chromosome turnover rate known in vertebrates[3]. Our findings thus corroborate that SD is a rapidly evolving trait in cichlids. We further found that the number of turnovers in a tribe is correlated with its species-richness (Fig. 2c, pGLS: P=0.0004, coeff=0.053), suggesting that the turnover rate has been relatively constant throughout the radiation, and that turnovers occur even between very closely related species.

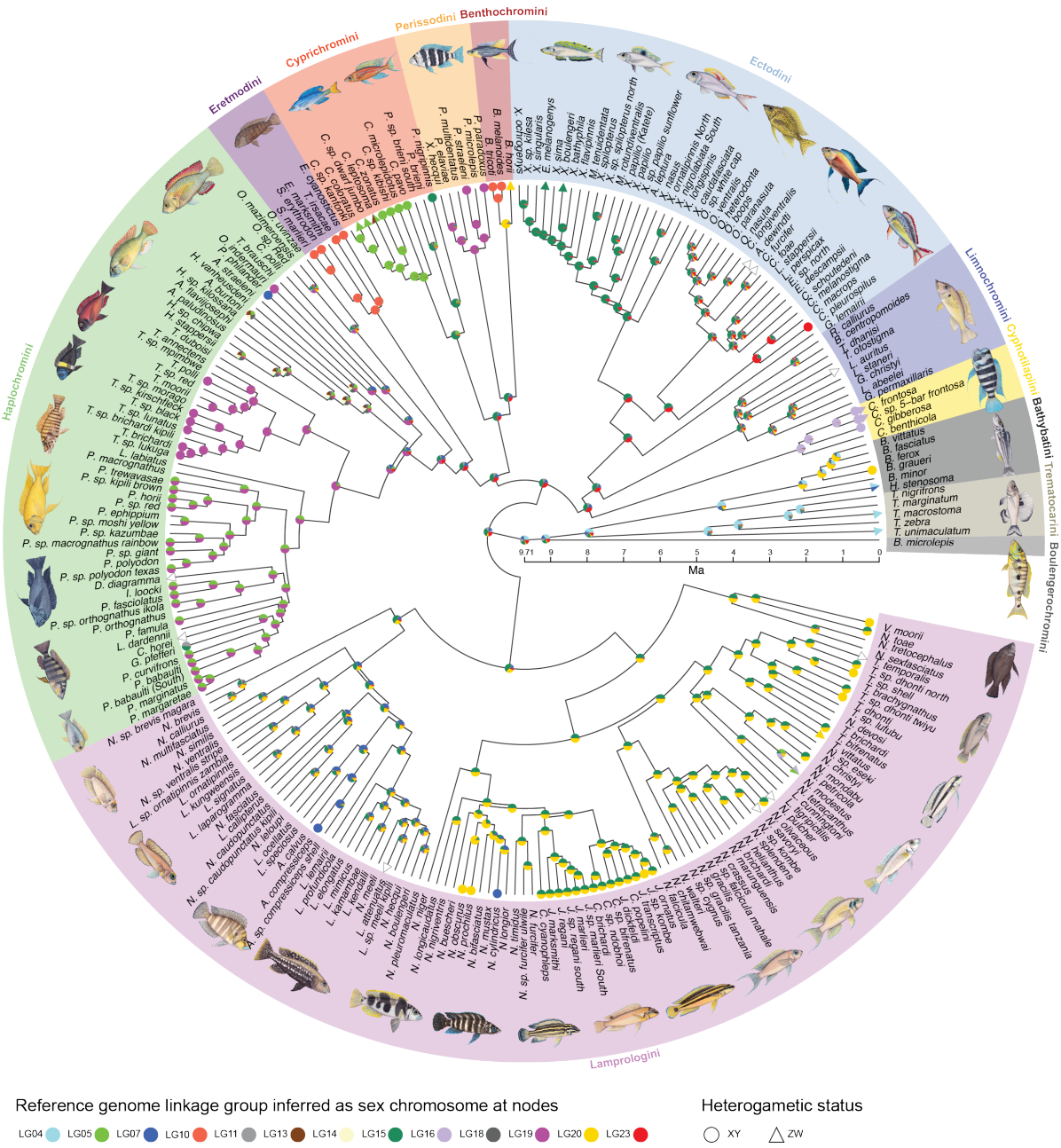

Fig. 2 | Non-random sex chromosome distribution in Lake Tanganyika cichlids. a, Recruitment of different LGs for sex determination. Bars represent the number of times a LG has been recruited as a sex chromosome at the species level and are coloured according to tribe. **b**, The occurrence of sex determination systems. Bars represent how often an XY or ZW SD system was identified at the species level and are coloured according to tribe. **c**, Correlation between species-richness and sex chromosome turnover. The number of sex chromosome turnovers leading to the tips of each tribe is correlated with the number of species investigated in each tribe (pGLS: P=0.0004, coeff=0.053). Dots are coloured according to tribes, the line represents the linear model fitted to the data.

Our reconstructions further revealed that XY is the ancestral state in the cichlid adaptive radiation in LT (Extended Data Fig. 2) and that more transitions occurred from XY to ZW than vice versa (15 versus 3). Transitions in heterogamety are predicted to be more likely when the new sex chromosome is dominant over the ancestral one[23,24], suggesting that in cichlids from LT – just like in some species from Lake Malawi[17] – the W chromosomes are dominant over Ys. Interestingly, we found heterogamety changes that were uncoupled from turnovers in LGs: A transitions from XY to ZW was detected on LG05 in Cyprichromini and on LG20 in Lamprologini (Fig. 1). On the other hand, most (21 versus 8) of the observed sex chromosome turnovers in LT cichlids preserved the heterogametic state, suggesting mutational load as driving force of sex chromosome turnover instead of sexual antagonism, in which case the heterogametic state would be expected to change as well[3].

Overall, the heterogamety transition rate in LT cichlids (0.044 transitions per Myr) was about six times higher than in ricefishes (0.007 transitions per Myr; ancestral state: ZW). To explore heterogamety changes on a greater taxonomic scale, we also calculated heterogamety transition rates for all ray-finned fishes available in the Tree of Sex database (http://www.treeofsex.org/) that were included in a recent comprehensive phylogeny[25] (544 species analysed in total). Our analysis revealed a rate of 0.009 transition per Myr for ray-finned fishes as a whole and identified XY as the ancestral state (Supplementary Table 2; Extended Data Fig. 3). Across the ray-finned fish phylogeny, transitions from XY to ZW were significantly younger than those from ZW to XY (Extended Data Fig. 3, P=0.005). A similar trend was observed in LT cichlids (Extended Data Fig. 3).

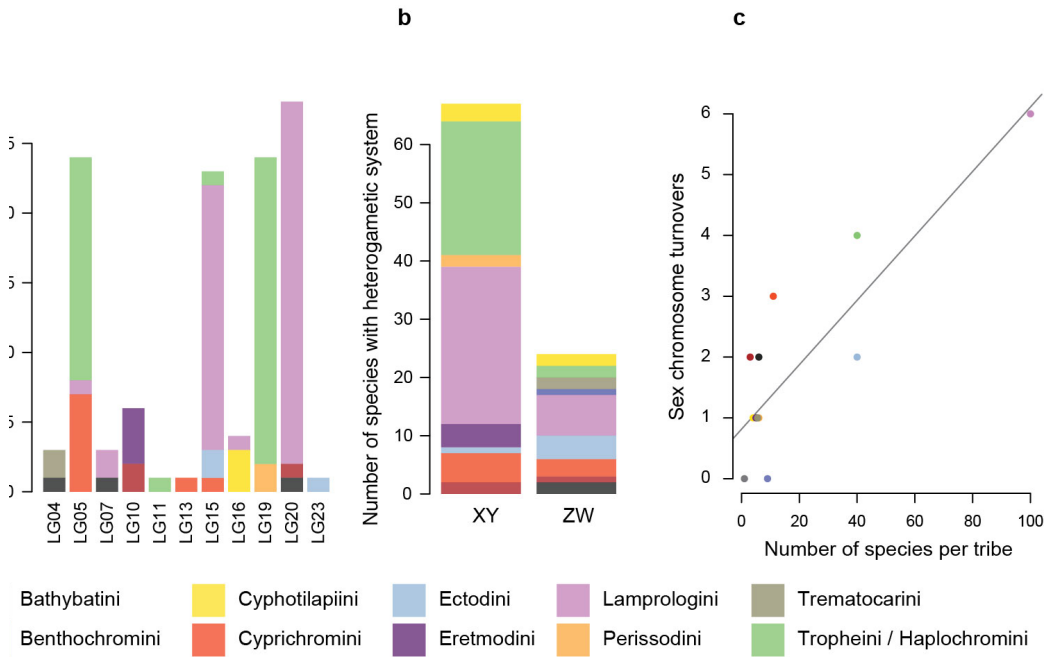

Fig. 2 | Non-random sex chromosome distribution in Lake Tanganyika cichlids. a, Recruitment of different LGs for sex determination. Bars represent the number of times a LG has been recruited as a sex chromosome at the species level and are coloured according to tribe. **b**, The occurrence of sex determination systems. Bars represent how often an XY or ZW SD system was identified at the species level and are coloured according to tribe. **c**, Correlation between species-richness and sex chromosome turnover. The number of sex chromosome turnovers leading to the tips of each tribe is correlated with the number of species investigated in each tribe (pGLS: P=0.0004, coeff=0.053). Dots are coloured according to tribes, the line represents the linear model fitted to the data.

Chromosome fusions and sex chromosomes

Our newly identified sex-chromosomal signatures suggest that chromosomal fusions have occurred in the course of the cichlid radiation in LT (Fig. 1, two-coloured symbols). For example, the distribution of sex-patterned genomic regions indicates a fusion between LGs 05 and 19 in Tropheini and between LGs 15 and 20 in Lamprologini (Fig. 1, Supplementary Information 1); further sex-patterned signatures point to species-specific fusion events (LG11/LG15 in *Gnathochromis pfefferi*, LG05/LG13 in *Cyprichromis leptosoma*, LG05/LG16 in *Neolamprologus modestus*). Chromosome fusions have previously been implicated with the evolution of novel sex chromosomes in other taxa, and it has been suggested that fusions can drive speciation through incompatibilities in genome structure[26-28]. However, while cytogenetics provided evidence for chromosome fusion and fissions in some cichlid species[29], we currently lack a comprehensive understanding of karyotype evolution in African cichlids, and, hence, of the interplay between fusions and the emergence of new sex chromosomes.

Convergent evolution of sex chromosomes

On some LGs and on LG19 in particular, the sex chromosome signatures largely overlapped between members of different tribes (Extended Data Fig. 4), which can either be explained by common ancestry or by the independent (convergent) recruitment of those LGs as sex chromosome. On LG19, several closely related species including six *Tropheus* species (tribe Tropheini, which is nested within the Haplochromini), the riverine haplochromine *Orthochromis indermauri*, and *Plecodus paradoxus* (tribe Perissodini) feature a similar XY signature (Extended Data Fig. 4). Our ancestral state reconstruction suggested an independent origin of the LG19 SD system in Perissodini and Tropheini, in each case early in the tribe's evolutionary histories, and another independent origin in the terminal branch leading to *O. indermauri*. We also inspected the genomes of these species for shared X- and Y-alleles, but did not find any. We then assessed how often each Perissodini genome is heterozygous at a polymorphism shared with Tropheini/Haplochromini versus heterozygous at private polymorphic sites (homozygous for the reference allele in Tropheini/Haplochromini) (Extended Data Fig. 5). We found an overrepresentation of heterozygous sites on LG19 in male *P. paradoxus*, as expected for an XY system. The proportion of private heterozygous sites in male P. paradoxus was larger than the proportion at ancestral polymorphic sites. If the Y chromosome was ancestral to Perissodini/Tropheini/Haplochromini, we would, however, expect the opposite pattern since species-specific patterns could only have accumulated later and, hence, in a much shorter evolutionary time frame. The comparison of *O. indermauri* with the six *Tropheus* species, on the other hand, revealed proportionally more male-specific heterozygous sites at shared polymorphic sites than at private sites (Extended Data Fig. 5), suggesting common ancestry (a scenario not supported by ancestral state reconstruction as it would require many losses within the Haplochromini) or introgression between Tropheus and *O. indermauri*.

The XY sex chromosome signature on LG05/19 of other Tropheini species is likely derived from another independent evolutionary event, since the regions on LG19 that show XY-patterning in the two Tropheini clades are not overlapping (Extended Data Fig. 4). Other convergent cases of sex chromosome recruitment supported by our ancestral state reconstruction involve LG05 (in Cyprichromini and the haplochromine *Astatotilapia burtoni*[16,30]) and LG07. LG07 has independently been recruited as a sex chromosome in *Hemibates stenosoma* (Bathybatini), in two distantly related Lamprologini clades (Fig.1), in several Lake Malawi cichlids[17] (Haplochromini) as well as in

Pseudocrenilabrus philander[15] (Haplochromini), making it the most widespread sex chromosome known in cichlids to date.

Sex chromosome differentiation

A comparison of the proportion of sex-patterned sites on the different sex chromosomes revealed a continuum of sex chromosome differentiation in the cichlid adaptive radiation in LT (Fig. 3, Extended Data Fig. 4) ranging from a few kb (LG20 in Lamprologini) to almost full chromosomal length (LG05 in Cyprichromini, LG19 in *Tropheus* species and Perissodini). Varying lengths of sex-differentiated regions were even detected in the same LG when being used as sex chromosome by different lineages (e.g., the sex-differentiated region on LG05 spans only 8 Mb in Tropheini versus the entire LG in Cyprichromini).

The canonical model of sex chromosome evolution predicts progressing differentiation of sex chromosomes with time[6]. Contrastingly, we found no correlation between the estimated age of origin of a sex chromosome and its degree of differentiation (Fig. 3, pGLS: P=0.8177, coeff=0.0012). Some very young sex chromosomes showed signs of differentiation along almost the full length of a LG, which is indicative of suppressed recombination[3] along the entire chromosome.

Models[24] and empirical observations[31] suggest that, beyond a certain degree of differentiation, sex chromosome turnover becomes unlikely. On the other hand, frequent turnovers, sex reversal, and continued recombination can contribute to counteract sex chromosome differentiation[32,33]. That turnovers have occurred frequently in the course of the cichlid adaptive radiation in LT indicates that the cichlids' sex chromosomes have not yet reached a threshold preventing turnover, but that their sex chromosomes remain dynamic.

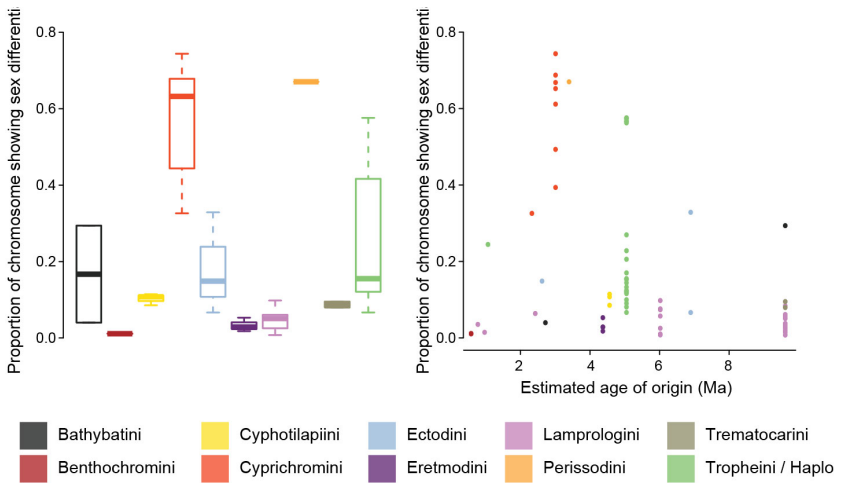

Fig. 3 | Sex chromosome differentiation in Lake Tanganyika cichlids. a, Size distribution of SD regions. The size of SD regions corresponds to the proportion of the LG with windows that have more sex-patterned SNPs than two times the mean across all windows. **b**, Per species proportion of the chromosome(s) showing sex differentiation and corresponding estimated ages of the sex chromosomal system based on ancestral state reconstructions on a time-calibrated species tree. The degree of differentiation is not correlated with the estimated age of origin (pGLS: P= 0.8177, coeff=0.0012).

The amount of sex-specific sequences inferred from a subtraction of expressed male and female sequences[34] was higher in XY than ZW systems, but only when not accounting for phylogenetic signal (phylogenetic ANOVA: P=0.2, Extended Data Fig. 6a). The observed pattern suggests that Y-chromosomal genes are more highly expressed in closely related species in adult tissues than W genes but it does not reflect a difference in the degree of differentiation between the two heterogametic types (Extended Data Fig. 6b, phylogenetic ANOVA: P=1).

Candidate genes of sex determination

Our inspection of known genes implicated in SD revealed that such genes were located on all LGs, including those for which no sex chromosome signature was detected, with no particular overrepresentation on certain LGs (Extended Data Fig. 7), and the regions with the strongest signal for being sex-differentiated did not contain any of these genes (Supplementary Table 1). However, through the inspections of the regions with the strongest signs of sex differentiation we identified promising new candidate genes for SD in these regions, such as tox2 in Lamprologini, a HMG-box transcription factor involved in the hypothalamo-pituitary-gonadal system. Tox2 resembles the mammalian master SD gene Sry[35], which also codes for an HMG-box protein.

In cichlids from lakes Malawi[17] and Victoria[36], sexually antagonistic colour genes underlying a characteristic orange-blotched colour pattern are linked to SD genes, creating the potential for speciation by sexual selection. In LT cichlids, which in general do not feature the orange-blotched phenotypes, we did not find any obvious pattern in the localization of colour genes on sex chromosomes (Extended Data Fig. 7). However, we found that species of sexually dichromatic tribes (n=5) showed a higher sex chromosome turnover rate compared to those of monochromatic tribes (n=6) (0.19 versus 0.09 turnovers per Myr), suggesting that sexual antagonism might account for some of the sex chromosome turnovers in LT, too.

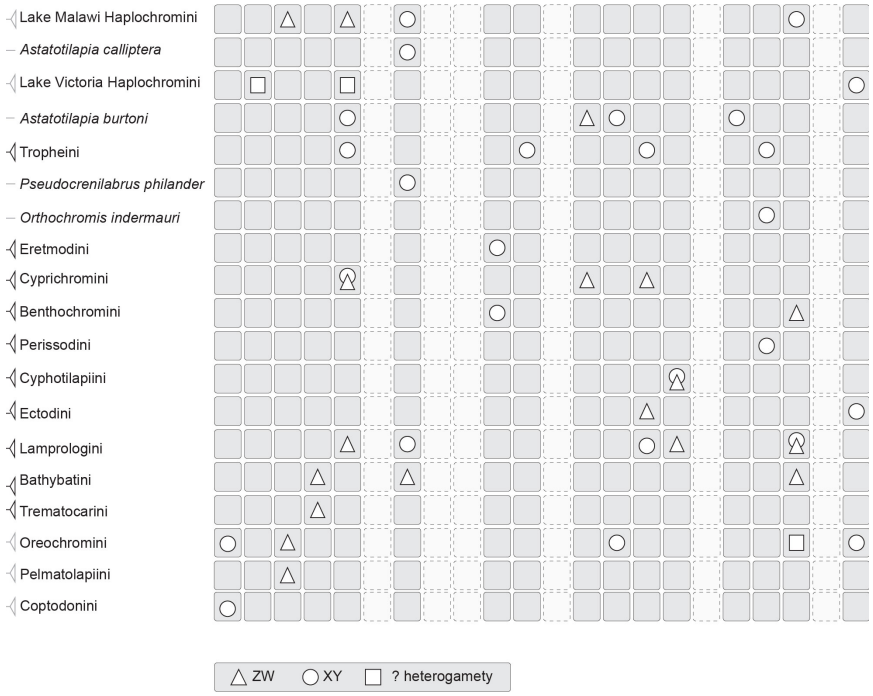

Fig. 4 | Sex chromosome evolution in African cichlids. Phylogenetic relationships and sex chromosome occurrence with reference to the genome of the Nile tilapia (*O. niloticus*) in African cichlids. Cichlid lineages found in Lake Tanganyika are indicated in black, cichlids from other lakes or rivers in grey. Sex chromosome information is derived from this study, and from summaries in and.

Conclusions

In the cichlid adaptive radiation of LT, sex chromosome turnovers have occurred extremely frequently and are non-random with respect to the recruited chromosome. This pattern becomes even more apparent when the LT cichlids are compared to other African cichlid species (Fig. 4), revealing that some LGs (in particular LGs 05, 07, and 20) emerged multiple times as sex chromosomes whereas others never appeared as such. This corroborates the hypothesis that particular chromosomes are preferentially[4] or even cyclically[32,33] recruited as sex chromosomes. Within LT cichlids, many of the turnovers have likely been driven by mutational load rather than sexual antagonism since male heterogametic SD is prevailing. The rapidity of sex chromosome turnover within (LT) cichlids confirms that SD mechanisms, albeit serving the unifying function of sex determination, can be extremely labile.

Main references

1. Bachtrog, D. et al. Sex determination: Why so many ways of doing It? PLoS Biol. 12, e1001899 (2014).
2. Charlesworth, D. Young sex chromosomes in plants and animals. New Phytol. 224, 1095-1107 (2019).
3. Jeffries, D. L. et al. A rapid rate of sex-chromosome turnover and non-random transitions in true frogs. Nat. Commun. 9, 4088 (2018).
4. Marshall Graves, J. A. & Peichel, C. L. Are homologies in vertebrate sex determination due to shared ancestry or to limited options? Genome Biol. 11, 205 (2010).
5. Rice, W. R. Sex chromosomes and the evolution of sexual dimorphism. Evolution 38, 735-742 (1984).
6. Charlesworth, B., Coyne, J. A. & Barton, N. H. The relative rates of evolution of sex chromosomes and autosomes. Am. Nat. 130, 113-146 (1987).
7. Irwin, D. E. Sex chromosomes and speciation in birds and other ZW systems. Mol. Ecol. 27, 3831-3851 (2018).
8. Bull, J. J. & Charnov, E. L. Changes in the heterogametic mechanism of sex determination. Heredity 39, 1-14 (1977).
9. Myosho, T. et al. Tracing the emergence of a novel sex-determining gene in medaka, Oryzias luzonensis. Genetics 191, 163-170 (2012).
10. Tennessen, J. A. et al. Repeated translocation of a gene cassette drives sex-chromosome turnover in strawberries. PLoS Biol. 16, e2006062 (2018).
11. Pennell, M. W. et al. Y fuse? Sex chromosome fusions in fishes and reptiles. PLoS Genet 11, e1005237 (2015).
12. Veyrunes, F. et al. A novel sex determination system in a close relative of the house mouse. Proc. Biol. Sci. 277, 1049-1056 (2010).
13. Heule, C., Salzburger, W. & Böhne, A. Genetics of sexual development – an evolutionary playground for fish. Genetics 196, 579-591 (2014).
14. Ronco, F., Indermaur, A., Büscher, H. & Salzburger, W. The taxonomic diversity of the cichlid fish fauna of ancient Lake Tanganyika, East Africa. Journal of Great Lakes Research in press (2019).
15. Böhne, A. et al. Repeated evolution versus common ancestry: Sex chromosome evolution in the haplochromine cichlid Pseudocrenilabrus philander. Genome Biol. Evol. 11, 439–458 (2019).
16. Böhne, A., Wilson, C. A., Postlethwait, J. H. & Salzburger, W. Variations on a theme: Genomics of sex determination in Astatotilapia burtoni. BMC Genomics 17, 883 (2016).
17. Roberts, R. B., Ser, J. R. & Kocher, T. D. Sexual conflict resolved by invasion of a novel sex determiner in Lake Malawi cichlid fishes. Science 326, 998-1001 (2009).
18. Ronco, F. et al. Drivers, dynamics and progression of a massive adaptive radiation in African cichlid fish. co-submitted (2019).
19. El Taher, A. et al. The evolution of gene expression levels during rapid organismal diversification. co-submitted (2019).

20. Pennell, M. W., Mank, J. E. & Peichel, C. L. Transitions in sex determination and sex chromosomes across vertebrate species. Mol. Ecol. 27, 3950-3963 (2018).
21. Lande, R., Seehausen, O. & van Alphen, J. J. Mechanisms of rapid sympatric speciation by sex reversal and sexual selection in cichlid fish. Genetica 112-113, 435-443 (2001).
22. Hilgers, L. & Schwarzer, J. The natural history of model organisms: The untapped potential of medaka's wild relatives. eLIFE 8, e46994 (2019).
23. van Doorn, G. S. & Kirkpatrick, M. Transitions between male and female heterogamety caused by sex-antagonistic selection. Genetics 186, 629-645 (2010).
24. Veller, C., Muralidhar, P., Constable, G. W. A. & Nowak, M. A. Drift-induced selection between male and female heterogamety. Genetics 207, 711-727 (2017).
25. Rabosky, D. L. et al. An inverse latitudinal gradient in speciation rate for marine fishes. Nature 559, 392-395 (2018).
26. King, M. Species Evolution - the Role of Chromosome Change. (Cambridge University Press, 1993).
27. Lucek, K. Evolutionary mechanisms of varying chromosome numbers in the radiation of Erebia butterflies. Genes 9 (2018).
28. Kitano, J. et al. A role for a neo-sex chromosome in stickleback speciation. Nature 461, 1079-1083 (2009).
29. Ozouf-Costaz, C. et al. New insights into the chromosomal differentiation patterns among cichlids from Africa and Madagascar. Cybium 41, 35-43 (2017).
30. Roberts, N. B. et al. Polygenic sex determination in the cichlid fish Astatotilapia burtoni. BMC Genomics 17, 835 (2016).
31. Pokorná, M. & Kratochvíl, L. Phylogeny of sex-determining mechanisms in squamate reptiles: are sex chromosomes an evolutionary trap? Zoological Journal of the Linnean Society 156, 168-183 (2009).
32. Rodrigues, N., Studer, T., Dufresnes, C. & Perrin, N. Sex-chromosome recombination in common frogs brings water to the fountain-of-youth. Mol. Biol. Evol. (2018).
33. Blaser, O., Neuenschwander, S. & Perrin, N. Sex-chromosome turnovers: The hot-potato model. Am. Nat. 183, 140-146 (2014).
34. Mahajan, S. & Bachtrog, D. Convergent evolution of Y chromosome gene content in flies. Nat. Commun. 8, 785 (2017).
35. Koopman, P., Gubbay, J., Vivian, N., Goodfellow, P. & Lovell-Badge, R. Male development of chromosomally female mice transgenic for Sry. Nature 351, 117 - 121 (1991).
36. Seehausen, O., van Alphen, J. J. M. & Lande, R. Color polymorphism and sex ratio distortion in a cichlid fish as an incipient stage in sympatric speciation by sexual selection. Ecol. Lett. 2, 367-378 (1999).
37. Gammerdinger, W. J., Conte, M. A., Sandkam, B. A., Penman, D. J. & Kocher, T. D. Characterization of sex chromosomes in three deeply diverged species of Pseudocrenilabrinae (Teleostei: Cichlidae). Hydrobiologia 832, 397-408 (2019).

Methods

Sequencing data. We used whole genome sequencing (WGS) data from[18] and transcriptome data from[19] (Supplementary Table 1). Based on a recent compilation of LT cichlid species[14], we included 180 described species, 29 undescribed species, and 19 local variants. We further included 14 riverine cichlid species (473 individuals in total, Supplementary Table 1). Transcriptome data were available for 74 of these species[19] (70 described and 4 undescribed species), from which we used three males and three females per species and three tissues per individual (brain, gonad, gills). WGS data are Illumina TruSeq DNA PCR-free 150 bp paired-end and transcriptome data are Illumina TruSeq RiboZero 125 bp single-end.

Variant calling for WGS data. Mapped reads were derived from[18]. In brief, adapters were removed with Trimmomatic[38] (v.0.36) in PE mode with the settings ILLUMINACLIP:${adapter_file}:2:30:12:8:true MINLEN:30. We used the Nile tilapia (*Oreochromis*

niloticus) genome (NBI RefSeq GCF_001858045.1_ASM185804v2) as reference for mapping and variant calling. Unplaced scaffolds were concatenated lexicographically into an "UNPLACED" super chromosome. DNA reads were aligned against this customized reference with BWA-MEM BWA[39] (v.0.7.12, parameters: -t 16, -M and -R). Alignments were coordinate-sorted and indexed with SAMtools[40] (v.1.3.1), duplicate reads per sample were marked with the function MarkDuplicates of Picard Tools (v.2.7.1, http://broadinstitute.github.io/picard) and local realignment around indels was performed with RealignerTargetCreator and IndelRealigner of GATK[41] (v.3.6). Repetitive regions were masked with a mappability mask generated with SNPable (http://lh3lh3.users.sourceforge.net/snpable.shtml), setting k=100 bp. This masked 207 Mb.

Variants were called for each tribe separately with GATK's[41] (v.3.7) HaplotypeCaller (per individual and per chromosome) and GenotypeGVCFs (per 1 Mb window), and merged with GATK's CatVariants. Variants were further filtered with BCFtools (v.1.6, https://github.com/samtools/bcftools), applying the settings ReadPosRankSum<-0.5, MQRankSum<-0.5, FS<20.0, QD>2.0, MQ>20.0 and placing tribe-specific thresholds on minimum and maximum read depths to account for varying sample sizes (Bathybatini: 50-300; Benthochromini: 25-100; Cyphotilapiini: 50-200, Cyprichromini: 100-400; Ectodini: 250-1500; Eretmodini: 50-200; Tropheini/Haplochromini: 375-1375; Lamprologini: 700-3000; Limnochromini: 50-300; Trematocarini: 50-300). For the tribes Lamprologini, Tropheini/Haplochromini, Ectodini, and Limnochromini we further applied InbreedingCoeff>-0.8.

Indels were normalized with BCFtools's norm function, monomorphic sites were excluded, and SNPs around indels were masked depending on the size of the indel: for indels with a size of 1 bp, 2 bp were masked on both sides, and 3, 5, and 10 bp were masked for indels with sizes of 3 bp, 4-5 bp, and >5 bp, respectively. Individual genotypes were then masked with VCFtools[42] (v.0.1.14) if they had low quality (--minGQ 20) or depth (--minDP 4). Finally, we only kept SNPs. Filtered variants were phased and missing genotypes were imputed with Beagle[43] (v.4.1). We then retained only sites that had no more than 50% missing data prior to phasing. For sites that were polymorphic but no individual had the reference genome allele, we set the first alternative allele as reference allele. We then only kept biallelic sites.

Tribe-wise association tests for sex on WGS data. The phased sets of variants for tribes with at least 10 species (Lamprologini: 196 individuals representing 100 species; Ectodini: 81 individuals representing 40 species; Tropheini/Haplochromini: 99 individuals of 55 species; and Cyprichromini: 21 individuals of 11 species) were transformed into bim and bed format with PLINK[44] (v.1.90b). We applied four approaches to identify sex chromosomes (approach 1-4). For approach 1 (GWAS, Supplementary Information 1), we ran association tests for sex using the univariate linear mixed model integrated in GEMMA[45] (v.0.97) accounting for population stratification. Genotypes of outlier sites were visualized with the R package Pheatmap (v.1.0.12, https://cran.r-project.org/web/packages/pheatmap/index.html) in R[46] (v.3.5.2).

Within all tribes, we also tested for an accumulation of sex-patterned sites (approach 2, Supplementary Information 2), assuming that a SD region will show an accumulation of sex-patterned sites due to linkage caused by suppressed recombination. To this end, we subset the unphased, filtered sets of variants to keep only information from species for which we had individuals of both sexes. We removed sites with more than 20% missing data and more than two alleles with VCFtools[42] (v.0.1.14). The resulting files were loaded into R[46] (v.3.5.0) with VCFR[47] (v.1.8.0.9). Each variant site was recoded per species as a "nosex" site if the male and the female individual had the

same genotype; as "noinfo" if one or both individuals had no genotype call; as "XY" if the male was heterozygous and the female homozygous; and as "ZW" if the female was heterozygous and the male homozygous. Next, we calculated per tribe the sum of "nosex", "ZW", and "XY" sites per window of 50 SNPs. We calculated the mean genomewide percentage of "nosex", "ZW", and "XY" sites. These values were multiplied with the number of called sites per window to obtain expected values for "XY", "ZW", and "nosex" under the assumption that most of the genome has no particular sex-pattern. The expected values per window were compared to the observed values using a Fisher's Exact test. A window was designated "XY" if the observed "XY" value was larger than the expected one and the observed "ZW" value smaller than the expected; "ZW" if the observed "ZW" value was larger than the expected and the observed "XY" value smaller than the expected. If both, observed "XY" and observed "ZW" values were larger than the expected value, a window was declared "ambiguous". If both, observed "XY" and observed "ZW" values were equal or smaller than the expected values, a window was declared "nosex". Fisher's Exact test P-values of XY, ZW, and ambiguous sites were plotted separately as Manhattan plots in comparison to a significance threshold using Bonferroni correction based on the number of windows. The resulting plots were inspected for an accumulation of sex-patterned sites after Bonferroni correction. To investigate sex-patterning on the species level, we ran the same test with the same settings per window per species.

Species-specific association tests for sex on transcriptome data. For species-specific association tests (approach 3, Supplementary Information 3), we pooled RNA sequencing reads of three tissues per individual and quality filtered and trimmed them with Trimmomatic[38] (v.0.33) with a 4 bp window size, a required window quality of 15 and a minimum read length of 30 bp. We performed reference free de novo variant calling per species with KisSplice[48] (v.2.4.0) with settings "-s 1 -t 4 -u" and "--experimental". The identified SNPs were placed on the Nile tilapia genome assembly with STAR[49] (v.2.5.2a) (settings "--outFilterMultimapxNmax 1 --outFilterMatchNminOverLread 0.4 --outFilterScoreMinOverLread 0.4"). The genome index used for this mapping was generated with the corresponding STAR parameters: --runMode genomeGenerate, --sjdbOverhang 124, --sjdbGTFfeatureExon exon and the genome annotation file (RefSeq GCF_001858045.1_ASM185804v2). Kiss2Reference[48] was used to classify KisSplice variants aligned to the Nile tilapia reference genome, and kissDE[48] (v.1.4.0) was applied to determine variants that differ between the two sexes. The resulting files were loaded into R. The KisSplice events were filtered with the following attributes: Only SNPs were kept; SNPs placed on mitochondrial DNA or on unplaced scaffolds of the reference genome were removed; only SNPs with significant P-values for an allele difference between the sexes ($P \leq 0.05$ after adjustment for multiple testing following the Benjamini and Hochberg method[50]) were retained. These SNPs were classified as “XY patterned” if they had zero read counts in all females and a minimum of one count in at least two males or as “ZW patterned” if they had zero counts in all males and a minimum of one count in at least two females. Next, the density of XY- and ZW-patterned SNPs was assessed in 10 kb non-overlapping windows and a Mann-Whitney test was run to compare the two obtained distributions using a significance threshold of 0.05. We also quantified sex-patterned SNPs per reference LG and normalized the obtained numbers by LG length.

Inference of heterogamety from sex-specific sequence subtraction. For species, which had both, transcriptome and WGS data available, we adapted a subtraction pipeline (approach 4) from[34] to infer sex-specific transcripts. Draft genomes from[18] were used as species-specific references. For each species, we pooled all male and female transcriptome data of all three tissues and quality

filtered them with Trimmomatic[38] (v.0.33) with a 4 bp window size, a required minimum window Phred score quality of 15, and a minimum read length of 80 bp. Next, the following steps were modified from[34]: In step 1, we used STAR[49] (v.2.5.2a) to map RNA reads of one sex to the DNA de novo assembly of the opposite sex (--outFilterMultimapNmax 10 --outFilterMatchNminOverLread 0.4 --outFilterScoreMinOverLread 0.4 --outFilterMismatchNmax 100 --seedSearchStartLmax 20 --seedPerReadNmax 100000 --seedPerWindowNmax 1000 --alignTranscriptsPerReadNmax 100000 --alignTranscriptsPerWindowNmax 10000). Step 2 was applied as described in[34]. In step 3, we used GMAP-GSNAP[51] (v.2017-08-15) with a minimum trimmed coverage of 0.9 and a minimum identity of 0.98, to map sex-specific *de novo* assembled transcripts to the genome of the opposite sex. In step 4, we used STAR[49] (v.2.5.2a) and BEDTools[52] (v.2.26.0) to remove presumed sex-specific transcripts that had more than 50% of their length covered with RNA-reads from the opposite sex. In step 5, we used the CD-HIT-EST function of Cd-hit[53] (v.4.6.4) to merge and extend sex-specific transcripts. Step 6 was applied as described in[34]. In step 7, we used RSEM[54] (v.1.2.31) to calculate RPKM values. We did not apply steps 8 (a repeat filter) and 9 (a transcript length filter). We tested for a correlation between the type of heterogametic system and the difference in the number of sex-specific contigs with a phylogenetic ANOVA using phytools[55] (v.0.6-67).

Sex chromosome systems definition and sex chromosome turnovers. Sex chromosomes and heterogametic state (XY/ZW) were inferred from sex-association in GWAS (approach 1), the sex-patterned site test (approach 2), species-specific sex-patterned site accumulations identified by allele differences test based on transcriptomes (approach 3), and the ratio of sex-specific transcripts (approach 4). The final sex chromosome set was coded as a probability matrix including 13 different LGs identified in at least one species as sex-linked, including published data for the two species *A. burtoni*[16,30] and *P. philander*[15]. Species for which we could not unambiguously identify a sex-linked LG were attributed equal probability for all 13 LGs.

In order to reconstruct sex chromosome evolution across the LT radiation, we placed sex chromosome identities onto the time-calibrated phylogeny of LT cichlids[18]. This phylogeny was pruned to include only the 244 species studied here, using phytools[55] in R[46]. We followed the approach described in[3] and inferred ancestral sex chromosome states using a stochastic mapping approach implemented in phytools. We compared the likelihood scores (based on the Akaike Information Criterion (AIC)) for three different transition rate models, equal rates (ER), symmetrical (SYM), and all rates different (ARD), which identified ARD as the best model for transition rates between states. We simulated 1'000 stochastic character maps along the phylogeny. In addition, we ran stochastic mapping for each chromosome separately, coding the use of the chromosome as a sex chromosome in a given species as a binary (yes/no) trait to account for the fact that some tips of the phylogeny are in two states rather than having the equal probability of being in one out of two states. We then combined the 13 separate reconstructions into one phylogenetic representation. The results obtained with the two approaches were very similar and we hence continued calculations with the binary reconstructions.

We determined the timepoints of sex chromosome turnover events as points on branches where the inferred probability of using a given chromosome as a sex chromosome dropped below 0.5 for the first time starting from the tips of the phylogeny using the function densityMap of phytools. Based on[3] we did not consider species that had no detectable sex chromosome as having losses but only considered transition events that led to the emergence of a new sex chromosome, i.e., gains. The reconstructions for LG15 and LG04 suggested the presence of this sex chromosome at the root of

the tree (probability of 0.632 and 1, respectively), with retention of these sex chromosomes in Lamprologini (LG15) and Trematocarini and Bathybatini (LG04). Due to this binary state at the root, we decided to place the origins of LGs 15 and 04 as sex chromosomes early in the radiation on the first branches after the root, for LG15 on the branch leading to the clade formed by all tribes except Boulengerochromini, Trematocarini, and Bathybatini, and for LG04 on the branch leading to the clade formed by the latter three tribes. This assumed scenario of LG04 and LG15 emerging early on in the radiation is also congruent with the ancestral state reconstruction of all potential sex chromosomes jointly, supporting a later origin (data not shown). Removing those two turnover events had little effect on the estimated turnover rate (0.15 versus 0.16 per Myr). Likewise, we ran 1'000 stochastic mappings for the type of heterogamety (XY/ZW).

We then ran the same analyses for ricefishes (Adrianichthyidae), which, to the best of our knowledge, are the only fish family with detailed data on sex chromosomes with synteny inference based on a comparison to a common reference genome (medaka). Information on sex chromosomes was taken from[22] and placed on a time-calibrated phylogeny of the family Adrianichthyidae (19 species, Supplementary Table 2), extracted from a recent comprehensive ray-finned fish phylogeny[25]. We could not include sex chromosome data of three species (*O. skaizumii*, *O. wolasi*, and *O. woworae*), as these were not included in the phylogeny and no other comprehensive time-calibrated tree comprising these fishes was available to us. To compare our data on a larger scale, we calculated transitions rates for ray-finned fishes of the Tree of Sex database (http://www.treeofsex.org/). We used all Tree of Sex species that were also included in the recent comprehensive ray-finned fish phylogeny[25] (Supplementary Table 3). As some species names were not initially included in the phylogeny of[25], we inspected species names of Tree of Sex for typos, older versions of species names and synonyms in FishBase (www.fishbase.org) and Eschmeyer's Catalog of Fishes Online Database (https://www.calacademy.org/scientists/projects/eschmeyers-catalog-of-fishes), and corrected the names accordingly. This allowed us to map sex determination data for 472 species from the Tree of Sex database onto the phylogeny. We further added data for cichlids based on[15,16,30,56,57] and this study, resulting in an additional 72 species. Sex determination data from the Tree of Sex database were simplified and coded as a probability matrix with three states, namely "XY" (including species classified by Tree of Sex as "XY heteromorphic", "XY homomorphic", "XO", "XY polygenic"), "ZW" (including species classified by Tree of Sex as "ZW heteromorphic" and "ZW homomorphic", "ZO", "ZW polygenic") and "NonGSD" (including species classified by Tree of Sex as "apomictic", "hermaphrodite", "ESD_other", "pH", "size", "density", "TSD", "other"). The final matrix is provided in Supplementary Table 3. Similar to our approach described above, all other species with no information on sex determination were included with an equal probability for all three states.

To test if gene content or chromosome size drives the observed pattern of sex chromosome recruitment in LT cichlids, we randomly picked 29 times (the number of sex chromosome recruitments derived from ancestral state reconstruction) a window of 10 kb of the reference genome and attributed the LG containing this window as sex chromosome to a species. We simulated this operation 10'000 times and counted how many times each LG was recruited in each simulation. We than counted in how many simulations 10 or more LGs were not recruited, as this was the observed pattern.

Defining sex-determining regions and candidate genes. On the above-defined sex chromosomes, we characterized the species-specific SD regions by counting the numbers of XY- and ZW-patterned SNPs identified within the association tests (see above) in non-overlapping windows of 10 kb. The density of XY- or ZW-patterned windows is shown in Extended Data Fig. 4. We defined the size of the SD region as the proportion of the LG covered by windows that have a density of sex-patterned SNPs that is more than twice as high as the mean over all windows. The sum of the sex-patterned windows defines the cumulative length of the sex-differentiated regions and the minimum and maximum window coordinates define the range of the sex-differentiated region on the LG. We tested for a correlation between sex chromosome differentiation and estimated age of origin of the sex chromosome derived from the turnover point with a phylogenetic generalized linear model (pGLS) using the R package ape[58] (v.5.2). From the results of the association tests (see above), we identified SD regions shared between several species and overlaid these with candidate genes involved in sex determination and pigmentation. Pigmentation genes in the reference genome were defined over gene ontology annotations including the term "pigmentation" and its child terms. We also retrieved orthologous sequences of the Nile tilapia to the medaka pigmentation genes defined by[59] over Biomart, Ensembl release 96. Since this Nile tilapia genome is a different genome release than the reference genome used by us, we searched the NCBI database for the obtained Ensembl gene IDs and translated them to the assembly version that we used with the NCBI Genome Remapping Service. Candidate genes for sex determination included genes previously identified through a literature search[60,61] and gene ontology analysis based on a GO annotation matching the word “sex” (list of gene IDs of candidate genes for SD and pigmentation in Supplementary Table 3). We further investigated all annotated genes that were partially or fully included in the window(s) with the maximum number of sex-patterned SNPs on the sex chromosome (Supplementary Table 1).

Methods References

38. Bolger, A. M., Lohse, M. & Usadel, B. Trimmomatic: A flexible trimmer for Illumina sequence data. Bioinformatics 30, 2114-2120 (2014).
39. Li, H. & Durbin, R. Fast and accurate short read alignment with Burrows-Wheeler transform. Bioinformatics 25, 1754-1760 (2009).
40. Li, H. et al. The sequence alignment/map format and SAMtools. Bioinformatics 25, 2078-2079 (2009).
41. McKenna, A. et al. The Genome Analysis Toolkit: A MapReduce framework for analyzing next-generation DNA sequencing data. Genome Res. 20, 1297-1303 (2010).
42. Danecek, P. et al. The variant call format and VCFtools. Bioinformatics 27, 2156-2158 (2011).
43. Browning, S. R. & Browning, B. L. Rapid and accurate haplotype phasing and missing-data inference for whole-genome association studies by use of localized haplotype clustering. Am. J. Hum. Genet. 81, 1084-1097 (2007).
44. Chang, C. C. et al. Second-generation PLINK: rising to the challenge of larger and richer datasets. Gigascience 4, 7 (2015).
45. Zhou, X. & Stephens, M. Genome-wide efficient mixed-model analysis for association studies. Nat. Genet. 44, 821-824 (2012).
46. Team, R. R: A language and environment for statistical computing. (R Foundation for Statistical Computing, 2008).
47. Knaus, B. J. & Grunwald, N. J. VCFR: a package to manipulate and visualize variant call format data in R. Mol. Ecol. Resour. 17, 44-53 (2017).
48. Lopez-Maestre, H. et al. SNP calling from RNA-seq data without a reference genome: identification, quantification, differential analysis and impact on the protein sequence. Nucleic Acids Res. 44, e148-e148 (2016).
49. Dobin, A. et al. STAR: ultrafast universal RNA-seq aligner. Bioinformatics 29, 15-21 (2013).

50. Benjamini, Y. & Hochberg, Y. Controlling the false discovery rate - a practical and powerful approach to multiple testing. J R Stat Soc B 57, 289-300 (1995).
51. Wu, T. D. & Watanabe, C. K. GMAP: a genomic mapping and alignment program for mRNA and EST sequences. Bioinformatics 21, 1859-1875 (2005).
52. Quinlan, A. R. & Hall, I. M. BEDTools: a flexible suite of utilities for comparing genomic features. Bioinformatics 26, 841-842 (2010).
53. Li, W. & Godzik, A. Cd-hit: a fast program for clustering and comparing large sets of protein or nucleotide sequences. Bioinformatics 22, 1658-1659 (2006).
54. Li, B. & Dewey, C. RSEM: accurate transcript quantification from RNA-Seq data with or without a reference genome. BMC Bioinformatics 12, 323 (2011).
55. Revell, L. J. phytools: an R package for phylogenetic comparative biology (and other things). Methods Ecol. Evol. 3, 217-223 (2012).
56. Gammerdinger, W. J. & Kocher, T. D. Unusual Diversity of Sex Chromosomes in African Cichlid Fishes. Genes 9, 480 (2018).
57. Ser, J. R., Roberts, R. B. & Kocher, T. D. Multiple interacting loci control sex determination in Lake Malawi cichlid fish. Evolution 64, 486-501 (2010).
58. Paradis, E. & Schliep, K. ape 5.0: an environment for modern phylogenetics and evolutionary analyses in R. Bioinformatics 35, 526-528 (2019).
59. Braasch, I., Brunet, F., Volff, J.-N. & Schartl, M. Pigmentation pathway evolution after whole-genome duplication in fish. Genome Biol. Evol. 1, 479-493 (2009).
60. Böhne, A., Heule, C., Boileau, N. & Salzburger, W. Expression and sequence evolution of aromatase cyp19a1 and other sexual development genes in East African cichlid fishes. Mol. Biol. Evol. 30, 2268-2285 (2013).
61. Heule, C., Göppert, C., Salzburger, W. & Böhne, A. Genetics and timing of sex determination in the East African cichlid fish Astatotilapia burtoni. BMC Genet. 15, 140 (2014).

Acknowledgements. We thank Daniel Jeffries and Guillaume Lavanchy for code sharing for ancestral state reconstructions, Julie Himes for fish illustrations, and Milan Malinsky for discussions on convergent evolution and sex-patterned sites. Calculations were performed at the sciCORE (http://scicore.unibas.ch/) scientific computing center at the University of Basel, with support by the SIB (Swiss Institute of Bioinformatics), and at the Abel computer cluster at the University of Oslo. This work was funded by the Swiss National Science Foundation (SNSF, Ambizione grant PZ00P3_161462) to A.B. and the European Research Council (ERC, CoG 617585 'CICHLID~X') to W.S.

Author Contributions. A.B. designed the study with input from A.E., F.R., and W.S.; A.E. and A.B. analysed all data, M.M. performed variant calling, and helped with ancestral state reconstructions as well as with statistics, F.R. helped in analysing data for ancestral state reconstructions and sex-specific site identifications, A.B. and A.E. wrote the manuscript with final contributions from all authors. All authors read and approved the final manuscript.

Competing interest declaration. The authors declare no competing interests.

Additional Information

Data availability. The genome and transcriptome sequencing and assembly datasets analysed during this study are available from NCBI under the BioProject accession numbers PRJNA552202 and PRJNA550295. All other data are provided in this paper and its Supplementary Information.

Code availability. Data were analysed with open-source software and their included functions as detailed in the methods section.

Supplementary Information is available for this paper.

Correspondence and requests to materials should be addressed to a.boehne@leibniz-zfmk.de

Chapter 8 | Extended Data

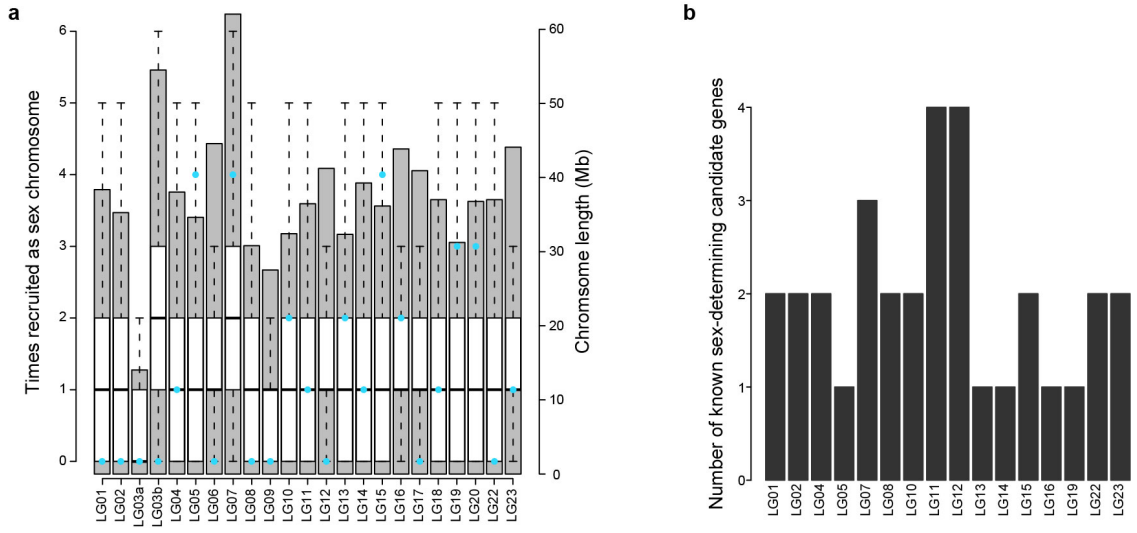

Extended Data Fig. 1 | Non-random sex chromosome evolution. a, Boxplots showing the expected number of sex chromosome recruitments if recruitment was random (10'000 permutations). Boxplot centre lines represent the median, box limits the upper and lower quartiles, and whiskers the 1.5x interquartile range. Outliers are not shown. We found that 10 LGs were never recruited as sex chromosomes in LT cichlids, under random recruitment this pattern occurred only in 3.45% of all simulations. Turquoise dots indicate the number of observed sex chromosome recruitments per LG derived from ancestral state reconstructions, grey bars represent chromosome length in Mb. **b**, Number of previously described candidate genes for sex determination on each reference LG.

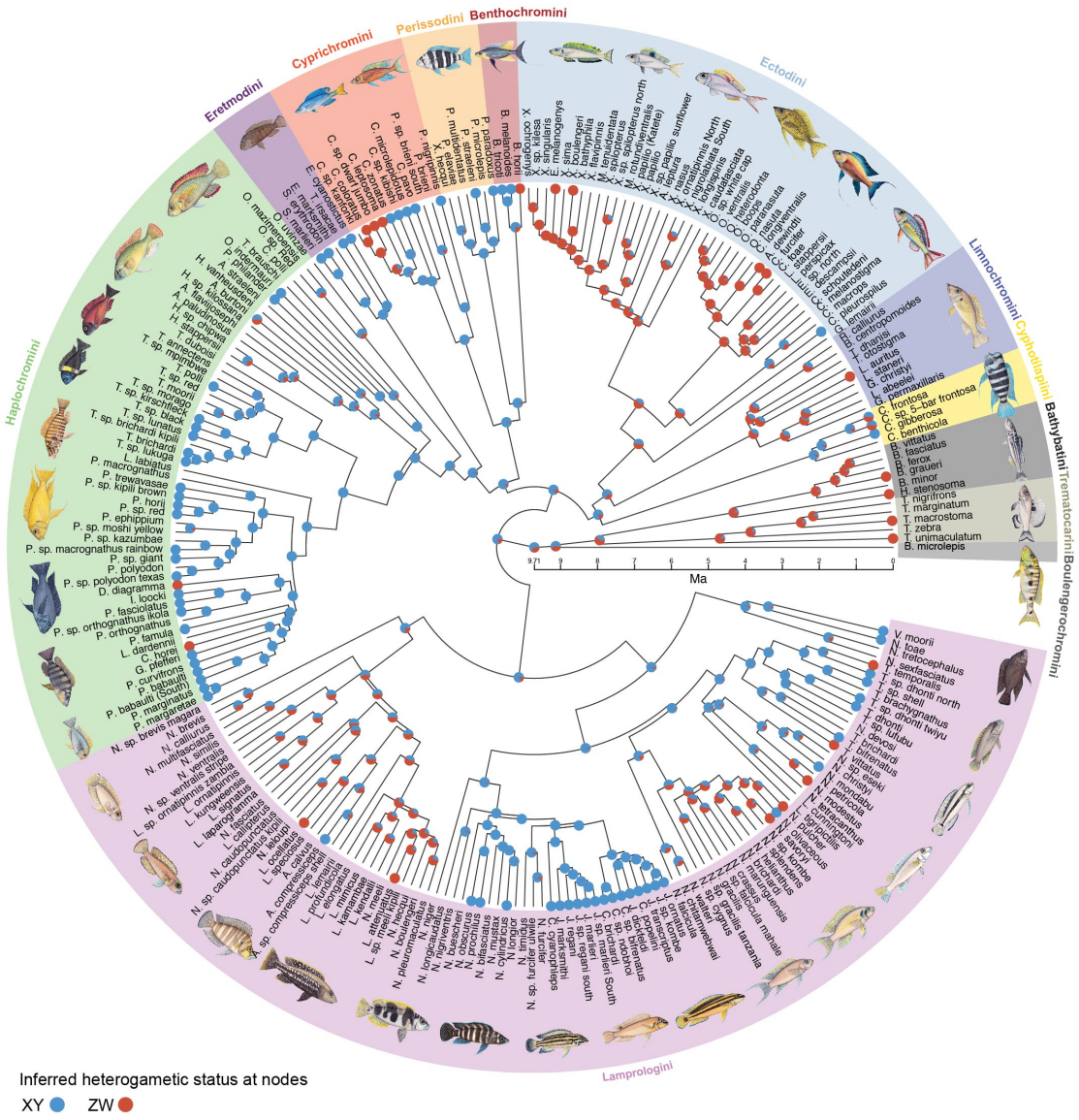

Extended Data Fig. 2 | Stochastic character mapping for heterogametic status. Circles at the tips of the phylogeny represent the heterogametic status (blue: XY, red: ZW). Pie charts at internal nodes represent the reconstructed heterogametic state in 1'000 simulations. Coloured shadings refer to the assignment of species into tribes.

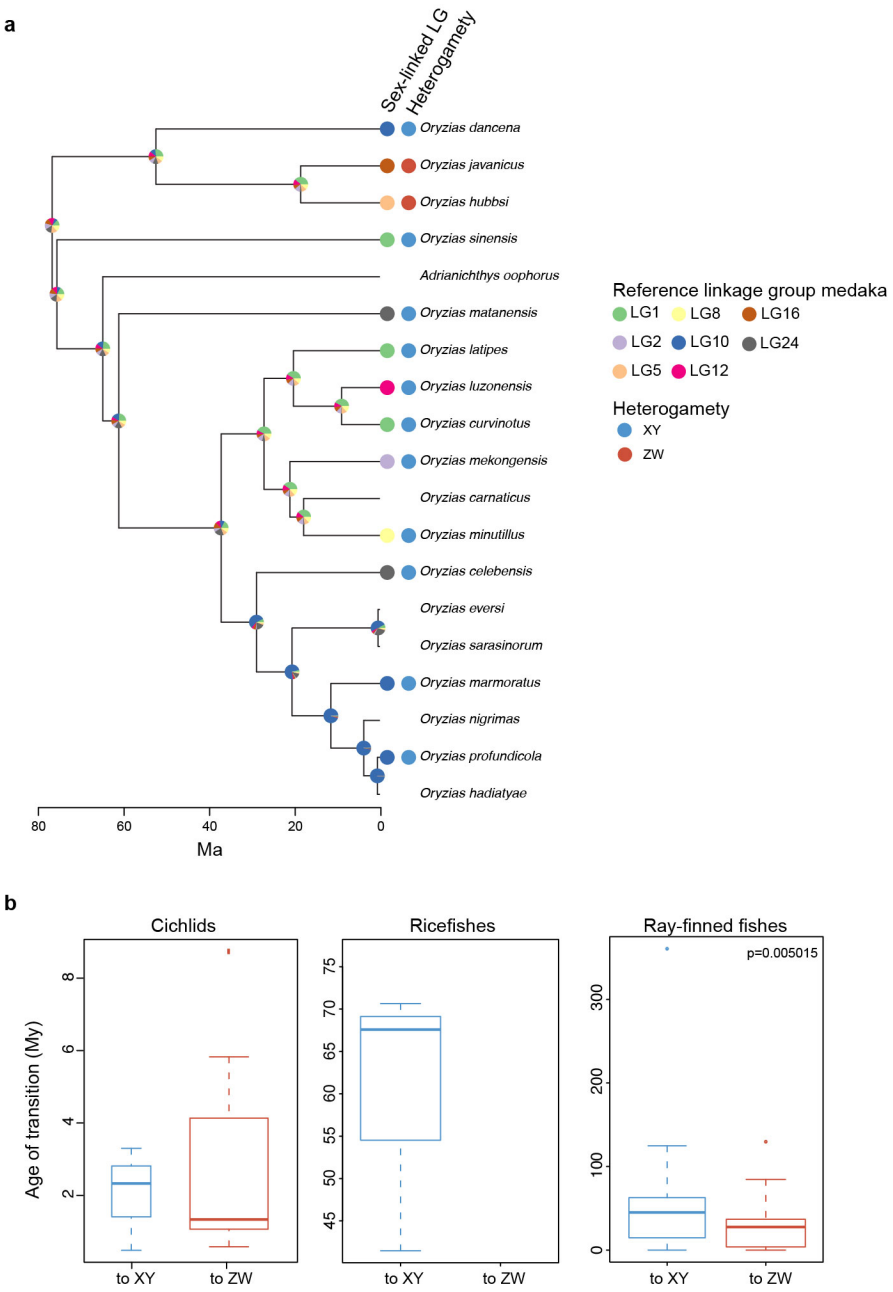

Extended Data Fig. 3 | Sex chromosome evolution in fishes. a, Stochastic character mapping for sex chromosomes in ricefishes. Circles at tips represent heterogametic status and sex-associated LGs with respect to the medaka genome. Pie charts at nodes represent the probability for an LG being a sex chromosome at this time. Colours refer to LGs of the reference genome. **b**, Age of heterogametic transitions. In cichlids (left panel) and in ray-finned fishes in general (right panel), transitions to ZW systems are younger than transitions to XY systems (significant difference in ray-finned fishes, Kruskal-Wallis rank sum test: P=0.005). In ricefishes (central panel), we reconstructed only three transitions to XY, none to ZW. Boxplot centre lines represent the median, box limits the upper and lower quartiles, and whiskers the 1.5x interquartile rang, points represent outliers. The size of boxes within a plot is proportional to the number of transition events.

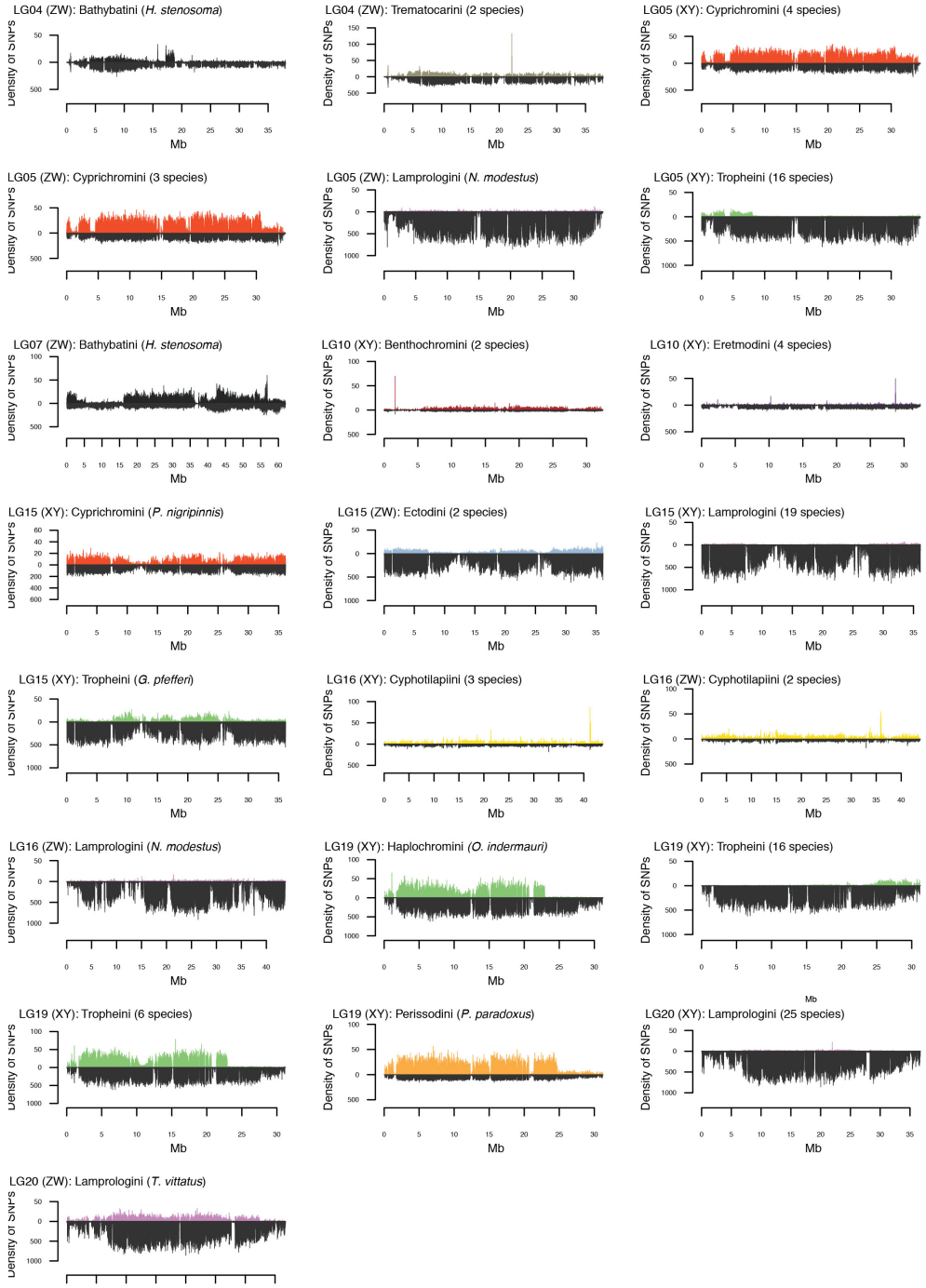

Extended Data Fig. 4 | Distribution of sex-patterned SNPs along the sex-associated LGs. Each plot represents one identified sex chromosomal system. In each plot, upper panels show the density of XY- or ZW-patterned SNPs, lower panels show the distribution of the total number of SNPs called for each window along the LG. Coloured bars represent the number of sex-linked SNPs along the linkage group, colour coding is according to tribe. For LG04 we show ZW-SNPs of *H. stenosoma* (Bathybatini), ZW-SNPs of Trematocarini (mean of two species); for LG05 we show XY-SNPs of Cyprichromini (mean of four species) and ZW-SNPs of Cyprichromini (mean of three species), ZW-SNPs of *N. modestus* (Lamprologini), XY-SNPs of Tropheini (mean of 16 species); for LG07 we show ZW-SNPs for *H. stenosoma* (Bathybatini); XY-SNPs for Benthochromini (mean of two species), for LG10 we show XY-SNPs of Eretmodini (mean of four species); for LG15 we show XY-SNPs of *P. nigripinnis* (Cyprichromini), ZW-SNPs of Ectodini (mean of two species), XY-SNPs of Lamprologini (mean of 19 species), XY-SNPs of *G. pfefferi* (Tropheini); for LG16 we show XY-SNPs of Cyphotilapiini (mean of three species), ZW-SNPs of Cyphotilapiini (mean of two species), ZW-SNPs of *N. modestus* (Lamprologini); for LG19 we show XY-SNPs of *O. indermauri* (Haplochromini), XY-SNPs of Tropheini (species with a XY system on LG05 and LG19, mean of 16 species), XY-SNPs of Tropheini (species with a signal on LG19 only genus *Tropheus*, mean of six species), XY-SNPs of *P. paradoxus* (Perissodini); for LG20 we show XY-SNPs of Lamprologini (mean of 25 species) and ZW-SNPs of *T. vittatus* (Lamprologini).

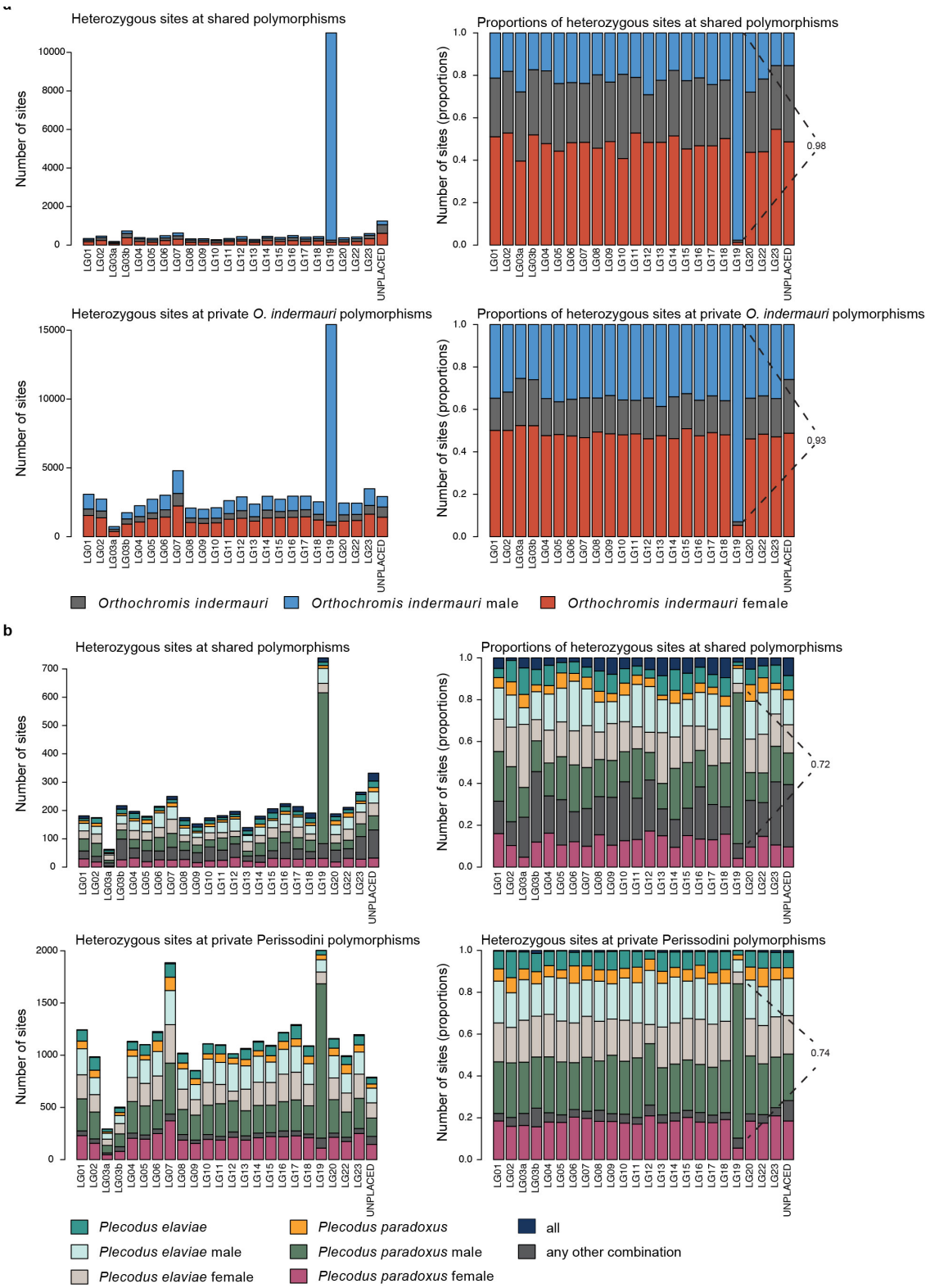

Extended Data Fig. 5 | Sex chromosome LG19 in Tropheini/Haplochromini and Perissodini. Analyses to test for convergent or shared sex chromosome recruitment in Perissodini and Tropheini/Haplochromini. LG19 carries an XY system in the same large region in six LT Tropheini (genus *Tropheus*), the riverine Haplochromini *O. indermauri* and in two Perissodini. a, Barplots representing the number of heterozygous sites in the *O. indermauri* individuals at sites with a shared polymorphism between *O. indermauri* and the *Tropheus* species (upper panels, plots left in counts, right in proportion) and at polymorphisms private to *O. indermauri* (lower panel). b, Barplots representing the number of heterozygous sites in Perissodini individuals at sites with a shared polymorphism between Perissodini and Tropheini/Haplochromini (upper panels, plots left in counts, right in proportion) and at polymorphisms private to the Perissodini (lower panel). The panel depicts *P. paradoxus*, which has the LG19 XY SD system and *P. elaviae*, which does not have it.

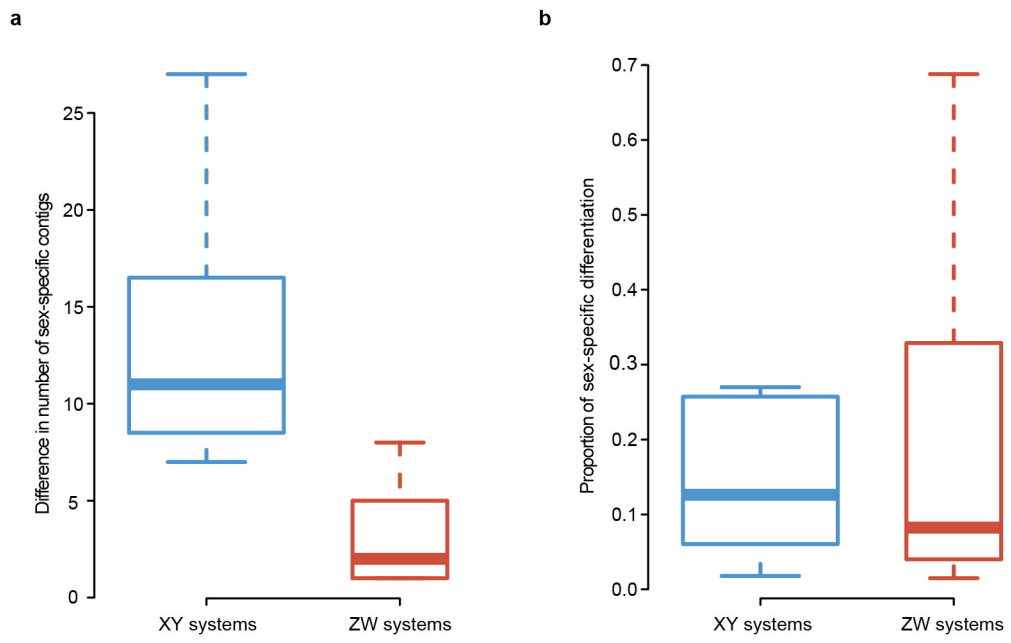

Extended Data Fig. 6 | Difference in identified sex-specific transcripts and degree of differentiation for XY and ZW systems. a, Boxplots of the difference in the number of sex-specific transcripts identified for XY and ZW systems, respectively, with the approach described in-. Boxplot centre lines represent the median, box limits the upper and lower quartiles, and whiskers the 1.5x interquartile range. The width of the boxes is proportional to the number of observations. Outliers are not shown. **b**, Boxplots of the percentage of differentiation of the sex chromosome for XY and ZW SD systems, respectively. Boxplot centre lines represent the median; box limits the upper and lower quartiles and whiskers the 1.5x interquartile range. The width of the boxes is proportional to the number of observations. Outliers are not shown.

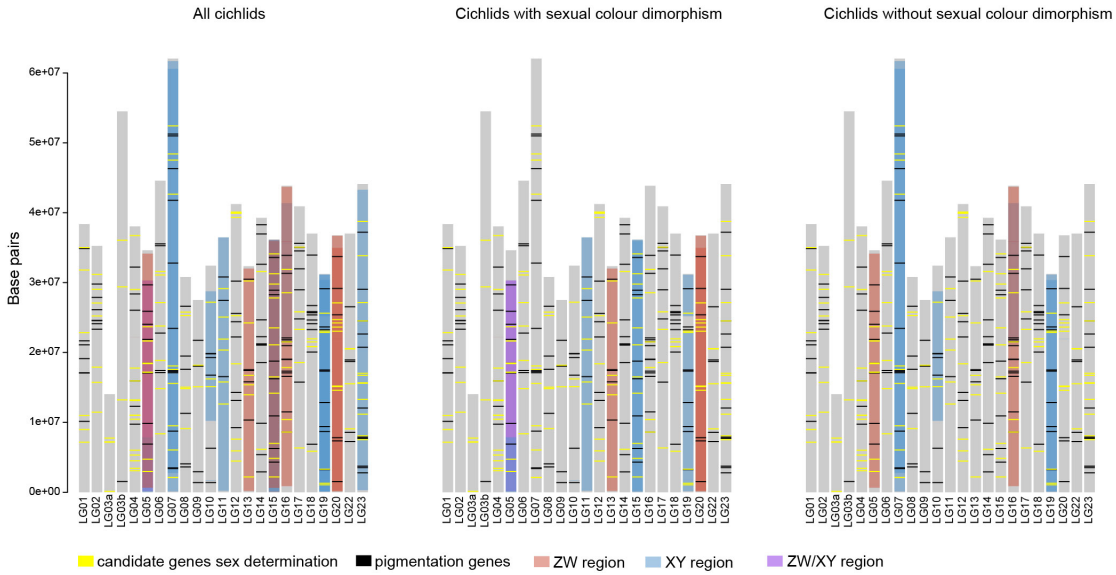

Extended Data Fig. 7 | Distribution of candidate genes for sex determination and pigmentation. Grey bars represent LGs and lines candidate genes for sex determination and pigmentation. Sex-determining regions are indicated with coloured shadings.

Chapter 8 | Supplementary Material

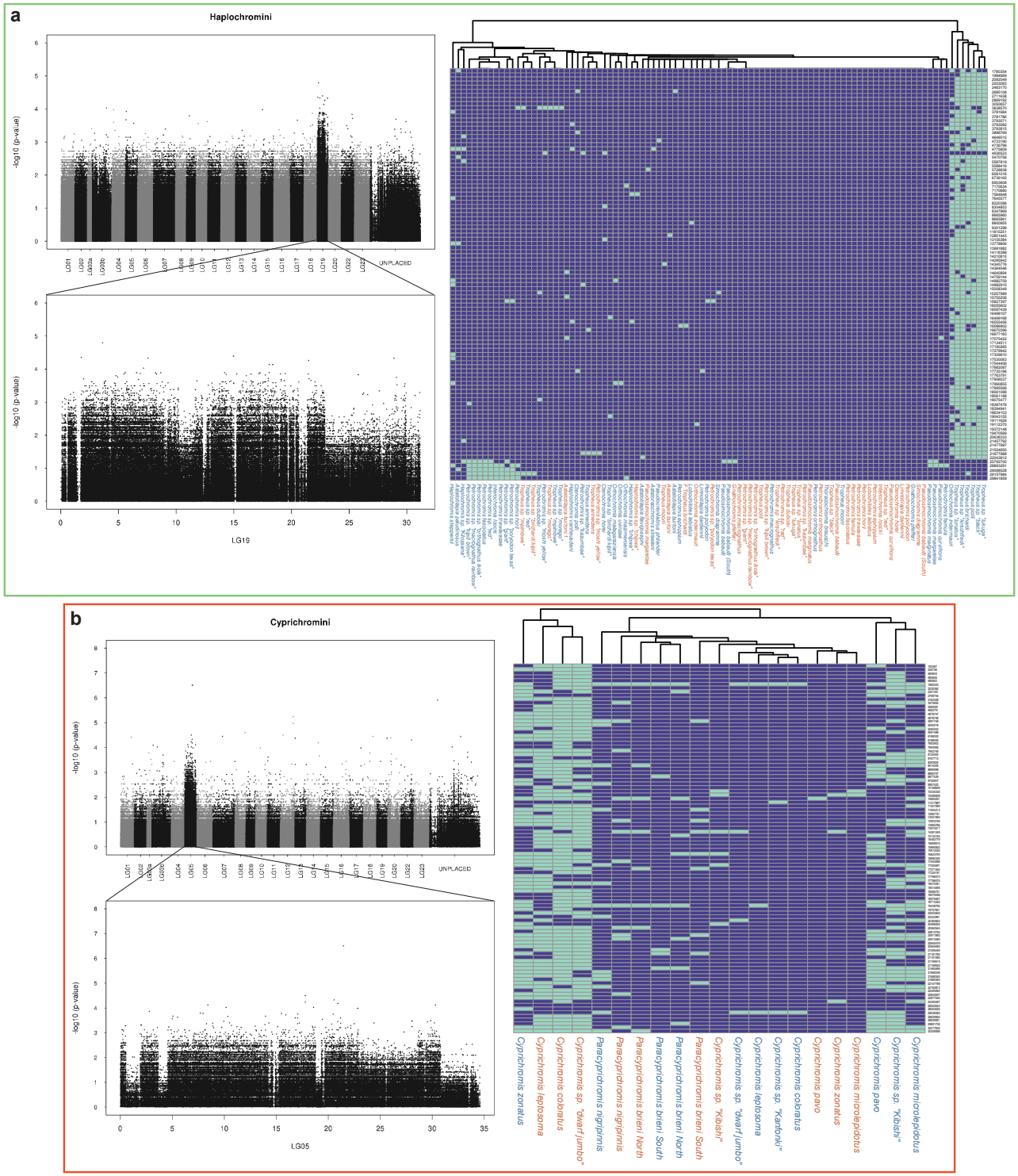

Fig. S1 GWAS for sex and underlying genotypes. Each panel shows a Manhattan plot for a GWAS to test for an association with sex, dark and light grey shadings indicate linkage groups of the reference genome (*O. niloticus*). Heatmaps show individual genotypes for outlier SNPs of sex-associated regions (purple: homozygous, green: heterozygous). **a** Haplochromini show an association with sex on LG19. A zoom on LG19 shows that there is broad region of increased association with sex. A heatmap of the genotypes of the 100 most significant SNPs indicates that this signal stems from an XY (male heterogametic, female homogametic) signal in species of the genus *Tropheus*. **b** Cyprichromini show an association with sex on LG05. A zoom on LG05 shows that almost the full length of LG05 shows an increased signal for association with sex. A heatmap of the genotypes of the 100 most significant SNPs indicates that LG05 is an XY system in four species of the genus *Cyprichromis* (male heterogametic, female homogametic) and a ZW system in three other species of the same genus (male homogametic, female heterogametic). Species of the genus *Paracyprichromis* seem not to show sex differentiation on LG05. **c** Lamprologini show an association with sex on LGs 15 and 20. A zoom on LG20 shows that there is a narrow region of increased association with sex. A heatmap of the genotypes of all outlier SNPs indicates that this signal stems from an XY (male heterogametic, female homogametic) system in 21 species and a ZW patterning in one species. **d** Ectodini did not show an accumulation of an association with sex on any LG

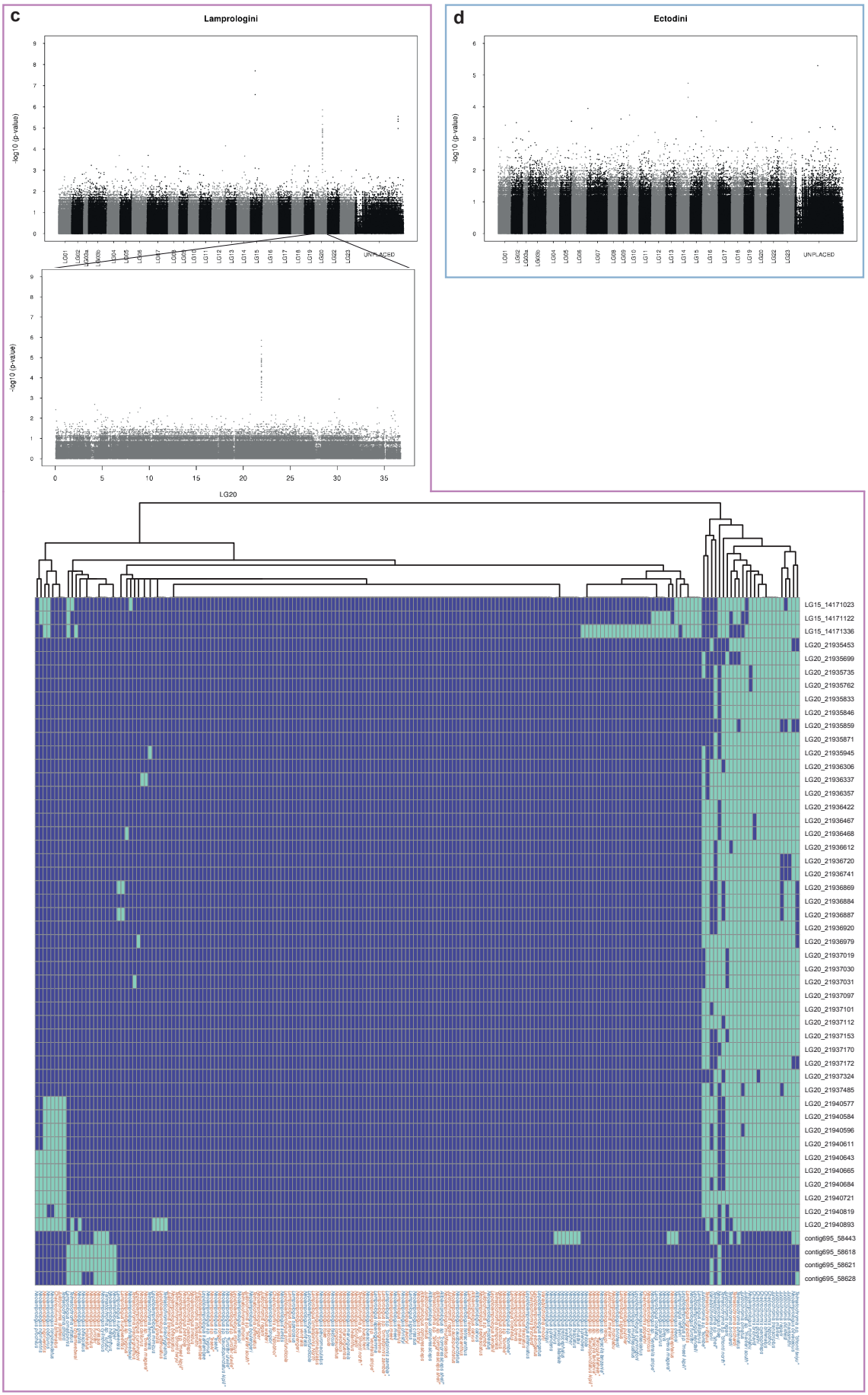
c
Lamprologini
-log10 (p-value)
UNPLACED
LG20
d
Ectodini
-log10 (p-value)
UNPLACED
LG15_14171023
LG15_14171122
LG15_14171336
LG20_21935453
LG20_21935699
LG20_21935735
LG20_21935762
LG20_21935833
LG20_21935846
LG20_21935859
LG20_21935871
LG20_21935945
LG20_21936306
LG20_21936337
LG20_21936357
LG20_21936422
LG20_21936467
LG20_21936468
LG20_21936612
LG20_21936720
LG20_21936741
LG20_21936869
LG20_21936884
LG20_21936887
LG20_21936920
LG20_21936979
LG20_21937019
LG20_21937030
LG20_21937031
LG20_21937097
LG20_21937101
LG20_21937112
LG20_21937153
LG20_21937170
LG20_21937172
LG20_21937324
LG20_21937485
LG20_21940577
LG20_21940584
LG20_21940596
LG20_21940611
LG20_21940643
LG20_21940665
LG20_21940684
LG20_21940721
LG20_21940819
LG20_21940893
contig695_58443
contig695_58618
contig695_58621
contig695_58628

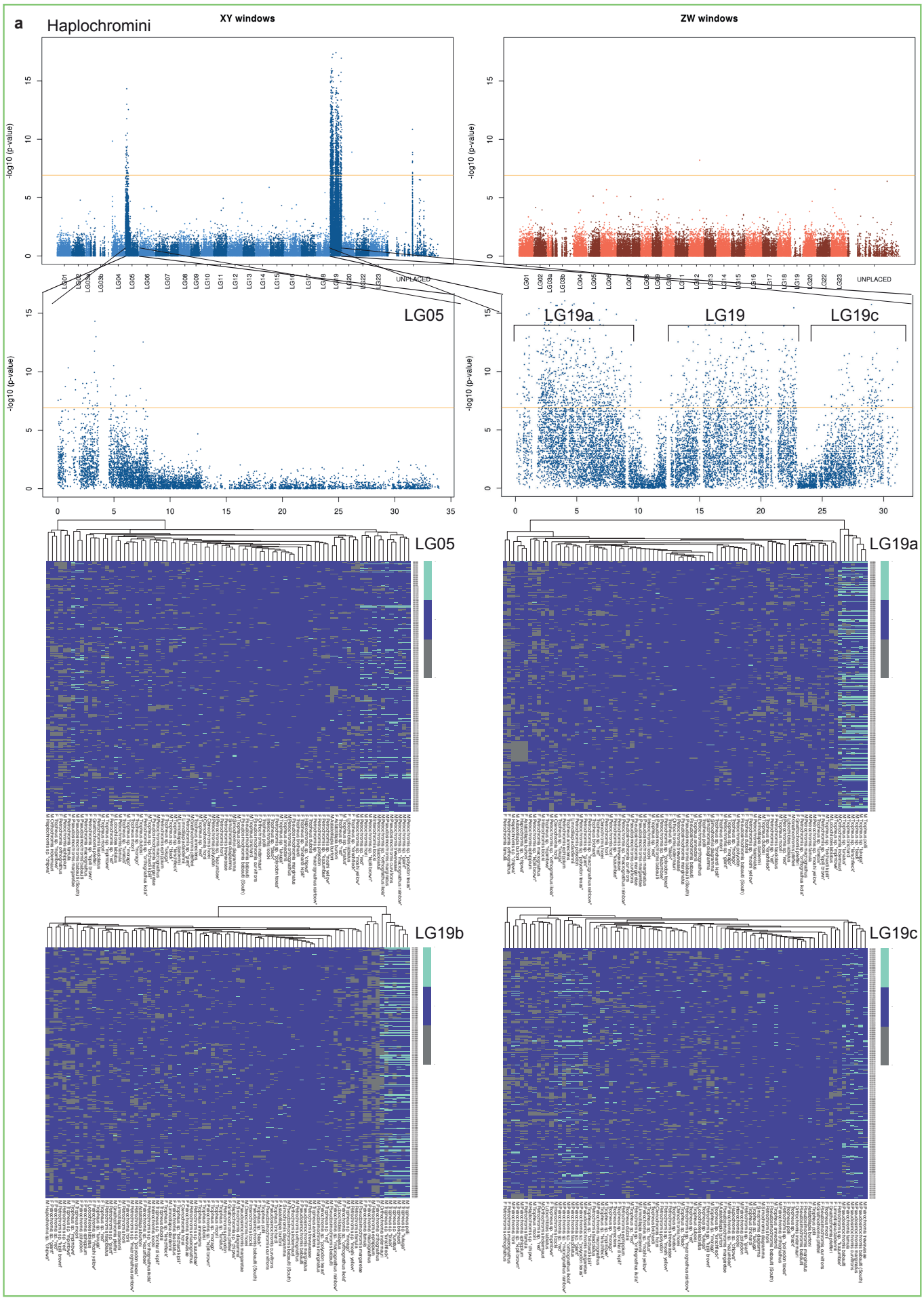
a
Haplochromini
XY windows
ZW windows
-log10 (p-value)
LG01
LG02
LG03a
LG03b
LG04
LG05
LG06
LG07
LG08
LG09
LG10
LG11
LG12
LG13
LG14
LG15
LG16
LG17
LG18
LG19
LG20
LG22
LG23
UNPLACED
LG05
LG19a
LG19
LG19c
LG19b

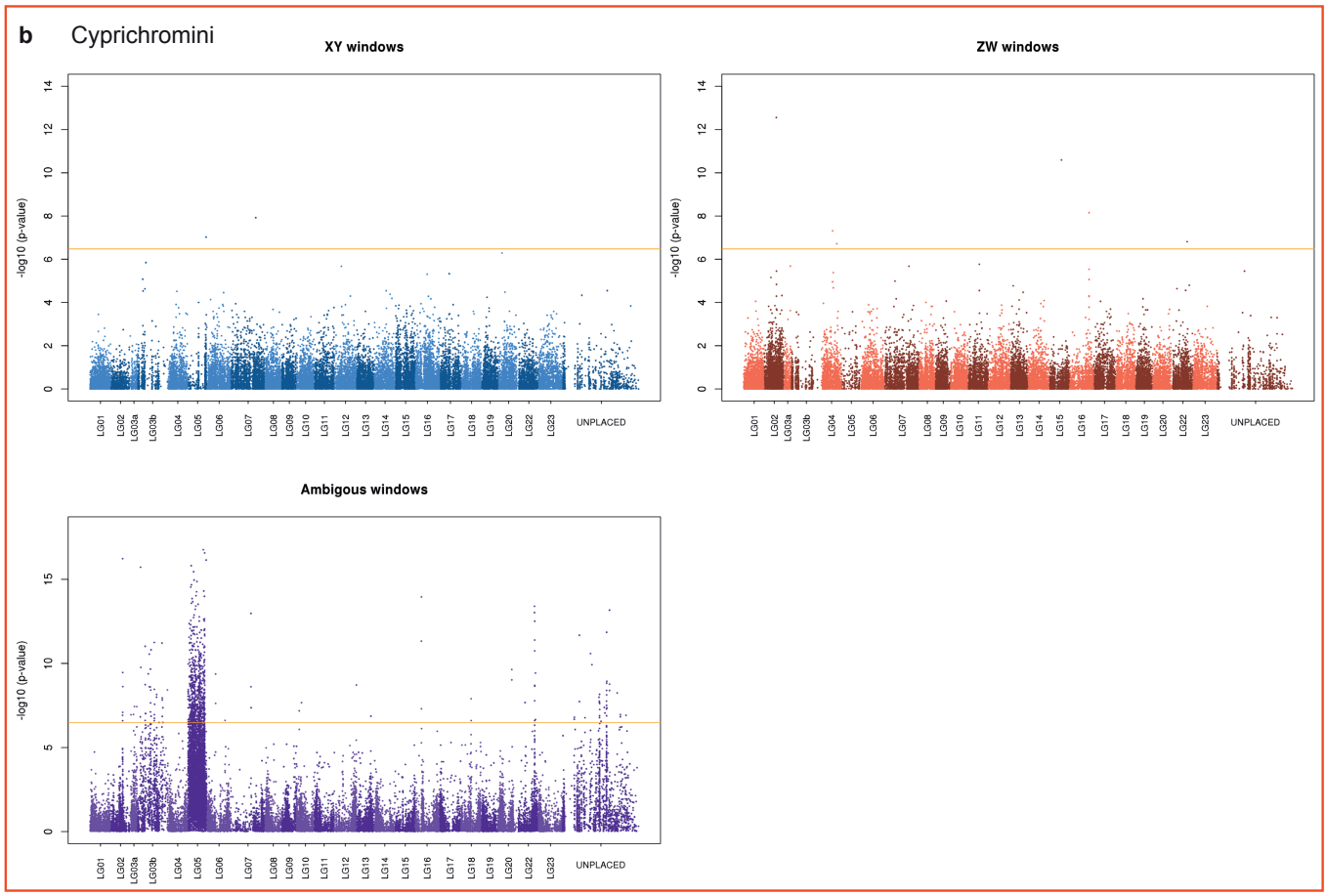
b
Cyprichromini
XY windows
ZW windows
Ambigous windows
-log10 (p-value)
LG01
LG02
LG03a
LG03b
LG04
LG05
LG06
LG07
LG08
LG09
LG10
LG11
LG12
LG13
LG14
LG15
LG16
LG17
LG18
LG19
LG20
LG22
LG23
UNPLACED

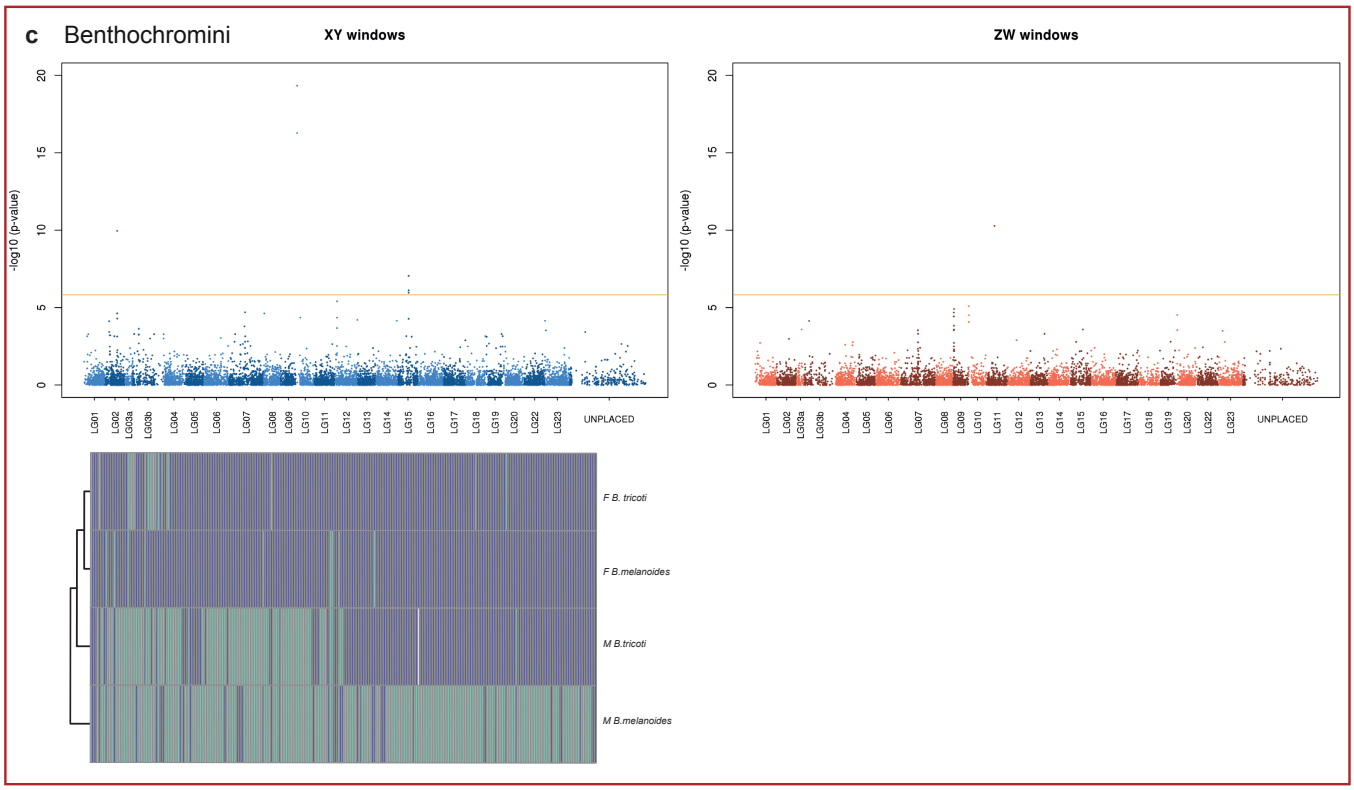
c
Benthochromini
XY windows
ZW windows
-log10 (p-value)
UNPLACED
F B. tricoti
F B.melanoides
M B.tricoti
M B.melanoides

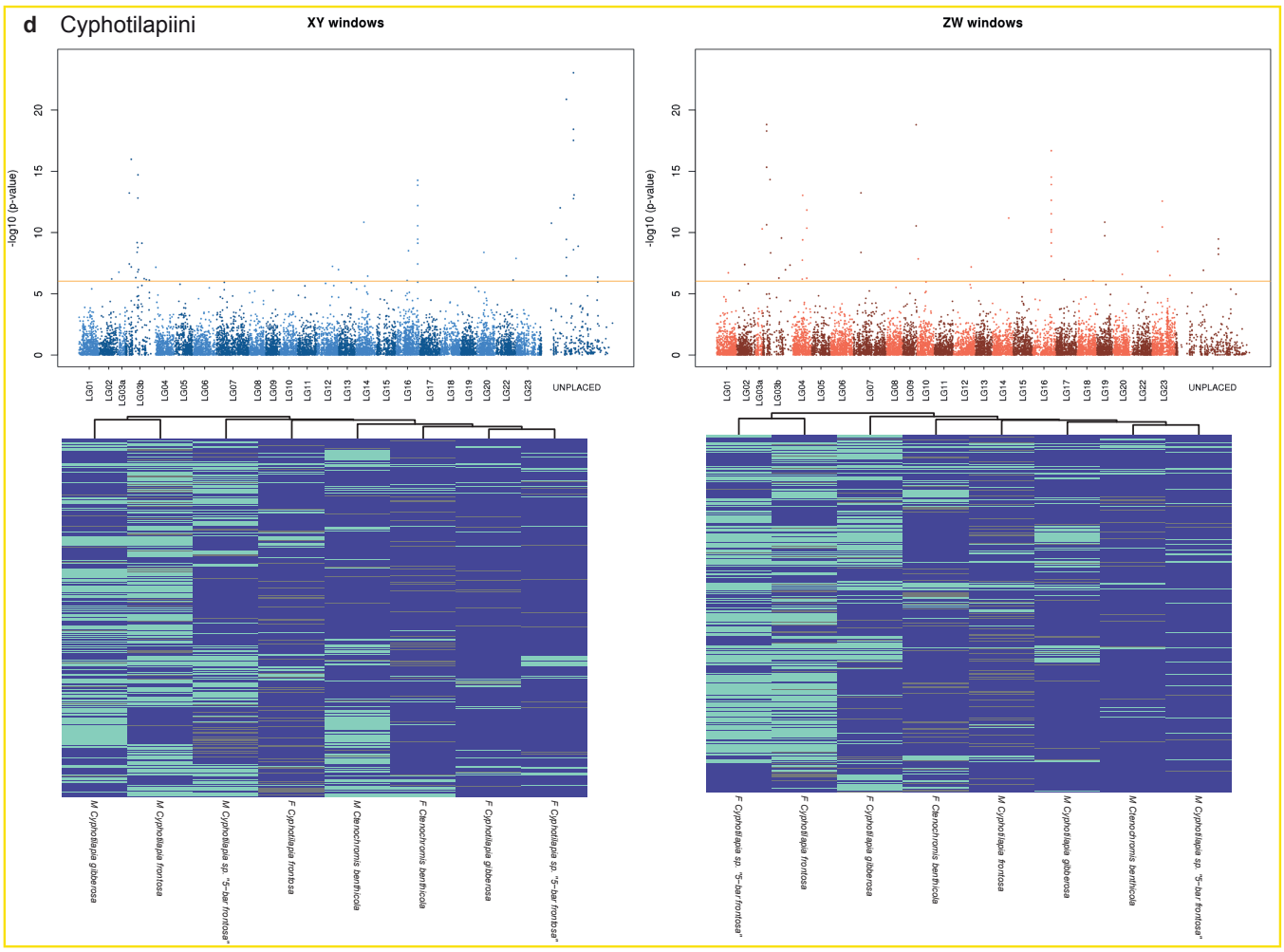
d Cyphotilapiini
XY windows
ZW windows
-log10 (p-value)
0
5
10
15
20
LG01
LG02
LG03a
LG03b
LG04
LG05
LG06
LG07
LG08
LG09
LG10
LG11
LG12
LG13
LG14
LG15
LG16
LG17
LG18
LG19
LG20
LG22
LG23
UNPLACED
M Cyphotilapia gibberosa
M Cyphotilapia frontosa
M Cyphotilapia sp. "5–bar frontosa"
F Cyphotilapia frontosa
M Ctenochromis benthicola
F Ctenochromis benthicola
F Cyphotilapia gibberosa
F Cyphotilapia sp. "5–bar frontosa"

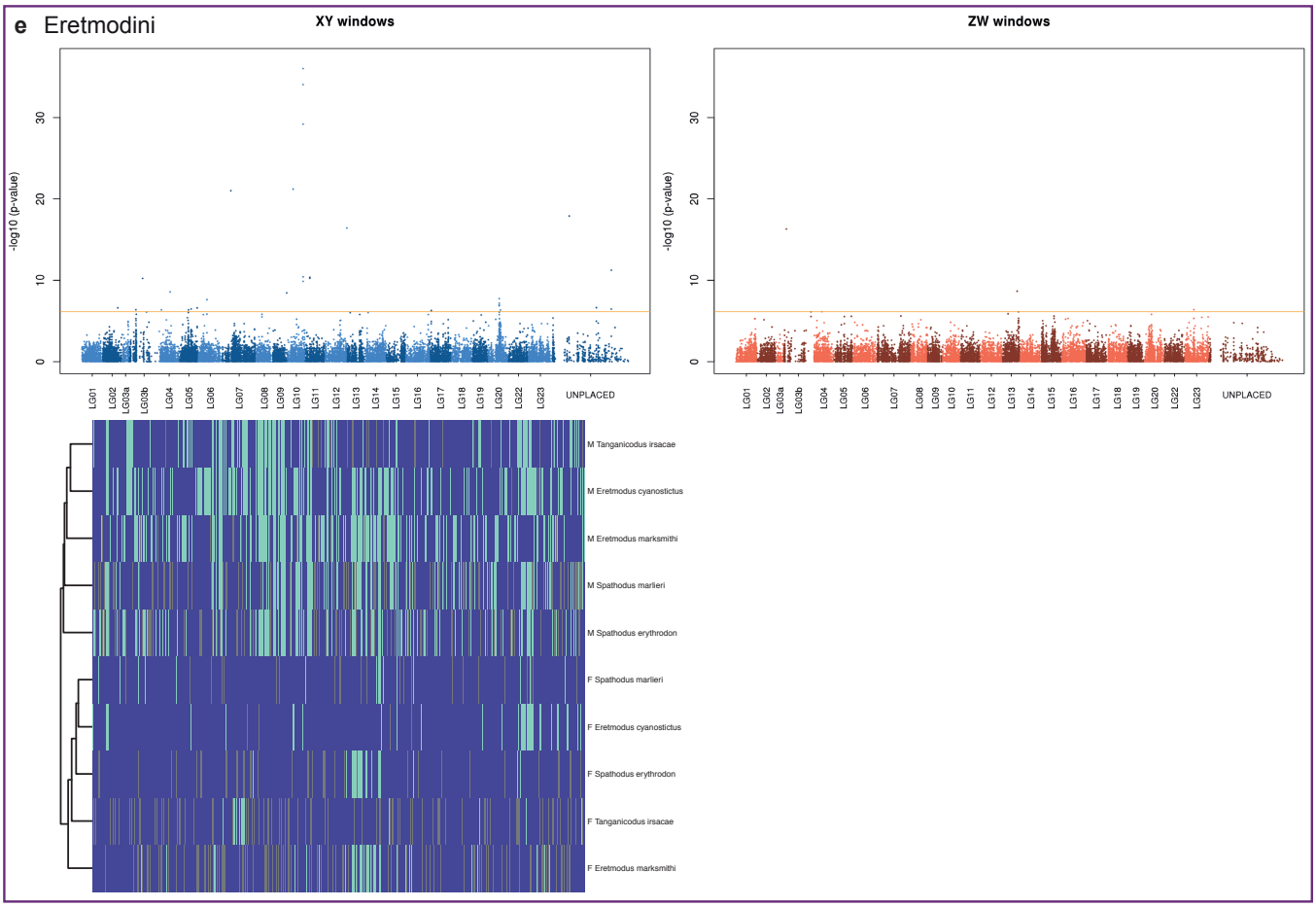
e Eretmodini
XY windows
ZW windows
-log10 (p-value)
0
10
20
30
LG01
LG02
LG03a
LG03b
LG04
LG05
LG06
LG07
LG08
LG09
LG10
LG11
LG12
LG13
LG14
LG15
LG16
LG17
LG18
LG19
LG20
LG22
LG23
UNPLACED
M Tanganicodus irsacae
M Eretmodus cyanostictus
M Eretmodus marksmithi
M Spathodus marlieri
M Spathodus erythrodon
F Spathodus marlieri
F Eretmodus cyanostictus
F Spathodus erythrodon
F Tanganicodus irsacae
F Eretmodus marksmithi

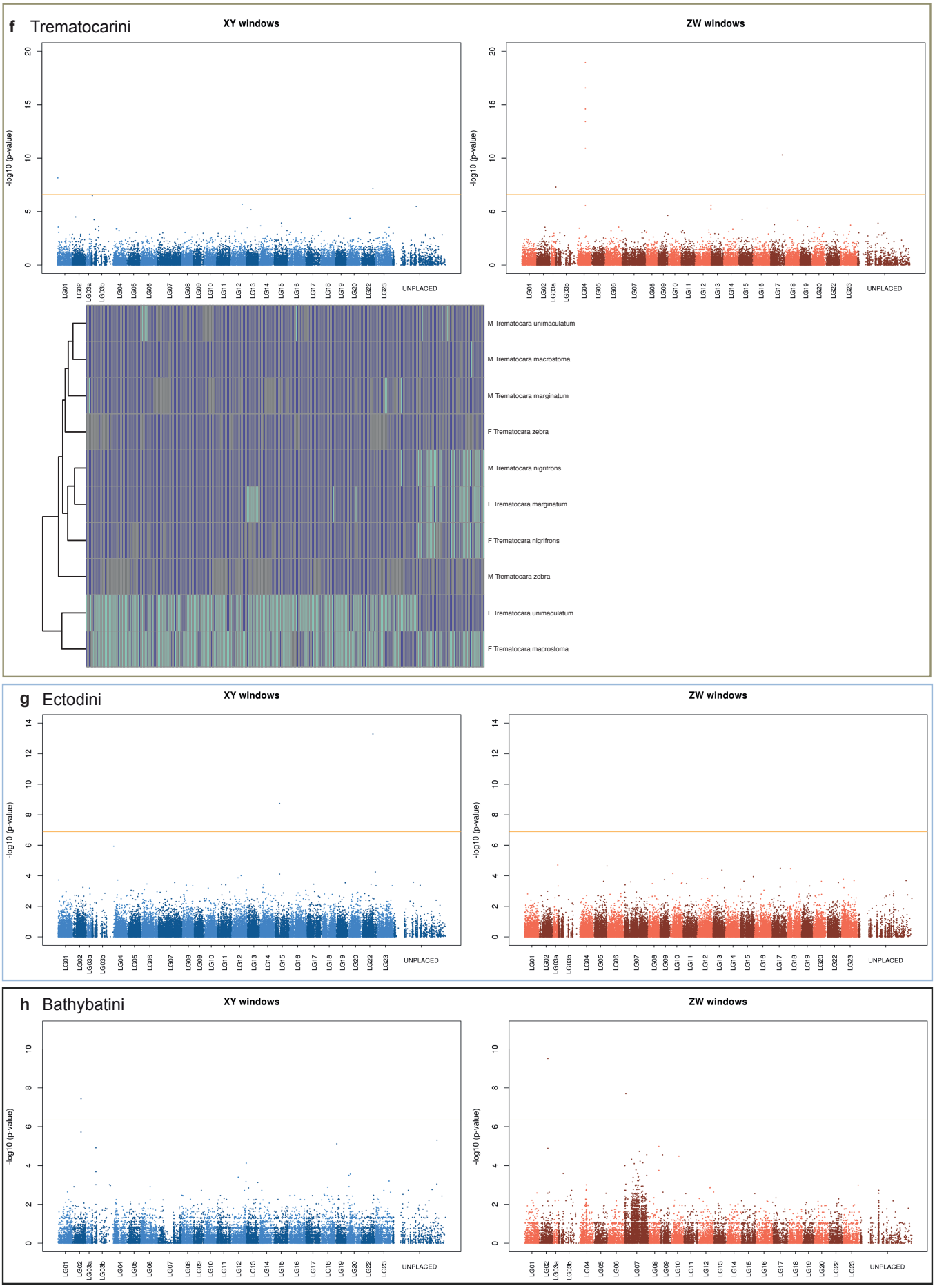
f Trematocarini
XY windows
ZW windows
-log10 (p-value)
LG01 LG02 LG03a LG03b LG04 LG05 LG06 LG07 LG08 LG09 LG10 LG11 LG12 LG13 LG14 LG15 LG16 LG17 LG18 LG19 LG20 LG22 LG23 UNPLACED
M Trematocara unimaculatum
M Trematocara macrostoma
M Trematocara marginatum
F Trematocara zebra
M Trematocara nigrifrons
F Trematocara marginatum
F Trematocara nigrifrons
M Trematocara zebra
F Trematocara unimaculatum
F Trematocara macrostoma
g Ectodini
XY windows
ZW windows
h Bathybatini
XY windows
ZW windows

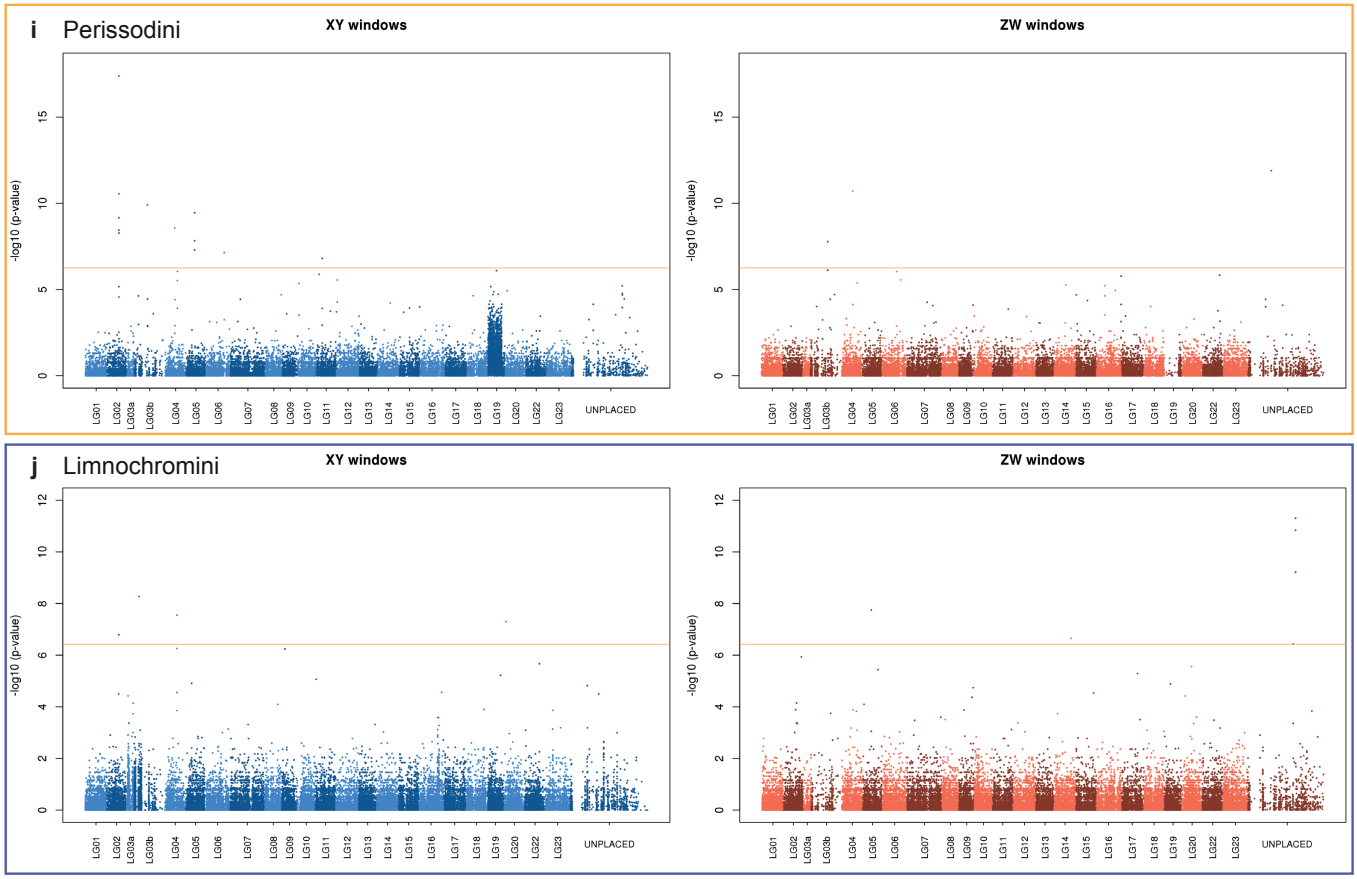
i Perissodini
XY windows
ZW windows
-log10 (p-value)
LG01 LG02 LG03a LG03b LG04 LG05 LG06 LG07 LG08 LG09 LG10 LG11 LG12 LG13 LG14 LG15 LG16 LG17 LG18 LG19 LG20 LG22 LG23
UNPLACED
j Limnochromini
XY windows
ZW windows
-log10 (p-value)
LG01 LG02 LG03a LG03b LG04 LG05 LG06 LG07 LG08 LG09 LG10 LG11 LG12 LG13 LG14 LG15 LG16 LG17 LG18 LG19 LG20 LG22 LG23
UNPLACED

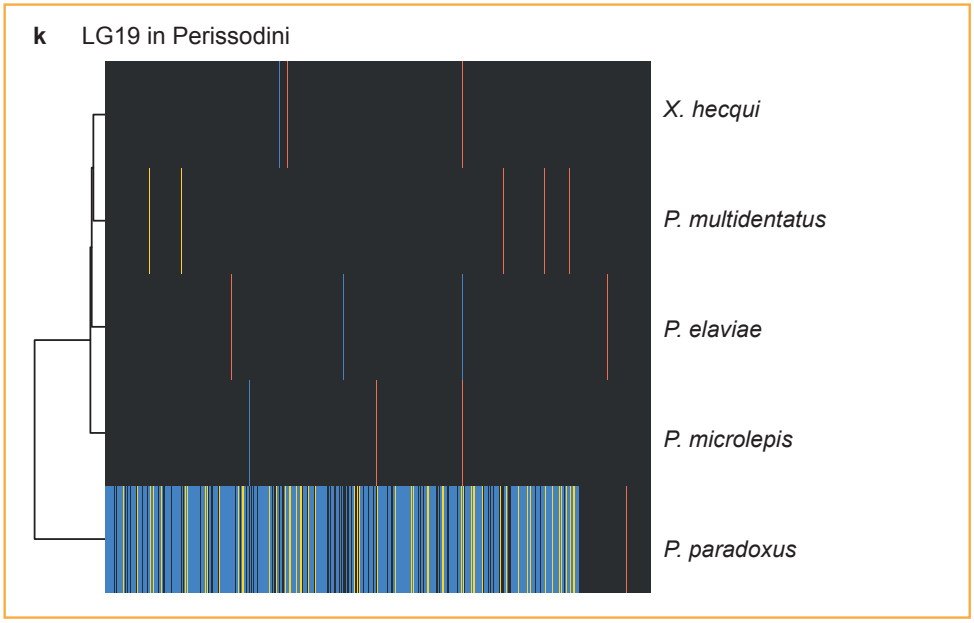
k LG19 in Perissodini
X. hecqui
P. multidentatus
P. elaviae
P. microlepis
P. paradoxus

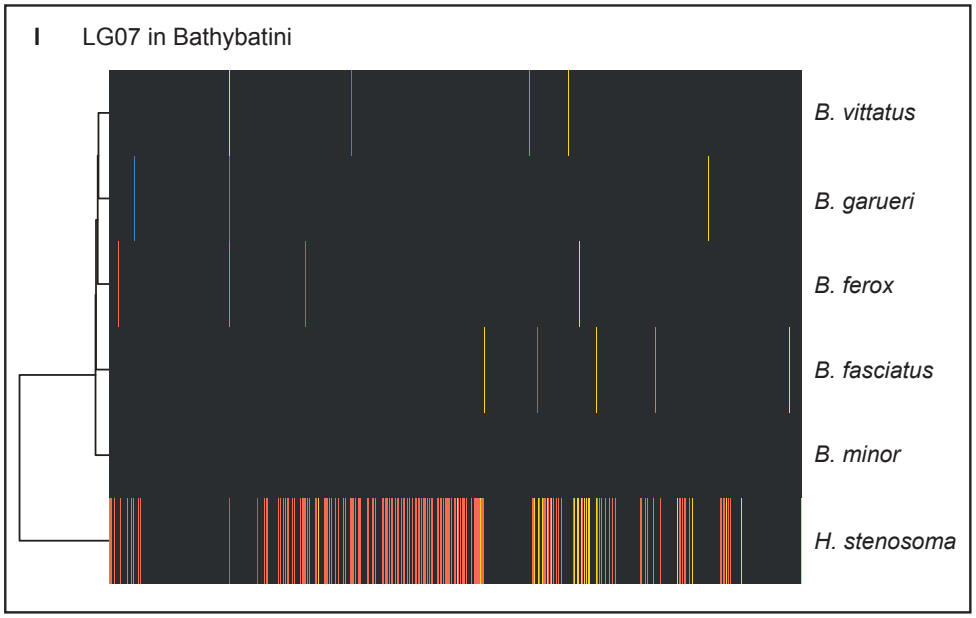

Fig. S2 Test for overrepresentation of sex-patterned sites per tribe. Each panel shows two Manhattan plots for a test of overrepresentation of XY (blue shadings) and ZW (red shadings) patterned sites with respect to the linkage groups of the reference genome (*O. niloticus*). Heatmaps show individual genotypes for outlier SNPs of sex-associated regions (purple: homozygous, green: heterozygous, grey: missing data). The orange line indicates the significance threshold after Bonferroni correction for multiple-testing. **a** Haplochromini show an accumulation of XY-patterned sites on LG05 and LG19. A zoom on LG05 shows that there is an association within the first ~7Mb of this LG. A zoom on LG19 indicates three large blocks of an increase of XY sites (referred to as LG19a, b and c). Genotype heatmaps of the outlier SNP windows indicate that LG06 is a n XY system in several Tropheini species not belonging to the genus *Tropheus*. The same species show an increase in XY-patterned sites in region LG19c. Regions LG19a and b represent an XY system in several species of the genus *Tropheus* as previously detected by a GWAS approach (Fig. S1). **b** Cyprichromini show an overrepresentation of windows which are both, XY- and ZW-patterned (referred to as ambiguous windows, see Methods for details and shaded in purple) indicating that the same regions on LG05 can be an XY as well as an ZW system, as already identified by the GWAS approach. **b** Benthochromini show outlier windows with an XY-patterning on LG10 and LG15. The underlying genotypes indicate an XY system in both *Benthochromis* species investigated. **d** Cyphotilapiini show an accumulation of both, XY- and ZW-patterned windows on LG16. **e** Eretmodini show an accumulation of XY-patterned windows on LG10. **f** Trematocarini show an accumulation of ZW-patterned windows on LG04. **g** Ectodini do not show an accumulation of sex-patterned windows. **h** Bathybatini do not show an accumulation of sex-patterned windows above Bonferroni correction. LG07 is increased for ZW-patterned sites. **i** Perissodini do not show an accumulation of sex-patterned windows above Bonferroni correction. LG19 is increased for XY-patterned sites. **j** Limnochromini do not show an accumulation of sex-patterned windows. **k** and **l** A species-specific analysis of sex-patterned windows shows that the signals observed for Perissodini (Fig. S2i) and Bathybatini (Fig. S2h) stems from one species in each case (ZW system on LG07 in *H. stenosoma* and XY system on LG18 in *P. paradoxus*). The heatmaps show sex-patterned windows along the two LGs for all species investigated in the two tribes, blue for XY-patterned windows, red for ZW-patterned windows, black for no-sex windows and yellow for ambiguous windows

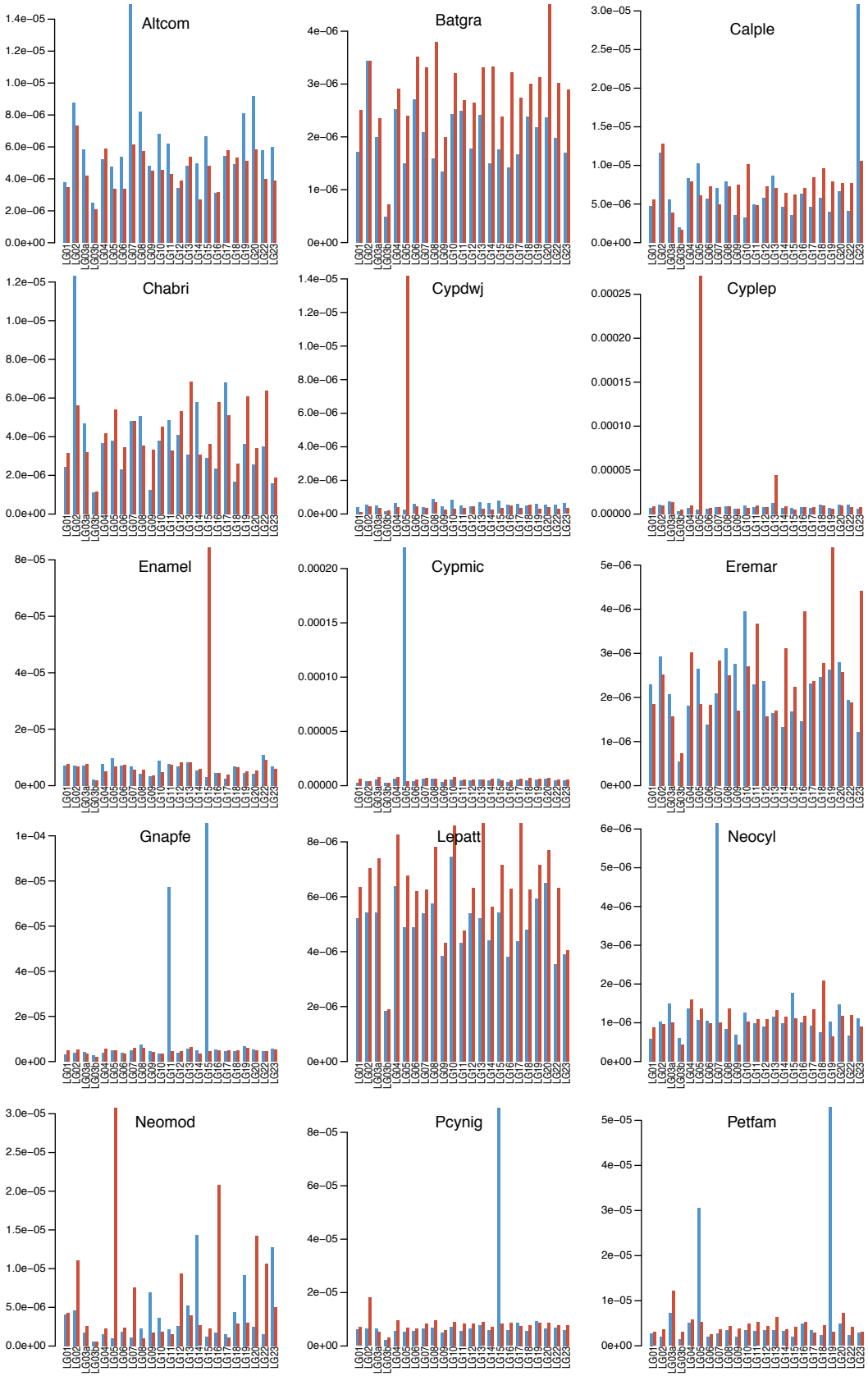
Altcom
Batgra
Calple
Chabri
Cypdwj
Cyplep
Enamel
Cypmic
Eremar
Gnapfe
Lepatt
Neocyl
Neomod
Pcynig
Petfam

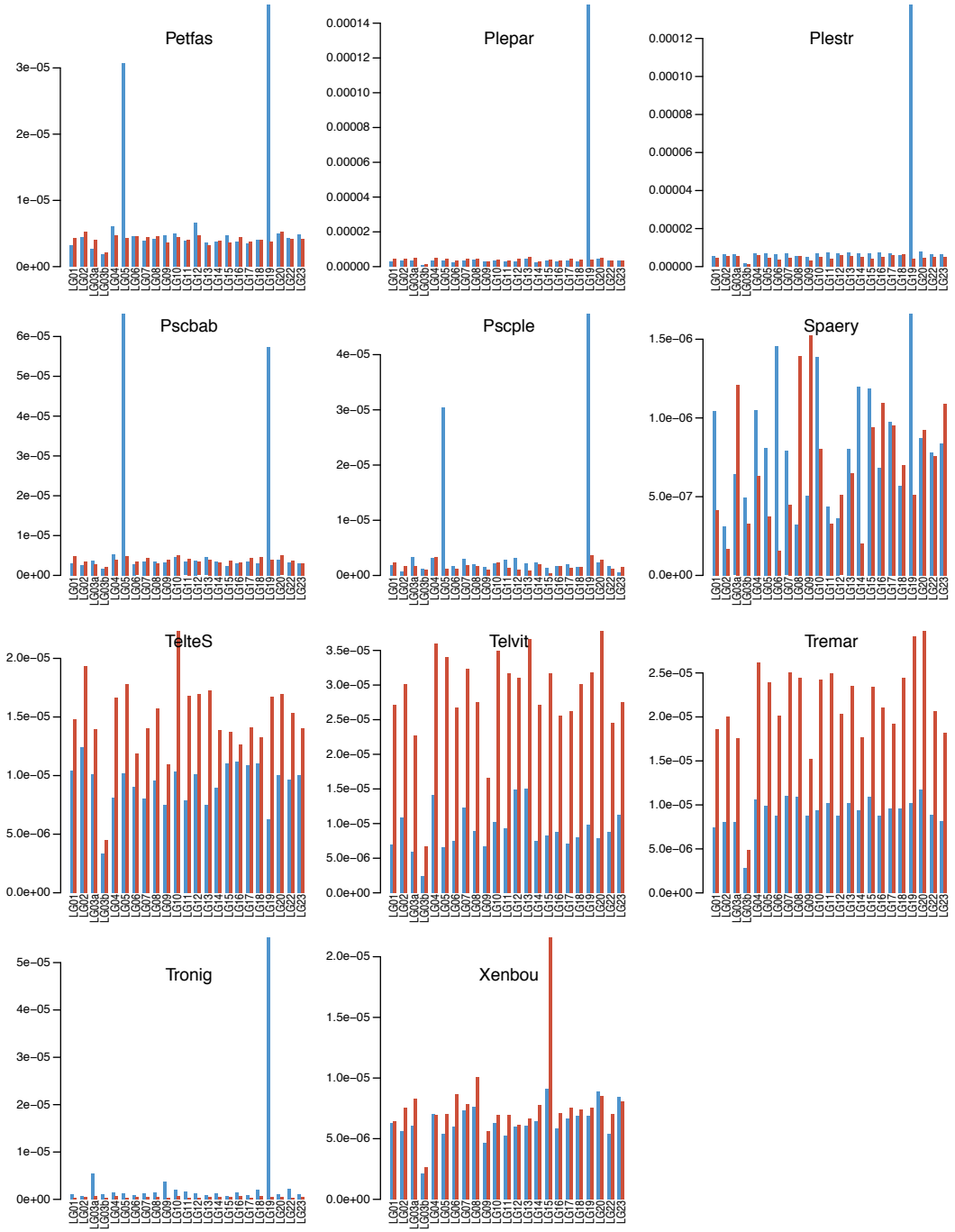

Fig. S3 Barplots showing the number of sex-patterned SNPs (RNA data) per linkage-group for species for which a sex-determining region was detected or corroborated using RNA data. The number of XY-patterned SNPs is represented with blue bars and the number of ZW-patterned SNPs in the red bars. The number of sex-pattern SNPs are corrected for the length of the respective linkage-group. See Table S1 for full species names

Table S1 Taxon list and main findings. For each taxon, the type of data used (genomes included from Ronco et al. (in prep); RNAseq data included from El Taher et al. (in prep)) and the main findings is given

			data used			Sex chromosome characterization			
Tribe	ID	Full Name	Genome (M)	Genome (F)	RNAseq data	Final Call System	Final Call LG	Final Call Stringent	Types of evidence
Bathybatini	Batfas	Bathybates fasciatus	ITH3	GPB2	no	XY	LG06	NA	only BarplotDNA
Bathybatini	Batfer	Bathybates ferox	LCD6	LCD7	no	NA	NA	NA	only BarplotDNA
Bathybatini	Batgra	Bathybates graueri	ILG7	IUI8	yes	ZW	LG20	ZW, LG20	RNA
Bathybatini	Batmin	Bathybates minor	JBG3	IXA5	no	NA	NA	NA	NA
Bathybatini	Batvit	Bathybates vittatus	JDE6	JDE7	no	NA	NA	NA	NA
Bathybatini	Hemste	Hemibates stenosoma	IXC2	IXC3	no	ZW	LG04, LG07	ZW, LG07, LG04	BarplotDNA+literature
Benthochromini	Benhor	Benthochromis horii			no	ZW	LG20	ZW, LG20	RNA
Benthochromini	Benmel	Benthochromis melanoides	IXB8	IZA2	no	ZW/XY	LG10, LG02	XY, LG10	Fisher, same signal two species
Benthochromini	Bentri	Benthochromis tricoti	LDA7	LDA9	no	XY	LG10	XY, LG10	Fisher, same signal two species
Boulengerochromini	Boumic	Boulengerochromis microlepis	JCF2	JAE7	yes	NA	NA	NA	NA
Cyphotilapiini	Cphfr5	Cyphotilapia sp. "5-bar frontosa"	KAG3	KDG2	no	XY/ZW	LG16	XY/ZW, LG16	Fisher same signal multiple species
Cyphotilapiini	Cphfro	Cyphotilapia frontosa	LEI9	LEI6	no	XY/ZW	LG16, LG23	XY/ZW, LG16	Fisher same signal multiple species
Cyphotilapiini	Cphgib	Cyphotilapia gibberosa	INH7	INH9	yes	XY	LG05, LG16	XY, LG16	BarplotDNA+Fisher
Cyphotilapiini	Cteben	Ctenochromis benthicola	DMD1	IYA8	no	NA	NA	NA	NA
Cyprichromini	Cypcol	Cyprichromis coloratus	JEC7	JED2	no	ZW/XY	LG05, LG07	ZW, LG05	GWAS+BarplotDNA
Cyprichromini	Cypdwj	Cyprichromis sp. "dwarf jumbo"	KFA7	KFA9	yes	ZW	LG05	ZW, LG05	GWAS+BarplotDNA+RNAsuggestive
Cyprichromini	Cypkan	Cyprichromis sp. "kanfonki"	INH1		no	NA	NA	NA	NA
Cyprichromini	Cypkib	Cyprichromis sp. "kibishi"	Bel16	Bel18	no	XY	LG05, LG02, LG15	XY, LG05	GWAS+BarplotDNA
Cyprichromini	Cyplep	Cyprichromis leptosoma	ISI2	ISI6	yes	ZW	LG05, LG13	ZW, LG05, LG13	GWAS+BarplotDNA+RNA
Cyprichromini	Cypmic	Cyprichromis microlepidotus	JVE1	JVF2	yes	XY/ZW	LG01, LG05, LG16	XY, LG05	GWAS+Barplot+RNA
Cyprichromini	Cyppav	Cyprichromis pavo	JEB2	JEB4	no	XY	LG05	XY, LG05	GWAS+BarplotDNA
Cyprichromini	Cypzon	Cyprichromis zonatus	GPC9	GPD1	no	XY	LG01, LG02, LG05	XY, LG05	GWAS+BarplotDNA
Cyprichromini	Pcybri	Paracyprichromis sp. "brieni south"	IQB9	IQC1	no	ZW	LG04	NA	Barplot DNA
Cyprichromini	PcybrN	Paracyprichromis brieni	JXI2	JXI4	yes	NA	NA	NA	NA
Cyprichromini	Pcynig	Paracyprichromis nigripinnis	GPC4	GPC6	yes	XY	LG15	XY, LG15	BarplotDNA+RNA
Ectodini	Asplep	Asprotilapia leptura	INF2	INF1	no	NA	NA	NA	Barplot DNA
Ectodini	Auldew	Aulonocranus dewindti		AUA1, AUA9	yes	ZW	NA	ZW	RNA
Ectodini	Calmac	Callochromis macrops	BND3	BND5	yes	NA	NA	NA	Barplot DNA + RNA
Ectodini	Calmel	Callochromis melanostigma	KAF3	KAF4	no	XY	LG04	NA	Barplot DNA
Ectodini	Calple	Callochromis pleurospilus	JZE2	JZE4	yes	XY	LG23	XY, LG23	BarplotDNA+RNAsuggestive
Ectodini	Carsch	Cardiopharynx schoutedeni	KAF1	KAF2	no	NA	NA	NA	Barplot DNA
Ectodini	Cunlon	Cunningtonia longiventralis	IWD7	IWD8	no	NA	NA	NA	Barplot DNA
Ectodini	Cyafoa	Cyathopharynx foae	IOD6	IOD4	no	NA	NA	NA	Barplot DNA
Ectodini	Cyafur	Cyathopharynx furcifer	AVH2	AYE5	yes	ZW	NA	ZW	RNA
Ectodini	Ectdes	Ectodus descampsii	IRD7	IRD8	no	NA	XY	NA	Barplot DNA
Ectodini	EctspN	Ectodus sp. "north"	KHC4	KHC5	no	ZW	LG07	NA	Barplot DNA
Ectodini	Enamel	Enantiopus melanogenys	AWC5	BNC5	yes	ZW	LG15, LG18	ZW, LG15	BarplotDNA+RNA
Ectodini	Gralem	Grammatotria lemairii	JDD7	JDD8	no	ZW	LG05	NA	BarplotDNA
Ectodini	Lesper	Lestradea perspicax	IRA1	IRA2	no	NA	NA	NA	NA
Ectodini	Lessta	Lestradea stappersii	JVH3	JVH2	no	NA	NA	NA	NA
Ectodini	Mdcrot	Microdontochromis rotundiventralis	JBE6	JBE7	no	NA	NA	NA	NA
Ectodini	Mdcten	Microdontochromis tenuidentata	LHG4	LHG6	no	ZW/XY	LG15, LG18, LG06, LG08	NA	NA
Ectodini	Ophboo	Ophthalmotilapia boops	LFI4	LFI6	no	ZW	LG18	NA	BarplotDNA
Ectodini	Ophhet	Ophthalmotilapia heterodonta	Bel06, Bel12		no	NA	NA	NA	NA
Ectodini	Ophnas	Ophthalmotilapia nasuta	AXH6	AXH8	no	ZW/XY	LG04, LG23, LG18	NA	Barplot DNA
Ectodini	Ophpar	Ophthalmotilapia paranasuta	JYF7	JYG5	no	ZW/XY	LG16; LG04,	NA	Barplot DNA
Ectodini	Ophven	Ophthalmotilapia ventralis	IQD3	IQE4	yes	XY	LG04	NA	Barplot DNA
Ectodini	Ophwhi	Ophthalmotilapia sp. "white cap"	LGH1	LGH3	no	NA	NA	NA	NA
Ectodini	Xenbat	Xenotilapia bathyphila	IVB4	IVB5	no	ZW	LG16	NA	Barplot DNA
Ectodini	Xenbou	Xenotilapia boulengeri	IPE3	IPE7	yes	ZW	LG15	ZW, LG15	RNA
Ectodini	Xencau	Xenotilapia caudafasciata	IXB9	IXC1	no	NA	NA	NA	NA
Ectodini	Xenfla	Xenotilapia flavipinnis	JAF7	JAF9	no	XY	LG10	NA	Barplot DNA
Ectodini	Xenkil	Xenotilapia sp. "kilesa"	Bel01, Bel03		no	NA	NA	NA	NA
Ectodini	Xenlon	Xenotilapia longispinis	KAF5	KAF6	no	NA	NA	NA	NA
Ectodini	Xennas	Xenotilapia nasus	IMF7	IMF8	yes	NA	NA	NA	NA
Ectodini	XenniS	Xenotilapia nigrolabiata South	IZC7	IXF4	no	XY	LG16	NA	Barplot DNA
Ectodini	Xenoch	Xenotilapia ochrogenys	JVH4	JVI5	no	XY/ZW	LG16, LG02, LG12, LG23	NA	BarplotDNA
Ectodini	Xenorn	Xenotilapia ornatipinnis North	JZE6	JZE8	no	NA	NA	NA	NA
Ectodini	XenpaK	Xenotilapia papilio		A206	no	NA	NA	NA	NA
Ectodini	Xenpap	Xenotilapia papilio (Katete population)	IVF4	IVF5	no	XY	LG06, LG11	NA	Barplot DNA
Ectodini	Xensim	Xenotilapia sima (location Chipwa)	IUF7	IUF8	no	ZW/XY	LG12, LG16	NA	Barplot DNA
Ectodini	Xensim	Xenotilapia sima (location Toby's)	LBE2	LBE9	no	XY	LG04	NA	Barplot DNA
Ectodini	Xensin	Xenotilapia singularis	IRD9	IRE3	no	ZW	LG23	NA	BarplotDNA
Ectodini	Xenspi	Xenotilapia spilopterus	AXB5	AXB8	yes	NA	NA	NA	NA
Ectodini	XenspN	Xenotilapia sp. "spilopterus north"	LEA3	LEA4	no	ZW	LG16	NA	BarplotDNA
Ectodini	Xensun	Xenotilapia sp. "papilio sunflower"	GPF8	GPF9	no	ZW/XY	LG02, LG12	NA	BarplotDNA
Eretmodini	Erecya	Eretmodus cyanostictus	IZH7	IZI3	yes	XY/ZW	LG10,LG14, LG16, LG22	XY, LG10	Fisher several species
Eretmodini	Eremar	Eretmodus marksmithi	JXE9	JXF4	yes	XY/ZW	LG10, LG19	NA	Fisher several species+RNA
Eretmodini	Spaery	Spathodus erythrodon	JUB6	JUB7	yes	XY/ZW	LG02, LG05, LG07, LG10, LG13, LG15, LG20	XY, LG10	Fisher several species+RNA
Eretmodini	Spamar	Spathodus marlieri	JZB7	JZD3	no	XY/ZW	LG10, LG16	XY, LG10	Fisher several species
Eretmodini	Tanirs	Tanganicodus irsacae	JYH3	JYH7	yes	XY	LG10, LG18	XY, LG10	Fisher several species
Haplochromini	Arcstr	Astatoreochromis straeleni	KAE8		no	NA	NA	NA	NA
Haplochromini	Astbur	Astatotilapia burtoni	IZA1	IZC5, JYD5	no	XY/ZW	LG05, LG14, LG18, LG13	XY, LG05, LG14, LG1	literature
Haplochromini	Astfla	Astatotilapia flaviijosephi	LJD2		no	NA	NA	NA	NA
Haplochromini	Astpal	Astatotilapia paludinosus	KYG1		no			NA	NA
Haplochromini	Ctepol	Ctenochromis polli	JWG2		no	NA	NA	NA	NA
Haplochromini	Hplkil	Haplochromis sp. "kilossana"	LJE8		no	NA	NA	NA	NA
Haplochromini	HplspC	Haplochromis sp. "chipwa"	HXC4	HXC5	no	NA	NA	NA	NA
Haplochromini	Hplsta	Haplochromis stappersii	JYD3		no	NA	NA	NA	NA
Haplochromini	Hplvan	Haplochromis vanheusdeni	JWG3		no	NA	NA	NA	NA
Haplochromini	Ortcho	Orthochromis indermauri	HXC7	HXC6	no	XY	LG19	XY, LG19	GWAS+Fisher+StackedBarplot
Haplochromini	Ortmaz	Orthochromis mazimeroensis	KDC6		no	NA	NA	NA	NA
Haplochromini	Ortred	Orthochromis malagaraziensis	KYE2		no	NA	NA	NA	NA
Haplochromini	Ortuvi	Orthochromis uvinzae	KYE7		no	NA	NA	NA	NA
Haplochromini	Psephi	Pseudocrenilabrus philander	JWG1		no	XY	LG07	XY, LG07	Literature
Haplochromini	Thobra	Thoracochromis brauschi	JWF8		no	NA	NA	NA	NA
Lamprologini	Altcal	Altolamprologus calvus	IOE2	IOE3	no	NA	NA	NA	NA
Lamprologini	Altcom	Altolamprologus compressiceps	ISB1	ISC9	yes	XY	LG07	XY, LG07	RNA
Lamprologini	Altshe	Altolamprologus sp. "compressiceps shell"	IRH2	IRH4	no	NA	NA	NA	NA
Lamprologini	Chabif	Chalinochromis sp. "bifrenatus"	LDE1	LDD9	no	XY	LG15, LG20	XY, LG15, LG20	GWAS+Fisher several species
Lamprologini	Chabri	Chalinochromis brichardi	AVB2	AVA9	yes	XY	LG07, LG15, LG19, LG20	XY, LG15, LG20	GWAS+Fisher several species+RNA
Lamprologini	Chacya	Chalinochromis cyanophleps	LGG6	LGG7	no	XY	LG15, LG20, LG22	XY, LG15, LG20	GWAS+Fisher several species
Lamprologini	Chando	Chalinochromis sp. "ndobhoi"	KEE9	KEF1	no	XY	LG15, LG20	XY, LG15, LG20	GWAS+Fisher several species
Lamprologini	Chapop	Chalinochromis popelini	Bel07	Bel09	no	XY	LG15, LG20	XY, LG15, LG20	GWAS+Fisher several species
Lamprologini	Juldic	Julidochromis dickfeldi	IRC4	IRC5	yes	XY	LG15, LG20	XY, LG15, LG20	GWAS+Fisher several species
Lamprologini	Julkom	Julidochromis sp. "kombe"	ILD9	INA6	no	XY	LG20	XY, LG20	GWAS+Fisher several species
Lamprologini	JulmaN	Julidochromis marlieri	JXB5	JXC1	no	XY	LG15, LG18, LG20	XY, LG15, LG20	GWAS+Fisher several species
Lamprologini	JulmaS	Julidochromis sp. "marlieri South"	LBF3	LBA1	no	XY	LG15, LG20	XY, LG15, LG20	GWAS+Fisher several species
Lamprologini	Julmrk	Julidochromis marksmithi	LFG8	LFH1	no	XY/ZW	LG15, LG20, LG11	XY, LG15, LG20	GWAS+Fisher several species

→ Table continuous on the next page

			data used			Sex chromosome characterization			
Tribe	ID	Full Name	Genome (M)	Genome (F)	RNAseq data	Final Call System	Final Call LG	Final Call Stringent	Types of evidence
Lamprologini	Julorn	Julidochromis ornatus	ISB7	ISC1	yes	XY	LG15, LG20	XY, LG15, LG20	GWAS+Fisher several species
Lamprologini	Julreg	Julidochromis sp. "regani south"	IRB8	IRB2	yes	XY/ZW	LG15, LG20, LG22	XY, LG15, LG20	GWAS+Fisher several species
Lamprologini	JulreK	Julidochromis regani	KHE6	KFF4	no	XY	LG10, LG15, LG20	XY, LG15, LG20	GWAS+Fisher several species
Lamprologini	Jultra	Julidochromis transcriptus	HFG1287	LJC2	no	XY	LG15, LG20	XY, LG15, LG20	GWAS+Fisher several species
Lamprologini	Lamcal	Lamprologus callipterus	IPH2	JAB1	no	NA	NA	NA	NA
Lamprologini	Lamkun	Lamprologus kungweensis	JXG8	JXH2	yes	XY	LG14	NA	Barplot DNA
Lamprologini	Lamlap	Lamprologus laparogramma	JDI2	JDI1	no	NA	NA	NA	NA
Lamprologini	Lamlem	Lamprologus lemairii	IZI7	IPD6	yes	ZW	NA	NA	RNA
Lamprologini	Lamoce	Lamprologus ocellatus	ILC1	ILD3	yes	ZW	NA	ZW	RNA
Lamprologini	Lamorn	Lamprologus ornatipinnis	JZF3	JZF4	no	XY	LG23	NA	Barplot DNA
Lamprologini	LamorS	Lamprologus sp. "ornatipinnis zambia"	JDF5	JDG4	no	NA	NA	NA	NA
Lamprologini	Lamsig	Lamprologus signatus	IWD5	IWD6	no	NA	NA	NA	NA
Lamprologini	Lamspe	Lamprologus speciosus	KCG2	KCG3	no	NA	NA	NA	NA
Lamprologini	Lamtig	Lamprologus tigripictilis		JWF6	no	NA	NA	NA	NA
Lamprologini	Lepatt	Lepidiolamprologus attenuatus	AVD4	AVG5	yes	ZW/XY	LG08	ZW	RNA
Lamprologini	Lepcun	Lepidiolamprologus cunningtoni	IOH5	IOH4	no	NA	NA	NA	NA
Lamprologini	Lepelo	Lepidiolamprologus elongatus	AUE6	Aug.08	yes	NA	NA	NA	NA
Lamprologini	Lepkam	Lepidiolamprologus kamambae	LFF7	LFF8	no	NA	NA	NA	NA
Lamprologini	Lepken	Lepidiolamprologus kendalli	IMD1	IMD2	no	NA	NA	NA	BarplotDNA
Lamprologini	LepmeK	Lepidiolamprologus sp. "meeli kipili"	LHA5	LHA2	no	NA	NA	NA	NA
Lamprologini	Lepmim	Lepidiolamprologus mimicus	LDD1	LDD6	no	NA	NA	NA	NA
Lamprologini	Leppro	Lepidiolamprologus profundicola	KAD2	KEB8	no	NA	NA	NA	NA
Lamprologini	Neobif	Neolamprologus bifasciatus	LHF6	LHF7	no	XY/ZW	LG04, LG19	NA	Barplot DNA
Lamprologini	Neobou	Neolamprologus boulengeri	KYB9	KCE5	no	NA	NA	NA	NA
Lamprologini	Neobre	Neolamprologus brevis	ILB6	ILB7	yes	NA	NA	NA	NA
Lamprologini	Neobri	Neolamprologus brichardi	JUI1	JUH9	no	NA	NA	NA	NA
Lamprologini	NeobrM	Neolamprologus sp. "brevis magara"	KCI6	KCI7	no	NA	NA	NA	NA
Lamprologini	Neobue	Neolamprologus buescheri	JEI4	JEI5	yes	NA	NA	NA	NA
Lamprologini	NeocaK	Neolamprologus sp. "caudopunctatus kipili	LDG2	LDG3	no	NA	NA	NA	NA
Lamprologini	Neocal	Neolamprologus calliurus	ILA7	INC7	no	NA	NA	NA	NA
Lamprologini	Neocau	Neolamprologus caudopunctatus	IQA3	IQA4	yes	XY	LG02	NA	Barplot DNA
Lamprologini	Neochi	Neolamprologus chitamwebwai	KHA7	KHA9	no	ZW	LG13	NA	Barplot DNA
Lamprologini	Neochr	Neolamprologus christyi	IZI8	ITG2	no	XY	LG19	NA	Barplot DNA
Lamprologini	Neocra	Neolamprologus crassus	IVE8	IVF1	no	ZW	LG07, LG08	NA	BarplotDNA
Lamprologini	Neocyg	Neolamprologus sp. "cygnus"	LFD2	LFD4	yes	NA	NA	NA	RNA
Lamprologini	Neocyl	Neolamprologus cylindricus	GPH1	GPH2	yes	XY	LG02, LG07	XY, LG07	RNA+BarplotDNA
Lamprologini	Neodev	Neolamprologus devosi	LEH2		no	NA	NA	NA	NA
Lamprologini	Neoese	Neolamprologus sp. "eseki"	LFB7	LFB9	no	NA	NA	NA	NA
Lamprologini	Neofal	Neolamprologus falcicula	JXD4	JXD7	no	NA	NA	NA	NA
Lamprologini	NeofaM	Neolamprologus sp. "falcicula mahale"	LCC2	LCB5	no	NA	NA	NA	NA
Lamprologini	Neofas	Neolamprologus fasciatus	AUE7	AXD5	yes	ZW	NA	NA	RNA
Lamprologini	Neofur	Neolamprologus furcifer	JEI6	JEI8	yes	XY	LG06, LG07	NA	Barplot DNA
Lamprologini	NeofuU	Neolamprologus sp. "furcifer ulwile"	LDF5	LDF4	no	NA	NA	NA	NA
Lamprologini	Neogra	Neolamprologus gracilis	JWH2	JWH1	no	XY/ZW	LG01, LG10, LG08, LG15, LG18	NA	Barplot DNA
Lamprologini	NeogrM	Neolamprologus sp. "gracilis tanzania"	LCB4	LCC6	no	XY	LG07, LG17, LG23	NA	Barplot DNA
Lamprologini	Neohec	Neolamprologus hecqui	A142		no	NA	NA	NA	NA
Lamprologini	Neohel	Neolamprologus helianthus	JWG9	JWG8	no	NA	NA	NA	NA
Lamprologini	Neokom	Neolamprologus sp. "kombe"	ILE5	ILE6	no	ZW	NA	NA	Barplot DNA
Lamprologini	Neoleu	Neolamprologus longior	KEH3	LEE1	no	NA	NA	NA	NA
Lamprologini	Neolon	Neolamprologus longicaudatus	JWI2	JWI3	no	NA	NA	NA	NA
Lamprologini	Neolou	Neolamprologus leloupi	LCA1	LCA2	no	NA	NA	NA	NA
Lamprologini	Neomar	Neolamprologus marunguensis	JWH3	JWH4	no	ZW	NA	NA	NA
Lamprologini	Neomee	Neolamprologus meeli	JDF3	JDF4	no	NA	NA	NA	NA
Lamprologini	Neomod	Neolamprologus modestus	IMG9	IMH3	yes	ZW	LG05, LG16	ZW, LG05, LG16	RNA
Lamprologini	Neomon	Neolamprologus mondabu	JVB4	JVB8	no	XY/ZW	LG14, LG15, LG20	XY, LG15, LG20	GWAS+Fisher several species
Lamprologini	Neomul	Neolamprologus multifasciatus	IRF6	IRF8	yes	XY	LG07	NA	BarplotDNA
Lamprologini	Neomux	Neolamprologus mustax	ILH1	ILB4	no	NA	NA	NA	NA
Lamprologini	Neonig	Neolamprologus niger	KYA1	KYA5	yes	NA	NA	NA	NA
Lamprologini	Neonve	Neolamprologus nigriventris	LJC3	A108	no	NA	NA	NA	NA
Lamprologini	Neoobs	Neolamprologus obscurus	IMA2	IMA1	no	XY	LG07, LG20	XY, LG20	Fisher several species, BarplotDNA strong outlier
Lamprologini	Neooli	Neolamprologus olivaceous	JWH6	JWH5	no	XY	LG12, LG15, LG20, LG23, LG18	XY, LG15, LG20	GWAS+Fisher several species
Lamprologini	Neopet	Neolamprologus petricola	LGH8	LGI1	no	XY/ZW	LG02, LG22	NA	Barplot DNA
Lamprologini	Neople	Neolamprologus pleuromaculatus	JZF1	JZF2	no	NA	NA	NA	NA
Lamprologini	Neopro	Neolamprologus prochilus	IVH1	IVH2	no	XY	LG20	XY, LG20	Fisher several species
Lamprologini	Neopul	Neolamprologus pulcher	ISA6	ISB3	yes	ZW	NA	ZW	RNA
Lamprologini	Neosav	Neolamprologus savoryi	ISA8	IYA4	yes	ZW	NA	ZW	RNA
Lamprologini	Neosex	Neolamprologus sexfasciatus	IND7	IND8	no	NA	NA	NA	NA
Lamprologini	Neosim	Neolamprologus similis	KEC1	KEC2	no	NA	NA	NA	NA
Lamprologini	Neospl	Neolamprologus splendens	A188, LJD3		no	NA	NA	NA	NA
Lamprologini	Neotet	Neolamprologus tetracanthus	IPF7	IPG3	yes	ZW	LG04	NA	Barplot DNA
Lamprologini	Neotim	Neolamprologus timidus	LGE2	LGE3	no	NA	NA	NA	NA
Lamprologini	Neotoa	Neolamprologus toae	JZD5	JZD6	yes	XY	LG15, LG20	XY, LG15, LG20	GWAS
Lamprologini	Neotre	Neolamprologus tretocephalus	KFH4	KFH5	no	XY	LG23	NA	BarplotDNA
Lamprologini	NeoveB	Neolamprologus ventralis	KAG7	KAG8	no	ZW	LG04, LG06	NA	BarplotDNA
Lamprologini	NeoveS	Neolamprologus sp. "ventralis stripe"	JED4	JED5	no	XY	LG07, LG20	NA	BarplotDNA
Lamprologini	Neowal	Neolamprologus walteri	KFD4	KFD2	yes	XY	LG17	NA	Barplot DNA
Lamprologini	Telbif	Telmatochromis bifrenatus	KYB7	KYB8	no	XY	LG15, LG20	XY, LG15, LG20	GWAS+Fisher several species
Lamprologini	Telbra	Telmatochromis brachygnathus	JBE8	JBE9	no	ZW	LG20	NA	Barplot DNA
Lamprologini	Telbri	Telmatochromis brichardi	JVI9	JXA4	no	XY/ZW	LG15, LG20, LG08, LG10, LG13	NA	GWAS+Fisher several species
Lamprologini	TeldhN	Telmatochromis sp. "dhonti north"	JUD4	JUD5	no	XY	LG15, LG20	XY, LG15, LG20	GWAS+Fisher several species
Lamprologini	TeldhS	Telmatochromis dhonti	LBF8	LBF7	yes	XY	LG20	XY, LG20	Fisher several species
Lamprologini	TeldhT	Telmatochromis sp. "dhonti twiyu"	LHC1	LHF2	no	XY	LG15,LG20	XY, LG15, LG20	GWAS+Fisher several species
Lamprologini	Telluf	Telmatochromis sp. "lufubu"	HXC8		no	NA	NA	NA	NA
Lamprologini	Telshe	Telmatochromis sp. "shell"	IRI8	IRI9	no	XY	LG20	XY, LG20	GWAS+Fisher several species
Lamprologini	TelteS	Telmatochromis temporalis	IMB3	IMB4	yes	ZW	LG12	ZW	RNA+BarplotDNA
Lamprologini	Telvit	Telmatochromis vittatus	JBD5	JBD6	yes	ZW	LG20	ZW, LG20	GWAS+Fisher several species+RNA
Lamprologini	Varmoo	Variabilichromis moorii	AUC4	AUC3	yes	XY	LG20	XY, LG20	GWAS+Fisher several species
Limnochromini	Baicen	Baileychromis centropomoides	JAB7	JAE9	no	XY	NA	NA	BarplotDNA
Limnochromini	Gnaper	Gnathochromis permaxillaris	IUI5	ITA4	no	NA	NA	NA	NA
Limnochromini	Gwcchr	Greenwoodochromis christyi	IZE4	IZF1	no	NA	NA	NA	NA
Limnochromini	Lchabe	Limnochromis abeelei	ITB4	ITB3	no	NA	NA	NA	NA
Limnochromini	Lchaur	Limnochromis auritus	JAF5	ITB1	yes	ZW	NA	ZW	RNA+BarplotDNA
Limnochromini	Lchsta	Limnochromis staneri	ITC2	ITA6	no	ZW	NA	NA	BarplotDNA
Limnochromini	Regcal	Reganochromis calliurus	IUI1	IUI4	no	XY	LG05	NA	BarplotDNA
Limnochromini	Tchdha	Tangachromis dhanisi	LJA7	LJA8	no	XY/ZW	LG11, LG16, LG17, LG10	NA	NA
Limnochromini	Trioto	Triglachromis otostigma	JEG6	JEG5	no	XY	LG19	NA	NA
Oreochromini	Oretan	Oreochromis tanganicae	JAB6	JAC7	yes	NA	NA	NA	NA
Perissodini	Permic	Perissodus microlepis	IQC4	IQI4	yes	XY	LG02	NA	BarplotDNA
Perissodini	Pleela	Plecodus elaviae	LHI4	LHI6	no	XY	LG12	NA	Barplot DNA
Perissodini	Plemul	Plecodus multidentatus	IZA9	IZA8	no	ZW	NA	NA	BarplotDNA
Perissodini	Plepar	Plecodus paradoxus	JDI4	LEC7	yes	XY	LG02, LG19	XY, LG19	BarplotDNA+RNA
Perissodini	Plestr	Plecodus straeleni			yes	XY	LG19	XY, LG19	RNA
Perissodini	Xchhec	Xenochromis hecqui	IUI7	JAH7	no	NA	NA	NA	NA
Trematocarini	Tremac	Trematocara macrostoma	IUD8	IUD9	no	ZW/XY	LG04/LG23	ZW, LG04	Fisher signal in two species

→ Table continuous on the next page

			data used			Sex chromosome characterization			
Tribe	ID	Full Name	Genome (M)	Genome (F)	RNAseq data	Final Call System	Final Call LG	Final Call Stringent	Types of evidence
Trematocarini	Tremar	Trematocara marginatum	ISA1	ISA3	yes	XY/ZW	LG14	NA	Barplot DNA, RNA
Trematocarini	Trenig	Trematocara nigrifrons	IUE5	GPA1	yes	NA	NA	NA	NA
Trematocarini	Treuni	Trematocara unimaculatum	IXA3	IXA6	no	ZW	LG04, LG12	ZW, LG04	Fisher signal in two species
Trematocarini	Trezeb	Trematocara zebra	LFC9	LFE4	no	NA	NA	NA	NA
Tropheini	Ctehor	Ctenochromis horei	AVA8	AXA7	yes	ZW	NA	ZW	RNA
Tropheini	Gnapfe	Gnathochromis pfefferi	AWB7	AWE2	yes	XY	LG11, LG15	XY, LG11, LG15	StackedBarplot+RNA
Tropheini	Intloo	Interochromis loocki	IPF3	IPB6	yes	XY	LG05, LG19	XY, LG05, LG19	GWAS+Fisher
Tropheini	Limdar	Limnotilapia dardennii	AWI6	AWI5	no	NA	NA	NA	NA
Tropheini	Loblab	Lobochilotes labiatus	ISD8	ISE5	yes	NA	NA	NA	NA
Tropheini	Peteph	Petrochromis ephippium	IYA5	IPC1	yes	NA	NA	NA	NA
Tropheini	Petfam	Petrochromis famula	IYA7	IYA6	yes	XY	LG05, LG19	XY, LG05, LG19	Fisher+StackedBarplot+RNA
Tropheini	Petfas	Petrochromis fasciolatus	GPH7	JAE1	yes	XY	LG05, LG19	XY, LG05, LG19	GWAS+Fisher+StackedBarplot+RNA
Tropheini	Petgia	Petrochromis sp. "giant"	LDC6	LHD2	no	XY	LG05, LG19	XY, LG05, LG19	GWAS+Fisher+StackedBarplot
Tropheini	Pethor	Petrochromis horii	IWB5	IWB6	no	XY	LG05, LG19	XY, LG05, LG19	Fisher+BarplotDNA
Tropheini	Petiko	Petrochromis sp. "orthognathus ikola"	LFA6	LFA8	no	XY	LG05, LG19	XY, LG05, LG19	GWAS+Fisher+StackedBarplot
Tropheini	Petkas	Petrochromis sp. "kazumbae"	KEB4	KEA4	no	NA	NA	NA	NA
Tropheini	Petkip	Petrochromis sp. "kipili brown"	LDE3	LDE4	no	XY	LG05, LG19, LG22	XY, LG05,LG19	GWAS+Fisher+StackedBarplot
Tropheini	Petmac	Petrochromis macrognathus	LDA4	LJB1	yes	NA	NA	NA	NA
Tropheini	Petmos	Petrochromis sp. "moshi yellow"	LCF6	LCF8	no	ZW	LG02	NA	Barplot DNA
Tropheini	Petort	Petrochromis orthognathus	JXH5	JXH4	no	NA	NA	NA	NA
Tropheini	Petpol	Petrochromis polyodon	AWB9	AWI4	yes	NA	NA	NA	NA
Tropheini	Petrai	Petrochromis sp. "macrognathus rainbow"	LGB5	LGB8	no	XY	LG05, LG19	XY, LG05, LG19	GWAS+Fisher+StackedBarplot
Tropheini	Petred	Petrochromis sp. "red"	LCD1	LCD5	no	XY	LG05, LG19	XY, LG05, LG19	GWAS+Fisher+StackedBarplot
Tropheini	Pettex	Petrochromis sp. "polyodon texas"	LHB1	LHB3	no	XY	LG05, LG19	XY, LG05, LG19	GWAS+Fisher+StackedBarplot
Tropheini	Pettre	Petrochromis trewavasae	IWC9	IWD4	no	XY	LG05, LG19	XY, LG05, LG19	GWAS+Fisher+StackedBarplot
Tropheini	Pscbab	Pseudosimochromis babaulti	JUA3	JUA4	yes	XY	LG05, LG19	XY, LG05, LG19	GWAS+Fisher+StackedBarplot+RNA
Tropheini	Psccur	Pseudosimochromis curvifrons	AYC7	AXF8	no	XY	LG05, LG19	XY, LG05, LG19	Fisher+StackedBarplot
Tropheini	Pscmar	Pseudosimochromis marginatus	KCE7	KCF3	no	XY	LG05, LG19	XY, LG05, LG19	Fisher+StackedBarplot
Tropheini	Pscmrg	Pseudosimochromis marginatus (North)	KFE8	KFF1	no	XY	LG05, LG19	XY, LG05, LG19	Fisher+StackedBarplot
Tropheini	Pscple	Pseudosimochromis babaulti (South)	AUB6	AVB6	yes	XY	LG05, LG19	XY, LG05, LG19	Fisher+StackedBarplot+RNA
Tropheini	Simdia	Simochromis diagramma	AUE1	AUD8	yes	ZW	NA	ZW	RNA
Tropheini	Troann	Tropheus annectens	JWG4	JWG5	no	NA	NA	NA	NA
Tropheini	Trobri	Tropheus brichardi	JYI8	JZA3	no	XY	LG19	XY, LG19	GWAS+Fisher+StackedBarplot
Tropheini	TrobrK	Tropheus sp. "brichardi kipili"	LGA5	LGA6	no	NA	NA	NA	NA
Tropheini	Trodub	Tropheus duboisi	KHA4	KHA5	no	NA	NA	NA	NA
Tropheini	Trokir	Tropheus sp. "kirschfleck"	LCF1	LCF3	no	XY	LG19	XY, LG19	GWAS+Fisher+StackedBarplot
Tropheini	Troluk	Tropheus sp. "lukuga"	KEF2	KEF3	no	XY	LG19	XY, LG19	GWAS+Fisher+StackedBarplot
Tropheini	Trolun	Tropheus sp. "lunatus"	KED6	KED7	no	XY	LG19	XY, LG19	GWAS+Fisher+StackedBarplot
Tropheini	Tromoo	Tropheus moorii	JBH4	JBH5	yes	NA	NA	NA	NA
Tropheini	Tromor	Tropheus sp. "morago"	LHD9	LHE3	no	XY	LG19	NA	Barplot DNA
Tropheini	Trompi	Tropheus sp. "mpimbwe"	LDI5	LDI7	no	NA	NA	NA	NA
Tropheini	Tronig	Tropheus sp. "black"	JVC9	JVC3	yes	XY	LG19	XY, LG19	GWAS+Fisher+StackedBarplot+RNA
Tropheini	Tropol	Tropheus polli	LEF8	LEF9	no	XY	LG19	XY, LG19	GWAS+Fisher+StackedBarplot
Tropheini	Trored	Tropheus sp. "red"	IOD9	IOE1	no	NA	NA	NA	NA

Table S2 Information on sex chromosome and heterogamety in the family Adrianichthyidae

Species	Chromosome of O. latipes reference genome showing sex-linkage	Heterogametic status	Sex-determining gene	Presence in ray-finned fish phylogeny Rabosky et al.
Oryzias latipes	1	XY	dmY	yes
Oryzias curvinotus	1	XY	dmY	yes
Oryzias skaizumii	1	XY	dmy	no
Oryzias sinensis	1	XY	dmY	yes
Oryzias mekongensis	2	XY	NA	yes
Oryzias hubbsi	5	ZW	NA	yes
Oryzias minutillus	8	XY	NA	yes
Oryzias dancena	10	XY	Sox3Y	yes
Oryzias marmoratus	10	XY	Sox3Y	yes
Oryzias profundicola	10	XY	Sox3Y	yes
Oryzias luzonensis	12	XY	gsdfY	yes
Oryzias javanicus	16	ZW	NA	yes
Oryzias matanensis	24	XY	NA	yes
Oryzias celebensis	24	XY	NA	yes
Oryzias wolasi	24	XY	NA	no
Oryzias woworae	24	XY	NA	no
Oryzias carnaticus	NA	NA	NA	yes
Oryzias hadiatyae	NA	NA	NA	yes
Oryzias sarasinorum	NA	NA	NA	yes
Oryzias eversi	NA	NA	NA	yes
Adrianichthys oophorus	NA	NA	NA	yes
Oryzias nigrimas	NA	NA	NA	yes

Table S3 Sex determination data in ray-finned fish species included in ohylogeny from Rabosjy et al. 2018

SpeciesName	ZW	XY	NonGSD
Acanthopagrus australis	0	0	1
Acanthopagrus berda	0	0	1
Acanthopagrus bifasciatus	0	0	1
Acanthopagrus butcheri	0	0	1
Acanthopagrus latus	0	0	1
Acanthopagrus schlegelii schlegelii	0	0	1
Achoerodus viridis	0	0	1
Acipenser transmontanus	1	0	0
Alepes djedaba	1	0	0
Allodontichthys hubbsi	0	1	0
Allodontichthys tamazulae	0	0	1
Altolamprologus compressiceps	0	1	0
Amphiprion bicinctus	0	0	1
Amphiprion clarkii	0	0	1
Amphiprion frenatus	0	0	1
Amphiprion melanopus	0	0	1
Amphiprion ocellaris	0	0	1
Amphiprion perideraion	0	0	1
Amphiprion polymnus	0	0	1
Amphiprion sandaracinos	0	0	1
Anampses geographicus	0	0	1
Anguilla anguilla	1	0	0
Anguilla japonica	1	0	0
Anguilla rostrata	1	0	0
Apareiodon affinis	1	0	0
Apeltes quadracus	1	0	0
Aphyosemion loennbergii	0	1	0
Aphyosemion malumbresi	0	1	0
Aphyosemion melanogaster	0	1	0
Apistogramma agassizii	0	0	1
Apistogramma caetei	0	0	1
Apistogramma hoignei	0	0	1
Aplocheilus panchax	1	0	0
Apolemichthys trimaculatus	0	0	1
Arctoscopus japonicus	0	1	0
Argentina silus	0	1	0
Arothron nigropunctatus	0	1	0
Astatotilapia burtoni	0.5	0.5	0
Astatotilapia calliptera	0	1	0
Aulonocara baenschi	0	1	0
Aulonocranus dewindti	1	0	0
Baldwinella vivanus	0	0	1
Barbonymus gonionotus	0	1	0
Bathybates graueri	1	0	0
Benthochromis horii	1	0	0
Benthochromis melanoides	0	1	0
Benthochromis tricoti	0	1	0
Beryx splendens	0	1	0
Betta splendens	0	0	1
Bidyanus bidyanus	0	0	1
Bodianus diplotaenia	0	0	1
Bodianus eclancheri	0	0	1
Bodianus rufus	0	0	1
Boleophthalmus boddarti	1	0	0
Boops boops	0	0	1
Bothus podas	0	1	0
Brachyhypopomus pinnicaudatus	0	1	0
Brevoortia aurea	0	1	0
Brienomyrus brachyistius	0	1	0
Bryaninops yongei	0	0	1
Calamus nodosus	0	0	1
Callionymus curvicornis	0	1	0
Callochromis pleurospilus	1	0	0
Calotomus carolinus	0	0	1
Calotomus spinidens	0	0	1
Carassius auratus	0	1	0
Carassius carassius	0	0.5	0.5
Carassius gibelio	0	0	1
Carassius langsdorfii	0	0	1
Centropomus undecimalis	0	0	1
Centropristis striata	0	0	1
Centropyge acanthops	0	0	1
Centropyge ferrugata	0	0	1
Centropyge flavissima	0	0	1
Centropyge multispinis	0	0	1
Centropyge potteri	0	0	1
Centropyge tibicen	0	0	1
Cephalopholis cruentata	0	0	1
Cephalopholis fulva	0	0	1
Chaenodraco wilsoni	0	1	0
Chaetodon multicinctus	0	0	1
Chalinochromis brichardi	0	1	0
Characidium fasciatum	1	0	0
Cheimerius nufar	0	0	1
Chionobathyscus dewitti	0	1	0
Chionodraco hamatus	0	1	0
Chionodraco myersi	0	1	0
Chlorophthalmus albatrossis	0	0	1
Chlorurus gibbus	0	0	1
Chlorurus sordidus	0	0	1
Choerodon azurio	0	0	1
Choerodon schoenleinii	0	0	1
Chrysoblephus cristiceps	0	0	1
Chrysoblephus laticeps	0	0	1
Chrysoblephus puniceus	0	0	1
Chrysophrys major	0	0	1
Cichlasoma bimaculatum	0	0	1
Cirrhitichthys falco	0	0	1
Clarias batrachus	1	0	0
Clarias fuscus	0	1	0
Clarias gariepinus	0	1	0
Clepticus parrae	0	0	1
Cobitis bilineata	0	0	1
Cobitis elongatoides	0	0	1
Cobitis hankugensis	0	0	1
Cobitis lutheri	0	0	1
Cobitis striata	0	1	0
Cobitis taenia	0	0	1
Cobitis tanaitica	0	0	1

SpeciesName	ZW	XY	NonGSD
Coilia nasus	1	0	0
Conger myriaster	1	0	0
Coregonus sardinella	0	1	0
Coris julis	0	0	1
Coryphopterus alloides	0	0	1
Coryphopterus dicrus	0	0	1
Coryphopterus eidolon	0	0	1
Coryphopterus glaucofraenum	0	0	1
Coryphopterus hyalinus	0	0	1
Coryphopterus lipernes	0	0	1
Coryphopterus personatus	0	0	1
Coryphopterus thrix	0	0	1
Cottus pollux	0	1	0
Crenicara punctulatum	0	0	1
Cryptotomus roseus	0	0	1
Ctenochromis horei	1	0	0
Ctenopharyngodon idella	0	1	0
Culaea inconstans	0	0	1
Cyathopharynx furcifer	1	0	0
Cyclothone atraria	0	0	1
Cyclothone microdon	0	0	1
Cynoglossus puncticeps	1	0	0
Cyphotilapia frontosa	0.5	0.5	0
Cyphotilapia gibberosa	0	1	0
Cyprichromis coloratus	1	0	0
Cyprichromis leptosoma	1	0	0
Cyprichromis microlepidotus	0	1	0
Cyprichromis pavo	0	1	0
Cyprichromis zonatus	0	1	0
Cyprinus carpio	0	1	0
Cyprinus pellegrini	0	1	0
Danio rerio	0	0	1
Dascyllus aruanus	0	0	1
Dascyllus carneus	0	0	1
Dascyllus marginatus	0	0	1
Dascyllus reticulatus	0	0	1
Dascyllus trimaculatus	0	1	0
Decodon melasma	0	0	1
Dentex gibbosus	0	0	1
Diademichthys lineatus	0	1	0
Dicentrarchus labrax	0	0.5	0.5
Diplectrum formosum	0	0	1
Diplodus annularis	0	0	1
Diplodus sargus sargus	0	0	1
Dormitator maculatus	0	1	0
Echidna nebulosa	0	0	1
Eigenmannia virescens	0	1	0
Eleginops maclovinus	0	0	1
Eleotris pisonis	1	0	0
Epibulus insidiator	0	0	1
Epinephelus adscensionis	0	0	1
Epinephelus aeneus	0	0	1
Epinephelus akaara	0	0	1
Epinephelus bruneus	0	0	1
Epinephelus chlorostigma	0	0	1
Epinephelus coioides	0	0	1
Epinephelus diacanthus	0	0	1
Epinephelus fasciatus	0	0	1
Epinephelus guttatus	0	0	1
Epinephelus malabaricus	0	0	1
Epinephelus marginatus	0	0	1
Epinephelus morio	0	0	1
Epinephelus polyphekadion	0	0	1
Epinephelus rivulatus	0	0	1
Epinephelus striatus	0	0	1
Epinephelus tauvina	0	0	1
Eretmodus cyanostictus	0	1	0
Erythrinus erythrinus	0	1	0
Eviota afelei	0	0	1
Evynnis tumifrons	0	0	1
Fundulus diaphanus diaphanus	0	1	0
Fundulus heteroclitus heteroclitus	0	1	0
Fundulus parvipinnis	0	1	0
Fusigobius neophytus	0	0	1
Galaxias platei	0	1	0
Gambusia affinis	1	0	0
Gambusia gaigei	1	0	0
Gambusia hurtadoi	1	0	0
Gambusia puncticulata	1	0	0
Garmanella pulchra	0	1	0
Garra lamta	1	0	0
Gasterosteus aculeatus	0	1	0
Gasterosteus wheatlandi	0	1	0
Genicanthus bellus	0	0	1
Genicanthus caudovittatus	0	0	1
Genicanthus lamarck	0	0	1
Genicanthus watanabei	0	0	1
Genidens barbus	0	1	0
Geophagus brasiliensis	0	1	0
Gnathochromis pfefferi	0	1	0
Gnathopogon caerulescens	0	0.5	0.5
Gobiodon citrinus	0	1	0
Gobiodon quinquestrigatus	0	0	1
Gobius bucchichi	0	1	0
Gobius cobitis	0	1	0
Gobius niger	0	1	0
Gobius paganellus	0	1	0
Gonostoma elongatum	0	0	1
Gramma loreto	0	0	1
Gymnomuraena zebra	0	0	1
Gymnothorax eurostus	0	1	0
Gymnothorax fimbriatus	0	0	1
Gymnothorax flavimarginatus	0	0	1
Gymnothorax margaritophorus	0	0	1
Gymnothorax pictus	0	0	1
Gymnotus pantanal	0	1	0
Halichoeres bivittatus	0	0	1
Halichoeres garnoti	0	0	1
Halichoeres marginatus	0	0	1

SpeciesName	ZW	XY	NonGSD
Halichoeres pictus	0	0	1
Halichoeres poeyi	0	0	1
Halichoeres prosopeion	0	0	1
Halichoeres radiatus	0	0	1
Halichoeres scapularis	0	0	1
Harttia carvalhoi	0	1	0
Hemibates stenosoma	1	0	0
Hime japonica	1	0	0
Hipposcarus longiceps	0	0	1
Hisonotus leucofrenatus	1	0	0
Holacanthus tricolor	0	0	1
Hoplias malabaricus	0	1	0
Hoplosternum littorale	0	0	1
Hucho hucho	0	1	0
Hypoplectrus chlorurus	0	0	1
Hypoplectrus nigricans	0	0	1
Hypoplectrus puella	0	0	1
Hypoplectrus unicolor	0	0	1
Hyporthodus niveatus	0	0	1
Hyporthodus septemfasciatus	0	0	1
Hypostomus ancistroides	0	1	0
Ictalurus punctatus	0.5	0	0.5
Ilyodon whitei	1	0	0
Imparfinis mirini	1	0	0
Iniistius pavo	0	0	1
Iniistius pentadactylus	0	0	1
Julidochromis dickfeldi	0	1	0
Julidochromis marlieri	0	1	0
Julidochromis ornatus	0	1	0
Julidochromis regani	0	1	0
Julidochromis transcriptus	0	1	0
Kajikia albida	0	1	0
Kryptolebias marmoratus	0	0	1
Labeotropheus trewavasae	1	0	0
Labroides dimidiatus	0	0	1
Labrus bergylta	0	0	1
Lamprologus ocellatus	1	0	0
Lates calcarifer	0	0	1
Lepidiolamprologus attenuatus	1	0	0
Lepidocephalichthys guntea	1	0	0
Lepomis cyanellus	0	1	0
Leporinus conirostris	1	0	0
Leporinus elongatus	1	0	0
Leporinus lacustris	0	1	0
Leporinus macrocephalus	1	0	0
Leporinus obtusidens	1	0	0
Leporinus reinhardti	1	0	0
Lethrinus lentjan	0	0	1
Lethrinus mahsena	0	0	1
Lethrinus miniatus	0	0	1
Lethrinus rubrioperculatus	0	0	1
Limia melanogaster	0	0	1
Limnochromis auritus	1	0	0
Lipolagus ochotensis	0	1	0
Lithognathus aureti	0	0	1
Lithognathus lithognathus	0	0	1
Lithognathus mormyrus	0	0	1
Lophogobius cyprinoides	0	0	1
Loricariichthys platymetopon	1	0	0
Lutjanus kasmira	0	0	1
Lutjanus quinquelineatus	0	1	0
Lythrypnus dalli	0	0	1
Lythrypnus nesiotes	0	0	1
Lythrypnus spilus	0	0	1
Lythrypnus zebra	0	0	1
Macrognathus aculeatus	0	1	0
Maylandia mbenjii	0	0	1
Maylandia zebra	0	1	0
Megupsilon aporus	0	1	0
Melamphaes parvus	0	1	0
Menidia menidia	0	0	1
Menidia peninsulae	0	0	1
Microchirus ocellatus	0	1	0
Misgurnus anguillicaudatus	0	0	1
Monodactylus argenteus	0	0	1
Monopterus albus	0	0	1
Mycteroperca bonaci	0	0	1
Mycteroperca interstitialis	0	0	1
Mycteroperca microlepis	0	0	1
Mycteroperca phenax	0	0	1
Mycteroperca rubra	0	0	1
Mycteroperca tigris	0	0	1
Mycteroperca venenosa	0	0	1
Mystus tengara	1	0	0
Nannobrachium ritteri	0	1	0
Nemipterus japonicus	0	0	1
Nemipterus peronii	0	0	1
Nemipterus virgatus	0	0	1
Neocirrhites armatus	0	0	1
Neolamprologus cylindricus	0	1	0
Neolamprologus modestus	1	0	0
Neolamprologus mondabu	0	1	0
Neolamprologus obscurus	0	1	0
Neolamprologus olivaceous	0	1	0
Neolamprologus prochilus	0	1	0
Neolamprologus pulcher	1	0	0
Neolamprologus savoryi	1	0	0
Neolamprologus toae	0	1	0
Nothobranchius orthonotus	0	1	0
Noturus taylori	0	1	0
Odontesthes argentinensis	0	0	1
Odontesthes bonariensis	0	0	1
Odontesthes hatcheri	0	0	1
Odontobutis obscura	0	1	0
Odonus niger	0	1	0
Ompok bimaculatus	0	1	0
Oncorhynchus gorbuscha	0	1	0
Oncorhynchus keta	0	1	0
Oncorhynchus kisutch	0	1	0

→ Table continuous on the next page

SpeciesName	ZW	XY	NonGSD
Oncorhynchus mykiss	0	1	0
Oncorhynchus nerka	0	0.5	0.5
Oncorhynchus tshawytscha	0	1	0
Oreochromis aureus	1	0	0
Oreochromis karongae	1	0	0
Oreochromis mossambicus	0	1	0
Oreochromis niloticus	0	1	0
Oreochromis tanganicae	1	0	0
Oryzias curvinotus	0	1	0
Oryzias dancena	0	1	0
Oryzias hubbsi	1	0	0
Oryzias javanicus	1	0	0
Oryzias latipes	0	1	0
Oryzias luzonensis	0	1	0
Oryzias mekongensis	0	1	0
Oryzias minutillus	0	1	0
Osteoglossum bicirrhosum	0	1	0
Pachymetopon aeneum	0	0	1
Pachymetopon grande	0	0	1
Pagellus acarne	0	0	1
Pagellus bogaraveo	0	0	1
Pagellus erythrinus	0	0	1
Pagetopsis macropterus	0	1	0
Pagothenia borchgrevinki	0	1	0
Pagrus auriga	0	0	1
Pagrus caeruleostictus	0	0	1
Pagrus pagrus	0	0	1
Parablennius tentacularis	0	1	0
Paracentropogon rubripinnis	0	1	0
Paracyprichromis nigripinnis	0	1	0
Paragobiodon echinocephalus	0	0	1
Paralabrax humeralis	0	0	1
Paralabrax maculatofasciatus	0	0	1
Paralichthys olivaceus	0	0.5	0.5
Parodon hilarii	1	0	0
Parodon nasus	1	0	0
Parvilux ingens	0	1	0
Pelmatolapia mariae	1	0	0
Pelvicachromis pulcher	0	0	1
Petrochromis famula	0	1	0
Petrochromis fasciolatus	0	1	0
Petrochromis polyodon	0	1	0
Petrochromis trewavasae	0	1	0
Phoxinus neogaeus	0	0	1
Plecodus paradoxus	0	1	0
Plecodus straeleni	0	1	0
Plectropomus leopardus	0	0	1
Plectropomus maculatus	0	0	1
Poecilia latipinna	1	0	0
Poecilia reticulata	0	0.5	0.5
Poecilia sphenops	1	0	0
Poecilia velifera	1	0	0
Poeciliopsis lucida	0	0	1
Poeciliopsis monacha	0	0	1
Pomoxis nigromaculatus	0	1	0
Ponticola kessleri	0	1	0
Priolepis eugenius	0	0	1
Priolepis hipoliti	0	0	1
Pronotogrammus martinicensis	0	0	1
Proterorhinus marmoratus	0	1	0
Pseudanthias squamipinnis	0	0	1
Pseudobathylagus milleri	0	1	0
Pseudocrenilabrus multicolor	0	1	0
Pseudocrenilabrus philander	0	1	0
Pseudolabrus miles	0	0	1
Pseudopleuronectes yokohamae	0	0	1
Pseudosimochromis curvifrons	0	1	0
Pseudotocindus tietensis	0	1	0
Pterogymnus laniarius	0	0	1
Pterolebias hoignei	0	1	0
Pungitius pungitius	0	1	0
Puntius johorensis	0	0	1
Rhabdosargus globiceps	0	0	1
Rhabdosargus haffara	0	0	1
Rhabdosargus sarba	0	0	1
Rhinecanthus aculeatus	0	1	0
Rhinecanthus rectangulus	0	1	0
Rhinecanthus verrucosus	0	1	0
Rhinogobiops nicholsii	0	0	1
Salmo salar	0	1	0
Salmo trutta	0	1	0
Salvelinus alpinus alpinus	0	1	0
Salvelinus namaycush	0	1	0
Sarotherodon melanotheron	0	1	0
Sarpa salpa	0	0	1
Satanoperca jurupari	0	1	0
Saurida undosquamis	1	0	0
Scardinius erythrophthalmus	1	0	0
Scarus dubius	0	0	1
Scarus festivus	0	0	1
Scarus flavipectoralis	0	0	1
Scarus forsteni	0	0	1
Scarus frenatus	0	0	1
Scarus ghobban	0	0	1
Scarus globiceps	0	0	1
Scarus iseri	0	0	1
Scarus niger	0	0	1
Scarus oviceps	0	0	1
Scarus prasiognathos	0	0	1
Scarus psittacus	0	0	1
Scarus rivulatus	0	0	1
Scarus rubroviolaceus	0	0	1
Scarus schlegeli	0	0	1
Scarus taeniopterus	0	0	1
Scatophagus argus	0	1	0
Scolecenchelys gymnota	0	1	0
Scolopsis bilineata	0	0	1
Scolopsis monogramma	0	0	1
Scolopsis taenioptera	0	0	1

SpeciesName	ZW	XY	NonGSD
Scopelengys tristis	0	1	0
Scopeloberyx robustus	0	1	0
Scopelogadus mizolepis bispinosus	0	1	0
Semaprochilodus taeniurus	1	0	0
Semicossyphus pulcher	0	0	1
Serranus baldwini	0	0	1
Serranus cabrilla	0	0	1
Serranus hepatus	0	0	1
Serranus phoebe	0	0	1
Serranus scriba	0	0	1
Serranus tigrinus	0	0	1
Serranus tortugarum	0	0	1
Sigmops bathyphilus	0	0	1
Sigmops gracilis	0	0	1
Simochromis babaulti	0	1	0
Simochromis diagramma	1	0	0
Sorubim lima	0	0	1
Sparidentex hasta	0	0	1
Sparisoma atomarium	0	0	1
Sparisoma aurofrenatum	0	0	1
Sparisoma chrysopterum	0	0	1
Sparisoma radians	0	0	1
Sparisoma rubripinne	0	0	1
Sparisoma viride	0	0	1
Sparodon durbanensis	0	0	1
Sparus aurata	0	0	1
Spathodus erythrodon	0	1	0
Spathodus marlieri	0	1	0
Spicara maena	0	0	1
Spicara smaris	0	0	1
Spondyliosoma cantharus	0	0	1
Squalius carolitertii	1	0	0
Squalius pyrenaicus	1	0	0
Stenobrachius leucopsarus	0	1	0
Stephanolepis cirrhifer	0	1	0
Stephanolepis hispidus	0	1	0
Sternoptyx diaphana	0	0	1
Stethojulis trilineata	0	0	1
Symbolophorus californiensis	0	1	0
Symphodus melanocercus	0	0	1
Symphodus roissali	0	0	1
Symphodus tinca	0	0	1
Symphurus plagiusa	0	1	0
Synodontis budgetti	1	0	0
Synodontis courteti	1	0	0
Synodontis filamentosus	1	0	0
Synodontis membranacea	1	0	0
Synodontis ocellifer	1	0	0
Synodontis sorex	1	0	0
Synodontis violaceus	1	0	0
Synodus hoshinonis	1	0	0
Synodus ulae	1	0	0
Takifugu rubripes	0	1	0
Tanganicodus irsacae	0	1	0
Telmatochromis bifrenatus	0	1	0
Telmatochromis dhonti	0	1	0
Telmatochromis temporalis	1	0	0
Tenualosa macrura	0	0	1
Tenualosa toli	0	0	1
Terapon jarbua	0	0	1
Tetraodon nigroviridis	0	0	1
Thalassoma bifasciatum	0	0	1
Thalassoma cupido	0	0	1
Thalassoma duperrey	0	0	1
Thalassoma lucasanum	0	0	1
Thalassoma lutescens	0	0	1
Thalassoma pavo	0	0	1
Thalassoma purpureum	0	0	1
Thoracocharax stellatus	1	0	0
Tigrigobius multifasciatus	0	0	1
Tilapia zillii	0	1	0
Trachinotus ovatus	1	0	0
Trematocara macrostoma	1	0	0
Trematocara unimaculatum	1	0	0
Trematomus hansoni	0	1	0
Trematomus newnesi	0	1	0
Trematomus nicolai	0	1	0
Triacanthus biaculeatus	0	1	0
Trichogaster fasciata	1	0	0
Trichogaster lalius	0.5	0.5	0
Trichonotus filamentosus	0	0	1
Trimma caesiura	0	0	1
Trimma okinawae	0	0	1
Triportheus albus	1	0	0
Triportheus angulatus	1	0	0
Triportheus guentheri	1	0	0
Tropheus brichardi	0	1	0
Tropheus polli	0	1	0
Tropidophoxinellus alburnoides	0	0	1
Variabilichromis moorii	0	1	0
Verasper moseri	0	0	1
Vimba vimba	0	1	0
Xenotilapia boulengeri	1	0	0
Xenotilapia melanogenys	1	0	0
Xiphophorus alvarezi	1	0	0
Xiphophorus cortezi	0	1	0
Xiphophorus hellerii	0	0	1
Xiphophorus maculatus	0	1	0
Xiphophorus milleri	0	1	0
Xiphophorus nezahualcoyotl	0	1	0
Xiphophorus nigrensis	0	1	0
Xiphophorus pygmaeus	0	1	0
Xiphophorus variatus	0	1	0
Xiphophorus xiphidium	0	1	0
Xyrichtys martinicensis	0	0	1
Zeus faber	0	1	0
Zingel zingel	0	1	0

Species ID	Sex Chromosome	Percentage Differentiation	All sex chromosomes of the species	Heterogametic type
Altcom	LG07	6.4	LG07	XY
Batgra	LG20	4.0	LG20	ZW
Benmel	LG10	1.2	LG10, LG02	XY
Bentri	LG10	1.1	LG10	XY
Calple	LG23	14.9	LG23	XY
Chabif	LG15	0.8	LG15, LG20	XY
Chabif	LG20	3.0	LG15, LG20	XY
Chabri	LG15	6.9	LG07, LG15,LG19, LG20	XY
Chabri	LG20	5.0	LG07, LG15,LG19, LG20	XY
Chacya	LG15	1.5	LG15, LG20, LG22	XY
Chacya	LG20	1.4	LG15, LG20, LG22	XY
Chando	LG15	2.6	LG15, LG20	XY
Chando	LG20	2.8	LG15, LG20	XY
Chapop	LG15	5.1	LG15, LG20	XY
Chapop	LG20	5.7	LG15, LG20	XY
Cphfr5	LG16	10.8	LG16	ZW
Cphfro	LG16	11.4	LG16, LG23	ZW
Cphgib	LG16	8.5	LG05, LG16	XY
Cypcol	LG05	66.8	LG05, LG07	ZW
Cypdwj	LG05	68.8	LG05	ZW
Cypkib	LG05	49.4	LG05, LG02, LG15	XY
Cyplep	LG05	65.1	LG05, LG13	ZW
Cyplep	LG13	11.9	LG05, LG13	ZW
Cypmic	LG05	65.3	LG01, LG05, LG16	XY
Cyppav	LG05	74.4	LG05	XY
Cypzon	LG05	61.2	LG01, LG02, LG05	XY
Enamel	LG15	32.9	LG15, LG18	ZW
Erecya	LG10	5.3	LG10,LG14, LG16, LG22	XY
Gnapfe	LG11	24.8	LG11, LG15	XY
Gnapfe	LG15	24.1	LG11, LG15	XY
Hemste	LG04	6.2	LG04, LG07	ZW
Hemste	LG07	43.6	LG04, LG07	ZW
Intloo	LG05	15.0	LG05, LG19	XY
Intloo	LG19	15.6	LG05, LG19	XY
Juldic	LG15	4.6	LG15, LG20	XY
Juldic	LG20	3.0	LG15, LG20	XY
Julkom	LG20	5.7	LG20	XY
JulmaN	LG15	5.3	LG15, LG18, LG20	XY
JulmaN	LG20	6.8	LG15, LG18, LG20	XY
JulmaS	LG15	3.4	LG15, LG20	XY
JulmaS	LG20	2.8	LG15, LG20	XY
Julmrk	LG15	3.8	LG15, LG20, LG11	XY
Julmrk	LG20	3.5	LG15, LG20, LG11	XY
Julorn	LG15	5.6	LG15, LG20	XY
Julorn	LG20	6.7	LG15, LG20	XY
Julreg	LG15	5.1	LG15, LG20, LG22	XY
Julreg	LG20	5.8	LG15, LG20, LG22	XY
JulreK	LG15	4.8	LG10, LG15, LG20	XY
JulreK	LG20	7.0	LG10, LG15, LG20	XY
Jultra	LG15	3.8	LG15, LG20	XY
Jultra	LG20	6.3	LG15, LG20	XY
Neocyl	LG07	3.5	LG02, LG07	XY
Neomod	LG05	1.5	LG05, LG16	ZW
Neomod	LG16	1.4	LG05, LG16	ZW
Neomon	LG15	2.6	LG14, LG15, LG20	XY
Neomon	LG20	2.6	LG14, LG15, LG20	XY
Neoobs	LG20	0.8	LG07, LG20	XY
Neooli	LG15	3.5	LG12. LG15. LG20. LG23. LG18	XY
Neooli	LG20	0.1	LG12, LG15, LG20, LG23, LG18	XY
Neopro	LG20	1.0	LG20	XY
Neotoa	LG15	1.0	LG15, LG20	XY
Neotoa	LG20	0.5	LG15, LG20	XY
Ortcho	LG19	56.1	LG19	XY
Pcynig	LG15	32.6	LG15	XY
Petfam	LG05	10.3	LG05, LG19	XY
Petfam	LG19	13.7	LG05, LG19	XY
Petfas	LG05	13.5	LG05, LG19	XY
Petfas	LG19	13.1	LG05, LG19	XY
Petgia	LG05	10.8	LG05, LG19	XY
Petgia	LG19	12.5	LG05, LG19	XY
Pethor	LG05	9.2	LG05, LG19	XY
Pethor	LG19	6.9	LG05, LG19	XY
Petiko	LG05	14.1	LG05, LG19	XY
Petiko	LG19	14.7	LG05, LG19	XY
Petkip	LG05	6.7	LG05, LG19, LG22	XY
Petkip	LG19	6.6	LG05, LG19, LG22	XY
Petrai	LG05	7.6	LG05, LG19	XY
Petrai	LG19	10.7	LG05, LG19	XY
Petred	LG05	10.5	LG05, LG19	XY
Petred	LG19	9.4	LG05, LG19	XY
Pettex	LG05	12.1	LG05, LG19	XY
Pettex	LG19	12.9	LG05, LG19	XY
Pettre	LG05	11.1	LG05, LG19	XY
Pettre	LG19	13.5	LG05, LG19	XY
Plepar	LG19	67.0	LG02, LG19	XY
Psccur	LG05	19.9	LG05, LG19	XY
Psccur	LG19	13.8	LG05, LG19	XY
Pscbab	LG05	31.1	LG05, LG19	XY
Pscbab	LG19	22.5	LG05, LG19	XY
Pscmar	LG05	28.0	LG05, LG19	XY
Pscmar	LG19	17.1	LG05, LG19	XY
Pscmrg	LG05	25.6	LG05, LG19	XY
Pscmrg	LG19	15.1	LG05, LG19	XY
Pscple	LG05	14.9	LG05, LG19	XY
Pscple	LG19	16.2	LG05, LG19	XY
Spaery	LG10	1.8	LG02. LG05. LG07. LG10. LG13. LG15. LG20	XY
Spamar	LG10	2.8	LG10, LG16	XY
Tanirs	LG10	2.9	LG10, LG18	XY
Telbif	LG15	7.2	LG15, LG20	XY
Telbif	LG20	9.5	LG15, LG20	XY
TeldhN	LG15	4.6	LG15, LG20	XY
TeldhN	LG20	6.8	LG15, LG20	XY
TeldhS	LG20	7.6	LG20	XY
TeldhT	LG15	7.2	LG15,LG20	XY
TeldhT	LG20	9.1	LG15,LG20	XY
Telshe	LG20	7.4	LG20	XY
Telvit	LG20	9.8	LG20	ZW
Tremac	LG04	9.5	LG04, LG23	ZW
Treuni	LG04	8.0	LG04, LG12	ZW
Trobri	LG19	56.3	LG19	XY
Trokir	LG19	56.7	LG19	XY
Troluk	LG19	57.6	LG19	XY
Trolun	LG19	57.2	LG19	XY
Tronig	LG19	56.6	LG19	XY
Tropol	LG19	57.6	LG19	XY
Varmoo	LG20	2.5	LG20	XY
Xenbou	LG15	6.7	LG15	ZW

Table S4 Percentage of sex chromosome that shows sex-patterning. See Table S1 for full species names

Table S5 Candidate genes in the Nile tilapia genome for pigmentation and sex determination from literature and gene ontology

Candidate genes pigmentation GeneID Nile tilapia	Candidate genes pigmentation GeneID Nile tilapia (continued)	Candidate genes sex determination GeneID Nile tilapia	Candidate genes sex determination GeneID Nile tilapia (continued)
100534400	100701350	100533461	100700864
100534421	100701459	100533980	100701078
100534521	100701529	100534396	100701204
100534525	100701925	100534409	100701546
100534534	100702095	100534410	100701738
100534539	100702733	100534420	100701898
100534551	100702862	100534476	100702085
100534568	100702877	100534501	100702222
100534572	100703183	100534505	100702247
100689801	100703664	100534511	100702522
100689915	100704034	100534514	100702716
100690172	100704305	100534515	100702736
100690195	100704318	100534517	100702892
100690201	100704365	100534524	100702996
100690331	100704769	100534552	100703050
100690388	100704843	100534553	100703102
100690674	100704913	100534554	100703430
100690943	100704989	100534555	100703469
100690990	100705045	100534556	100703825
100691019	100705184	100534568	100704060
100691393	100705334	100628563	100704482
100691799	100705449	100628565	100705298
100691832	100705454	100653404	100705426
100691841	100705498	100689842	100705609
100691937	100705846	100690187	100705631
100691948	100706331	100690205	100705633
100692011	100706405	100690484	100705740
100692051	100706409	100690744	100705870
100692056	100706422	100691116	100706100
100692323	100706475	100691214	100706254
100692440	100706831	100691300	100706281
100692455	100707268	100691335	100706379
100692535	100707629	100691883	100706391
100692718	100707648	100692044	100706428
100692726	100707700	100692270	100706586
100692783	100707819	100692377	100706751
100693240	100707982	100692437	100706903
100693323	100708186	100692594	100706984
100693792	100708301	100692717	100707206
100693840	100708620	100692788	100707265
100693914	100708659	100693077	100707328
100694037	100708725	100693196	100707770
100694149	100708782	100693336	100707856
100694709	100709052	100693400	100707964
100694866	100709256	100693716	100708217
100694978	100709369	100693799	100708876
100695033	100709428	100693845	100709316
100695041	100709502	100693957	100709514
100695090	100709654	100693960	100709588
100695655	100709724	100694010	100709682
100695709	100709907	100694017	100709711
100695773	100709964	100694036	100710109
100696095	100710383	100694119	100710262
100696381	100710555	100694284	100710461
100696488	100710855	100694286	100710608
100696552	100711096	100694390	100710661
100696675	100711133	100694426	100711345
100697010	100711145	100694473	100711743
100697052	100711224	100694644	100712010
100697112	100711267	100694811	100712297
100697366	100711312	100695155	100712506
100697446	100711415	100695177	100712519
100697603	100711455	100695190	102077220
100697810	100711613	100695473	102078926
100697949	100711675	100695663	102081481
100697996	100711795	100695998	106096424
100698441	100711800	100696015	106096450
100698565	100711910	100696339	106096473
100699023	100711924	100696358	106097998
100699102	100711932	100696603	109194203
100699306	100712046	100696935	109194288
100699365	100712541	100698575	109195369
100699367	101168312	100698665	109196330
100699557	101171736	100698702	109196674
100699731	102076536	100698766	109196675
100699759	102076808	100699731	109198092
100699836	102077476	100699759	109198093
100700142	106097084	100700021	109201890
100700374	109194146	100700140	109202790
100700431	109194164	100700173	
100700935	109194169	100700424	
100700971	109194371	100700465	
100701076	109194820	100700556	
100701300	109199026	100700657	
100701349	109199183	100700736	

Table S6 Candidate genes located in the sex-determining regions of cichlids. See Table S1 for full species names

Linkage group	Species	GeneID Nile tilapia	biotype	Gene name	Gene description
LG04	Hemste	109201825	protein coding	LOC109201825	B-cell receptor CD22-like
LG04	Hemste	100707371	protein coding	rnf213	E3 ubiquitin-protein ligase RNF213
LG04	Tremac	100701209	protein coding	LOC100701209	BUB3-interacting and GLEBS motif-containing protein ZNF207 isoform X2
LG04	Tremac	102081930	protein coding	LOC102081930	sterile alpha motif domain-containing protein 9-like
LG04	Treuni	100701209	protein coding	LOC100701209	BUB3-interacting and GLEBS motif-containing protein ZNF207 isoform X2
LG04	Treuni	102081930	protein coding	LOC102081930	sterile alpha motif domain-containing protein 9-like
LG05	Cypkib	100700221	protein coding	LOC100700221	metabotropic glutamate receptor 4 isoform X2
LG05	Cypkib	100690326	protein coding	atp2b2	plasma membrane calcium-transporting ATPase 2 isoform X3
LG05	Cypzon	100707387	protein coding	LOC100707387	immunoglobulin-like and fibronectin type III domain-containing protein 1
LG05	Cypzon	100707652	protein coding	LOC100707652	immunoglobulin-like and fibronectin type III domain-containing protein 1 isoform X1
LG05	Cyplep	100692152	protein coding	camkv	caM kinase-like vesicle-associated protein
LG05	Cypcol	100699505	protein coding	LOC100699505	synaptotagmin-2 isoform X1
LG05	Cypcol	100699773	protein coding	LOC100699773	protein phosphatase 1 regulatory subunit 12B isoform X1
LG05	Cypmic	100700221	protein coding	LOC100700221	metabotropic glutamate receptor 4 isoform X2
LG05	Cypdwj	100692353	protein coding	ptprt	receptor-type tyrosine-protein phosphatase T isoform X6
LG05	Neomod	102082092	protein coding	LOC102082092	protein shisa-4-like
LG05	Neomod	102082295	protein coding	LOC102082295	protein shisa-5
LG05	Neomod	102082209	protein coding	LOC102082209	protein shisa-5-like isoform X1
LG05	Intloo	100695551	protein coding	LOC100695551	contactin-4 isoform X3
LG05	Intloo	102081487	lncRNA	LOC102081487	uncharacterized LOC102081487
LG05	Petfas	100712000	protein coding	snrpe	small nuclear ribonucleoprotein E
LG05	Petfas	100691174	protein coding	LOC100691174	cell division control protein 42 homolog isoform X2
LG05	Petfas	100695551	protein coding	LOC100695551	contactin-4 isoform X3
LG05	Petfas	102081487	lncRNA	LOC102081487	uncharacterized LOC102081487
LG05	Petgia	100712465	protein coding	LOC100712465	copine-9%2C transcript variant X3
LG05	Pethor	100694025	protein coding	LOC100694025	voltage-dependent calcium channel subunit alpha-2/delta-3 isoform X2
LG05	Pethor	102081140	protein coding	LOC102081140	uncharacterized protein LOC102081140
LG05	Petiko	100695551	protein coding	LOC100695551	contactin-4 isoform X3
LG05	Petiko	102081487	lncRNA	LOC102081487	uncharacterized LOC102081487
LG05	Petkip	100695551	protein coding	LOC100695551	contactin-4 isoform X3
LG05	Petkip	102081487	lncRNA	LOC102081487	uncharacterized LOC102081487
LG05	Petrai	100700928	protein coding	LOC100700928	deoxyribonuclease-1
LG05	Petrai	109194541	protein coding	LOC109194541	deoxyribonuclease-1-like isoform X2
LG05	Petred	100690920	protein coding	LOC100690920	fibulin-2 isoform X2
LG05	Pettex	100694025	protein coding	LOC100694025	voltage-dependent calcium channel subunit alpha-2/delta-3 isoform X2
LG05	Pettex	102081140	protein coding	LOC102081140	uncharacterized protein LOC102081140
LG05	Pettre	100691723	protein coding	iqsec1	IQ motif and SEC7 domain-containing protein 1 isoform X7
LG05	Psccur	100692152	protein coding	camkv	caM kinase-like vesicle-associated protein
LG05	Pscbab	100705135	protein coding	etnk2	ethanolamine kinase 2 isoform X2
LG05	Pscmar	100691877	protein coding	LOC100691877	copine-5 isoform X2
LG05	Pscmrg	100697401	protein coding	LOC100697401	phosphatidate phosphatase LPIN2 isoform X1
LG05	Pscmrg	100697131	protein coding	LOC100697131	myosin regulatory light polypeptide 9
LG05	Pscple	100696343	protein coding	LOC100696343	contactin-3 isoform X2
LG07	Altcom	100703688	protein coding	LOC100703688	uncharacterized protein LOC100703688
LG07	Altcom	100703956	protein coding	rbm28	RNA-binding protein 28
LG07	Neocyl	100702599	protein coding	LOC100702599	aminopeptidase N
LG07	Neocyl	100708592	protein coding	LOC100708592	uncharacterized protein LOC100708592
LG10	Benmel	102075614	protein coding	LOC102075614	uncharacterized protein LOC102075614 isoform X3
LG10	Bentri	102075614	protein coding	LOC102075614	uncharacterized protein LOC102075614 isoform X3
LG10	Erecya	100698711	protein coding	cxadr	coxsackievirus and adenovirus receptor
LG10	Spaery	100698711	protein coding	cxadr	coxsackievirus and adenovirus receptor
LG10	Tanirs	100698711	protein coding	cxadr	coxsackievirus and adenovirus receptor
LG10	Spamar	100698711	protein coding	cxadr	coxsackievirus and adenovirus receptor
LG11	Gnapfe	102079720	lncRNA	LOC102079720	uncharacterized LOC102079720
LG13	Cyplep	102076913	lncRNA	LOC102076913	uncharacterized LOC102076913
LG13	Cyplep	102076743	protein coding	lg13h7orf72	uncharacterized protein C7orf72 homolog
LG15	Enamel	100707161	protein coding	gpcpd1	LOW QUALITY PROTEIN: glycerophosphocholine phosphodiesterase GPCPD1
LG15	Enamel	100699458	protein coding	LOC100699458	solute carrier family 23 member 1
LG15	Xenbou	102077429	protein coding	LOC102077429	E3 ubiquitin-protein ligase rnf213-alpha isoform X1
LG15	Chabif	100707634	protein coding	snx9	sorting nexin-9 isoform X4
LG15	Chabif	100708179	protein coding	LOC100708179	angiopoietin-related protein 1
LG15	Chabri	100701731	protein coding	LOC100701731	up-regulator of cell proliferation
LG15	Chacya	109194911	lncRNA	LOC109194911	uncharacterized LOC109194911
LG15	Chando	100705243	protein coding	LOC100705243	LOW QUALITY PROTEIN: NHS-like protein 1
LG15	Chapop	100700034	protein coding	LOC100700034	deoxyribonuclease-2-beta
LG15	Chapop	100699770	protein coding	rpf1	ribosome production factor 1
LG15	Chapop	100710956	protein coding	LOC100710956	deoxyribonuclease-2-alpha isoform X1
LG15	JulmaN	100704690	protein coding	LOC100704690	nesprin-1 isoform X8
LG15	JulmaS	100700169	protein coding	LOC100700169	synapse differentiation-inducing gene protein 1-like
LG15	Julmrk	100702552	protein coding	sash1	SAM and SH3 domain-containing protein 1 isoform X4
LG15	Julorn	100690374	protein coding	tmem151b	transmembrane protein 151B
LG15	Julorn	100690647	protein coding	tcte1	T-complex-associated testis-expressed protein 1 isoform X3
LG15	Julreg	100700078	protein coding	LOC100700078	tripartite motif-containing protein 35 isoform X1
LG15	JulreK	100692480	protein coding	LOC100692480	low density lipoprotein receptor adapter protein 1 isoform X6
LG15	Jultra	100701168	protein coding	pde7b	cAMP-specific 3'%2C5'-cyclic phosphodiesterase 7B isoform X1
LG15	Neomon	102078051	protein coding	LOC102078051	uncharacterized protein LOC102078051 isoform X23
LG15	Neomon	100696959	protein coding	akap7	A-kinase anchor protein 7 isoform X4
LG15	Neotoa	100692749	protein coding	blk	tyrosine-protein kinase Blk
LG15	Neotoa	100692480	protein coding	LOC100692480	low density lipoprotein receptor adapter protein 1 isoform X6
LG15	Telbif	100695925	protein coding	LOC100695925	low affinity immunoglobulin gamma Fc region receptor II isoform X2
LG15	Telbif	102076702	protein coding	LOC102076702	CD276 antigen homolog
LG15	TeldhN	100691138	protein coding	ptk2b	protein-tyrosine kinase 2-beta isoform X1
LG15	TeldhT	102075576	protein coding	gen1	flap endonuclease GEN homolog 1
LG15	TeldhT	100697962	protein coding	msgn1	mesogenin-1
LG15	TeldhT	102075938	protein coding	LOC102075938	wiskott-Aldrich syndrome protein homolog
LG15	Gnapfe	100690290	protein coding	LOC100690290	T-lymphoma invasion and metastasis-inducing protein 2
LG15	Gnapfe	109194883	lncRNA	LOC109194883	uncharacterized LOC109194883
LG16	Cphfro	100704412	protein coding	LOC100704412	fas apoptotic inhibitory molecule 1 isoform X2

→ Table continuous on the next page

Linkage group	Species	GeneID Nile tilapia	biotype	Gene name	Gene description
LG16	Cphfro	100704679	protein coding	LOC100704679	poly [ADP-ribose] polymerase 9
LG16	Cphfro	100704412	protein coding	LOC100704412	fas apoptotic inhibitory molecule 1 isoform X2
LG16	Cphfro	100704679	protein coding	LOC100704679	poly [ADP-ribose] polymerase 9
LG16	Cphgib	100704412	protein coding	LOC100704412	fas apoptotic inhibitory molecule 1 isoform X2
LG16	Cphgib	100704679	protein coding	LOC100704679	poly [ADP-ribose] polymerase 9
LG16	Neomod	102080033	protein coding	LOC102080033	immunoglobulin superfamily member 3 isoform X6
LG16	Neomod	100692381	protein coding	klhl6	kelch-like protein 6
LG16	Neomod	102080119	protein coding	LOC102080119	protein IWS1 homolog
LG19	Plepar	100711379	protein coding	LOC100711379	leucine-rich repeat and fibronectin type-III domain-containing protein 2
LG19	Plestr	100703884	protein coding	fbxo33	F-box only protein 33
LG19	Intloo	100712469	protein coding	lg19h20orf194	uncharacterized protein C20orf194 homolog
LG19	Petfas	100701842	protein coding	arhgap5	rho GTPase-activating protein 5
LG19	Petgia	100696567	protein coding	LOC100696567	LOW QUALITY PROTEIN: neurexin-3a
LG19	Petgia	100694978	protein coding	dio2	type II iodothyronine deiodinase
LG19	Pethor	100689992	protein coding	LOC100689992	cathepsin L1-like
LG19	Pethor	100705883	protein coding	LOC100705883	cathepsin L1 isoform X1
LG19	Petiko	100692806	protein coding	LOC100692806	exocyst complex component 3-like protein 4 isoform X1
LG19	Petiko	102080950	protein coding	LOC102080950	titin%2C transcript variant X5
LG19	Petkip	100700490	protein coding	sgpp1	sphingosine-1-phosphate phosphatase 1
LG19	Petkip	109195774	lncRNA	LOC109195774	uncharacterized LOC109195774%2C transcript variant X1
LG19	Petrai	109195939	protein coding	LOC109195939	tumor necrosis factor alpha-induced protein 2-like
LG19	Petrai	100692806	protein coding	LOC100692806	exocyst complex component 3-like protein 4 isoform X1
LG19	Petrai	100695513	protein coding	arid4a	AT-rich interactive domain-containing protein 4A
LG19	Petred	100696567	protein coding	LOC100696567	LOW QUALITY PROTEIN: neurexin-3a
LG19	Petred	100694978	protein coding	dio2	type II iodothyronine deiodinase
LG19	Pettex	100699944	protein coding	kcnh5	potassium voltage-gated channel subfamily H member 5 isoform X2
LG19	Pettex	102083216	protein coding	LOC102083216	transcription regulator protein BACH2
LG19	Pettex	100710823	protein coding	LOC100710823	gap junction alpha-10 protein
LG19	Pettre	100689992	protein coding	LOC100689992	cathepsin L1-like
LG19	Pettre	100705883	protein coding	LOC100705883	cathepsin L1 isoform X1
LG19	Psccur	100696567	protein coding	LOC100696567	LOW QUALITY PROTEIN: neurexin-3a
LG19	Psccur	100694978	protein coding	dio2	type II iodothyronine deiodinase
LG19	Pscmar	100693880	protein coding	LOC100693880	tumor necrosis factor alpha-induced protein 2
LG19	Pscmar	102078469	protein coding	LOC102078469	uncharacterized protein LOC102078469 isoform X1
LG19	Pscmar	100702378	protein coding	npas3	neuronal PAS domain-containing protein 3 isoform X2
LG19	Pscmrg	100702378	protein coding	npas3	neuronal PAS domain-containing protein 3 isoform X2
LG19	Pscple	100702378	protein coding	npas3	neuronal PAS domain-containing protein 3 isoform X2
LG19	Pscple	100696567	protein coding	LOC100696567	LOW QUALITY PROTEIN: neurexin-3a
LG19	Trobri	100692368	protein coding	LOC100692368	connector enhancer of kinase suppressor of ras 1 isoform X2
LG19	Trobri	100703833	protein coding	pgf	placenta growth factor isoform X3
LG19	Trokir	100692368	protein coding	LOC100692368	connector enhancer of kinase suppressor of ras 1 isoform X2
LG19	Troluk	100692368	protein coding	LOC100692368	connector enhancer of kinase suppressor of ras 1 isoform X2
LG19	Trolun	100692368	protein coding	LOC100692368	connector enhancer of kinase suppressor of ras 1 isoform X2
LG19	Tronig	100692368	protein coding	LOC100692368	connector enhancer of kinase suppressor of ras 1 isoform X2
LG19	Tropol	100703833	protein coding	pgf	placenta growth factor isoform X3
LG19	Ortcho	102079941	protein coding	apob	apolipoprotein B-100 isoform X1
LG20	Batgra	100705676	protein coding	LOC100705676	helicase ARIP4 isoform X2
LG20	Benhor	100704556	protein coding	tpd52l2	tumor protein D54 isoform X12
LG20	Benhor	100700644	protein coding	LOC100700644	pancreatic progenitor cell differentiation and proliferation factor B
LG20	Benhor	109196283	tRNA	trnas-aga	tRNA-Ser
LG20	Benhor	109196288	tRNA	trnae-cuc	tRNA-Glu
LG20	Chabif	100697510	protein coding	LOC100697510	TOX high mobility group box family member 2 isoform X6
LG20	Chabri	100697510	protein coding	LOC100697510	TOX high mobility group box family member 2 isoform X6
LG20	Chacya	100697510	protein coding	LOC100697510	TOX high mobility group box family member 2 isoform X6
LG20	Chando	100697510	protein coding	LOC100697510	TOX high mobility group box family member 2 isoform X6
LG20	Chapop	100697510	protein coding	LOC100697510	TOX high mobility group box family member 2 isoform X6
LG20	Juldic	100697510	protein coding	LOC100697510	TOX high mobility group box family member 2 isoform X6
LG20	Julkom	100693869	protein coding	acot7	cytosolic acyl coenzyme A thioester hydrolase isoform X2
LG20	Julkom	100694854	protein coding	LOC100694854	transcription factor HES-2-like
LG20	JulmaN	100697510	protein coding	LOC100697510	TOX high mobility group box family member 2 isoform X6
LG20	JulmaS	102080478	protein coding	LOC102080478	fez family zinc finger protein 1
LG20	Julmrk	100704486	protein coding	plekhg5	pleckstrin homology domain-containing family G member 5 isoform X2
LG20	Julorn	100711882	protein coding	r3hdml	peptidase inhibitor R3HDML
LG20	Julorn	109196246	lncRNA	LOC109196246	uncharacterized LOC109196246
LG20	Julorn	100706245	protein coding	hnf4a	hepatocyte nuclear factor 4-alpha isoform X3
LG20	Julorn	100697510	protein coding	LOC100697510	TOX high mobility group box family member 2 isoform X6
LG20	Julreg	100712099	protein coding	cacna1d	voltage-dependent L-type calcium channel subunit alpha-1D isoform X9
LG20	JulreK	100705978	protein coding	pkig	cAMP-dependent protein kinase inhibitor gamma isoform X1
LG20	JulreK	100705718	protein coding	ada	adenosine deaminase
LG20	Jultra	100692677	protein coding	LOC100692677	proto-oncogene tyrosine-protein kinase Src isoform X4
LG20	Neomon	100697510	protein coding	LOC100697510	TOX high mobility group box family member 2 isoform X6
LG20	Neoobs	100705978	protein coding	pkig	cAMP-dependent protein kinase inhibitor gamma isoform X1
LG20	Neoobs	100705718	protein coding	ada	adenosine deaminase
LG20	Neooli	100697510	protein coding	LOC100697510	TOX high mobility group box family member 2 isoform X6
LG20	Neopro	100705852	protein coding	LOC100705852	suppressor of tumorigenicity 14 protein homolog%2C transcript variant X4
LG20	Neotoa	100697510	protein coding	LOC100697510	TOX high mobility group box family member 2 isoform X6
LG20	Telbif	100690165	protein coding	cpsf3l	integrator complex subunit 11
LG20	TeldhN	100697510	protein coding	LOC100697510	TOX high mobility group box family member 2 isoform X6
LG20	TeldhS	106098587	lncRNA	LOC106098587	uncharacterized LOC106098587%2C transcript variant X2
LG20	TeldhT	102079006	protein coding	LOC102079006	uncharacterized protein LOC102079006 isoform X2
LG20	TeldhT	100708900	protein coding	LOC100708900	sentrin-specific protease 1
LG20	TeldhT	100712023	protein coding	mfsd5	molybdate-anion transporter
LG20	TeldhT	100709170	protein coding	faim2	protein lifeguard 2
LG20	Telshe	100710491	protein coding	sema3g	semaphorin-3G isoform X1
LG20	Telvit	100690165	protein coding	cpsf3l	integrator complex subunit 11
LG20	Telvit	100697510	protein coding	LOC100697510	TOX high mobility group box family member 2 isoform X6
LG20	Varmoo	100702780	protein coding	LOC100702780	protein phosphatase 1 regulatory subunit 3A isoform X3
LG23	Calple	100692863	protein coding	lnx1	E3 ubiquitin-protein ligase LNX isoform X4

Table S7 Sex-specific transcripts based on Mahajan & Bachtrog 2017. See Table S1 for full species names

			Heterogametic type	
Species ID	Male specific contigs	Female specific contigs	According to SNP data	According to Mahajan & Bachtrog 2017
Altcom	41	30	XY	homomorphic
Neofas	1	6	ZW	ZW
Batfas	15	5	NA	XY
Batgra	3	4	ZW	homomorphic
Benhor	3	30	ZW	ZW
Boumic	3	1	NA	homomorphic
Calmac	36	17	NA	XY
Calple	4	3	XY	homomorphic
Chabri	12	1	XY	XY
Cphgib	8	14	XY	homomorphic
Ctehor	39	13	ZW	XY
Cyafur	74	22	ZW	XY
Cypdwj	6	11	ZW	homomorphic
Cyplep	72	45	ZW	homomorphic
Cypmic	19	11	XY	homomorphic
Enamel	15	16	ZW	homomorphic
Erecya	0	3	XY	ZW
Eremar	8	1	NA	XY
Gnapfe	29	2	XY	XY
Intloo	49	28	XY	homomorphic
Juldic	4	17	XY	ZW
Julorn	27	9	XY	XY
Julreg	5	7	XY	homomorphic
Lamkun	11	17	NA	homomorphic
Lamlem	7	7	NA	homomorphic
Lamoce	6	3	ZW	XY
Lchaur	4	8	ZW	ZW
Lepatt	2	16	ZW	ZW
Lepelo	7	6	NA	homomorphic
Loblab	53	56	NA	homomorphic
Neobre	3	11	NA	ZW
Neobue	0	1	NA	ZW
Neocau	27	4	NA	XY
Neocyg	8	8	NA	homomorphic
Neocyl	7	0	XY	XY
Neofur	1	1	NA	homomorphic
Neomod	1	2	ZW	ZW
Neomul	12	NA	NA	homomorphic
Neonig	9	4	NA	XY
Neopul	11	46	ZW	ZW
Neosav	41	17	ZW	XY
Neotet	35	31	NA	homomorphic
Neotoa	0	0	XY	homomorphic
Neowal	10	22	NA	ZW
Ophven	99	49	NA	XY
Oretan	8	8	NA (literature: XY)	homomorphic
PcybrN	9	8	NA	homomorphic
Pcynig	8	11	XY	homomorphic
Permic	2	10	NA	XY
Peteph	41	6	NA	XY
Petfam	65	50	XY	homomorphic
Petfas	36	25	XY	homomorphic
Petmac	19	10	NA	homomorphic
Petpol	20	38	NA	homomorphic
Plepar	8	1	XY	XY
Plestr	6	2	XY	XY
Pcsbab	22	10	XY	XY
Simdia	27	26	ZW	homomorphic
Pscple	19	11	XY	homomorphic
Spaery	10	1	XY	XY
Tanirs	12	13	XY	homomorphic
TeldhS	24	15	XY	homomorphic
TelteS	16	19	ZW	homomorphic
Telvit	5	8	ZW	homomorphic
Tremar	19	11	NA	homomorphic
Trenig	134	19	NA	XY
Tromoo	38	8	NA	XY
Tronig	124	33	XY	XY
Tylpol	6	6	NA	homomorphic
Varmoo	15	0	XY	XY
Xenbou	30	38	ZW	homomorphic
Xennas	59	10	NA	XY
Xenspi	19	2	NA	XY

Part III | Outreach

Chapter 9

Speciation: Genomic Archipelagos in a Crater Lake

Fabrizia Ronco & Walter Salzburger

Current Biology (2016)

Current Biology
Dispatches

5. Boothby, T.C., Tenlen, J.R., Smith, F.W., Wang, J.R., Patanella, K.A., Osborne Nishimura, E., Tintori, S.C., Li, Q., and Jones, C.D. (2015). Evidence for extensive horizontal gene transfer from the draft genome of a tardigrade. Proc. Natl. Acad. Sci. USA *112*, 15976–15981.

6. Koutsovoulos, G., Kumar, S., Laetsch, D.R., Stevens, L., Daub, J., Conlon, C., Maroon, H., Thomas, F., Aboobaker, A., and Blaxter, M. (2015). The genome of the tardigrade Hypsibius dujardini. bioRxiv, http://dx.doi.org/10.1101/033464.

7. Martin, A., Serano, J.M., Jarvis, E., Bruce, H.S., Wang, J., Ray, S., Barker, C.A., O'Connell, L.C., and Patel, N.H. (2016). CRISPR/Cas9 mutagenesis reveals versatile roles of Hox genes in crustacean limb specification and evolution. Curr. Biol. *26*, 14–26.

8. Averof, M., and Patel, N.H. (1997). Crustacean appendage evolution associated with changes in Hox gene expression. Nature *388*, 682–686.

9. Mendivil Ramos, O., Barker, D., and Ferrier, D.E.K. (2012). Ghost loci imply Hox and paraHox existence in the last common ancestor of animals. Curr. Biol. *22*, 1951–1956.

10. Duboule, D. (2007). The rise and fall of Hox gene clusters. Development *134*, 2549–2560.

11. Aboobaker, A.A., and Blaxter, M.L. (2003). Hox gene loss during dynamic evolution of the nematode cluster. Curr. Biol. *13*, 37–40.

12. Cook, C.E., Jiménez, E., Akam, M., and Saló, E. (2004). The Hox gene complement of acoel flatworms, a basal bilaterian clade. Evol. Dev. *6*, 154–163.

13. Campbell, L.I., Rota-Stabelli, O., Edgecombe, G.D., Marchioro, T., Longhorn, S.J., Telford, M.J., Philippe, H., Rebecchi, L., Peterson, K.J., and Pisani, D. (2011). MicroRNAs and phylogenomics resolve the relationships of Tardigrada and suggest that velvet worms are the sister group of Arthropoda. Proc. Natl. Acad. Sci. USA *108*, 15920–15924.

14. Budd, G.E. (2001). Tardigrades as "stem-group arthropods": the evidence from the Cambrian fauna. Zool. Anz. J. Comp. Zool. *240*, 265–279.

15. Dewel, R.A., and Dewel, W.C. (1996). The brain of Echiniscus viridissimus Peterfi, 1956 (Heterotardigrada): a key to understanding the phylogenetic position of tardigrades and the evolution of the arthropod head. Zool. J. Linn Soc. *116*, 35–49.

16. Mayer, G., Martin, C., Rüdiger, J., Kauschke, S., Stevenson, P.A., Poprawa, I., Hohberg, K., Schill, R.O., Pflüger, H.J., and Schlegel, M. (2013). Selective neuronal staining in tardigrades and onychophorans provides insights into the evolution of segmental ganglia in panarthropods. BMC Evol. Biol. *13*, 230.

17. Maas, A., and Waloszek, D. (2001). Cambrian derivatives of the early arthropod stem lineage, pentastomids, tardigrades and lobopodians an "Orsten" perspective. Zool. Anz. J. Comp. Zool. *240*, 451–459.

18. Ortega-Hernández, J. (2015). Lobopodians. Curr. Biol. *25*, R873–R875.

19. Telford, M.J., Budd, G.E., and Philippe, H. (2015). Phylogenomic insights into animal evolution. Curr. Biol. *25*, R876–R887.

20. Chang, E.S., Neuhof, M., Rubinstein, N.D., Diamant, A., Philippe, H., Huchon, D., and Cartwright, P. (2015). Genomic insights into the evolutionary origin of Myxozoa within Cnidaria. Proc. Natl. Acad. Sci. USA *112*, 14912–14917.

Speciation: Genomic Archipelagos in a Crater Lake

Fabrizia Ronco and Walter Salzburger*
Zoological Institute, University of Basel, Vesalgasse 1, 4051 Basel, Switzerland
*Correspondence: walter.salzburger@unibas.ch
http://dx.doi.org/10.1016/j.cub.2016.01.057

The opening stages of speciation remain poorly understood, especially from a genomic perspective. The genomes of newly discovered crater-lake cichlid fish shed light on the early phases of diversification and suggest that selection acts on multiple genomic regions.

Despite decades of research into the topic, evolutionary biologists are still struggling to understand — let alone to predict — how, when, and under which circumstances one biological unit (species) splits into two (or more) such units. While it is well established that ecology, via divergent natural selection, can play a pivotal role in this process [1,2], we know relatively little about what happens to the genomes of diversifying lineages [3,4].

A new study by Malinsky *et al.* [5] makes use of an impressive set of more than one hundred whole-genome sequences to examine, from a genomic perspective, the early phases of divergence between two ecomorphs of cichlid fishes that have recently been discovered in a small crater lake in Tanzania. Volcanic crater lakes are fascinating natural laboratories for evolutionary biologists — especially for those with a keen interest in cichlids [5–9]. These lakes form when volcanic craters — so called 'calderas' or 'maars' — become filled with water, which is often the case in areas of high precipitation in the tropics or subtropics. Owing to their volcanic origin, crater lakes are geologically well datable, they are typically small in size, yet deep, and they lack in- and outflows, which impedes their colonization by aquatic organisms. If colonized, however, e.g. by a cichlid fish population, one can survey adaptation and, in some cases, divergence of that population in a closed setting and within a known time frame.

The investigation of Malinsky *et al.* [5] is situated in crater lake Massoko, which belongs to a series of maar lakes about 40 km north of Lake Malawi in the area of the East African Rift Valley (Figure 1A). Massoko is tiny (only about 700 m in diameter), up to 37 m deep, completely isolated from surrounding water bodies and around 50,000 years old [10]. Nevertheless, it contains two distinct ecomorphs belonging to the widely distributed cichlid genus *Astatotilapia*. These ecomorphs differ, as shown by Malinsky *et al.* [5], in male breeding coloration, mate preference, habitat preference, overall morphology, the

CellPress

Current Biology
Dispatches

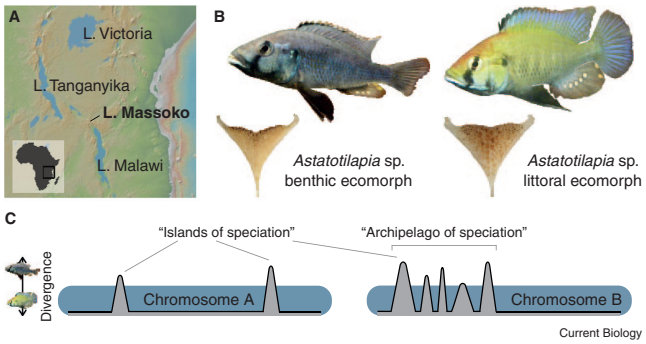

Figure 1. The genomics of sympatric speciation in East African crater lake cichlids.
(A) Map of eastern Africa showing the three largest lakes in the area and the position of the crater Lake Massoko. (B) The two ecomorphs of *Astatotilapia* sp. in Lake Massoko. For each ecomorph, a male in breeding coloration is shown, as well as the lower pharyngeal jaw bone. The pharyngeal jaw apparatus constitutes a second set of jaws in the pharynx, which is functionally decoupled from the oral jaws, and used to process food (see [18,20] and Supplementary Movie in [20]). Images by Alexandra M. Tyers. (C) Schematic view of the signature of genomic divergence between the cichlid ecomorphs in Lake Massoko. Malinsky *et al.* [5] identified more than 50 "islands of speciation", which are characterized by high levels of divergence between the two ecomorphs. About half of these islands are organized in "archipelagos" on five linkage groups.

morphology of the trophic apparatus, and diet. A form with an elongated head and blue-colored males, feeding on (more) planktonic food, occurs in the deeper benthic zone of the lake, whereas a short-headed form with yellow males and a more littoral-based diet is primarily found in the shallow-water habitat (Figure 1B). Importantly, a phylogeny based on several thousand single nucleotide polymorphisms (SNPs) derived from restriction associated DNA (RAD) sequencing revealed common ancestry of the Lake Massoko cichlids, suggesting that they have evolved *in situ* in this isolated maar lake.

To investigate the genomic signature of divergence in Lake Massoko's cichlids in more detail, Malinsky *et al.* [5] inspected whole-genome sequences of 146 individuals representing the two Massoko ecomorphs, as well as small specimens from within that lake that could not be unambiguously assigned to any of the two ecomorphs, plus additional *Astatotilapia* specimens from outside Lake Massoko. A phylogeny on the basis of these genomes confirmed the monophyly of the Lake Massoko cichlids and identified a fish from nearby Mbaka River as their closest relative, suggesting an initial colonization of Lake Massoko by Mbaka River fish. Coalescence analyses further support this scenario and suggest that the split between the two ecomorphs in Lake Massoko occurred only within the past 500–1,000 years. The authors then applied three measures to study the patterns of genomic differentiation between the two ecomorphs along the genome, relative divergence (F_{ST}), absolute sequence divergence (d_{XY}) and the difference in nucleotide diversity (π). While there was not a single fixed difference between the ecomorphs, the authors could identify close to one hundred regions in the genome that are highly diverged. Fifty-five of those highly diverged regions (HDRs) featured high d_{XY} values, while showing normal values of π, making them strong candidates for genomic regions causally implicated with speciation. These 'islands of speciation' were not randomly distributed across the genome, though. Instead, 27 of these clustered on only five chromosomes, forming some sort of 'genomic archipelagos of speciation' (Figure 1C).

The work by Malinsky *et al.* [5] provides an unprecedented view into the genomic changes associated with the early phases of adaptive divergence between a pair of cichlid ecomorphs. This is made possible because of their strategy of applying whole-genome sequencing to a large number of individuals, which enabled full resolution genome scans, and of integrating this precise genomic information with data on ecology, morphology and behavior. The study thus exemplifies the power — and feasibility — of using whole genomes to survey adaptation and organismal diversification at the population level [11,12]. Lower resolution genome scans, designed to capture only a fraction of the genome so that the distances between individual markers are comparably large, would almost certainly have failed to recover most of these HDRs (in case of the Massoko cichlids, HDRs can be as small as 4.4 kB [5]). Lower resolution genome scans, e.g. involving RAD sequencing, should thus be seen as a temporary phenomenon that, at least in the field of population and speciation genomics, will soon be replaced by whole-genome sequencing – especially, as sequencing is becoming more and more automated.

The findings of Malinsky *et al.* [5] findings are in line with previous studies investigating the genetic architecture of adaption (and diversification), which revealed that, just as seen in the Massoko cichlids [5], multiple loci on several chromosomes are involved in divergent evolution [11,13–15]. A burning question emerging from these studies relates to the actual function and phenotypic effect of these genomic regions — individually and jointly. Malinsky *et al.* [5] exerted the common approach [11,16] of subjecting the regions in question to a gene-ontology enrichment analysis, hinting at a significant enrichment for the gene-ontology terms morphogenesis, cytoskeleton, protein translation, hormone signaling and sensory systems (the latter includes a rhodopsin gene that occurs in two variants with different allele frequencies in the ecomorphs). It is fairly easy to envisage how each of these gene-ontology categories may relate to a particular trait or phenotype previously implicated with cichlid diversification [17,18]. However, only functional experiments will inform about the phenotypes associated with these HDRs and their relative contributions to adaptation and divergence. Now that these regions have been identified, such functional tests should be performed.

One aspect that has not been explored in detail by Malinsky *et al.* [5] is that of

Current Biology
Dispatches

sympatric speciation, although the system has all the ingredients to become yet another textbook example of speciation in the absence of geographical barriers and involving cichlids in a crater lake [6–9]. The geographical and taxonomic context makes the case of the Lake Massoko cichlids particularly exciting. While the previously known examples of sympatric speciation in cichlids come from crater lakes in Cameroon and Nicaragua and involve lineages that are phylogenetically rather distant to the cichlid faunas in the East African Great Lakes, the ecomorphs discovered in Lake Massoko belong to the haplochromines and, hence, to the by far most species-rich cichlid clade that is famous for its adaptive radiations in Lake Victoria and Lake Malawi [19]. It is questionable, however, whether the study of small cichlid radiations in crater lakes — even if founded by haplochromines — will tell us much about what happened with the cichlids in Lake Victoria, Lake Malawi and Lake Tanganyika. To answer this question, it will probably be necessary to examine an entire massive cichlid adaptive radiation in similar detail as has been done for the Lake Massoko cichlids.

REFERENCES

1. Nosil, P. (2012). Ecological Speciation (Oxford: Oxford University).
2. Schluter, D. (2009). Evidence for ecological speciation and its alternative. Science *323*, 737–741.
3. Berner, D., and Salzburger, W. (2015). The genomics of organismal diversification illuminated by adaptive radiations. Trends Genet. *31*, 491–499.
4. Seehausen, O., Butlin, R.K., Keller, I., Wagner, C.E., Boughman, J.W., Hohenlohe, P.A., Peichel, C.L., Saetre, G., Bank, C., Brannstrom, A., *et al*. (2014). Genomics and the origin of species. Nat. Rev. Genet. *15*, 176–192.
5. Malinsky, M., Challis, R.J., Tyers, A.M., Schiffels, S., Terai, Y., Ngatunga, B.P., Miska, E.A., Durbin, R., Genner, M.J., and Turner, G.F. (2015). Genomic islands of speciation separate cichlid ecomorphs in an East African crater lake. Science *350*, 1493–1498.
6. Schliewen, U.K., Tautz, D., and Pääbo, S. (1994). Sympatric speciation suggested by monophyly of crater lake cichlids. Nature *368*, 629–632.
7. Barluenga, M., Stölting, K.N., Salzburger, W., Muschick, M., and Meyer, A. (2006). Sympatric speciation in Nicaraguan crater lake cichlid fish. Nature *439*, 719–723.
8. Elmer, K.R., Fan, S., Kusche, H., Spreitzer, M.L., Kautt, A.F., Franchini, P., and Meyer, A. (2014). Parallel evolution Nicaraguan crater lake cichlid fishes via non-parallel routes. Nat. Comm. *5*, 5168.
9. Martin, C.H., Cutler, J.S., Friel, J.P., Touokong, C.D., Coop, G., and Wainwright, P.C. (2015). Complex histories of repeated gene flow in Cameroon crater lake cichlids cast doubt on one of the clearest examples of sympatric speciation. Evolution *69*, 1406–1422.
10. Barker, P., Williamson, D., Gasse, F., and Gibert, E. (2003). Climatic and volcanic forcing revealed in a 50,000-year diatom record from Lake Massoko, Tanzania. Quat. Res. *60*, 368–376.
11. Jones, F.C., Grabherr, M.G., Chan, Y.F., Russell, P., Mauceli, E., Johnson, J., Swofford, R., Pirun, M., Zody, M.C., White, S., *et al*. (2012). The genomic basis of adaptive evolution in threespine sticklebacks. Nature *484*, 55–61.
12. Soria-Carrasco, V., Gompert, Z., Comeault, A.A., Farkas, T.E., Parchman, T.L., Johnston, J.S., Buerkle, C.A., Feder, J.L., Bast, J., Schwander, T., *et al*. (2014). Stick insect genomes reveal natural selection's role in parallel speciation. Science *344*, 738–742.
13. Arnegard, M.E., McGee, M.D., Matthews, B., Marchinko, K.B., Conte, G.L., Kabir, S., Bedford, N., Bergek, S., Chan, Y.F., Jones, F.C., *et al*. (2014). Genetics of ecological divergence during speciation. Nature *511*, 307–311.
14. Lawniczak, M.K.N., Emrich, S.J., Holloway, A.K., Regier, A.P., Olson, M., White, B., Redmond, S., Fulton, L., Appelbaum, E., Godfrey, J., *et al*. (2010). Widespread divergence between incipient *Anopheles gambiae* species revealed by whole genome sequences. Science *330*, 512–514.
15. Fournier-Level, A., Korte, A., Cooper, M.D., Nordborg, M., Schmitt, J., and Wilczek, A.M. (2011). A map of local adaptation in *Arabidopsis thaliana*. Science *334*, 86–89.
16. Brawand, D., Wagner, C.E., Li, Y.I., Malinsky, M., Keller, I., Fan, S., Simakov, O., Ng, A.Y., Lim, Z.W., Bezault, E., *et al*. (2014). The genomic substrate for adaptive radiation in African cichlid fish. Nature *513*, 375–381.
17. Kocher, T.D. (2004). Adaptive evolution and explosive speciation: the cichlid fish mode. Nat. Rev. Genet. *5*, 288–298.
18. Salzburger, W. (2009). The interaction of sexually and naturally selected traits in the adaptive radiations of cichlid fishes. Mol. Ecol. *18*, 169–185.
19. Salzburger, W., Van Bocxlaer, B., and Cohen, A.S. (2014). Ecology and evolution of the African Great Lakes and their faunas. Annu. Rev. Ecol. Evol. Syst. *45*, 519–545.
20. Muschick, M., Indermaur, A., and Salzburger, W. (2012). Convergent evolution within an adaptive radiation of cichlid fishes. Curr. Biol. *22*, 2362–2368.

Visual Neuroscience: The Puzzle of Perceptual Stability

Eckart Zimmermann[1] and Frank Bremmer[2,*]
[1]Cognitive Neuroscience (INM3), Institute of Neuroscience and Medicine, Research Centre Juelich, D-52428 Juelich, Germany
[2]Department of Neurophysics, University of Marburg, Karl-v-Frisch Str. 8a, D-35043 Marburg, Germany
*Correspondence: frank.bremmer@physik.uni-marburg.de
http://dx.doi.org/10.1016/j.cub.2016.01.050

Our world appears stable, although our eyes constantly shift its image across the retina. What brain mechanisms allow for this perceptual stability? A recent study has brought us a step closer to answering this millennial question.

While reading this dispatch, your eyes constantly jump across the text at high speed by means of fast eye-movements, so-called saccades. Moving a camera at that speed would result in a blurred mesh that would not allow detection of any single character. Yet the perception of our world is anything but blurred: instead, the foveae of our eyes guarantee high resolution snapshots not only of this paragraph, but also of the world around us. While the past hundred years have seen an increasing

Discussion

This doctoral thesis work has led to a number of important insights contributing to a better understanding of the evolutionary mechanisms and processes behind the origin of the spectacular taxonomic, eco-morphological, and genetic diversity of the Lake Tanganyika cichlid adaptive radiation. By combining a broad set of methodologies this work represents an integrative approach addressing fundamental questions on components and the dynamics of adaptive radiations. Here, I review the main results and conclusions of part I, the main chapters of this thesis, and their implications to the field and address future perspectives.

Taxonomic Diversity

The Lake Tanganyika cichlid adaptive radiation is considered the most outstanding example of adaptive radiation (Fryer and Iles, 1972) and thus constitutes one of the prime model systems for speciation research. However, most studies on the Lake Tanganyika species flock either focused on one particular species, on a group of taxa (e.g. a genus or a tribe), or on a subset of species occurring in a particular area of the lake as a representation for the entire radiation. Consequently, some species and/or geographic regions are thoroughly investigated, whereas others remain understudied. One of the main goals of this thesis was to incorporate for the first time the *entire* Tanganyikan cichlid adaptive radiation in a comparative study (see chapter 2). However, the scientific literature is vague when it comes to the actual number of cichlid species found in Lake Tanganyika and more importantly, many taxa are undescribed. In line with this, I first reviewed the taxonomic diversity of the Lake Tanganyika cichlid assemblage and its taxonomic history (Chapter 1: The taxonomic diversity of the cichlid fish fauna of ancient Lake Tanganyika, East Africa). Based on the available literature and extensive observations and collections around the lake we compiled a species inventory of Lake Tanganyika cichlids. This chapter thus provides a complete list of all currently valid described species of the Lake Tanganyika cichlid assemblage and an additional 55 putatively undescribed species and local varieties. According to our accounts, 208 cichlid species belonging to 57 genera and 16 tribes are described from Lake Tanganyika to date and we classified another 33 taxa as potential species (undescribed). Hence, we estimate that Lake Tanganyika's cichlid species flock comprises at least 241 species, most of which (99.2%) are endemic to the basin. The presented timely species inventory of the cichlid fauna of Lake Tanganyika will facilitate future research on the taxonomy, the ecology and evolution of the species flock, as well as its

conservation. As a start, the species list provided the basis for the taxonomic sampling for chapter 2 and 8, as well as for species assignments in the transect surveys presented in chapter 4 and 5.

Eco-Morphological Disparity

Besides the shear taxonomic diversity (speciation), adaptive radiations involve adaptation to a variety of ecological niches as a key component (Gavrilets and Losos, 2009). Hence, a phenotype-environment correlation as a consequence of ecological adaptation is a prerequisite of any adaptive radiation (Schluter, 2000). In this thesis I establish such phenotype-environment associations for several morphological traits – overall fish body shape, oral jaw morphology, lower pharyngeal jaw shape, and gill raker length (see Chapters 2 and 3). As an estimate for niche use, we used stable isotope signatures of carbon (C) and nitrogen (N), which integrate over the two major components in an aquatic ecosystem (the benthic-pelagic trajectory and the trophic levels) (Post, 2002). It has previously been shown that each of the mentioned morphological traits is related to different aspects of ecology (Clabaut et al., 2007; Muschick et al., 2014, 2012, see also Chapter 4), however none of them have been investigated in a radiation-wide study. As part of this thesis I characterized the morphological disparity of virtually the entire Lake Tanganyika cichlid radiation in terms of body shape, oral jaw morphology and lower pharyngeal jaw shape (see Chapter 2: Drivers, dynamic and progression of a massive adaptive radiation in African cichlid fish). Each trait measurement is based on geometric morphometric analyses, capturing multivariate differences in skeleton or bone morphology. By and large the 'morphospace' of each trait as well as the 'ecospace' are remarkably uniformly but densely packed, showing a striking diversity in the different morphological components as well as in niche use.

The phenotype-environment correlation for gill raker length and niche use was established on a subset of species (65 taxa from the southern basin of the lake) revealing an extraordinary disparity in gill raker morphology, which is associated with trophic ecology (see Chapter 3: A functional trade-off between trophic adaptation and parental care predicts sexual dimorphism in cichlid fish). Further, in this chapter we detect a sexual dimorphism in gill raker length in some of the species. By contrasting the extent of sexual dimorphism in gill raker length among the different breeding modes of Lake Tanganyika cichlids (uni-parental mouthbrooders, bi-parental mouthbrooders, and nest guarding species) the study revealed several important findings: First, our results suggest that gill raker length is not only related to trophic ecology, but also influenced by mouthbrooding. Second, we provide insights into mechanisms and the complexity of sexual dimorphism. Evolutionary causes of sexual dimorphism are usually attributed to sexual selection (Andersson, 1994; Darwin, 1871) or initial niche divergence (Slatkin, 1984; Temeles et al., 2000). However, we report a case where a sex-specific functional trade-off related to parental care explains sexual dimorphism in a primarily trophic trait. This study not only contributes to the understanding of the evolution of sexual dimorphism but also opens a new perspective on how a functional trade-off can act as an additional source of morphological variation in a trophic trait.

Temporal Dynamics of Eco-Morphological Adaptation

Based on the ecological theory of adaptive radiation, adaptation to ecological niches is the major driver of speciation in adaptive radiations and ecological opportunity is a primary factor regulating the temporal pattern of diversification (Gavrilets and Losos, 2009; Gavrilets and Vose, 2005; Schluter, 2000). Comparing rates of eco-morphological evolution and trait disparity through

phylogenetic history can provide important insights into the temporal dynamics of adaptive radiations and the relative importance of different trajectories of adaptation to lineage accumulation.

As part of this thesis I investigated the temporal dynamics of eco-morphological adaptation through the phylogenetic history of the Lake Tanganyika cichlid radiation (Chapter 2: Drivers, dynamics and progress of a massive adaptive radiation in African cichlid fish). In a comparative approach I trace back patterns of morphospace filling (expansion and packing) in three ecological relevant traits (body shape, oral jaw morphology, and lower pharyngeal jaw shape) and estimate rates of eco-morphological evolution through time.

This study revealed a similar pattern across all three traits, that is, a burst in morphospace expansion, followed by a period of increased morphospace packing. However, the timing of the pulses differs among the traits, resulting in a consecutive order of morphospace expansion of the different ecologically relevant traits. Contrasting this pattern of morphospace filling with evolutionary rates of the different traits and the lineage accumulation through time revealed a number of important insights into the succession of eco-morphological adaptation of the Lake Tanganyika cichlid radiation. First, for body shape disparity we find a burst very early in radiation alongside with elevated evolutionary rates, both decreasing over time with increasing number of lineages. This corresponds with the 'early burst' model of adaptive radiations, which predicts diversification to be faster at early stages of a radiation and to slow down as free niche space – and thus the ecological opportunity – gets reduced (Gavrilets and Losos, 2009; Gavrilets and Vose, 2005). Interestingly, a metanalysis showed that such a signal of an 'early burst' is rather rare and previous studies of Tanganyika cichlids revealed rather constant rates of body shape evolution (Harmon et al., 2010; Muschick et al., 2012). This emphasized the important of a complete taxon sampling for comparative analysis (see e.g. Harmon et al., 2003).

Second, we find empirical support that ecological specialisation in an adaptive radiation proceeds in stages. However, while the classical three-stages model predicts a third stage of diversification along a signalling axes (Danley and Kocher, 2001; Streelman and Danley, 2003), we find a second pulse of differentiation along the trophic axes – the divergence in LPJ shape. This burst in LPJ morphospace expansion seems to be paralleled by the major peak of speciation events and maps on a temporal trend of accelerating rate of trait evolution through time. Together this suggests that the LPJ appears to have played a key role late in evolutionary history when niche space was already limited and was thus likely involved in (micro-) niche partitioning. These findings not only emphasize the pharyngeal jaw apparatus as a 'key-innovation' of the cichlid radiations, but also provide a novel perspective on the *role* of key-innovations in adaptive radiations: The 'key-innovation' might not have *provided* the ecological opportunity, but rather *allowed* a finer resource-partitioning, resulting in a densely packed niche space.

Future perspectives

The extensive dataset presented in this thesis, constitutes a valuable resource for many more projects to follow:

The sequenced genomes of virtually all members of the Tanganyika radiation provide a powerful tool for a comparative approach to pinpoint genomic regions contributing to variation within different phenotypes.

The detailed information on different trophic traits provide an ideal dataset to investigate the degree of modularity of the pharyngeal jaw apparatus and the oral jaw. Thus, testing to what degree

the functional decoupling of the oral jaw apparatus (specialized for food uptake) and the pharyngeal jaw apparatus (specialized for food processing) (Liem, 1973) is reflected in these two traits.

The extensive data collected of nearly all extant taxa of Lake Tanganyika cichlids (three-dimensional information on the lower pharyngeal jaw apparats, the CT-scans of the heads, and the X-ray images) will serve as useful reference dataset for the upcoming Tanganyika deep drilling project (Cohen and Salzburger, 2017; Russell et al., 2012).

I would also like to mention here, that work presented in this thesis and the related collection activities resulted in the foundation of the *'Ichthyological collection on Tanganyika cichlids of the University of Basel'*. With around 3'000 specimens – covering 183 of the 208 described species (88%) and nearly all of the 55 potential species and variants reported in chapter 1 – the collection ranks among the most complete scientific collections of Tanganyikan cichlids in the world. As part of my work over the past years I substantially contributed to the build-up and management of this collection, which represents an important resource for ongoing and future research projects.

References

Andersson, M., 1994. Sexual Selection. Princeton Univ. Press, Princeton, NJ.

Clabaut, C., Bunje, P.M.E., Salzburger, W., Meyer, A., 2007. Geometric morphometric analyses provide evidence for the adaptive character of the Tanganyikan cichlid fish radiations. Evolution 61, 560–578. https://doi.org/10.1111/j.1558-5646.2007.00045.x

Cohen, A.S., Salzburger, W., 2017. Scientific drilling at Lake Tanganyika, Africa: A transformative record for understanding evolution in isolation and the biological history of the African continent, University of Basel, 6-8 June 2016. Sci. Drill. 22, 43–48. https://doi.org/10.5194/sd-22-43-2017

Danley, P.D., Kocher, T.D., 2001. Speciation in rapidly diverging systems: lessons from Lake Malawi. Mol. Ecol. 10, 1075–1086.

Darwin, C.R., 1871. The descent of man and selection in relation to sex. John Murray, London, U.K.

Fryer, G., Iles, T.D., 1972. The Cichlid Fishes of the Great Lakes of Africa. T.F.H. Publications, Neptune City, NJ.

Gavrilets, S., Losos, J.B., 2009. Adaptive Radiation: Contrasting Theory with Data. Science (80-.). 323, 732–737.

Gavrilets, S., Vose, A., 2005. Dynamic patterns of adaptive radiation. PNAS 102, 18040–18045. https://doi.org/10.1073/pnas.0506330102

Harmon, L.J., Losos, J.B., Jonathan Davies, T., Gillespie, R.G., Gittleman, J.L., Bryan Jennings, W., Kozak, K.H., McPeek, M.A., Moreno-Roark, F., Near, T.J., Purvis, A., Ricklefs, R.E., Schluter, D., Schulte, J.A., Seehausen, O., Sidlauskas, B.L., Torres-Carvajal, O., Weir, J.T., Mooers, A.T., 2010. Early bursts of body size and shape evolution are rare in comparative data. Evolution (N. Y). 64, 2385–2396. https://doi.org/10.1111/j.1558-5646.2010.01025.x

Harmon, L.J., Schulte, J. a, Larson, A., Losos, J.B., 2003. Tempo and Mode of Evolutionary Radiation in Iguanian Lizards - Supporting Online Material Materials and methods. Science (80-.). 10, 1–25.

Liem, K.F., 1973. Evolutionary Strategies and Morphological Innovations: Cichlid Pharyngeal Jaws. Syst. Zool. 22, 425–441.

Muschick, M., Indermaur, A., Salzburger, W., 2012. Convergent evolution within an adaptive radiation of cichlid fishes. Curr. Biol. 22, 2362–8. https://doi.org/10.1016/j.cub.2012.10.048

Muschick, M., Nosil, P., Roesti, M., Dittmann, M.T., Harmon, L., Salzburger, W., 2014. Testing the stages model in the adaptive radiation of cichlid fishes in East African Lake Tanganyika. Proc. R. Soc. B Biol. Sci. 281, 20140605–20140605. https://doi.org/10.1098/rspb.2014.0605

Post, D.M., 2002. Using stable isotopes to estimate trophic position: models, methods, and assumptions. Ecology 83, 703–718. https://doi.org/10.2307/3071875

Russell, J.M., Cohen, A., Johnson, T.C., Scholz, C.A., 2012. Scientific drilling in the East African rift lakes: A strategic planning workshop. Sci. Drill. 49–54. https://doi.org/10.2204/iodp.sd.14.08.2012

Schluter, D., 2000. The ecology of adaptive radiation. Oxford University Press, New York.

Slatkin, M., 1984. Ecological Causes of Sexual Dimorphism. Evolution (N. Y). 38, 622–630.

Streelman, J.T., Danley, P.D., 2003. The stages of vertebrate evolutionary radiation. Trends Ecol. Evol. 18, 126–131. https://doi.org/10.1016/S0169-5347(02)00036-8

Temeles, E.J., Pan, I.L., Brennan, J.L., Horwitt, J.N., 2000. Evidence for ecological causation of sexual dimorphism in a hummingbird. Science (80-.). 289, 441–443. https://doi.org/10.1126/science.289.5478.441

Acknowledgement

The work presented in this thesis would not have been possible without the help and the support from various people I would like to acknowledge here.

First, I would like to thank **Walter Salzburger** for giving me the opportunity to work on this amazing system, for his support whenever needed and at the same time granting freedom to realize my own ideas. He is a mentor and a good friend simultaneously! I am very thankful for all the time we spent together conducting fieldwork in various places around the world: collecting samples, meeting people, and get once more inspiration for new questions and projects. Walter always encouraged me to work in an integrative way, learning new methods, advance in acquired expertise, and never loose connection to the biological system and the questions fueling my research.

Next, I would like to thank **Adrian Indermaur** for being a good friend and "the fish guy". Without him, my work would not have been possible in several aspects. First of all, I greatly appreciate his contribution during fieldwork: helping with collecting my samples and building up the Tanganyika cichlid collection as a by-product of my thesis. But equally important, he "infected" me with the fascination for cichlids. He guided me through the world of cichlids, showed and taught me this fascinating group of fish.

The same applies for **Heinz H. Büscher**. I am very grateful for his contribution to my thesis work with helping during fieldwork, and sharing his deep knowledge about Tanganyika cichlids and the data he acquired over the years. His documentation of species occurrence along the Tanganyika shoreline made a large-scale sampling possible at the first place. I always enjoy and appreciate our discussions about various aspects of cichlid biology, evolution, and taxonomy. His fascination and knowledge of Tanganyika cichlids inspires me over and over again.

I would like to thank all my collaborators and coauthors and especially **Bernd Egger** and **Anya Theis** my supervisors during my master Thesis with whom I could continue to work with during the early phase of my PhD. The positive experiences during my time as a master student, their advice and support encouraged me to do my PhD in the first place. I would also like to thank **Astrid Böhne** for her great support (scientifically and private) during my time as a PhD student.

I am very thankful to all (past and present) members of **the Salzburger Lab** for the great working atmosphere and the amazing time we spent together, and all the moments we share. The time in the Salzburger Lab shaped and influenced me in many ways – as a scientist and as a person. It would go to far to mention everyone separately but a special thanks to all my office mates (Anya, Lukas, Adrian, Attila, and Alexandra) for a lot of fun and valuable discussions. Further I am very grateful to **Marco Colombo**, **Hugo Gante**, and **Daniel Berner** for interesting und valuable discussions on various topics and projects.

The extensive fieldwork at various places around Lake Tanganyika would not have been possible without the help and support of Dinny Mwanakulya, Jimmy Sichilima, Humphery D Sichilima Jr., Gerald Katai (Zambia), George Kazumbe and his family (Tanzania), as well as Mireille Schreyen-Brichard, and Adolfe Irakoze (Burundi).

Finally, a special thank-you to Dino and my family for being my support system, helping and encouraging me through this intense time. Thank you for always being there for me!

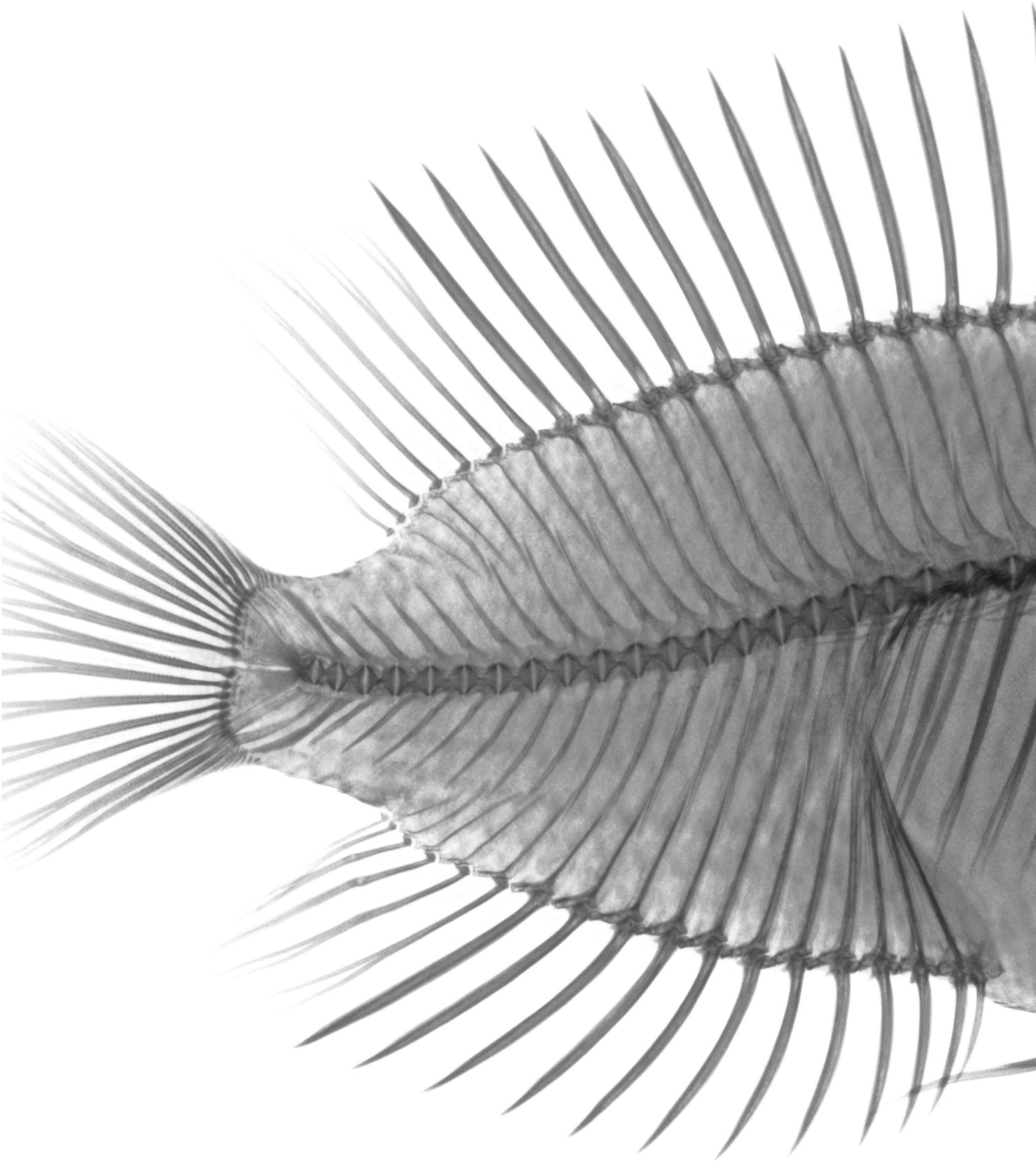

Altolamprologus calvus